

**SYNTHESIS AND CHARACTERISATION OF NOVEL
THIENYLPHOSPHINES AND THEIR GOLD(I)
COMPLEXES**

by

Elena Lakoba, M.Sc. (Moscow)

A thesis submitted in partial fulfilment of the requirements for the degree of
Doctor of Philosophy in the Faculty of Science and Agriculture
University of Natal, Pietermaritzburg

School of Chemistry and Physics


University of Natal

Pietermaritzburg

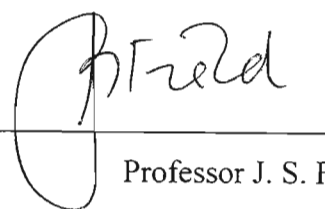
September 2000

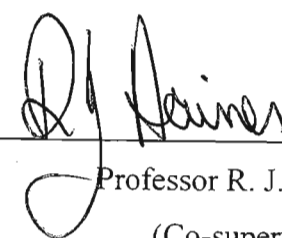
DECLARATION

I hereby certify that this research is the result of my own investigation which has not already been accepted for any other degree and is not being submitted in candidature for any other degree:

Signed  _____
E. I. Lakoba

I hereby certify that this statement is correct:

Signed  _____
Professor J. S. Field
(Supervisor)

Signed  _____
Professor R. J. Haines
(Co-supervisor)

School of Chemistry and Physics
University of Natal
Pietermaritzburg
September 2000

ACKNOWLEDGEMENTS

I wish to express my sincere gratitude to **Professors J. S. Field** and **R. J. Haines** for providing me with the great opportunity to do this research project, for their invaluable support and guidance throughout the course of this work!

I also would like to thank a number of other people who one way or another contributed towards completion of this project:

My parents, for introducing me to joys of Chemistry, for always encouraging me in my studies and for their constant support.

Drs. G. Berjzkin, S. Vinogradov, V. Djumajev and Ye. Nejmerovets, my former colleagues at the Department of Chemistry, Moscow State University, for initiating me into the art of Organometallic Chemistry, especially, Phosphine Chemistry!

Dr Hal Sosabowski, for sparking off an idea, which led to formulation of this project, as well as his friendship, interest and support.

Mr Martin Watson, for invaluable training and assistance with regards to NMR spectroscopy and mass-spectrometry, for inspiration and moral support.

Mr Paul Forder, for always being there to help, wherever glassware was concerned.

Dr Nicola Brown and **Ms Niyum Ramesar**, for their much needed help in solving and refining the X-ray crystal structures discussed herein.

Professor Mthembeni Zulu (of late), of University of Zululand, for providing the facilities for luminescent measurements.

Dr Colin Southway, for his help with gas chromatographic analysis.

Mr James Ryan, for his help with elemental analysis.

Mr Raj Somaru, for his help with preparation for running centrifugal chromatography.

Mr Dave Gregory, of the Mechanical Instrument Workshop, for technical assistance.

Mr Alistair Nixon, of the Audio Visual Centre (UNP), for drawing diagrams for Appendix B.

Mr Anil Chuturgoon, of the Department of Physiology (UND), for making facilities for cytotoxic testing available, and **Ms Thilo Pillay**, for conducting the cytotoxicity measurements.

The Foundation for Research and Development and the **University of Natal**, for financial assistance.

Professor and Dr T.M. Letcher, for encouragement, kindness and understanding.

Dr and Mrs R.A. Daneel, for their love and support throughout these years, for providing me with home away from home and becoming my second family.

My colleagues and friends in the Department of Chemistry, **Dr Florence Ajulu, Mr Francesco Bernardis, Mr Garth Cripps, Mr Jan Gertenbach, Mr Craig Grimmer, Mrs Marion Horn, Mrs Karina Kriel, Ms Noelene May, Ms Anne-Mary Poulton, Ms Niyum Ramesar, Mr Werner Shauerte and Ms Frances van Staden**, for sharing their knowledge and good times with me during these years.

And last, but not the least, my husband, **Dr Ashley Nevines**, for his undying support, through thick and thin, and for believing in me.

LIST OF ABBREVIATIONS

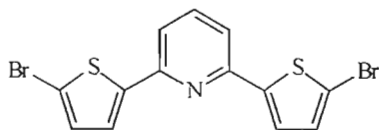
Å	angström
Ac	acetyl
Ad=Ad	adamantylidene adamantane
Ad=O	adamantanone
Ar	aryl group
b.p.	boiling point
br	broad
BrSNSBr	2,6-bis(5'-bromo-2'-thienyl)pyridine
BTDPA	2,2'-bithien-5,5'-diyl di(phenylphosphinic acid)
Bu	butyl
BuLi	<i>n</i> -butyl lithium
cm	centimetre
°C	degree Celsius
CCS	coordination chemical shift
COSY	correlated spectroscopy
d	doublet
D_c	calculated density
DEPT	distortionless enhancement by polarisation transfer
dppb	1,4-bis(diphenylphosphino)butane
dppe	1,2-bis(diphenylphosphino)ethane
dppm	bis(diphenylphosphino)methane
dppp	1,3-bis(diphenylphosphino)propane
DMF	dimethyl formamide
DMSO	dimethyl sulfoxide
DTPA	bis[5-(diphenylphosphino)-2-thienyl]phosphinic acid
ε	extinction coefficient
Et	ethyl
EtOH	ethanol
g	gram
GC	gas chromatography
GCMS	gas chromatography/mass-spectroscopic detection
{¹H}	proton noise decoupled

Het	heteroaryl group
HETCOR	heteronuclear correlated spectroscopy
HPSSPH	5,5'-bis(phenylphosphino)-2,2'-bithiophene
Hz	Hertz, s ⁻¹
IR	infra-red
J	coupling constant (Hz)
K	Kelvin
L	ligand
LDA	lithium di-(<i>iso</i> -propyl)amide
λ	radiation wavelength
m	multiplet <i>or</i> medium
max	maximum
M	mol/l <i>or</i> metal
M⁺	molecular ion
Me	methyl
MeCN	acetonitrile
MeOH	methanol
m.p.	melting point
NBS	N-bromosuccinimide
nm	nanometer
NMR	nuclear magnetic resonance
P	monodentate phosphine
PDS	phenyldi(2-thienyl)phosphine
PDSP	phenylbis[(5-diphenylphosphino)-2-thienyl]phosphine
Ph	phenyl
PhCN	benzonitrile
PNS	diphenyl[6-(2'-thienyl)-2-pyridyl]phosphine
PP	bidentate diphosphine
ppm	parts per million
Pr	propyl
PS	diphenyl(2-thienyl)phosphine
PSBr	diphenyl(5-bromo-2-thienyl)phosphine
PSN	diphenyl[5-(2'-pyridyl)-2-thienyl]phosphine
PSNP	diphenyl[5-(2'-{6'-diphenylphosphino}pyridyl)-2-thienyl]phosphine

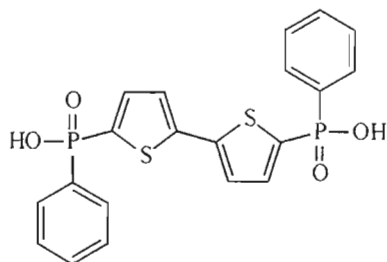
PSNSP	2,6-bis[(5'-diphenylphosphino)-2'-thienyl]pyridine
PSP	2,5-bis(diphenylphosphino)thiophene
PSS	diphenyl[5-(2,2'-bithienyl)]phosphine
PSSP	5,5'-bis(diphenylphosphino)-2,2'-bithiophene
PSSS	diphenyl[5-(2,2':5',2''-terthienyl)]phosphine
PSSSP	5,5''-bis(diphenylphosphino)-2,2':5',2''-terthiophene
PTS	tris(2-thienyl)phosphine
PTSP	tris[(5-diphenylphosphino)-2-thienyl]phosphine
Py	pyridine or pyridyl
R	alkyl group
s	singlet <i>or</i> strong
sh	shoulder
SiSSSi	5,5'-bis(trimethylsilyl)-2,2'-bithiophene
SN	2-(2'-pyridyl)thiophene [\equiv 2-(2'-thienyl)pyridine]
SNS	2,6-bis(2'-thienyl)pyridine
SS	2,2'-bithiophene
SSS	2,2':5',2''-terthiophene
tdg	thiodiethylene glycol (2,2'-thiodiethanol)
TDPA	thien-2,5-diyl di(phenylphosphinic acid)
Th	thienyl or thiophene
THF	tetrahydrofuran
tht	tetrahydrothiophene
TLC	thin layer chromatography
TMEDA	tetramethylenediamine
tr	triplet
UV	ultra-violet
vs	very strong
vw	very weak
w	weak

LIST OF STRUCTURAL FORMULAE OF PHOSPHINES AND RELATED COMPOUNDS

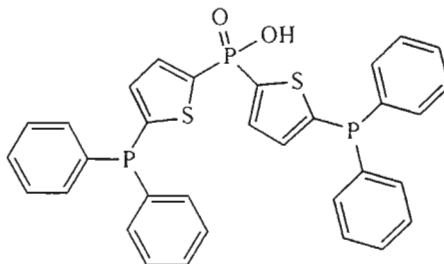
BrSNSBr :



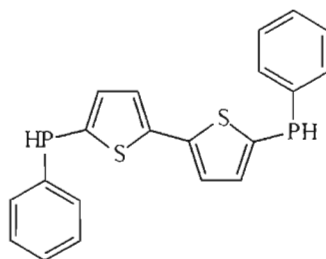
BTDPA :



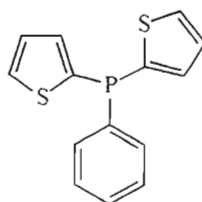
DTPA :



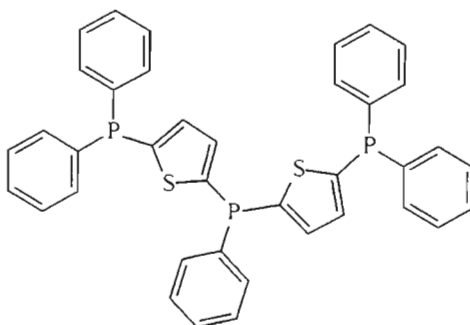
HPSSPH :



PDS :

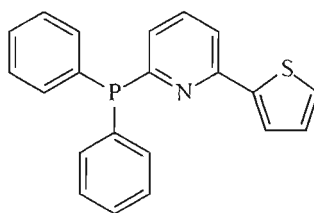


PDSP :



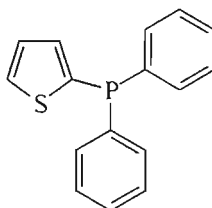
PNS

:



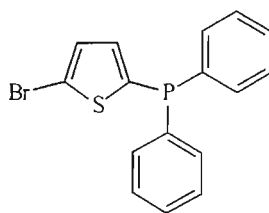
PS

:



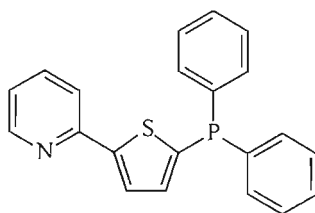
PSBr

:



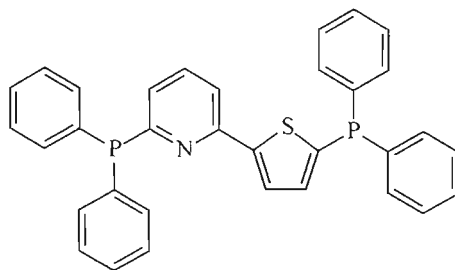
PSN

:



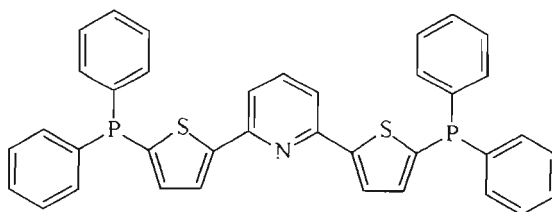
PSNP

:



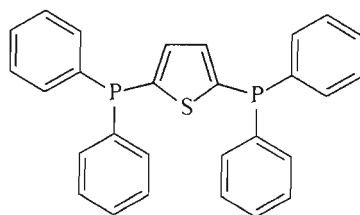
PSNSP

:



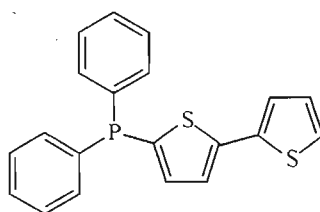
PSP

:



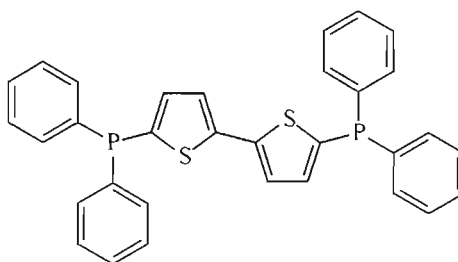
PSS

:



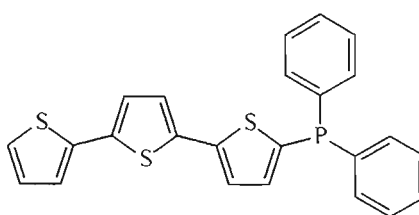
PSSP

:



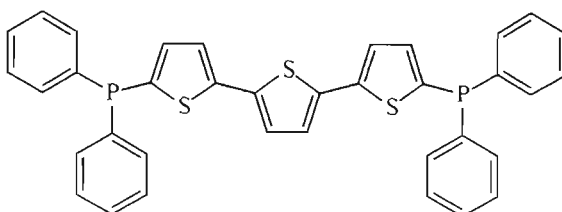
PSSS

:



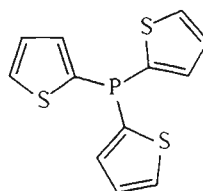
PSSSP

:



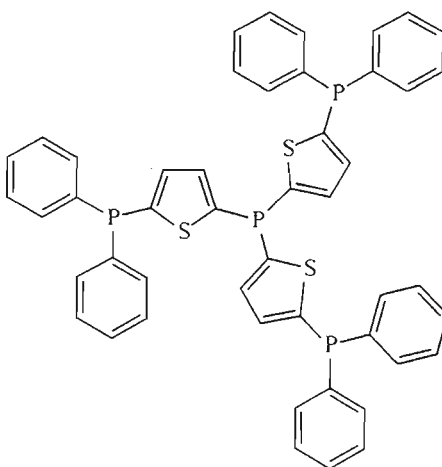
PTS

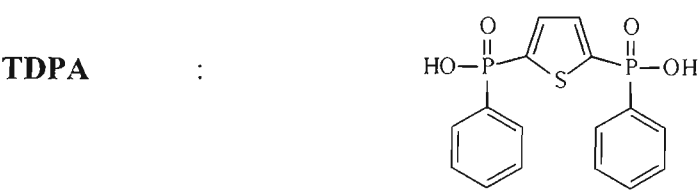
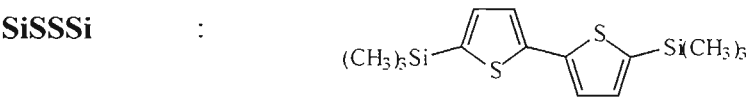
:



PTSP

:





LIST OF GOLD(I) COMPLEXES

- [1] : [ClAuPS]
- [2] : [ClAuPDS]
- [3] : [ClAuPTS]
- [4] : [ClAuPSBr]
- [5] : [ClAuPSS]
- [6] : [ClAuPSSS]
- [7] : [ClAuPSN]
- [8] : [ClAuPNS]
- [9] : [ClAu(PS)₂]
- [10] : [ClAu(PDS)₂]
- [11] : [ClAu(PTS)₂]
- [12] : [ClAu(PSN)₂]
- [13] : [ClAu(PS)₃]·2CH₂Cl₂
- [14] : [Au(η¹-PSN)₂]SbF₆
- [15] : [Au₂(μ-PSN)₂](SbF₆)₂
- [16] : [Au(η¹-PNS)₂]SbF₆
- [17] : [Au₂(μ-PNS)₂](PF₆)₂
- [18] : [ClAu(μ-PSP)AuCl]
- [19] : [ClAu(μ-PSSP)AuCl]
- [20] : [ClAu(μ-PSSSP)AuCl]
- [21] : [ClAu(μ-PSNP)AuCl]
- [22] : [ClAu(μ-PSNSP)AuCl]
- [23] : [ClAu(μ-PSP)₂AuCl]
- [24] : [ClAu(μ-PSSSP)₂AuCl]
- [25] : [Au(η¹-PSSSP)₂]PF₆
- [26] : [Au₂(μ-PSP)₂](PF₆)₂
- [27] : [Au₂(μ-PSP)₃](PF₆)₂

SUMMARY

This study comprises the preparation and characterisation of various novel tertiary mono- and polyphosphines as well as their gold(I) complexes. The possible modes of coordination of mono-, bi- and tridentate phosphine ligands to gold(I) are summarised in Chapter One, thus serving as an introduction to coordination behaviour of the new ligands to gold(I).

The synthesis and characterisation of twelve novel, tertiary mono- and polyphosphines as well as the three previously known thienylphosphines, diphenyl(2-thienyl)phosphine (PS), phenyldi(2-thienyl)phosphine (PDS) and tris(2-thienyl)phosphine (PTS), are reported in Chapter Two. There are four phosphines derived from a monothiophene unit *i.e.*, diphenyl(5-bromo-2-thienyl)phosphine (PSBr), 2,5-bis(diphenylphosphino)thiophene (PSP), phenylbis[(5-diphenylphosphino)-2-thienyl]phosphine (PDSP) and tris[(5-diphenylphosphino)-2-thienyl]phosphine (PTSP); two from a 2,2'-bithiophene unit *i.e.*, diphenyl[5-(2,2'-bithienyl)]phosphine (PSS) and 5,5'-bis(diphenylphosphino)-2,2'-bithiophene (PSSP); two phosphines from a 2,2':5',2''-terthiophene unit *i.e.*, diphenyl[5-(2,2':5'.2''-terthienyl)]phosphine (PSSS) and 5,5''-bis(diphenylphosphino)-2,2':5',2''-terthiophene (PSSSP); three phosphines from a 2-(2'-thienyl)pyridine unit *i.e.*, diphenyl[5-(2'-pyridyl)-2-thienyl]phosphine (PSN), diphenyl[6-(2'-thienyl)-2-pyridyl]phosphine (PNS) and diphenyl[5-(2'-{6'-diphenylphosphino}pyridyl)-2-thienyl]phosphine (PSNP); and one phosphine from a 2,6-bis(2'-thienyl)pyridine unit *i.e.*, 2,6-bis[(5'-diphenylphosphino)-2'-thienyl]pyridine (PSNSP). A combination of ^1H , ^{13}C and ^{31}P NMR spectroscopy as well as mass spectrometry and microanalysis is employed to establish the structures for all the compounds, while in three cases (for the ligands PSSP, PSNP and PSNSP) the structural assignment is confirmed by X-ray crystallography.

The synthetic strategies used for the preparation of the phosphine ligands vary widely from a traditional reaction between a metallated thiophene and a chlorophosphine on one hand, to a Ni-catalysed coupling reaction involving phosphine-substituted heterocycles on the other, the choice depending not only on the parent heterocyclic molecule, but also on the number of phosphorus atoms present. A new synthetic methodology leading to a potentially water-soluble diphosphine ligand is also explored. Although the target compound itself is not isolated, the preparation of its precursor, 5,5'-bis(phenylphosphino)-

2,2'-bithiophene (HPSSPH), represents the first example of the synthesis of a secondary phosphine containing a thiophene moiety.

In Chapter Three the reactions of the mono- and diphosphine ligands PS, PDS, PTS, PSBr, PSS, PSSS, PSN, PNS, PSP, PSSP, PSNP, PSSSP and PSNSP with the gold(I) precursors (such as HAuCl_4 , reduced *in situ* with thiodiglycol, and $[\text{Au}\{\text{MeCN}\}_2]\text{SbF}_6$) are studied. The structures of the products are elucidated by means of ^1H and ^{31}P NMR and IR spectroscopy as well as X-ray crystallography in the case of $[\text{ClAuPSS}]$, $[\text{ClAuPNS}]$, $[\text{ClAu}(\text{PDS})_2]$, $[\text{ClAu}(\text{PS})_3]$ and $[\text{Au}_2(\mu\text{-PSN})_2](\text{SbF}_6)_2$. Neutral complexes containing two-coordinate gold(I) are obtained for all the ligands, having general formulae $[\text{ClAuP}]$ and $[\text{ClAu}(\mu\text{-PP})\text{AuCl}]$, where P and PP represent a mono- and a diphosphine respectively. Isolation of neutral complexes with three-coordinate gold(I) proved more difficult and is only achieved for the complexes $[\text{ClAuP}_2]$ (P = PS, PDS, PTS and PSN) and $[\text{ClAu}(\mu\text{-PP})]_n$ (PP = PSP and PSSSP). A ^{31}P NMR study of the behaviour of complexes in solution shows the complexes with three-coordinate gold to be very labile with respect to dissociation of the third ligand. The complex $[\text{ClAu}(\text{PS})_3]$, where gold(I) exhibits a coordination number intermediate between 3 and 4 in the solid state (as shown by the X-ray crystallographic analysis), is serendipitously obtained from a reaction of $[\text{ClAu}(\text{PPh}_3)]$ and PS in a 1:1 molar ratio.

Both mono- and dinuclear complexes with two-coordinate gold(I) are formed when the monophosphines PSN and PNS are reacted with suitable precursors (*viz.* $[\text{ClAuPNS}]$ and $[\text{Au}\{\text{MeCN}\}_2]\text{SbF}_6$). The mononuclear complexes are of formula $[\text{Au}(\eta^1\text{-P})_2]\text{SbF}_6$, as confirmed by ^1H and ^{31}P NMR and IR spectroscopy. In the case of the dinuclear complexes, $[\text{Au}_2(\mu\text{-P})_2]\text{X}_2$ (P = PSN, X = SbF_6 ; P = PNS, X = PF_6), bridging is achieved via the phosphorus atom and nitrogen atom of the pyridine ring in both ligands. This coordination mode is consistent with the ^1H and ^{31}P NMR data for both complexes, and it is also confirmed by an X-ray structure determination of the former complex. The diphosphine ligands PSSP, PSNP and PSNSP tend to produce insoluble polymeric products when reacted with cationic gold(I) precursors, while the diphosphines PSP and PSSSP allow discrete species (*e.g.* $[\text{Au}\{\eta^1\text{-PSSSP}\}_2]\text{PF}_6$ and $[\text{Au}_2\{\mu\text{-PSP}\}_3]\{\text{PF}_6\}_2$) to be isolated under similar conditions. None of the gold(I) complexes synthesised in this work displays any evidence of the thiophene ring being one way or the other coordinated to the metal.

Chapter Three concludes with a short description of the luminescence properties of a selection of gold(I)-phosphine complexes both in solution and in the solid state. Our results confirm the previously established trend that complexes containing three-coordinate gold(I) tend to luminesce. They also show, for the first time, that a dinuclear complex with no metal-metal interaction, and where each gold atom is coordinated to one phosphorus and one nitrogen donor atom *i.e.*, $[\text{Au}_2(\mu\text{-PSN})_2](\text{SbF}_6)_2$, exhibits luminescent properties.

The results of the cytotoxic testing of a number of mono- and diphosphines (PS, PDS, PTS, PSS, PSSH, PSSP, PSSSP, PSNSP and dppe) as well as of some heterocyclic compounds and the gold(I) complexes $[\text{ClAuPSS}]$ and $[\text{ClAu}(\mu\text{-PP})\text{AuCl}]$ (PP = PSSP and dppe) against two cell lines are presented in Chapter Four. The complex $[\text{ClAuPSS}]$ shows great potency against the HepG2 (liver cancer) cell line, far exceeding that of the known cytotoxic agent, $[\text{ClAu}(\mu\text{-dppe})\text{AuCl}]$. For the other cell line, A549 (lung cancer), the cytotoxicity measurements are compared for 'in the dark' and under UVA light conditions. The results show that application of UVA light generally increases the cytotoxic properties of the compounds tested. Although there appears to be a link between the phototoxic properties of a compound and its photosensitising ability (a photophysical property of thienylphosphine ligands and their gold(I) complexes, reported at the beginning of Chapter Four), it is not yet possible to establish a quantitative correlation between the two.

TABLE OF CONTENTS

Acknowledgements	i
List of Abbreviations	iii
List of Structural Formulae of Phosphines and Related Compounds	vi
List of Gold(I) Complexes	x
Summary	xi

Chapter I MONO-, DI- AND TRINUCLEAR PHOSPHINE COMPLEXES OF GOLD(I)

I.1 INTRODUCTION	1
I.2 GOLD(I) COMPLEXES WITH MONODENTATE PHOSPHINES	4
I.2.1 Neutral mononuclear complexes	5
I.2.2 Neutral dinuclear complexes	14
I.2.3 Cationic mononuclear complexes	14
I.2.4 Cationic dinuclear complexes	19
I.3 GOLD(I) COMPLEXES WITH BIDENTATE PHOSPHINES	21
I.3.1 Mononuclear complexes	21
I.3.1.1 Neutral mononuclear complexes	22
I.3.1.2 Cationic mononuclear complexes	23
I.3.2 Dinuclear complexes of gold(I) containing bridging bidentate phosphine ligands	26
I.3.2.1 Neutral dinuclear complexes	26
I.3.2.2 Cationic dinuclear complexes	30
I.3.3 Trinuclear complexes of gold(I) containing bridging bidentate phosphine ligands	35
I.4 GOLD(I) COMPLEXES WITH TRIDENTATE PHOSPHINES	36
I.4.1 Mononuclear complexes	36
I.4.2 Dinuclear complexes	37
I.4.3 Trinuclear complexes	38
I.4.3.1 Neutral complexes	38
I.4.3.2 Cationic complexes	39
I.5 OBJECTIVES OF THIS STUDY	40

Chapter II LIGAND SYNTHESIS

II.1 INTRODUCTION TO GENERAL METHODS FOR PHOSPHINE SYNTHESIS	42
II.1.1 Addition of primary and secondary phosphines to unsaturated C-C bonds	43
II.1.2 Nucleophilic substitution at the carbon atom by metallated phosphines	43
II.1.3 Nucleophilic substitution at the phosphorus atom by organometallic reagents	46
II.1.4 Nucleophilic substitution by phosphorus(III) compounds	48
II.1.5 Electrophilic substitution by phosphorus(III) compounds	48
II.2 PREPARATION OF THIENYLPHOSPHINE LIGANDS	50
II.2.1 Preparation of monodentate phosphines with monothiophene units	50
II.2.1.1 Synthesis of PS, PDS and PTS	51
II.2.1.2 Characterisation of PS, PDS and PTS	54
II.2.2 Preparation of new mono- and polydentate tertiary phosphines with monothiophene units	60
II.2.2.1 Synthesis and characterisation of PSP	60
II.2.2.2 Synthesis and characterisation of the polydentate phosphines PDSP and PTSP	66
II.2.2.3 Synthesis and characterisation of the monodentate precursor, PSBr	75
II.2.2.4 Attempted synthesis of bis(5-diphenylphosphino-2-thienyl)-methane	78
II.2.3 Preparation of the mono- and bidentate phosphines with polythiophene units	83
II.2.3.1 Synthesis and characterisation of PSSP	84
II.2.3.2 Synthesis and characterisation of PSS	89
II.2.3.3 Synthesis and characterisation of PSSSP	95
II.2.3.4 Synthesis and characterisation of PSSS	97
II.2.4 Attempted synthesis of thienylphosphines with highly polar substituents	101
II.2.5 Synthesis of thienylphosphines containing a pyridine ring in their structure	114
II.2.5.1 Synthesis of PSN and PSNSP	115
II.2.5.2 Characterisation of PSN and PSNSP	120
II.2.5.3 Synthesis of PNS and PSNP	124
II.2.5.4 Characterisation of PNS and PSNP	127

II.3 SUMMARY AND CONCLUSION	132
II.3.1 Properties of the new thienylphosphines	132
II.3.2 Methods of synthesis	136
II.4 EXPERIMENTAL	138
II.4.1 Syntheses	138
II.4.2 Crystal structure determinations	163
 Chapter III SYNTHESIS OF GOLD(I) COMPLEXES CONTAINING NOVEL THIENYLPHOSPHINE LIGANDS	
III.1 INTRODUCTION	186
III.2 SYNTHESIS AND CHARACTERISATION OF GOLD(I) COMPLEXES WITH THE NOVEL THIENYLPHOSPHINE LIGANDS	191
III.2.1 Gold(I) complexes with monophosphine ligands	192
III.2.1.1 Neutral mononuclear complexes containing two-coordinate gold	192
III.2.1.2 Neutral mononuclear complexes containing three-coordinate gold	207
III.2.1.3 Neutral mononuclear complexes containing four-coordinate gold	215
III.2.1.4 Cationic complexes containing two-coordinate gold	224
III.2.2 Gold(I) complexes with diphosphine ligands	232
III.2.2.1 Neutral dinuclear complexes containing two-coordinate gold	232
III.2.2.2 Neutral dinuclear complexes containing three-coordinate gold	238
III.2.2.3 The cationic mononuclear complex $[\text{Au}(\eta^1\text{-PSSSP})_2]\text{PF}_6$ ([25])	241
III.2.2.4 Cationic dinuclear complexes	244
III.2.2.5 Attempted preparation of cationic dinuclear and trinuclear complexes using the PSNP ligand	247
III.3 LUMINESCENT PROPERTIES OF A SELECTION OF GOLD(I) COMPLEXES WITH THIENYLPHOSPHINE LIGANDS	250
III.4 SUMMARY AND CONCLUSION	254
III.4.1 Properties of the new gold(I) complexes	254
III.4.2 Conclusion	257

III.5 EXPERIMENTAL	259
III.5.1 Syntheses	259
III.5.2 Crystal structure determinations	272
 Chapter IV PRELIMINARY STUDIES OF THE BIOLOGICAL ACTIVITY OF SELECTED THIENYLPHOSPHINES AND THEIR GOLD(I) COMPLEXES	
IV.1 INTRODUCTION	319
IV.1.1 Biological activity of α -bi- and terthiophenes	319
IV.1.2 Biological activity of gold(I)-phosphine complexes	322
IV.1.3 Design of new antitumour-active compounds	324
IV.2 PHOTSENSITISING PROPERTIES OF THIENYLPHOSPHINES AND THEIR GOLD(I) COMPLEXES	326
IV.2.1 Introduction	326
IV.2.2 Photochemical oxidation of adamantylidene adamantane in presence of selected thiophene-based compounds	327
IV.3 CYTOTOXIC PROPERTIES OF THIENYLPHOSPHINES AND THEIR GOLD(I) COMPLEXES	333
IV.3.1 Cytotoxic effects of selected compounds against the HepG2 cell line	334
IV.3.2 Cytotoxic effects of selected compounds against the A549 cell line	336
IV.4 CONCLUSION	347
IV.5 EXPERIMENTAL	350
IV.5.1 Photochemical studies	350
IV.5.2 Gas chromatographic analysis of adamantylidene adamantane and adamantanone mixtures	350
IV.5.3 Cytotoxicity measurements	352
 Appendix A EXPERIMENTAL DETAILS	356
A.1 GENERAL	356
A.2 CHEMICALS	359
 Appendix B CONE ANGLE CALCULATIONS	367
 References	376

CHAPTER ONE

MONO-, DI- AND TRINUCLEAR PHOSPHINE COMPLEXES OF GOLD(I)

I.1 INTRODUCTION

Gold has attracted the attention of scientists since time immemorial. Its role during the Middle Ages as a driving force behind alchemical research, which eventually led to the development of modern Chemistry, is well known. During this century the interest in gold has not subsided, but has in fact experienced an upsurge in the number of publications dealing with gold and gold compounds over the last two decades.

The new interest in gold complexes can be attributed to the following facts:

- a) rich photophysical and photochemical properties exhibited by polynuclear gold(I) complexes can be potentially utilised in new technologies such as nonlinear optics,
- b) gold(I) and also reportedly gold(III) complexes show remarkable medicinal potential, especially in the field of rheumatoid arthritis and antitumour treatment,
- c) the phenomenon of metal-metal attractive interactions is very common between closed shell gold(I) atoms ($[\text{Xe}]4f^{14}5d^{10}$) in polynuclear gold compounds, though it still remains poorly understood.

Gold can exist in the oxidation states -1 , 0 , $+1$, $+2$, $+3$ and even $+4$ and $+5$, the most stable being gold(0), gold(I) and gold(III), and hence these oxidation states have the greatest practical significance. Both gold(I) and gold(III) can be reduced to the free metal by reaction with relatively mild reducing agents. Whilst gold(III) compounds are generally considered to be powerful oxidizing agents, gold(I) complexes – especially with soft ligands such as thiolates and tertiary phosphines – can be quite thermodynamically stable.¹

Gold(I) comprises a soft metal centre, where binding to ligands is achieved by means of both σ and π -bonding. Here gold is in a low oxidation state and hence the degree of π -bonding between the filled $5d$ -orbitals of the metal and empty $d\pi$ -orbitals of the ligand's binding atom can significantly affect the strength of the newly formed bond.

As a rule, gold(I) has an affinity for soft ligands with π -accepting properties such as cyanides, phosphines, arsines and various sulfur compounds.² Cases of coordination to nitrogen compounds such as aliphatic and heterocyclic amines are also known, as well as examples of complexes with weakly bonded oxygen donor ligands such as nitrates and perchlorates. However the latter complexes are generally reactive and much less stable.³

Although gold is certainly the most famous of all metals, its coordination chemistry has not been explored to such an extent as that of other precious metals such as platinum, for example. It is well known however, that the chemistry of gold differs considerably from that of other members of Group 11 in their monovalent state (d^{10} electronic configuration). To illustrate: for gold(I), linear coordination is by far the most common coordination geometry, whereas for copper(I) and silver(I), tetrahedral four-coordination is the most frequently encountered. This phenomenon has been attributed to the contribution of relativistic effects. Pyykkö *et al.*⁴ proved that the inner shell electrons of gold move with speeds approaching the velocity of light causing expansion of the 5d and contraction of the 6s orbitals. This apparently results in a reduction of the expected size of a gold atom, an enhancement of the possibility of metal-metal interactions and a predominance of linear coordination for gold(I).

Much of the information known about gold complexes is derived from solid state studies mainly by X-ray crystallography, but also by means of such esoteric techniques as EXAFS/XANES^{5,6} (Extended X-ray Absorption Fine Structure spectroscopy and X-ray Absorption Near Edge Spectroscopy - respectively); Mössbauer⁷ and far-infrared spectroscopy⁸ and, more recently, by means of ^{31}P cross-polarization magic angle spinning (CPMAS)^{8,9} NMR techniques. The X-ray diffraction techniques normally provide information about the coordination number, oxidation state and ligating atoms of gold complexes, while Mössbauer spectroscopy allows the determination of the coordination number, geometry and oxidation state of the gold atom.

Considerably less is known regarding solutions of gold(I) complexes. Numerous investigations have shown that although several species may be present in solution, the compounds that crystallize out do not necessarily correspond to the major species in solution. For example, the crystallographically characterized four-coordinate gold(I) complex $[\text{Au}(\text{PMePh}_2)_4]\text{PF}_6$ ¹⁰ dissociates in solution into two- or three-coordinate species;

even two-coordinate gold complexes can exhibit fluxional behaviour – the exchange of monodentate ligands bound to gold(I) has been observed in solution¹¹ possibly via an intermediate three-coordinate state.

Gold(I) has a d^{10} -electronic configuration, which precludes ESR studies. It also eliminates the possibility of using UV-visible spectroscopy for characterization of gold(I) complexes at least insofar as d-d electronic transitions including the gold atom are concerned. The ^{197}Au isotope is 100% abundant, with $I = 3/2$ and a quadrupole moment $Q = 0.59 \cdot 10^{-28} \text{ m}^2$. As a consequence of the large value of the quadrupole moment, the gold relaxation time is short and no spin coupling of gold with other nuclei has ever been observed. Since gold does not have an isotope suitable for NMR studies, the characterization of complexes in solution depends solely upon other nuclei present in the gold complex, most importantly ^{31}P and ^1H . This general lack of characterization methods was one of the reasons behind making phosphines the ligands of choice for studying the coordination chemistry of gold(I). Due to the simplicity of ^{31}P NMR spectra and the sensitivity of ^{31}P shifts to substitution at the metal in *trans* positions to the phosphorus nuclei, ^{31}P NMR spectroscopy has served as a convenient probe for monitoring gold(I) phosphine complexes. The latter are normally labile on the NMR time scale at room temperature and the solution needs to be cooled to observe individual compounds. A viable alternative to NMR solution studies was proposed by Colton *et al.*¹² The authors reported that electrospray mass-spectrometry (ESMS) allows the observation of individual gold(I)-phosphine species present in solution even at room temperature. ESMS is able to reveal individual components provided they carry either a negative or positive charge.

At present coordination of phosphines to gold(I) is a fast developing area due to the wealth of interesting properties exhibited by gold(I) tertiary phosphine complexes. Many of them have been found to luminesce both in solid state and solution, while others have proved to be cytotoxic and even active against a number of tumour cell lines *in vivo* (even those cell lines which are resistant to other known cytotoxic agents *e.g.*, cisplatin).

A number of gold chemistry reviews^{1,2,13-15} can be found in the literature. However at present, no comprehensive survey of gold(I) phosphine complexes with up to date information is available. The objective of this Chapter is to describe coordination

behaviour of gold(I) towards various types of tertiary phosphines, namely mono-, bi- and tridentate phosphines.

1.2 GOLD(I) COMPLEXES WITH MONODENTATE PHOSPHINES

Both mono- and polydentate phosphines can give rise to a variety of interesting species upon coordination to gold(I), the structures of which are a function of the ligand and also of the preparation scheme. The compounds vary both in nuclearity, charge and coordination number.

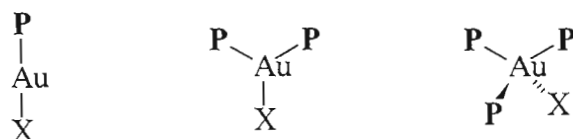
Monodentate phosphines lead almost exclusively to formation of mononuclear gold complexes in the absence of other bridging ligands with neutral and cationic complexes being the most common. The lack of anionic gold(I) phosphine complexes is not surprising: in order to achieve the negative charge, gold(I) should be coordinated to at least two anionic ligands (and a phosphine), *i.e.* it should have a coordination number not less than three. The three-coordinate geometry around gold(I) is not a thermodynamically stable arrangement, with only very few chelating dithiolate ligands having demonstrated the ability to form such complexes, *e.g.* $(\text{NBu}_4)[\text{Au}(\text{dmit})\text{PPh}_3]$,¹⁶ where dmit = 2-thioxo-1,3-dithiole-4,5-dithiolate. In fact, thiolate ligands generally possess lower coordinating ability towards gold than phosphines.

Neutral complexes have the general formula $[\text{AuL}_n\text{X}]$, where L is a monodentate phosphine ligand, X is a halide, pseudohalide or a thio-compound and $n = 1-3$. Ionic complexes have a somewhat different formula $[\text{AuL}_n]^+\text{X}^-$, where X is a poorly coordinating or non-coordinating ion such as perchlorate, tetrafluoroborate, hexafluoroantimonate *etc.* and $n = 2-4$.

Formally ionic gold(I) phosphine complexes may be classified as neutral or cationic depending on the solid state structure, the complex being considered neutral if there is evidence for a bond between the positively charged gold(I) and the negatively charged counterion (note that in solution this bond is either retained or broken).

I.2.1 Neutral mononuclear complexes

Monodentate tertiary phosphines have been used to form mononuclear gold(I) complexes with different coordination numbers – two, three and four – corresponding to linear, triangular and tetrahedral geometries. Different types of neutral mononuclear gold complexes are presented in Scheme I.1.



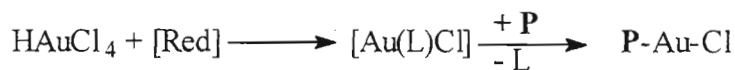
P = monodentate phosphine

X = Cl^- , Br^- , SCN^- , I^- , SR^- , R^- etc.

SCHEME I.1

Two-coordinate complexes

Amongst the above mentioned three types, the first is the most common and also the best studied. There are numerous examples of X-ray crystal structure studies on neutral two-coordinate gold(I)-phosphine complexes. The most typical scenario involves a gold(I)-phosphine complex with a halogen ion as a second ligand. Synthesis of this type of complex is achieved by substitution of an easily replaceable ligand from a chlorogold(I) precursor (Scheme I.2).



Red = reducing agent,

P = monodentate phosphine,

L = Me_2S , tetrahydrothiophene etc.

SCHEME I.2

Neutral two-coordinate chlorogold(I)-phosphine complexes are air- and moisture-stable solids at room temperature. Many of them only decompose at $T > 150^\circ$. Their acetone solutions are non-conductive, while solubility patterns largely depend on the phosphine ligand. The structural integrity of neutral two-coordinate gold(I) complexes is retained in

solution as indicated by ^{31}P , ^{13}C and ^1H NMR studies. The solutions show that only one type of species is present at both low and high temperatures.

Figure I.1 below shows as an example of two-coordination the molecular structure of $[\text{Au}(\text{2-MBPA})\text{Cl}]$, where 2-MBPA = methyl 4.6-*O*-benzylidene-2-deoxy-2-(diphenylphosphino)- α -D-altropyranoside.¹⁷

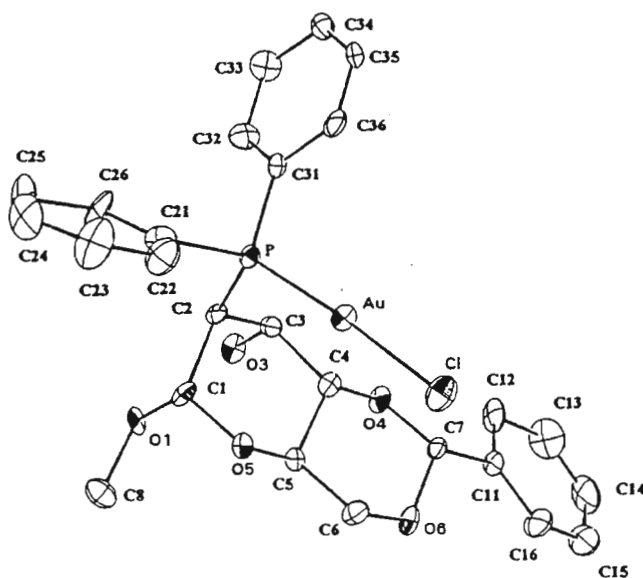


Fig. I.1 Molecular structure of $[\text{Au}(\text{2-MBPA})\text{Cl}]$ ¹⁷. 2-MBPA = methyl 4.6-*O*-benzylidene-2-deoxy-2-(diphenylphosphino)- α -D-altropyranoside.

The gold atom exists in the expected linear geometry as defined by the P atom of the 2-MBPA ligand and the chlorine atom, with the P-Au-Cl angle being $174.5(3)^\circ$. The Au-P and Au-Cl distances are $2.232(6)$ Å and $2.275(7)$ Å respectively. These values are characteristic for two-coordinate neutral gold(I) complexes. Table I.1 lists the bond lengths encountered in these complexes as determined by X-ray analysis.

It can be seen from Table I.1 that the Au-P bond lengths vary from 2.220 Å for a gold(I)-phosphole complex to 2.253 Å for a complex with a bulky phosphine ligand. The values can be used as a rough indication of bond strengths between gold and phosphorus atoms. The Au-Cl bond lengths also vary, exhibiting values from 2.275 to 2.310 Å; there being no apparent correlation between the Au-P and Au-Cl distances in the same molecule.

Table I.1 Bond lengths for $[\text{Au}(\text{PR}_3)\text{X}]$ complexes

PR_3, X	$\text{Au-P}, \text{\AA}$	$\text{Au-X}, \text{\AA}$	Reference
$\text{PMe}_3, \text{X} = \text{Cl}$	2.233(3)	2.306(4)	18
	2.234(4)	2.310(4)	
	2.234(4)	2.310(4)	
$\text{PMe}_3, \text{X} = \text{I}$	2.256(3)	2.583(1)	19
$\text{PEt}_3, \text{X} = \text{Cl}$	2.232(9)	2.305(8)	20
$\text{PPh}_3, \text{X} = \text{Cl}$	2.235(3)	2.279(3)	21
$\text{PPh}_3, \text{X} = \text{Br}$	2.252(6)	2.407(2)	22
$\text{PPh}_3, \text{X} = \text{I}$	2.249(2)	2.553(1)	19
$\text{P}(\text{c-C}_6\text{H}_{11})_3, \text{X} = \text{Cl}$	2.242(4)	2.279(5)	23
$\text{P}(2,4,6\text{-trimethoxyphenyl})_3, \text{X} = \text{Cl}$	2.253(5)	2.303(6)	8
$\text{P}(2,4,6\text{-trimethoxyphenyl})_3, \text{X} = \text{I}$	2.239(7)	2.586(2)	8
2-MBPA [*] , $\text{X} = \text{Cl}$	2.232(6)	2.275(7)	17
DBP ^{**} , $\text{X} = \text{Cl}$	2.220(9)	2.285(10)	9
	2.221(8)	2.282(9)	
DMPP ^{***} , $\text{X} = \text{Cl}$	2.227(2)	2.288(2)	9

^{*} 2-MBPA = methyl 4.6-*O*-benzylidene-2-deoxy-2-(diphenylphosphino)- α -D-altropyranoside

^{**} DBP = 1-phenyldibenzophosphole

^{***} DMPP = 1-phenyl-3.4-dimethylphosphole

The structure presented on Figure I.1 is characteristic for two-coordinate gold(I) complexes provided the phosphine ligand is sufficiently bulky. For ligands with a small cone angle,

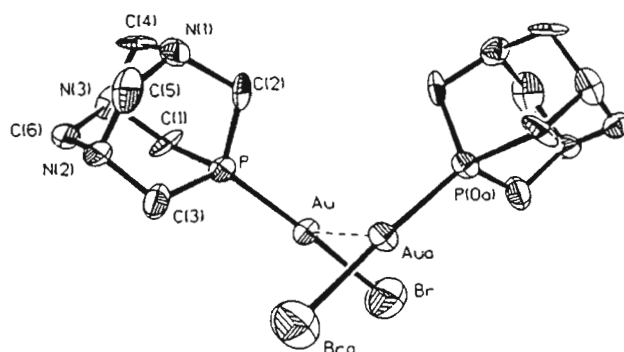


Fig. I.2 ORTEP diagram of $[\text{Au}(\text{TPA})\text{Br}]_2$.²⁴ TPA = 1.3.5-triaza-7-phosphaadamantane.

such as 1,3,5-triaza-7-phosphaadamantane²⁴ (TPA) or Me₂PPh²⁵ or DBP (*vide supra*), the coordination behaviour in the solid phase is somewhat different. There, individual two-coordinate units associate to produce dimeric and even trimeric species that involve weak Au-Au bonds (Figures I.2 and I.3).

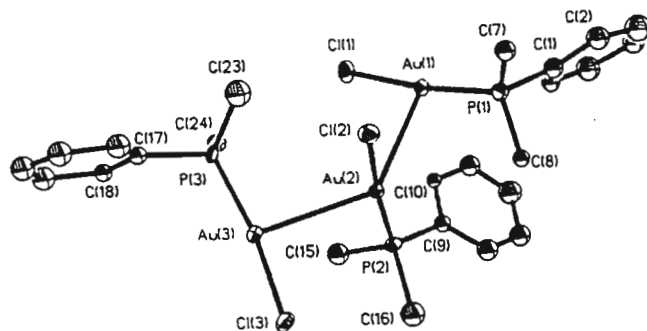
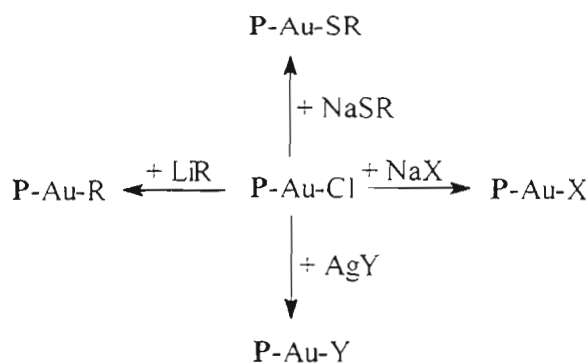


Fig. I.3 ORTEP diagram of [Au(Me₂PPh)Cl]₃.²⁵

Association of individual mononuclear units through Au-Au contacts, where Au-Au distances are less than 3.3 Å is a demonstration of so-called 'auriophilicity' phenomenon.²⁶ The interaction between closed shell (d¹⁰) gold atoms has been estimated in a number of experiments²⁷ and is of order 5-10 kcal/mol. The small size of the ligands does not impede the mutual approach of the gold(I) complex molecules, with the result that aggregation is observed in the solid phase. On the other hand, analytical and spectroscopic data for solutions of these complexes indicate complete dissociation of aggregates into monomeric species.^{24,25}

The chlorogold(I) phosphine complexes are convenient starting materials for the synthesis of a host of other two-coordinate complexes (Scheme I.3):



R = alkyl aryl

X = Br, I; Y = NO₃, ClO₄ in non-coordinating solvents

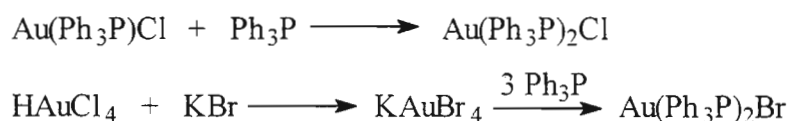
SCHEME I.3

The conversion is normally achieved by selection of an appropriate metathesis reagent: organo-lithium compounds,^{28,29} silver salts,^{11,30,31} sodium, potassium or ammonium salts^{9,32} and also basic solutions of aliphatic and aromatic thiols.^{16,33,34}

Three- and four-coordinate complexes

Examples of three- and four-coordinate mononuclear gold(I) complexes are considerably more scarce than those of the two-coordinate species. As a rule, they are much less stable and therefore their chemistry has not been so thoroughly studied. It makes sense to discuss both types together though, as they share some common features.

To prepare a three-coordinate gold(I) complex, a two-coordinate complex is normally combined with a stoichiometric amount of the ligand. Alternatively, a suitable gold(III) precursor is prepared from tetrachloroauric acid and subsequently reacted with three or more equivalents of the ligand (Scheme I.4):



SCHEME I.4

Similarly, four-coordinate neutral complexes could be synthesised using one of the above routes with the only modification being the number of equivalents of the ligand.

There are a variety of parameters controlling the formation of complexes with coordination number higher than two:

- The steric and electronic features of the tertiary phosphine,
- The coordinating ability of the non-phosphine ligand and,
- The choice of solvent and reactant concentrations.

As expected, sterically demanding phosphines, such as *n*-Bu₂PPh or (*c*-C₆H₁₁)₃P, should lead to complexes with lower coordination numbers. This was indeed confirmed by Parish,³⁵ who established that monodentate phosphine ligands with large cone angles were not capable of forming complexes with ligand to metal ratios greater than 3:1. For example, both [Au(Ph₃P)₂X] and [Au(Ph₃P)₃X] (X = Cl, SCN) have been structurally

confirmed to show three- and four-coordination respectively, while the gold atom in $\{\text{Au}[(\text{c-C}_6\text{H}_{11})_3\text{P}]_2\}\text{X}$ was found to be essentially two-coordinate with some weak interaction between the anion and the gold atom being observed for $\text{X} = \text{SCN}$.³⁶ This theory stayed unchallenged until 1994 when Fackler *et al.*^{37,38} structurally characterised two three-coordinate gold(I) complexes with the CEP ligand, where CEP = tris(cyanoethyl)phosphine. CEP has a cone angle smaller than that of Ph_3P , but tends to form linear two-coordinate complexes under the same conditions for which Ph_3P would typically form a linear three-coordinate complex. Fackler *et al.*³⁸ proposed an alternative explanation based on the influence of the electronic properties of the ligand. From the accumulated data regarding Au-P bonding it appears that two-coordinate gold(I)-phosphine complexes with good σ -donors tend to resist increased coordination while those with good π -accepting ligands prefer to form higher coordination number complexes. As CEP is a better σ -donor but weaker π -acid than Ph_3P , gold(I)-CEP complexes are not likely to accommodate a third ligand within the inner sphere.

The coordinating ability of the non-phosphine ligands also plays a significant role in determining the geometry of the complexes. For example, three-coordinate gold(I)-phosphine complexes may be obtained from a monodentate phosphine and a chelating ligand. With the bidentate nitrogen donor ligand 2,2'-bipyridine, a distorted trigonal species is obtained upon bonding to $[\text{Au}(\text{Ph}_3\text{P})]^+$,³⁹ but with dithiocarbamate ligands only linear two-coordination results.⁴⁰ A number of three-coordinate neutral complexes $[\text{Au}(\text{R}_3\text{P})_2\text{X}]$ ($\text{R} = \text{alkyl, aryl; X} = \text{Br, I}$) are known, but it has proved impossible to synthesise analogous four-coordinate compounds with the same counter ions. The bromide and iodide anions seem to be 'pushed' outside the coordination sphere of the metal and cationic complexes are formed instead.

The role of the solvent during the synthesis of higher coordination number complexes should not be underestimated. Even the choice of recrystallisation solvent(s) is sometimes crucial in obtaining the desired species. For example Malatesta³¹ found that $[\text{Au}(\text{Ph}_3\text{P})_2\text{Cl}]$ could be recrystallised from dichloromethane/hexane, but attempts to do the same from THF or warm methanol led to precipitation of the initial two-coordinate complex $[\text{Au}(\text{Ph}_3\text{P})\text{Cl}]$. On the other hand, whereas $[\text{Au}(\text{Ph}_3\text{P})_3]\text{Cl}$ cannot be recrystallised from dichloromethane/hexane as it loses one of its ligands, it has been successfully obtained from acetonitrile.

CHAPTER ONE

MONO-, DI- AND TRINUCLEAR PHOSPHINE COMPLEXES OF GOLD(I)

I.1 INTRODUCTION

Gold has attracted the attention of scientists since time immemorial. Its role during the Middle Ages as a driving force behind alchemical research, which eventually led to the development of modern Chemistry, is well known. During this century the interest in gold has not subsided, but has in fact experienced an upsurge in the number of publications dealing with gold and gold compounds over the last two decades.

The new interest in gold complexes can be attributed to the following facts:

- a) rich photophysical and photochemical properties exhibited by polynuclear gold(I) complexes can be potentially utilised in new technologies such as nonlinear optics,
- b) gold(I) and also reportedly gold(III) complexes show remarkable medicinal potential, especially in the field of rheumatoid arthritis and antitumour treatment,
- c) the phenomenon of metal-metal attractive interactions is very common between closed shell gold(I) atoms ($[\text{Xe}]4f^{14}5d^{10}$) in polynuclear gold compounds, though it still remains poorly understood.

Gold can exist in the oxidation states -1 , 0 , $+1$, $+2$, $+3$ and even $+4$ and $+5$, the most stable being gold(0), gold(I) and gold(III), and hence these oxidation states have the greatest practical significance. Both gold(I) and gold(III) can be reduced to the free metal by reaction with relatively mild reducing agents. Whilst gold(III) compounds are generally considered to be powerful oxidizing agents, gold(I) complexes – especially with soft ligands such as thiolates and tertiary phosphines – can be quite thermodynamically stable.¹

Gold(I) comprises a soft metal centre, where binding to ligands is achieved by means of both σ and π -bonding. Here gold is in a low oxidation state and hence the degree of π -bonding between the filled $5d$ -orbitals of the metal and empty $d\pi$ -orbitals of the ligand's binding atom can significantly affect the strength of the newly formed bond.

As a rule, gold(I) has an affinity for soft ligands with π -accepting properties such as cyanides, phosphines, arsines and various sulfur compounds.² Cases of coordination to nitrogen compounds such as aliphatic and heterocyclic amines are also known, as well as examples of complexes with weakly bonded oxygen donor ligands such as nitrates and perchlorates. However the latter complexes are generally reactive and much less stable.³

Although gold is certainly the most famous of all metals, its coordination chemistry has not been explored to such an extent as that of other precious metals such as platinum, for example. It is well known however, that the chemistry of gold differs considerably from that of other members of Group 11 in their monovalent state (d^{10} electronic configuration). To illustrate: for gold(I), linear coordination is by far the most common coordination geometry, whereas for copper(I) and silver(I), tetrahedral four-coordination is the most frequently encountered. This phenomenon has been attributed to the contribution of relativistic effects. Pyykkö *et al.*⁴ proved that the inner shell electrons of gold move with speeds approaching the velocity of light causing expansion of the 5d and contraction of the 6s orbitals. This apparently results in a reduction of the expected size of a gold atom, an enhancement of the possibility of metal-metal interactions and a predominance of linear coordination for gold(I).

Much of the information known about gold complexes is derived from solid state studies mainly by X-ray crystallography, but also by means of such esoteric techniques as EXAFS/XANES^{5,6} (Extended X-ray Absorption Fine Structure spectroscopy and X-ray Absorption Near Edge Spectroscopy - respectively); Mössbauer⁷ and far-infrared spectroscopy⁸ and, more recently, by means of ^{31}P cross-polarization magic angle spinning (CPMAS)^{8,9} NMR techniques. The X-ray diffraction techniques normally provide information about the coordination number, oxidation state and ligating atoms of gold complexes, while Mössbauer spectroscopy allows the determination of the coordination number, geometry and oxidation state of the gold atom.

Considerably less is known regarding solutions of gold(I) complexes. Numerous investigations have shown that although several species may be present in solution, the compounds that crystallize out do not necessarily correspond to the major species in solution. For example, the crystallographically characterized four-coordinate gold(I) complex $[\text{Au}(\text{PMePh}_2)_4]\text{PF}_6$ ¹⁰ dissociates in solution into two- or three-coordinate species:

even two-coordinate gold complexes can exhibit fluxional behaviour – the exchange of monodentate ligands bound to gold(I) has been observed in solution¹¹ possibly via an intermediate three-coordinate state.

Gold(I) has a d^{10} -electronic configuration, which precludes ESR studies. It also eliminates the possibility of using UV-visible spectroscopy for characterization of gold(I) complexes at least insofar as d-d electronic transitions including the gold atom are concerned. The ^{197}Au isotope is 100% abundant, with $I = 3/2$ and a quadrupole moment $Q = 0.59 \cdot 10^{-28} \text{ m}^2$. As a consequence of the large value of the quadrupole moment, the gold relaxation time is short and no spin coupling of gold with other nuclei has ever been observed. Since gold does not have an isotope suitable for NMR studies, the characterization of complexes in solution depends solely upon other nuclei present in the gold complex, most importantly ^{31}P and ^1H . This general lack of characterization methods was one of the reasons behind making phosphines the ligands of choice for studying the coordination chemistry of gold(I). Due to the simplicity of ^{31}P NMR spectra and the sensitivity of ^{31}P shifts to substitution at the metal in *trans* positions to the phosphorus nuclei, ^{31}P NMR spectroscopy has served as a convenient probe for monitoring gold(I) phosphine complexes. The latter are normally labile on the NMR time scale at room temperature and the solution needs to be cooled to observe individual compounds. A viable alternative to NMR solution studies was proposed by Colton *et al.*¹² The authors reported that electrospray mass-spectrometry (ESMS) allows the observation of individual gold(I)-phosphine species present in solution even at room temperature. ESMS is able to reveal individual components provided they carry either a negative or positive charge.

At present coordination of phosphines to gold(I) is a fast developing area due to the wealth of interesting properties exhibited by gold(I) tertiary phosphine complexes. Many of them have been found to luminesce both in solid state and solution, while others have proved to be cytotoxic and even active against a number of tumour cell lines *in vivo* (even those cell lines which are resistant to other known cytotoxic agents *e.g.*, cisplatin).

A number of gold chemistry reviews^{1,2,13-15} can be found in the literature. However at present, no comprehensive survey of gold(I) phosphine complexes with up to date information is available. The objective of this Chapter is to describe coordination

behaviour of gold(I) towards various types of tertiary phosphines, namely mono-, bi- and tridentate phosphines.

1.2 GOLD(I) COMPLEXES WITH MONODENTATE PHOSPHINES

Both mono- and polydentate phosphines can give rise to a variety of interesting species upon coordination to gold(I), the structures of which are a function of the ligand and also of the preparation scheme. The compounds vary both in nuclearity, charge and coordination number.

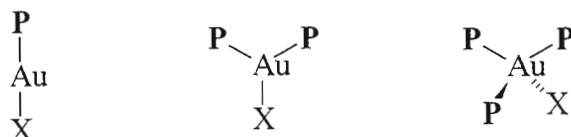
Monodentate phosphines lead almost exclusively to formation of mononuclear gold complexes in the absence of other bridging ligands with neutral and cationic complexes being the most common. The lack of anionic gold(I) phosphine complexes is not surprising: in order to achieve the negative charge, gold(I) should be coordinated to at least two anionic ligands (and a phosphine), *i.e.* it should have a coordination number not less than three. The three-coordinate geometry around gold(I) is not a thermodynamically stable arrangement, with only very few chelating dithiolate ligands having demonstrated the ability to form such complexes, *e.g.* $(\text{NBu}_4)[\text{Au}(\text{dmit})\text{PPh}_3]$,¹⁶ where dmit = 2-thioxo-1,3-dithiole-4,5-dithiolate. In fact, thiolate ligands generally possess lower coordinating ability towards gold than phosphines.

Neutral complexes have the general formula $[\text{AuL}_n\text{X}]$, where L is a monodentate phosphine ligand, X is a halide, pseudohalide or a thio-compound and $n = 1-3$. Ionic complexes have a somewhat different formula $[\text{AuL}_n]^+\text{X}^-$, where X is a poorly coordinating or non-coordinating ion such as perchlorate, tetrafluoroborate, hexafluoroantimonate *etc.* and $n = 2-4$.

Formally ionic gold(I) phosphine complexes may be classified as neutral or cationic depending on the solid state structure, the complex being considered neutral if there is evidence for a bond between the positively charged gold(I) and the negatively charged counterion (note that in solution this bond is either retained or broken).

I.2.1 Neutral mononuclear complexes

Monodentate tertiary phosphines have been used to form mononuclear gold(I) complexes with different coordination numbers – two, three and four – corresponding to linear, triangular and tetrahedral geometries. Different types of neutral mononuclear gold complexes are presented in Scheme I.1.



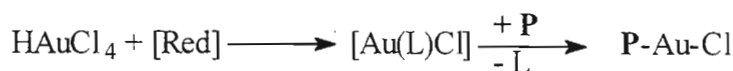
P = monodentate phosphine

X = Cl^- , Br^- , SCN^- , I^- , SR^- , R^- etc.

SCHEME I.1

Two-coordinate complexes

Amongst the above mentioned three types, the first is the most common and also the best studied. There are numerous examples of X-ray crystal structure studies on neutral two-coordinate gold(I)-phosphine complexes. The most typical scenario involves a gold(I)-phosphine complex with a halogen ion as a second ligand. Synthesis of this type of complex is achieved by substitution of an easily replaceable ligand from a chlorogold(I) precursor (Scheme I.2).



Red = reducing agent,

P = monodentate phosphine,

L = Me_2S , tetrahydrothiophene etc.

SCHEME I.2

Neutral two-coordinate chlorogold(I)-phosphine complexes are air- and moisture-stable solids at room temperature. Many of them only decompose at $T > 150^\circ$. Their acetone solutions are non-conductive, while solubility patterns largely depend on the phosphine ligand. The structural integrity of neutral two-coordinate gold(I) complexes is retained in

solution as indicated by ^{31}P , ^{13}C and ^1H NMR studies. The solutions show that only one type of species is present at both low and high temperatures.

Figure I.1 below shows as an example of two-coordination the molecular structure of $[\text{Au}(\text{2-MBPA})\text{Cl}]$, where 2-MBPA = methyl 4.6-*O*-benzylidene-2-deoxy-2-(diphenylphosphino)- α -D-altropyranoside:¹⁷

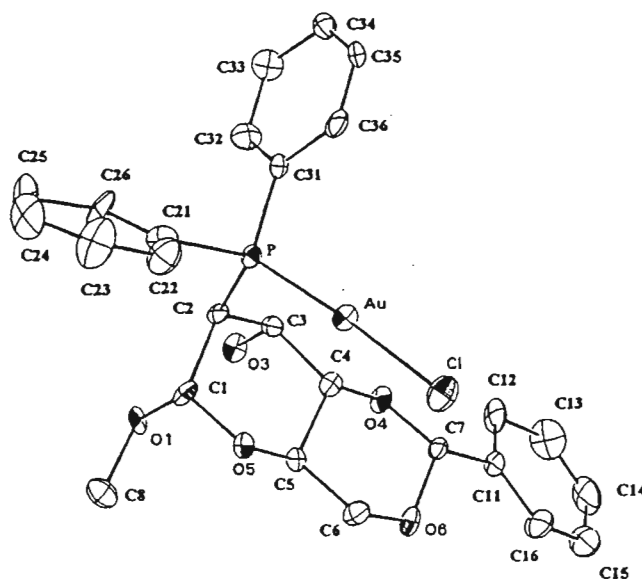


Fig. I.1 Molecular structure of $[\text{Au}(\text{2-MBPA})\text{Cl}]$ ¹⁷. 2-MBPA = methyl 4.6-*O*-benzylidene-2-deoxy-2-(diphenylphosphino)- α -D-altropyranoside.

The gold atom exists in the expected linear geometry as defined by the P atom of the 2-MBPA ligand and the chlorine atom, with the P-Au-Cl angle being $174.5(3)^\circ$. The Au-P and Au-Cl distances are $2.232(6)$ Å and $2.275(7)$ Å respectively. These values are characteristic for two-coordinate neutral gold(I) complexes. Table I.1 lists the bond lengths encountered in these complexes as determined by X-ray analysis.

It can be seen from Table I.1 that the Au-P bond lengths vary from 2.220 Å for a gold(I)-phosphole complex to 2.253 Å for a complex with a bulky phosphine ligand. The values can be used as a rough indication of bond strengths between gold and phosphorus atoms. The Au-Cl bond lengths also vary, exhibiting values from 2.275 to 2.310 Å: there being no apparent correlation between the Au-P and Au-Cl distances in the same molecule.

Table I.1 Bond lengths for $[\text{Au}(\text{PR}_3)\text{X}]$ complexes

PR_3, X	$\text{Au-P}, \text{\AA}$	$\text{Au-X}, \text{\AA}$	Reference
$\text{PMe}_3, \text{X} = \text{Cl}$	2.233(3)	2.306(4)	18
	2.234(4)	2.310(4)	
	2.234(4)	2.310(4)	
$\text{PMe}_3, \text{X} = \text{I}$	2.256(3)	2.583(1)	19
$\text{PEt}_3, \text{X} = \text{Cl}$	2.232(9)	2.305(8)	20
$\text{PPh}_3, \text{X} = \text{Cl}$	2.235(3)	2.279(3)	21
$\text{PPh}_3, \text{X} = \text{Br}$	2.252(6)	2.407(2)	22
$\text{PPh}_3, \text{X} = \text{I}$	2.249(2)	2.553(1)	19
$\text{P}(\text{c-C}_6\text{H}_{11})_3, \text{X} = \text{Cl}$	2.242(4)	2.279(5)	23
$\text{P}(2,4,6\text{-trimethoxyphenyl})_3, \text{X} = \text{Cl}$	2.253(5)	2.303(6)	8
$\text{P}(2,4,6\text{-trimethoxyphenyl})_3, \text{X} = \text{I}$	2.239(7)	2.586(2)	8
2-MBPA [*] , $\text{X} = \text{Cl}$	2.232(6)	2.275(7)	17
DBP ^{**} , $\text{X} = \text{Cl}$	2.220(9)	2.285(10)	9
	2.221(8)	2.282(9)	
DMPP ^{***} , $\text{X} = \text{Cl}$	2.227(2)	2.288(2)	9

^{*} 2-MBPA = methyl 4.6-*O*-benzylidene-2-deoxy-2-(diphenylphosphino)- α -D-altropyranoside

^{**} DBP = 1-phenyldibenzophosphole

^{***} DMPP = 1-phenyl-3,4-dimethylphosphole

The structure presented on Figure I.1 is characteristic for two-coordinate gold(I) complexes provided the phosphine ligand is sufficiently bulky. For ligands with a small cone angle.

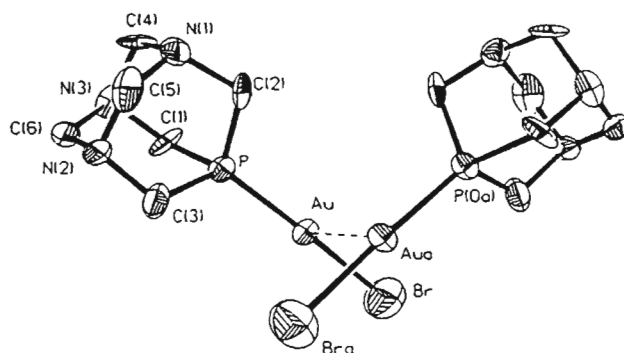


Fig. I.2 ORTEP diagram of $[\text{Au}(\text{TPA})\text{Br}]_2$.²⁴ TPA = 1.3.5-triaza-7-phosphaadamantane.

such as 1.3.5-triaza-7-phosphaadamantane²⁴ (TPA) or Me₂PPh²⁵ or DBP (*vide supra*), the coordination behaviour in the solid phase is somewhat different. There, individual two-coordinate units associate to produce dimeric and even trimeric species that involve weak Au-Au bonds (Figures I.2 and I.3).

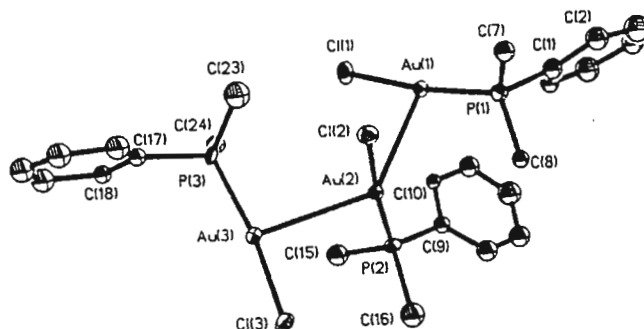
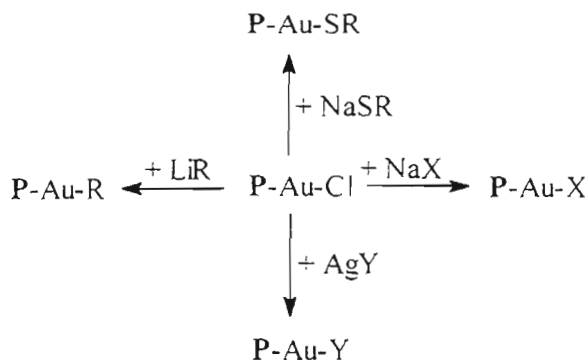


Fig. I.3 ORTEP diagram of [Au(Me₂PPh)Cl]₃.²⁵

Association of individual mononuclear units through Au-Au contacts, where Au-Au distances are less than 3.3 Å is a demonstration of so-called 'auriophilicity' phenomenon.²⁶ The interaction between closed shell (d¹⁰) gold atoms has been estimated in a number of experiments²⁷ and is of order 5-10 kcal/mol. The small size of the ligands does not impede the mutual approach of the gold(I) complex molecules, with the result that aggregation is observed in the solid phase. On the other hand, analytical and spectroscopic data for solutions of these complexes indicate complete dissociation of aggregates into monomeric species.^{24,25}

The chlorogold(I) phosphine complexes are convenient starting materials for the synthesis of a host of other two-coordinate complexes (Scheme I.3):



R = alkyl aryl

X = Br, I; Y = NO₃, ClO₄ in non-coordinating solvents

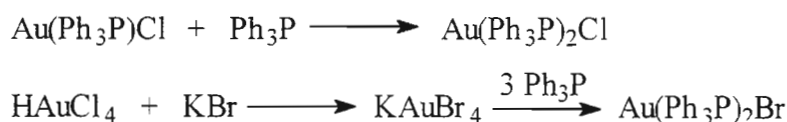
SCHEME I.3

The conversion is normally achieved by selection of an appropriate metathesis reagent: organo-lithium compounds,^{28,29} silver salts,^{11,30,31} sodium, potassium or ammonium salts^{9,32} and also basic solutions of aliphatic and aromatic thiols.^{16,33,34}

Three- and four-coordinate complexes

Examples of three- and four-coordinate mononuclear gold(I) complexes are considerably more scarce than those of the two-coordinate species. As a rule, they are much less stable and therefore their chemistry has not been so thoroughly studied. It makes sense to discuss both types together though, as they share some common features.

To prepare a three-coordinate gold(I) complex, a two-coordinate complex is normally combined with a stoichiometric amount of the ligand. Alternatively, a suitable gold(III) precursor is prepared from tetrachloroauric acid and subsequently reacted with three or more equivalents of the ligand (Scheme I.4):



SCHEME I.4

Similarly, four-coordinate neutral complexes could be synthesised using one of the above routes with the only modification being the number of equivalents of the ligand.

There are a variety of parameters controlling the formation of complexes with coordination number higher than two:

- a) The steric and electronic features of the tertiary phosphine,
- b) The coordinating ability of the non-phosphine ligand and,
- c) The choice of solvent and reactant concentrations.

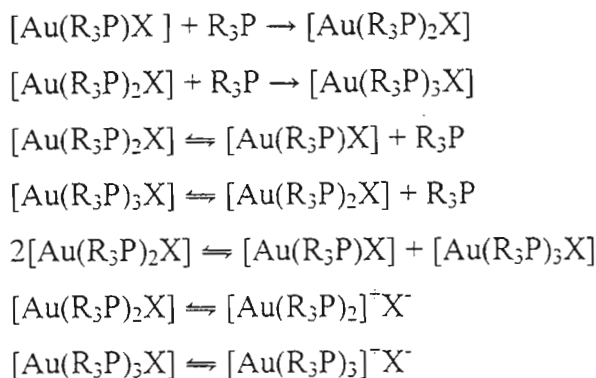
As expected, sterically demanding phosphines, such as *n*-Bu₂PPh or (*c*-C₆H₁₁)₃P, should lead to complexes with lower coordination numbers. This was indeed confirmed by Parish,³⁵ who established that monodentate phosphine ligands with large cone angles were not capable of forming complexes with ligand to metal ratios greater than 3:1. For example, both [Au(Ph₃P)₂X] and [Au(Ph₃P)₃X] (X = Cl, SCN) have been structurally

confirmed to show three- and four-coordination respectively, while the gold atom in $\{\text{Au}[(c\text{-C}_6\text{H}_{11})_3\text{P}]_2\}\text{X}$ was found to be essentially two-coordinate with some weak interaction between the anion and the gold atom being observed for $\text{X} = \text{SCN}$.³⁶ This theory stayed unchallenged until 1994 when Fackler *et al.*^{37,38} structurally characterised two three-coordinate gold(I) complexes with the CEP ligand, where CEP = tris(cyanoethyl)phosphine. CEP has a cone angle smaller than that of Ph_3P , but tends to form linear two-coordinate complexes under the same conditions for which Ph_3P would typically form a linear three-coordinate complex. Fackler *et al.*³⁸ proposed an alternative explanation based on the influence of the electronic properties of the ligand. From the accumulated data regarding Au-P bonding it appears that two-coordinate gold(I)-phosphine complexes with good σ -donors tend to resist increased coordination while those with good π -accepting ligands prefer to form higher coordination number complexes. As CEP is a better σ -donor but weaker π -acid than Ph_3P , gold(I)-CEP complexes are not likely to accommodate a third ligand within the inner sphere.

The coordinating ability of the non-phosphine ligands also plays a significant role in determining the geometry of the complexes. For example, three-coordinate gold(I)-phosphine complexes may be obtained from a monodentate phosphine and a chelating ligand. With the bidentate nitrogen donor ligand 2,2'-bipyridine, a distorted trigonal species is obtained upon bonding to $[\text{Au}(\text{Ph}_3\text{P})]^+$,³⁹ but with dithiocarbamate ligands only linear two-coordination results.⁴⁰ A number of three-coordinate neutral complexes $[\text{Au}(\text{R}_3\text{P})_2\text{X}]$ ($\text{R} = \text{alkyl, aryl; X} = \text{Br, I}$) are known, but it has proved impossible to synthesise analogous four-coordinate compounds with the same counter ions. The bromide and iodide anions seem to be 'pushed' outside the coordination sphere of the metal and cationic complexes are formed instead.

The role of the solvent during the synthesis of higher coordination number complexes should not be underestimated. Even the choice of recrystallisation solvent(s) is sometimes crucial in obtaining the desired species. For example Malatesta³¹ found that $[\text{Au}(\text{Ph}_3\text{P})_2\text{Cl}]$ could be recrystallised from dichloromethane/hexane, but attempts to do the same from THF or warm methanol led to precipitation of the initial two-coordinate complex $[\text{Au}(\text{Ph}_3\text{P})\text{Cl}]$. On the other hand, whereas $[\text{Au}(\text{Ph}_3\text{P})_3]\text{Cl}$ cannot be recrystallised from dichloromethane/hexane as it loses one of its ligands, it has been successfully obtained from acetonitrile.

Numerous solution studies have shown that complex equilibria (see Scheme I.5) are established upon addition of one or more equivalents of a phosphine ligand to $[\text{Au}(\text{R}_3\text{P})\text{X}]$ ($\text{R} = \text{alkyl, aryl}; \text{X} = \text{Br, Cl}$):^{9,11,35,41-44}



SCHEME I.5

The relative importance of the equilibria above depends on the solvent used. Parish *et al.*¹¹ found that strongly solvating media such as acetone and acetonitrile were suitable for the preparation of higher coordination number complexes by means of a stoichiometric reaction, while with a less polar solvent a 4-5 fold excess of the ligand was necessary.⁴²

Three- and four-coordinate neutral gold(I) complexes typically deviate from their respective idealised geometries of a regular triangle and a regular tetrahedron. Examples of each complex type are shown on Figures I.4 and I.5.

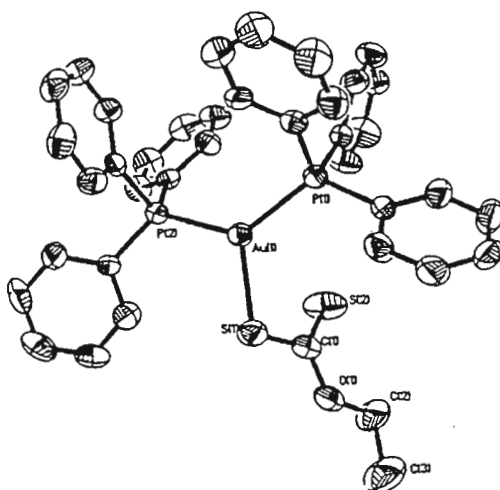


Fig. I.4 Molecular structure of the three-coordinate $[\text{Au}(\text{Ph}_3\text{P})_2\text{S}_2\text{COEt}]$.³⁸

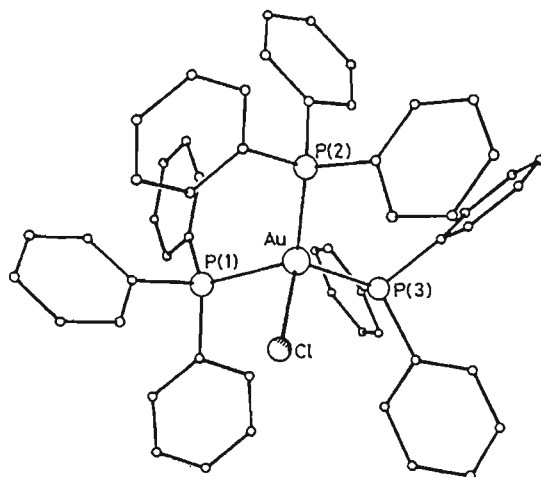


Fig. I.5 Molecular structure of the four-coordinate $[\text{Au}(\text{Ph}_3\text{P})_3]\text{Cl}$.⁴⁵

The $[\text{Au}(\text{Ph}_3\text{P})_2\text{S}_2\text{COEt}]^{38}$ complex has a geometry which can be described as almost trigonal planar with the bond angles around the gold atom being $130.1(1)^\circ$ [P(1)-Au-P(2)], $118.1(1)^\circ$ [S(1)-Au-P(2)] and $110.8(1)^\circ$ [S(1)-Au-P(1)]. The four-coordinate compound $[\text{Au}(\text{Ph}_3\text{P})_3\text{Cl}]^{45}$ is even further from its idealised geometry and may be considered as an intermediate case between three- and four-coordination due to large non-equivalencies in the values of bond angles: $119.6(1)^\circ$ [P(1)-Au-P(2)], $116.6(1)^\circ$ [P(2)-Au-P(3)], $116.1(1)^\circ$ [P(1)-Au-P(3)], $107.7(1)^\circ$ [P(3)-Au-Cl], $98.3(1)^\circ$ [P(2)-Au-Cl] and $92.0(1)^\circ$ [P(1)-Au-Cl]. In both complexes the non-phosphine ligands appear to be slightly shifted away from their theoretical positions. *i.e.* compared to the Au-P bonds the Au-X bonds are longer than expected. In fact in three-coordinate complexes the Au-Cl bond is known to correlate with the P-Au-P bond angles in the sense that the widest angle lies opposite to the longest bond.

The limited amount of crystallographic data does not allow the compilation of a comprehensive table of the bond lengths encountered in three- and four-coordinate gold(I) complexes. However, the general trend is that the distances are somewhat longer than those in two-coordinate complexes. The expected increase in bond lengths is the result of intramolecular steric effects due to the higher coordination number of the gold atom.

When X-ray data are not available, information on the coordination mode of gold(I) in the solid phase can be provided by far-infrared and ^{197}Au Mössbauer spectroscopic studies. The studies of gold(I)-ligand IR stretching and other vibrations can yield useful information about the metal-ligand bond strength and the degree of covalence in the metal-

ligand bond. Gold-halogen stretching frequencies decrease as the coordination number of gold(I) increases, consistent with weakening of the Au-X bond⁴⁶ (Fig. I.6). On the other hand Au-P frequencies do not seem to correlate closely with changes in the coordination number.

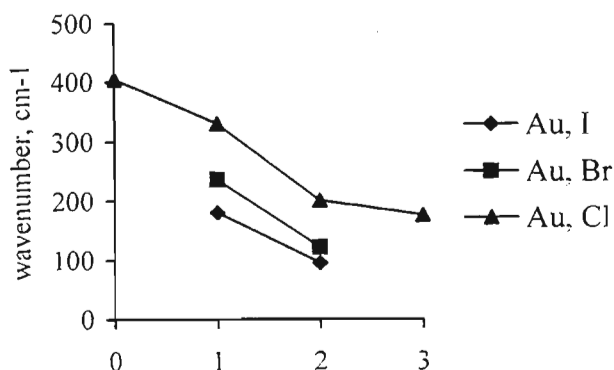


Fig. I.6 Dependence of the frequencies of Au-X bond stretching, $\nu(\text{Au-X})$, in two-coordinate halogold(I) phosphine complexes on the number of coordinated ligands.

¹⁹⁷Au Mössbauer spectroscopy is also a good means for obtaining information about bonding and geometry in gold complexes. Isomer shift (I.S.) and quadrupole splitting (Q.S.) values are respectively employed to characterise the electronic effects of the ligands in the complex and the differences in electronic density between the bonds. I.S. values tend to decrease in going from two- to four-coordinate complexes, while Q.S. values are the highest for three-coordinate and the lowest for four-coordinate complexes^{7,35} (in the ideal case of a regular tetrahedral geometry the quadrupole splitting is equal to zero). However, despite being informative and easily interpretable, Mössbauer spectroscopy does not always allow one to distinguish between subtle differences in coordination mode, *i.e.* whether the compound is a chelated monomer, ring dimer or polymeric species.

It has already been mentioned, that three- and four-coordinate gold(I)-monodentate phosphine complexes are not very stable in solution and readily dissociate or disproportionate into other species. Generally, more species are capable of existence in solution than can be crystallised from that same solution. To 'observe' the individual compounds, low temperature ³¹P NMR spectroscopy is normally employed. Chemical shifts for the neutral gold(I)-phosphine complexes have been found to follow the trend: three- > two- > four-coordinate. So far there has been no evidence of association of three-

and four-coordinate complexes into dimers or trimers in either solution or the solid state by means of gold-gold interactions.

I.2.2 Neutral dinuclear complexes

Clearly, monodentate phosphine ligands cannot be employed to stabilise dinuclear complexes of gold(I). However, neutral digold(I) complexes stabilised by bridging ligands and containing a monodentate phosphine do exist; these will now be discussed.

The examples include dinuclear gold(I) complexes with dithiolate and ethynediyl bridges: *e.g.* $[(\text{Ph}_3\text{P})\text{Au}]_2[\text{S}_2\text{C}=\text{C}(\text{CN})_2]$ ⁴⁷ and $[(\text{RPh}_2\text{P})\text{Au}-\text{C}\equiv\text{C}-\text{Au}(\text{PPh}_2)]$ ³⁰ (R = naphthyl). In the first complex there is a weak Au-Au interaction (metal-metal distance equal to 3.156 Å), while in the latter neither intra- nor inter-molecular Au...Au interactions were observed due to its dumbbell geometry and bulkiness of the phosphine ligand. In all other respects, the compounds appear to have structural features as well as chemical properties close to that of corresponding mononuclear complexes. Attempts to increase the coordination number of gold(I) in these compounds by adding more equivalents of the ligands have not been successful as the Au-S and Au-C bonds were cleaved by the added phosphines.

I.2.3 Cationic mononuclear complexes

It is convenient to divide the discussion on mononuclear cationic gold(I) complexes with monodentate phosphines into two parts as it was done for the neutral complexes. Two-coordinate cationic complexes are found in great abundance, while three- and four-coordinate compounds are rarely found.

Two-coordinate complexes

Monodentate phosphines can coordinate to gold(I) forming cationic species where the metal is bonded to one or two phosphine ligands. The former - of the type $[\text{Au}(\text{Ph}_3\text{P})\text{L}]^+$ - are fairly reactive, especially when L is a neutral non-phosphine and labile ligand such as tetrahydrothiophene or amine.⁴⁸ They are not stable in solution for a considerable length of time and thus make convenient precursors for substitution reactions. The latter, on the other hand, are particularly stable complex types of gold(I).

Two-coordinate cationic complexes show the expected linear geometry and are normally accompanied by the presence of centre of symmetry when identical ligands are bonded to the gold atom³⁷ (Figure I.7). Examples abound: *e.g.* $[\text{Au}\{(\text{c-C}_6\text{H}_{11})_3\text{P}\}_2]\text{SCN}$,³⁶ $[\text{Au}(\text{MePh}_2\text{P})_2]\text{PF}_6$.⁴⁹ However, there are exceptions, such as $[\text{Au}((\text{Me}_2\text{Ph})\text{P})_2]\text{SnCl}_3$: in this compound the P-Au-P angle is 158.3° , there being no evidence for counterion coordination.⁵⁰ The Au-P bond length of $2.314(2) \text{ \AA}$ in the compound depicted on Figure I.7 is comparable to that in neutral two-coordinate as well as in other cationic two-coordinate complexes.^{29,32}

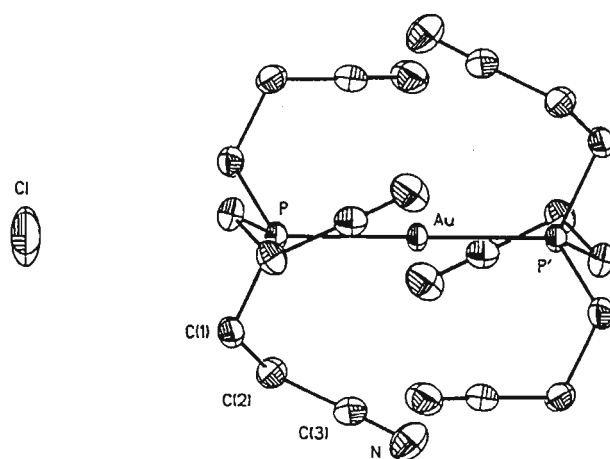


Fig. I.7 Structure of $[\text{Au}(\text{CEP})_2]\text{Cl}$,³⁷ CEP = tris(2-cyanoethyl)phosphine.

Unlike amongst neutral mononuclear two-coordinate gold(I) complexes with small ligands, the aurophilicity phenomenon has not been observed in the related cationic species. A possible explanation is that often bulky counterion present in the solid state impedes intermolecular attractions between two gold atoms.

Synthesis of bis(phosphine) cationic complexes of gold(I) can be achieved through one of the following two routes:

- Addition of two equivalents of the phosphine ligand to a neutral gold(I) precursor followed by an inorganic salt (if required),
- Addition of two equivalents of the phosphine ligand to a cationic gold precursor with readily replaceable ligands.

Examples are shown in Scheme I.6.

	Reference:
1) $[\text{Au}(\text{MePh}_2\text{P})\text{Cl}] + \text{MePh}_2\text{P} + \text{AgNO}_3 \rightarrow [\text{Au}(\text{MePh}_2\text{P})_2]\text{NO}_3$	51
$[\text{Au}(\text{Ph}_3\text{P})_2\text{Cl}] + \text{NaBPh}_4 \rightarrow [\text{Au}(\text{Ph}_3\text{P})_2][\text{BPh}_4]$	31
2) $[\text{Au}(\text{MeCN})_2][\text{BF}_4] + 2 \text{Ph}_3\text{P} \rightarrow [\text{Au}(\text{Ph}_3\text{P})_2][\text{BF}_4]$	52
$[\text{Au}(\text{MeCN})_2][\text{ClO}_4] + 2 (\text{t-Bu})_3\text{P} \rightarrow [\text{Au}(\text{t-Bu}_3\text{P})_2][\text{ClO}_4]$	53

SCHEME I.6

For the first route, conditions which favour the formation of cationic as opposed to neutral species should be employed. They usually include the use of polar solvents and the introduction of the excess of a weakly or non-coordinating anion. But even strongly coordinating counterions such as Cl^- and SCN^- can be forced outside the inner coordination sphere of the complex. This normally occurs when the phosphine ligand is very bulky, *e.g.* $(\text{c-C}_6\text{H}_{11})_3\text{P}$,³⁶ or a sufficiently strong donor to cause an excess of electron density on the gold ion, *e.g.* CEP ³⁷ (*vide supra*), thus discouraging coordination of the counterion.

The properties of two-coordinate cationic complexes are as expected different from those of the neutral complexes. For instance, they are much more soluble in polar solvents such as ethanol, acetonitrile, THF, acetone and dichloromethane but are not soluble in chloroform or ether. The ionic compounds appear to be ionised in solution – partially or fully depending on the ligand and solvent used,¹¹ with the cation retaining its structural integrity.

An interesting example of the tendency of gold(I) to be two-coordinate was demonstrated recently by Zotto *et al.*³² The authors were studying the coordination behaviour of an unsymmetrical ligand, 1-(diphenylphosphino)-2-(2-pyridyl)ethane (ppye), that contains P and N donor atoms. This ligand exhibits versatile coordination behaviour with a number of transition metals: it can act as both a chelating and monodentate (N- or P-) ligand. However with gold(I) the ligand only forms a complex where it is monodentate and

terminally bonded through one P-atom (Figure I.8). Coordination of the pyridyl arm even in solution is ruled out by both IR and low temperature NMR studies.

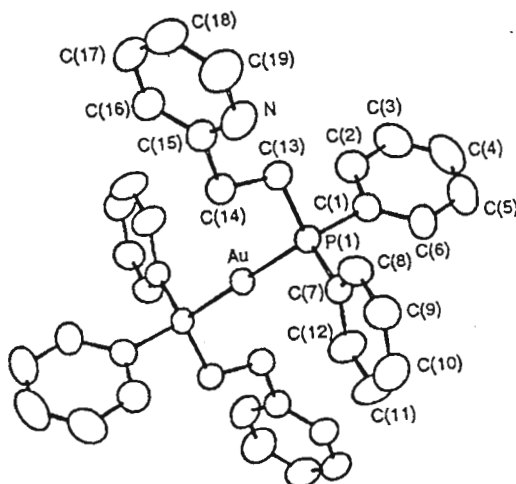


Fig. I.8 ORTEP diagram of the $[\text{Au}(\text{ppye})_2]^+$ cation.⁵² ppye = 1-(diphenylphosphino)-2-(2-pyridyl)ethane.

Three- and four-coordinate complexes

Examples of three- and four-coordinate gold(I) complexes with monodentate phosphines are very scarce due to the difficulties associated with their preparation. As a rule, they are obtained from the corresponding two-coordinate cationic precursors by adding a specific amount of the ligand. However, the complexes are labile and readily dissociate in solution often producing equilibrium mixtures.⁵¹

In contrast to neutral three-coordinate gold(I) complexes, which give rise to distorted trigonal geometries for the complex in the solid state, three-coordinate cationic compounds with identical ligands exhibit nearly ideal trigonal geometries. Figure I.9 shows the structure of the $[\text{Au}(\text{Ph}_3\text{P})_3]^+$ cation of the compound $[\text{Au}(\text{Ph}_3\text{P})_3][\text{BPh}_4]$.⁵⁴

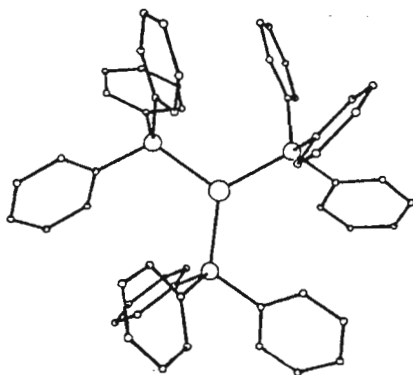


Fig. I.9 Structure of $[\text{Au}(\text{Ph}_3\text{P})_3]^+$ cation.⁵⁴

The Au-P distances here are 2.365(3), 2.384(3) and 2.403(3) Å, while the angles between the bonds are 115.2(2), 119.3(2) and 125.4(2)°, *i.e.* the arrangement is very close to idealised trigonal geometry.

A related complex with four triphenylphosphine ligands has also been prepared. However investigation of its crystal structure⁵⁵ revealed three different crystal modifications with different degrees of distortion from the ideal tetrahedral geometry. The ligands either seem to be arranged in a trigonal pyramidal fashion or 'loosely' bonded at approximate tetrahedral sites. This is most likely due to the relative steric bulk of the triphenylphosphine ligand. In fact a smaller ligand such as methyldiphenylphosphine affords a complex¹⁰ with a geometry nearly that of regular tetrahedron (Figure I.10), the Au-P distance being 2.449(1) Å and the two independent P-Au-P angles 105.24(4) and 118.3(2)°. It can be noted that the Au-P distances increase with increasing coordination number of gold(I) in a cation in accordance with the phenomenon observed for the neutral gold(I)-phosphine complexes.

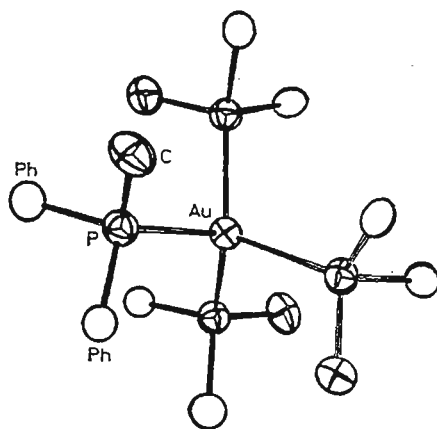
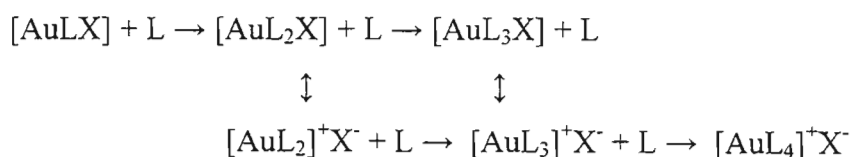


Fig.I.10 Structure of the cation $[\text{Au}(\text{MePh}_2\text{P})_4]^+$.¹⁰ Phenyl ring positions are indicated by open ellipses for the carbon atom bound to phosphorus.

Various authors have shown that four-coordinate complexes are formed with small phosphine ligands, such as Me_2PhP , MePh_2P , Et_2PhP and Et_3P .^{35,41-43,51} On the other hand gold(I) complexes with slightly bulkier ligands – $n\text{-Bu}_3\text{P}$, $n\text{-Bu}_2\text{PhP}$, $i\text{-Pr}_2\text{PhP}$, $(c\text{-C}_6\text{H}_{11})\text{Ph}_2\text{P}$ – exhibit three-coordination at most as shown by low temperature ^{31}P NMR and Mössbauer spectroscopy. Counterions also play part in determining of the coordination number: for instance, tris(*p*-tolyl)phosphine can form two- and three-coordinate gold(I) complexes with perchlorate as an anion. Substitution of perchlorate by $\text{B}_9\text{H}_{12}\text{S}^-$ allows all

three cations $[\text{AuL}_n]^+$ ($n = 2, 3, 4$, $\text{L} = (p\text{-CH}_3\text{C}_6\text{H}_4)_3\text{P}$) to be observed. With even larger anions such as $\text{B}_{10}\text{H}_{15}^-$ only $[\text{AuL}_4]^+$ is obtained.⁵⁶

Although very few four-coordinate cationic gold(I) complexes with monodentate phosphine ligands have been successfully isolated and structurally characterised, ^{31}P NMR spectroscopic studies have provided unambiguous proof of their presence in solution. In most cases complexes identified in solution cannot be isolated because they exist in equilibrium with other species. Any attempt to crystallise the solids leads to precipitation of the least soluble components – not necessarily the highest coordination number complex (Scheme I.7).⁴¹⁻⁴³



SCHEME I.7

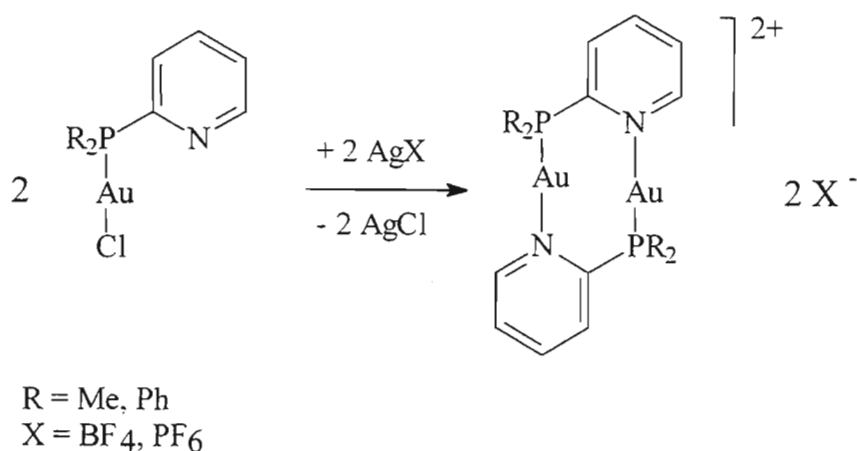
To obtain meaningful information on the behaviour of complexes in solution, the temperature is reduced to 180-200 K in order to prevent rapid ligand exchange. Under such conditions assignment of individual species becomes possible as the ^{31}P chemical shifts for the phosphine ligands obey the following trend: $[\text{AuLCl}] < [\text{AuL}_2]^+ > [\text{AuL}_3]^+ > [\text{AuL}_4]^+ > \text{L}$ (L = phosphine ligand). Low temperature ^{31}P NMR spectroscopy is essentially the only method that allows the identification of the individual cationic gold(I)-phosphine complexes in solution, other spectroscopic methods not providing valuable information. Electrospray mass spectroscopy (ESMS) can help with the detection and assignment of individual cationic species in solution.¹² However, the result does not always correlate with the one obtained from the low temperature NMR studies, *e.g.* $[\text{Au}(\text{Ph}_3\text{P})_4]^+$ could not be observed by ESMS, while it was identified at -100°C by ^{31}P NMR spectroscopy.

I.2.4 Cationic dinuclear complexes

Ligands containing in their structure an extra uncharged donor atom other than phosphorus are capable of stabilising dinuclear cationic gold(I) complexes by bridging via both phosphorus and the other donor atom. Nitrogen is normally a poor donor as far as

coordination to gold(I) is concerned, and no bond is formed when competing ligands such as halogens or sulfur compounds are present. However, by using conditions favouring the formation of cationic species, *i.e.* where the gold(I) precursor is bound to very weak ligands as well as polar reaction media, it is possible to achieve bonding of nitrogen to gold.

Schmidbaur *et al.*⁵⁷ have prepared several complexes with 2-pyridylphosphine ligands where both P and N are coordinated to gold (Scheme I.8). Removal of the chloride ion with a silver salt from the starting neutral mononuclear complex resulted in a head-to-tail dimerisation. X-ray analysis of one of the complexes showed an almost planar and centrosymmetric ring system coplanar with the two attached pyridine rings. The Au-Au intramolecular distance appeared to be very short at 2.776(1) Å. (Two-coordinate gold(I) complexes with Au...Au separations less than 3.6 Å in the solid state are considered to experience attractive aurophilic interactions.)⁵⁸



SCHEME I.8

A similar result was obtained by Field and co-workers⁵⁹ when using 2-(diphenylphosphino)quinoline as a ligand, although via a different synthetic route. Again the two gold atoms are bridged by the ligand in a head-to-tail fashion. The solution studies (by means of ^{31}P NMR spectroscopy) indicated that this was the only species in solution, and no head-to-head isomer was present. This fact is hardly surprising as phosphines are much better ligands than pyridines in stabilising gold in its lower oxidation state and, therefore, a $[\text{N-Au-N}]^+$ fragment is not to be expected.

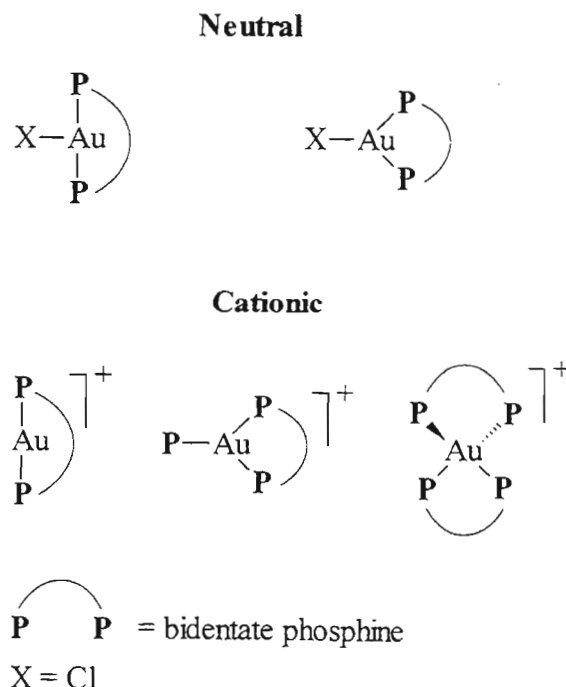
I.3 GOLD(I) COMPLEXES WITH BIDENTATE PHOSPHINES

Bidentate tertiary phosphines have proved to be very versatile when coordinating to gold(I). They promote the formation of mono-, di- and even trinuclear complexes that are either neutral or cationic.

In general, the physical properties (*e.g.* solubility and conductivity) of gold(I) complexes with bidentate phosphines as well as the methods employed for their synthesis and characterisation, strongly resemble those of corresponding complexes with monodentate phosphines, provided they have the same coordination arrangement around the gold atoms.

I.3.1 Mononuclear complexes

Contrary to the behaviour exhibited by bidentate phosphines with other transition metals, so far there have been no examples reported of bidentate phosphines bonding to gold(I) through one of the two phosphorus atoms only, leaving the other one pendant. Thus, in mononuclear complexes, only the chelating mode is found. The structural types that have been observed are illustrated below (Scheme I.9).



SCHEME I.9

I.3.1.1 Neutral mononuclear complexes

These complexes normally contain a chelating diphosphine as well as one coordinated anionic ligand, therefore exhibiting three-coordination around the gold atom.

The ligand 2,11-bis(diphenylphosphinomethyl)benzo[*c*]phenanthrene⁶⁰ is known to chelate to gold(I) via two phosphorus atoms in *trans* positions to each other thus forming a three-coordinate T-shaped complex with a chloride as the third ligand. In this complex, the P-Au-P' angle of 175.7(3)° is very close to linear, while both P-Au-Cl angles are about 90°.

To date there has been no reported isolation of three-coordinate chelated species containing phosphines with a less rigid backbone of the $R_2P(CH_2)_nPR_2$ type ($n \geq 2$). For example, Baker *et al.*⁶¹ obtained a compound formulated as $[Au(DiPPE)Cl]$, where DiPPE = 1,2-bis(diisopropylphosphino)ethane. However, a closer look – by means of single crystal X-ray studies – revealed that the complex exists as a polymer with a three-coordinate T-shape geometry around the gold atoms, but with the ligands bridging rather than chelating. Similar coordination behaviour was encountered for $[Au(dppf)Cl]$ which also proved to be a polymer with bridging diphosphine ligands.⁶²

The first example of a truly three-coordinate neutral mononuclear gold(I) complex with a *cis*-chelating diphosphine appeared in 1995, when Parish *et al.*⁷ prepared the permethylated derivative of dppf and coordinated it to gold(I) (Figure I.11).

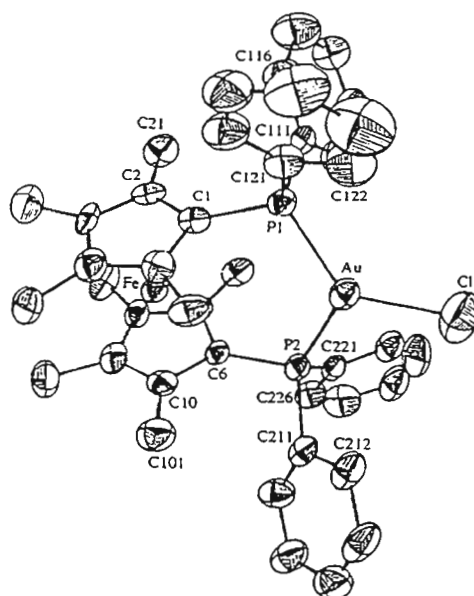


Fig. I.11 Molecular structure of $[Au(dppomf)Cl]$.⁷ dppomf = 1,1'-bis(diphenylphosphino)-octamethylferrocene.

The complex is obtained from $[\text{Au}(\text{tht})\text{Cl}]$ and the ligand under carefully controlled conditions (low temperature, non-complexing solvent, slow addition) and can be easily converted into a dinuclear species with the ligand bridging rather than chelating by addition of extra $[\text{Au}(\text{tht})\text{Cl}]$.

I.3.1.2 Cationic mononuclear complexes

There are examples of two-, three- and four-coordination in mononuclear cationic complexes of gold(I) with bidentate phosphines.

Two-coordinate complexes

Two-coordination is achieved with *trans*-chelating ligands, such as 1,8-bis(diphenylphosphino)-3,6-dioxaoctane (Figure I.12).⁶³

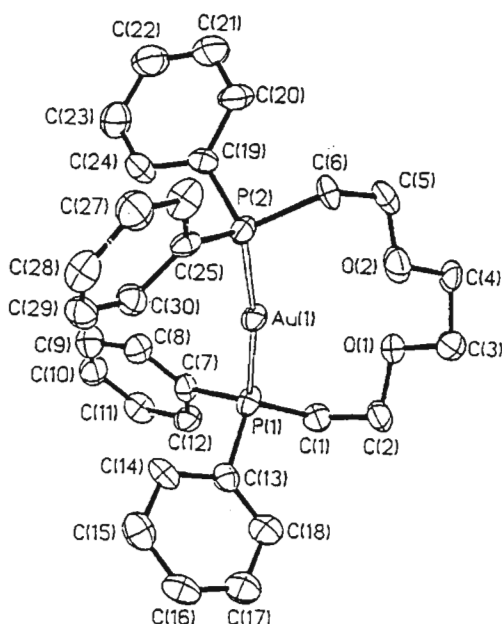


Fig. I.12 ORTEP diagram of $[\text{Au}(\text{dpdo})]^+$ cation.⁶³ dpdo = 1,8-bis(diphenylphosphino)-3,6-dioxaoctane.

The P-Au-P' angle of 172° in $[\text{Au}(\text{dpdo})]^+$ deviates from the ideal linear geometry because of geometric constraints imposed by the chelating ligand. The complex was prepared by a method analogous to that employed to obtain complexes with two monodentate phosphine

ligands. The resulting compound is, however, less prone to ligand exchange or dissociation in solution due to the chelating nature of the ligand.

Three-coordinate complexes

Addition of a monodentate phosphine – Ph_3P – to the above compound $\{i.e. [\text{Au}(\text{dpdo})]^+\}^{63}$ led to the formation of a three-coordinate species as determined by ^{31}P NMR spectroscopy. The compound unfortunately could not be isolated. It seems probable that in the solid state it would adopt T-shaped geometry.

Addition of the *cis*-chelating dhp ligand [dhp = 1,2-bis(di-*iso*-propylphosphino)benzene] to $[\text{ClAuPEt}_3]$ afforded a complex with an irregular trigonal geometry (Figure I.13).⁶¹

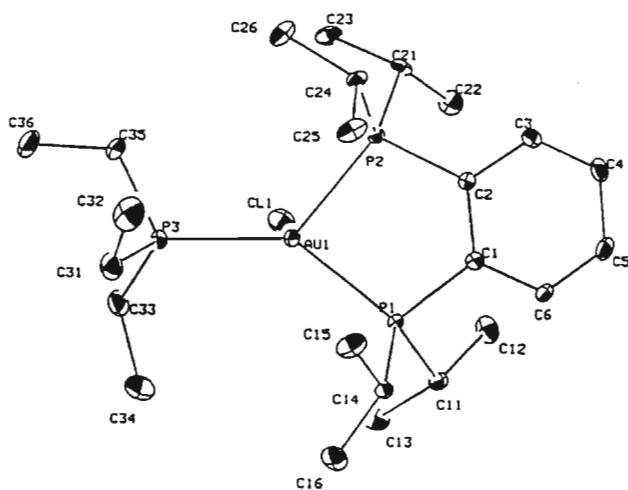


Fig. I.13 The molecular structure of $[\text{Au}(\text{dhp})(\text{PEt}_3)]\text{Cl}$.⁶¹ dhp = 1,2-bis(di-*iso*-propylphosphino)benzene.

It is interesting to consider the bond lengths and angles in this complex: $\text{P}(1)\text{-Au-P}(2) = 87.82(5)$, $\text{P}(1)\text{-Au-P}(3) = 139.37(6)$, $\text{P}(2)\text{-Au-P}(3) = 129.16(6)^\circ$; $\text{Au}(1)\text{-P}(1) = 2.366(2)$, $\text{Au}(1)\text{-P}(2) = 2.394(1)$ and $\text{Au}(1)\text{-P}(3) = 2.296(2)$ Å. The very small $\text{P}(1)\text{-Au-P}(2)$ angle reflects the significant constraint imposed by the *o*-benzene moiety and may explain the lack of examples of three-coordination for ligands with P_2C_2 backbones. It is also known that the strongest bond within three-coordinate gold(I) complexes lies opposite to the largest angle.⁶⁴ However, in this compound, the bond between the gold atom and the phosphorus atom of the monodentate phosphine is somewhat stronger than those to the phosphorus atoms of the bidentate phosphine, as evidenced by the shortest bond length being $\text{Au}(1)\text{-P}(3)$. This contradicts the expected trend. An analogous complex was

prepared with the dppf instead of the dhp ligand⁶⁵ and the structural features were found to be very similar, although distortion from the trigonal geometry in the former case was not as large [$P(1)-Au-P(2) = 109$ vs. 87°].

Four-coordinate complexes

Tetrahedral gold(I) cations with two chelating diphosphine ligands is the most common structural type in this class of gold(I) compound. One of the first examples reported in the literature is $[Au(dppe)_2]Cl$, which was crystallographically characterised by Bates and Waters⁶⁶ in 1984. The coordination at each gold atom approximates to ideal tetrahedral geometry (see Figure I.14), the dihedral angles between the two planes defined by $Au, P(1), P(2)$ and $Au, P(3), P(4)$ being 89.7° . However distortion from the ideal is observed since the 'bite' angles within each chelate ring are $87.1(1)$ and $86.4(1)^\circ$. The four $Au-P$ distances are not identical varying from $2.384(2)$ to $2.412(2)$ Å with an average of 2.397 Å. This value is significantly shorter than the bond lengths determined in 'classical' four-coordinate gold(I) complexes such as $[Au(MePh_2P)_4][PF_6]$ ($2.449(1)$ Å)¹⁰ and $[Au(Ph_3P)_4][BPh_4]$ (average, 2.606 Å).⁵⁵ On this basis bis-chelated complexes appear more stable than their four-coordinate analogues with monodentate phosphines.

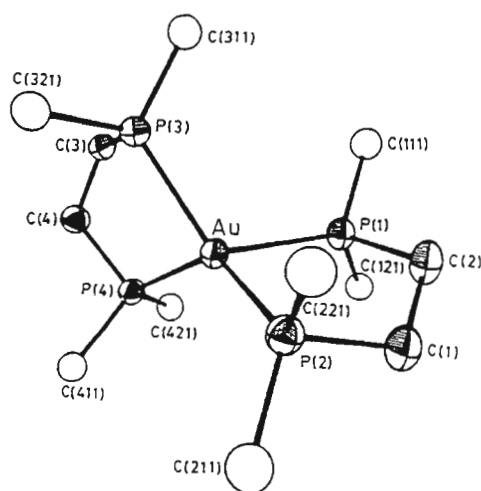


Fig. I.14 The molecular structure of the $[Au(dppe)_2]^+$ cation.⁶⁶ The first atom only of each phenyl ring is shown.

Berners-Price and Sadler⁶⁷ investigated the stability of various $[Au\{R_2P(CH_2)_nPR'_2\}_2]^+$ complexes ($n = 1-4$, $R = R' = Ph, Et$; $R = Ph, R' = Et$) in solution. The stability was found

to be influenced by several factors: the ring size of the chelate complex, steric requirements of the substituents on the phosphorus atoms and the solvent. Only complexes containing either five- or six-membered chelate rings were found to exist in solution. For the ligands dppe, dppp and eppe ($n = 2$, $R = \text{Ph}$, $R' = \text{Et}$) chelation appears to be extremely favourable especially in non-polar solvents such as chloroform, as four-coordinate complexes were detected in solutions even with ligand to gold ratios less than 1:1. Other examples of bis-chelated gold(I) complexes contain *o*-phenylene and *cis*-ethylene based ligands,^{61,68} bis[(diphenylphosphino)methyl]phenylarsine⁶⁹ and the dppf ligand.⁶⁵ It is interesting to note that the permethylated derivative of the last ligand (dppomf⁷ - see Section I.3.1.1 of this Chapter) is not capable of forming bis-chelated species probably due to its greater steric demands.

I.3.2 Dinuclear complexes of gold(I) containing bridging bidentate phosphine ligands

This is the most abundant type of gold(I) complexes formed by bidentate phosphines. According to the classification adopted so far, complexes of this type can be divided into two main subcategories: neutral and cationic, and within these subcategories further subdivided according to structural type. The various structural types possible are presented in Scheme I.10 (on the next page).

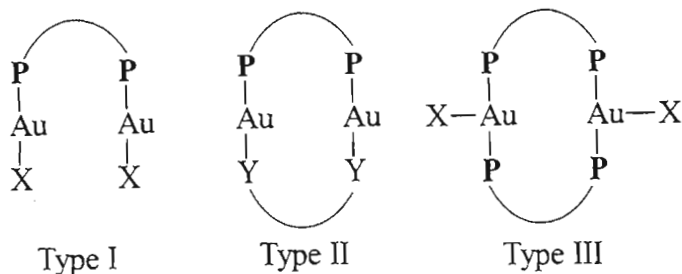
I.3.2.1 Neutral dinuclear complexes

These will be discussed according to the structural types illustrated in Scheme I.10.

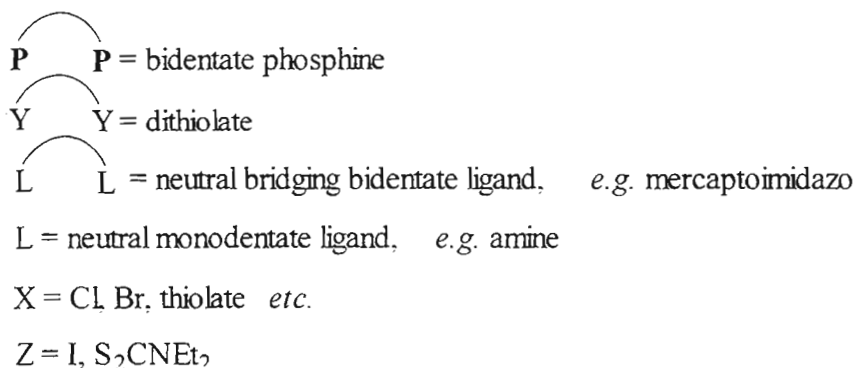
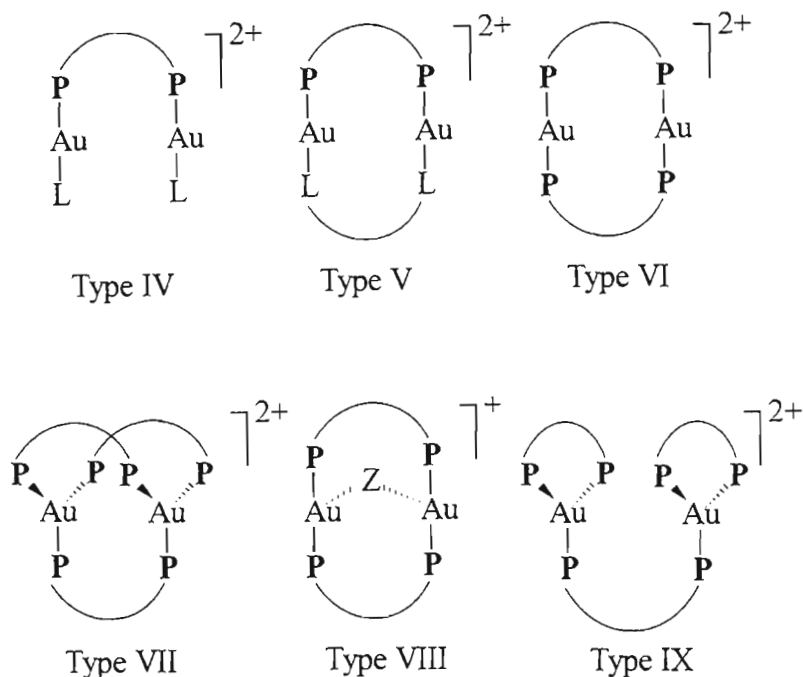
Complexes of type I and II

The most common type of dinuclear neutral gold(I) complexes with bridging diphosphine ligands is $[\text{Au}_2(\mu\text{-PP})\text{X}_2]$ (Type I), where $\mu\text{-PP}$ is a bidentate phosphine and X is a monodentate anion such as a halogen atom,^{7,70} an acetylide group^{28,71,72} or a thiolate group.^{73,74} These complexes received considerable attention during the late 1980's when Mirabelli *et al.*⁷⁵ prepared a large variety of compounds with the above formula and tested their antitumour activity. It appeared that the dinuclear complexes (in particular those containing the dppe ligand) showed much greater potency than their mononuclear analogues.

Neutral



Cationic



SCHEME I.10

A large number of X-ray crystal structures have been reported for compounds of the type [Au₂(μ-PP)Cl₂]. In these molecules the gold(I) atoms are two-coordinate with the expected

linear geometry. One of the first determinations was carried out by Schmidbaur *et al.*⁷⁶ for the complex containing dppm as a bridging ligand (Figure I.15).

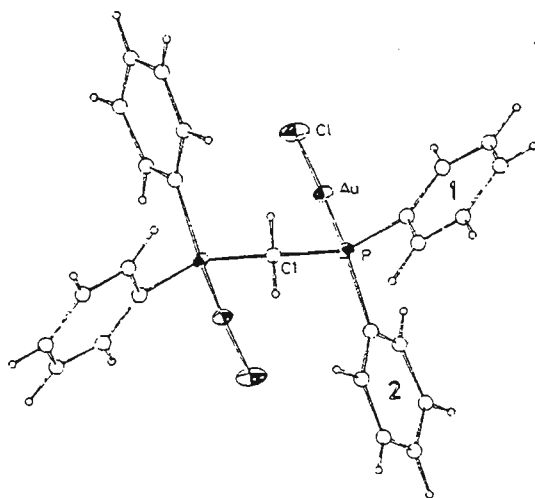


Fig. I.15 Molecular structure of $[\text{Au}_2(\mu\text{-dppm})\text{Cl}_2]$.⁷⁶

Structurally, the molecule did not exhibit any unusual features as both the P-Au-Cl angle, Au-Cl and Au-P bond lengths fell within the normal range of values characteristic for two-coordinate chlorogold(I) complexes with monodentate phosphines ($175.2[2]^\circ$, $2.288[1]$ and $2.238[1]$ Å respectively). The interaction between two gold atoms was not significant, as their separation was as large as $3.351(2)$ Å, a value believed to be consequent to the adopted conformation of the dppm ligand in the solid state.

It should be noted here, that dinuclear gold(I) compounds, such as $[\text{Au}_2\{\mu\text{-R}_2\text{P}(\text{CH}_2)_n\text{PR}_2\}\text{X}_2]$ (where R = alkyl or aryl, $n = 1\text{-}3$ and X_2 represents either two anionic ligands or a bridging diphosphine ligand) present very good opportunity for the study of gold-gold interactions. Short intermetallic contacts have generated much interest during the past decade, especially as Au-Au contacts which are shorter than the sum of the Van der Waals radii of two gold atoms (3.5 Å) are indicative of weak attractive interactions. An interesting physical property exhibited by most gold(I) compounds with close Au-Au contacts is the visible luminescence observed under UV excitation.⁴⁷ Not surprisingly, the observed luminescence has been associated with the Au-Au interaction, which is thought to cause metal-centred emission. However recent results⁷⁴ altered this popular opinion and demonstrated that a gold(I)-gold(I) interaction is not a necessary condition for luminescence, though in many cases the direct correlation between the Au-Au distance and emission wavelength can be found.⁷⁷

Later studies revealed that in other chlorogold(I) complexes with higher homologues of dppm (such as dppb and dppp) intramolecular Au-Au interactions were often absent. However interactions between gold atoms in adjacent molecules (Au-Au distances from 3.04 to 3.32 Å) were frequently observed to take place, thus yielding tetramers⁷⁸ or polymer-like chains.⁷⁹⁻⁸¹ On the other hand, intramolecular gold-gold contacts *are* exhibited by complexes with ligands containing a rigid backbone with one or two carbon atoms connecting the two phosphorus atoms, such as *cis*-1,2-bis(diphenylphosphino)ethylene,⁸² 1,1'-bis(diphenylphosphino)cyclopropane⁸³ and [bis-(diphenylphosphino)methylene]trimethylphosphorane.⁸⁴

The type II complexes $[\text{Au}_2(\mu\text{-PP})(\mu\text{-YY})]$ (H_2YY = xanthine derivatives,⁸⁵ *p*-thiocresol or 1,3-propanedithiol²⁷) are prepared from the reaction of the corresponding type I complex with the potassium or ammonium salt of the ligand.^{27,85} The success in preparation of these complexes depends on the structure of both the phosphine and the other ligand so that closure of metallamacrocyclic ring can be achieved. Examples of such compounds are very scarce and they can be considered as curiosities.

Complexes of type III

Three-coordination in neutral dinuclear gold(I) complexes leads to quite unexpected geometries. Thus, addition of an extra equivalent of the dppm ligand to $[\text{Au}_2(\mu\text{-dppm})\text{Cl}_2]$ results in the formation of an 8-membered macrocyclic ring as well as shortening of the gold-gold bond to 2.962(1) Å in $[\text{Au}_2(\mu\text{-dppm})_2\text{Cl}_2]$. One chloride is associated with each gold atom forming an Au-Au-Cl angle of 97.0(1)°, while the other forms a similar angle but on the other side of the Au_2P_4 plane;⁸⁶ in this way a T-shaped geometry is adopted around each gold atom (Figure I.16).

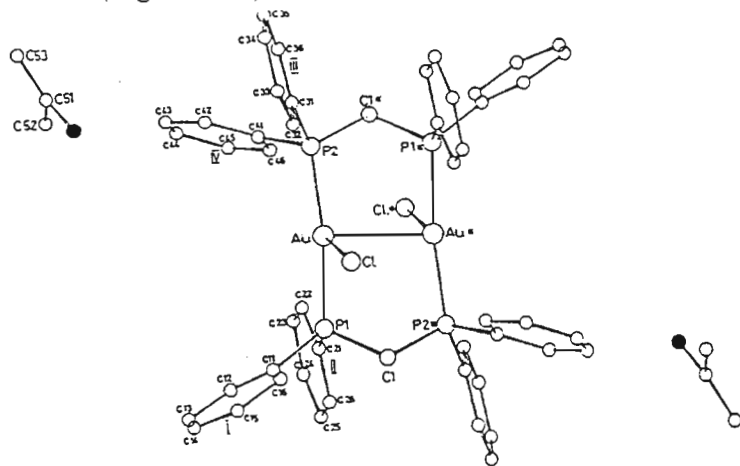


Fig. I.16 Molecular structure of $[\text{Au}_2(\mu\text{-dppm})_2\text{Cl}_2]$.⁸⁶

The dibromide compound was found to have a similar structure.⁸⁷ However, the diiodide analogue, $[\text{Au}_2(\mu\text{-dppm})_2(\mu\text{-I})]\text{I}$, is not neutral but rather adopts the cationic structural type VIII (see Scheme I.10).⁸⁷ Presumably the change in coordination is associated with the increased bulk of the iodide ligand.

The neutral three-coordinate complexes with two bridging phosphine ligands appear to be relatively stable in both solution and the solid state. But addition of an excess of a non-coordinating counterion, such as PF_6^- , results in the loss of the halide ligand and the formation of an ionic complex.⁸⁸ The thermodynamic driving force for this reaction is a more stable linear coordination around gold(I). There have been no reports of attempts to react the above complexes with another non-phosphine bridging ligand in order to produce triply-bridged neutral compounds.

I.3.2.2 Cationic dinuclear complexes

Dinuclear cationic gold(I) complexes with bridging diphosphine ligands can be both two- and three-coordinate in respect to the gold atoms.

Complexes of type IV, V and VI

The complexes of these three types have two-coordinate gold(I) atoms with either one or two diphosphine molecules connecting the two metal centres (see Scheme I.10). In the first case - $[\text{Au}_2(\mu\text{-PP})\text{L}_2]^{2+}$ - the neutral ligands L normally contain nitrogen or sulfur donor atoms, forming a relatively labile bond with gold. Complexes of these type are generally obtained from the corresponding type I complexes by first removing the halogen with a silver salt of a non-coordinating anions followed by an *in situ* reaction with the non-phosphine ligands. As an example, complexes of the general formula $[\text{Au}_2(\mu\text{-dppe})(\text{NH}_2\text{R})_2]$ have been prepared in this manner.⁴⁸

For the preparation of type V complexes, a single neutral bridging bidentate ligand is used instead of two monodentate ones, while the general synthetic strategy remains the same as for the type IV complexes. Burini *et al.*⁸⁹ studied the reactions of " $[\text{Au}_2\{\mu\text{-Ph}_2\text{P}(\text{CH}_2)_n\text{PPh}_2\}]^{2+}$ " ($n = 1\text{-}3$) with asymmetric $\mu\text{-}1,3$ (P,N or N,S) or symmetric $\mu\text{-}1,5$ ligands (N,N) such as thioimidazole and dipyrazole derivatives. They found that the reactions successfully produce metallamacrocycles even with a large ring size (10 to 12 atoms), but only with N- or S-donor atom ligands. The presence of a phosphorus atom

causes cleavage of dinuclear gold(I) ring compounds and results in a mixture of products. Unfortunately, no crystal structures of this type of compounds have ever been published, and most of information about them is obtained from ^{31}P NMR studies.

The more conventional type VI complexes contain two equivalent bridging diphosphine ligands and are consequently thermodynamically much more stable. Dissociation of the diphosphine ligands from gold(I) in solution can be observed by means of ^{31}P NMR spectroscopy, but it is much slower than that for the corresponding mononuclear complexes with monodentate phosphines. The metallamacrocycle can be prepared from either a mono- or dinuclear neutral gold(I) precursor by addition of a certain amount of the diphosphine ligand followed by metathesis of the anion – if required. Extensive research⁹⁰⁻⁹² has been conducted regarding dinuclear ligand-bridged complexes of dppm, dppe, dppp and their analogues (ring size 10-14 atoms) as most of these compounds show interesting photoluminescent properties. An example of a crystal structure for one of the complexes – $[\text{Au}_2(\mu\text{-dcpe})_2](\text{PF}_6)_2$ [dcpe = 1,2-bis(dicyclohexylphosphino)ethane] – is shown on Figure I.17.⁹³

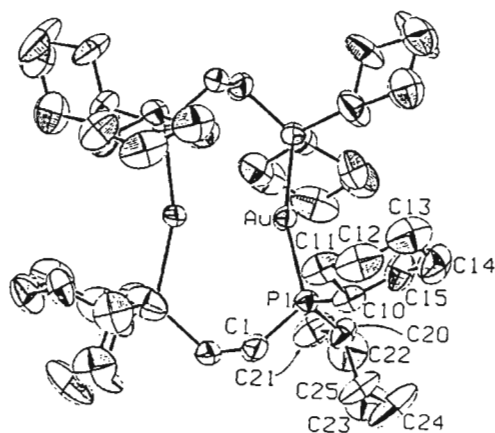


Fig. I.17 ORTEP diagram of $[\text{Au}_2(\mu\text{-dcpe})_2]^{2+}$.⁹³ dcpe = 1,2-bis(dicyclohexylphosphino)-ethane.

A very pronounced feature of this structure is a strong bonding between the two gold atoms – they seem to be pulled towards each other by this bonding as evidenced by a very short Au-Au distance of 2.935(1) Å. This causes the geometry around the gold atom to deviate significantly from linearity, the P-Au-P' angle being equal to 160.6(1)°. However

the rest of the structure remains unaffected, *e.g.* the Au-P bond lengths of 2.314(2) Å are not very different to those in corresponding mononuclear complexes.

Not all diphosphines are capable of stabilising complexes of type VI. In spite of extensive synthetic efforts using the ligands dppf⁶⁵ and dpma [dpma = bis(diphenylphosphinomethyl)phenylarsine]⁹⁴ it has not been possible to produce the desired symmetrical ring compounds. The reason for this behaviour remains to be understood, as even the dppb ligand is capable of stabilising 14-membered metallamacrocycles of gold(I) in solution.⁴³

Complexes of type VII and VIII

These complexes contain two three-coordinate gold atoms bridged by either two or three diphosphine ligands.

The inadvertently obtained $[\text{Au}_2(\mu\text{-dppm})_2(\mu\text{-I})][\text{Au}(\text{CN})_2]$ complex provides an example of the structural type VIII compound (see Scheme I.10), where bridging of two gold atoms is achieved through two diphosphine ligands and an iodide ion (Figure I.18).⁹⁵

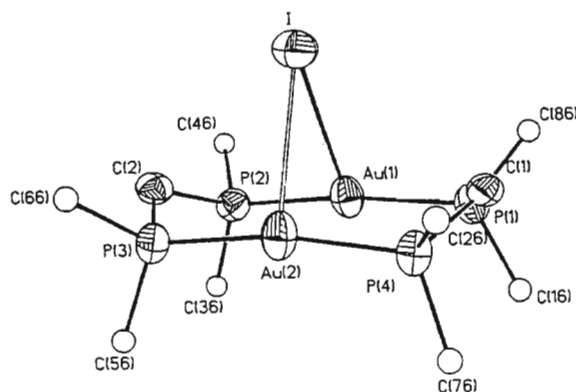


Fig. I.18 Structure of the cation $[\text{Au}_2(\mu\text{-dppm})_2(\mu\text{-I})]^+$.⁹⁵

The crystal structure shows that the iodide asymmetrically bridges the two gold atoms with Au-I distances of 3.161(3) and 3.342(3) Å, the Au-Au-I angle being 73°. The geometry around gold can be considered as nearly linear, as the P-Au-P angles at 170.0(1) and 171.3(1)° are quite close to 180°. The gold-gold separation of 3.16 Å is typical for digold

compounds containing two bridging diphosphine ligands. This cation retains its integrity in solution as indicated by ^1H and ^{31}P NMR spectroscopic data.⁹⁵

Interestingly, in the complexes $[\text{Au}_2\{\mu\text{-Ph}_2\text{PC(=CH}_2\text{)PPh}_2\}_2\text{Cl}]^+$ and $[\text{Au}_2\{\mu\text{-Ph}_2\text{PC(CH}_2\text{CH}_2\text{)PPh}_2\}_2\text{Cl}]^+$,^{96,97} which are formally analogous to the just described complex, the chloride ions were found to coordinate to only one of the two gold atoms. The Au-Au-Cl angles in these complexes are equal to 96 and 75° respectively, while in the symmetrically bridged complex $[\text{Au}_2(\mu\text{-dppm})_2(\mu\text{-I})]\text{I}$ the corresponding angle is 66°.⁹⁵ The coordinated chlorides interact only weakly with the gold atoms as shown by long Au-Cl distances ranging from 2.72 to 2.96 Å, which is notably longer than 2.50 Å in the mononuclear three-coordinate complex $[\text{Au}(\text{Ph}_3\text{P})_2\text{Cl}]$.⁹⁸ Thus in spite of the general formula similarity with $[\text{Au}_2(\mu\text{-dppm})_2(\mu\text{-I})]^+$, the above complexes cannot be considered as type VIII complexes and should rather be considered as cases with mixed geometry around two gold(I) atoms.

Complexes of the type VII $\{[\text{Au}_2(\mu\text{-PP})_3]^{2+}\}$ are generally prepared by addition of an extra equivalent of the diphosphine ligand to the type VI complexes of dppm, dppe and their analogues.⁴³ These complexes are not always easy to crystallise from solution and selection of the counterion often plays an important role in the successful determination of the crystal structure. Figure I.19 shows the structure of $[\text{Au}_2(\mu\text{-Me}_2\text{PCH}_2\text{PMe}_2)_3]^{2+}$ cation.⁹⁹

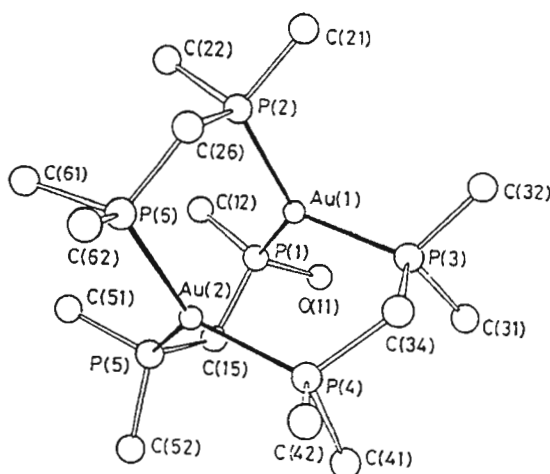


Fig. I.19 The structure of the cation $[\text{Au}_2(\mu\text{-Me}_2\text{PCH}_2\text{PMe}_2)_3]^{2+}$.⁹⁹

The complex is made up by two nearly trigonal planar gold atoms connected via P-C-P bridges. The deviation from ideal trigonal geometry is small with the P-Au-P angles ranging from 114.7 to 124.9° and what makes it nearly trigonal is that the Au-P distances are nearly the same (average 2.358 Å). The Au-Au interaction [Au-Au = 3.04(1) Å] as well as the presence of three strongly bonding bridging diphosphine ligands make this cation very stable, so that it does not decompose in solution even after a considerable length of time.

Che *et al.*^{100,101} have prepared interesting examples of type VII complexes using 2,6-bis(diphenylphosphino)pyridine and 2,7-bis(diphenylphosphino)naphthyridine as the bridging ligands. examples being $\{\text{Au}_2[\mu\text{-}2,6\text{-(Ph}_2\text{P)}_2\text{(C}_5\text{H}_3\text{N)}]_3\}(\text{ClO}_4)_2$ ¹⁰⁰ and $\{\text{Au}_2[\mu\text{-}2,7\text{-(Ph}_2\text{P)}_2\text{(C}_8\text{H}_4\text{N}_2)]_3\}(\text{ClO}_4)_2$ ¹⁰¹ respectively. Both are large macrocyclic compounds with nearly trigonal planar geometry around the gold atoms, but without intramolecular (or intermolecular) metal-metal interactions. the intramolecular Au-Au distances in the complexes being 4.87 and 7.20 Å respectively. The large separation between two gold atoms in both complexes provides cavities for small inorganic ions such as K^+ .¹⁰¹

Not surprisingly, larger diphosphine ligands such as dppe⁶⁵ and dcpe¹⁰² are not able to achieve a triply-bridged arrangement between the two gold atoms. The structure that results in those two cases (structural type IX – see Scheme I.10) is a combination of bridging and chelation by the diphosphine ligands as illustrated in Figure I.20.

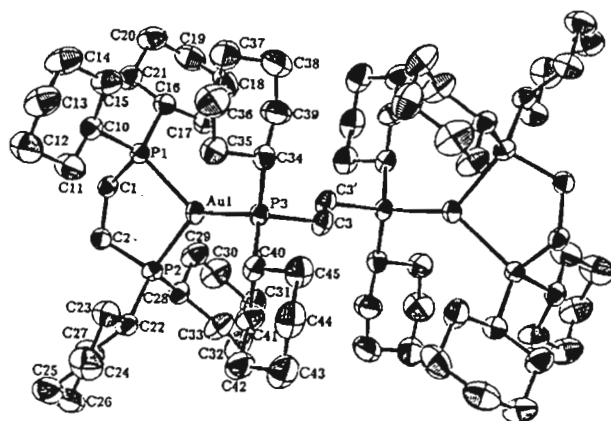


Fig. I.20 ORTEP view of the cation $[\{\text{Au}(\text{dcpe})\}_2(\mu\text{-dcpe})]^{2+}$.¹⁰²

The geometry around the gold atoms is trigonal planar with slightly higher than expected values for Au-P bond lengths – presumably the consequence of the steric constraints. Again, no Au-Au interactions are observed.

I.3.3 Trinuclear complexes of gold(I) containing bridging bidentate phosphine ligands

The first example of a trinuclear complex with a bidentate phosphine ligand was reported in 1983 by Uson *et al.*¹⁰³ They prepared $[\text{ClAu}(\mu\text{-dppm})\text{Au}(\mu\text{-dppm})\text{AuCl}]\text{X}$ ($\text{X} = \text{ClO}_4^-$ or $[\text{Au}(\text{C}_6\text{F}_5)_3\text{Cl}]^-$) from $[\text{Au}_2(\mu\text{-dppm})\text{Cl}_2]$ by carefully selecting conditions for step-by-step substitution: *e.g.* for the perchlorate complex, one chloride ligand of the starting complex was removed by using AgClO_4 and the reactive intermediate was treated consecutively with equimolar amounts of dppm and $[\text{Au}(\text{tht})\text{Cl}]$. Later studies^{104,105} showed that the chloride species, $[\text{ClAu}(\mu\text{-dppm})\text{Au}(\mu\text{-dppm})\text{AuCl}]\text{Cl}$, exists in equilibrium in solution with dinuclear dppm ligand-bridged gold(I) complexes. The trinuclear complexes with perchlorate or tri(pentafluorophenyl)chloroaurate as counterions, can be characterised in solution and, in addition, can be successfully isolated as solids. The chloride complex, however, is less stable than its analogues and could not be characterised in solution. The reason for the instability of the chloride complex in solution is believed to be the reaction of the chloride anion with the trinuclear compound via the central gold atom, affording $[\text{Au}_2(\mu\text{-dppm})\text{Cl}_2]$ and $[\text{Au}_2(\mu\text{-dppm})_2\text{Cl}_2]$. However precipitation with ethanol allowed the crystallisation of the intact trinuclear species and the determination of its X-ray structure (Figure I.21).¹⁰⁵

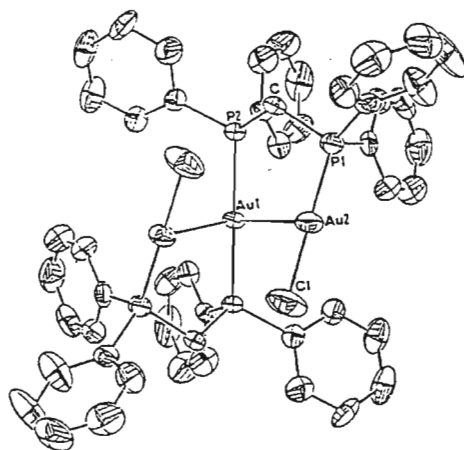


Fig. I.21 ORTEP diagram of the cation $[\text{ClAu}(\mu\text{-dppm})\text{Au}(\mu\text{-dppm})\text{AuCl}]^+$ in $[\text{ClAu}(\mu\text{-dppm})\text{Au}(\mu\text{-dppm})\text{AuCl}]\text{Cl}$.¹⁰⁴

The three gold atoms are in a V-shape arrangement with two short [3.076(1) Å] and one long [3.729(1) Å] Au-Au distances. The values are comparable to the gold-gold distances [3.067(5) and 3.164(5) Å – the short distances and 3.676(5) Å – the long distance] reported by Uson¹⁰³ for the $[\text{ClAu}(\mu\text{-dppm})\text{Au}(\mu\text{-dppm})\text{AuCl}][\text{Au}(\text{C}_6\text{F}_5)_3\text{Cl}]$ complex. The bent geometry is believed to arise from the incorporation of two empty *p*-orbitals on gold in the Au-Au bonding. The two P-Au-Cl 'arms' are pointing toward opposite directions such that further reaction with dppm to close up the triangle of gold atoms is unlikely.

Attempts to apply the method suitable for the preparation of the dppm-based trinuclear complex using the dppe ligand were not successful, as the target compound was formed only as a minor product.¹⁰⁵

I.4 GOLD(I) COMPLEXES WITH TRIDENTATE PHOSPHINES

The coordination behaviour of tridentate phosphine ligands towards gold(I) has not been extensively studied. There are several reports in the literature describing the coordination modes of a few tridentate phosphine ligands to gold(I), but they do not amount to a systematic investigation of the subject. The coordination mode appears to be a function of both the backbone structure of the ligand and the conditions of the synthesis, with the former playing the major role. The examples of complexes characterised to date include mono-, di- and trinuclear compounds.

I.4.1. Mononuclear complexes

The only known example of a mononuclear gold(I) complex of this type was reported by Fackler *et al.*¹⁰⁶ with the tripodal ligand tris{2-(diphenylphosphino)ethyl}amine (NP_3). The compound was obtained by reacting $[\text{Au}(\text{PPh}_3)\text{Cl}]$ with TIPF_6 in order to remove the chloride counterion, followed by addition of one equivalent of the ligand. The outcome of the reaction was not sensitive to the solvent, but to the nature of the starting material, yielding a dinuclear compound under slightly different conditions. The compound is stable in solution, producing a single peak in the ^{31}P NMR spectrum, and it does not undergo rearrangement into other species. The structure of the $[\text{Au}(\text{NP}_3)]^+$ cation is shown on Figure I.22.

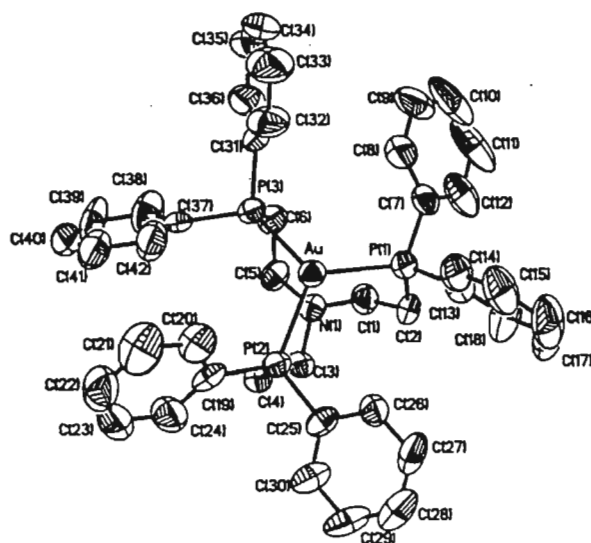


Fig. I.22 ORTEP diagram of $[\text{Au}(\text{NP}_3)]^+$ cation.¹⁰⁶ NP_3 = tris{2-(diphenylphosphino)-ethyl}amine.

The geometry around the gold centre is roughly trigonal planar, with the gold atom being slightly removed from P(1)-P(2)-P(3) plane in a direction opposite to the nitrogen atom. The Au-N distance is 2.683(6) Å and is considered to be very weakly bonding. The Au-P distances average at 2.356 Å, which is very close to normal values for three-coordinate gold complexes (2.384 Å,⁵⁴ average in $[\text{Au}\{\text{PPh}_3\}_3]^+$).

I.4.2 Dinuclear complexes

The same authors¹⁰⁶ obtained a dinuclear gold(I) complex with the NP_3 ligand. They used a somewhat different reaction conditions: $[\text{Au}(\text{tht})\text{Cl}]$ as a starting material and an excess of sodium salt for the removal of the chloride, while the gold/phosphine ratio was kept unchanged at 1:1. The result was the dinuclear compound $[\text{Au}_2(\text{NP}_3)_3](\text{BPh}_4)_2$. This compound is also stable in solution, but shows two separate singlets in the ^{31}P NMR spectrum, indicating that two different sets of phosphorus atoms are present in that molecule. Figure I.23 illustrates the structure of this dinuclear complex.

Two of the phosphorus atoms of each ligand chelate to one gold atom, while the third phosphorus atom bridges to the other metal centre, resulting in three-coordination around both gold atoms. The geometry can be described as distorted trigonal planar, as one of the

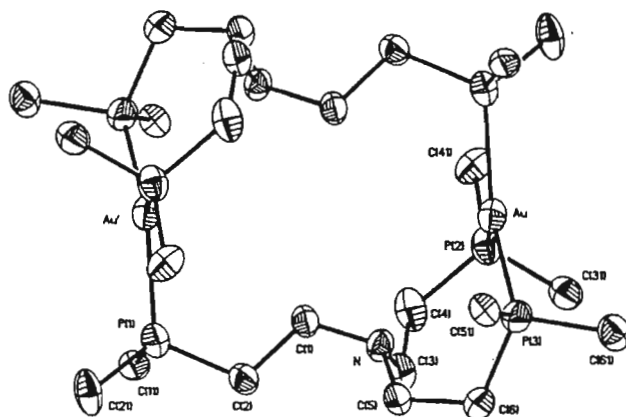


Fig. I.23 ORTEP diagram of $[\text{Au}_2(\text{NP}_3)]^{2+}$ cation.¹⁰⁶ NP_3 = tris{2-(diphenylphosphino)-ethyl}amine.

Au-P bonds is longer than two others (2.399 vs. 2.364 Å). No Au-Au interaction – either intra- or intermolecular - has been observed for this compound. Unlike in the previously discussed mononuclear complex with the NP_3 ligand, there was no evidence of Au-N bonding.

A similar example of the coordination mode described above was reported by Balch¹⁰⁷ with the tetradentate phosphorus analogue of NP_3 , *i.e.* PP_3 . This ligand also causes the formation of a dinuclear species in which one of the arms of the PP_3 ligand functions as a bridge and the other three phosphorus atoms chelate one of the gold centres. This results in four-coordination (distorted tetrahedral geometry) at each gold atom.

I.4.3 Trinuclear complexes

I.4.3.1 Neutral complexes

The tripod-like ligands 1,1,1-tris(diphenylphosphino)methane (tpm)¹⁰⁸ and 1,1,1-tris(diphenylphosphinomethyl)ethane (tdme)¹⁰⁹ form the neutral species $[(\mu\text{-tpm})(\text{AuCl})_3]$ and $[(\mu\text{-tdme})(\text{AuCl})_3]$ respectively upon reaction with a stoichiometric amount of a chlorogold(I) precursor. The only unusual feature of the crystal structure of the second molecule is the interaction between just two of the three gold atoms: two 'arms' of the tripod molecule are crossed almost orthogonally, which brings the metal atoms into very close proximity, the short Au-Au distance being 3.091 Å. It appears that steric constraints

imposed by the backbone of the tripod ligand prevent close approach between all three of the gold atoms.

I.4.3.2 Cationic complexes

Che *et al.*^{110,111} have been successful in synthesising trinuclear gold(I) complexes where all the gold atoms are involved in intramolecular bonding. They used bridging ligands such as dmmp [dmmp = bis(dimethylphosphinomethyl)methylphosphine] and dpmp [dpmp = bis(diphenylphosphinomethyl)phenylphosphine]. The cationic trinuclear compounds $[\text{Au}_3(\mu\text{-L})_2]^{3+}$ (L = dpmp or dmmp) were obtained by reacting a chlorogold(I) precursor *in situ* with one equivalent of the ligand followed by metathesis with a sodium/lithium salt. In both complexes the gold atoms are two-coordinate, therefore providing a very stable arrangement. This was confirmed by observation of only one species in solution. The complexes have common features in their crystal structures, such as three linear P-Au-P units held together by P-C-P bridges with comparable Au-Au distances (2.981[1] and 2.962[1] Å in the dmmp complex,¹¹⁰ and 3.0137[8] and 3.0049[8] Å in the dpmp complex¹¹¹). However they differed quite markedly in the Au-Au-Au angles, which were found to be 167.21(2) and 136.26(4)° for the dpmp and dmmp complexes respectively. No reasonable explanation for the observed differences has been proposed, especially taking into account the fact that dpma – the ligand nearly identical to dpmp, the only difference being the middle phosphorus substituted by an arsenic atom – forms a similar type of complex $[\text{Au}_3\text{Cl}_3(\mu\text{-dpma})]^{94}$ with a Au-Au-Au angle as low as 110.9°.

A somewhat different arrangement of three P-Au-P units in a cationic complex was reported by Che.¹¹² The tripodal ligand tpm (*vide supra*) forms an interesting compound $[\text{Au}_3(\mu\text{-tpm})_2\text{Cl}]^{2+}$ with different coordination numbers for gold atoms. The crystal structure of the compound is shown on Figure I.24.

The complex has two distinctly different environments around the gold atoms: linear [P(1)-Au(1)-P(2) = 175.6(1)°] and T-shaped [P(3)-Au(2)-P(3') = 170.0(1)°, Cl(1)-Au(2)-P(3) = 94.97(8)°]. The Au-Cl interaction is quite strong, with the Au(2)-Cl(1) contact of only 2.642(6) Å being shorter than that in the similar bis(T-shaped) complex $[\text{Au}_2(\mu\text{-dppm})_2\text{Cl}_2]$, *i.e.* 2.771(4) Å.⁸⁶ The three gold atoms are arranged in a nearly equilateral triangle with the Au-Au-Au angles being around 60°; however the sides of the triangle,

which are adjacent to the Cl-Au bond, are slightly longer [$\text{Au}(1)\text{-Au}(1') = 2.9220(8) \text{ \AA}$, while $\text{Au}(1)\text{-Au}(2) = 3.0889(8) \text{ \AA}$] as a result of the chloride coordination to Au(2).

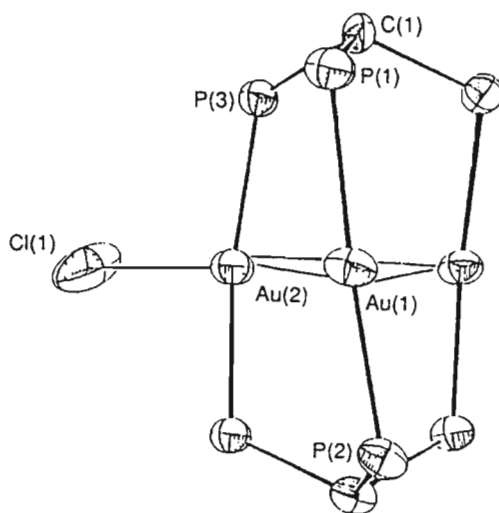
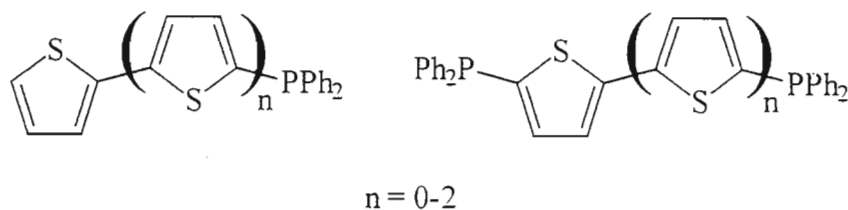


Fig. I.24 ORTEP diagram of $[\text{Au}_3(\mu\text{-tpm})_2\text{Cl}]^{2+}$ cation.¹¹²

I.5 OBJECTIVES OF THIS STUDY

The initial aim of this project was to synthesise various mono- and diphosphines containing mono- and polythiophene structural units. For this study 2,2'-bithiophene and 2,2':5,2''-terthiophene fragments were selected as polythiophene moieties and phosphine substituents were introduced at position 2 of the thiophenes (Scheme I.11). The class of thienylphosphines described to date has been limited to 2- and 3-(diphenylphosphino)thiophenes and a handful of their derivatives.^{113,114} Their chemistry has been poorly studied and, furthermore, nothing is known regarding their coordination behaviour towards gold(I). Thus, another aim of this project was to investigate the coordination chemistry of mono- and polythiophene based phosphines with gold(I).



SCHEME I.11

During the course of this study it was discovered that several thiophene-based phosphines and their gold(I) complexes – particularly the ones with a polythiophene fragment – were poorly soluble. Also, numerous attempts to induce the sulfur of a thiophene to coordinate to the metal failed. Therefore, it was decided to extend the range of compounds studied and to introduce substituents allowing for different solubility properties and an improved scope of coordination behaviour. Thus, 2-pyridyl was substituted for 2-thienyl in 2,2'-bithiophene and 2,2':5',2''-terthiophene fragments giving rise to the synthesis of four more new phosphines. As expected, the introduction of a pyridine unit led to improved solubility as well as increased possibilities for the ligands' coordination to gold(I).

Finally, the combination of thiophene, phosphine and gold(I) moieties in the same molecule appears to have a biological potential: in the past decade considerable attention has been drawn to the medicinal properties of gold(I)-phosphine complexes and, independently, to the biological properties of thiophenes. Gold(I)-phosphine complexes are known to be active against rheumatoid arthritis^{1,115} and have potential as antitumour drugs.^{75,116-119} Thiophene compounds have shown potential applications as neumatocidal, pesticidal and insecticidal agents. Furthermore, α -linked bi- and terthiophenes have been found to possess antiviral and cytotoxic properties.¹²⁰⁻¹²² To the best of our knowledge there have been no attempts to combine the biological properties of gold(I) and polythiophenes; however, we believe that this approach could produce biologically active compounds as similar strategies employing gold(I) and a ligand with known antitumour properties, such as 5-fluorouracil and 2-diphenylphosphinoethyl-methyl sulfoxide, were successfully used recently by a number of workers.^{17,123,124}

With this in mind, a pilot study of the cytotoxic properties of the new thiophene-based phosphines and their gold(I) complexes was initiated, where special emphasis was made on correlating the properties of the parent polythiophenes with the toxicity of the final gold(I) complexes. As the mechanism of cytotoxicity in bi- and terthiophenes is known to be largely phototoxicity-based,¹²⁵ the photochemical properties of a number of thiophene-based phosphines were briefly studied.

CHAPTER TWO

LIGAND SYNTHESIS

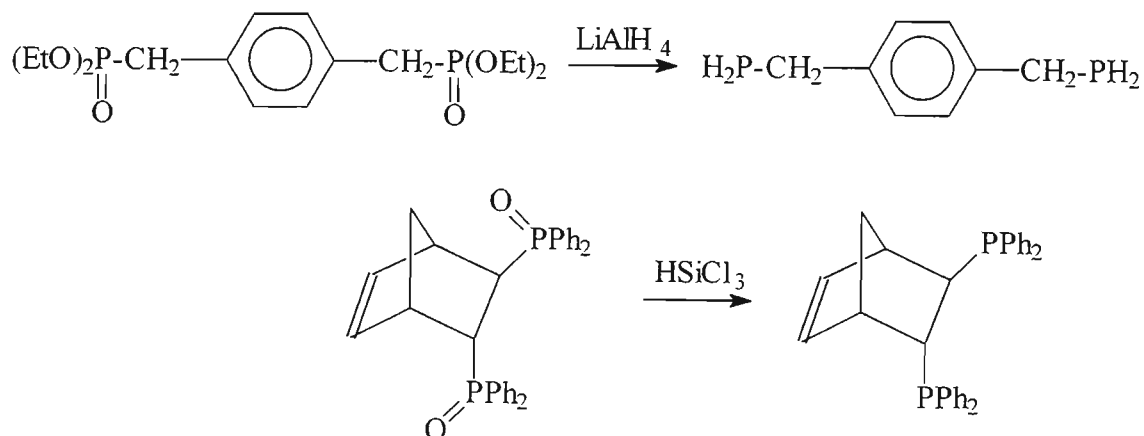
II.1 INTRODUCTION TO GENERAL METHODS FOR PHOSPHINE SYNTHESIS

This introduction is focused on the most direct and general methods for synthesis of tertiary phosphines. Primary and secondary phosphines often serve as precursors to tertiary phosphines, so their preparation is included in the discussion where relevant.

The methods for tertiary phosphine synthesis can be divided into two main groups:

- 1) where the skeleton of the precursor molecule remains unchanged after the reaction, *i.e.* no new C-P bonds are created and
- 2) where new C-P bonds are created as the result of the reaction.

The first group involves the reduction of P-O and P-S bond containing compounds of phosphorus(V). Typically, phosphinic or phosphonic acid esters or chlorides, phosphine oxides and sulfides are reduced with lithium aluminium hydride¹²⁶ and trichlorosilane¹²⁷ (see Scheme II.1).

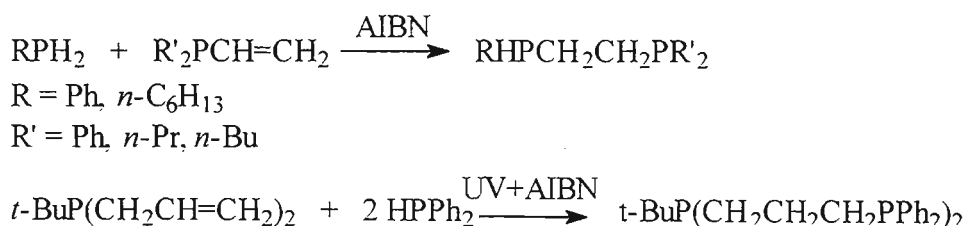


SCHEME II.1

The second, larger group contains five subgroups arranged on the basis of the mechanism involved in the creation of the new P-C bond. These will now be described.

II.1.1 Addition of primary and secondary phosphines to unsaturated C-C bonds

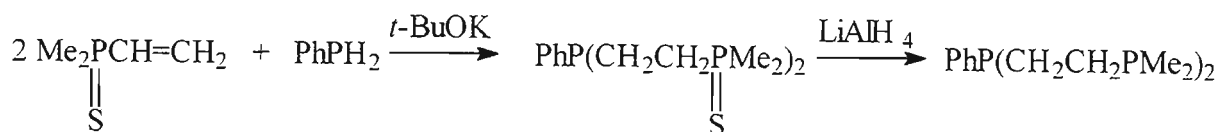
The first method is extensively used in the preparation of bi- and polydentate phosphines. AIBN-assisted (AIBN = azo-*iso*-butyronitrile) free radical catalysed addition of a P-H bond to a carbon-carbon double bond affords a polymethylene-bridged phosphine which may be symmetrical or asymmetrical (Scheme II.2):^{128,129}



SCHEME II.2

The addition can also proceed in the presence of a basic catalyst, such as *t*-BuOK. In this case, however, the reaction cannot be stopped at the intermediate stage of the secondary phosphine formation, but always proceeds to the tertiary product.¹³⁰

Very often this method is used in conjunction with the reduction of P-S and P-O bonds in order to prepare ligands with particularly air-sensitive groups (see Scheme II.3).¹³¹

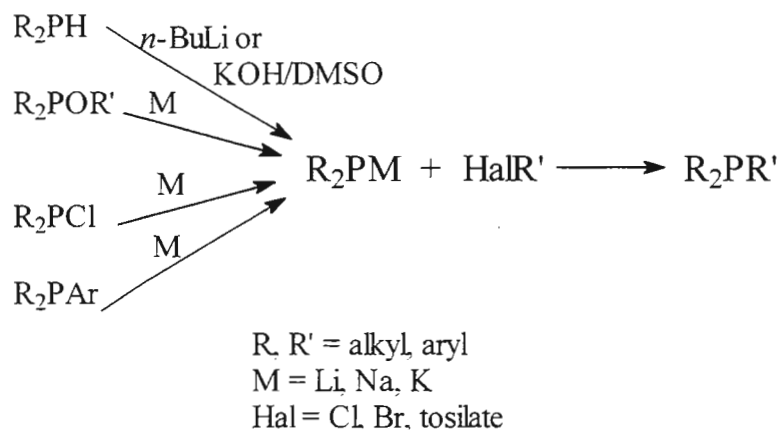


SCHEME II.3

II.1.2. Nucleophilic substitution at the carbon atom by metallated phosphines

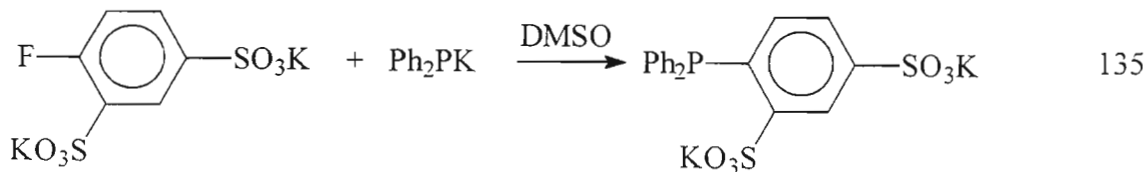
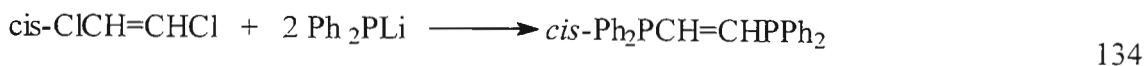
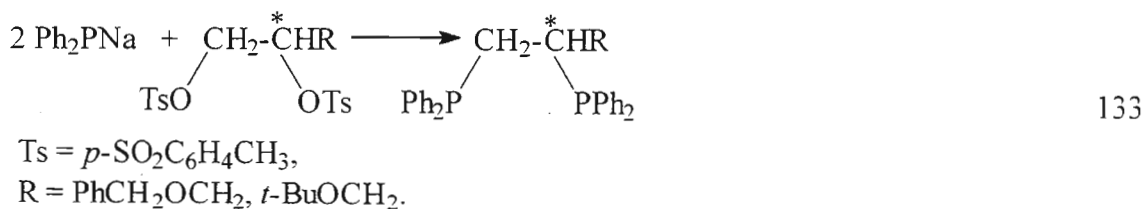
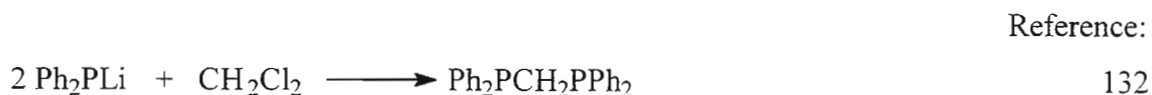
The second method is extensively developed and studied, and is currently one of the most widely used synthetic routes. The general reaction scheme is shown below (Scheme II.4):

The metal phosphides are normally prepared *in situ* by cleavage of a P-X bond (where X can be H, Cl or Ar) with a metal or an organometallic compound and then reacted with a

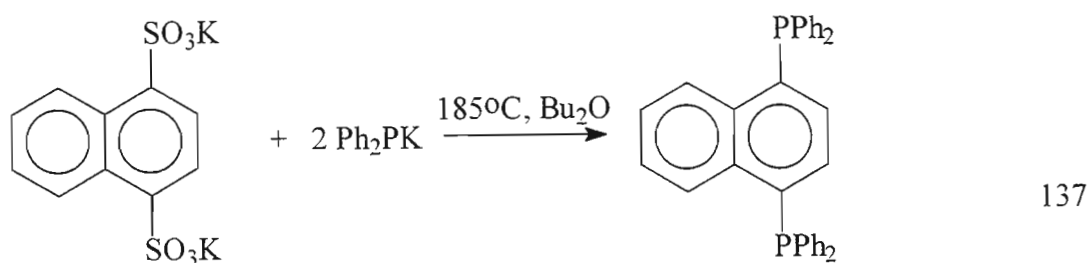
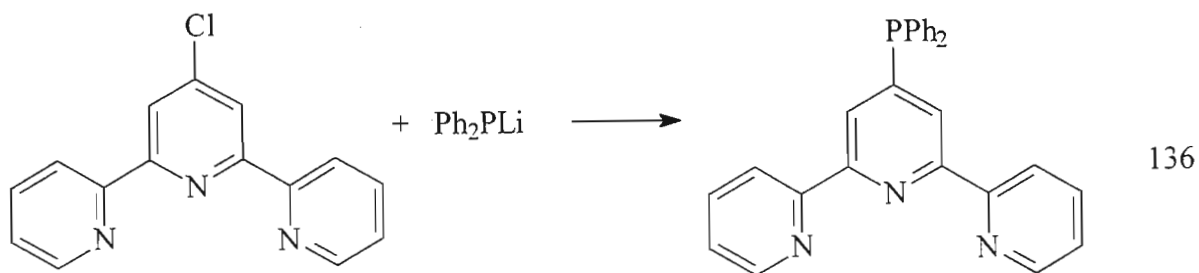


SCHEME II.4

variety of alkylating agents: alkyl halides or tosylates, allyl and benzyl halides, alkenyl and acyl chlorides and also aromatic halides or sulfonates. Typical examples of these reactions are given in Scheme II.5:



SCHEME II.5



SCHEME II.5 (continued)

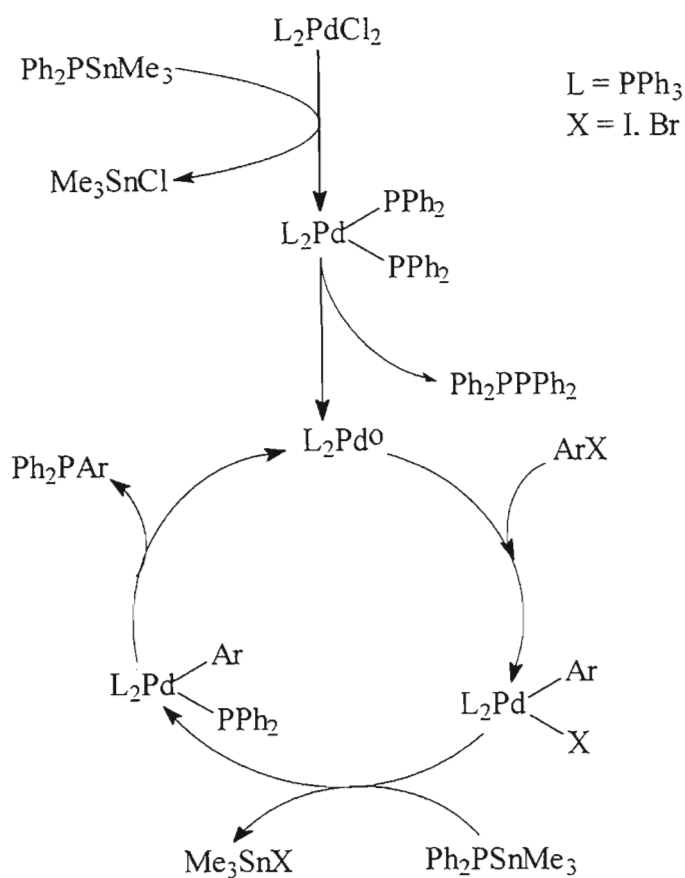
Alkali metal derivatives of phosphines are generally very reactive, so their use is limited to substrates which do not contain nucleophile or base sensitive functional groups such as aryl alkyl ethers, nitriles or keto-groups.

(Trimethylsilyl)diphenylphosphine is a much milder reagent and it can be used in a similar way for the preparation of phosphines from acid chlorides,¹³⁸ α -halocarbonyls¹³⁹ and α -chloronitriles.¹⁴⁰ The chemistry of (trimethylstannyl)diphenylphosphine is very similar, and the target phosphines with sensitive groups can be prepared under even milder conditions in the presence of a palladium catalyst. The mechanism of the coupling reaction is presented in Scheme II.6.¹⁴¹ It includes formation of a zero-valent palladium complex, oxidative addition of the haloaromatic substrate, transmetallation and reductive elimination of the product.

This reaction cannot be classified as involving true nucleophilic attack by a metallated phosphine on a carbon atom: it evidently has a more complex mechanism and takes place only for aryl iodides and some bromides.¹⁴¹ Nevertheless, it is discussed here as the stoichiometry of the overall reaction is as for the metallated phosphines, *i.e.*:



where $\text{M} = \text{Me}_3\text{Si}$ or Me_3Sn , $\text{X} = \text{Br, I}$ and $\text{R}' = \text{Ar}$.

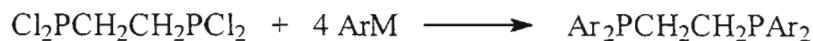


SCHEME II.6

II.1.3 Nucleophilic substitution at the phosphorus atom by organometallic reagents

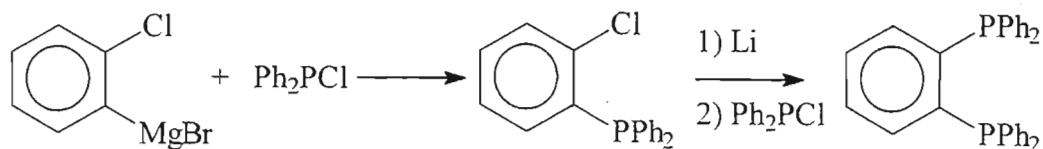
This is the oldest method used for the preparation of tertiary phosphines and involves reaction between organometallic reagents and phosphine halides. Examples are presented in Scheme II.7.

Reference:



74

M = Li: Ar = 2-pyridyl, 4-pyridyl, 2-furanyl, 2-thienyl

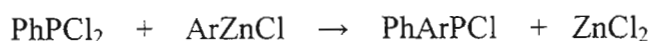
M = MgBr: Ar = 4-FC₆H₄, 4-CH₃OC₆H₄, 4-CH₃SC₆H₄ etc.

142

SCHEME II.7

A significant number of heterocyclic phosphines have been prepared via this route: *e.g.*, tris(2-pyrrolyl)phosphines,¹⁴³ 2,5-bis(diphenylphosphino)furan,¹⁴⁴ tris(2-methyl-3-thienyl)phosphine,¹¹⁴ tris(2-pyridyl)phosphine¹⁴⁵ and tris(5-trimethylsilyl-2-thienyl)phosphine.¹⁴⁶

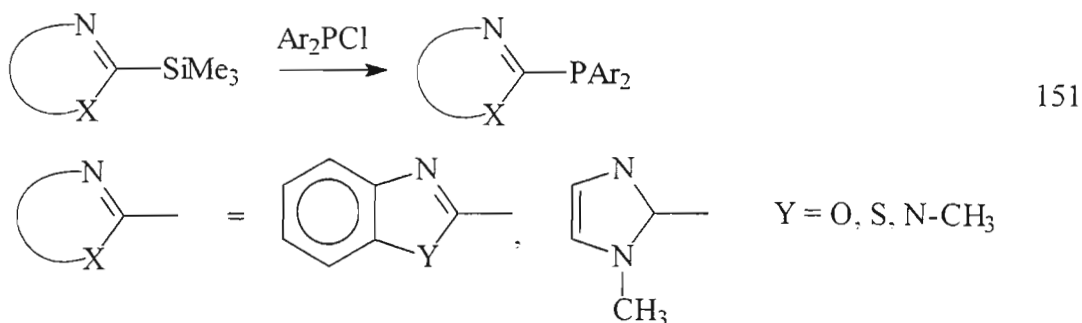
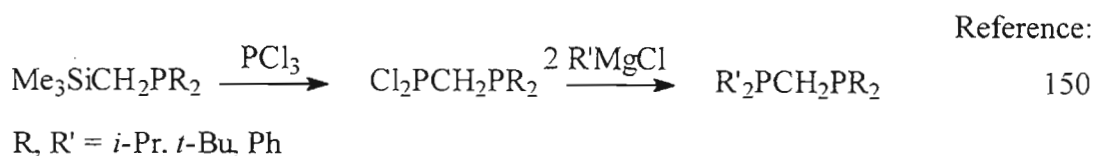
The use of organolithium over the Grignard reagents is preferred when the synthesis of sterically hindered phosphines is required. Organozinc compounds, on the other hand, are used when selective and partial substitution is required (Scheme II.8).¹⁴⁷



SCHEME II.8

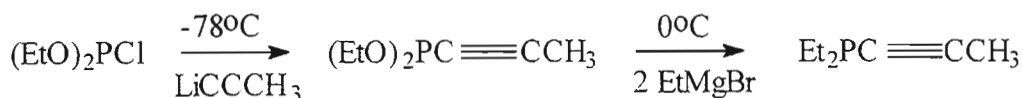
Variations of the Grignard route have been explored. For example Richter *et al.*^{148,149} have studied the reactions of metal derivatives of conjugated polyenes, such as butadienyl magnesium or cyclooctatetraenyl magnesium with diphenylchlorophosphine. These reactions selectively afford single products, *viz* 1,2-bis(diphenylphosphino)but-3-ene and 1,2-bis(diphenylphosphino)cycloocta-3,5,7-triene respectively, despite the fact that the double bonds in the original organomagnesium compounds are delocalised.

Silyl compounds have also been employed as organometallic reagents for the synthesis of phosphines (Scheme II.9), their use is limited however, as only substrates with very reactive Si-C bond succeed in reactions with phosphine chlorides.



SCHEME II.9

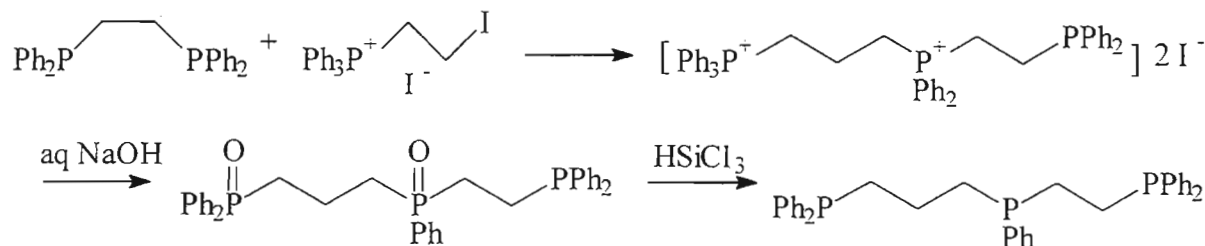
Phosphorus (III) esters can be good alternatives to phosphine halides for the preparation of tertiary phosphines. For example, triphenylphosphite $(\text{PhO})_3\text{P}$ is a common starting material that is successfully employed for the synthesis of tris(cyclopropyl)phosphine.¹⁵² At low temperatures, alkoxy and aryloxy substituents at the phosphorus atom can serve as protecting groups, which are replaced at higher temperatures (Scheme II.10).¹⁵³



SCHEME II.10

II.1.4. Nucleophilic substitution by phosphorus(III) compounds

This subgroup of synthetic methods is based on the high affinity of non-metallated phosphines for electron-deficient centres - due to the lone electron pair on the phosphorus atom. The nucleophilicity in the series primary, secondary and tertiary phosphine increases with the increase of the number of organic substituents: $\text{PH}_3 < \text{RPH}_2 < \text{R}_2\text{PH} < \text{R}_3\text{P}$. As it is with amines, alkylation of a primary phosphine is very difficult to stop at a partial alkylation level, and a quaternary salt is normally formed as a result. The quaternary salt can be converted to a tertiary phosphine by hydrolysis. During the hydrolytic procedure one of the substituents is normally lost and a phosphine oxide is formed, which has to be subsequently reduced to the corresponding phosphine. Aromatic substituents and hydrogen show a greater tendency to leave than alkyl groups. An example of an elegant synthesis of an asymmetrical triphosphine via this route is presented in Scheme II.11.¹⁵⁴



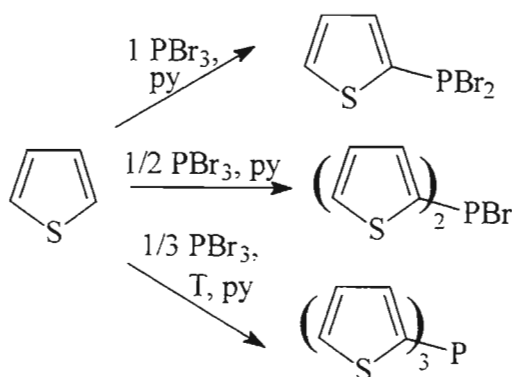
SCHEME II.11

II.1.5. Electrophilic substitution by phosphorus(III) compounds

This last group of methods involves reactions between electron-deficient phosphine derivatives and electron-rich centres. It is based on the known ability of phosphorus to

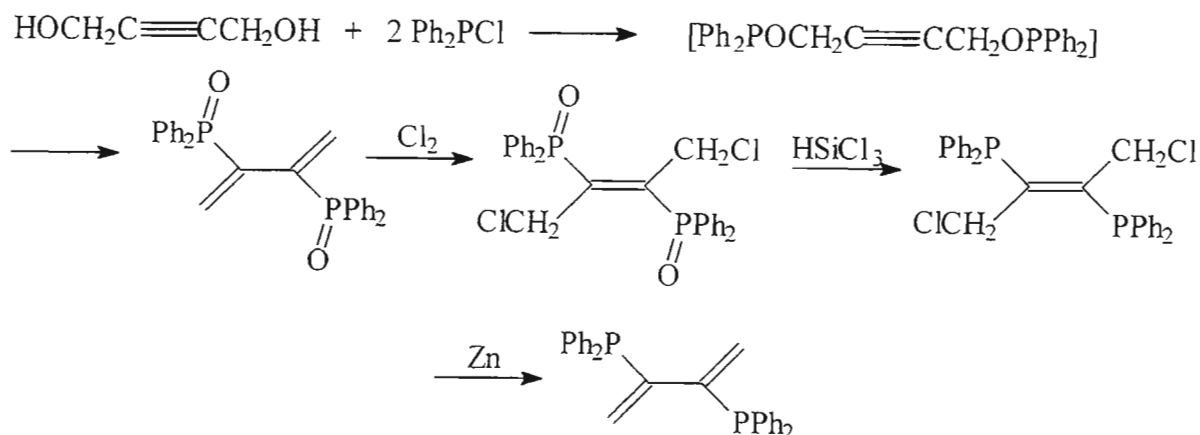
accommodate an extra pair of electrons on its empty 3d-orbital. The commonly used electron-deficient compounds of phosphorus are chlorides and bromides, while aromatic rings, double bonds and even heteroatoms (*e.g.* oxygen) fulfil the role of electron-rich centres.

The reaction of mono-, di- and trihalogenated phosphines with aromatic and heteroaromatic compounds under Friedel-Crafts conditions produces tertiary phosphines, albeit as a mixture of isomers and, sometimes, together with subalkylated compounds. Lewis acids such as ZnCl_2 , AlCl_3 and SnCl_4 are normally used as catalysts for these reactions.^{155,156} In a recent report pyridine was used as a catalyst for the phosphorylation of furan and thiophene (Scheme II.12).¹⁵⁷



SCHEME II.12

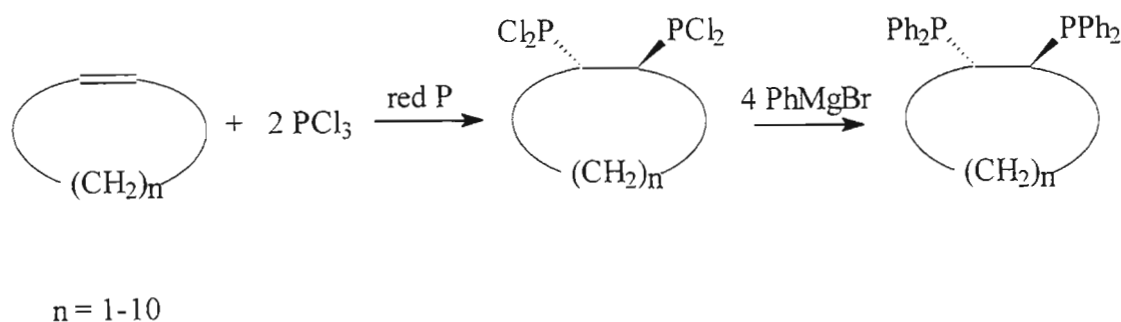
An example of the synthesis where the chlorophosphine reacted with the substrate via a heteroatom is shown in Scheme II.13.¹⁵⁸



SCHEME II.13

The above reaction sequence is also of note due to the characteristic rearrangement that the diphenylphosphite moiety undergoes, producing finally the diphenylphosphoryl fragment.

The synthetic methods listed so far are not exhaustive: there is still a number of phosphine preparation schemes in the literature which do not formally fall under any of the described methods, *e.g.* Scheme II.14.¹⁵⁹



SCHEME II.14

To summarise, the choice of the synthetic strategy leading to a particular tertiary phosphine is determined by the nature of the substituents which are to be incorporated in its structure. For example, preparation of a trialkylphosphine normally involves the Grignard route, while for a phosphine with π -electron-deficient heteroaromatic substituents the reaction of a metallated phosphine with the corresponding heteroaromatic halide is more appropriate.

II.2 PREPARATION OF THIOPHENE-BASED PHOSPHINE LIGANDS

II.2.1 Preparation of monodentate phosphines with monothiophene units

Amongst tertiary phosphines containing a thiophene moiety, only monodentate phosphines with one or more monothiophene substituents have been previously reported. These phosphines normally have from one to three variously substituted monothiophene nuclei linked to the phosphorus atom via the 2- or 3-position of the thiophene ring. They are fairly well studied and their coordination behaviour with certain transition metals such as Rh,¹⁴⁶ Pd,^{160,161} Ni(II),¹⁶² Co(II),¹⁶³ and Pt^{151,161,164} has been recorded.

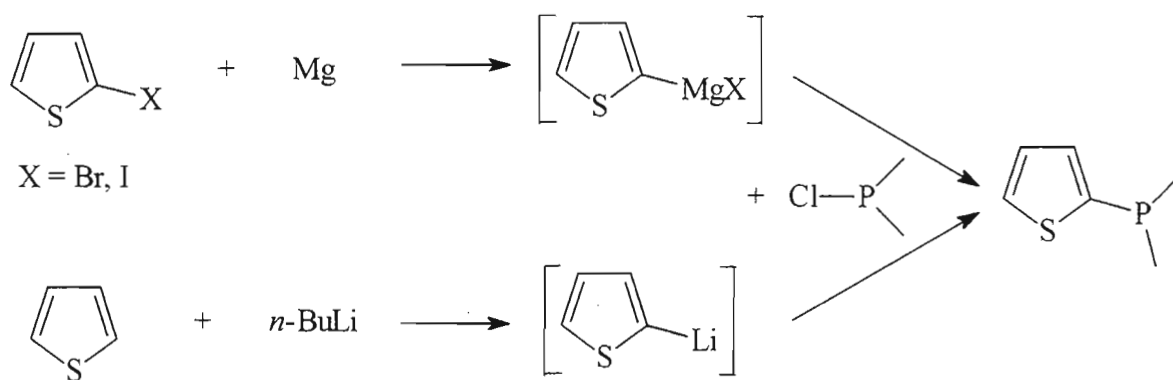
During this work, three of the previously known monothiophene-based phosphines were synthesised: namely, diphenyl(2-thienyl)phosphine (PS), phenyldi(2-thienyl)phosphine

(PDS) and tris(2-thienyl)phosphine (PTS). Their synthesis was undertaken with the following intentions:

- to develop a general method for the preparation and characterisation of tertiary phosphines linked to thiophene units via the 2-position,
- to provide synthetic intermediates for the preparation of more complex polythiophene-substituted phosphines,
- to study the coordination behaviour of thiophene-based phosphines with gold(I), using the above compounds as easily available models.

II.2.1.1 Synthesis of diphenyl(2-thienyl)phosphine (PS), phenyldi(2-thienyl)phosphine (PDS) and tris(2-thienyl)phosphine (PTS)

Tertiary phosphines with 2-thienyl substituents are usually prepared from lithium or magnesium derivatives of thiophene and a chlorophosphorus compounds^{143,160,161,165} (Scheme II.15). The reaction is normally a one-pot synthesis which involves the preparation of an organometallic reagent followed by the addition of a phosphorus compound, the mechanism of the last step being an ordinary nucleophilic substitution at the P(III) atom.

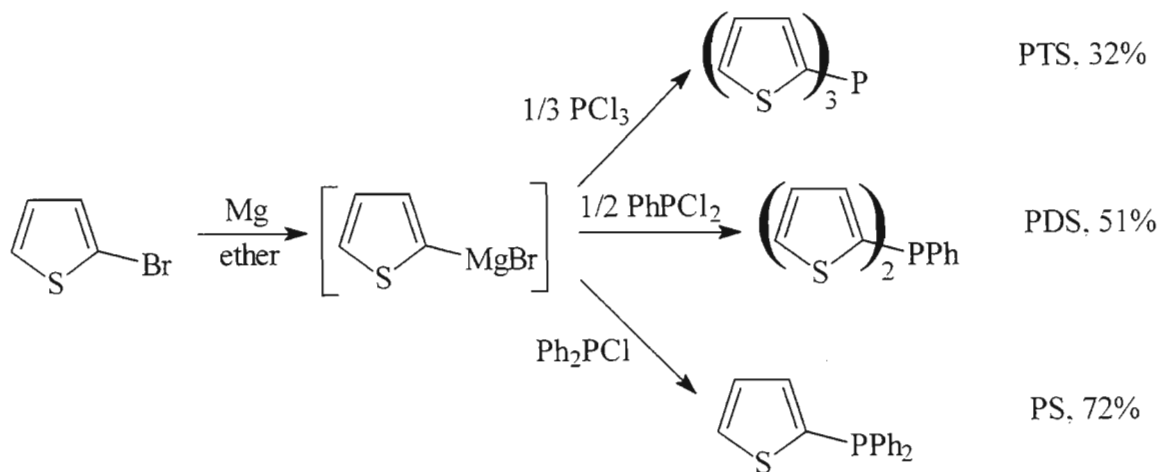


SCHEME II.15

The reaction is not very sensitive to the choice of the organometallic reagent and the yields are normally good, 60 to 80%.^{143,160,165}

During this work the first method utilising a Grignard reagent was chosen as it offered the advantage of convenience in the handling of the reactants: 2-bromothiophene is less volatile and disagreeable in odour than thiophene itself, while Mg metal possesses less working hazard in comparison to *n*-BuLi. In addition the Grignard method leads to

selective metallation of the thiophene ring in only one position, while with the butyllithium dimetallation can also occur,¹⁶⁶ with the formation of undesired by-products. Scheme II.16 shows the synthetic sequence used to obtain PS, PDS and PTS.



SCHEME II.16

Various conditions were employed in order to optimise the yields of the target phosphines. Both ether and THF were used as reaction solvents, and it was found that pure ether is superior to THF as the former causes minimal decomposition of the organometallic intermediate thus producing a purer final product. However, during the preparation of bulk amounts of the phosphine pure ether has a disadvantage, in that it causes precipitation of the inorganic by-product (MgBrCl) thus making efficient stirring very difficult. This leads to local overheating and, consequently, partial decomposition and lower yield. In such cases addition of 30% THF helps to minimise precipitation without compromising the yield.

The effect of the temperature during the addition to the Grignard reagent step was also studied. Diphenylchlorophosphine was allowed to react with 2-thienylmagnesium bromide at -70 , -20 , 0°C and at room temperature. The lowest temperature reaction proceeded instantly but gave rise to a large amount of MgBrCl precipitate which, as noted above, is detrimental to the yield. As expected, at room temperature the reaction mixture overheated and significant discoloration was observed, with the yield being poor again. The reactions carried out at -20 and 0°C gave the best results with the latter temperature being selected for preparative purposes due to experimental convenience. Changing the reaction times (from 1 to 14 hours) hardly affects the yields, as the formation of the target phosphines was

essentially complete after the last drop of a chlorophosphine was added (as monitored by ^{31}P NMR spectroscopy).

The procedures employed for the purification of the 2-thienyl substituted phosphines included a combination of crystallisation and chromatographic techniques such as flash column or centrifugal chromatography with a hexane-based eluent on a silica stationary phase. This is in contrast to literature methods,^{143,160,165} which employ distillation. Distillation was found to be less suitable than the former two methods due to partial oxidation of the phosphines by residual oxygen at the high temperatures.

As far as the yields are concerned, they become progressively lower with the introduction of each subsequent 2-thienyl group into the phosphine moiety (Scheme II.16). This is chiefly attributed to the physical properties of this class of phosphines: their melting points decrease with an increase in the number of thiophene rings in the molecule, being 45-46° for PS, 29-30° for PDS and 25-26°C for PTS. Substances with lower melting points are in general more difficult to crystallise and hence present problems during the isolation step. It should be noted here that the melting points of the PDS and PTS were determined for the first time during this study. It is quite probable that other researchers did not isolate these compounds in a crystalline and pure form.

With regard to the chemical properties of the PS, PDS and PTS, their relative lack of reactivity towards oxygen is noteworthy, the majority of tertiary phosphines being very prone to oxidation, especially in solution. The thiophene-based phosphines, however, are not only stable for an indefinite periods of time in the solid state at room temperature (one sample of PS was stored in air without appreciable deterioration for two years), but can also withstand mild heating for a limited period of time in non-deoxygenated solutions. On the other hand, exposure to light (sunlight) causes gradual decomposition, being more pronounced in the phosphines with the greater number of thiophene units. Therefore, PTS had to be kept in the dark at all the times to prevent discoloration.

All three phosphines are white solids, with PS being of a crystalline nature and the other two being rather amorphous. They are soluble in most organic solvents, such as ether, benzene, THF, dichloromethane, chloroform and acetone. They are moderately soluble in hydrocarbons and warm alcohols, though they precipitate out (very slowly!) from chilled

methanol solutions. In summary, the chemical properties of the three phosphines are very similar in most respects.

II.2.1.2 Characterisation of PS, PDS and PTS

The purified phosphines were characterised by various spectroscopic techniques, such as ^1H , $^{13}\text{C}\{^1\text{H}\}$ and $^{31}\text{P}\{^1\text{H}\}$ NMR (later referred to simply as ^{13}C and ^{31}P , respectively) spectroscopy, IR spectroscopy and UV-vis spectroscopy as well as by means of mass-spectrometry. The results are presented in Tables II.1a and II.1b.

Among the three kinds of nuclear magnetic resonance spectroscopies used, ^{31}P NMR spectroscopy gives the clearest indication of the phosphine structure. The signal for each phosphine in the ^{31}P NMR spectrum appears as a sharp singlet with a chemical shift in the region characteristic for tertiary phosphines ($-70 < \delta < 0$ ppm) (Table II.1a). It can be noted that substitution of each phenyl ring in triphenylphosphine with a 2-thienyl group leads to progressive shielding of the phosphorus nucleus by approximately 13 ppm. (The chemical shifts for PPh_3 and its derivatives are commonly reported to be close to -6 ppm¹⁴¹).

Such large changes in chemical shifts upon substituting one organic residue by another are believed to be the result of a combination of at least three factors: the electronegativity of the substituent, the effects of π -bonding between the substituent and the phosphorus atom and the bond angles at the phosphorus atom. Allen and Griffin^{164,167-169} demonstrated on the basis of the evidence obtained from UV-vis and ^1H NMR spectroscopic data that there is very little π -bonding between a phenyl and/or a 2-thienyl group and the phosphorus atom. The bond angles at the phosphorus substituted with either phenyl or 2-thienyl group are not significantly different (see Tables II.24, II.30 and II.36 at the end of the Experimental section of this Chapter). However, 2-thienyl groups are well-established as being electron withdrawing relative to phenyl ones,¹⁶⁵ thus the progressive shielding at the phosphorus atom upon introduction of thienyl groups can be attributed to the strong electronegative effect of the sulfur incorporated in the thiophene ring.

To the best of our knowledge, ^1H NMR spectra of PS and PDS have not been previously reported. Jakobsen and Nielsen¹⁷⁰ have, however, carried out a detailed analysis of the ^1H NMR spectrum of PTS. During this work, the assignment of the ^1H NMR signals due to

Table II.1a Nuclear magnetic resonance data for PS, PDS and PTS, as measured in CDCl₃

Compound	$\delta^{31}\text{P}$, ppm	$\delta^1\text{H}$, ppm	$\delta^{13}\text{C}$, ppm
PS	-19.90 (-19.3 [*])	7.13 (ddd, 1 H, H _{Th-4}), 7.35 (ddd, 1 H, H _{Th-3}), 7.30-7.45 (m, 10 H, H _{Ph}), 7.59 (dd, 1 H, H _{Th-5})	128.0 (d, C _{Th-4}), 128.4 (d, C _{Ph-3}), 128.8 (s, C _{Ph-4}), 132.0 (s, C _{Th-5}), 133.1 (d, C _{Ph-2}), 136.3 (d, C _{Th-3}), 137.8 (d, C _{Ph-1}), 138.0 (d, C _{Th-2})
PDS	-33.26 (-33.6 [*])	7.13 (ddd, 2 H, H _{Th-4}), 7.37 (ddd, 2 H, H _{Th-3}), 7.30-7.45 (m, 5 H, H _{Ph}), 7.61 (dd, 2 H, H _{Th-5})	127.9 (d, C _{Th-4}), 128.3 (d, C _{Ph-3}), 128.8 (s, C _{Ph-4}), 131.9 (d, C _{Ph-2}), 132.1 (s, C _{Th-5}), 136.2 (d, C _{Th-3}), 138.4 (d, C _{Th-2}), 138.6 (d, C _{Ph-1})
PTS	-46.27 (-45.8 [*])	7.08 (ddd, 3 H, H _{Th-4}), 7.35 (ddd, 3 H, H _{Th-3}), 7.56 (dd, 3 H, H _{Th-5})	127.9 (d, C _{Th-4}), 131.9 (s, C _{Th-5}), 135.4 (d, C _{Th-3}), 138.8 (d, C _{Th-2})

Literature values are taken from the reference 164, as measured in dichloromethane

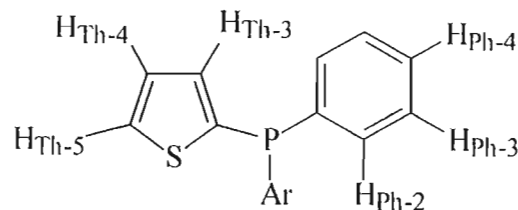


Fig. II.1 This is generally accepted numbering scheme for hydrogen atoms in the thiophene and benzene nuclei. The numbering of carbon atoms is done analogously, *e.g.* C_{Th-3} is the carbon attached to the H_{Th-3}.

Table II.1b Remaining spectroscopic data for PS, PDS and PTS

Compound	UV [*] : λ_{max} , nm (ϵ , M ⁻¹ ·cm ⁻¹)	IR ^{**} : ν , cm ⁻¹	GCMS: m/z (molar mass, g·mol ⁻¹)
PS	238 (1.2·10 ⁴)	490 (s), 694 (s), 716 (s), 741 (s), 750 (s), 849 (w), 991 (w), 1215 (w), 1400 (m), 1433 (m), 1475 (m)	267.95 (268.31)
PDS	240 (1.5·10 ⁴), 270 (sh [#] , 0.9·10 ⁴)	492 (s), 575 (m), 708 (vs), 741 (s), 850 (w), 995 (w), 1217 (m), 1406 (m), 1433 (m)	273.95 (274.34)
PTS	240 (1.8·10 ⁴), 270 (sh [#] , 1.1·10 ⁴)	496 (s), 577 (m), 704 (vs), 742 (m), 850 (m), 997 (m), 1217 (m), 1332 (w), 1406 (m)	279.80 (280.36)

* UV measurements were carried out in dichloromethane

** IR data were obtained as KBr discs

shoulder on the main peak

the thiophene hydrogens was based on their assignment (see Table II.1a). The proton signals of 7.32 and 7.48 ppm for H_{Th-3} and H_{Th-5} , respectively, are deshielded in comparison to those in thiophene itself (7.20 and 7.31 ppm, respectively). This is due to the electronegative effect of the phosphine substituent. The chemical shift of H_{Th-4} (in unsubstituted thiophene $\delta[H_{Th-3}] = \delta[H_{Th-4}] = 7.20$ ppm) remained essentially unaffected. As expected, the phenyl proton signals appear as a non-resolvable multiplet. The three protons of the thiophene units, on the other hand, represent a well-defined ABMX coupling system with the phosphorus atom as the fourth nucleus. This is essentially a first-order system and thus all coupling constants can be easily determined. The coupling constants found in this work for all three phosphines as well as the literature values for PTS and its phosphine oxide, $PTS=O$,¹⁷⁰ are summarised in Table II.2.

Table II.2 Absolute values for hydrogen-phosphorus coupling constants in thienyl rings of 2-thienylphosphines

Compound J_{H-P} , Hz	PS	PDS	PTS	PTS ¹⁷⁰	PTS=O ¹⁷⁰
$^3J_{H-P}$	4.93	4.88	5.85	6.17	8.01
$^4J_{H-P}$	1.28	1.27	1.40	1.33	2.10
$^5J_{H-P}$	0.00	0.00	0.00	0.19	4.63

It can be seen from the Table II.2 that the relevant coupling constants in all three phosphines are very similar, the only exception being the larger $^3J_{H-P}$ value for PTS. Due to the fact that the NMR spectrometer used in this study was not able to resolve any fine line splitting below 0.5 Hz (see Appendix A), the magnitude of hydrogen-phosphorus coupling through five bonds, $^5J_{H-P}$, could not be determined and was recorded as zero. Within the phosphine series the coupling constants were found to decrease in the order: $^3J_{H-P} > ^4J_{H-P} > ^5J_{H-P}$, while in the phosphine oxide the order was somewhat different: $^3J_{H-P} > ^5J_{H-P} > ^4J_{H-P}$, with the absolute values for each constant being correspondingly greater than their equivalent in the phosphine molecule. Thus, the interactions between hydrogen and phosphorus nuclei appear to be weaker in phosphines than in the related phosphine oxide and follow the expected trend of decreasing in magnitude with an increase in the number of bonds between the nuclei.

The assignments of peaks in the ^{13}C NMR spectra of the three phosphines were made by means of HETCOR and DEPT experiments as no relevant data were available in the literature. Analysis of the spectrum for PTS as well as peak intensity considerations allowed the separation of peaks due to the carbons in the 2-thienyl and phenyl rings. The signals at the lowest field strengths are assigned to the quaternary carbons, $\text{C}_{\text{Th-2}}$ and $\text{C}_{\text{Ph-1}}$ (for PS and PDS only). The chemical shifts of the carbons in the thiophene ring follow the sequence $\delta_{\text{C3}} > \delta_{\text{C5}} > \delta_{\text{C4}}$, while in the benzene ring $\delta_{\text{C-ipso}} > \delta_{\text{C-ortho}} > \delta_{\text{C-para}} > \delta_{\text{C-met}}$, which correlate well with the data obtained by Jakobsen for 3-thienylphosphines and triphenylphosphine.¹⁷¹ A comparison of the carbon-phosphorus coupling constants in the three thienylphosphines and triphenylphosphine is presented in Table II.3. The signs of the coupling constants have not been determined as it exceeded the scope of this work, but normally $^1J_{\text{C-P}}$ is accepted to be negative, while $^2J_{\text{C-P}}$, $^3J_{\text{C-P}}$ and $^4J_{\text{C-P}}$ are positive. As in the instance of ^1H NMR spectra, the magnitude of long-range $^4J_{\text{C-P}}$ coupling constants could not be determined due to the low resolving power of the instrument (*vide supra*) and were recorded as zero.

Table II.3 Absolute values for carbon-phosphorus coupling constants in 2-thienyl and phenyl substituted phosphines

Compound $J_{\text{C-P}}$, Hz	PS	PDS	PTS	PPh_3 ¹⁷¹
$^1J_{\text{Th}}^*$	20.8	21.6	20.0	-
$^2J_{\text{Th}}^*$	26.4	28.6	26.7	-
$^3J_{\text{Th}}^*$	8.1	8.2	8.8	-
$^4J_{\text{Th}}^*$	0.0	0.0	0.0	-
$^1J_{\text{Ph}}^{**}$	14.7	11.8	-	12.51
$^2J_{\text{Ph}}^{**}$	19.4	20.4	-	19.65
$^3J_{\text{Ph}}^{**}$	6.4	6.9	-	6.80
$^4J_{\text{Ph}}^{**}$	0.0	0.0	-	0.33

* refers to the coupling between a carbon of a thiophene ring and phosphorus

** refers to the coupling between a carbon of a benzene ring and phosphorus

The UV-vis spectra of PS, PDS and PTS in dichloromethane look quite similar, exhibiting broad bands between 220 (beginning of the scan) and 300 nm with maxima at around 240 nm. This spectra strongly resemble those of the parent aromatic compounds, benzene and thiophene. Thus, the absorption bands exhibited by PS, PDS and PTS can be attributed to π - π^* and n - π^* electronic transitions in the aromatic rings. Interestingly, the spectra of the individual phosphines can be distinguished from each other by the shoulder on the main band at around 270 nm that becomes more pronounced as the thiophene 'fraction' in the molecule increases.

The infrared spectra of PS, PDS and PTS recorded as KBr disks are not very informative. This is expected as tertiary phosphines do not have characteristic absorption bands in the IR region of the spectrum - unlike phosphine oxides, phosphinic or phosphonic acid esters. The three spectra have common absorption bands at around 1400 cm^{-1} due to the P-Ph or P-(2-Th) stretching frequencies as well as bands in the 'fingerprint' part of the spectra at 1215 cm^{-1} and below.

The GCMS data presented in Table II.1b does not call for a special comment as all thienylphosphines gave the molecular ion fragment under the ionisation conditions employed for their analysis. It should be noted, though, that during the fragmentation of these phosphines upon the electron impact, the phenyl group breaks off much easier than the 2-thienyl group. This conclusion is based on a comparison of intensities of P(Ph)^+ ($m/z = 108$) vs. P(2-Th)^+ peaks ($m/z = 114$) as well as $(\text{M-Ph})^+$ vs. $(\text{M-[2-Th]})^+$ peaks for PS and PDS: the first peaks in each of the two pairs are approximately 30% more intense than the respective second ones.

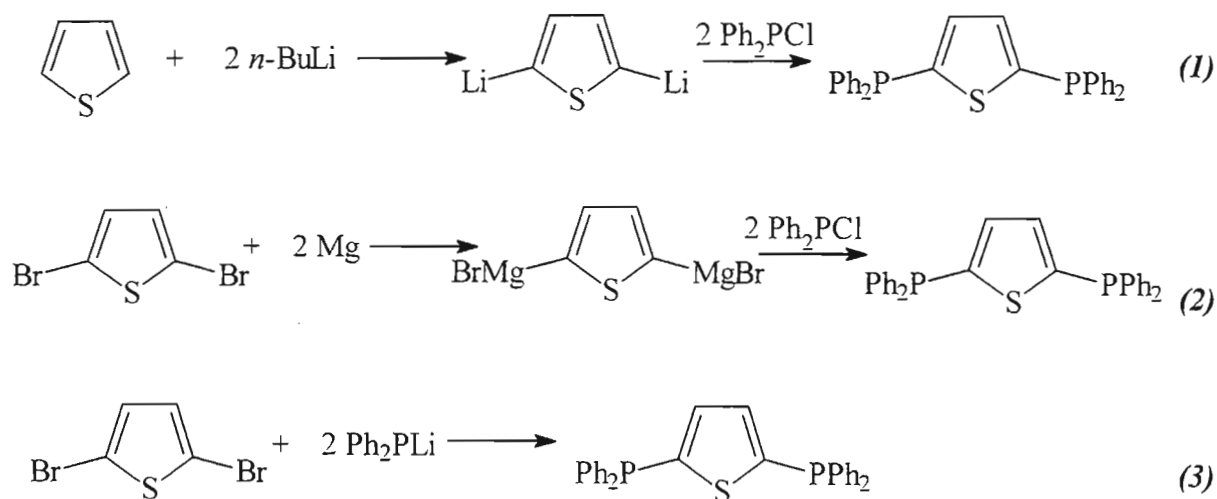
In conclusion, the results of the detailed characterisation of the three phosphines, PS, PDS and PTS, demonstrate that the NMR spectroscopic data (especially, ^1H and ^{31}P) carry the most significant information and allows one to unequivocally establish the structures of the individual phosphines. Mass-spectrometry and UV-vis spectroscopy are instrumental in confirming the structure of the molecule, while IR-spectroscopy appears to be of little use for the characterisation of 2-thienylphosphines. For this reason, in the following chapters, the discussion of the characterisation of the novel thiophene-based phosphines, characterisation will focus on data from the most informative techniques.

II.2.2 Preparation of new mono- and polydentate tertiary phosphines with monothiophene units

II.2.2.1 Synthesis and characterisation of 2,5-bis(diphenylphosphino)thiophene (PSP)

Reference is made to the 2,5-bis(diphenylphosphino)thiophene (PSP) ligand in a 1986 paper by Brown *et al.*¹⁷² In this paper the coordination of PSP to silver(I) is compared to that of 2,5-bis(diphenylphosphino)furan and *trans*-1,2-bis(diphenylphosphino)-cyclopropane ligands. However no details for the synthesis of the PSP ligand are supplied nor is any firm evidence for the existence of the ligand given, beyond the ³¹P chemical shift for the silver(I) complex containing the PSP ligand. Therefore, a novel synthetic procedure had to be designed in order to prepare the PSP ligand.

Several approaches were considered based on the known methods of phosphine synthesis (Scheme II.17):



SCHEME II.17

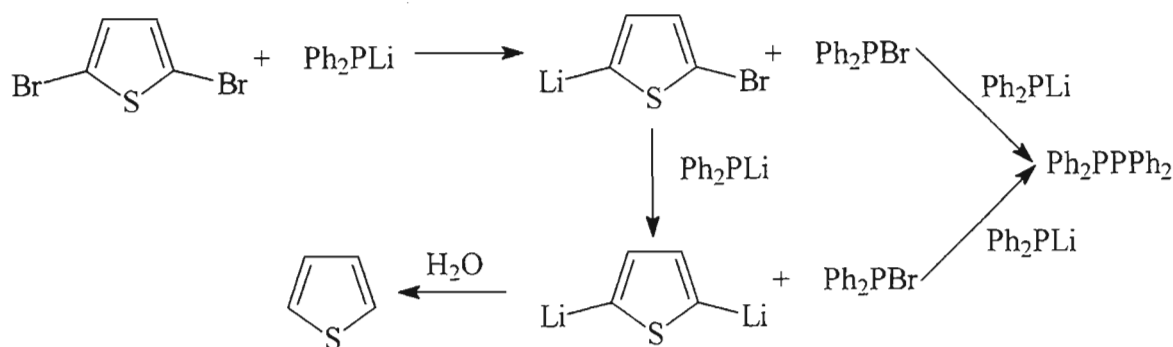
The first method is similar to that employed by Brown *et al.* for preparation of 2,5-bis(diphenylphosphino)furan:¹⁴⁴ *i.e.* dilithiation of the parent heterocycle with subsequent quenching of the intermediate with diphenylchlorophosphine. The method proved to be unsatisfactory not only due to the necessity of handling unpleasant starting materials, but also due to the production of large amount of by-products, possibly as a result of cleavage of the thiophene nucleus during metallation with an excess of BuLi.

It was hoped that the second method would be more advantageous in comparison to the first one – by analogy with the synthesis of PS. The method indeed provided the desired diphosphine, PSP, but the yield was substantially lower (40%) than in the case of PS. One problem is that it is difficult to selectively prepare the bis-Grignard reagent, as even harsh conditions of boiling the dibromide in THF with excess of magnesium for 6 hours did not bring the reaction to completion. Another is that the high temperature employed for the preparation of the bis-Grignard reagent leads to some decomposition of the latter, as evidenced by discoloration of the reaction mixture and a concomitant reduction in the total yield of PSP. The poor solubility of the bis-Grignard reagent in a number of solvents (ether, THF, benzene, toluene) also affects the yield negatively.

In order to avoid the unstable dimetallated Li- or BrMg-intermediates, the third method was tested. Nucleophilic substitution of a bromo- or a chloro-group in an aromatic ring by a phosphide ion is well known (see Section II.1.2 of this Chapter) and it has been used for preparation of tertiary phosphines, such as polypyridylphosphines.¹⁷³ Unlike pyridine, thiophene is a π -electron rich heteroaromatic compound; nevertheless, it was anticipated that the electron-withdrawing effect of the bromine atom will make the positions 2 and 5 of the 2,5-dibromothiophene sufficiently susceptible to the attack by the phosphorus containing nucleophile.

The analysis of the reaction products showed that although the attack did occur, the outcome of the reaction was totally different from the anticipated: *i.e.*, the only identified phosphine formed was tetraphenyldiphosphine, Ph_2PPPh_2 . The authenticity of this compound was confirmed by comparing its ^{31}P NMR and GCMS data with those of the tetraphenyldiphosphine synthesised from Ph_2PLi and Ph_2PCl ($\delta = -14.9$ ppm in C_6D_6 , $m/z = 370 - \text{M}^+$).¹⁷⁴ The possible mechanism of this transformation is presented below (Scheme II.18).

The formation of thiophene as a product of this reaction was confirmed by the ^1H NMR spectrum of the organic fraction distilled from the reaction mixture, this being in full agreement with the spectrum of the authentic material.

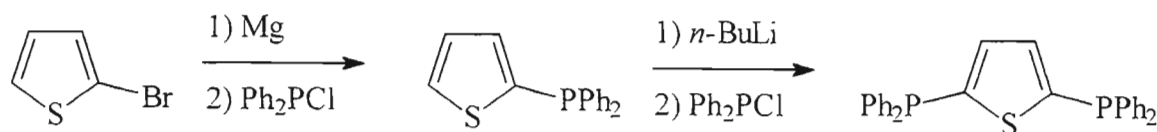


SCHEME II.18

It has been reported¹⁶⁶ that halogenated thiophenes undergo halogen-metal exchange in the presence of $n\text{-BuLi}$ even at -70°C . It seems to be likely that in this case Ph_2PLi plays a similar role to that of $n\text{-BuLi}$, causing bromine-lithium exchange at the thiophene nucleus. The driving force behind the formation of such lithiated thiophene is the remarkable stability of a 2-thienyl anion: the negative charge on the second carbon atom is effectively delocalised by the electron-withdrawing nature of sulfur. The second product of this undesired reaction, Ph_2PBr , instantaneously reacts with the excess of Ph_2PLi present in the reaction mixture to form tetraphenyldiphosphine, thus preventing any reverse halogen-metal exchange from taking place.

Later in the course of this study, several attempts were made to react other brominated thiophenes, such as 2-bromothiophene and 5,5'-dibromo-2,2'-bithiophene, with Ph_2PLi . In majority of the cases, the outcome was identical to that described above: *i.e.* tetraphenyldiphosphine was the major phosphine product of the reaction. The only exception was observed during the reaction of 2-bromo-5-(2-pyridyl)thiophene with Ph_2PLi , where the desired thienylphosphine was the major product. This case will be described in detail in the Section 2.5.1 of this Chapter.

A different synthetic route was investigated in order to find the optimal preparation method for PSP. It consisted of two steps, thus eliminating the necessity of formation of a dimetallated species (Scheme II.19):



SCHEME II.19

The reaction sequence afforded a much purer product than the previous methods.

The stoichiometry of the second step was found to be crucial in ensuring the least possible contamination of the desired phosphine with by-products. It became apparent that a BuLi : PS ratio less than 1 resulted in insufficient metallation of PS, with the latter having to be separated from the final product, thus reducing the total yield. Addition of an exact stoichiometric amount of BuLi to PS significantly improved the conversion of PS into PSP. The reaction was monitored by means of ^{31}P NMR spectroscopy, as PS and PSP exhibit clearly distinct peaks in deuteriochloroform solution at -19.9 and -18.8 ppm, respectively. However, even at this ratio, there was still a noticeable amount of PS present. It was assumed at first, that origin of this PS is the reaction of traces of water or acid (present in the solvent) with the 5-lithiated PS. Interestingly, increasing the proportion of BuLi (1.2 : 1 ratio) did not help to overcome the problem; on the contrary, it led to an increase in the ratio of PS to PSP in the final product mixture.

This observation can be explained as being the result of the P-C_{Th} cleavage in the starting phosphine, taking into account the remarkable stability of 2-thienyl anion. In other words, during metallation of PS with *n*-BuLi two lithiated species are formed: 2-(diphenylphosphino)-5-lithiothiophene (major) and 2-lithiothiophene (minor). The reaction of the former with diphenylchlorophosphine leads to the desired product, PSP, while the latter reacts with diphenylchlorophosphine to afford PS, *i.e.* the starting material. This analysis explains why PSP obtained through this last method is always going to be contaminated with PS, although contamination can be minimised by selecting a BuLi : PS ratio close to 1.

The cleavage of the P-C bond with alkali metals is not a new or rare phenomenon: cleavage of triphenylphosphine with lithium metal has been extensively used in the past to produce lithium diphenylphosphide.¹⁷⁵ However, no reports could be found where the P-C bond in a tertiary phosphine was cleaved by *n*-BuLi. It seems that the reason here lies in the nature of the cleaved bond. It has been shown¹⁷⁶ that carbon-phosphorus bonds in aromatic systems are much more susceptible to cleavage upon treatment with a base than those in aliphatic systems. Amongst the aromatic systems, heterocyclic compounds, such as furan and thiophene, are particularly labile. For example, tris(2-thienyl)phosphine oxide undergoes significant P-C cleavage upon heating with aqueous NaOH with the formation

of a mixture of di-(2-thienyl)phosphinic acid and thiophene, while triphenylphosphine oxide can withstand vigorous base treatment without any appreciable change. The greater degree of cleavage in the former case is the reflection of the greater stability of the 2-thienyl anion (*vide supra*) in comparison with the phenyl anion.^{168,176} The observations obtained during the preparation of PSP are entirely consistent with these findings, as no product arising from a possible cleavage of P-C_{Ph} bond has been detected in this work. Had the phenyl anion formed it would have reacted with diphenylchlorophosphine producing triphenylphosphine with an easily recognisable ³¹P chemical shift of -6 ppm).

In practice, there is little advantage to using the method just described as compared to Method 2 described above, the yields of PSP in both cases being about 40 %. The only bonus to using the method in Scheme II.19 is the better quality of the reaction product. Nevertheless, this has proved to be a significant factor insofar as the isolation of PSP is concerned as it directly affects the ability of the phosphine to crystallise or even to solidify. Although the melting point of this phosphine was found to be as high as 77°C, it normally precipitates from solution as an amorphous thick white liquid. It took anything from 3 days to 3 months at -20°C to crystallise different batches of PSP, with cleaner samples solidifying quicker. It might be due to its poor solidifying properties, that PSP was not fully described and characterised before.

Similar to the phosphines PS, PDS and PTS, PSP appears to be oxidation resistant and does not require any special precautions during the work-up or even storage, proving to be stable for at least a year in a powdered form at room temperature and in contact with air. The same techniques were used to characterise the diphosphine as were for the first three thienylphosphines, *i.e.* ¹H, ¹³C and ³¹P NMR spectroscopy as well as UV-vis and IR spectroscopy; GC-mass spectrometry was also used. The data can be found in Tables II.4a and II.4b.

Table II.4a NMR data for 2,5-bis(diphenylphosphino)thiophene, as measured in CDCl₃

δ ³¹ P, ppm	δ ¹³ C, ppm	δ ¹ H, ppm
-18.84	129.1 (d, C _{Ph-3}), 129.6 (s, C _{Ph-4}), 133.7 (d, C _{Ph-2}), 137.1 (dd, C _{Th-3}), 137.9 (d, C _{Ph-1}), 145.6 (d, C _{Th-2})	7.16-7.21 (m, 2 H, H _{Th}), 7.29-7.41 (m, 20 H, H _{Ph}),

The assignments of the signals in the NMR spectra were done on the basis of the established values for PS. The numbering scheme is the same as shown in Figure II.1.

Table II.4b Spectroscopic data for 2,5-bis(diphenylphosphino)thiophene

UV*: λ_{\max} , nm (ϵ , $\text{M}^{-1}\cdot\text{cm}^{-1}$)	IR**: ν , cm^{-1}	GCMS: m/z (molar mass, $\text{g}\cdot\text{mol}^{-1}$)
	430 (s), 501 (vs), 534 (vs), 550 (s), 558 (s), 694 (vs), 744 (vs), 820 (s), 966 (w), 1003 (s), 1026 (s), 1090 (m), 1180(s), 1203 (s), 1280 (w), 1433 (s), 1475 (s), 1583 (m)	452.50 (452.49)
231 ($3.0\cdot 10^4$)		
256 (br sh [#] , $2.3\cdot 10^4$)		

* UV-vis measurements were carried out in dichloromethane

** IR data were obtained as KBr discs

[#] shoulder on the main peak

The data in Tables II.4a and II.4b, taken together confirm that the structure of the new phosphine corresponds to 2,5-bis(diphenylphosphino)thiophene. First of all, a singlet in the ^{31}P NMR spectrum is indicative of single environment for the phosphorus atoms, the shift value being characteristic for a diphenylphosphine substituted at the position 2 of a thiophene ring [$\delta(\text{PS}) = -19.9$ ppm]. The large multiplet in the ^1H NMR spectrum between 7.29 and 7.41 ppm is due to the hydrogens of the phenyl rings, while a poorly resolved signal (a the limitation of the available NMR spectrometer) between 7.16 and 7.21 ppm represents an AA'XX' system for the two chemically, but not magnetically equivalent, hydrogens on the thiophene ring – these couple to both phosphorus nuclei with different strength. The integration of these two sets of signals gave the expected 10 : 1 ratio. The ^{13}C NMR spectrum of the diphosphine is somewhat different from that of PS, the phosphine structurally very close to PSP. The principal difference lies in the symmetrical nature of PSP in relation to the thiophene nucleus, which results in coalescence of signals due to $\text{C}_{\text{Th-5}}$ and $\text{C}_{\text{Th-2}}$ as well as $\text{C}_{\text{Th-4}}$ and $\text{C}_{\text{Th-3}}$ (refer to Figure II.1 for the numbering scheme). The assignment of the signals is based on the assumption that the introduction of the second diphenylphosphino substituent on the thiophene ring should not influence strongly the chemical shifts of the carbons on the phenyl rings, as was indeed observed, and can be easily seen by comparing the $\delta \text{C}_{\text{Ph}}$ values of PS and PSP (Tables II.1a and II.4a). Coupling

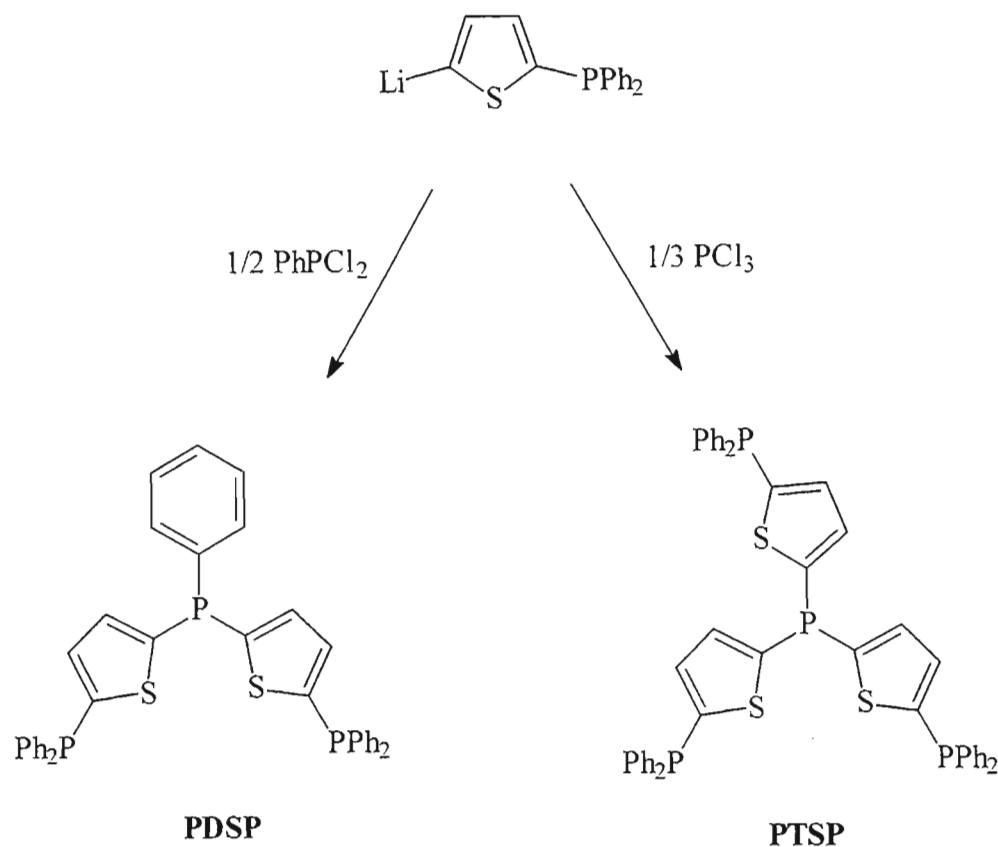
between the C_{Th-2} carbon and the phosphorus nucleus attached to the C_{Th-5} carbon is negligible, which results in the signal for C_{Th-2} (as well as that for the chemically equivalent C_{Th-5}) appearing as a doublet - due to coupling to the *ipso*-phosphorus only. At the same time C_{Th-3} (and, likewise, C_{Th-4}) couples to both phosphorus nuclei, affording a doublet of doublets in the ¹³C NMR spectrum.

The mass-spectrometric analysis of the new diphosphine gave the expected molecular ion, 452, which ties well with the NMR data and confirms the proposed structure. On the other hand, the UV and IR spectra were of little interest as they showed only general features characteristic to thienylphosphines (similar to what was observed during characterisation of PS, PDS and PTS): *i.e.* one broad absorption band between 220 and 300 nm in the UV region of the spectrum and several absorption bands in the 'fingerprint' section of the IR region.

II.2.2.2 Synthesis and characterisation of polydentate phosphines phenylbis[(5-diphenylphosphino)-2-thienyl]phosphine (PDSP) and tris[(5-diphenylphosphino)-2-thienyl]phosphine (PTSP)

The synthetic route employed for the preparation of PSP via the monophosphine precursor, PS (see Scheme II.19), *i.e.* lithiation of the vacant position 5 of the thiophene ring followed by quenching with diphenylchlorophosphine, appeared to show a potential as a general method for preparation of a variety of phosphines. During the last step, the quenching reagent diphenylchlorophosphine may be substituted for other chlorophosphorus compounds, thus giving rise to previously unknown thiophene-based phosphines.

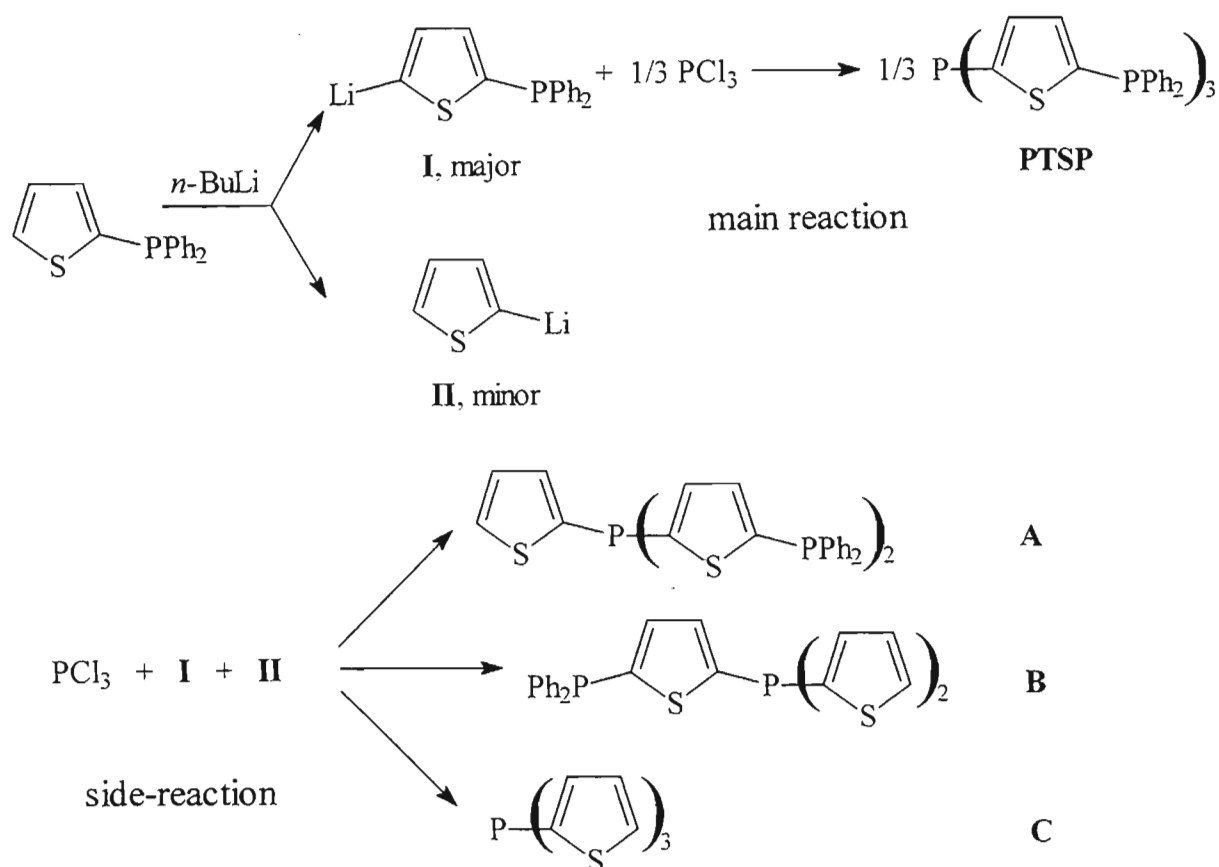
Dichlorophenylphosphine and phosphorus trichloride were chosen to react with the metallated PS in order to produce the tri- and tetraphosphines PDSP and PTSP respectively (Scheme II.20), in a manner analogous to that used for the preparation of PDS and PTS. The ³¹P NMR spectroscopic analysis of the products obtained via this method indicated that a tridentate and a tetradentate phosphine each with non-equivalent phosphorus nuclei had indeed formed. Evidenced for this was the appearance of signals due to the phosphorus nuclei in the characteristic region of the ³¹P NMR spectrum and with the desired peak area ratios (2:1 and 3:1 respectively).



SCHEME II.20

However, neither of these reactions produced the desired compounds in pure form. Even after rigorous purification, the elemental analysis of the products showed a lower percentage carbon content to what was required according to the formulae, and ^1H NMR analysis showed higher thiophene/phenyl hydrogen ratios than the ones one would derive theoretically for PDSP and PTSP.

All this indicated that PDSP and PTSP obtained via the above route must be contaminated with compounds having very similar chemical and physical nature. As the relative number of phenyl hydrogens was found to be slightly less than expected and the percentage carbon lower, a hypothesis was put forward that the contaminants must have been phosphines with a partial deficiency of diphenylphosphino groups. The occurrence of these by-products could be the result of the side reaction between *n*-BuLi and diphenyl(2-thienyl)phosphine described earlier, *i.e.* the cleavage of P-C bond between the phosphorus and the thiophene ring. Scheme II.21 illustrates the formation of plausible by-products during the attempted synthesis of pure PTSP. Similar reaction sequences can be drawn to explain by-product formation in the case of PDSP.



SCHEME II.21

As can be seen from the Scheme II.21, the by-products A, B and C are indeed chemically very close to the tetraphosphine PTSP. Furthermore, as a direct consequence of their structures, the ^{31}P NMR spectra of the by-products A, B and C will have the following signals in common with PTSP: a peak at around -19 ppm due to the phosphorus atoms bonded to two benzene and one thiophene unit; and one at around -45 ppm due to the phosphorus atoms bonded to three thiophene units. (Note that by-product C is in fact the previously characterised phosphine PTS with a ^{31}P chemical shift of -46.3 ppm.) A thorough ^{31}P NMR analysis of the "purified" PTSP showed the presence of several lines of low intensity at around both -19 and -45 ppm, in addition to two major peaks at -18.62 and -44.73 ppm due to the PTSP itself.

For compounds A, B and C the ratios of diphenylphosphino groups to thiophene units are 2:3, 1:3 and 0 respectively, *i.e.* less than the ratio of 1:1 for PTSP. This would lead to a reduced ratio of phenyl to thienyl hydrogens in the ^1H NMR spectrum of PTSP, as well as to an increased contribution of the thiophene's sulfur to the observed 'molecular mass' of

the product, thus resulting in apparently lower values for the percentage of carbon in the molecule. All this agrees well with the experimental results, strongly suggesting that Scheme II.21 is an accurate reflection of the by-product formation in this approach to the synthesis of PTSP. Indeed, the formation of by-products with a lower content of diphenylphosphino groups seems to be an intrinsic drawback of the chosen method which could not be overcome by subsequent steps of purification. Therefore, in order to eliminate the formation of contaminants, a different synthetic strategy had to be employed.

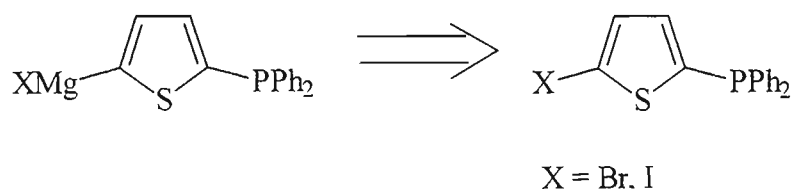
An obvious solution to the problem lies with a use of a base strong enough to abstract the hydrogen at the 5-position of the thiophene unit, but too weak to cleave the P-C bond (a so-called non-nucleophilic base). There are a number of examples of such bases in the literature. Amongst them, lithium di(*iso*-propyl)amide (LDA) and the TMEDA (TMEDA = tetramethylenediamine) complex of *n*-BuLi are most commonly used. The former was chosen for our synthetic purposes as its reactions with various thiophenes are well documented.^{177,178}

The first step of the synthesis involved *in situ* formation of LDA from di(*iso*-propyl)amine and *n*-BuLi at -78°C followed by addition of the starting phosphine, PS. After a time period optimised at one hour, to ensure clean formation of the lithiated species, the mixture was treated with PCl₃ and worked up as before. This preparation proved successful with PTSP being obtained in sufficiently pure form and in 45% yield. The ratio of phenyl to thienyl hydrogens in the molecule obtained from the ¹H NMR spectrum was found to correspond to the desired value of 5:1, while no 'satellite' peaks were observed in the ³¹P NMR spectrum near the two major peaks in the region of -19 and -45 ppm. The microanalysis of the compound also gave a result very close to the expected values; however, although being within the accepted limits, the carbon content was still slightly lower than required. Perhaps, even under much milder conditions (LDA instead of *n*-BuLi) some P-C cleavage still takes place. Thus, though this method gives satisfactory results, further attempts were made to improve on the outcome of the synthesis.

The alternative approach adopted recognises that there is a better solution to the problem of introducing a metal substituent in the 5-position of the PS molecule. Specifically, the introduction of a bromomagnesium substituent in the 5-position of the thienyl ring via a Grignard reaction should not lead to P-C bond cleavage: magnesium is much less reactive

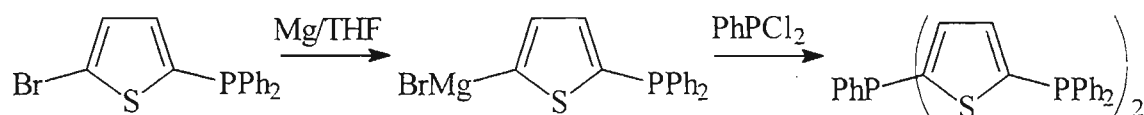
than the alkali metals and their organometallic compounds. It has been shown elsewhere that magnesium is not even capable of cleaving the P-P bond in Ph_2PPPh_2 ¹⁷⁴ which is definitely weaker than a P-C bond.

In order to prepare the desired Grignard reagent, the corresponding halothiénylphosphine must be obtained first.



It proved to be experimentally easier to prepare the bromo derivative rather than the iodo one – due to the generally poorer stability of iodothiophenes. The synthesis and characterisation of diphenyl(5-bromo-2-thienyl)phosphine (PSBr) will be discussed in the next section of this Chapter (Section 2.3).

After the successful preparation of PSBr it became possible to carry out the synthesis of PDSP through a Grignard route (Scheme II.22).



SCHEME II.22

The first step in the reaction proceeded smoothly in refluxing THF forming an insoluble dark oil of the phosphine-containing Grignard reagent. After cooling to 10°C (as further cooling leads to solidification of the oil) the organometallic compound was quenched with dichlorophenylphosphine producing the desired triphosphine. Carrying out a reaction at a temperature considerably higher than zero is not ideal. However, the negative impact on the yield appears to be less pronounced than the alternative of removing the THF and redissolving the Grignard reagent in a more appropriate solvent (*e.g.*, benzene). For this reason the reaction sequence was conducted as one-pot-synthesis in a single solvent.

The formation of a small amount of PS was detected during the work-up of the reaction mixture using a combination of GC-mass spectrometric and ^{31}P NMR spectroscopic methods. However no other impurities of the type observed before (see Scheme II.21) were found. Thus, the appearance of PS must have been the consequence of an ordinary quenching of the Grignard reagent with small amounts of moisture in the solvent. The by-product was easily separated from the PDSP by column chromatography on silica.

The microanalysis and ^1H NMR spectroscopy of the product PDSP after the final purification step confirmed that no contaminants involving a partial loss of diphenylphosphino groups were present. This, together with the reasonably good yield of 60%, makes this method of using a bromomagnesium derivative a very good alternative to the previous one, where the lithiated precursor was employed. However this method has the disadvantage of being laborious, relying on the preparation and careful purification of at least one phosphine as the starting material (PSBr and possibly PS).

In spite of the high molecular weight of the newly synthesised triphosphine, PDSP, all attempts at crystallising the material failed. No amount of purification or 'precipitation' from different solvents or freezing to -25°C achieved the formation of even an amorphous solid form of the phosphine. On the other hand, PTSP precipitates out easily from cold alcohols and acetone solution as a microcrystalline solid. The spectroscopic properties of PDSP and PTSP are summarised in Tables II.5a and II.5b. The stability towards oxidation of PDSP and PTSP is as good as that of the other thienylphosphines.

The ^{31}P NMR spectra of each of the two phosphines consist of two singlets with unequal intensities. The intensity ratio for the PDSP molecule is 2:1 for the peaks at -18.68 and -32.17 ppm, respectively. Based on the intensities and on the chemical environment of the two phosphorus nuclei, the former peak was assigned to the phosphorus atom attached to two phenyl and one thiophene rings, P_B , while the latter - to the phosphorus atom attached to two thiophene and one phenyl rings, P_A . (The atom labelling scheme for these two phosphines is given in Figure II.2.) Similarly, in the PTSP molecule, the peak at -18.62 ppm was assigned to the phosphorus atom attached to two phenyl and one thiophene rings (P_B), while the one at -44.73 ppm was assigned to the phosphorus bonded to three thiophene units (P_A). The values of the P_B chemical shifts (around -18.6 ppm) in both PDSP and PTSP molecules are close to those for phosphorus nuclei in PS and other

diphenylphosphines with a 2-thienyl substituents which will be discussed later in this Chapter (-18 to -19 ppm). There is also a good correlation between the values for P_A chemical shifts in PDSP and PTSP with those for the respective phosphorus atoms in PDS and PTS ligands: *i.e.* -32.17 and -33.26 ppm for PDSP/PDS pair and -44.73 and -46.27 ppm for the PTSP/PTS pair. It is interesting to note that inspite of large differences in the ^{31}P NMR chemical shifts for P_A and P_B of both PDSP and PTSP, no detectable coupling could be observed between them. This is unexpected as two phosphorus nuclei are known to couple through as many as 6 bonds, while in this case there are only 5 (no interaction is transmitted via a heteroatom such as S). Originally it was attributed to thermal broadening of the signal at ambient temperature. But even after lowering the temperature to -50°C (CDCl_3 solution) the signals did not resolve. The reason behind this behaviour is not understood. The literature on the subject is extremely scarce: known examples of interacting phosphorus nuclei concern primarily aliphatic polyphosphines rather than heterocyclic ones. It is very likely, though, that the coupling cannot be observed simply due to its low value, which is not detectable by an instrument running at only 32 MHz (in respect to the phosphorus nuclei).

The ^1H NMR spectra of the two phosphines strongly resemble that of the PSP. First, a set of peaks appear consistent with the presence of an ABXY system due to the hydrogens $\text{H}_{\text{Th-3}}$ and $\text{H}_{\text{Th-4}}$ on the thiophene rings. These hydrogens are non-equivalent, couple to each other and to the both phosphorus nuclei attached to the thiophene unit. Second, a large multiplet due to phenyl protons is visible. The ratio of the integrated intensities of the thienyl to the phenyl protons corresponds to the expected values of 4:25 and 1:5 for PDSP and PTSP respectively. It was difficult to assign individual signals due to $\text{H}_{\text{Th-3}}$ and $\text{H}_{\text{Th-4}}$ as no NMR method could help to identify these protons. So, a tentative assignment was made based on the observation that in going from PSP to PTSP the thiophene hydrogen signals shift slightly upfield, which is probably caused by an increasing electron-withdrawing effect of a phosphorus attached to several thiophene units. Thus, hydrogens closest to the phosphorus with the highest number of thiophene rings (P_A) should have the lower value of the chemical shift. This is analogous to what was observed for bromo-substituted phosphine PSBr (*vide infra*).

Table II.5a NMR data for PDSP and PTSP, as measured in CDCl₃

Compound	$\delta^{31}\text{P}$, ppm	$\delta^{13}\text{C}$, ppm	$\delta^1\text{H}$, ppm
PDSP	-18.68 (s, P _B), -32.17 (s, P _A) (2:1 intensity ratio)	128.4 (d, C _{Ph'-3}), 128.5 (d, C _{Ph-3}), 129.0 (s, C _{Ph-4}), 129.1 (s, C _{Ph'-4}), 133.1 (d, C _{Ph-2}), 133.2 (d, C _{Ph'-2}), 136.2 (d, C _{Ph-1}), 136.4 (dd, C _{Th-4}), 136.7 (d, C _{Ph'-1}), 137.0 (dd, C _{Th-3}), 144.8 (d, C _{Th-5}), 145.1 (d, C _{Th-2})	7.14-7.27 (m, ABXY system; 4 H, H _{Th-3} + H _{Th-4}), 7.28-7.41 (m, 25 H, H _{Ph})
PTSP	-18.62 (s, P _B), -44.73 (s, P _A) (3:1 intensity ratio)	128.5 (d, C _{Ph-3}), 130.0 (s, C _{Ph-4}), 133.2 (d, C _{Ph-2}), 135.9 (dd, C _{Th-1}), 136.3 (d, C _{Ph-1}), 137.0 (dd, C _{Th-3}), 144.9 (d, C _{Th-5}), 145.4 (d, C _{Th-2})	7.10-7.16 (m, part of ABXY system; 3 H, H _{Th-3}), 7.21-7.27 (m, part of ABXY system; 3 H, H _{Th-4}), 7.28-7.41 (m, 30 H, H _{Ph})

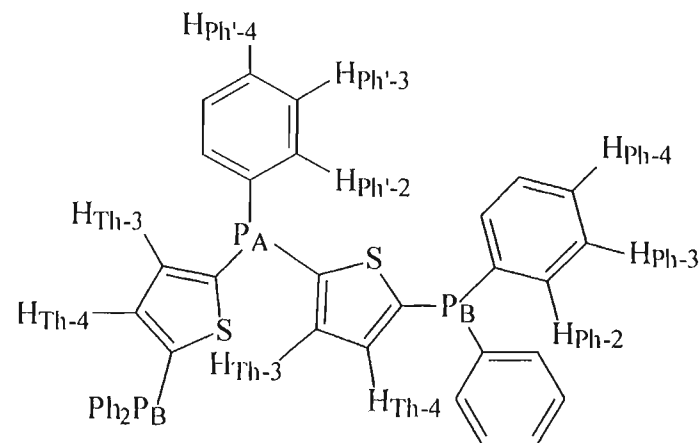


Fig. II.2 This is the numbering scheme for the thiophene and benzene nuclei in the molecule of PDSP (the carbon atoms are given the same number as the hydrogens they are attached to). Likewise, numeration starts from the central P_A atom in the molecule of PTSP.

Table II.5b Mass-spectrometric, UV-vis and IR spectroscopic data for PDSP and PTSP

Compound	UV [*] :	IR ^{**} :	MS (direct injection):
	λ_{max} , nm (ϵ , M ⁻¹ ·cm ⁻¹)	ν , cm ⁻¹	m/z (molar mass, g·mol ⁻¹)
PDSP	230 (3.2·10 ⁴),	501 (m), 519 (m), 536 (m), 551 (m), 696 (vs), 742 (s), 813	642.40 (642.69)
	251 (sh [#] , 2.6·10 ⁴), 295 (1.8·10 ⁴)	(m), 964 (w), 1002 (m), 1026 (w), 1068 (vw), 1089 (w), 1203 (m), 1284 (w), 1325 (w), 1414 (w), 1435 (s), 1479 (w)	
PTSP	229 (3.2·10 ⁴),	505 (m), 528 (m), 561 (s), 582 (w), 696 (vs), 746 (s), 813	833.40 (832.89)
	252 (2.7·10 ⁴), 302 (2.0·10 ⁴)	(m), 966 (vw), 1001 (m), 1024 (m), 1070 (w), 1091(m), 1205 (m), 1284 (w), 1325 (w), 1410 (w), 1433 (s), 1477 (w)	

* UV-vis measurements were carried out in dichloromethane

** IR data were obtained as KBr discs

shoulder on the main peak

Once the assignment of hydrogen atoms was complete, the assignment of the carbon atoms in both PDSP and PTSP was done on the basis of HETCOR two-dimensional and DEPT experiments. Unlike the ^1H NMR spectra, the two ^{13}C NMR spectra are distinctly different due to the presence of a unique phenyl group attached to P_A in the molecule of PDSP. The signals due to the carbon atoms of this group are seen as shoulders, or barely resolved shadow peaks, of signals due to the carbon atoms of the phenyl rings attached to P_B .

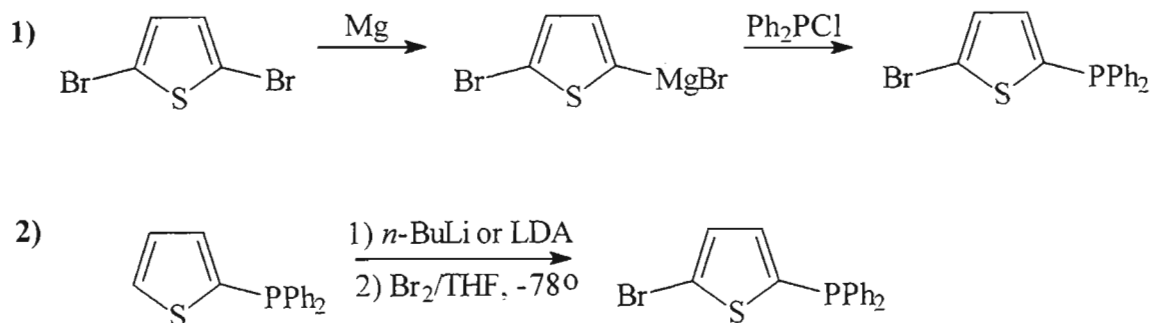
The use of mass-spectrometry for the characterisation of these two polyphosphines proved to be critical because of the ambiguity of the NMR data, *i.e.* it was necessary to confirm that the compounds obtained were not mixtures showing accidentally correct spectral patterns, but were the whole target molecules. The molecular ion values (see Table II.5b) have provided a proof that PDSP and PTSP have indeed been synthesised. The fragmentation pattern of these molecules under electron impact conditions included characteristic consecutive loss of diphenylphosphino ($M = 185$) and (diphenylphosphino)thienyl groups ($M = 267$) as well as a phenyl group in case of PDSP, further confirming the proposed structures.

Although, as before, the IR spectroscopic data did not yield any important information and was very similar to that obtained for the other four phosphines studied so far, the UV-vis spectra recorded for PDSP and PTSP revealed some interesting features. Both spectra now have a second absorption maximum at ± 300 nm and a pronounced shoulder at ± 252 nm (the latter can even be considered as a shallow peak for PTSP) which distinguish them from those of the previously characterised phosphines PS, PSP, PDS and PTS.

II.2.2.3 Synthesis and characterisation of the monophosphine precursor, diphenyl(5-bromo-2-thienyl)phosphine (PSBr)

Diphenyl(5-bromo-2-thienyl)phosphine (PSBr) is a novel compound and thus it was necessary to develop an efficient synthetic route to this compound. Two possible reaction sequences were considered (see Scheme II.23 on the next page):

Both methods were found to possess certain advantages and disadvantages. The first method makes use of the commercially available starting materials, 2,5-dibromothiophene, Mg and Ph_2PCl . The second requires the initial synthesis of PS from 2-bromothiophene and BuLi or LDA. Though the yield of the latter reaction is good (70%) it does demand



SCHEME II.23

extra preparative time. On the other hand, the second method was found to give a cleaner reaction mixture, which resulted in a shorter purification time and a slightly higher yield (45 vs. 40%). A minor side reaction was observed while preparing PSBr according to the second method, *i.e.* the formation of oxidised phosphines, as determined by ^{31}P NMR spectroscopy: several small peaks appeared in the 20-25 ppm region, characteristic of oxidised tertiary phosphines. This was confirmed by GCMS measurements. The latter method also allowed identification of two of the impurities according to their molecular masses *i.e.*, diphenyl(2-thienyl)phosphine oxide and diphenyl(5-bromo-2-thienyl)-phosphine oxide. The presence of these phosphine oxides did not affect the outcome of the purification step as they were retained on the silica during column chromatography of the product mixture. Finally note that there was neither loss of selectivity nor isomer formation during the bromination step employed in the second method for the preparation of PSBr.

The products obtained via both methods were shown to be identical, as proved by application of a combination of GC-mass spectrometric, microanalytical, ^1H and ^{31}P NMR and UV-vis spectroscopic techniques. However, the first method was given preference as the preparative technique for PSBr – mainly due to the easy availability of large quantities of the starting materials for bulk synthesis.

The choice of solvent and temperature is critical to the success of the first step in the first method for the synthesis of PSBr (Scheme II.23). Thus, this reaction is carried out in a relatively dilute and refluxing diethyl ether solution to prevent formation of dimagnesium species. Using THF as a solvent or a concentrated ether solution led to an increase in temperature above 40°C , allowing the formation of the bis(Grignard) reagent, thus generating by-products and decreasing the final yield.

Introduction of a bromine substituent in the 5-position of the thiophene ring of the thienylphosphine PS, results in significant changes to the physical properties. The phosphine PSBr appears to be much more polar than PS, being readily soluble in methanol and insoluble in hexane, in contrast to the behaviour of parent molecule. The melting point increases to 69°C and the ability to crystallise - as opposed to formation of an amorphous substance - is significantly improved. However, the ability to resist oxidation by atmospheric oxygen is common to both PS and PSBr.

The spectroscopic data for PSBr are given in Tables II.6a and II.6b.

Table II.6a NMR data for diphenyl(5-bromo-2-thienyl)phosphine, as measured in CDCl₃

$\delta^{31}\text{P}$, ppm	$\delta^{13}\text{C}$, ppm	$\delta^1\text{H}$, ppm
	118.2 (d, C _{Th-5}), 128.6 (d, C _{Ph-3}), 129.1 (s, C _{Ph-4}),	7.03-7.18 (ABX system, 2
-17.88	131.0 (d, C _{Th-4}), 131.8 (d, C _{Th-2}), 133.0 (d, C _{Ph-2}),	H, H _{Th-4} + H _{Th-5}),
	136.9 (d, C _{Th-3}), 137.2 (d, C _{Ph-1})	7.32-7.44 (m, 10 H, H _{Ph})

Table II.6b Spectroscopic data for diphenyl(5-bromo-2-thienyl)phosphine

UV [*] : λ_{max} , nm (ϵ , M ⁻¹ ·cm ⁻¹)	IR ^{**} : ν , cm ⁻¹	GCMS: m/z (molar mass, g·mol ⁻¹)
	490 (s), 503 (vs), 532 (m), 551 (m),	
232 (1.25·10 ⁴),	565 (m), 694 (vs), 741 (s), 804 (s), 949	
252 (sh [‡] , 1.17·10 ⁴)	(m), 999 (m), 1026 (w), 1066 (w),	345.85 and 347.85, d
	1087 (w), 1120 (w), 1201 (m), 1404	(347.2)
	(m), 1433 (m), 1473 (m)	

^{*} UV measurements were carried out in dichloromethane

^{**} IR data were obtained as KBr discs

[‡] shoulder on the main peak

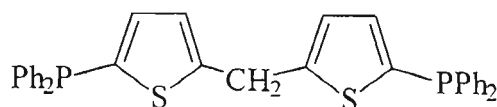
The ³¹P chemical shift for the phosphorus atom in PSBr is located noticeably downfield (by about 2 ppm) to that recorded for PS (-19.90 ppm). This is due to the electron-withdrawing effect of the bromo-substituent in the position-5 of the thiophene ring. However the resonance is still in a region characteristic of a phosphorus atom to which two phenyl and one thienyl substituents are attached.

As can be seen from Table II.6a, the two thiophene hydrogens give rise to a pattern comprising a doublet of doublets of equal intensity. This is indicative of an ABX system in which the hydrogens couple strongly to each other and to the phosphorus nucleus, the logical conclusion being that the thiophene ring is substituted in the positions 2 and 5. The introduction of the bromine atom significantly influences the ^1H and ^{13}C chemical shifts of the nuclei of the thiophene ring: the signals for both $\text{H}_{\text{Th-3}}$ and $\text{H}_{\text{Th-4}}$ in the PSBr molecule become deshielded (by approximately 0.2 ppm), when compared to the corresponding signals in PS, as do the signals due to $\text{C}_{\text{Th-4}}$ and $\text{C}_{\text{Th-3}}$ in the ^{13}C NMR spectrum. At the same time the signal due to $\text{C}_{\text{Th-5}}$ (the carbon attached to the bromine) moved upfield by as much as 14 ppm and $\text{C}_{\text{Th-2}}$ - by 6 ppm. The phenyl ring resonances remain essentially unaffected. The low ^{13}C chemical shift value for the $\text{C}_{\text{Th-5}}$ nucleus (118.2 ppm) is not out of range as has been proved on a number of occasions during this work through the synthesis and characterisation of various 5-bromo-substituted thiophenes. Thus, for 5,5'-dibromo-2,2'-bithiophene $\delta(\text{C}_{\text{Th-5}}) = 111.3$, for 2-(5'-bromo-2'-thienyl)pyridine $\delta(\text{C}_{\text{Th-5}}) = 115.0$ and for 5-bromo-2,2':5',2''-terthiophene $\delta(\text{C}_{\text{Th-5}}) = 111.0$ ppm.

The mass-spectrum of the phosphine yielded the expected molecular ion doublet due to the two isotopes of bromine, ^{79}Br and ^{81}Br . The loss of bromine led to a fragment at 267.05 (equivalent to $\text{M}[\text{PS}]-1$), with the rest of fragmentation pattern being very similar to that of the PS. Although the UV-vis and IR spectra of the PSBr show certain characteristic features, they largely resemble those of PS.

II.2.2.4 Attempted synthesis of bis(5-diphenylphosphino-2-thienyl)methane

The particular characteristic of the new polydentate phosphines synthesised so far, PSP, PDSP and PTSP, is the rigidity of their structure, as the backbone connecting two adjacent phosphorus atoms in all these molecules is a heterocyclic ring (thiophene). This implies that they possess limited coordination abilities in complexes with metals, *i.e.* they are not likely to form chelates. In order to overcome this limitation and to create a more flexible polydentate thienylphosphine, synthesis of bis(5-diphenylphosphino-2-thienyl)methane (PSCSP) was undertaken.



PSCSP

As can be seen from the above structure, the diphosphine contains two thiophene units each substituted with a diphenylphosphino group in position-5. The two rings are separated by a methylene group which allows for a greater degree of flexibility within the molecule. The selection of the methylene group (as opposed to ethylene or 1,3-propylene, for example) as a spacer between the thiophene rings was made with a view to

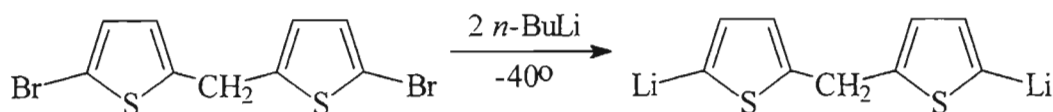
- a) keeping the distance between the phosphorus atoms to a minimum and
- b) ensuring that the preparation of a suitable precursor is feasible.

Originally it was envisaged that the synthesis would involve the preparation of the dibromo compound, bis(5-bromo-2-thienyl)methane, and its subsequent conversion to the diphosphine. The preparation of bis(5-bromo-2-thienyl)methane is well documented^{179,180} and was easily reproduced during this work, albeit with some minor modifications (see Appendix A).

The next step of the traditional route from a bromothiophene to a diphenylphosphino thiophene involved conversion into a Grignard reagent. After several attempts it was established that introduction of magnesium into the C-Br bond of this molecule requires considerable effort and could only be achieved with a use of an entrainer, such as ethyl bromide. The reaction was carried out in ether, but after the formation of the Grignard reagent was complete, the latter was redissolved in dry benzene and diphenylchlorophosphine added in the usual manner. After the hydrolytic work-up the mixture was subjected to mass-spectrometric analysis. This showed the presence of several compounds containing a diphenylphosphino group: (5-bromo-2-thienyl)(5-diphenylphosphino-2-thienyl)methane ($m/z = 442.35$ and 444.45 – doublet, M^+), (5-diphenylphosphino-2-thienyl)(2-thienyl)methane ($m/z = 363.75$, M^+), ethyldiphenylphosphine ($m/z = 214.25$, M^+), diphenylphosphine ($m/z = 185.85$, M^+) as well as the desired product, PSCSP ($m/z = 547.75$, M^+). The ^{31}P NMR spectroscopic analysis confirmed the mass-spectrometric results by showing several peaks at *ca.* -18 ppm (the region characteristic of diphenylthienylphosphines), as well as peaks at *ca.* -40 ppm (Ph_2PH) and *ca.* -16 ppm (the region characteristic of alkyl diphenylphosphines, as the fact confirmed by running the ^{31}P NMR spectrum of *n*-BuPPh₂). Although PSCSP was the major product of this reaction, all attempts to separate the components of this complex mixture proved fruitless: neither crystallisation from different solvents, nor

chromatography on silica gel with various mobile phases led to isolation of the target phosphine in its pure form.

The failure of the traditional Grignard route prompted a different approach which was to use a dilithium rather than a di(bromomagnesium) species as the synthetic precursor (Scheme II.24).

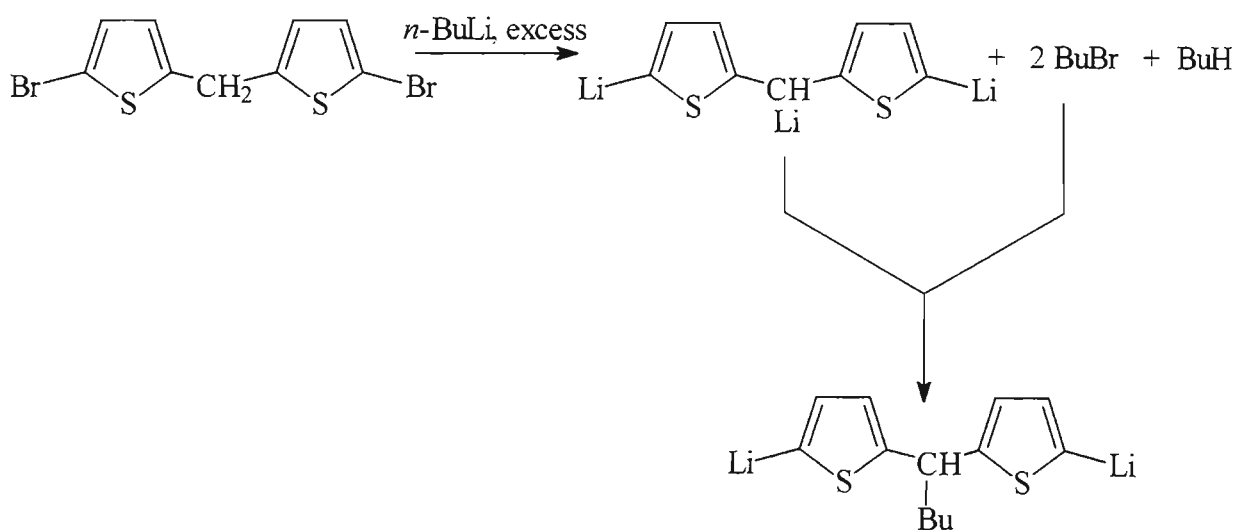


SCHEME II.24

The addition of *n*-BuLi to the dibromo compound was carried out at -40°C in order to minimise side reactions, in particular the abstraction of a proton from the methylene group, as the hydrogens of this methylene group are quite acidic due to the presence of two electron-withdrawing thiophene rings. The dilithium species formed in this reaction were successfully quenched with diphenylchlorophosphine. After the work-up of the reaction mixture, the mass-spectrometric analysis (together with ^{31}P NMR spectroscopy) revealed the presence of the following compounds: (butyl)(2-thienyl)(5-diphenylphosphino-2-thienyl)methane ($m/z = 420.65$, M^+), (5-diphenylphosphino-2-thienyl)(2-thienyl)methane ($m/z = 363.75$, M^+), diphenyl(2-thienyl)phosphine ($m/z = 268.05$, M^+), {bis(2-thienyl)}-(butyl)methane ($m/z = 236.30$, M^+), bis(2-thienyl)methane ($m/z = 179.80$, M^+) and the desired product PSCSP ($m/z = 547.75$, M^+), the latter being present in the largest amount. Chromatography of the mixture on silica with hexane/ether 1:1 as eluent enabled the removal of the minor impurities while, after extraction with hot hexane, only bis(5-diphenylphosphino-2-thienyl)methane (PSCSP) and (5-diphenylphosphino-2-thienyl)(2-thienyl)methane remained. However these two compounds could not be successfully separated by chromatography or other means.

The formation of the unsymmetrical by-products, (5-diphenylphosphino-2-thienyl)(2-thienyl)methane and butyl(2-thienyl)(5-diphenylphosphino-2-thienyl)methane, can be attributed to partial hydrolysis of the dilithiated species by residual moisture in the solvent or diphenylchlorophosphine. This moisture is very difficult to eliminate completely, especially from the latter chemical. Likewise, bis(2-thienyl)methane must have been

formed as the result of hydrolysis. The combination of ^{31}P NMR spectroscopy and GC-Mass spectrometry does not allow one to determine the position at which a butyl substituent was introduced into the molecules of butyl(2-thienyl)(5-diphenylphosphino-2-thienyl)methane and {bis(2-thienyl)}(butyl)methane. However, it seems logical to propose that substitution occurred at the methylene part of the molecule, given that butyl substitution did not occur during any other reaction of a brominated thiophene with *n*-BuLi (at least not in this work!). A plausible mechanism is shown in the Scheme II.35 below.



SCHEME II.35

Thus, both methods of conversion of bis(5-bromo-2-thienyl)methane into the desired diphosphine, PSCSP, through dimetallated intermediates proved to be unsatisfactory.

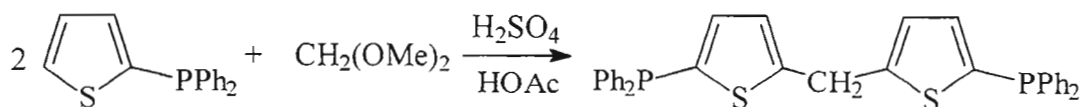
At this point it was decided to change the strategy and to react bis(5-bromo-2-thienyl)methane with a phosphinating reagent. Quite expectedly, the reaction between the dibromo compound and lithium diphenylphosphide yielded tetraphenyldiphosphine as the major product due to bromine-lithium exchange (see Section 2.2.1 of this Chapter). Therefore, alternative diphenylphosphino reagents were tested.

The Pd-catalysed reaction between a bromothiophene and (trimethylsilyl)- or (trimethylstannyl)diphenylphosphine introduced by Stille *et al.*,¹⁴¹ was described in the introduction to this chapter. Both diphenylphosphino compounds are much milder reagents than lithium diphenylphosphide. As the first compound was less toxic and easier to prepare than the second, it was tried first in the reaction with bis(5-bromo-2-thienyl)methane. The

reaction was carried out in dry oxygen-free refluxing toluene with $\text{Pd}(\text{CH}_3\text{CN})_2\text{Cl}_2$ as the catalyst. A sample of the mixture was analysed every 24 hours. A peak due to a thienylphosphine (^{31}P NMR $\delta = \pm -19$ ppm) only appeared after 48 hours. At the end of 120 hours, the conversion of (trimethylsilyl)diphenylphosphine (^{31}P NMR $\delta = -58$ ppm) still did not reach 30%. At this point the reaction was abandoned, as the reaction time was not practically viable.

Due to the high toxicity of (trimethylstannyl)diphenylphosphine and its synthetic precursor, Me_3SnCl , a tributyl derivative was prepared instead. (Tributylstannyl)-diphenylphosphine was reacted with bis(5-bromo-2-thienyl)methane in dry oxygen-free refluxing toluene with $\text{Pd}(\text{PPh}_3)_2\text{Cl}_2$ as a catalyst. Analysis of the reaction mixture after 36 hours showed that conversion of (tributylstannyl)diphenylphosphine (^{31}P NMR $\delta = -56$ ppm) was not greater than 65-70%. After refluxing for 24 more hours the reaction was complete. The work-up of the mixture afforded a very dark tarry residue. Attempts to purify it using column chromatography proved unsuccessful. No compound could be isolated from the mixture.

The failure of the Pd-catalysed reaction led to another change in synthetic approach. It was decided to introduce diphenylphosphino substituents on the thiophene moieties first and then join the two units with a methylene bridge. The reaction shown in Scheme II.36 was carried out in order to achieve the desired product (a similar reaction is used for preparation of bis{5-bromo-2-thienyl}methane).¹⁸⁰



SCHEME II.36

Unfortunately, this reaction also did not afford the target compound. This is due to protonation of the phosphino groups in the highly acidic reaction medium, evidence for this being a shift in the ^{31}P chemical shift for PS to ± 40 ppm. In view of the protonated molecule being positively charged aromatic electrophilic substitution becomes impossible. No thiophene compound containing a methylene bridge could be isolated after basification of the reaction mixture.

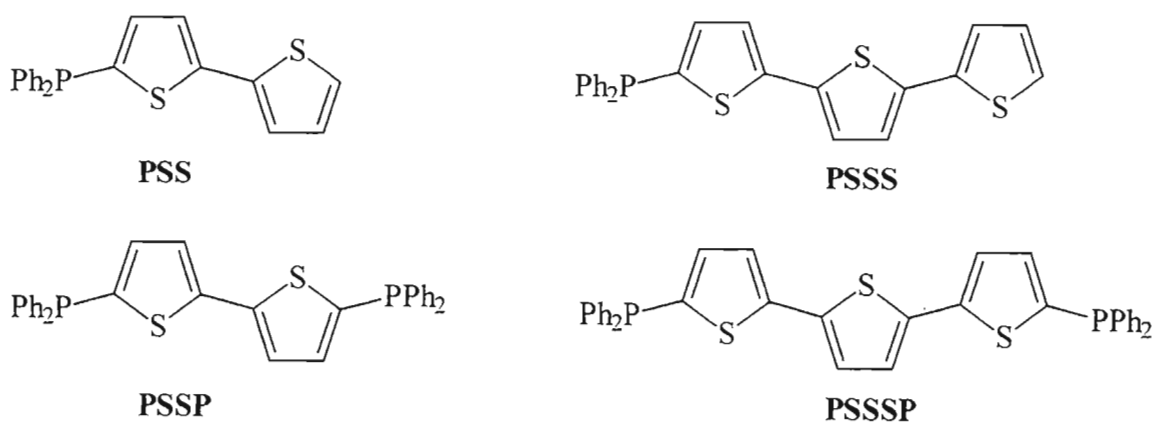
In order to protect the phosphine group from protonation, the phosphine was converted into the corresponding phosphine sulfide with the intention of reducing the latter back to the phosphine after the final step of the reaction. Preparation of the phosphine sulfide was easily achieved by refluxing PS with powdered sulfur in toluene for 2 hours. However, the phosphine sulfide proved to be completely unreactive towards bis(methoxy)methane (Scheme II.36); again probably due to the strong electron-withdrawing effect of the diphenylthiophosphoryl group and the consequent inhibition of electrophilic substitution on the thiophene ring.

No further attempts were made to synthesise PSCSP.

II.2.3 Preparation of the mono- and bidentate phosphines with polythiophene units

No examples of mono- or polydentate phosphines containing a polythiophene moiety have been reported in the literature to date. Although some of the phosphines described in the preceding Chapters do contain two or more thiophene rings in their structure *e.g.*, PTS and PDSP, the thiophene rings are separated from each other by a phosphorus atom. In the strictest sense, polythiophenes contain thiophene units directly linked to each other.

Of particular interest here are polythiophenes with two and three thiophene rings joined through the α -position, as they are known to be biologically active, exhibiting phototoxic activity against nematodes, larvae and eggs of insects, bacteria, algae, certain viruses and fungi.^{181,182} The four target diphenylphosphino substituted compounds based on these polythiophenes are shown below (Scheme II.37).

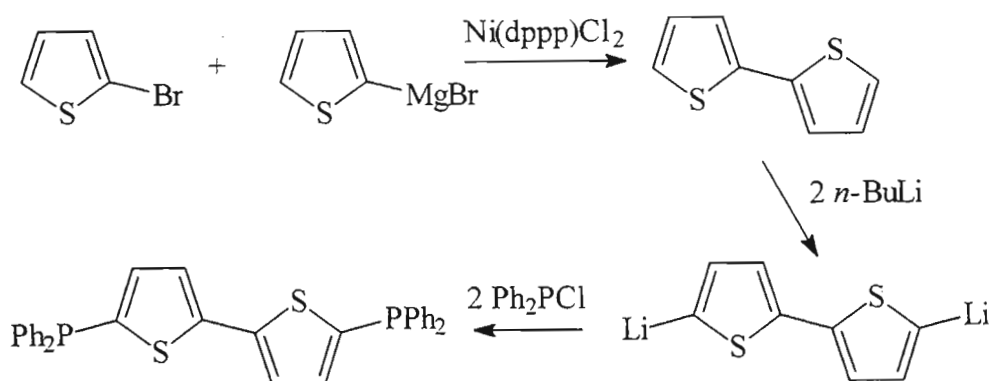


SCHEME II.37

II.2.3.1 Synthesis and characterisation of 5,5'-bis(diphenylphosphino)-2,2'-bithiophene (PSSP)

In order to prepare the target compounds, the already well-established route via metallated thiophenes and diphenylchlorophosphine was considered.

Lithiation of the bithiophene, SS, with 2 molar equivalents of *n*-BuLi under mild conditions can be carried out in either ether or THF, yielding 5,5'-dilithio-2,2'-bithiophene – the ideal precursor for PSSP. The starting material for the reaction, SS is easily prepared from 2-bromothiophene according to the method by Kumada *et al.*¹⁸³ (see Appendix A). The full reaction sequence for the synthesis of PSSP is shown below (Scheme II.38).



SCHEME II.38

The amount of *n*-BuLi used for dimetallation of the bithiophene during the second step was optimised during this study. It was found that using 2 or slightly fewer equivalents of the reagent results in incomplete formation of 5,5'-dilithio-2,2'-bithiophene. Use of 2.5 or more equivalents results not only in metallation at the 2-positions of the bithiophene, but in other positions as well. The latter fact was confirmed by treating SS with approximately 3 equivalents of *n*-BuLi. After a period of 4 hours, the reaction mixture was treated with excess diphenylchlorophosphine and analysed using ³¹P NMR spectroscopy. The analysis showed the presence of not only a signal due to a 2-thienyl substituted phosphine ($\delta = \pm -19$ ppm), but also unidentified peaks at -23, -27 and -35 ppm. After the normal work up, the crude reaction mixture was analysed using mass-spectrometry. A compound(s) with a molecular mass of 718.4 was found amongst the products together with the target phosphine, PSSP. The former corresponds to a bithiophene with 3 diphenylphosphino groups.

In this way it was established that use of 2.2 molar equivalents of *n*-BuLi achieves complete lithiation of bithiophene at positions-5 and -5' without noticeable contamination by polymetallated species. After quenching the reaction mixture with the corresponding amount of diphenylchlorophosphine (2.2 molar equivalents) and a traditional work up, pure PSSP was obtained in 62% yield.

Purification of PSSP did not prove to be difficult, as the compound is highly crystalline and stable (oxidation resistant); moreover it is easily purified by recrystallisation from chloroform and methanol. The diphosphine has limited solubility, dissolving mostly in chlorinated solvents and benzene and precipitating easily from alcohols, acetone and saturated hydrocarbons. Off-white crystals of PSSP grew spontaneously from a semi-saturated chloroform solution left standing in air. They appeared to be of good quality and were successfully used for collecting X-ray data and determination of the compound's crystal structure (*vide infra*).

The ^1H , ^{13}C and ^{31}P NMR data as well as the results of UV-vis and IR spectroscopies and mass-spectrometric measurements for PSSP are given in Tables II.7a and II.7b respectively.

Table II.7a NMR data for 5,5'-bis(diphenylphosphino)-2,2'-bithiophene, as measured in CDCl_3

$\delta^{31}\text{P}$, ppm	$\delta^{13}\text{C}$, ppm	$\delta^1\text{H}$, ppm
	124.8 (d, $\text{C}_{\text{Th-3}}$), 128.5 (d, $\text{C}_{\text{Ph-3}}$), 129.0 (s, $\text{C}_{\text{Ph-4}}$),	7.11-7.22 (ABX system; 4
-18.75 (s)	133.0 (d, $\text{C}_{\text{Ph-2}}$), 137.3 (d, $\text{C}_{\text{Th-4}}$), 137.6 (d, $\text{C}_{\text{Ph-1}}$),	H, $\text{H}_{\text{Th-3}} + \text{H}_{\text{Th-4}}$,
	137.8 (d, $\text{C}_{\text{Th-5}}$), 143.4 (s, $\text{C}_{\text{Th-2}}$)	7.29-7.44 (m, 20 H, H_{Ph})

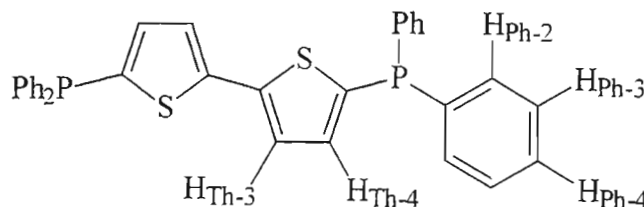


Fig. II.3 Numbering scheme for hydrogen atoms in the PSSP molecule

Table II.7b Spectroscopic data for 5,5'-bis(diphenylphosphino)-2,2'-bithiophene

UV*: λ_{max} , nm (ϵ , M ⁻¹ ·cm ⁻¹)	IR**: ν , cm ⁻¹	MS (direct injection): m/z (molar mass, g·mol ⁻¹)
230 (1.9·10 ⁴), 350 (1.95·10 ⁴)	486 (s), 499 (s), 514 (s), 551 (w), 571 (w), 696 (vs), 741 (vs), 798 (vs), 875 (m), 918 (w), 988 (s), 1026 (w), 1068 (w), 1073 (w), 1092 (m), 1198 (m), 1271 (w), 1308 (w), 1429 (m), 1435 (s), 1477 (m)	534.20 (534.61)

* UV-vis measurements were carried out in dichloromethane

** IR data were obtained as KBr discs

The ³¹P NMR spectrum of PSSP displays a singlet which is expected due to the symmetrical nature of the diphosphine. The chemical shift of -18.75 ppm is in the region characteristic of diphenyl(2-thienyl) phosphines.

As the molecule of PSSP is centrosymmetric, it consists of two chemically and magnetically equivalent halves. The atoms in the molecule can be relatively easily assigned to signals in both the ¹H and ¹³C NMR spectra. Half a PSSP molecule is nearly the same as a PS molecule; however, the NMR spectra of PSSP and PS do differ to some extent. Apart from the expected absence of a signal due to the hydrogen in the 2-position of the thiophene in the ¹H NMR spectrum of PSSP, there are other differences in the spectrum of this compound. In particular the signals due to H_{Th-3} and H_{Th-4} are shifted slightly upfield, compared to those in PS, which is most likely a consequence of the electron-withdrawing effect of the sulfur (through 4 and 5 bonds) in the neighbouring thiophene ring.

The ¹³C NMR spectrum of PSSP resembles that of both PS and the parent heterocycle, SS. For example, the "inner" C_{Th-2} and C_{Th-3} atoms in PSSP (δ = 137.8 and 124.8 ppm, respectively) have chemical shifts very similar to those for the same carbon atoms in SS (δ = 137.3 and 123.6 ppm for C_{Th-2} and C_{Th-3}, respectively). The only significant difference is the splitting of the C_{Th-3} signal in the ¹³C NMR spectrum of PSSP, due to coupling to the phosphorous nucleus through 4 bonds. As far as the "outer" carbons, C_{Th-4} and C_{Th-5}, are

concerned, they have chemical shifts and splitting patterns very similar to those for the equivalent carbons in PS (see Table II.1a).

On the other hand, the electronic absorption (UV-vis) spectrum of a dichloromethane solution of PSSP is markedly different from those recorded for both PS and SS. The spectrum has 2 pronounced absorption maxima at 230 and 350 nm, while PS exhibits only a single broad peak at 230 nm, and SS two peaks at 247 and 305 nm. In particular, the introduction of two diphenylphosphino groups in the 5- and 5'-position of the 2,2'-bithiophene molecule has led to a bathochromic shift in the long wavelength absorption band from 305 to 350 nm. This band is normally assigned to a $\pi \rightarrow \pi^*$ transition, the position of which being previously shown to be affected by the presence of substituents on the bithiophene molecule.¹⁸⁴ These authors¹⁸⁴ demonstrated that the stepwise introduction of bromine atoms in the 5- and 5'-positions of SS leads to bathochromic shifts in the absorption maxima from 302 to 309 nm and from 309 to 321 nm (these data were obtained in chloroform solution). The electronic properties of diphenylphosphino group are somewhat similar to those exhibited by bromine in that it can be mildly electron withdrawing ($-I$ effect), while possessing a $+M$ effect due to the lone pair on the phosphorus atom. The bathochromic shift is therefore expected. The IR and mass spectra for PSSP show no unusual features and are not discussed.

The most informative part of the characterisation of the diphosphine, PSSP, comes from the X-ray analysis of its crystals. Figure II.4 gives a perspective view of the ligand and also shows the atom labelling scheme. Tables II.23 and II.24 in the Experimental section list the interatomic distances and angles respectively. The PSSP molecules exist as discrete entities in the crystal, there being no non-bonded contact distances less than the sum of the van der Waals radii for the two atoms concerned. The geometry of the molecule includes a centre of symmetry which lies at the centre of the C(4)-C(4)* bond. As a consequence, the ligand adopts a planar *transoid* arrangement, which correlates well with the reported conformation of the parent heterocycle, SS, in the solid state.¹⁸⁵ In solution, however, the conformation is known to change, as proved by Veracini *et al.*¹⁸⁶ for 2,2'-bithiophene and its 5,5'-disubstituted derivatives. Both *trans*- and *cis*- conformers coexist in solution, with the former being more stable and thus, predominant. It is expected that PSSP will follow the same trend in solution.

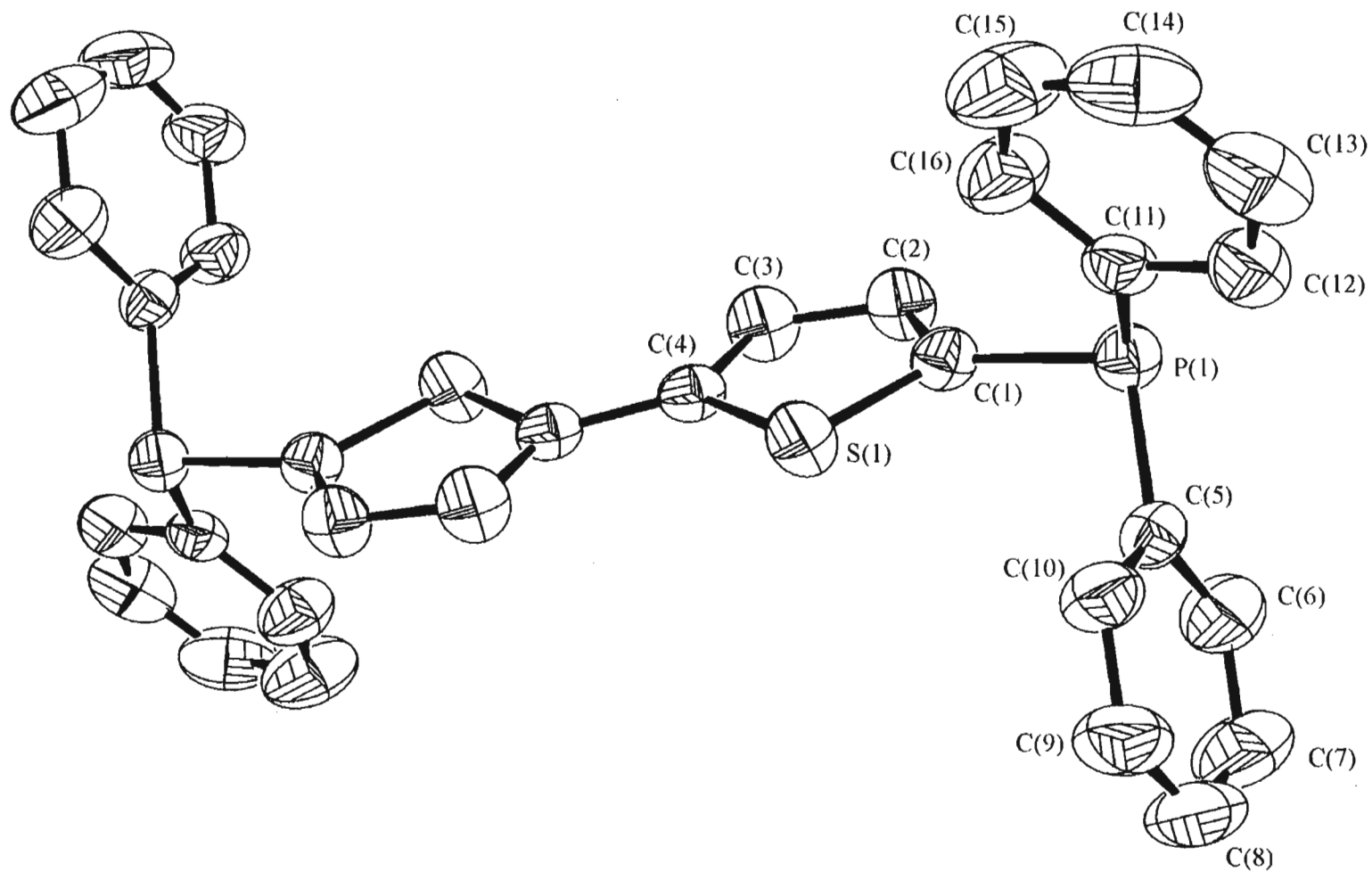


Fig. II.4 Structure of the PSSP ligand, showing the atom numbering scheme

The geometry around the phosphorus atom (only one half of the molecule is considered due to its inherent symmetry) is pyramidal, with the C-P-C angles being between 101.6(1) and 103.5(1)° and with the phenyl rings adopting orientations such that their planes are at dihedral angles of 77.3° [C(5) to C(10)] and 105.7° [C(11) to C(16)] to that of the thiophene ring. Remaining bonds and angles in the PSSP molecule are as expected (see Tables II.23 and II.24).

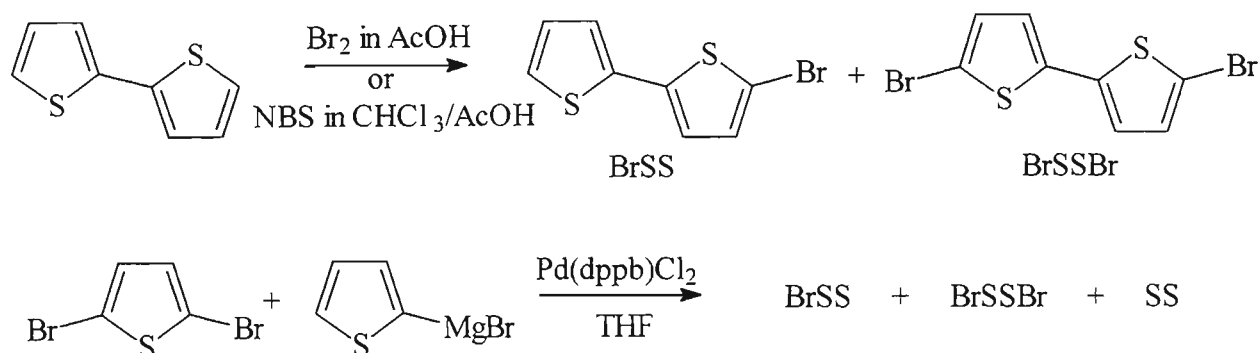
It is interesting to note, that the torsion angles [S(1)-C(1)-P(1)-C(5)] and [S(1)-C(1)-P(1)-C(11)] are 42.5(2) and 63.9(2)° respectively, implying that the phenyl rings on the phosphorus are turned towards the sulfur. This in turn indicates that the lone pair on the phosphorus atom in PSSP faces the direction opposite to that of the sulfur in the adjacent thiophene. As there are no reported crystal structures of free 2-thienylphosphine ligands in the literature, this finding can best be compared to the molecular structure of 6-diphenylphosphino-2,2'-bipyridine¹⁸⁷ as the only example of a diphenylphosphino group substituted in the α -position of a binuclear heterocycle. The analysis of the crystal structure of the latter compound shows that the lone pair on the phosphorus is turned towards the nitrogen of the adjacent pyridine ring. The exact opposite is true for the thienylphosphine PSSP, however: here the lone pair of the phosphorus points in the opposite direction to that of the sulfur. This comparison tends to suggest that the direction of the phosphorus lone pair is the direct result of the steric interaction with the lone pair on the heteroatom.

II.2.3.2 Synthesis and characterisation of diphenyl[5-(2,2'-bithienyl)]phosphine (PSS)

The introduction of a single diphenylphosphino substituent in the α -position of the 2,2'-bithiophene molecule proved to be substantially more difficult than the preparation of the disubstituted compound, PSSP. Monolithiation of the parent heterocycle, SS, has been described in the literature.^{188,189} However, all attempts to obtain PSS selectively following lithiation of the SS with 1 or fewer mole equivalents of *n*-BuLi or LDA, and subsequent quenching of the mixture with diphenylchlorophosphine, proved fruitless. Use of different temperatures and a range of solvents such as hexane, ether and THF did not help. The final result was always an inseparable mixture of PSS, PSSP and SS.

The next strategy applied to the synthesis of PSS was the Grignard route. This required the prior synthesis of a suitable precursor, viz. 5-bromo-2,2'-bithiophene. When followed, most

of the literature procedures^{177,190} claiming to have prepared this compound, led to formation of the disubstituted product in considerable amounts as well (Scheme II.39).



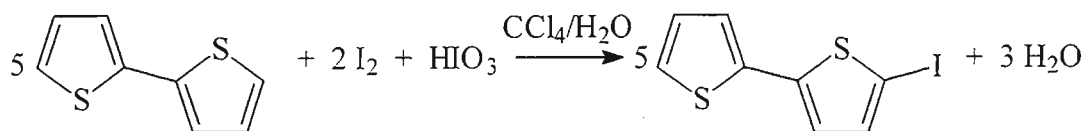
SCHEME II.39

Even the very effective method of selective monobromination of oligothiophenes developed by Bäuerle and Effenberger¹⁹¹ involving low temperature bromination with NBS in dimethylformamide in the absence of light, yielded noticeable amounts of the dibrominated by-product when applied to SS. The alternative procedure¹⁹² recommended by the Beilstein Reference Handbook guarantees the selective formation of the monobrominated compound, BrSS, but involves five intermediate low-yielding steps making it a tedious and an unattractive method.

Due to the lack of success in the synthesis of 5-bromo-2,2'-bithiophene, the decision was made to change the halogen substituent on the SS moiety from bromine to iodine. In fact, 5-iodo-2,2'-bithiophene (ISS) has been previously synthesised either by iodination of 2,2'-bithiophenyl-5-yl-mercuric chloride in chloroform,¹⁹³ or according to the Curtis' method¹⁹² *i.e.*, 2,2'-bithiophenyl-5-carboxylic acid methyl ester is treated with iodine and then NaOH and finally reacted with Hg(OAc)₂ in acetic acid to give ISS. Although it avoids formation of by-products, the second method is tedious and, moreover, results in a low total yield.

The yield of the first method is about 42%, which is normally quite acceptable. However it was decided to improve on this method, especially as it was found to be very time consuming (approximately 4-5 days were required to obtain 5-iodo-2,2'-bithiophene from SS). The method designed during the course of this work is roughly based on the method used for the selective monobromination of thiophene by a mixture of concentrated HBr and KBrO₃ in a two-phase solution.¹⁹⁴ Although the above method failed to produce

uncontaminated 5-bromo-2,2'-bithiophene, it was possible to obtain pure 5-iodo-2,2'-bithiophene (ISS) in 56% yield using I_2 in acetic acid instead of HBr, and HIO_3 instead of $KBrO_3$. The reaction sequence between the components is shown in Scheme II.40.

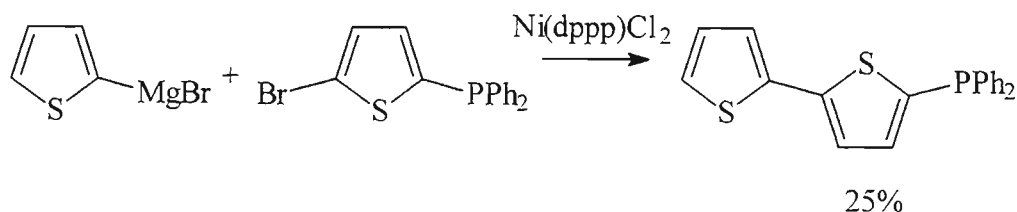


SCHEME II.40

This method provided not only a significant improvement in the yield (56 vs. 42%), but has also significantly reduced the time required for the synthesis, making it possible to obtain 5-iodo-2,2'-bithiophene within one day.

After the successful preparation of the iodo compound, the Grignard route to the target phosphine, PSS, was followed in a usual manner. The 5-iodo-2,2'-bithiophene was treated with magnesium in dry THF followed by reaction with diphenylchlorophosphine. The mixture obtained after the hydrolytic work up contained mostly PSS and SS, as established by GCMS analysis. The mixture was subjected to gradient elution on a silica column, which produced yellow oil. This oil solidified only after standing under methanol at -20° for 3 months. The final yield of PSS prepared according to this method was only 24%. The reason behind such a low reaction yield is not certain. A poor ability of PSS (unlike that of PSSP!) to solidify is most likely one of the reasons, while the tendency of ISS to decompose is responsible for the formation of by-products.

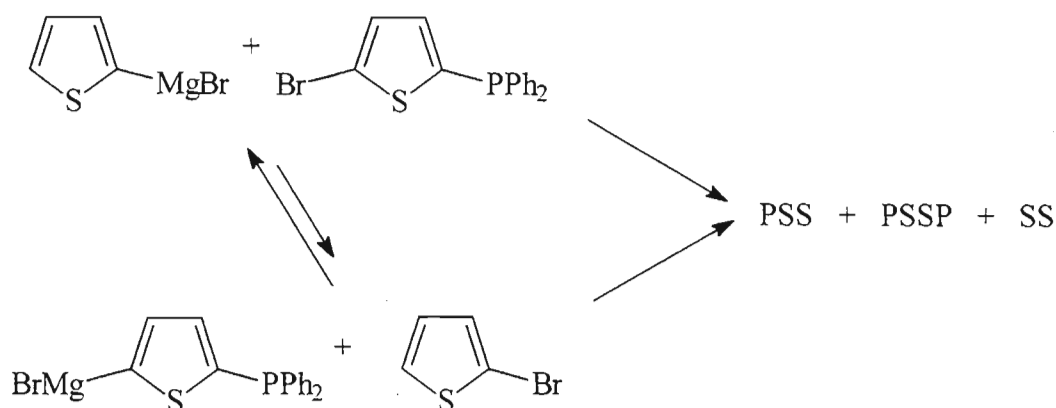
The low yield of the target phosphine prepared via the Grignard reaction led to attempts to create a more efficient route for the synthesis of PSS. A promising approach, which was selected for this purpose, utilised a Ni-catalysed cross-coupling reaction (Scheme II.41).



SCHEME II.41

The above reaction belongs to the same class of Ni-catalysed reactions as the ones reported by Kumada¹⁸³ as well as other authors¹⁹⁵ which are used for the coupling of various heterocycles, including 2,2'-bithiophene and 2,2':5,2''-terthiophene. The only advantage it seems to offer in comparison to the Grignard route is the cutting of a number of steps between commercially available chemicals and the target phosphine: 2,5-dibromothiophene→PSBr→PSS as opposed to 2-bromothiophene→SS→ISS→PSS. The combined yield of PSS via the first sequence is very similar to that attained via the second route (10% and 11%, respectively).

It is interesting to note, that 'swapping polarities', *i.e.* exchanging the bromo and bromomagnesium substituents on the reagents in Scheme II.41 leads to different reaction products. While the mixture obtained as the result of the original reaction contained more PSS together with some PSSP, SS and residual PSBr; SS, PSSP as well as PS were the major products of the reaction between 2-bromothiophene and 5-diphenylphosphino-2-thienyl-magnesium bromide (Scheme II.42).



SCHEME II.42

One feasible explanation which can be offered is that metal-halogen exchange takes place in either solution, as we observe apparent homo-coupling in both cases. However in the case of the second reaction, the exchange must go to a much larger extent, providing more of the compounds which can participate in cross-coupling reactions with 2-bromothiophene and 5-diphenylphosphino-2-thienyl-magnesium bromide. As the stability of the metallated thiophene is attributed to the electron-withdrawing ability of sulfur, which assists in charge delocalisation, introduction of substituents possessing some electron-donating properties (+*M* or +*I*) on the thiophene moiety is going to destabilise the

negatively charged species. As the diphenylphosphino group possesses $+M$ effect with poorly pronounced $-I$ effect, it renders 5-diphenylphosphino-2-thienyl-magnesium bromide less stable than 2-thienyl-magnesium bromide, thus promoting the exchange. (Formation of PS as a by-product of this reaction is simply the result of partial hydrolysis of 5-diphenylphosphino-2-thienyl-magnesium bromide with residual moisture or alcohol in the catalyst.)

The new phosphine possesses the same kind of stability towards oxidation by atmospheric oxygen as the other thienylphosphines described so far. As far as its solubility properties are concerned, it is easily dissolved in the majority of organic solvents (unlike PSSP).

The characterisation data for the PSS molecule are given in Tables II.8a and II.8b (^1H , ^{13}C and ^{31}P NMR data as well as the results of UV-vis and IR spectroscopic and mass-spectrometric measurements).

Table II.8a NMR data for 5-diphenylphosphino-2,2'-bithiophene, as measured in CDCl_3

$\delta^{31}\text{P}$, ppm	$\delta^{13}\text{C}$, ppm	$\delta^1\text{H}$, ppm
-18.83 (s)	124.1 (s, $\text{C}_{\text{Th-3'}}$), 124.5 (d, $\text{C}_{\text{Th-3}}$), 124.9 (s, $\text{C}_{\text{Th-5'}}$),	6.97 (dd, 1 H, $\text{H}_{\text{Th-4'}}$),
	127.8 (s, $\text{C}_{\text{Th-4'}}$), 128.5 (d, $\text{C}_{\text{Ph-3}}$), 129.0 (s, $\text{C}_{\text{Ph-4}}$),	7.10-7.25 (m, 4 H, $\text{H}_{\text{Th-3}}$ +
	133.0 (d, $\text{C}_{\text{Ph-2}}$), 136.8 (d, $\text{C}_{\text{Th-5}}$), 137.3 (d, $\text{C}_{\text{Th-4}}$),	$\text{H}_{\text{Th-4}} + \text{H}_{\text{Th-3'}}$ + $\text{H}_{\text{Th-5'}}$),
	137.4 (s, $\text{C}_{\text{Th-2'}}$), 137.6 (d, $\text{C}_{\text{Ph-1}}$), 143.9 (s, $\text{C}_{\text{Th-2}}$)	7.32-7.47 (m, 10 H, H_{Ph})

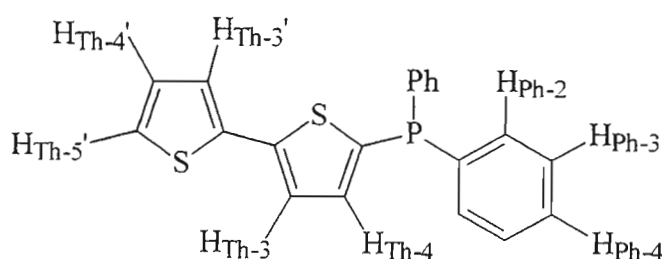


Fig. II.5 Numbering scheme for hydrogen atoms in the PSS molecule

Table II.8b Spectroscopic data for 5-diphenylphosphino-2,2'-bithiophene

UV*: λ_{max} , nm (ϵ , $\text{M}^{-1}\cdot\text{cm}^{-1}$)	IR**: ν , cm^{-1}	GCMS: m/z (molar mass, $\text{g}\cdot\text{mol}^{-1}$)
	482 (s), 494 (s), 504 (s), 550 (m), 692 (vs), 737 (s), 743 (vs), 804 (s), 839 (m), 908 (w), 988 (m), 1027 (w), 1045 (vw), 1066 (w), 1089 (w), 1155 (vw), 1180 (w), 1200 (w), 1215 (vw), 1420 (m), 1431 (m), 1478 (w)	349.80 (350.43)
230 ($1.34\cdot 10^4$), 330 ($1.60\cdot 10^4$)		

* UV-vis measurements were carried out in dichloromethane

** IR data were obtained as KBr discs

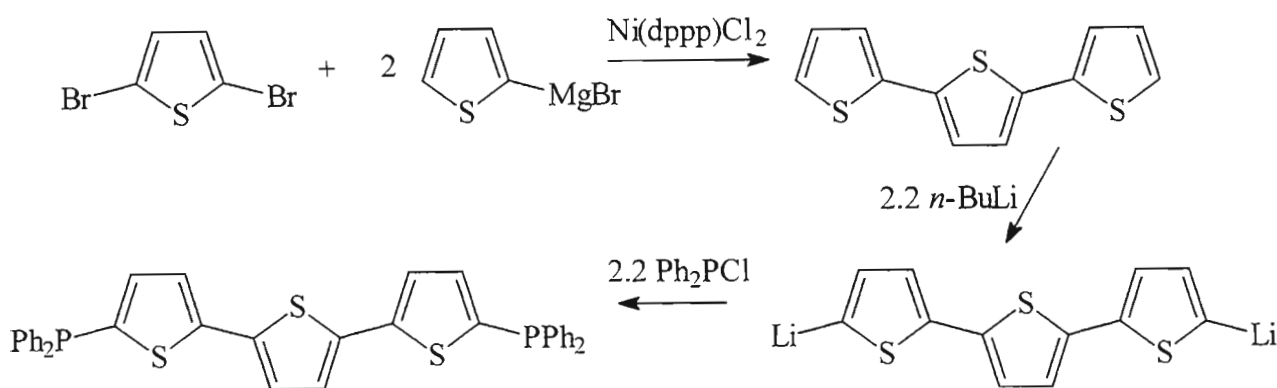
The spectroscopic data presented in the above Tables require little comment, as they are consistent with the structure of PSS being a combination of features from both PSSP and SS. The ^{31}P chemical shift of PSS is within experimental error that of PSSP, thus indicating that the second diphenylphosphino group in PSSP has no influence on the chemical shift of the phosphorus atom in the first diphenylphosphino group. This conclusion is supported by the fact that both the ^1H and ^{13}C NMR spectra of PSS can be interpreted as approximate superimpositions of equivalent spectra of SS and PSSP: PSS = one half of SS molecule + one half of PSSP molecule. (The spectroscopic properties of SS were measured in this work under conditions identical to those used to characterise PSS, so that their spectra could be meaningfully compared.)

The UV-vis spectrum of a solution of PSS in dichloromethane differs from that of PSSP and SS in that it has the higher wavelength absorption maximum at 330 nm, a value intermediate between the maxima of 350 and 305 nm, observed for PSSP and SS respectively. This observation is consistent with the finding of Zimmer *et al.*¹⁸⁴ that the second absorption maximum shifts systematically to the red as bromine substituents are introduced into positions 5 and 5' of SS. Noteworthy is that the extinction coefficients for both peaks in the spectrum of PSS are lower than those recorded for PSSP ($1.34\cdot 10^4$ vs. $1.95\cdot 10^4$ and $1.60\cdot 10^4$ vs. $1.90\cdot 10^4$ $\text{M}^{-1}\cdot\text{cm}^{-1}$). Presumably this is the result of reduction of the number of phenyl rings in the molecule.

II.2.3.3 Synthesis and characterisation of 5,5''- bis(diphenylphosphino)-2,2':5',2''-terthiophene (PSSSP)

Preparation of 5,5''-bis(diphenylphosphino)-2,2':5',2''-terthiophene (PSSSP) was carried out according to a procedure similar to the one used for the synthesis of PSSP. The starting material, *i.e.* the parent heterocycle SSS, was obtained using modification of Kumada's method¹⁸³ (see Appendix A).

The dimetallation of SSS with *n*-BuLi using a slight stoichiometric excess over the stoichiometric amount (2.2 molar equivalents) in dry ether at 0° followed by addition of the corresponding amount of diphenylchlorophosphine afforded the desired phosphine in 66% yield. The reaction sequence for the synthesis is shown in Scheme II.43.



SCHEME II.43

The amount of by-products formed as the result of this reaction is not large, and the target diphosphine is easily separated from impurities by a combination of precipitation and chromatographic methods. The pure PSSSP is a bright yellow crystalline compound. Unfortunately no crystals of suitable quality could be found to carry out an X-ray analysis.

The chemical stability of this diphosphine is the same as that of the previously described thienyl phosphines, *i.e.* it can be kept in contact with atmospheric oxygen for a very long time without noticeable changes. However, exposure to light even in the atmosphere of nitrogen soon leads to discoloration of the compound and the formation of unidentifiable by-products. Fortunately, they can be separated from PSSSP by chromatography on silica. The solubility of PSSSP in common organic solvents is somewhat better than that of PSSP, but not as good as that of the parent heterocycle, SSS: it dissolves easily in THF and

chlorinated solvents; partially in ether, petroleum ether and ethanol; and poorly in methanol and acetone.

The spectroscopic and mass spectrometric data for PSSSP are given in Tables II.9a and II.9b respectively.

Table II.9a NMR data for 5,5''-bis(diphenylphosphino)-2,2':5',2''-terthiophene, as measured in CDCl₃

$\delta^{31}\text{P}$, ppm	$\delta^{13}\text{C}$, ppm	$\delta^1\text{H}$, ppm
-18.71 (s)	124.4 (d, C _{Th-3}), 124.8 (s, C _{Th-3'}), 128.6 (d, C _{Ph-3}),	7.00 (s, 2 H, H _{Th-3'}),
	129.0 (s, C _{Ph-4}), 133.0 (d, C _{Ph-2}), 136.0 (s, C _{Th-2'}),	7.13-7.25 (ABX system,
	137.3 (d, C _{Th-4}), 137.4 (d, C _{Ph-1}), 138.0 (d, C _{Th-5}),	4 H, H _{Th-3} + H _{Th-4}),
	143.5 (s, C _{Th-2})	7.33-7.48 (m, 20 H, H _{Ph})

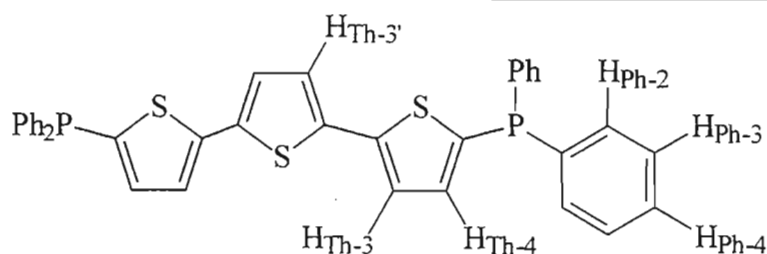


Fig. II.6 Numbering scheme for hydrogen atoms in the PSSSP molecule

Table II.9b Spectroscopic data for 5,5''-bis(diphenylphosphino)-2,2':5',2''-terthiophene

UV [*] : λ_{max} , nm (ϵ , M ⁻¹ ·cm ⁻¹)	IR ^{**} : ν , cm ⁻¹	MS (direct injection): m/z (molar mass, g·mol ⁻¹)
230 (1.90·10 ⁴), 253 (sh [‡] , 1.7·10 ⁴) 388 (2.45·10 ⁴)	482 (s), 499 (s), 507 (m), 551 (m), 694 (vs), 742 (vs), 798 (vs), 800 (s), 869 (w), 912 (m), 983 (s), 1001 (w), 1026 (w), 1070 (w), 1091 (m), 1157 (m), 1202 (m), 1213 (w), 1433 (s), 1480 (m), 1494 (w), 1583 (w)	616.07 (616.81)

^{*} UV-vis measurements were carried out in dichloromethane

^{**} IR data were obtained as KBr discs

[‡] shoulder on the main peak

The molecule of PSSSP is symmetrical, thus its NMR spectra are uncomplicated. The ^{31}P NMR chemical shift of PSSSP is very similar to that of both PSS and PSSP, indicating that the presence of the third thiophene ring has little effect on the local magnetic field at the phosphorus atom attached to the first thiophene. Both the ^1H and ^{13}C NMR spectra of PSSSP largely resemble those of PSSP with the only additions being signals due to the middle thiophene ring (compare Tables II.7a and II.9a). The assignment of these was made by comparison with the equivalent spectra of the parent compound, SSS.

The UV-vis spectrum of the PSSSP solution shows the same feature that was observed for the bithiophene based phosphines *i.e.*, in addition to the usual peak at 230 nm assigned to the phenyl groups, a second peak with a λ_{max} of 388 nm is visible that is red-shifted compared to the equivalent peak in SSS itself ($\lambda_{\text{max}} = 356$ nm). A further feature present in this spectrum but not in that of PSSP is a clearly pronounced shoulder on the first peak at 253 nm, this coinciding with the first absorption maximum in the spectrum of SSS.

As in previous cases, the IR spectrum of PSSSP does not provide any unique or specific information, while the mass spectrum simply confirms the molecular mass of the compound.

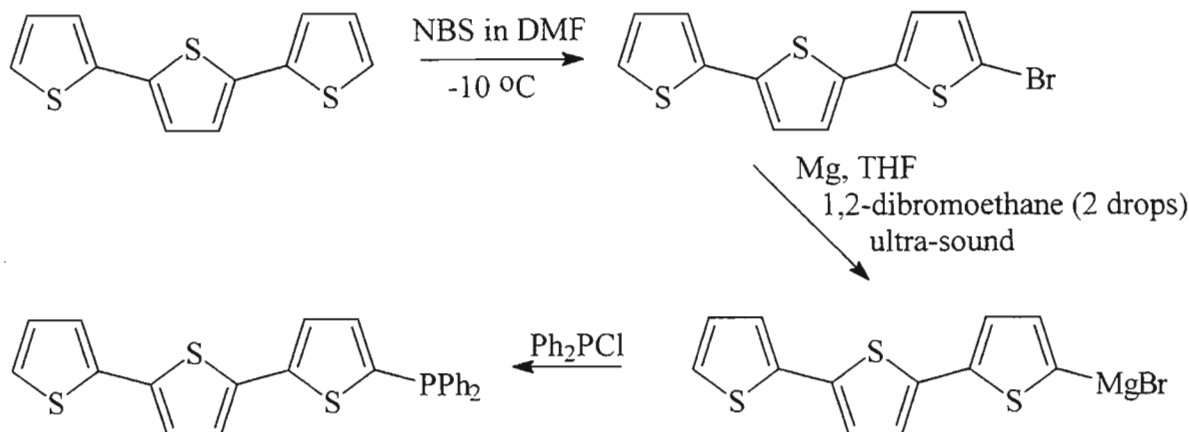
II.2.3.4 Synthesis and characterisation of diphenyl[5-(2,2':5',2''-terthienyl)]phosphine (PSSS)

It proved just as difficult to achieve selective monolithiation of SSS as was the case for SS (see Section 2.3.2 of this Chapter). For this reason, further efforts to synthesise the target phosphine, PSSS, focused on the Grignard route.

Preparation of 5-bromo-2,2':5',2''-terthiophene turns out to be far less difficult than that for 5-bromo-2,2'-bithiophene. The compound can be obtained in 77% yield according to a slight modification of the method of selective monobromination developed by Bäuerle and Effenberger,¹⁹¹ which involves low temperature bromination with NBS in dimethylformamide (see Appendix A).

However the subsequent step *i.e.*, the reaction between magnesium and the bromo-compound, required special conditions. It was found that the reaction only took place in the presence of an entrainer (1,2-dibromoethane) with continuous ultrasonic activation, and at a

temperature no less than 20°. After the formation of the Grignard reagent was complete, the mixture was quenched with diphenylchlorophosphine, producing the desired phosphine. The synthesis of PSSS is presented in Scheme II.44.



SCHEME II.44

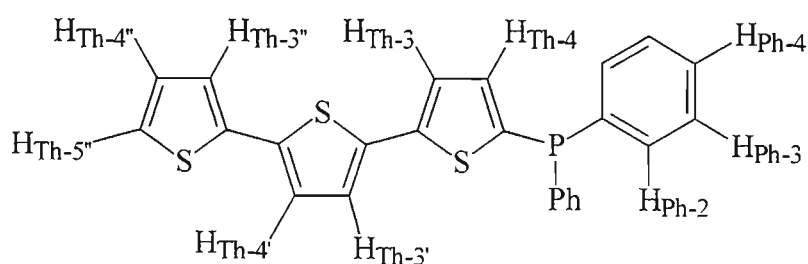
The total yield of PSSS, starting from SSS, is 30%. In particular, the yield during the final step of the synthesis is only 39%. Although the latter is considerably better than the yield of the PSS in the final step of the synthesis (approximately 25%), it still falls short of the yield of the related diphosphine, PSSSP (66%). It is believed that the drop of yield on going from a diphosphine to the corresponding monophosphine can be attributed to their very different physical properties. For example, while both PSSP and PSSSP are highly crystalline compounds, PSS and PSSS are amorphous powders, with the former even proving difficult to precipitate as a solid from solution. Also, diphosphines are much less soluble in common organic solvents than the corresponding monophosphines, which makes the recovery of the latter less efficient.

The PSSS compound retains the yellow colour of the parent compound, SSS, although it has a somewhat different tinge to it. The compound is stable in air, but decomposes in light, forming unidentifiable products. For this reason PSSS is best stored in the absence of light, especially in view of the difficulties experienced in crystallisation of the compound in reasonable quantities from solution.

The spectroscopic and mass spectrometric data for PSSS are given in Tables II.10a and II.10b.

Table II.10a NMR data for 5-diphenylphosphino-2,2':5',2''-terthiophene, as measured in CDCl_3

$\delta^{31}\text{P}$, ppm	$\delta^{13}\text{C}$, ppm	$\delta^1\text{H}$, ppm
	124.3-125.0 (m, $\text{C}_{\text{Th-3}'} + \text{C}_{\text{Th-4}'} + \text{C}_{\text{Th-4}''} + \text{C}_{\text{Th-5}''}$), 125.2 (d, $\text{C}_{\text{Th-3}}$), 128.6 (s, $\text{C}_{\text{Th-3}''}$), 129.2 (d, $\text{C}_{\text{Ph-3}}$), 129.6 (s, $\text{C}_{\text{Ph-4}}$), 133.8 (d, $\text{C}_{\text{Ph-2}}$), 137.7 (d, $\text{C}_{\text{Th-4}}$), 137.0-139.0 (m, $\text{C}_{\text{Th-5}} + \text{C}_{\text{Th-2}'} + \text{C}_{\text{Th-5}'} + \text{C}_{\text{Th-2}''} + \text{C}_{\text{Ph-1}}$), 144.2 (s, $\text{C}_{\text{Th-2}}$)	6.99-7.06 (m, 3 H, $\text{H}_{\text{Th-3}'} + \text{H}_{\text{Th-4}'} + \text{H}_{\text{Th-4}''}$), 7.15-7.27 (m, 4 H, $\text{H}_{\text{Th-3}} + \text{H}_{\text{Th-4}} + \text{H}_{\text{Th-3}''} + \text{H}_{\text{Th-5}''}$), 7.32-7.48 (m, 10 H, H_{Ph})

**Fig. II.7** Numbering scheme for hydrogen atoms in the PSSS molecule**Table II.10b** Spectroscopic data for 5-diphenylphosphino-2,2':5',2''-terthiophene

UV*: λ_{max} , nm (ϵ , $\text{M}^{-1}\cdot\text{cm}^{-1}$)	IR**: ν , cm^{-1}	MS (direct injection): m/z (molar mass, $\text{g}\cdot\text{mol}^{-1}$)
228 ($1.34\cdot 10^4$), 250 (sh [#] , $1.12\cdot 10^4$), 374 ($2.0\cdot 10^4$)	474 (m), 494 (s), 509 (m), 550 (w), 695 (vs), 746 (s), 793 (vs), 835 (m), 862 (w), 900 (vw), 984 (m), 1028 (vw), 1055 (vw), 1092 (w), 1155 (vw), 1196 (w), 1228 (w), 1422 (m), 1433 (s), 1454 (w), 1479 (m)	432.02 (432.55)

* UV-vis measurements were carried out in dichloromethane

** IR data were obtained as KBr discs

shoulder on the main peak

The data presented in the Table II.10a bear a close resemblance to the values obtained for the other polythiophene based phosphines, PSS and PSSSP. As expected, the ^{31}P NMR chemical shift of PSSS is equal (within experimental error) to those of the other three related phosphines, PSS, PSSP and PSSSP. The PSSS molecule does not possess any point

symmetry elements, which makes assignment of the peaks in its ^1H and ^{13}C NMR spectra difficult. Although the spectra contain peaks easily recognisable from the previous assignments, certain signals cannot be unequivocally ascribed to specific atoms, even when established trends are noted. This is in part due to the presence of nuclei with very similar chemical environments, *e.g.* atoms in the second and third thiophene rings give rise to signals that overlap and thus, unfortunately, can only be described as multiplets.

As was noted before with the other phosphines, the IR spectrum of PSSS contains little information. The UV-vis spectrum of PSSS has two absorption maxima as well as a shoulder on the peak of lower wavelength, corresponding to the λ_{max} for the highest energy peak in the spectrum of SSS. Again, there is a bathochromic shift (compared to SSS) of the second absorption maximum. Table II.11 gives a summary of the effect of diphenylphosphino substituents in positions 5 and 5'/5" of 2,2'-bithiophene and 2,2':5',2"-terthiophene on the value of the second absorption maxima.

Table II.11 The λ_{max} values of the long wavelength peak of the parent heterocycles SS and SSS and their diphenylphosphino substituted derivatives (all UV-vis spectra recorded in dichloromethane)

Compound	λ_{max} , nm	Δ^* , nm
SS	305	-
PSS	330	25
PSSP	350	45
SSS	355	-
PSSS	374	19
PSSSP	388	33

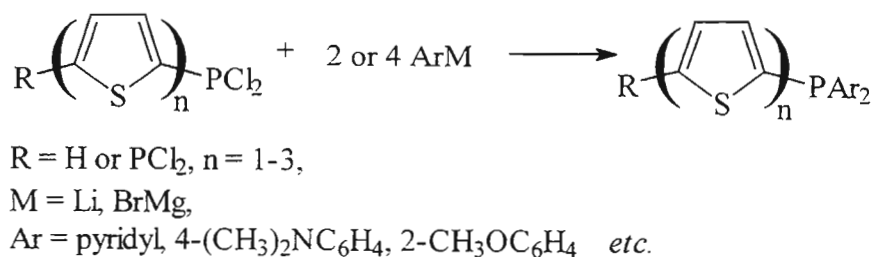
* Δ is the difference between the λ_{max} of the phosphine and its parent heterocycle

It is clear from Table II.11 that each added diphenylphosphino group causes a progressive red shift in λ_{max} . However, these shifts are different in the bithiophene and terthiophene series. This has been attributed to increased thermal motion with increasing the molecule size; increased thermal motion leads to a decrease in planarity and a concomitant increase in the energy of the $\pi \rightarrow \pi^*$ transition.¹⁸⁴

II.2.4 Attempted synthesis of thiophene-based phosphines with highly polar substituents

The novel mono- and polythiophene-based phosphines which have been synthesised so far (with the possible exception of PSBr), appear to exhibit an unfavourable solubility pattern *i.e.* they are much more soluble in non-polar rather than polar solvents. This markedly decreases the potential use of these thienyl-substituted phosphines in reactions carried out in strongly polar media. Recent trends, however, indicate that water-soluble phosphines are becoming increasingly important industrially as ligands for metal-based catalysts in two-phase organic syntheses.¹⁹⁶⁻²⁰¹ Furthermore, phosphine ligands with polar substituents^{17,124} confer promising biological activity on complexes with gold(I). In keeping with the general aims of this work and taking into account the benefits of the above applications, the synthesis of a water-soluble polythiophene-based phosphine or at least a thiophene-based phosphine with very polar substituents has been undertaken.

The first synthetic strategy that was considered is presented in Scheme II.45. According to this Scheme, the thiophene-substituted dichlorophosphine is reacted with an organometallic substrate containing polar aryl groups to produce the target phosphine (although the methoxyphenyl is not a very polar group, it can be modified by acid hydrolysis to yield the corresponding highly polar hydroxy derivative). This approach was favoured over the alternative one, where a metallated thiophene would have been reacted with a chlorophosphine containing two polar substituents, due to unavailability of the latter reagent.

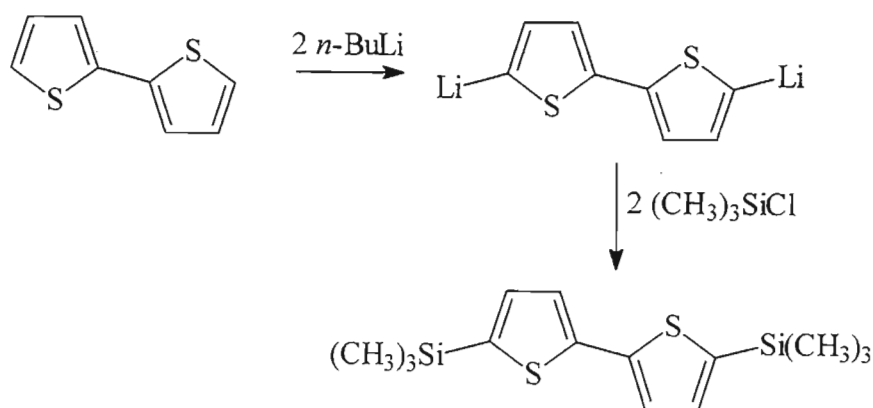


SCHEME II.45

The thiophene-substituted dichlorophosphine is clearly the key precursor in the proposed synthetic sequence. Hence several options of introducing a PCl_2 group onto a thiophene moiety have been studied.

The classic Friedel-Crafts method of phosphination of an aromatic ring with phosphorus trichloride in the presence of AlCl_3 or SnCl_4 as catalysts was tried first. Although Bentov *et al.*¹⁵⁵ have reported the successful preparation (40% yield) of 2-thienylphosphonous dichloride from thiophene and PCl_3 with SnCl_4 as a catalyst, our attempts to phosphinate SS (as a model thiophene moiety) with PCl_3 in the presence of either AlCl_3 or SnCl_4 led to inseparable complex mixtures (numerous peaks were observed in the ^{31}P NMR spectra throughout the spectral region of 200 to -50 ppm). The appearance of a number of phosphorus containing products is most likely the result of poor selectivity due to the use of AlCl_3 and SnCl_4 as catalysts, which leads not only to the formation of biarylated and triarylated PCl_3 derivatives, but also to possible introduction of the phosphorus substituent on different positions of the bithiophene molecule, thus giving rise to a large variety of peaks in the ^{31}P NMR spectrum. Distillation of the mixture under high vacuum did not lead to separation of products, because of the high temperature which was required, this resulting in decomposition of the products.

The next attempt at introducing a PCl_2 group into the molecule was based on the method described in the introduction to this Chapter, *i.e.* the substitution of trimethylsilyl groups attached to an organic moiety by chlorophosphines (see Section 1.3 of this Chapter). With this approach in mind, and with 2,2'-bithiophene serving again as the model polythiophene substrate, the novel bis(silylated) derivative, 5,5'-bis(trimethylsilyl)-2,2'-bithiophene (SiSSSi), was prepared (Scheme II.46).



SCHEME II.46

The product of the above reaction was characterised using ^1H NMR spectroscopic and GCMS analyses. The ^1H NMR spectrum of the compound is remarkably simple in

appearance consisting of one singlet at 0.33 ppm and a doublet of doublets at 7.17 ppm in the expected 9:2 ratio. The former signal undoubtedly belonged to the hydrogens of the methyl groups on the silyl substituents, while the latter corresponded to the hydrogens H_{Th-3} and H_{Th-4} of the bithiophene moiety (AB coupling pattern). The gas-chromatographic analysis of SiSSSi showed the largest intensity, highest molar mass peak at $m/z = 309.85$ which is easily assigned to the $(M^+ - 1)$ ion. The fragmentation pattern also confirmed the presence of the $Si(CH_3)_3$ groups, both $m/z = 72.95$ (due to the group itself) and $m/z = 237.20$ (due to the loss of the group from the molecule) being present in the spectrum. Also evident in the mass spectrum is a peak $m/z = 164.70$ corresponding to the mass of the 2,2'-bithiophene moiety less one unit.

Using the conditions employed by Whitesides *et al.*,¹⁵¹ a mixture of 5,5'-bis(trimethylsilyl)-2,2'-bithiophene and freshly distilled phosphorus trichloride was refluxed under an atmosphere of dry nitrogen for 5 hours. The volatile compounds were removed under vacuum and the residual oil was analysed for presence of the target dichlorophosphinated compound. The ^{31}P NMR spectroscopic analysis revealed the presence of only one phosphorus containing species – the starting material, PCl_3 ($\delta = 219$ ppm). Acid hydrolysis of the reaction residue resulted in an 88% recovery of 2,2'-bithiophene, confirming that the reaction did not proceed. Increasing the reaction time from 5 to 24 hours did not affect the outcome of the experiment nor did the substitution of PCl_3 by Ph_2PCl or $(-OCH_2CH_2O-)PCl$ (2-chloro-1,3,2-dioxaphospholane - *vide infra*). Attempts to carry out the reaction in an inert solvent such as THF, benzene and toluene at various reaction temperatures also failed. The reason why it was not possible to make this reaction work is not clear: the thiophene backbone structure does not appear to be any worse a substrate for electrophilic attack by PCl_3 as the other compounds used previously with this method (see Section 1.3 of this Chapter). Unfortunately, there was no research conducted concerning the mechanism of the above reaction and the available selection of the substrates for which the method did work was very limited, thus it seems impossible to suggest a reason why the reaction failed in our case.

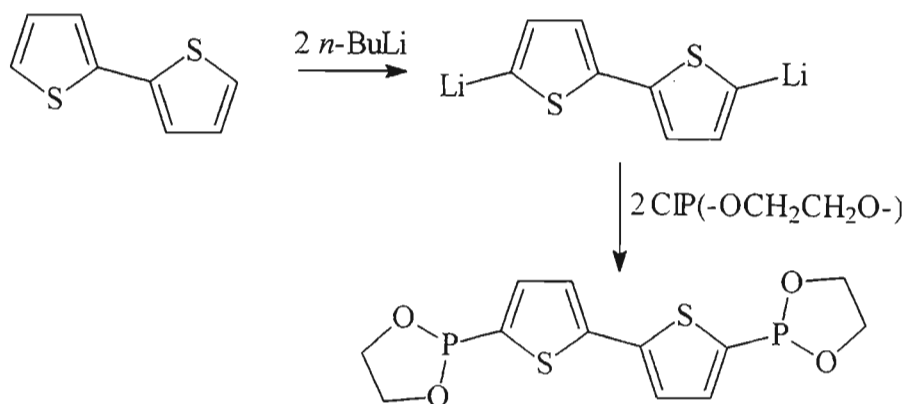
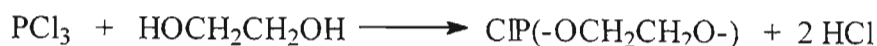
Although PCl_3 could not substitute a trimethylsilyl group in position 5 of 2,2'-bithiophene, it exhibited much greater activity in its reaction with the chloromercurated derivative, 5-chloromercurio-2,2'-bithiophene. This compound can be easily prepared in pure form from SS, mercuric chloride and sodium acetate (see Appendix A for details). A mixture of 5-

chloromercuro-2,2'-bithiophene and excess of phosphorus trichloride was thoroughly degassed and sealed in a glass bomb. The mixture was heated at 140°C for 72 hours, during which time the solution became yellow and a grey precipitate separated. The bomb was cooled down slowly and opened under atmosphere of dry nitrogen. A vacuum was applied until a very viscous oil was obtained. The ^{31}P NMR spectroscopic analysis of the neat oil showed the presence of several compounds, including the starting material, PCl_3 ($\delta = \pm 219$ ppm), one major ($\delta = \pm 142$ ppm) and 3 minor ($\delta = \pm 51, 19$ and 10 ppm) components. The major compound is believed to be the target species on the basis of its ^{31}P NMR chemical shift, as the chemical shift for PhPCl_2 was measured to be ± 157 ppm and the resonance of the thiophene analogue was expected to be 10-15 ppm further upfield. In order to effect its separation, a distillation under vacuum was attempted. Unfortunately, as the temperature in the distillation flask reached 150°C ($p = 0.4$ mm Hg), polymerisation occurred and the product could not be recovered. A similar reaction was carried out with diphenylchlorophosphine instead of phosphorus trichloride. However, after opening the bomb and examining the dark oily mixture, very little of the target phosphine (PSS, $\delta = \pm -18$ ppm) was observed. At the same time there were a large number of other peaks in the ^{31}P NMR spectrum that could not be successfully assigned. No attempts to isolate the phosphine from this complex mixture were made.

As all attempts to introduce a PCl_2 group on a polythiophene molecule proved to be unsuccessful, our interest shifted to preparation of a PBr_2 -substituted species instead. Recently Tolmachev *et al.*¹⁵⁷ reported a method of phosphination of furan and thiophene compounds with PBr_3 in the presence of pyridine. The reaction was very successful in the case of furan and could even be carried out under mild conditions. In the case of thiophene, however, the reaction had to be carried out at a high temperature in a sealed bomb. We used SSS as a model polythiophene compound during this work. Stoichiometric amounts of 2,2':5',2''-terthiophene and degassed phosphorus tribromide (1:2 molar ratio) were placed in dry pyridine and heated to 150°C for 24 hours. A dark viscous oil was obtained which could not be distilled under vacuum. The ^{31}P NMR spectroscopic analysis of the part of the mixture extracted into dry benzene revealed the presence of many peaks, mainly in the region between 5 and 25 ppm, which did not correspond to the expected value of ± 150 ppm. Lowering the reaction temperature to 120°C resulted in the reaction not proceeding at all. The failure of the reaction was attributed to possible polymerisation of any disubstituted product formed and to possible oxidation of the mixture with residual

oxygen in the pyridine solution. For these reasons, in the next experiment the SSS was substituted by 5-bromo-2,2':5',2''-terthiophene to block one of the two active sites of the heterocycle and the pyridine was thoroughly degassed. The outcome however did not change: the reaction failed to proceed below 115°, while heating above 125°C led to appearance of an insoluble brown precipitate, which was different from the expected pyridine hydrobromide and most likely was polymeric in nature.

It was mentioned in the introduction to this Chapter that phosphites could be used as an alternatives to halophosphines in reactions with Grignard reagents. Thus the next attempt at the synthesis of a substrate for the sequence shown in Scheme II.47 involved preparation of a polythiophene substituted with dialkoxyphosphino group. To derivatise the 2,2'-bithiophene with dialkoxyphosphino groups, 2-chloro-1,3,2-dioxaphospholane was used. Chlorodialkylphosphites are usually highly reactive compounds, which quickly undergo hydrolysis, oxidation and rearrangement reactions. However, the presence of a 5-membered ring in its structure results in 2-chloro-1,3,2-dioxaphospholane being relatively stable, and for this reaction it was used. The reactions leading to the synthesis of the target compound are presented in Scheme II.47.



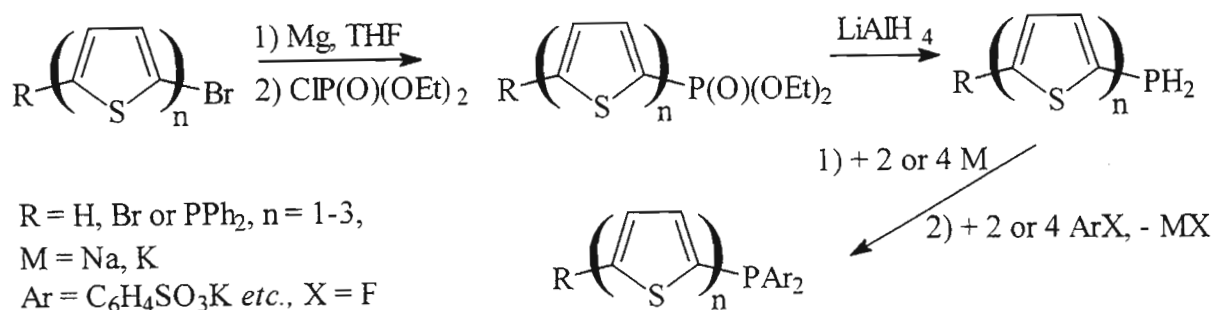
SCHEME II.47

The preparation of the reagent 2-chloro-1,3,2-dioxaphospholane is described in the literature.²⁰² A THF solution containing 5,5'-dilithium-2,2'-bithiophene was added slowly to a solution of the reagent (1:2 mole ratio). The addition was carried out at -78°C, but no reaction could be observed at this temperature and therefore, the temperature was increased to -20°C. After stirring at this temperature for 0.5 hour, there was still no sign of any

reaction and the solution was warmed to -5°C . After 0.5 hour at that temperature, the solution started changing its appearance and an oily precipitate appeared. This precipitate was insoluble in benzene or chloroform and was most likely to be polymeric in nature. The mother liquor was analysed by ^{31}P NMR spectroscopy and only 2 compounds were detected. The major compound was the starting material ($\delta = \pm 169\text{ ppm}$) and the minor had a chemical shift of $\pm 19\text{ ppm}$, which made it unlikely be the target compound as the shift was more characteristic of P(V) derivatives.

At this stage attempts to synthesise a suitable substrate for the reaction shown in the Scheme II.47 were terminated and the strategy was changed.

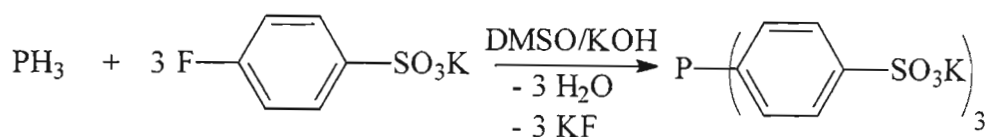
The new approach involved phosphorylation of a thiophene precursor to afford a P(V) compound which would subsequently be reduced to the P(III) state and then modified with polar substituents (Scheme II.48).



SCHEME II.48

The phosphorylation of thiophene was best achieved by Allen *et al.* in 1972,²⁰³ when they reported the preparation of diethyl (2-thienyl)phosphate via the reaction of 2-thienylmagnesium bromide with diethyl chlorophosphate at 40°C . Although they did not carry out a reduction of the P(V) derivative to the primary phosphine, the second step of the reaction sequence outlined above does not appear to be difficult, as it is a standard technique in phosphine synthesis. The last step in the Scheme II.48 involves metallation of the primary phosphine followed by reaction with an arene containing a highly polar sulfonate group. This part of the strategy is based on the recently developed method for the preparation of water-soluble phosphines, which has received considerable attention in the past ten years. Most of the work has been devoted to development of aromatic phosphines

such as trisulfonated triphenylphosphine²⁰⁴ Traditionally, phosphines with *meta*-sulfonated phenyl groups have been obtained by direct sulfonation with oleum of neutral phosphines bearing aromatic substituents. The drawback of that method is not only the formation of derivatives with variable degree of sulfonation, but also the oxidation of phosphorus. However newer methods avoid the direct sulfonation of aromatic rings and employ alternative synthetic strategies for the introduction of sulfonyl groups into the molecule. The recent synthetic approach^{205,206} involves nucleophilic aromatic phosphination of either *para*- or *ortho*-fluorosubstituted benzene containing one or two SO₃K or SO₃Na groups with PH₃, primary and secondary phosphines in superbasic media (*e.g.* DMSO/KOH) as shown in Scheme II.49.

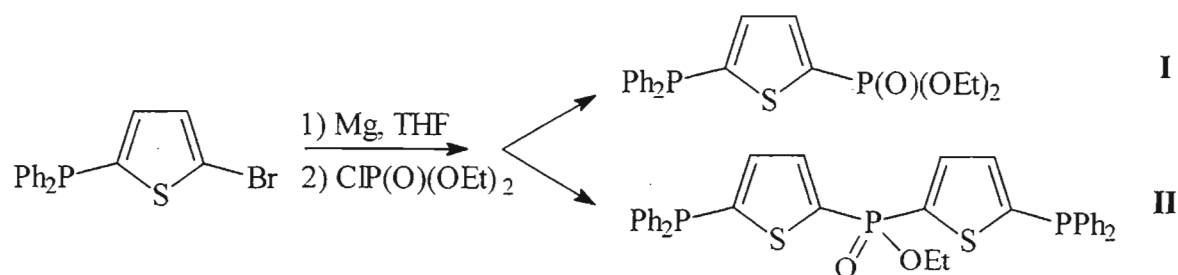


SCHEME II.49

The phosphorylation strategy was applied to several thiophene-containing compounds, selected on the basis of their availability in reasonable quantities at the time of the synthesis. Initially, 5,5'-dibromo-2,2'-bithiophene was treated with magnesium in order to furnish the di-Grignard reagent. However this reaction required additional activation in order to proceed, such as the use of an entrainer and ultrasonication, and on most occasions did not go to completion, *i.e.* both mono- and di-Grignard reagent were present in the reaction mixture. This led to a small change in the method, which involved lithiation instead. Lithiation of 2,2':5',2''-terthiophene at the positions 5 and 5'' was successfully achieved according to the technique described in the Section 2.3.3 of this Chapter. The solution of metallated heterocycle was added under nitrogen to a thoroughly degassed solution of diethyl chlorophosphate [ClP(O)(OEt)₂], present in 10% excess, refluxed for 30 minutes, then stirred at room temperature for 16 hours. After hydrolysis with dilute acid, an amorphous precipitate was observed which proved to be insoluble in organic solvents such as dichloromethane and acetone. This indicated possible formation of a polymeric compound. The mother liquor was analysed by ³¹P NMR spectroscopy, but no compounds containing a diethoxyphosphoryl group attached to a thiophene unit ($\delta = \pm 11 \text{ ppm}^{203}$) were detected. It is possible that diethyl chlorophosphate, having several active groups (one chloro and two ethoxy groups) might have reacted with two or more lithiated terthiophene

molecules, leading to the formation of a cross-linked polymer. Changing the solvent from THF to ether was not successful as 5,5''-dilithio-2,2':5',2''-terthiophene is very poorly soluble in ether and no reaction could be observed. Carrying out the reaction at ambient temperature proved to be fruitless as well.

The failure of the dimetallated species to furnish the desired diphosphorylated compound resulted in the new round of trials, this time with monometallated thiophenes. The novel phosphine PSBr has proved to be a good choice of a substrate for the production of a Grignard reagent (see Sections 2.2.1 and 2.2.2 of this Chapter), hence it was employed in the reaction with diethyl chlorophosphate using the conditions described above and as outlined in Scheme II.50. After hydrolysis of the product mixture with 0.1 M HCl and washing with NaHCO₃ solution, the mixture was extracted with dichloromethane and the solvent evaporated affording some white crystals. According to GCMS and ³¹P NMR spectroscopic methods, the mother liquor contained the target compound (**I**) with *m/z* = 404.20 (*M*⁺) and δ (³¹P) = 10.21 and -18.15 ppm *i.e.*, two singlets in a 1:1 intensity ratio. Unfortunately, the major component of the mother liquor was identified to be PS, formed most likely as the result of quenching of the Grignard reagent with HCl which is always present in diethyl chlorophosphate. Numerous attempts to separate the desired compound from PS on silica gel proved unsuccessful.



SCHEME II.50

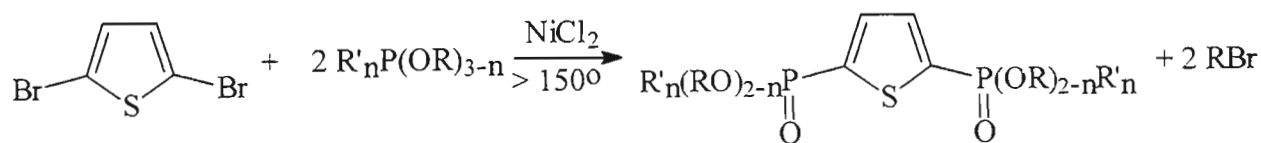
On the other hand, the precipitate separated from the mother liquor could be purified by chromatography on a Chromatotron®. The ¹H NMR spectrum recorded in CDCl₃ of the isolated compound showed that it did not contain ethyl groups, although phenyl and thienyl hydrogens were present as evidenced by a multiplet at 7.27-7.40 ppm and two doublets of doublets at 7.21 and 7.47 ppm, respectively. Also present was a broad signal at \pm 3 ppm assigned to a hydrogen of an OH group. The ³¹P NMR spectrum revealed two peaks at 4.85 and -18.24 ppm in a 1:2 intensity ratio. The compound did not produce any

response during GCMS analysis, indicating it either had a very high molar mass or was very polar and thus was retained on the column of the gas chromatograph. The combination of all these data showed clearly that the compound was different from the target species. With the aid of microanalysis results, it was finally established that the new compound corresponded to bis[5-(diphenylphosphino)-2-thienyl]phosphinic acid (DTPA); this acid is derived from compound **II** in Scheme II.50 as a result of acid hydrolysis (10% yield). It is interesting to note, that even in a compound with two phosphorus atoms in very different chemical environments and located not very far from each other, no phosphorus-phosphorus coupling is observed, even at low temperatures (-50°C , CDCl_3). The reason behind this phenomenon is not understood, although it correlates well with previous observations that the magnitude of coupling between atoms in the positions 2 and 5 of the thiophene ring is essentially negligible (see Sections 2.1 and 2.2 of this Chapter).

A brief study of the properties of the newly isolated compound, DTPA, showed that it dissolves to some extent in both polar solvents, like ethanol and acetone, and not very polar solvents such as chloroform and dichloromethane. It is air-stable like all the previously synthesised thiophene-based phosphines; thus, due to its interesting chemical nature and amphiphilic properties, it might turn out to be useful either as a precursor for a polyphosphine or in its own right.

The presence of the compound **II** in the reaction mixture is attributable to the substitution by the metallated thiophene of not only the chloro group on diethyl chlorophosphate, but also of one of the two ethoxy groups. It is likely that the product of exhaustive substitution *i.e.* of the chloro and both ethoxy groups, which would correspond to the PTSP oxide, was also formed during the reaction, but it must have been present in too small a quantity to be identified. The occurrence of this side reaction rendered the first step of the strategy proposed in the Scheme II.48 unsuitable and a new approach was investigated.

The new approach involved a modification of the Arbuzov's reaction for aromatic halocompounds. This method of introduction of phosphorus into a molecule of an aromatic compound was recently 'rediscovered' by a group of Russian chemists²⁰⁷ who reported the phosphorylation of 2,5-dibromothiophene with various phosphinic acid esters in the presence of a Ni(II) catalyst (Scheme II.51).



R = alkyl

R' = alkyl, phenyl, 2-thienyl

n = 0-2

SCHEME II.51

The product of the above reaction should serve as a good precursor for the synthesis of a primary (or a secondary) phosphine, which can be converted to the desired water-soluble phosphine according to the method in Scheme II.49. For our purposes, diethyl phenylphosphonite (R = Et, R' = Ph, n = 1) was chosen as the phosphorylating reagent due to its commercial availability as well as due to the high yield (67%) of the corresponding 2,5-diphosphorilated thiophene reported by Krasil'nikova and co-workers.²⁰⁷

However, several attempts to reproduce the results obtained by Krasil'nikova *et al.* proved totally fruitless: not even a trace of the target diphosphorylated compound was formed, although judging by the ³¹P NMR spectrum of the crude reaction mixture, some reaction definitely took place. We questioned the reported results as too few experimental details were given in the paper; moreover no characterisation data (apart from the microanalysis) was presented for the supposed products. After searching the literature, it was found that the Russian group was not the first to use this modified Arbuzov's reaction for the phosphorylation of thiophenes. In 1970 Tavs²⁰⁸ prepared various aromatic phosphonites by the reaction of trialkylphosphites and aryl halides in presence of anhydrous NiCl₂ or NiBr₂ at 150-160°C. Although at least 25 benzene-based phosphinic acid esters were successfully prepared by this method, the thiophene-based products could only be isolated as the corresponding acids after hydrolysis of the reaction mixture with methanolic NaOH followed by acidification with HCl. Tavs used 2-bromothiophene as the precursor for phosphorylated thiophenes.

We applied a slightly modified version of Tav's phosphorylation procedure²⁰⁸ (anhydrous NiCl₂ as a catalyst, 170-180°C) to 2,5-dibromothiophene, using diethyl phenylphosphonite as a phosphorylating agent. The reaction was successful and thien-2,5-diyl di(phenylphosphinic acid) (TDPA) was obtained in 24% yield. When 5,5'-dibromo-2,2'-

bithiophene was used as the starting compound, 2,2'-bithien-5,5'-diyl di(phenylphosphinic acid) (BTDP) was obtained in 34% yield. The chemical structures of TDPA and BTDP are shown in Figure II.8. Both compounds are believed to be new as their characterisation has never been reported before. The ^1H and ^{31}P NMR spectroscopic data for both compounds are given in Table II.12. (Note that the assignments of the peaks in the ^1H NMR spectrum are tentative).

Table II.12 ^1H and ^{31}P NMR data for thien-2,5-diyl and 2,2'-bithien-5,5'-diyl di(phenylphosphinic acids), as measured in CD_3OD

Compound	$\delta^{31}\text{P}$, ppm	$\delta^1\text{H}$, ppm
TDPA	19.86 (s)	7.43-7.65 (m, 8 H, $\text{H}_{\text{Ph}(m-p)} + \text{H}_{\text{Th}}$), 7.76-7.93 (m, 4 H, $\text{H}_{\text{Ph}(o)}$)
BTDP	20.08 (s)	7.56 (dd, 2 H, $\text{H}_{\text{Th-3}}$), 7.65-7.80 (m, 8 H, $\text{H}_{\text{Ph}(m-p)} + \text{H}_{\text{Th-4}}$), 7.96-8.10 (m, 4 H, $\text{H}_{\text{Ph}(o)}$)

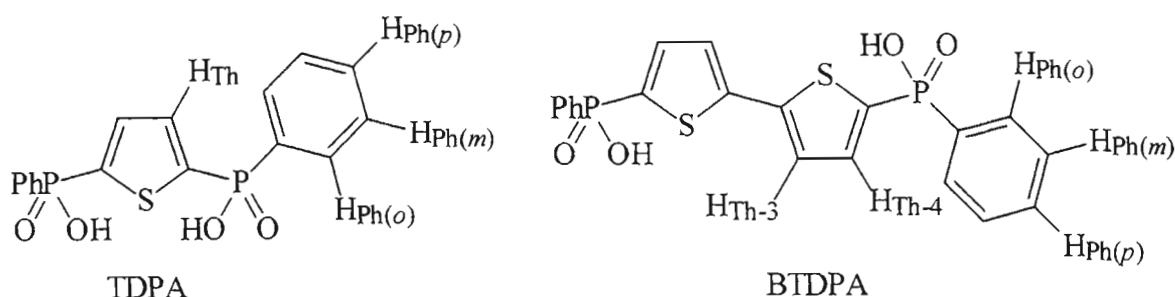


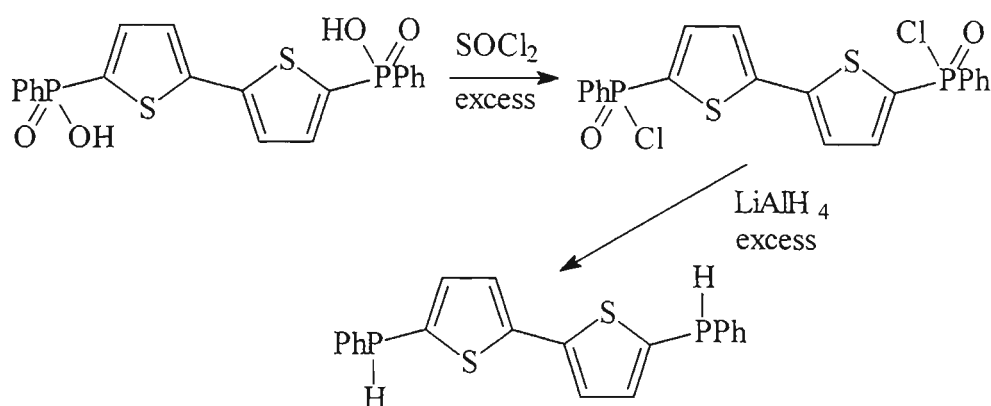
Fig. II.8 Numbering scheme for hydrogen atoms in the TDPA and BTDP molecules

Their ^{31}P NMR chemical shifts indicate that the compounds are P(V) derivatives since their δ values are very close to the value of ± 21 ppm for diphenylphosphinic acid. The IR spectrum of BTDP recorded as KBr pellet exhibited peaks characteristic of P-OH ($\nu = 2673\text{ cm}^{-1}$, w, br), P=O ($\nu = 1200\text{ cm}^{-1}$, s) and P-Ph ($\nu = 1425\text{ cm}^{-1}$, s) bonds.²⁰⁹

As the compounds are only intermediates in the synthesis of the target water-soluble phosphines, a full characterisation was not carried out. The acids are crystalline air-stable compounds, soluble with difficulty in non-polar solvents (dichloromethane) and easily soluble in polar solvents such as methanol and ethanol.

The next step of the synthetic sequence was the conversion of the phosphinic acid into a secondary phosphine, BTDP being selected as it was obtained in greater yield. Acids

cannot be converted directly into the secondary phosphines, thus BTDDPA had to be converted first in an acid chloride which would then be reduced by LiAlH_4 . General techniques from the Houben Weyl Handbook²¹⁰ were used for these reactions. Heating BTDDPA with thionyl chloride afforded a pale-yellow amorphous compound [$\delta(^{31}\text{P}) = 33$ ppm, measured as a neat liquid], which fumed in air and which was used in the next step as received, because attempts to distil it resulted in decomposition of the substance. The reduction of the acid chloride by LiAlH_4 in THF was completed in 12 hours. The reaction did not produce many by-products and 5,5'-bis(phenylphosphino)-2,2'-bithiophene (HPSSPH) was obtained in an overall 70% yield. The overall synthetic sequence is shown in Scheme II.52.



SCHEME II.52

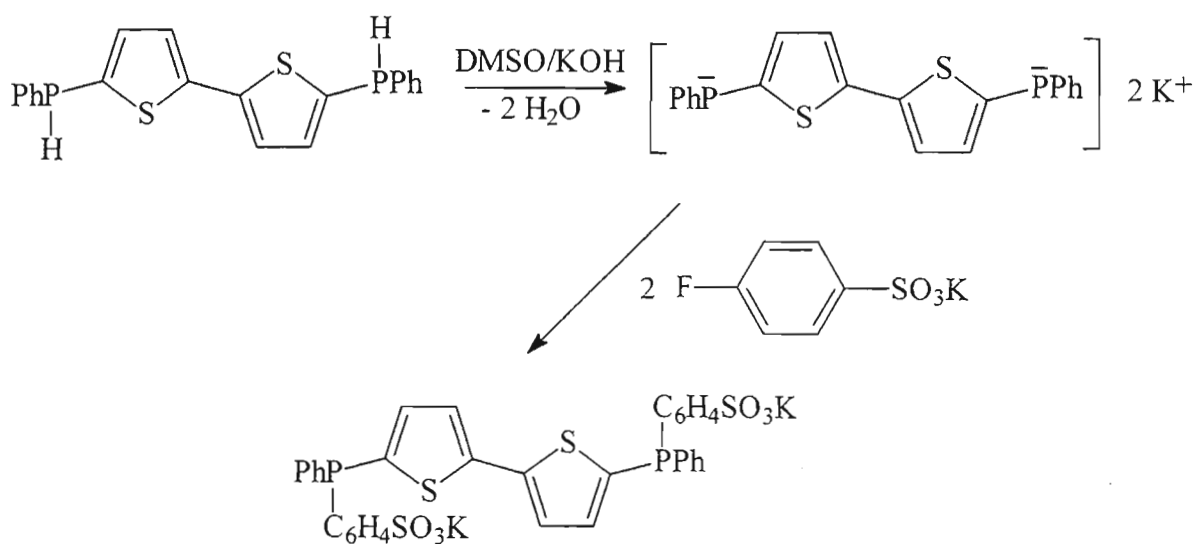
This is the first example of a thiophene-based secondary phosphine. Unfortunately, like most other secondary phosphines, this one was readily oxidised by contact with atmospheric oxygen and thus could not be completely characterised by those methods requiring prolonged handling in air, such as microanalysis and GCMS. The ^1H and ^{31}P NMR spectroscopic data for the new phosphine are given in Table II.13.

Table II.13 ^1H and ^{31}P NMR data for 5,5'-bis(phenylphosphino)-2,2'-bithiophene (HPSSPH), as measured in CDCl_3 (the numbering of the atoms corresponds to that in the Table II.12)

$\delta^{31}\text{P}$, ppm	$\delta^1\text{H}$, ppm
-64.34 (s)	5.35 (d, 2 H, $\underline{\text{H}}\text{-P}$), 7.04-7.15 (ABX system; 4 H, $\text{H}_{\text{Th-3}} + \text{H}_{\text{Th-4}}$), 7.27-7.37 (m, 6 H, $\text{H}_{\text{Ph(m-p)}}$), 7.43-7.55 (m, 4 H, $\text{H}_{\text{Ph(o)}}$)

The chemical shift value of the ^{31}P NMR signal (-64 ppm) leaves no doubt as to the identity of this compound, being characteristic for secondary phosphines. Interestingly, the signal is shifted upfield by *ca.* 23 ppm from that recorded at -41 ppm for Ph_2PH in CDCl_3 . This is somewhat higher than expected since upfield shift in the ^{31}P NMR signal associated with the replacement of a phenyl group with a thiophene group in a tertiary phosphine, is typically *ca.* 13 ppm. The assignment of the ^1H NMR signals of the new secondary phosphine was carried out as before, *i.e.* with reference to the data for its precursor, BTDPA as well as to that of the related tertiary phosphine, PSSP. Though these assignments are not certain, the doublet due to the hydrogen attached to the phosphorus atom could be unmistakably identified due to the large H-P coupling constant of 225 Hz. The signals due to the $\text{H}_{\text{Th-4}}$ and $\text{H}_{\text{Th-3}}$ atoms appear as complex multiplets in this spectrum, rather than as the expected doublet of doublets, which is probably the result of long-range coupling to the hydrogen attached to phosphorus. It should be noted that a more comprehensive NMR spectroscopic investigation of the secondary phosphine was hindered by its tendency to decompose in deuterated solvents over a period of time.

Finally the secondary phosphine was subjected to the last step in the synthesis of a water-soluble tertiary phosphine (see Scheme II.53). The compound was treated with a superbasic solution of KOH in DMSO for 30 minutes. The solution turned a deep blue colour following which the metallated intermediate was quenched with potassium 4-fluorophenylsulfonate (Scheme II.53).



SCHEME II.53

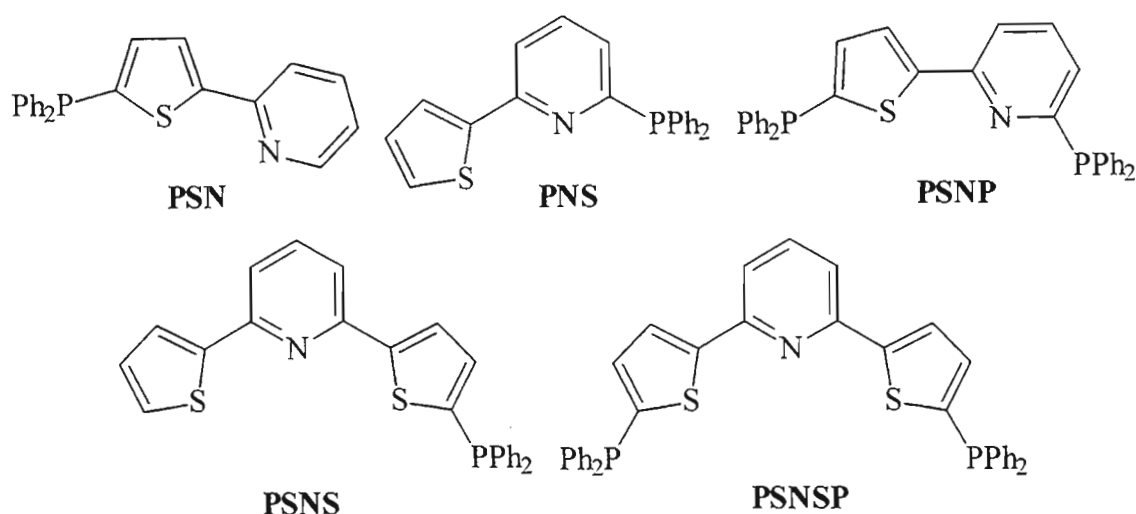
The solution was stirred at room temperature for 24 hours and a 1:1 *iso*-propanol/water mixture added. The ^{31}P NMR spectroscopic analysis of the resulting solution revealed the presence of several phosphorus-containing species as evidenced by peaks at $\delta = 25, 8, 5, -18, -27$ and -64 ppm. These data suggest the possible formation of a tertiary phosphine with two phenyl and one thiophene groups ($\delta = -18$ ppm) during the reaction. The solvent was evaporated under vacuum and neat *iso*-propanol added. However no precipitation occurred. Attempts to use chromatography to isolate the desired phosphine or any other thiophene-based phosphine for this matter were also unsuccessful. Eventually, the synthesis was abandoned.

As to why the reaction was not successful one can only speculate given the scarcity of characterisation data available. Oxidation of the secondary phosphine appears to have taken place as evidenced by appearance of several peaks in the ^{31}P NMR spectrum at ± 25 ppm, the region characteristic of P(V). Also, the peak at -64 ppm is for the starting compound, showing that metallation of the secondary phosphine by the KOH was not complete. The other peaks in the ^{31}P NMR spectrum at *ca.* 5 and -27 ppm remain to be assigned and may prove crucial in understanding the metallation of a thiophene-derived secondary phosphine. However, due to the lack of time no further investigation of this reaction was carried out.

II.2.5 Synthesis of thiophene-based phosphines containing a pyridine ring in their structure

As previous attempts to introduce a phosphino moiety with one or two highly polar substituents onto a polythiophene backbone (Schemes II.48 and II.53) proved fruitless, it was decided to introduce a polar fragment in the backbone structure instead. Aliphatic and aromatic amine substituents are potentially good candidates for increasing a molecule's affinity for polar solvents. Indeed, recent work by Leeuwen *et al.*²¹¹ revealed that phosphines modified by dialkylamino or pyridyl groups (*e.g.* 2,2'-bis[phenyl{3-pyridyl}phosphinomethyl]-3,3'-bipyridine and 2,2'-bis{[4-(diethylaminomethyl)phenyl]-phenylphosphinomethyl}-1,1'-biphenyl) show amphiphilic properties *i.e.* they are soluble in both polar and non-polar media. However aliphatic amino-substituted thiophenes are known to be unstable, thus leaving a pyridine moiety as the fragment of choice.

Although there are several ways of attaching a pyridine ring to a thiophene molecule, the 2,2-link was chosen as it matched most closely the original link between thiophene units in polythiophene (*i.e.* 2,2'-bithiophene and 2,2':5',2''-terthiophene) structures. Therefore, the synthesis of the following pyridine and thiophene containing phosphines was undertaken (Scheme II.54):



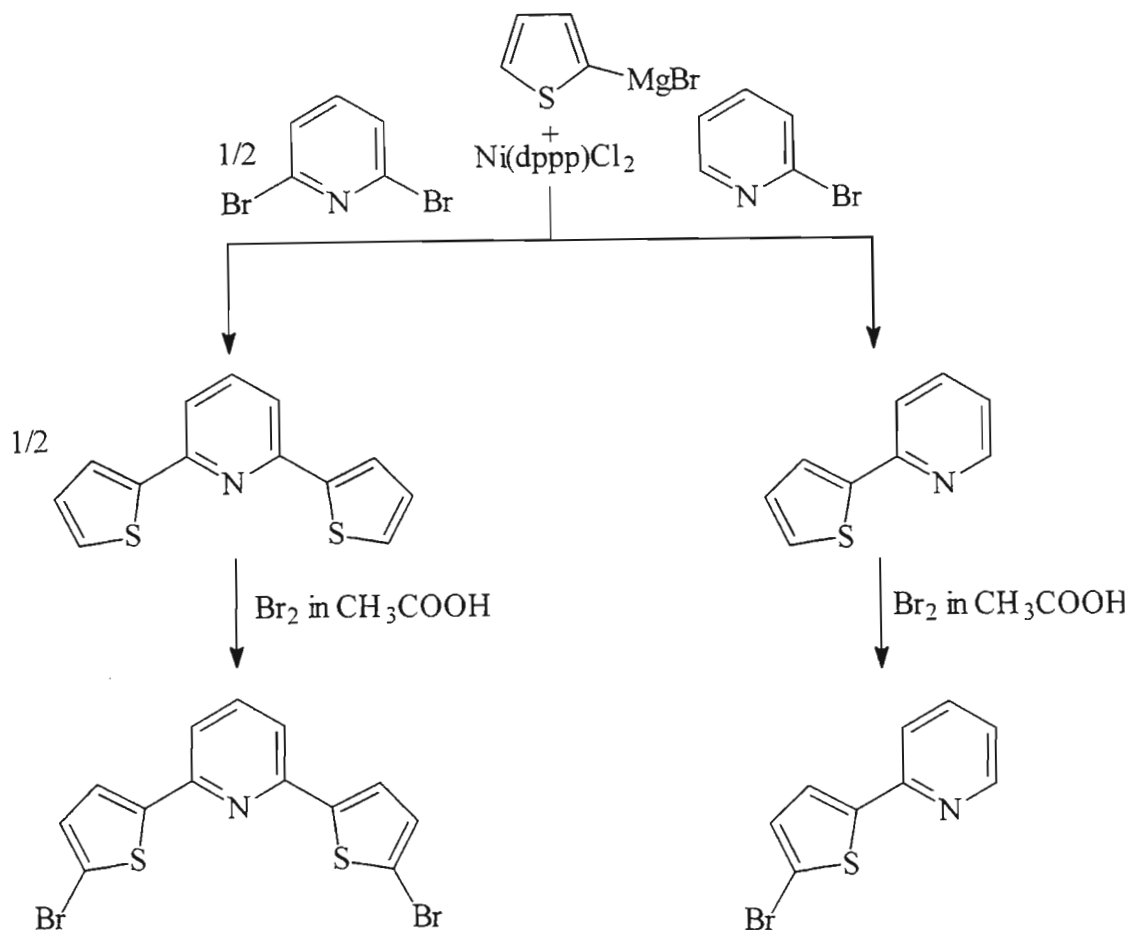
SCHEME II.54

None of the above mono- and diphosphines has been synthesised before, although there are numerous examples of the preparation of pyridine-based phosphines in the literature.^{136,173,187} It should be noted that the most widely used method for synthesis of the latter involves the reaction between a metallated phosphine and a 2-halosubstituted pyridine. This synthetic approach is totally different from the method generally used for the preparation of thiophene-based phosphines.

II.2.5.1 Synthesis of diphenyl[5-(2'-pyridyl)-2-thienyl]phosphine (PSN) and 2,6-bis((5'-diphenylphosphino)-2'-thienyl)pyridine (PSNSP)

The starting point for the synthesis of the target pyridine and thiophene-containing phosphines is the preparation of the parent non-phosphino group substituted polyheterocyclic compound. The initial strategic approach was based on the reactions which had been proven to work for the corresponding bithiophene and terthiophene phosphines.

The parent polyheterocyclic compounds SN [2-(2'-thienyl)pyridine] and SNS [2,6-bis(2'-thienyl)pyridine], were prepared according to the general methods by Kumada *et al.*¹⁸³ using a Ni(II)-catalysed coupling reaction (see Scheme II.55). Bromination at position 5 of the thiophene rings with bromine in glacial acetic acid²¹² led to formation of the corresponding bromides (Scheme II.55).



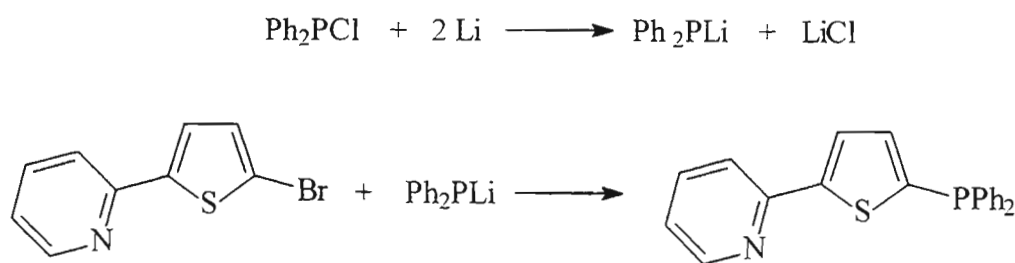
SCHEME II.55

It proved impossible to obtain a pure monobrominated derivative of SNS, even by using a variety of reagents such as KBrO_3/HBr , NBS or Br_2 in CHCl_3 or DMF.

This is the first report of the synthesis of the dibrominated compound, 2,6-bis(5'-bromo-2'-thienyl)pyridine, and thus it was duly characterised using ^1H and ^{13}C NMR, IR and UV-vis spectroscopic methods as well as by means of microanalysis for %C, %H and %N. The data can be found in the Experimental section.

The next step in the pathway towards the target phosphines involved preparation of the corresponding Grignard reagents followed by reaction with diphenylchlorophosphine. However a serious problem was encountered during the attempts to carry out these reactions: both brominated SN and SNS 'resisted' conversion to the bromomagnesium species even under activated conditions (using ultrasound and an entrainer). It was believed to be the consequence of presence of a pyridine ring which deactivated the surface of magnesium as the latter was observed to turn dull and flaky during the course of the reaction. It is also possible that the electronic effect of a pyridine substituent in the position 5 (or 2) of the thiophene plays a role; indeed, it has been shown that the electron density in the thiophene nucleus is markedly changed upon introduction of a pyridine substituent.²¹³

As the traditional Grignard route failed, it was decided to apply the method suitable for preparation of pyridine-based phosphines to obtain the desired compounds. Reaction of lithium diphenylphosphide (prepared from diphenylchlorophosphine and excess lithium metal in THF) with 2-(5'-bromo-2'-thienyl)pyridine produced a dark coloured reaction mixture, which contained (on the basis of a ^{31}P NMR spectroscopic analysis) a thiophene-based phosphine as well as tetraphenyldiphosphine, the impurity normally associated with this method of synthesis (see Section 2.2 of this Chapter). Due to the presence of a basic pyridine moiety in the molecule, the compound was successfully extracted from the complex mixture by an acidification/basification sequence, allowing it to be separated from less polar impurities. The phosphine obtained after this procedure was still not 100% pure as the ^{31}P NMR spectrum revealed the presence of several small peaks at around -18 ppm together with the main peak at -18.34 ppm. The use of column chromatography on silica with hexane-ether as eluent allowed the isolation of the desired compound, PSN, in its pure form (66% yield). The reaction sequence is presented in Scheme II.56.



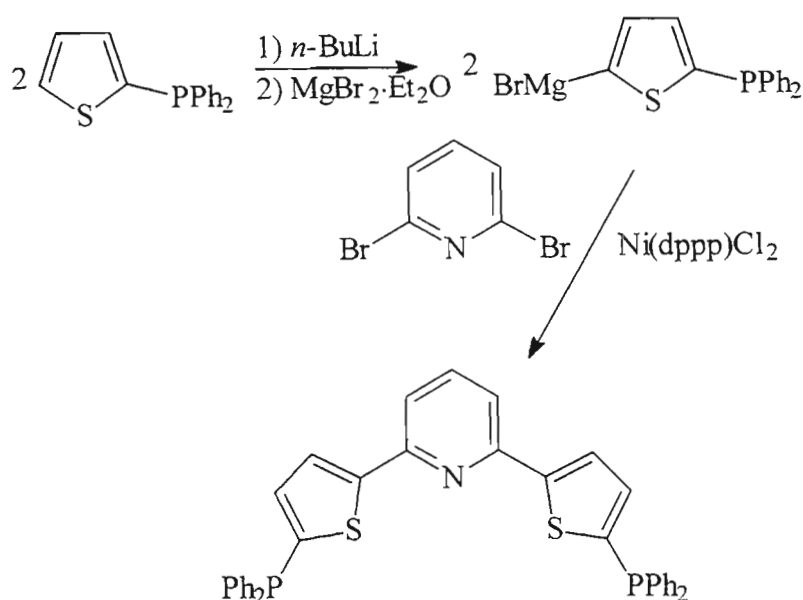
SCHEME II.56

A similar procedure was applied to 2,6-bis(5'-bromo-2'-thienyl)pyridine. The ^{31}P NMR spectrum of this reaction mixture also revealed the presence of thiophene-based phosphines as evidenced by peaks at δ ca. -18 ppm. Tetraphenyldiphosphine is also present (δ = -14 ppm). However, attempts to extract the desired compound into an aqueous phase by acidification with strong acid did not work, possibly due to the highly non-polar nature of the molecule arising from the presence of two thiophene substituents. A more conventional work-up for thiophene-based phosphines (acidic hydrolysis, followed by extraction into chloroform or dichloromethane) was then used. This removes the tetraphenyldiphosphine. The product obtained was not pure as it showed several peaks in the desired region of the ^{31}P NMR spectrum. Also microanalysis gave results different from the expected values. Chromatography of the product on silica with a variety of eluents (chloroform/ethyl acetate or dichloromethane/ethyl acetate and hexane/ether in various ratios) was not successful. Attempts to use crystallisation from different solvents also proved to be fruitless.

An alternative procedure had to be designed in order to prepare the desired PSNSP compound. It was decided to "assemble" the diphosphine in a similar manner to that used for the preparation of the parent heterocycle, in other words, to couple 2,6-dibromopyridine and the Grignard reagent of 2-diphenylphosphinothiophene (PS). The latter reagent has been used before on a number of occasions (see Sections 2.2-2.4 of this Chapter) and has been proven to provide good results. The bromomagnesium species was prepared *in situ* from lithiated PS by remetallation with MgBr_2 . The Grignard reagent thus obtained was reacted with 2,6-dibromopyridine in the presence of the $\text{Ni}(\text{dppp})\text{Cl}_2$ catalyst, affording the desired diphosphine in 54% yield. The reaction sequence leading to the synthesis of PSNSP is shown in Scheme II.57.

Due to the failure of the attempted synthesis of monobrominated SNS, the compound which would serve as a precursor for PSNS, and also due to low probability that alternative routes to the compound would prove successful (*e.g.* coupling between PSMgBr and 6-bromo-2-(2'-thienyl)pyridine*), the synthesis of PSNS was not studied during this work.

* This latter compound was never obtained in a 100% pure form (*vide infra*), being contaminated with at least 2 structurally related impurities. Thus the reaction mixture obtained after reacting it with PSMgBr would be



SCHEME II.57

Examination of the properties of the new phosphines, PSN and PSNSP, revealed that they are as resistant to oxidation as the purely thiophene-based phosphines *i.e.*, as solids, they can be kept indefinitely in air at room temperature and, as solutions in non-degassed solvents, they can withstand mild heating. Compared to the corresponding monophosphine PSS, the PSN ligand is more crystalline, manifested not only by the higher melting point (60 vs. 70°C, respectively), but also the ease with which it precipitates out of solution. It is also somewhat more soluble in polar solvents, such as methanol and ethanol, but much less soluble in hydrocarbon solvents. The PSNSP ligand also shows a considerable increase in the degree of crystallinity in comparison with its thiophene analogue, PSSSP. Again, not only is the melting point of the former compound much higher (176 vs. 149°C, respectively), but it also produces good quality single crystals upon slow evaporation from a number of solvents. The solubility of PSNSP, on the other hand, does not follow the same tendency as that of PSN. In fact, the compound exhibits poor affinity for most solvents, both polar and non-polar, which is most likely the result of the molecule's large size. It is also possible that the lone pair on the pyridine nitrogen might be shielded to some extent from interaction with the solvent molecules by the lone pair electrons of the two sulfur atoms of the neighbouring thiophene rings. That this might be the case is indicated

more difficult to separate. Taking into account that the target compound, PSNS is not symmetrical, it is unlikely to crystallise easily, suggesting that the isolation of the pure material would be extremely difficult.

by the molecule's structure, as determined by X-ray diffraction methods (*vide infra*), which shows that the lone pairs on nitrogen and both sulfur atoms 'face' the same direction. It is interesting to note that PSNSP has only a light, pale-greenish colour compared to the strong yellow of PSSSP, which indicates that substitution of a thiophene ring by pyridine significantly changes the electron energy levels in the molecule.

II.2.5.2 Characterisation of PSN and PSNSP

The ^1H , ^{13}C and ^{31}P NMR spectroscopic data for the new phosphines PSN and PSNSP are given in Table II.14. The assignments of the signals in the ^1H and ^{13}C NMR spectra were made on the basis of COSY and HETCOR spectra of both the phosphines as well as the ^1H and ^{13}C NMR spectra of the parent heterocycles.

Table II.14 NMR data for PSN, as measured in CDCl_3 , and PSNSP, as measured in CD_2Cl_2

Compound	$\delta^{31}\text{P}$, ppm	$\delta^{13}\text{C}$, ppm	$\delta^1\text{H}$, ppm
PSN	-18.35 (s)	118.8 (s, $\text{C}_{\text{Py-3}}$), 122.2 (s, $\text{C}_{\text{Py-5}}$)	7.15 (ddd, 1 H, $\text{H}_{\text{Py-5}}$), 7.29-
		125.2 (d, $\text{C}_{\text{Th-3}}$), 128.5 (d, $\text{C}_{\text{Ph-3}}$),	7.50 (m, 11 H, $\text{H}_{\text{Ph}} + \text{H}_{\text{Th-4}}$),
PSNSP	-18.28 (s)	129.0 (s, $\text{C}_{\text{Ph-4}}$), 133.1 (d, $\text{C}_{\text{Ph-2}}$),	7.57 (dd, 1 H, $\text{H}_{\text{Th-3}}$), 7.61-
		136.7 (s, $\text{C}_{\text{Py-4}}$), 137.3 (d, $\text{C}_{\text{Th-4}}$),	7.70 (m, 2 H, $\text{H}_{\text{Py-3}} + \text{H}_{\text{Py-4}}$),
		137.6 (d, $\text{C}_{\text{Ph-1}}$), 140.6 (d, $\text{C}_{\text{Th-5}}$),	8.50-8.56 (m, 1 H, $\text{H}_{\text{Py-6}}$)
		149.5 (s, $\text{C}_{\text{Py-6}}$), 150.9 (s, $\text{C}_{\text{Th-2}}$),	
		152.1 (s, $\text{C}_{\text{Py-2}}$)	
		117.8 (s, $\text{C}_{\text{Py-3}}$), 126.0 (d, $\text{C}_{\text{Th-3}}$),	7.25 (dd, 2 H, $\text{H}_{\text{Th-4}}$), 7.31-
		128.8 (d, $\text{C}_{\text{Ph-3}}$), 129.3 (s, $\text{C}_{\text{Ph-4}}$),	7.48 (m, 22 H, $\text{H}_{\text{Ph}} +$
		133.4 (d, $\text{C}_{\text{Ph-2}}$), 137.4 (d, $\text{C}_{\text{Th-4}}$),	$\text{H}_{\text{Py-3}}$), 7.59 (dd, 2 H, $\text{H}_{\text{Th-3}}$),
		137.8 (s, $\text{C}_{\text{Py-4}}$), 138.0 (d, $\text{C}_{\text{Ph-1}}$),	7.64 (dd*, 1 H, $\text{H}_{\text{Py-4}}$)
		141.2 (d, $\text{C}_{\text{Th-5}}$), 150.9 (s, $\text{C}_{\text{Th-2}}$),	
		152.0 (s, $\text{C}_{\text{Py-2}}$)	

* This is in fact an 'A' part of an AB_2 spectrum, not a real doublet of doublets.

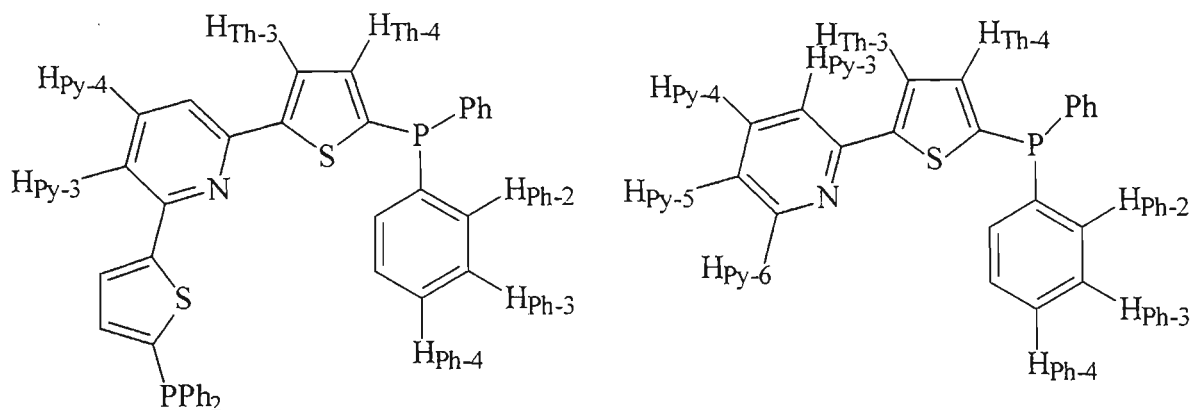


Fig. II.9 Numbering scheme for hydrogen atoms in the PSN and PSNSP molecules, the numbering of the carbon atoms coincides with that for the hydrogen atoms

It can be noticed from the above Table, that the ^{31}P NMR chemical shifts of these thienylpyridine-based phosphines are shifted very slightly to lower field, in comparison with PSS and PSSSP for which $\delta = -18.7$ ppm. This is an expected result as the pyridine substituent in the 5 (or 2) position of thiophene plays a similar role to bromine in PSBr *i.e.*, it withdraws some electron density from the thiophene ring.

The effect of the introduction of the pyridine substituent on the chemical shifts of the hydrogen atoms of the thiophene ring is even more pronounced. The signal due to the H_{Th-3} proton is shifted considerably downfield (7.6 vs. 7.1 ppm) in both phosphines, while that of H_{Th-4} is slightly shifted from 7.15 to 7.32 (in PSN) and from 7.15 to 7.25 (in PSNSP). The former effect is due to the influence of the aromatic ring current of pyridine on the adjacent hydrogen atoms of thiophene, while the latter is probably due to the inductive electron-withdrawing effect of pyridine. Through space interaction between the hydrogen atoms, H_{Py-3} of the pyridine and H_{Th-3} of the thiophene, was confirmed by differential Nuclear Overhauser Effect (NOE) NMR experiment.

As far as the thiophene and phenyl regions in the ^{13}C NMR spectra of PSN and PSNSP are concerned, these are not that different from the corresponding regions in the ^{13}C NMR spectra of PSS and PSSSP. The only significant change in the chemical shift is experienced by C_{Th-2}, the carbon adjacent to the pyridine ring (151 vs. 143.5 ppm, respectively). The chemical shifts of the pyridine carbons resemble those of the parent heterocycle, SN.

The UV-vis spectra of the thienylpyridine-based phosphines show a similar trend to that observed in purely thiophene-based phosphines. The former also exhibit bathochromic shifts of their longest wavelength absorption maxima ($\pi \rightarrow \pi^*$ electron transfer, *vide supra*) when compared to the longest wavelength absorption maxima of the parent heterocycles (compare SN and PSN, SNS and PSNSP in Table II.15).

Table II.15 The UV-vis data for SN, SNS, PSN and PSNSP, as measured in dichloromethane

Compound	SN	PSN	SNS	PSNSP
λ_{max} , nm	270 (sh [#] ,	231 ($1.3 \cdot 10^4$)	260 ($1.1 \cdot 10^4$)	230 ($3.3 \cdot 10^4$)
	$0.83 \cdot 10^4$)	271 ($1.3 \cdot 10^4$)	287 ($1.3 \cdot 10^4$)	265 ($2.7 \cdot 10^4$)
(ϵ , $\text{M}^{-1} \cdot \text{cm}^{-1}$)	303 ($1.5 \cdot 10^4$)	324 ($1.8 \cdot 10^4$)	333 ($1.0 \cdot 10^4$)	323 ($2.7 \cdot 10^4$)
				345 ($2.8 \cdot 10^4$)

[#] shoulder on the main peak

Although the combination of NMR and microanalysis data conclusively proved the formation of the desired compounds, the structure of the diphosphine, PSNSP, was further confirmed by means of a single crystal X-ray diffraction study. Suitable crystals were obtained by slow evaporation of a dichloromethane-methanol solution. Figure II.10 gives a perspective view of the ligand and also shows the atom labelling scheme. Tables II.29 and II.30 list the interatomic distances and angles respectively.

The PSNSP molecules exist as discrete entities in the crystal, there being no non-bonded contact distances less than the sum of the van der Waals radii for the two atoms concerned. Unlike PSSP, the molecule does not possess any point symmetry elements, as might have been anticipated from its symmetrical formula. The SNS fragment of the PSNSP molecule adopts a nearly planar *cisoid* arrangement, with the angles between the outer two thiophene planes and the central pyridine plane being 1.33 and 4.32° , that between the two thiophene rings being 4.97° . The distances between the N(1) atom and each of the two S atoms are $2.932(2)$ and $2.950(2)$ Å, which indicates that they are conveniently spaced to chelate to a metal atom, while the distance between the S atoms is $4.628(1)$ Å. The P(1)...P(2) distance is much greater at $9.928(1)$ Å.

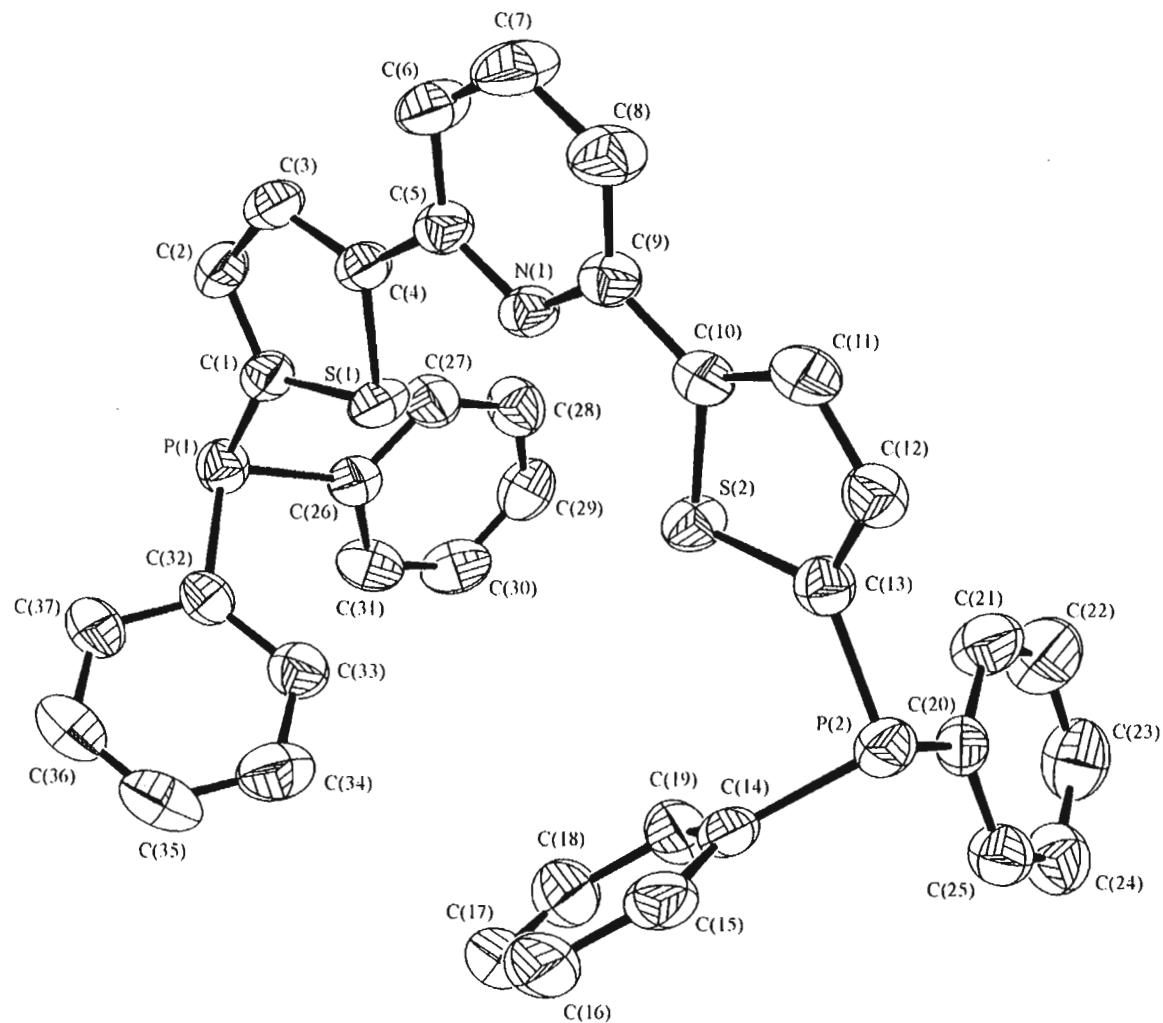


Fig. II.10 Structure of the PSNSP ligand, showing the atom numbering scheme

The geometry around the phosphorus atoms is pyramidal, with the C-P-C angles being between 100.9(1) and 104.8(1)° and with the phenyl rings adopting orientations such that their planes are at dihedral angles of 78.7° [C(14) to C(19)] and 106.0° [C(20) to C(25)] to the plane of the S(2)..C(13) thiophene ring; and 76.6° [C(26) to C(31)] and 76.9° [C(32) to C(37)] to the plane of the S(1)..C(4) thiophene ring. The lengths of all C-S, C-P, C-C and C-N bonds are within expected boundaries, as are the remaining angles within the molecule (see Tables II.29 and II.30).

As it was observed for the PSSP molecule, the phenyl rings on both phosphorus atoms are turned towards the sulfur, the torsion angles S(1)-C(1)-P(1)-C(26), S(1)-C(1)-P(1)-C(32), S(2)-C(13)-P(2)-C(14) and S(2)-C(13)-P(2)-C(20) being 61.6(2), 45.6(2), 33.6(2) and 71.2(2)°, respectively. This fact supports the earlier conclusion drawn from the PSSP structure *i.e.*, that the direction of the lone pair on the phosphorus atom is opposite to the direction of the in-plane electron pair on sulfur, an observation ascribed to the steric effect of the heteroatom (see Section 2.3.1 of this Chapter).

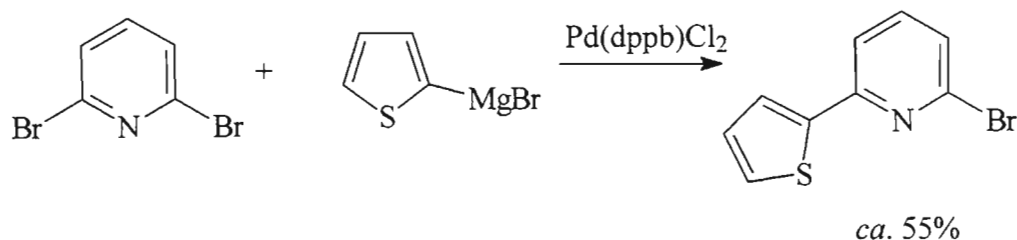
The shape of the cavity in the PSNSP molecule (Figure II.10) suggests that the ligand might be able to chelate to a metal atom via the S(1), N(1) and S(2) donor atoms *i.e.*, providing the metal is capable of coordinating to a thiophene sulfur atom. It is questionable however, whether chelation via N- and one (or two) of the P-atoms could be achieved, as their lone pairs appear facing opposite directions - at least in the solid state for the free ligand. Of course, the situation can change in the solution in the presence of a metal ion, but chelation through the P and N seems less likely than a situation where these two atoms bridge two metals. In fact, bridging two metal atoms via the P- and N-atoms of a PSN fragment is a distinct possibility and one confirmed by the crystal structure of [Au₂(μ-PSN)₂](SbF₆)₂ (see Section III.2.1.3).

II.2.5.3 Synthesis of diphenyl[6-(2'-thienyl)-2-pyridyl]phosphine (PNS) and diphenyl[5-(2'-(6'-diphenylphosphino)pyridyl)-2-thienyl]phosphine (PSNP)

As PNS can be considered a pyridine-based phosphine, its synthesis was carried out according to the method commonly used for preparation of tertiary phosphines with pyridine substituents.^{136,187} For this approach the phosphine precursor must contain a chloro- or a bromo- substituent in the position 6 of 2-(2'-thienyl)pyridine. The required

chloro-derivative was obtained by Kumada *et al.*²¹⁴ from 2,6-dichloropyridine by selective coupling with 2-thienylmagnesium bromide in the presence of a Pd(II) catalyst.

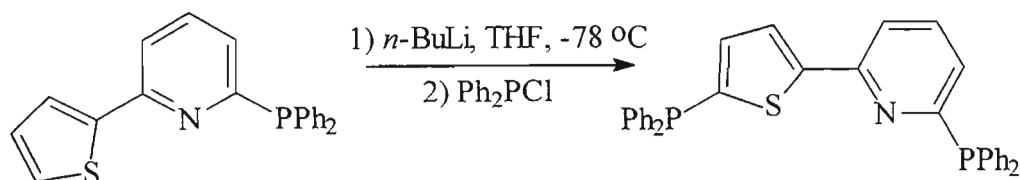
We repeated the synthesis using 2,6-dibromopyridine as the starting compound. The reaction is shown in Scheme II.58 below.



SCHEME II.58

The product mixture obtained as the result of the above reaction contained the target bromo-derivative as well as SNS (formed as a result of disubstitution) and unreacted 2,6-dibromopyridine. It proved relatively easy to remove the latter impurity, as most of it separated as a solid from the oily residue after keeping it at 10°C for 72 hours. However it proved very difficult to eliminate SNS from the mixture: cooling the residue to lower temperatures (less than -10°C) led to co-precipitation of the SNS with the bromo-derivative. An oily solution formed when the mixture was brought back to room temperature. Attempts to separate the components chromatographically were not very successful, nor were attempts to distil off one of the components, this resulting in a drastic drop in the final yield. As SNS was unlikely to interfere with the next step in the synthesis of the desired phosphine, it was decided to use the mixture as is, provided all the 2,6-dibromopyridine had been removed.

Reaction of this crude mixture with lithium diphenylphosphide proceeded smoothly and furnished the desired phosphine, PNS, in 42% yield. This phosphine was used as a starting material for the synthesis of PSNP. The strategy for the synthesis is shown in Scheme II.59. This route was preferred to an alternative one *i.e.*, the synthesis of 6-bromo-2-(5-bromo-2-thienyl)pyridine followed by reaction with two equivalents of lithium diphenylphosphide, because the dibromo compound would have been difficult to obtain pure.



SCHEME II.59

The conditions under which the thiophene ring is lithiated are crucial to the outcome of the reaction. It was shown by Queguiner *et al.*,²¹⁵ that lithiation of 2-(2'-thienyl)pyridine with *n*-BuLi preferably occurs in the position 5 of thiophene, if the solvent strongly coordinates the lithium atom. In poorly coordinating solvents such as ether, lithiation occurs in the position 3 of the thiophene ring.

The reaction shown in Scheme II.59 produced PSNP as expected. It was also established by means of ³¹P NMR spectroscopy that substituting THF for ether during the lithiation step led to a complex mixture, where the desired PSNP was a minor product (there were a number of unidentifiable peaks in the ³¹P NMR spectrum in the region between -18 and -40 ppm). Isolation of PSNP proved somewhat difficult: like PSNSP, PSNP resisted attempts to be transferred into the aqueous phase during acidification with a strong acid, thus ordinary hydrolytic procedure had to be employed. The product obtained after this step, however, resembled a very viscous oil. It took between 2 and 3 weeks in methanol at -25°C for the oil to become a crystalline material. Purification using chromatography on silica with hexane-ether as eluent eventually provided the pure phosphine in only 38% yield.

The new phosphines are off-white crystalline materials with high melting points (95 and 160°C for PNS and PSNP, respectively). Both are oxygen-sensitive and, as such, must be stored under an atmosphere of nitrogen (or argon) if kept for a long period of time. Short time exposure to atmospheric oxygen at ambient temperature, on the other hand, can be tolerated. Deoxygenated solvents must be used to prepare solutions of the two phosphines. The solubility of PNS in polar solvents such as methanol, acetonitrile and acetone is somewhat improved in comparison to that of PSS, while the solubility of PSNP is not significantly different from that of PSSP.

II.2.5.4 Characterisation of PNS and PSNP

The ^1H , ^{13}C and ^{31}P NMR spectroscopic data for the new phosphines PNS and PSNP are given in Table II.16. The assignments of the signals in the ^1H and ^{13}C NMR spectra were made on the basis of COSY and HETCOR spectra of the two phosphines as well as by comparison with the spectra of the parent heterocycle, SN, and the previously synthesised PSN. The numbering of the atoms corresponds to that shown in Figure II.9 (see Section 2.5.2 of this Chapter).

The ^{31}P NMR chemical shifts for the phosphorus atoms in PNS and PSNP (*i.e.*, the one bonded to the pyridine ring in the latter), appear in the region characteristic of that for pyridine based phosphines, *i.e.* at around -3 ppm (see Table II.16). The diphosphine, PSNP, has a second peak in the ^{31}P NMR spectrum at δ -18.3 ppm assigned to the phosphorus atom bonded to the thiophene ring.

Table II.16 NMR data for PNS and PSNP, as measured in CDCl_3

Compound	$\delta^{31}\text{P}$, ppm	$\delta^{13}\text{C}$, ppm	$\delta^1\text{H}$, ppm
PNS	-3.64 (s)	117.2 (s, $\text{C}_{\text{Py}-3}$), 124.6 (s, $\text{C}_{\text{Th}-3}$), 126.3 (d, $\text{C}_{\text{Py}-5}$), 127.9 (2 s, $\text{C}_{\text{Th}-4}$ + $\text{C}_{\text{Th}-5}$), 128.4 (d, $\text{C}_{\text{Ph}-3}$), 129.0 (s, $\text{C}_{\text{Ph}-4}$), 134.3 (d, $\text{C}_{\text{Ph}-2}$), 136.1 (d, $\text{C}_{\text{Py}-4}$), 136.4 (d, $\text{C}_{\text{Ph}-1}$), 147.3 (d, $\text{C}_{\text{Py}-6}$ *) 150.9 (s, $\text{C}_{\text{Th}-2}$), 151.8 (s, $\text{C}_{\text{Py}-2}$)	6.99 (ddd, 1 H, $\text{H}_{\text{Py}-5}$), 7.05 (dd, 1 H, $\text{H}_{\text{Th}-4}$), 7.30-7.40 (m, 7 H, $\text{H}_{\text{Ph}-3}$ + $\text{H}_{\text{Ph}-4}$ + $\text{H}_{\text{Th}-5}$), 7.42-7.58 (m, 7 H, $\text{H}_{\text{Ph}-2}$ + $\text{H}_{\text{Py}-3}$ + $\text{H}_{\text{Py}-4}$ + $\text{H}_{\text{Th}-3}$)
PSNP	-3.60 (s)	117.3 (s, $\text{C}_{\text{Py}-3}$), 125.6 (d, $\text{C}_{\text{Th}-3}$), 126.7 (d, $\text{C}_{\text{Py}-5}$), 128.4 (d, $\text{C}_{\text{Ph}-5}$), 128.9 (s, $\text{C}_{\text{Ph}-4}$), 134.3 (d, $\text{C}_{\text{Ph}-2}$), 136.1 (d, $\text{C}_{\text{Py}-4}$), 136.6 (d, $\text{C}_{\text{Ph}-1}$), 137.1 (d, $\text{C}_{\text{Th}-4}$), 137.8 (d, $\text{C}_{\text{Th}-5}$), 147.5 (d, $\text{C}_{\text{Py}-6}$ *) 150.7 (s, $\text{C}_{\text{Th}-2}$), 152.2 (s, $\text{C}_{\text{Py}-2}$)	7.01 (ddd, 1 H, $\text{H}_{\text{Py}-5}$), 7.28 (dd, 1 H, $\text{H}_{\text{Th}-4}$), 7.30-7.53 (m, 22 H, H_{Ph} + $\text{H}_{\text{Py}-3}$ + $\text{H}_{\text{Py}-4}$), 7.59 (dd, 1 H, $\text{H}_{\text{Th}-3}$)
	-18.34 (s)		

* The intensity of the signal is very close to the noise level, so this value must be treated with caution

The ^1H NMR spectra of PNS and PSNP are poorly resolved with several signals overlapping, making assignments of signals to individual hydrogens not always possible. We first note that all three pyridine hydrogens in PNS *i.e.*, $\text{H}_{\text{Py-3}}$, $\text{H}_{\text{Py-4}}$ and $\text{H}_{\text{Py-5}}$, experience an upfield shift by about 0.15 ppm in comparison to the chemical shifts recorded for the SN molecule ($\delta = 7.62\text{--}7.72$ ppm – for $\text{H}_{\text{Py-3}}$ and $\text{H}_{\text{Py-4}}$; $\delta = 7.14$ ppm for $\text{H}_{\text{Py-5}}$). The thiophene hydrogen signals remain at approximately the same values as they were in the parent heterocycle. In the PSNP molecule, the chemical shifts of hydrogen atoms of both heterocyclic rings are affected by the diphenylphosphino substituents: the chemical shift of the $\text{H}_{\text{Th-4}}$ is shifted downfield from the corresponding signal in the SN spectrum by 0.15 ppm, while the pyridine hydrogens experience an upfield shift of about the same value (similar to what was observed for PNS). The ^{13}C NMR spectra of the two phosphines show the expected changes in the carbon chemical shifts when compared to those recorded for unsubstituted SN. Specifically, the signals of carbon atoms within 3 bonds from the phosphorus atom split, producing doublets, and are generally shifted downfield.

The UV-vis spectra of the three phosphines derived from SN do not show the same trends as those observed for 2,2'-bithiophene based phosphines (see Table II.17). Firstly, the introduction of a diphenylphosphino substituent on the different rings of the SN moiety results in different electronic absorption spectra (compare PSN and PNS). A consequence of this is that there is no systematic red shift in the longest wavelength ($\pi \rightarrow \pi^*$) band on increasing the number of diphenylphosphino substituents. This was the case for SS, where the introduction of each diphenylphosphino group led to gradual increase in the wavelength of the band. This implies that the introduction of the second diphenylphosphino group on the pyridine ring of PSN does not lead to an improved delocalisation of electron density. This may be due to a distortion of the planarity of the molecule. An alternative explanation is that further delocalisation is disrupted because of the different extent of interaction between the phosphorus lone pair and the π -electrons of a pyridine ring, compared to the equivalent interaction between the phosphorus and a thiophene ring.

Table II.17 The UV-vis data for the 2-(2'-thienyl)pyridine based phosphines, PSN, PNS and PSNP, and the parent compound SN (spectra recorded in dichloromethane)

Compound	SN	PSN	PNS	PSNP
λ_{max} , nm	270 (sh [#] ,	231 ($1.3 \cdot 10^4$)	230 ($1.3 \cdot 10^4$)	233 ($2.5 \cdot 10^4$)
$(\epsilon, \text{M}^{-1} \cdot \text{cm}^{-1})$	$0.83 \cdot 10^4$)	271 ($1.3 \cdot 10^4$)	264 ($1.4 \cdot 10^4$)	265 ($2.0 \cdot 10^4$)
	303 ($1.5 \cdot 10^4$)	324 ($1.8 \cdot 10^4$)	278 ($1.4 \cdot 10^4$)	323 ($2.0 \cdot 10^4$)
			318 ($1.1 \cdot 10^4$)	

[#] shoulder on the main peak

It is difficult to verify or disprove the above statement in the absence of the accurate structural data for the SN derivatives. For this reason single crystals of PSNP were grown (by evaporation of hexane-ether solution) and its crystal structure determined by X-ray diffraction methods. Figure II.11 gives a perspective view of the diphosphine, while Tables II.35 and II.36 provide the information on bond lengths and angles in the molecule.

The heterocycle fragment of the PSNP molecule is approximately planar, the angle between the pyridine and the thiophene rings being only 3.56° . A *cisoid* arrangement of the thiophene S and pyridine N atoms about the interannular C(4)-C(5) bond is adopted. The distance between the two heteroatoms is $2.921(5) \text{ \AA}$, which is close to the values observed in the structure of PSNSP *i.e.*, $2.931(4)$ and $2.946(5) \text{ \AA}$. The distances between non-adjacent donor atoms, *i.e.* P(1)...N(1), P(2)...S(1) and P(1)...P(2) are $6.048(4)$, $5.203(2)$ and $8.250(2) \text{ \AA}$ respectively. The length of the interannular C-C bond between the heterocycles in this molecule is comparable to what was observed in the structure of the PSNSP ligand: $1.458(7) \text{ \AA}$ for the C(4)-C(5) bond in PSNP *vs* $1.468(4) \text{ \AA}$ for the C(4)-C(5) bond and $1.463(4) \text{ \AA}$ for the C(9)-C(10) bond in PSNSP.

The geometry around the phosphorus atoms is pyramidal with the C-P-C angles ranging from $101.2(3)$ and $105.2(2)^\circ$ and with the phenyl rings adopting orientations such that their planes are at dihedral angles of 63.42° [C(10) to C(15)] and 82.03° [C(16) to C(21)] to the plane of the S(1)..C(4) thiophene ring; and at 68.54° [C(22) to C(27)] and 43.56° [C(28) to C(33)] to the plane of the N(1)..C(9) pyridine ring. The lengths of the C-S, C-P, C-C and C-N bonds are within expected boundaries, as are the angles within the molecule (see Tables II.35 and II.36 in the Experimental section).

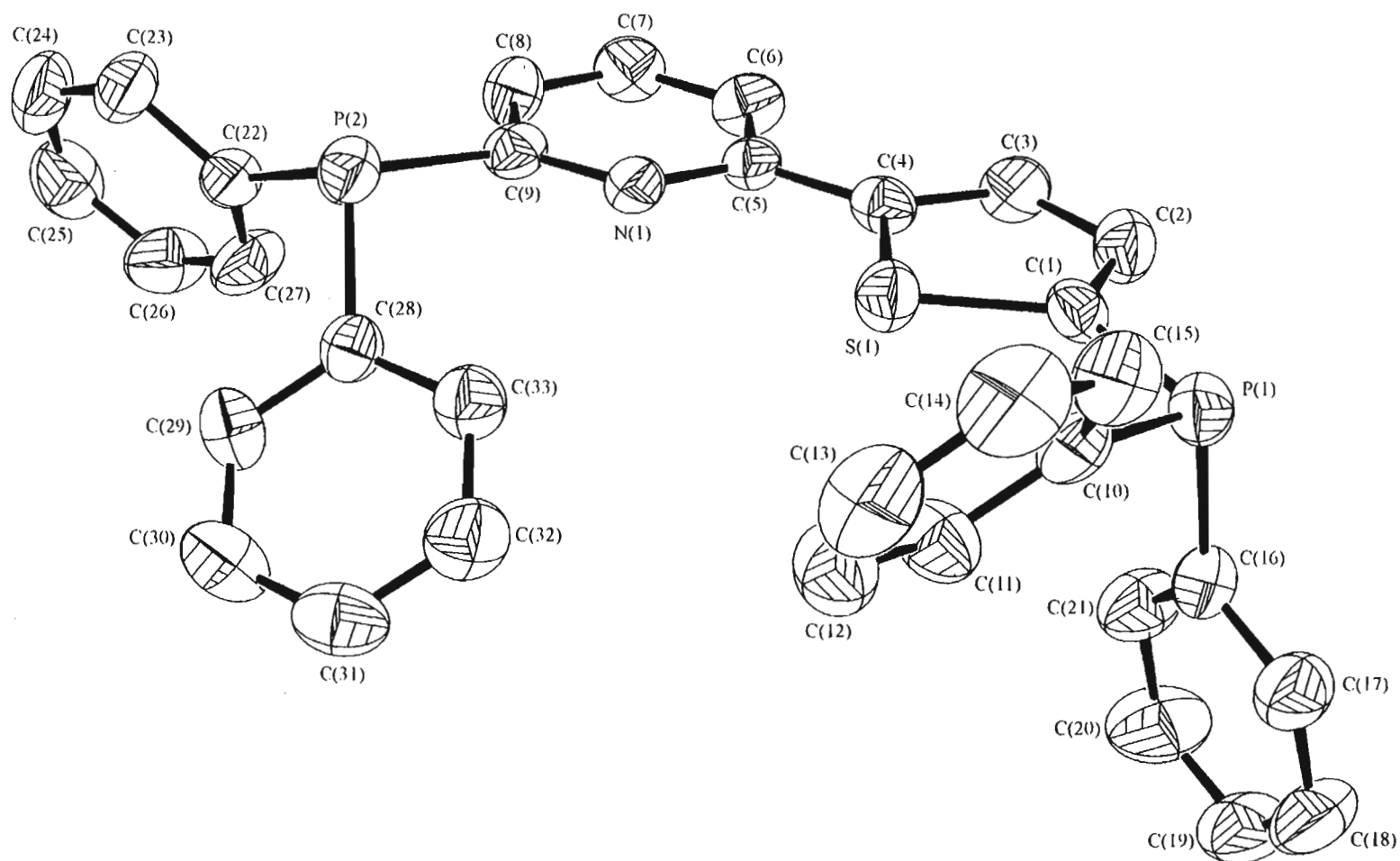


Fig. II.11 Structure of the PSNP ligand, showing the atom numbering scheme

Unlike the situation observed for the PSNSP ligand, the phenyl rings on the two phosphorus atoms are turned to a different degree towards the respective heterocycle rings. The torsion angles S(1)-C(1)-P(1)-C(10) and S(1)-C(1)-P(1)-C(16) are 13.9(4) and 91.7(3)°, while N(1)-C(9)-P(2)-C(22) and N(1)-C(9)-P(2)-C(28) are 158.1(4) and 51.6(4)°, respectively. Thus the direction of the lone pair on phosphorus attached to the thiophene ring is approximately opposite to that of the electron pair on sulfur - similar to what was observed for PSSP and PSNSP. However the lone pair on phosphorus attached to the pyridine ring, although it does not exactly point in the same direction as the lone pair on N(1), it definitely appears to be on the same side of the heterocycle as the nitrogen atom with respect to an imaginary plane drawn through P(2) and C(9) and perpendicular to the pyridine ring. This difference in conformations around the two phosphorus atoms can clearly be attributed to the difference in the steric effect imposed by S and N lone pairs as well as the different geometries of the respective heterocycles.

The PSNP ligand does not form a cavity similar to that of PSNSP. The ligand might be able to chelate to a suitable metal via the S and N atoms and it definitely possesses the potential to bridge two metal atoms via the N and P atoms. The juxtaposition of the P(2), N(1) and S(1) atoms on one hand, as well as the P(1), S(1) and N(1) atoms on the other, is such that it is unlikely that the ligand can adopt a conformation in which three donor atoms simultaneously coordinate to the same metal atom.

II.3 SUMMARY AND CONCLUSION

Given that the synthesis and characterisation of a number of new thiophene-based phosphines is reported in this Chapter, it seems appropriate to briefly summarise their properties as well as the methods used for their synthesis.

II.3.1 Properties of the new thienylphosphines

Table II.18 presents the basic characteristics of the newly synthesised thiophene-based phosphines and related compounds, such as colour, melting point, ^{31}P NMR shift and resistance to oxidation as well as the yield in which they were obtained.

As can be seen from the Table, the yields of the phosphorus compounds range from good (70%) to poor (10%). There does not seem to be any clear-cut relationship between the structure of the molecule and the successfulness of its preparation, as the latter is the direct result of the method chosen for the synthesis of that particular compound.

The phosphines exhibit a wide range of melting points (from below room temperature to 192°C) which appear to be structure related: generally phosphines with polar groups such as bromo or pyridyl substituents have higher melting points as well as a higher degree of crystallinity than those with thiophene groups only. The presence of centre of symmetry within the molecule also increases the melting point. A good example is PSSP which has the highest melting point and - as established by X-ray analysis - possesses a centre of symmetry. With regard to PSSP, it is likely that the planar arrangement of the two thiophene rings as well as the large distance between the two diphenylphosphino groups allows for convenient packing (and, therefore, strong interactions) of the molecules in the solid state. Comparison of the crystal structures of PSSP and PSNP confirms this suggestion. In the latter molecule the two heterocyclic rings are not coplanar (dihedral angle 4.5°); moreover the disposition of the two diphenylphosphino group with respect to the mean plane through the two rings is different, thus causing difficulty in close packing.

Table II.18 Selected properties of the novel phosphines and related compounds obtained during this work

Compound name	Yield, %	M.p., °C	Colour	Air- sensitivity	$\delta^{31}\text{P}$, ppm
Diphenyl(2-thienyl)phosphine (PS)	72	44-46	white	<i>a</i>	-19.90 (s)
Phenyldi(2-thienyl)phosphine (PDS)	51	29-30	white	<i>a</i>	-33.26 (s)
Tris(2-thienyl)phosphine (PTS)	32	25-26	white	<i>a</i>	-46.27 (s)
Diphenyl(5-bromo-2-thienyl)phosphine (PSBr)	45	69-70	white	<i>a</i>	-17.88 (s)
Diphenyl[5-(2,2'-bithienyl)]phosphine (PSS)	25	58-60	off-white	<i>a</i>	-18.83 (s)
Diphenyl[5-(2,2':5',2''-terthienyl)]phosphine (PSSS)	39	77-78	yellow	<i>a</i>	-18.71 (s)
2,5-Bis(diphenylphosphino)thiophene (PSP)	40	77-78	white	<i>a</i>	-18.84 (s)
5,5'-Bis(diphenylphosphino)-2,2'-bithiophene (PSSP)	61	191-192	off-white	<i>a</i>	-18.75 (s)
5,5''-bis(diphenylphosphino)-2,2':5',2''-terthiophene (PSSSP)	66	148-149	yellow	<i>a</i>	-18.71 (s)
Phenylbis[(5-diphenylphosphino)-2-thienyl]phosphine (PDSP)	60	- (oil)	colourless	<i>a</i>	-18.68 (s) & -32.17 (s), 2:1
Tris[(5-diphenylphosphino)-2-thienyl]phosphine (PTSP)	45	137-138	white	<i>a</i>	-18.62 (s) & -44.73 (s), 3:1
Diphenyl[5-(2'-pyridyl)-2-thienyl]phosphine (PSN)	66	69-70	white	<i>a</i>	-18.35 (s)
Diphenyl[6-(2'-thienyl)-2-pyridyl]phosphine (PNS)	42	94-95	off-white	<i>b</i>	-3.64 (s)
Diphenyl[5-(2'-{6'-diphenylphosphino}pyridyl)-2-thienyl]-phosphine (PSNP)	38	159-160	off-white	<i>b</i>	-3.60 (s) & -18.34 (s), 1:1
2,6-Bis[(5'-diphenylphosphino)-2'-thienyl]pyridine (PSNSP)	54	175-176	greenish-white	<i>a</i>	-18.28 (s)

Table II.18 continued...

Bis[5-(diphenylphosphino)-2-thienyl]phosphinic acid (DTPA)	10	n.d. [*]	white	<i>a</i>	4.85 (s) & -18.24 (s), 1:2
Thien-2,5-diyl di(phenylphosphinic acid) (TDPA)	24	n.d. [*]	white	<i>a</i>	19.86 (s)
2,2'-Bithien-5,5'-diyl di(phenylphosphinic acid) (BTDPA)	34	n.d. [*]	yellow	<i>a</i>	20.08 (s)
5,5'-Bis(phenylphosphino)-2,2'-bithiophene (HPSSPH)	70	- (oil)	colourless	<i>c</i>	-64.34 (s)

^{*} the m.p. of the compound was not determined

a the compound is stable in air for considerable periods of time

b the compound is resistant to oxidation at reduced temperatures and under a layer of solvent, but is easily oxidised in solution and at elevated temperatures

c the compound is quickly oxidised both in pure form and in solution, irrespective of the temperature

As a result the melting point of PSNP is lower than that of PSSP, although one would expect it to be greater on the basis of the substitution of a thiophene group by the more polar pyridine group.

Tertiary phosphines where a phosphorus atom is attached to the 2-position of the thiophene ring show a remarkable stability towards oxidation. On the other hand, the phosphines with the phosphorus atom at the 2-position of a pyridine ring are far less stable, quickly oxidising in solution and even in solid state if left standing in air for prolonged periods of time. As expected, the phosphinic acid derivatives, bis[5-(diphenylphosphino)-2-thienyl]phosphinic acid (DTPA), thien-2,5-diyl di(phenylphosphinic acid) (TDPA) and 2,2'-bithien-5,5'-diyl di(phenylphosphinic acid) (BTDPa), are resistant towards oxidation, as the phosphorus atoms in those molecules are already in the highest oxidation state (+5). The secondary phosphine, 5,5'-bis(phenylphosphino)-2,2'-bithiophene (HPSSPH), is readily oxidised even when only traces of oxygen are present, the property characteristic of secondary aromatic phosphines *e.g.*, diphenylphosphine. Although the thiophene-based phosphines appear to be perfectly air-stable, they show a certain light-sensitivity, which becomes more pronounced with an increase in the number of thiophene rings in the molecule *e.g.*, PSSSP, PSSS and PTSP. Replacing a thiophene by a pyridine moiety decreases the sensitivity to light by the molecule.

The original goal behind the preparation of thiophene-based tertiary phosphines containing a pyridine substituent was to obtain compounds soluble in both non-polar and polar solvents. However, it was found that the introduction of one pyridine ring only slightly improved the solubility in polar solvents. In fact, all the compounds listed in Table II.18 dissolve to some extent in solvents such as benzene, THF, chloroform and dichloromethane, *i.e.* both weakly polar and non-polar solvents. The only exceptions are thien-2,5-diyl di(phenylphosphinic acid) (TDPA) and 2,2'-bithien-5,5'-diyl di(phenylphosphinic acid) (BTDPa) which, being phosphinic acids, are soluble in alcohols and aqueous NaOH. The phosphines (apart from PSBr) are only marginally soluble in cold alcohols and none of them are soluble in aqueous media.

II.3.2 Methods of synthesis

Thiophene, bithiophene and terthiophene derived diphenylphosphines with the phosphorus atom attached to 2-position of a thiophene nucleus have been successfully prepared either directly from the parent heterocycle or (as in the case of PSS) by coupling of two thiophene containing fragments. The former is the traditional approach used for the preparation of a variety of phosphines with electron-rich heterocycle substituents and involves metallation of the parent heterocycle, followed by reaction with a suitable chlorophosphine. It was established during the syntheses of PS, PDS, PTS, PSBr, PSSP, PSSS and PSSSP that both Li and Mg thiophene derivatives are effective as precursors, the selection of the appropriate organometallic reagent being largely dependent on the availability of a suitable intermediate and/or practical convenience. The method generally provides phosphines in good yields, although these vary due to differences in the physical properties of the compounds *e.g.*, the isolation of low-melting phosphines is difficult resulting in low yields.

When a suitable organometallic precursor for the reaction with a chlorophosphine is not available, it is sometimes possible to utilise an alternative route to the required phosphine. Thus, for the preparation of PSS, a Ni(II)-catalysed coupling reaction between two thiophene containing compounds (2-thienylmagnesium bromide and PSBr) was used. However the reaction gave low yields, possibly as a consequence of the competing homocoupling side reactions. Although coupling reactions between heterocycles are well documented, this is the first example of a reaction when one of the heterocycles includes a phosphine moiety in its structure.

During the course of this study it was found that metallation of the PS molecule at the unsubstituted 5-position with *n*-BuLi results in partial cleavage of the P-C bond. Thus, in order to metallate a thiophene which already has one phosphine substituent, one has to use a less nucleophilic reagent. Lithium di-*iso*-propylamide has been used as an alternative to *n*-BuLi. However a better method is based on the use of a thiophene-based phosphine containing a bromine substituent at the required position on the thiophene ring, which can be subsequently converted into the corresponding Grignard reagent. Preparation of the polyphosphines PDSP and PTSP became successful only due to the latter metallating procedure.

Preparation of phosphines with both thiophene and pyridine moieties in their structure, such as PSN, PNS, PSNP and PSNSP, can be considered as a significant development not only because novel phosphines have been prepared, *i.e.* phosphines containing both electron-rich and electron-poor nuclei in the molecule, but also because it has introduced different synthetic approaches. It was established that the selective attachment of a diphenylphosphino group to a heterocycle containing both pyridine and thiophene rings, could be achieved via the reaction between the haloheterocycle and lithium diphenylphosphide, the halogen atom being positioned on either the thiophene or pyridine ring*. The traditional Grignard reaction for the preparation of thiophene-based phosphines, as described above, can no longer be employed once there is a pyridine ring in the molecule.

The reaction between a halogenated heterocycle and lithium diphenylphosphide does not, however, always produce sufficiently clean product - which was the case during the attempted synthesis of PSNSP. In that instance, assembling the molecule by means of a Ni(II)-catalysed coupling reaction was more successful, providing a product with far fewer impurities.

During this work an attempt was made to prepare a water-soluble thiophene-based mono- or diphosphine containing sulfonated phenyl groups or, indeed, any other strongly polar aromatic groups. This was not achieved. However, the synthesis of the potential precursor, 5,5'-bis(phenylphosphino)-2,2'-bithiophene, has opened a convenient route to primary and secondary 2-thienylphosphines. This route consists of several steps, the first and most important one being the phosphorylation of a thiophene at the 2-position with a suitable P(III) reagent in the presence of an anhydrous Ni(II) salt. The expected product of the first step is a phosphinic or phosphonic acid, which can be converted to its chloroanhydride and finally reduced to a P(III) compound with one or two hydrogens bonded at the phosphorus atom. Whether the last named species can be converted into a novel tertiary phosphine is uncertain, since the reaction still needs to be studied.

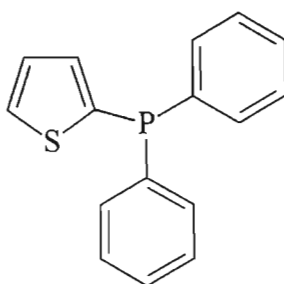
* Normally, with thiophene-only based heterocyclic systems, such a reaction would have resulted in a fast halogen-metal exchange and the formation of homocoupling products, with Ph_2PPPh_2 being the main phosphorus-containing compound.

II.4 EXPERIMENTAL

All reactions for phosphine syntheses were carried out under an atmosphere of dry nitrogen. Work-up procedures were normally performed in air unless otherwise stated due to generally air-stable nature of the phosphines. General experimental details and sources of chemicals are outlined in Appendix A.

II.4.1 Syntheses

II.4.1.1 Synthesis of diphenyl(2-thienyl)phosphine (PS)



$$M = 268.31 \text{ g}\cdot\text{mol}^{-1}$$

2-Bromothiophene (8.15 g, 50 mmol) was dissolved in 40 ml dry ether. The solution was added to a slurry of 1.25 g (52 mmol) of magnesium turnings in 10 ml dry ether in such a way as to maintain a gentle reflux. The addition was complete in 30 minutes. At this stage, 20 ml ether were added and the mixture was warmed up to reflux again and left refluxing until all magnesium disappeared (1-1.5 hours). It was cooled to 0°C and 9.0 ml (50 mmol) of diphenylchlorophosphine in 30 ml dry THF were added dropwise to the cold solution over a period of 40-50 minutes. After this, the cooling was removed and the mixture allowed to stir at room temperature for at least 2-3 hours. Most of the solvent was then evaporated *in vacuo* and 100 ml of ether added, followed by 200 ml dilute HCl. If the reaction appeared too vigorous, some ice was added. The product was extracted with ether (2 x 50 ml), the ethereal layers were combined, washed with brine and dried over MgSO₄. The solution was filtered from the drying agent and the solvent removed *in vacuo*. The resulting oil was allowed to crystallise by storing at -10°C for 1-3 days. Cold methanol was added to the solid and mother liquor removed. The solid was finely crushed and washed twice with small portions of cold methanol. A white crystalline product was obtained.

Yield = 9.6 g (72%), m.p. = 44-46°C (lit.¹⁴¹ 43-46°C).

Elemental analysis: calculated C 71.62 %, H 4.88 %;

found C 71.65 %, H 4.86 %.

³¹P{H} (CDCl₃) = -19.90 (s) ppm (lit.¹⁶⁴ -19.3 ppm).

^1H (CDCl_3), δ , ppm: 7.13 (ddd, $^4J_{\text{H-P}} = 1.28$, $^3J_{\text{H-H}} = 4.90$, $^3J_{\text{H-H}} = 2.73$; 1 H), 7.31 (ddd, $^3J_{\text{H-P}} = 4.93$, $^4J_{\text{H-H}} = 0.90$, $^3J_{\text{H-H}} = 2.73$; 1 H), 7.34-7.45 (m, 10 H), 7.59 (dd, $^4J_{\text{H-H}} = 0.90$, $^3J_{\text{H-H}} = 4.89$; 1 H).

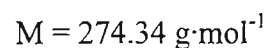
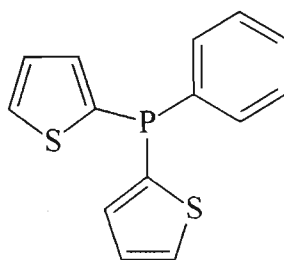
$^{13}\text{C}\{\text{H}\}$ (CDCl_3), δ , ppm: 128.0 (d, $^3J_{\text{C-P}} = 8.1$), 128.4 (d, $^3J_{\text{C-P}} = 6.4$), 128.8 (s), 132.0 (s), 133.1 (d, $^2J_{\text{C-P}} = 19.4$), 136.3 (d, $^2J_{\text{C-P}} = 26.4$), 137.8 (d, $^1J_{\text{C-P}} = 14.7$), 138.0 (d, $^1J_{\text{C-P}} = 20.8$).

GCMS: $m/z = 267.95$ (M^+).

IR (KBr disk): 490 (s), 694 (s), 716 (s), 741 (s), 750 (s), 849 (w), 991 (w), 1215 (w), 1400 (m), 1433 (m), 1475 (m).

UV-vis (dichloromethane), λ_{max} , nm (ϵ , $\text{M}^{-1}\cdot\text{cm}^{-1}$): 238 ($1.2\cdot 10^4$).

II.4.1.2 Synthesis of phenyldi(2-thienyl)phosphine (PDS)



2-Bromothiophene (16.3 g, 100 mmol) dissolved in 40 ml dry ether was added to 2.43 g (100 mmol) of magnesium turnings suspended in 15 ml dry ether. Preparation of the Grignard reagent was carried out in a similar fashion to that described for synthesis of diphenyl(2-thienyl)phosphine (PS) (Section 4.1.1). A solution of 6.8 ml (50 mmol) of PhPCl_2 in 30 ml dry THF was added dropwise to the Grignard solution cooled to 0°C . After the addition was complete, the mixture was allowed to warm up to room temperature and stirred overnight. The solution was hydrolysed by adding dilute HCl/ice slush. The ether layer was collected, while the acid solution was extracted with ether (2 x 100 ml). The combined ethereal layers were washed with brine and dried over MgSO_4 . Evaporation of the solvent produced a pale orange oil. It was purified by column chromatography (silica; hexane/ether, 10:1, v:v). The final product was a white microcrystalline solid.

Yield = 7.0 g (51%), m.p. = $29\text{--}30^\circ\text{C}$.

Elemental analysis: calculated C 61.31 %, H 4.05 %;

found C 61.06 %, H 3.78 %.

$^{31}\text{P}\{\text{H}\}$ (CDCl_3) = -33.26 (s) ppm.

^1H (CDCl_3), δ , ppm (J , Hz): 7.13 (ddd, $^4J_{\text{H-P}} = 1.27$, $^3J_{\text{H-H}} = 4.70$, $^3J_{\text{H-H}} = 3.57$; 2 H), 7.37 (ddd, $^3J_{\text{H-P}} = 4.88$, $^4J_{\text{H-H}} = 1.05$, $^3J_{\text{H-H}} = 3.57$; 2 H), 7.30-7.45 (m, 5 H), 7.61 (dd, $^4J_{\text{H-H}} = 1.05$, $^3J_{\text{H-H}} = 4.69$; 2 H).

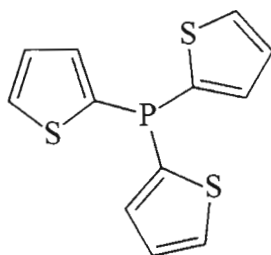
$^{13}\text{C}\{\text{H}\}$ (CDCl_3), δ , ppm (J , Hz): 127.9 (d, $^3J_{\text{C-P}} = 8.2$), 128.3 (d, $^3J_{\text{C-P}} = 6.9$), 128.8 (s), 131.9 (d, $^2J_{\text{C-P}} = 20.4$), 132.1 (s), 136.2 (d, $^2J_{\text{C-P}} = 28.6$), 138.4 (d, $^1J_{\text{C-P}} = 21.6$), 138.6 (d, $^1J_{\text{C-P}} = 11.8$).

GCMS: $m/z = 273.95$ (M^+).

IR (KBr disk): 492 (s), 575 (m), 708 (vs), 741 (s), 850 (w), 995 (w), 1217 (m), 1406 (m), 1433 (m).

UV-vis (dichloromethane), λ_{max} , nm (ϵ , $\text{M}^{-1}\cdot\text{cm}^{-1}$): 240 ($1.5\cdot 10^4$), 270 (sh, $0.9\cdot 10^4$).

II.4.1.3 Synthesis of tris(2-thienyl)phosphine (PTS)



$\text{C}_{12}\text{H}_9\text{PS}_3$

$M = 280.36 \text{ g}\cdot\text{mol}^{-1}$

The Grignard reagent based on 24.5 g (150 mmol) of 2-bromothiophene was prepared as described previously for preparation of PS (see Section 4.1.1). After all metal had reacted, the mixture was cooled to 0°C , and a solution of 5.0 ml (50 mmol) of phosphorus trichloride in 30 ml of dry THF were added dropwise over one hour. The reaction mixture was allowed to reach the room temperature slowly and was stirred overnight. The hydrolytic work-up procedure was similar to that described for phenyldi(2-thienyl)phosphine (PDS) (Section 4.1.2). Evaporation of ether in the final step yielded a pale yellow oil. It was purified by column chromatography (silica; hexane/ether, 10:1, v:v). The purified oil slowly crystallised out over several days at -10°C . The product was not stable on exposure to sunlight and discoloured within a few days.

Yield = 4.5 g (32%), m.p. = $25\text{--}26^\circ\text{C}$.

Elemental analysis: calculated C 51.41 %, H 3.24 %;

found C 51.84 %, H 3.10 %.

$^{31}\text{P}\{\text{H}\}$ (CDCl_3) = -46.27 (s) ppm.

^1H (CDCl_3), δ , ppm (J , Hz): 7.123 (ddd, $^4J_{\text{H-P}} = 1.40$, $^3J_{\text{H-H}} = 4.99$, $^3J_{\text{H-H}} = 3.62$; 3 H), 7.385 (ddd, $^3J_{\text{H-P}} = 5.85$, $^3J_{\text{H-H}} = 3.58$, $^4J_{\text{H-H}} = 1.26$; 3 H), 7.603 (dd, $^3J_{\text{H-H}} = 4.98$, $^4J_{\text{H-H}} = 1.23$; 3 H).

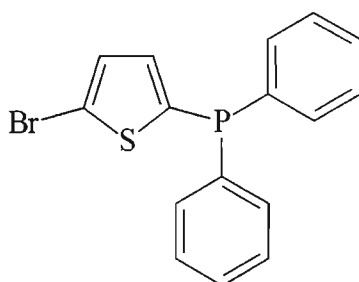
$^{13}\text{C}\{\text{H}\}$ (CDCl_3), δ , ppm (J , Hz): 127.9 (d, $^3J_{\text{C-P}} = 8.8$), 131.9 (s, $\text{C}_{\text{Th-5}}$), 135.4 (d, $^2J_{\text{C-P}} = 26.7$), 138.8 (d, $^1J_{\text{C-P}} = 20.0$).

GCMS: $m/z = 279.80$ (M^+).

IR (KBr disk): 496 (s), 577 (m), 704 (vs), 742 (m), 850 (m), 997 (m), 1217 (m), 1332 (w), 1406 (m).

UV-vis (dichloromethane), λ_{max} , nm (ϵ , $\text{M}^{-1}\cdot\text{cm}^{-1}$): 240 ($1.8\cdot 10^4$), 270 (sh, $1.1\cdot 10^4$).

II.4.1.4 Synthesis of diphenyl(5-bromo-2-thienyl)phosphine (PSBr)



$\text{C}_{16}\text{H}_{12}\text{BrPS}$

$M = 347.21 \text{ g}\cdot\text{mol}^{-1}$

METHOD A

A mixture of 6.08 g (25 mmol) of 2,5-dibromothiophene and 0.6 g (25 mmol) of magnesium turnings in 25 ml dry ether was refluxed for one hour or until all metal had dissolved. The solution was cooled to room temperature ($\pm 15^\circ\text{C}$, cooling below this temperature causes precipitation of the Grignard reagent) and a solution of 4.5 ml (25 mmol) of diphenylchlorophosphine in 20 ml THF added dropwise over a 30 minute period. When the addition was complete, the mixture was refluxed for 1 hour and then stirred overnight at room temperature. The solution was evaporated to a quarter of its original volume and 100 ml of ordinary ether added, followed by a semi-saturated NH_4Cl solution. The ether layer was separated and the aqueous layer was extracted with ether (2 x 50 ml). The combined ether extracts were washed with brine and dried over MgSO_4 . Three quarters of the solvent were evaporated *in vacuo* and cold methanol added to the mixture. After standing for 1 day at -25°C , an off-white precipitate was formed. It was quickly filtered and subsequently purified. Centrifugal chromatography on Chromatotron® (silica; hexane/ether, 8:1, v:v) yielded a white crystalline solid.

Yield = 3.4 g (40%), m.p. = $69\text{--}70^\circ\text{C}$.

Elemental analysis: calculated C 55.35 %, H 3.48 %;

found C 55.74 %, H 3.77 %.

$^{31}\text{P}\{\text{H}\}$ (CDCl_3) = -17.88 (s) ppm.

^1H (CDCl_3), δ , ppm (J , Hz): 7.03–7.18 (ABX system, $^4J_{\text{H-P}} = 1.30$, $^3J_{\text{H-P}} = 6.14$, $J_{\text{AB}} = 3.66$; 2 H), 7.32–7.44 (m, 10 H).

$^{13}\text{C}\{\text{H}\}$ (CDCl_3), δ , ppm (J , Hz): 118.2 (d, $^4J_{\text{C-P}} = 1.4$), 128.6 (d, $^3J_{\text{C-P}} = 7.1$), 129.1 (s), 131.0 (d, $^3J_{\text{C-P}} = 8.5$), 131.8 (d, $^1J_{\text{C-P}} = 10.5$), 133.0 (d, $^2J_{\text{C-P}} = 19.6$), 136.9 (d, $^2J_{\text{C-P}} = 30.1$), 137.2 (d, $^1J_{\text{C-P}} = 8.3$).

GCMS: $m/z = 345.85$ ($^{79}\text{Br-M}^+$), 347.85 ($^{81}\text{Br-M}^+$), 99 and 100% respectively.

IR (KBr disk): 490 (s), 503 (vs), 532 (m), 551 (m), 565 (m), 694 (vs), 741 (s), 804 (s), 949 (m), 999 (m), 1026 (w), 1066 (w), 1087 (w), 1120 (w), 1201 (m), 1404 (m), 1433 (m), 1473 (m).

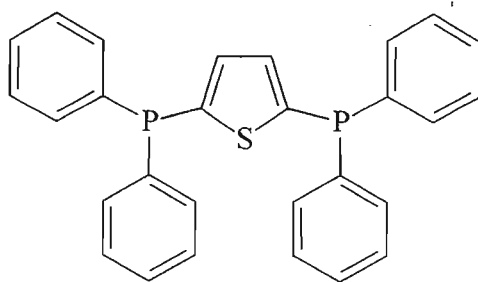
UV-vis (dichloromethane), λ_{max} , nm (ϵ , $\text{M}^{-1}\cdot\text{cm}^{-1}$): 232 ($1.25\cdot 10^4$), 252 (sh, $1.17\cdot 10^4$).

METHOD B

A solution of 0.603 g (2.25 mmol) of diphenyl(2-thienyl)phosphine (PS) in 30 ml dry ether was cooled to 0°C and a hexane solution (1.6 M) containing 2.40 mmol BuLi was added to it over a period of 10 minutes. The mixture was allowed to stir at room temperature for one hour and then cooled to -78°C . A solution of 0.13 ml (2.32 mmol) of bromine in 10 ml dry THF was added slowly with stirring. An off-white precipitate was formed, which subsequently dissolved when the mixture was warmed up to room temperature. It was allowed to stir for 14 hours at room temperature, after which the solvent was evaporated *in vacuo* and 5 ml of cold methanol added. After 3 hours at -25°C , the newly formed precipitate was filtered off and recrystallised from hot hexane.

Yield = 0.35 g (45%).

II.4.1.5 Synthesis of 2,5-bis(diphenylphosphino)thiophene (PSP)



$\text{C}_{28}\text{H}_{22}\text{P}_2\text{S}$

$M = 452.49 \text{ g}\cdot\text{mol}^{-1}$

METHOD A

Diphenyl(2-thienyl)phosphine (PS) (2.04 g, 7.6 mmol) was dissolved in 30 ml dry THF and added dropwise at 0°C to a hexane solution containing 8 mmol of BuLi. The solution gradually changed colour from yellow to dark reddish-brown. The mixture was allowed to warm up to room temperature and stirred for 2 more hours. After that the mixture was cooled to 0°C and a solution of 1.5 ml (8.3 mmol) diphenylchlorophosphine in dry THF

was added over 20 minutes. The solution was stirred overnight at room temperature. The solution volume was reduced to a quarter of its original value, and 30 ml dilute HCl with crushed ice added. The solution was extracted with ether (3 x 20 ml), the ethereal layers combined, washed with brine and dried over MgSO_4 . After removal of the solvent, a very viscous oil was obtained, which was extremely difficult to crystallise. Even prolonged storage at -25°C did not always yield crystalline product. Addition of 5-10 ml of acetonitrile helped somewhat to facilitate the crystallisation process. It took on average between 1 week and 2 months to obtain the precipitate. The product is a white microcrystalline solid.

Yield = 1.3 g (38%), m.p. = $77-78^\circ\text{C}$.

Elemental analysis: calculated C 74.32 %, H 4.90 %;
found C 73.97 %, H 4.96 %.

$^{31}\text{P}\{\text{H}\}$ (CDCl_3) = -18.84 (s) ppm.

^1H (CDCl_3), δ , ppm: 7.196 (m, AA'XX' system; 2 H), 7.30-7.42 (m, 20 H).

$^{13}\text{C}\{\text{H}\}$ (CDCl_3), δ , ppm (J , Hz): 129.1 (d, $^3J_{\text{C-P}} = 7.1$), 129.6 (s), 133.7 (d, $^2J_{\text{C-P}} = 19.9$), 137.1 (dd, $^3J_{\text{C-P}} = 5.8$, $^2J_{\text{C-P}} = 22.2$), 137.9 (d, $^1J_{\text{C-P}} = 9.0$), 145.6 (d, $^1J_{\text{C-P}} = 29.6$).

GCMS: $m/z = 452.50$ (M^+).

IR (KBr disk): 430 (s), 501 (vs), 534 (vs), 550 (s), 558 (s), 694 (vs), 744 (vs), 820 (s), 966 (w), 1003 (s), 1026 (s), 1090 (m), 1180(s), 1203 (s), 1280 (w), 1433 (s), 1475 (s), 1583 (m).

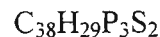
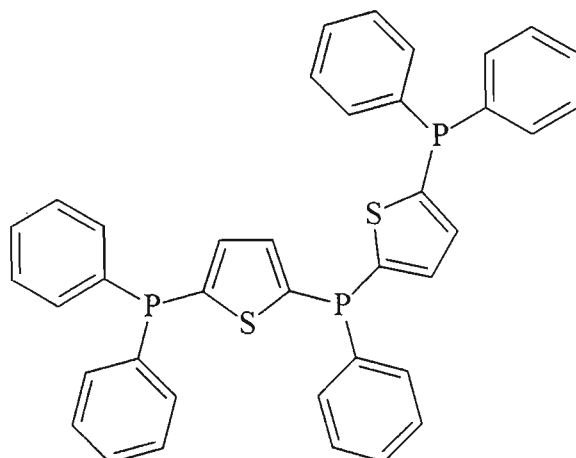
UV-vis (dichloromethane), λ_{max} , nm (ϵ , $\text{M}^{-1}\cdot\text{cm}^{-1}$): 231 ($3.0\cdot 10^4$), 256 (br sh, $2.3\cdot 10^4$).

METHOD B

2,5-Dibromothiophene (4.84 g, 20 mmol) and magnesium turnings (1.05 g, 44 mmol) were placed in a dry flask and 40 ml dry THF added. The mixture was refluxed for 4 hours, yielding yellow-brown precipitate. A solution of 7.2 ml (40 mmol) diphenylchlorophosphine in 30 ml dry THF was added quickly at room temperature. The reaction mixture was stirred at room temperature for 14 hours. A usual hydrolytic work-up followed (as described in Method A). The viscous dark brown oil was purified by passing through a layer of silica using acetone as eluent, the solvent removed, and the residue was left to solidify at -25°C . After 2 months an off-white solid was obtained, which was washed with cold methanol to give the final product.

Yield = 4.32 g (40%).

II.4.1.6 Synthesis of phenylbis[(5-diphenylphosphino)-2-thienyl]phosphine (PDSP)



$$M = 642.69 \text{ g}\cdot\text{mol}^{-1}$$

A mixture of 1.07 g (3 mmol) diphenyl(5-bromo-2-thienyl)phosphine (PSBr) and 0.073 g (3 mmol) magnesium turnings in 15 ml dry THF was refluxed for 3 hours or until all metal was dissolved. It was cooled to 10°C and a solution of 0.20 ml (1.5 mmol) dichlorophenylphosphine in 15 ml dry THF was added dropwise at this temperature. When the addition was complete, the mixture was allowed to stir at room temperature overnight. Usual hydrolytic work-up followed (as described in Section 4.1.5), with the only modification of using dichloromethane instead of ether for extraction. After evaporation of the solvent, viscous yellowish oil was obtained. It was purified on Chromatotron® (silica; hexane/ether, 10:1, v:v). The second band was collected. After evaporation of the solvent, colourless oil was obtained which failed to crystallise despite numerous efforts.

Yield = 0.57 g (60%).

Elemental analysis: calculated C 71.02 %, H 4.55 %;

found C 70.64 %, H 4.51 %.

$^{31}\text{P}\{\text{H}\}$ (CDCl_3) = -18.68 (s), -32.17 (s) ppm in 2:1 ratio.

^1H (CDCl_3), δ , ppm: 7.14-7.27 (m, ABXY system; 4 H), 7.28-7.41 (m, 25 H).

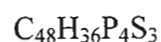
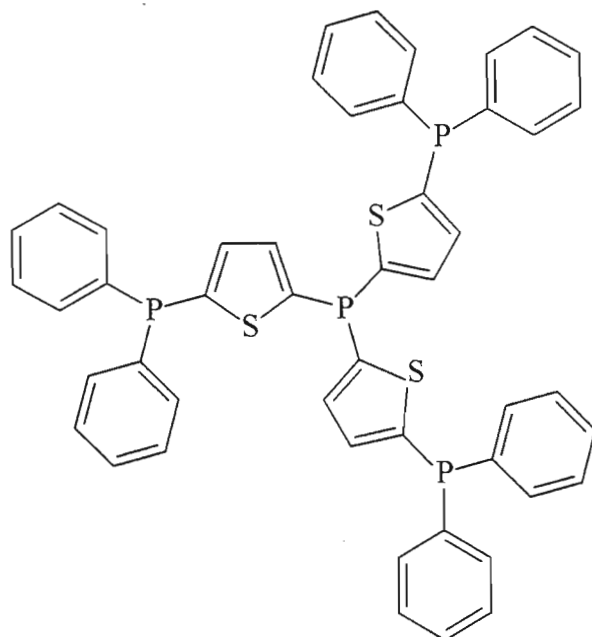
$^{13}\text{C}\{\text{H}\}$ (CDCl_3), δ , ppm (J , Hz): 128.4 (d, $^3J_{\text{C-P}} = 7.2$), 128.5 (d, $^3J_{\text{C-P}} = 7.2$), 129.0 (s), 129.1 (s), 133.1 (d, $^2J_{\text{C-P}} = 20.0$), 133.2 (d, $^2J_{\text{C-P}} = 19.9$), 136.2 (d, $^1J_{\text{C-P}} = 7.0$), 136.4 (dd, $^3J_{\text{C-P}} = 7.0$, $^2J_{\text{C-P}} = 22.0$), 136.7 (d, $^1J_{\text{C-P}} = 7.4$), 137.0 (dd, $^3J_{\text{C-P}} = 8.8$, $^2J_{\text{C-P}} = 28.6$), 144.8 (d, $^1J_{\text{C-P}} = 24.5$), 145.1 (d, $^1J_{\text{C-P}} = 29.9$).

MS (direct injection): $m/z = 642.40$ (M^+).

IR (KBr disk): 501 (m), 519 (m), 536 (m), 551 (m), 696 (vs), 742 (s), 813 (m), 964 (w), 1002 (m), 1026 (w), 1068 (vw), 1089 (w), 1203 (m), 1284 (w), 1325 (w), 1414 (w), 1435 (s), 1479 (w).

UV-vis (dichloromethane), λ_{\max} , nm (ϵ , $\text{M}^{-1}\cdot\text{cm}^{-1}$): 230 ($3.2\cdot 10^4$), 251 (sh, $2.6\cdot 10^4$), 295 ($1.8\cdot 10^4$).

II.4.1.7 Synthesis of tris[(5-diphenylphosphino)-2-thienyl]phosphine (PTSP)



$$M = 832.89 \text{ g}\cdot\text{mol}^{-1}$$

Freshly distilled diisopropylamine (0.84 g, 6 mmol) was dissolved in 20 ml dry THF. This solution was added dropwise to a hexane solution containing 6 mmol of BuLi at -78°C . When the addition was complete, the mixture was allowed to warm to 0°C and stirred at this temperature for 30 minutes, followed by cooling to -78°C . A solution containing 1.608 g (6 mmol) diphenyl(2-thienyl)phosphine (PS) in 15 ml dry THF was added slowly. After one hour, the mixture was allowed to gradually warm up to 0°C . A solution of 0.18 ml (2 mmol) phosphorus trichloride in 10 ml dry THF was added dropwise to the above mixture at 0°C . It was stirred at room temperature overnight. The mixture was hydrolysed with dilute HCl and extracted with ether in a usual way (see Sections 4.1.1 and 4.1.5). After evaporation of the solvent, the dark residue was dissolved in acetone (5 ml). Very dark brown oil remained undissolved and was subsequently discarded. The solution was poured in cold methanol, and off-white precipitate separated. It was purified by column chromatography (silica; hexane) and the first band was collected. Evaporation of the solvent gave a white solid.

Yield = 0.75 g (45%), m.p. = $137-8^\circ\text{C}$.

Elemental analysis: calculated C 69.22 %, H 4.36 %;

found C 68.38 %, H 4.26 %.

$^{31}\text{P}\{\text{H}\}$ (CDCl_3) = -18.62 (s), -44.73 (s) ppm in 3:1 ratio.

^1H (CDCl_3), δ , ppm: 7.10-7.16 (m, ABXY system; 3 H), 7.21-7.27 (m, ABXY system; 3 H), 7.27-7.38 (m, 30 H).

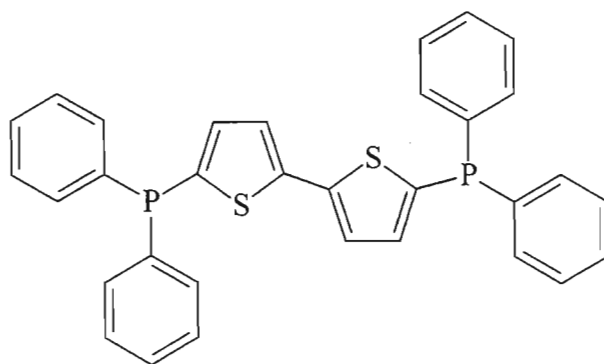
$^{13}\text{C}\{\text{H}\}$ (CDCl_3), δ , ppm (J , Hz): 128.5 (d, $^3J_{\text{C-P}} = 7.3$), 130.0 (s), 133.2 (d, $^2J_{\text{C-P}} = 20.0$), 135.9 (dd, $^3J_{\text{C-P}} = 6.9$, $^2J_{\text{C-P}} = 25.2$), 136.3 (d, $^1J_{\text{C-P}} = 6.7$), 137.0 (dd, $^3J_{\text{C-P}} = 9.1$, $^2J_{\text{C-P}} = 30.4$), 144.9 (d, $^1J_{\text{C-P}} = 24.1$), 145.4 (d, $^1J_{\text{C-P}} = 30.5$).

MS (direct injection): $m/z = 833.40$ (M^+).

IR (KBr disk): 505 (m), 528 (m), 561 (s), 582 (w), 696 (vs), 746 (s), 813 (m), 966 (vw), 1001 (m), 1024 (m), 1070 (w), 1091(m), 1205 (m), 1284 (w), 1325 (w), 1410 (w), 1433 (s), 1477 (w).

UV-vis (dichloromethane), λ_{max} , nm (ϵ , $\text{M}^{-1}\cdot\text{cm}^{-1}$): 229 ($3.2\cdot 10^4$), 252 ($2.7\cdot 10^4$), 302 ($2.0\cdot 10^4$).

II.4.1.8 Synthesis of 5,5'-bis(diphenylphosphino)-2,2'-bithiophene (PSSP)



$\text{C}_{32}\text{H}_{24}\text{P}_2\text{S}_2$

$M = 534.61 \text{ g}\cdot\text{mol}^{-1}$

A solution of 2.36 g (14.2 mmol) 2,2'-bithiophene (see Appendix A for the preparation method) in 30 ml dry ether was added dropwise to a solution containing 31.2 mmol of BuLi (1.6 M, hexane) at 0°C . The addition was complete in approximately 40 minutes, and yellowish precipitate was observed. The mixture was allowed to stir for two hours at room temperature, after which a solution of 5.2 ml (28.8 mmol) diphenylchlorophosphine in 20 ml dry ether was added dropwise with cooling (0°C). Then the mixture was gradually brought to ambient temperature and stirred for 14 hours. During the work-up procedure, 30 ml 0.1 M HCl solution were added followed by crushed ice. The product was extracted with dichloromethane (3 x 100 ml), washed with NaHCO_3 and NaCl solutions and dried over Na_2SO_4 . The organic layer was reduced *in vacuo* and 25 ml of a mixture of methanol/acetone (4:1, v:v) added. A yellowish precipitate separated after cooling the mixture to -25°C for 24 hours. It was purified on Chromatotron® (silica; hexane/ether, 8:1, v:v).

Yield = 4.65 g (61%), m.p. = $191\text{-}2^\circ\text{C}$.

Elemental analysis: calculated C 71.89 %, H 4.52 %;

found C 71.78 %, H 4.80 %.

$^{31}\text{P}\{\text{H}\}$ (CDCl_3) = -18.75 (s).

^1H (CDCl_3), δ , ppm (J , Hz): 7.10-7.22 (ABX system, $^4J_{\text{H-P}} = 1.46$, $^3J_{\text{H-P}} = 6.14$, $J_{\text{AB}} = 3.57$, 4 H), 7.30-7.44 (m, 20 H).

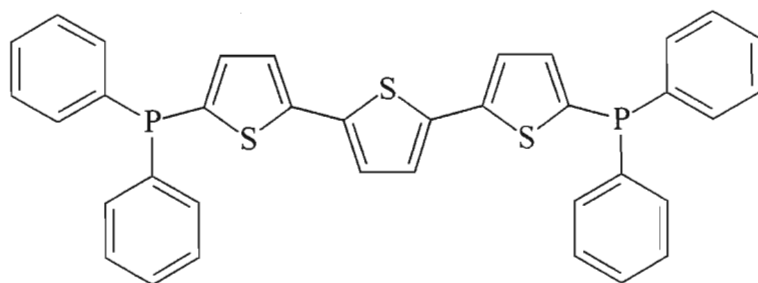
$^{13}\text{C}\{\text{H}\}$ (CDCl_3), δ , ppm (J , Hz): 124.8 (d, $^3J_{\text{C-P}} = 8.0$), 128.5 (d, $^3J_{\text{C-P}} = 7.1$), 129.0 (s), 133.0 (d, $^2J_{\text{C-P}} = 19.7$), 137.3 (d, $^2J_{\text{C-P}} = 18.3$), 137.6 (d, $^1J_{\text{C-P}} = 6.8$), 137.8 (d, $^1J_{\text{C-P}} = 30.2$), 143.4 (s).

MS (direct injection): $m/z = 534.38$ (M^+).

IR (KBr disk): 486 (s), 499 (s), 514 (s), 551 (w), 571 (w), 696 (vs), 741 (vs), 798 (vs), 875 (m), 918 (w), 988 (s), 1026 (w), 1068 (w), 1073 (w), 1092 (m), 1198 (m), 1271 (w), 1308 (w), 1429 (m), 1435 (s), 1477 (m).

UV-vis (dichloromethane), λ_{max} , nm (ϵ , $\text{M}^{-1}\cdot\text{cm}^{-1}$): 230 ($1.9\cdot 10^4$), 350 ($1.95\cdot 10^4$).

II.4.1.9 Synthesis of 5,5''-bis(diphenylphosphino)-2,2':5',2''-terthiophene (PSSSP)



$\text{C}_{36}\text{H}_{26}\text{P}_2\text{S}_3$

$M = 616.81 \text{ g}\cdot\text{mol}^{-1}$

2,2':5',2''-Terthiophene (3.72 g, 15 mmol) (see Appendix A for the preparation method) was suspended in 50 ml dry ether in a dropping funnel attached to a flask containing 33 mmol of BuLi (1.6 M solution in hexane). The addition of the suspension was carried out slowly – not allowing too much of the solid to go in the reaction flask at once and adding more ether when required, with the temperature being kept at 0°C . Greenish-yellow precipitate formed when approximately half amount of the terthiophene was added. After the addition was complete, the mixture was allowed to stir for 2.5 hours at room temperature. Then it was cooled down to 0°C and a solution of 5.5 ml (30.5 mmol) diphenylchlorophosphine in 30 ml dry ether was added slowly. It was allowed to warm up to room temperature gradually and left to stir for 15 hours. Dry dichloromethane (50 ml) was added, followed by addition of 100 ml dilute HCl and ice. The product was extracted several times with approximately 300 ml of dichloromethane (in total). The organic layer was washed with NaHCO_3 and NaCl solutions and dried over MgSO_4 . The solvent was

evaporated off and the residue was allowed to crystallise at -5°C for 24 hours. The precipitated solid was quickly washed with 50 ml a cold mixture of methanol and acetone (10:1, v:v), dissolved in small amount of dichloromethane and passed through a short silica column with hexane/ether (1:1, v:v) as eluent to remove discolouring impurities. It was purified further on Chromatotron® (silica; hexane/ether, 10:1, v:v). Bright yellow crystalline compound (second band) was obtained. (None of the crystals, however, proved to be suitable for X-ray crystallography.)

Yield = 6.1 g (66%), m.p. = $148-9^{\circ}\text{C}$.

Elemental analysis: calculated C 70.11 %, H 4.25 %;

found C 69.94 %, H 4.11 %.

$^{31}\text{P}\{\text{H}\}$ (CDCl_3) = -18.71 (s) ppm.

^1H (CDCl_3), δ , ppm: 7.00 (s, 2 H), 7.13-7.25 (m, ABX system; 4 H), 7.32-7.48 (m, 20 H).

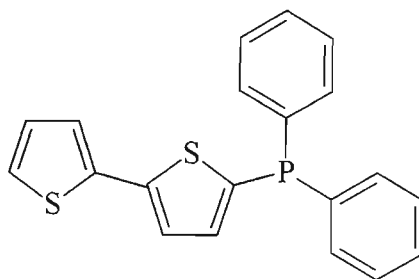
$^{13}\text{C}\{\text{H}\}$ (CDCl_3), δ , ppm (J , Hz): 124.4 (d, $^3J_{\text{C-P}} = 8.1$), 124.8 (s), 128.6 (d, $^3J_{\text{C-P}} = 7.0$), 129.0 (s), 133.0 (d, $^2J_{\text{C-P}} = 19.7$), 136.0 (s), 137.3 (d, $^2J_{\text{C-P}} = 28.1$), 137.4 (d, $^1J_{\text{C-P}} = 8.1$), 138.0 (d, $^3J_{\text{C-P}} = 29.4$), 143.5 (s).

MS (direct injection): $m/z = 616.07$ (M^+).

IR (KBr disk): 482 (s), 499 (s), 507 (m), 551 (m), 694 (vs), 742 (vs), 798 (vs), 800 (s), 869 (w), 912 (m), 983 (s), 1001 (w), 1026 (w), 1070 (w), 1091 (m), 1157 (m), 1202 (m), 1213 (w), 1433 (s), 1480 (m), 1494 (w), 1583 (w).

UV-vis (dichloromethane), λ_{max} , nm (ϵ , $\text{M}^{-1}\cdot\text{cm}^{-1}$): 230 ($1.90\cdot 10^4$), 253 (sh, $1.7\cdot 10^4$), 388 ($2.45\cdot 10^4$).

II.4.1.10 Synthesis of diphenyl[5-(2,2'-bithienyl)]phosphine (PSS)



$\text{C}_{20}\text{H}_{15}\text{PS}_2$

$M = 350.43 \text{ g}\cdot\text{mol}^{-1}$

METHOD A

2-Bromothiophene (1.63 g, 10 mmol) was dissolved in 20 ml dry ether and added to a slurry of 0.26 g (11 mmol) magnesium turnings at a such a speed as to maintain a gentle reflux. After the addition was complete, the reflux was continued until all the metal was

dissolved. Then the mixture was cooled down and added slowly to a solution of 3.47 g (10 mmol) diphenyl(5-bromo-2-thienyl)phosphine (PSBr, see Section 4.1.4 for the synthetic details) in 35 ml dry ether containing 0.05 g of Ni(dppp)Cl₂ at 0°C. When the addition was complete, the mixture was allowed to stir for 14 hours at ambient temperature, after which it was hydrolysed with semi-saturated NH₄Cl solution and ice. The product was extracted with dichloromethane (3 x 50 ml), washed with brine and dried over MgSO₄. Evaporation of dichloromethane left brownish oil, which was purified first by passing it through a short silica column with ether as eluent, isolating the first band and removing ether, and then 'recrystallisation' from 100 ml hot hexane/ethanol (1:1, v:v). Evaporation of three-quarter of the solvent, followed by cooling to -25°C for 20 hours, produced a small amount of precipitate of PSSP. It was filtered off and the residue left to solidify at -25°C for 10 weeks. Eventually a yellowish powder was obtained which was quickly washed with very cold methanol and dried under vacuum.

Yield = 0.87 g (25%), m.p. = 58-60°C.

Elemental analysis: calculated C 68.55 %, H 4.31 %;

found C 68.33 %, H 4.33 %.

³¹P{H} (CDCl₃) = -18.83 (s) ppm.

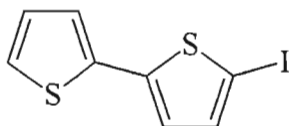
¹H (CDCl₃), δ, ppm (*J*, Hz): 6.97 (dd, ³*J*_{H-H} = 5.07, ³*J*_{H-H} = 3.60; 1 H), 7.10-7.25 (m, 4 H), 7.30-7.47 (m, 10 H).

¹³C{H} (CDCl₃), δ, ppm (*J*, Hz): 124.1 (s), 124.5 (d, ³*J*_{C-P} = 8.1), 124.9 (s), 127.8 (s), 128.5 (d, ³*J*_{C-P} = 6.8), 129.0 (s), 133.0 (d, ²*J*_{C-P} = 19.6), 136.8 (d, ¹*J*_{C-P} = 29.4), 137.3 (d, ²*J*_{C-P} = 28.1), 137.4 (s), 137.6 (d, ¹*J*_{C-P} = 8.4), 143.9 (s).

GCMS: *m/z* = 349.80 (M⁺).

IR (KBr disk): 482 (s), 494 (s), 504 (s), 550 (m), 692 (vs), 737 (s), 743 (vs), 804 (s), 839 (m), 908 (w), 988 (m), 1027 (w), 1045 (vw), 1066 (w), 1089 (w), 1155 (vw), 1180 (w), 1200 (w), 1215 (vw), 1420 (m), 1431 (m), 1478 (w).

UV-vis (dichloromethane), λ_{max}, nm (ε, M⁻¹·cm⁻¹): 230 (1.34·10⁴), 330 (1.60·10⁴).

METHOD B**Synthesis of 5-iodo-2,2'-bithiophene (ISS)**

$M = 292.15 \text{ g}\cdot\text{mol}^{-1}$

2,2'-Bithiophene (3.30 g, 20 mmol) was dissolved in a mixture of 8 ml CCl_4 and 10 ml glacial acetic acid. To this solution 0.7 g (4 mmol) HIO_3 was added, followed by 7 ml water. Then 2.3 g iodine (9 mmol) was introduced into the flask. And finally a catalytic amount of concentrated H_2SO_4 (0.1 ml) was added. The mixture was stirred at 40°C until the purple colour of iodine disappeared. Water (20 ml) was added, the organic layer collected and the rest was extracted with chloroform (2 x 20 ml). The combined extracts were washed with saturated solution of NaHCO_3 and semi-saturated solution of Na_2SO_3 , dried over CaCl_2 and filtered. After evaporation of the solvent, a brown solid mass was obtained. It was distilled under vacuum. The oil solidified and the off-yellow crystals were washed quickly with cold hexane to yield white product. It showed to be >95% the target compound by GC analysis.

Yield = 3.36 g (56%), m.p. = $30\text{--}32^\circ\text{C}$ (lit.¹⁹³ 32°C), b.p. = $165\text{--}70^\circ\text{C}/1.5 \text{ mmHg}$ (lit.¹⁹³ = $108\text{--}9^\circ\text{C}/0.03 \text{ mmHg}$).

^1H (CDCl_3), δ , ppm (J , Hz): 6.85 (d, $^3J_{\text{H-H}} = 3.85$; 1 H), 6.98-7.16 (m, AB system, $J_{\text{AB}} = 3.64$; 2 H), 7.18 (d, $^3J_{\text{H-H}} = 3.85$; 1 H), 7.23 (dd, $^4J_{\text{H-H}} = 1.18$, $^3J_{\text{H-H}} = 5.09$; 1 H).

GCMS: $m/z = 291.90$ (M^+).

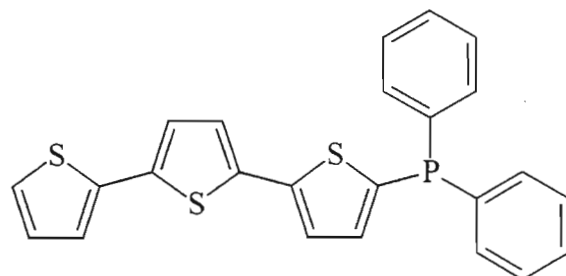
Synthesis of diphenyl[5-(2,2'-bithienyl)]phosphine

5-Iodo-2,2'-bithiophene (3.0 g, ± 10 mmol) was dissolved in 25 ml dry THF. To this solution 0.26 g (11 mmol) magnesium turnings were added. Iodine (\pm two crystals) was added as a catalyst, and the mixture was left refluxing for 5 hours or until practically all metal was dissolved. Then the mixture was cooled to 0°C and 2.0 ml (11 mmol) neat diphenylchlorophosphine were added slowly. The mixture was allowed to gradually warm up and was stirred at room temperature for 14 hours. A usual hydrolytic work up (*e.g.*, see Section 4.1.5) followed. After drying and evaporation of the solvent, the residue was applied to a silica column with hexane/ether (20:1, v:v) as eluent to remove 2,2'-bithiophene. Using hexane/ether (5:1, v:v) as eluent, the target compound was eluted from the column. This yielded yellow oil, which was left to solidify under a small layer of

methanol at -15°C . Crystallisation occurred after ± 3 months. The off-white powder was washed with very cold methanol and dried.

Yield = 0.84 g (24%), m.p. = $58-59^{\circ}\text{C}$.

II.4.1.11 Synthesis of diphenyl[5-(2,2':5',2''-terthienyl)]phosphine (PSSS)



$\text{C}_{24}\text{H}_{17}\text{PS}_3$

$M = 432.55 \text{ g}\cdot\text{mol}^{-1}$

5-Bromo-2,2':5',2''-terthiophene (0.82 g, 2.5 mmol) (see Appendix A for the preparation details) was dissolved in 10 ml dry THF and magnesium turnings (0.060 g, 2.5 mmol) were added. The reaction flask was placed in an ultrasonic bath and two drops of freshly distilled 1,2-dibromoethane were added. The mixture quickly turned brownish, but the reaction was complete only after an hour of sonication at room temperature. Then the flask was cooled to 0°C and 10 ml dry THF added, followed by dropwise addition of a solution of 0.45 ml (2.5 mmol) diphenylchlorophosphine in 5 ml dry THF. The mixture was allowed to reach ambient temperature and stirred for 1 hour. The solvent was evaporated off and cold methanol added, resulting in formation of an orange precipitate. This precipitate was placed on the top of a silica column and eluted with petroleum ether (60-80) to remove 2,2':5',2''-terthiophene (SSS) and the starting material. The next yellow band was collected using hexane/ether (20:1, v:v) as eluent, the solvent removed and methanol added. A bright yellow precipitate was formed after 1 day at -25°C . It was washed with methanol and dried under vacuum.

Yield = 0.42 g (39%), m.p. = $77-8^{\circ}\text{C}$.

Elemental analysis: calculated C 66.64 %, H 3.96 %;

found C 66.22 %, H 4.12 %.

$^{31}\text{P}\{\text{H}\}$ (CDCl_3) = -18.71 (s) ppm.

^1H (CDCl_3), δ , ppm: 6.99-7.06 (m, 3 H), 7.15-7.27 (m, 4 H), 7.32-7.48 (m, 10 H).

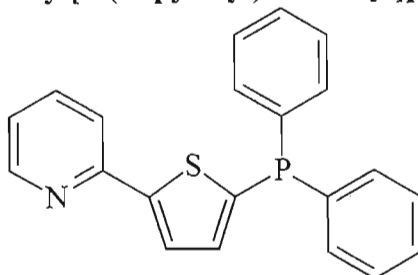
$^{13}\text{C}\{\text{H}\}$ (CDCl_3), δ , ppm (J , Hz): 124.3-125.0 (m, 4 C), 125.2 (d, $^3J_{\text{C-P}} = 7.0$), 128.6 (s), 129.2 (d, $^3J_{\text{C-P}} = 8.8$), 129.6 (s), 133.8 (d, $^2J_{\text{C-P}} = 19.7$), 137.7 (d, $^2J_{\text{C-P}} = 28.3$), 137.0-139.0 (m, 5 C), 144.2 (s).

MS (direct injection): $m/z = 432.02$ (M^+).

IR (KBr disk): 474 (m), 494 (s), 509 (m), 550 (w), 695 (vs), 746 (s), 793 (vs), 835 (m), 862 (w), 900 (vw), 984 (m), 1028 (vw), 1055 (vw), 1092 (w), 1155 (vw), 1196 (w), 1228 (w), 1422 (m), 1433 (s), 1454 (w), 1479 (m).

UV-vis (dichloromethane), λ_{\max} , nm (ϵ , $\text{M}^{-1}\cdot\text{cm}^{-1}$): 228 ($1.34\cdot 10^4$), 250 (sh, $1.12\cdot 10^4$), 374 ($2.0\cdot 10^4$)

II.4.1.12 Synthesis of diphenyl[5-(2'-pyridyl)-2-thienyl]phosphine (PSN)



$\text{C}_{26}\text{H}_{16}\text{NPS}$

$M = 345.40 \text{ g}\cdot\text{mol}^{-1}$

A solution of 3.6 ml (20 mmol) diphenylchlorophosphine in 20 ml dry THF was added carefully to a slurry of 0.7 g (100 mmol) lithium pieces in 10 ml dry THF under argon. When no reaction was observed for 10 minutes, the mixture was gently warmed up to $\pm 50^\circ\text{C}$ until the reaction started and the solution turned orange. After all diphenylchlorophosphine was added, the mixture was refluxed for further 3 hours. Then it was cooled to room temperature, decanted off the metal and placed in a reaction flask under nitrogen. A solution of 4.8 g (20 mmol) of 2-bromo-5-(2'-pyridyl)thiophene (see Appendix A for the preparation details) in 20 ml dry THF was added to it dropwise at -78°C over 1.5 hours. When the addition was complete, the mixture was allowed to warm up to room temperature and stirred for 14 hours. Two-thirds of the solvent were evaporated and 30 ml of degassed dry ether added. The solution was extracted with 2 x 20 ml of 5 M HCl and then carefully basified with concentrated ammonia solution at 0°C . The basified solution was extracted with ether (2 x 30 ml), ethereal layers combined, dried, filtered and evaporated to dryness. The residue was purified by column chromatography (silica; hexane/ether, 6:1, v:v), yielding a white microcrystalline compound.

Yield = 4.61 g (66%), m.p. = $69\text{--}70^\circ\text{C}$.

Elemental analysis: calculated C 73.03 %, H 4.67 %, N 4.06 %;

found C 72.61 %, H 4.44 %, N 4.01 %.

$^{31}\text{P}\{\text{H}\}$ (CDCl_3) = -18.35 (s) ppm.

^1H (CDCl_3), δ , ppm (J , Hz): 7.15 (ddd, $^4J_{\text{H-H}} = 1.96$, $^3J_{\text{H-H}} = 5.43$, $^3J_{\text{H-H}} = 7.08$; 1 H), 7.29-7.50 (m, 11 H), 7.57 (dd, $^4J_{\text{H-P}} = 1.32$, $^3J_{\text{H-H}} = 3.62$; 1 H), 7.61-7.70 (m, 2 H), 8.50-8.56 (m, 1 H).

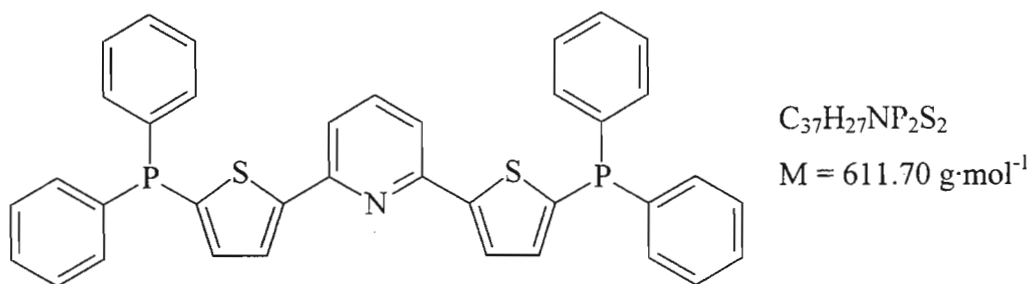
$^{13}\text{C}\{\text{H}\}$ (CDCl_3), δ , ppm (J , Hz): 118.8 (s), 122.2 (s), 125.2 (d, $^3J_{\text{C-P}} = 8.5$), 128.5 (d, $^3J_{\text{C-P}} = 7.2$), 129.0 (s), 133.1 (d, $^2J_{\text{C-P}} = 19.8$), 136.7 (s), 137.3 (d, $^2J_{\text{C-P}} = 29.2$), 137.6 (d, $^1J_{\text{C-P}} = 8.1$), 140.6 (d, $^1J_{\text{C-P}} = 22.5$), 149.5 (s), 150.9 (s), 152.1 (s).

GCMS: $m/z = 344.60$ ($\text{M}^+ - 1$).

IR (KBr disk): 476 (m), 497 (s), 504 (s), 553 (m), 692 (vs), 714 (m), 745 (vs), 777 (vs), 814 (m), 964 (m), 988 (s), 1004 (m), 1027 (w), 1045 (vw), 1081 (w), 1093 (w), 1151 (m), 1211 (w), 1292 (w), 1325 (w), 1427 (s), 1438 (m), 1466 (s), 1478 (m), 1533 (m), 1562 (m), 1585 (s).

UV-vis (dichloromethane), λ_{max} , nm (ϵ , $\text{M}^{-1}\cdot\text{cm}^{-1}$): 231 ($1.3\cdot 10^4$), 271 ($1.3\cdot 10^4$), 324 ($1.8\cdot 10^4$).

II.4.1.13 Synthesis of 2,6-bis((5'-diphenylphosphino)-2'-thienyl)pyridine (PSNSP)



A hexane solution containing 10 mmol of BuLi was added dropwise to a solution of 2.68 g (10 mmol) diphenyl(2-thienyl)phosphine (PS) in 20 ml dry ether at 0°C . The mixture was stirred for 2 hours and 2.58 g (10 mmol) solid $\text{MgBr}_2\cdot\text{Et}_2\text{O}$ were added portionwise under nitrogen blanket over 10 minutes. The solution was allowed to react for one hour and was then transferred to a dropping funnel via a cannula. The mixture was slowly added – keeping the temperature at 0°C – to a solution of 1.18 g (5 mmol) 2,6-dibromopyridine in 20 ml dry THF to which 0.10 g $\text{Ni}(\text{dppp})\text{Cl}_2$ had been added. The resulting solution was allowed to warm up to ambient temperature and stirred for 16 hours. The mixture was hydrolysed with semi-saturated NH_4Cl solution, extracted with dichloromethane (3 x 25 ml), washed with brine, dried and the solvent evaporated. After evaporation of the solvent, 15 ml cold methanol were added and the precipitate was filtered off. It was recrystallised from methanol or, alternatively, purified by column chromatography (silica; hexane/ether, 2:1, v:v). Greenish crystals were obtained.

Yield = 1.65 g (54%), m.p. = $175\text{--}6^\circ\text{C}$.

Elemental analysis: calculated C 72.65 %, H 4.45 %, N 2.29 %;

found C 72.78 %, H 4.29 %, N 2.31 %.

$^{31}\text{P}\{\text{H}\}$ (CD_2Cl_2) = -18.28 (s) ppm.

^1H (CD_2Cl_2), δ , ppm (J , Hz): 7.25 (dd, $^3J_{\text{H-P}} = 5.82$, $^3J_{\text{H-H}} = 3.66$; 2 H), 7.31-7.47 (m, 22 H), 7.58-7.68 (m, 3 H).

$^{13}\text{C}\{\text{H}\}$ (CD_2Cl_2), δ , ppm (J , Hz): 117.8 (s), 126.0 (d, $^3J_{\text{C-P}} = 7.7$), 128.8 (d, $^3J_{\text{C-P}} = 7.1$), 129.3 (s), 133.4 (d, $^2J_{\text{C-P}} = 19.9$), 137.4 (d, $^2J_{\text{C-P}} = 26.1$), 137.8 (s), 138.0 (d, $^1J_{\text{C-P}} = 7.8$), 141.2 (d, $^1J_{\text{C-P}} = 30.8$), 150.9 (s), 152.0 (s).

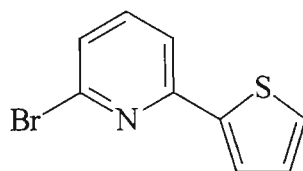
MS (direct injection): $m/z = 610.75$ ($\text{M}^+ - 1$).

IR (KBr disk): 496 (s), 504 (w), 537 (m), 553 (w), 694 (vs), 739 (vs), 791 (vs), 814 (vw), 955 (w), 988 (m), 1001 (m), 1026 (w), 1070 (w), 1089 (w), 1095 (w), 1120 (w), 1164 (m), 1209 (w), 1265 (m), 1313 (w), 1326 (vw), 1421 (s), 1435 (s), 1454 (s), 1477 (m), 1525 (w), 1562 (vs), 1580 (s).

UV-vis (dichloromethane), λ_{max} , nm (ϵ , $\text{M}^{-1}\cdot\text{cm}^{-1}$): 230 ($3.3\cdot 10^4$), 265 ($2.7\cdot 10^4$), 323 ($2.7\cdot 10^4$), 345 ($2.8\cdot 10^4$).

II.4.1.14 Synthesis of diphenyl[6-(2'-thienyl)-2-pyridyl]phosphine (PNS)

Synthesis of 2-bromo-6-(2'-thienyl)pyridine



$\text{C}_9\text{H}_6\text{BrNS}$

$M = 240.11 \text{ g}\cdot\text{mol}^{-1}$

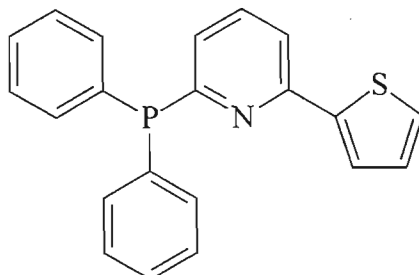
A solution of 8.1 g (50 mmol) 2-bromothiophene in 50 ml dry ether was added dropwise to 1.2 g (50 mmol) magnesium turnings in 10 ml dry ether to obtain 2-thienyl magnesium bromide in a usual manner (see Section 4.1.1). The solution of the Grignard reagent thus obtained was added slowly to a mixture containing 11 g (46 mmol) 2,6-dibromopyridine and 0.8 g (1 mmol) $\text{Pd}(\text{dppb})\text{Cl}_2$ (see Appendix A for preparation details) in 50 ml dry ether at 0°C . The reaction was sufficiently exothermal not to require external heating. The mixture was stirred at ambient temperature for 14 hours and then hydrolysed with semi-saturated NH_4Cl solution. After the usual work-up (see Section 4.1.2), evaporation of the solvent led to greenish oil which was kept at 10°C for 3 days. The precipitate was formed during this time, which was subsequently filtered off and the residual oil collected. GC analysis of the oil showed no presence of 2,6-dibromopyridine and $\pm 95\%$ of the target compound in the mixture.

Yield = 7.26 g ($\pm 55\%$).

^1H (CDCl_3), δ , ppm (J , Hz): 7.08 (dd, $^3J_{\text{H-H}} = 5.50$, $^3J_{\text{H-H}} = 3.81$; 1 H), 7.28 (dd, $^3J_{\text{H-H}} = 7.05$, $^4J_{\text{H-H}} = 1.65$; 1 H), 7.37-7.68 (m, 6 H).

GCMS: $m/z = 239.20$ (M^+ , ^{79}Br) and 241.20 (M^+ , ^{81}Br) - 98 and 100% respectively.

Synthesis of diphenyl[6-(2'-thienyl)-2-pyridyl]phosphine



$\text{C}_{21}\text{H}_{16}\text{NPS}$

$M = 345.40 \text{ g}\cdot\text{mol}^{-1}$

A hexane solution containing 30 mmol BuLi was added dropwise with cooling ($0-5^\circ\text{C}$) to a solution of 5.3 ml (30 mmol) diphenylphosphine in 50 ml dry THF. The mixture turned orange immediately. It was stirred at ambient temperature for at least 3.5 more hours to ensure completion of the reaction. The crude 2-bromo-6-(2'-thienyl)pyridine (7.26 g, approximately 30 mmol), obtained during the previous step, was dissolved in 50 ml dry THF and the solution was added slowly at 0°C to the orange mixture. The reaction mixture was allowed to reach room temperature and stirred for 14 hours.

The subsequent work-up operations were performed under an atmosphere of nitrogen with deoxygenated solvents wherever possible. Diluted HCl solution (20 ml, $\text{pH} = 2$) was added with cooling to the reaction mixture followed by 30 ml ether. The organic layer was separated and washed with water (50 ml) and dried over MgSO_4 . After the solvent was evaporated, methanol was added and the mixture was left to stand at 4°C for 2-3 days. The precipitate was filtered off, crushed finely under nitrogen and washed with cold methanol to give off-white microcrystalline compound.

Yield = 4.32 g (42%), m.p. = $94-5^\circ\text{C}$.

Elemental analysis: calculated C 73.03 %, H 4.67 %, N 4.06 %;

found C 72.55 %, H 4.57 %, N 3.86 %.

$^{31}\text{P}\{\text{H}\}$ (CDCl_3) = -3.64 (s) ppm.

^1H (CDCl_3), δ , ppm (J , Hz): 6.99 (ddd, $^3J_{\text{H-P}} = 2.40$, $^4J_{\text{H-H}} = 2.00$, $^3J_{\text{H-H}} = 6.02$; 1 H), 7.05 (dd, $^3J_{\text{H-H}} = 3.73$, $^3J_{\text{H-H}} = 5.05$; 1 H), 7.30-7.40 (m, 7 H), 7.42-7.58 (m, 7 H).

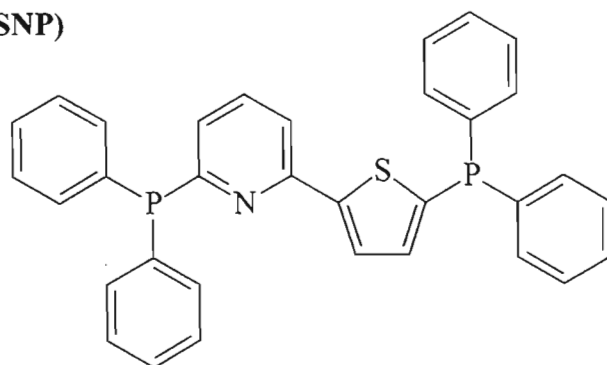
$^{13}\text{C}\{\text{H}\}$ (CDCl_3), δ , ppm (J , Hz): 117.2 (s), 124.6 (s), 126.3 (d, $^2J_{\text{C-P}} = 21.5$), 127.9 (2 s, 2 C), 128.4 (d, $^3J_{\text{C-P}} = 7.2$), 129.0 (s), 134.3 (d, $^2J_{\text{C-P}} = 19.7$), 136.1 (d, $^3J_{\text{C-P}} = 4.1$), 136.4 (d, $^1J_{\text{C-P}} = 10.0$), 147.3 (d, $^1J_{\text{C-P}} = 12.7$) 150.9 (s), 151.8 (s).

GCMS: $m/z = 344.60$ ($M^+ - 1$).

IR (KBr disk): 457 (w), 494 (s), 507 (m), 623 (w), 631 (w), 694 (vs), 715 (vs), 748 (vs), 800 (s), 862 (w), 993 (w), 1026 (vw), 1068 (vw), 1091 (w), 1164 (m), 1229 (w), 1273 (w), 1322 (vw), 1342 (w), 1418 (s), 1435 (s), 1445 (vs), 1477 (m), 1529 (w), 1554 (vs), 1573 (s).

UV-vis (dichloromethane), λ_{\max} , nm (ϵ , $M^{-1}\cdot\text{cm}^{-1}$): 230 ($1.3\cdot 10^4$), 264 ($1.4\cdot 10^4$), 278 ($1.4\cdot 10^4$), 318 ($1.1\cdot 10^4$).

II.4.1.15 Synthesis of diphenyl{5'-[2-(6-diphenylphosphino)pyridyl]-2'-thienyl}-phosphine (PSNP)



$C_{33}H_{25}NP_2S$

$M = 529.58 \text{ g}\cdot\text{mol}^{-1}$

Diphenyl[6-(2'-thienyl)-2-pyridyl]phosphine (PNS, 1.32 g, 3.82 mmol) was dissolved in 25 ml dry THF and cooled to -78°C . Then a solution of 3.85 mmol BuLi (1.6 M, hexane) was added slowly and the mixture stirred for one hour at this temperature. A solution of 0.70 ml (3.9 mmol) diphenylchlorophosphine in 10 ml dry THF was added to the mixture at -78°C and allowed gradually to warm up to room temperature. It was stirred for further 16 hours at ambient temperature. A hydrolytic work-up analogous to that described for the previous synthesis, in Section 4.1.14, followed. After evaporation of the solvent, 10 ml of cold methanol were added and the precipitated yellowish oil left to solidify at -25°C . After about 20-25 days the oil crystallised out. The solid was dissolved in a minimal volume of dichloromethane and purified using Chromatotron (silica; hexane/ether, 6:1, v/v). An off-white crystalline material was obtained as a final product.

Yield = 0.77 g (38 %), m.p. = $159-60^\circ\text{C}$.

Elemental analysis: calculated C 74.85 %, H 4.76 %, N 2.64 %;

found C 74.89 %, H 4.71 %, N 2.58 %.

$^{31}\text{P}\{\text{H}\}$ (CDCl_3) = -3.60 (s), -18.34 (s) ppm in 1:1 ratio.

^1H (CDCl_3), δ , ppm (J , Hz): 7.01 (ddd, $^3J_{\text{H-P}} = 1.74$, $^4J_{\text{H-H}} = 1.65$, $^3J_{\text{H-H}} = 7.05$; 1 H), 7.28 (dd, $^3J_{\text{H-H}} = 5.98$, $^3J_{\text{H-H}} = 3.67$; 1 H), 7.30-7.53 (m, 22 H), 7.59 (dd, $^4J_{\text{H-H}} = 1.35$, $^3J_{\text{H-H}} = 3.66$; 1 H).

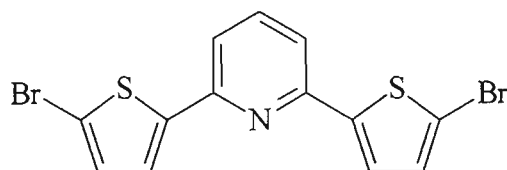
$^{13}\text{C}\{\text{H}\}$ (CDCl_3), δ , ppm (J , Hz): 117.3 (s), 125.6 (d, $^3J_{\text{C-P}} = 7.9$), 126.7 (d, $^2J_{\text{C-P}} = 21.8$), 128.4 (d, $^3J_{\text{C-P}} = 7.2$), 128.9 (s), 134.3 (d, $^2J_{\text{C-P}} = 19.6$), 136.1 (d, $^3J_{\text{C-P}} = 3.7$), 136.6 (d, $^1J_{\text{C-P}} = 8.9$), 137.1 (d, $^2J_{\text{C-P}} = 22.5$), 137.8 (d, $^1J_{\text{C-P}} = 13.6$), 147.5 (d, $^1J_{\text{C-P}} = 15.2$), 150.7 (s), 152.2 (s).

GCMS: $m/z = 529.28$ (M^+).

IR (KBr disk): 422 (m), 457 (w), 472 (w), 488 (m), 503 (m), 575 (w), 612 (w), 631 (m), 694 (vs), 741 (vs), 798 (vs), 816 (w), 973 (w), 987 (w), 999 (w), 1028 (w), 1078 (w), 1095 (w), 1164 (m), 1264 (vw), 1312 (w), 1421 (s), 1435 (s), 1442 (vs), 1479 (m), 1529 (vw), 1552 (vs), 1566 (s).

UV-vis (dichloromethane), λ_{max} , nm (ϵ , $\text{M}^{-1}\cdot\text{cm}^{-1}$): 233 ($2.5\cdot 10^4$), 265 ($2.0\cdot 10^4$), 323 ($2.0\cdot 10^4$).

II.4.1.16 Synthesis of 2,6-bis(5'-bromo-2'-thienyl)pyridine (BrSNSBr)



$\text{C}_{11}\text{H}_7\text{Br}_2\text{NS}_2$

$M = 401.22 \text{ g}\cdot\text{mol}^{-1}$

2,6-Bis(2'-thienyl)pyridine (3.7 g, 15 mmol) was dissolved in 100 ml glacial acetic acid. To this solution 1.7 ml (30 mmol) bromine in 50 ml glacial acetic acid was added gradually at room temperature during 2 hours. The mixture was left to stir for 14 hours at room temperature. To this mixture two litres of cold water were added and the precipitate collected. The precipitate was extracted with 3 x 50 ml of warm dichloromethane. The combined extracts were washed with NaHCO_3 solution until the effervescence ceased and dried over MgSO_4 . After removal of the solvent, the greenish residue was recrystallised from 1,2-dichloroethane with activated charcoal. Mica-like crystals of the final product were obtained.

Yield = 3.1 g (52%), m.p. = 220-1°C.

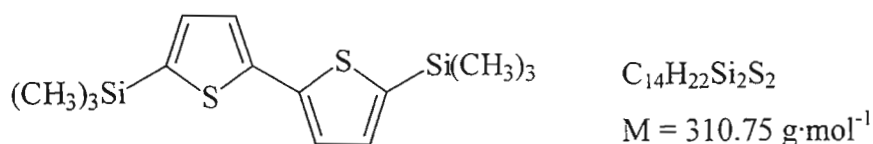
Elemental analysis: calculated C 38.90 %, H 1.75 %, N 3.49 %;

found C 38.59 %, H 1.45 %, N 3.40 %.

^1H ($\text{DMSO}-d_6$), δ , ppm (J , Hz): 7.32 (d, $^3J_{\text{H-H}} = 3.94$; 2 H), 7.69 (d, $^3J_{\text{H-H}} = 3.94$; 2 H), 7.72-7.95 (m, 3 H).

GCMS: $m/z = 398.50$ ($^{79}\text{Br} + ^{79}\text{Br}$: M^+-1), 400.50 ($^{79}\text{Br} + ^{81}\text{Br}$: M^+-1), 402.50 ($^{81}\text{Br} + ^{81}\text{Br}$: M^+-1) – triplet.

II.4.1.17 Synthesis of 5,5'-bis(trimethylsilyl)-2,2'-bithiophene (SiSSSi)



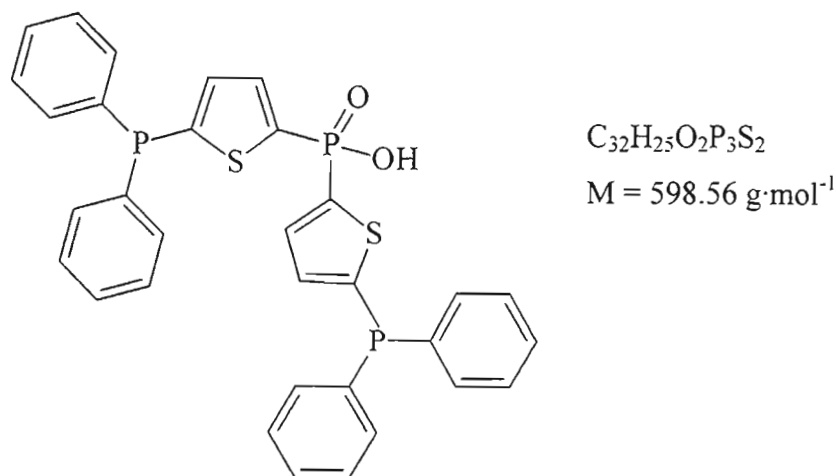
2,2'-Bithiophene (SS, 2.49 g, 15 mmol) was dissolved in 35 ml dry ether. The resulting solution was gradually added to a solution of BuLi (31 mmol) in hexane at 0°C. When the addition was complete, the mixture was stirred for 2 hours at 0°C. Freshly distilled trimethylchlorosilane (4 ml, >40 mmol) was added via a syringe. The mixture was gradually warmed up to room temperature and left to stir for 16 hours. It was hydrolysed using saturated NaHCO₃ solution, extracted with ether (2 x 50 ml) and dried over Na₂SO₄. After the solvent was evaporated, the yellow residue quickly crystallised as brownish crystals. They were recrystallised from hot methanol with activated charcoal, yielding pure white microcrystalline material.

Yield = 3.5 g (75%), m.p. = 63-64°C.

¹H (CDCl₃), δ, ppm (*J*, Hz): 0.33 (s, 18 H), 7.13-7.23 (m, AB system, *J*_{A-B} = 3.75; 4 H).

GCMS: *m/z* = 309.85 (*M*⁺-1).

II.4.1.18 Synthesis of bis[5-(diphenylphosphino)-2-thienyl]phosphinic acid (DTPA)



A solution of 2.08 g (6 mmol) diphenyl(5-bromo-2-thienyl)phosphine (PSBr) in 35 ml dry THF was refluxed with 0.15 g (>6 mmol) magnesium turnings under nitrogen for 4.5 hours. The solution was cooled down and transferred via a cannula to a dropping funnel connected to a flask containing 0.87 g (6 mmol) thoroughly degassed diethyl chlorophosphate in 35 ml dry THF. This mixture was brought to reflux while the Grignard reagent was being added (40 minutes). The solution was refluxed for a further hour and then stirred at ambient temperature for 15 hours. A solution of hydrochloric acid (20 ml,

pH = 1) was added followed by saturated NaHCO_3 solution until the effervescence ceased. The mixture was extracted with dichloromethane (3 x 30 ml) and dried over MgSO_4 . After evaporation of two-thirds of the solvent, a whitish precipitate separated. Both the precipitate and the mother liquor were subsequently investigated.

Analysis of the mother liquor showed the presence of the intended compound *i.e.*, 2-diethoxyphosphoryl-5-(diphenylphosphino)thiophene ($^{31}\text{P}\{\text{H}\}$ NMR: $\delta = 10.21$ and -18.15 ppm – two singlets in 1:1 ratio; GCMS: $m/z = 404.20 - \text{M}^+$). However it was present in a small amount in a mixture where the major component was identified as diphenyl(2-thienyl)phosphine (PS) ($^{31}\text{P}\{\text{H}\}$ NMR: $\delta = -19.90$ ppm). Numerous attempts of chromatographic separation with a variety of mobile phases on silica proved to be fruitless and the former compound was not isolated.

On the other hand, the precipitate separated from the mother liquor was purified on Chromatotron® using dichloromethane as eluent. By combination of analytical techniques the isolated compound was identified as bis[5-(diphenylphosphino)-2-thienyl]phosphinic acid. Yield = 0.36 g (10%).

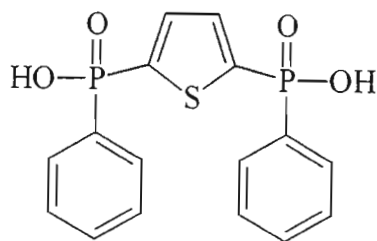
Elemental analysis: calculated C 64.21 %, H 4.21 %;

found C 64.14 %, H 4.10 %.

$^{31}\text{P}\{\text{H}\}$ (CDCl_3) = 4.85 (s), -18.24 (s) ppm in 1:2 ratio.

^1H (CDCl_3), δ , ppm (J , Hz): 7.21 (ddd, $^4J_{\text{H-P}} = 2.05$, $^3J_{\text{H-P}} = 5.83$, $^3J_{\text{H-H}} = 3.52$; 2 H), 7.27-7.40 (m, 20 H), 7.47 (ddd, $^4J_{\text{H-P}} = 1.03$, $^3J_{\text{H-P}} = 7.91$, $^3J_{\text{H-H}} = 3.52$; 2 H).

II.4.1.19 Synthesis of thien-2,5-diyl di(phenylphosphinic acid) (TDPA)



$\text{C}_{16}\text{H}_{14}\text{O}_4\text{P}_2\text{S}$

$M = 364.29 \text{ g}\cdot\text{mol}^{-1}$

Thoroughly degassed 2,5-dibromothiophene (3.6 g, 15 mmol) was placed in a flask under nitrogen followed by 0.75 g freshly calcified NiCl_2 . To this mixture, 10 g (>50 mmol) neat, degassed diethyl phenylphosphonite was added at 170°C over a period of one hour. The suspension slowly changed its colour to deep red and then purple. The temperature was maintained at $170\text{--}180^\circ\text{C}$ for another hour. Then the reaction flask was connected to a vacuum pump and all volatile impurities were removed leaving a dark residue.

To this residue solid NaOH (1.4 g) was added, followed by 50 ml methanol. The mixture was refluxed gently for 3 hours. Methanol was evaporated and 50 ml water added. The organic matter was extracted with ether (2 x 50 ml) and discarded. The aqueous layer was collected, heated to 45°C and purified with activated charcoal. The clear filtrate was acidified with dilute HCl solution (pH = 2). A white precipitate was isolated after cooling at -10°C for 24 hours. It was recrystallised from 30% aqueous methanol to obtain the pure material.

Yield = 1.20 g (24%).

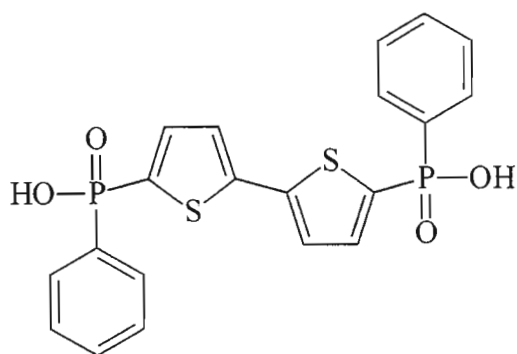
Elemental analysis: calculated C 52.75 %, H 3.85 %;

found C 53.50 %, H 3.84 %.

$^3\text{P}\{\text{H}\}$ (CD_3OD) = 19.86 (s) ppm.

^1H (CD_3OD), δ , ppm: 7.43-7.65 (m, 8 H), 7.76-7.93 (m, 4 H).

II.4.1.20 Synthesis of 2,2'-bithien-5,5'-diyl di(phenylphosphinic acid) (BTDPA)



$\text{C}_{20}\text{H}_{16}\text{O}_4\text{P}_2\text{S}_2$

$M = 446.37 \text{ g}\cdot\text{mol}^{-1}$

A 3-necked flask containing 4.9 g (15 mmol) 5,5'-dibromo(2,2'-bithiophene) and 0.9 g freshly calcified NiCl_2 was filled with nitrogen and heated to 150°C or until the solid started melting. Neat, degassed diethyl phenylphosphonite (10 g, >50 mmol) was added very slowly to the mixture at 170°C (1 hour). The mixture gradually changed its colour to dark brown-purple. The reaction was carried out at 175-185°C for 2 hours and volatile by-products were allowed to evaporate. The mixture was allowed to cool below 80°C, when 1.5 g NaOH and 50 ml methanol were added. The mixture was refluxed for 3 hours and the solvent was distilled off. Water (300 ml) was added to the residue at room temperature and the solution filtered. The yellow filtrate was extracted with ether to remove organic impurities and the aqueous layer was acidified with concentrated HCl/ice mixture. Yellowish flaky precipitate formed. It was allowed to coagulate at -10°C for 24 hours. After filtration the compound was recrystallised from hot ethanol.

Yield = 2.28 g (34%).

Elemental analysis: calculated C 53.81 %, H 3.61 %;
found C 53.53 %, H 3.47 %.

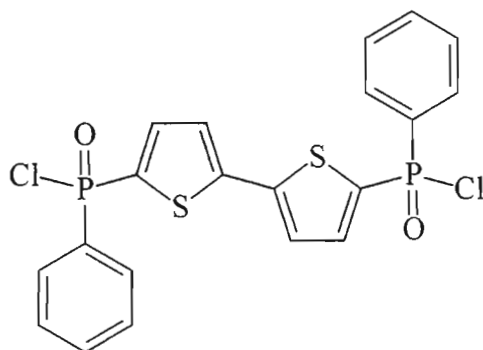
$^{31}\text{P}\{\text{H}\}$ (CD_3OD) = 20.08 (s) ppm.

^1H (CD_3OD), δ , ppm (J , Hz): 7.56 (dd, $^4J_{\text{H-P}} = 2.54$, $^3J_{\text{H-H}} = 3.71$; 2 H), 7.63-7.80 (m, 8 H), 7.76-7.93 (m, 4 H).

IR (KBr disk): 476 (w), 501 (w), 524 (s), 546 (vs), 562 (m), 579 (m), 646 (m), 692 (s), 719 (s), 748 (w), 804 (m), 881 (m), 962 (vs), 1020 (vs), 1095 (s), 1128 (s), 1190 (br, s), 1275 (w), 1319 (vw), 1424 (m), 1438 (s), 1637 (br, m), 2240 (br, w), 2673 (br, w).

II.4.1.21 Synthesis of 5,5'-bis(phenylphosphino)-2,2'-bithiophene (HPSSPH)

Synthesis of 5,5'-bis(*P*-chloro-phenylphosphoryl)-2,2'-bithiophene

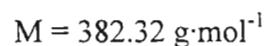
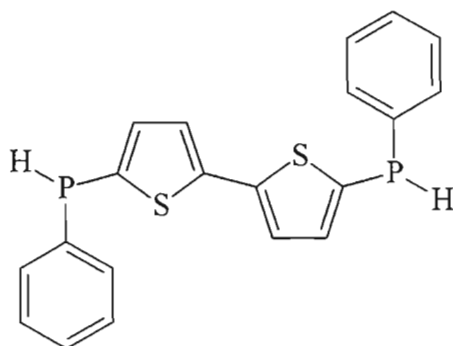


$\text{C}_{20}\text{H}_{14}\text{Cl}_2\text{O}_2\text{P}_2\text{S}_2$

$M = 483.24 \text{ g}\cdot\text{mol}^{-1}$

2,2'-Bithien-5,5'-diyl di(phenylphosphinic acid) (BTDDPA, 1.42 g, 3.2 mmol) was placed in a dry flask and 100 ml freshly distilled thionyl chloride added. The mixture was kept at 40°C for 1 hour or until the solid dissolved. The excess of thionyl chloride was removed under vacuum. Dry THF (10 ml) was added to the residue and the solvent removed under vacuum, this procedure being repeated twice. A pale-yellow compound was used in the next step as obtained, since all distillation attempts resulted in decomposition or hydrolysis of at least some of the product.

$^{31}\text{P}\{\text{H}\}$ (neat) = 33 (br s) ppm.

Synthesis of 5,5'-bis(phenylphosphino)-2,2'-bithiophene (HPSSPH)

The residue obtained in the previous step was dissolved in 40 ml dry THF. Large excess of LiAlH_4 (± 1 g) was added. The mixture was refluxed for 12 hours. It was cooled down and hydrolysed with wet, oxygen-free THF. The solution was decanted from the precipitate and evaporated to dryness. Warm, degassed hexane was added to the solid, the mixture was ultrasonicated and the undissolved residue was filtered off. The remaining solution was evaporated to dryness under vacuum. Neither elemental nor MS analyses could be performed on the compound due to its air-sensitive nature.

Yield = 0.86 g (70%).

$^{31}\text{P}\{\text{H}\}$ (CDCl_3) = -64.34 (s) ppm.

^1H (CDCl_3), δ , ppm (J , Hz): 5.35 (d, $^1J_{\text{H-P}} = 225$ Hz; 2 H), 7.04-7.15 (ABX system, $^4J_{\text{H-P}} = 1.28$, $^3J_{\text{H-P}} = 4.92$, $J_{\text{AB}} = 3.55$; 4 H), 7.27-7.37 (m, 6 H), 7.43-7.55 (m, 4 H).

II. 4. 2 Crystal structure determinations

II.4.2.1 Single crystal X-ray diffraction study on PSSP

Colourless blocks of PSSP were grown by slow evaporation of chloroform solution. Data were collected using an Enraf-Nonius CAD4 diffractometer (Appendix A). SHELXS-97²¹⁶ and SHELXL-97²¹⁷ were employed for the structure solution calculations (Appendix A). Half the molecule is generated by a centre of symmetry between C(4) and C(4)*. In the least-squares refinement, the hydrogen atoms were included as ideal contributors with standard idealisation parameters. The anisotropic thermal factors of the non-hydrogen atoms indicated that there was no disorder in the crystal structure. Crystallographic data are given in Table II.19, the non-hydrogen atomic coordinates in Table II.20, the hydrogen atomic coordinates in Table II.21, the anisotropic thermal factors in Table II.22, the interatomic distances in Table II.23 and the interatomic angles in Table II.24. The observed and calculated structure factors may be found on the disk in an envelope fixed to inside back cover.

Table II.19 Crystal data and details of data collection and structure refinement for PSSP

Empirical formula	C ₃₂ H ₂₄ P ₂ S ₂
Colour and description	Colourless rectangular block
Crystal dimensions (mm)	0.46 x 0.23 x 0.27
Molecular mass (g·mol ⁻¹)	534.57
Crystal system	Monoclinic
Space Group	P2 ₁ /c
a (Å)	8.954(2)
b (Å)	19.678(3)
c (Å)	8.877(2)
α (°)	90
β (°)	117.93(2)
γ (°)	90
V (Å ³)	1381.9(6)
Z	2
D _c (g·cm ⁻³)	1.285

Table II.19 continued...

F(000)	556
T (K)	293(2)
λ (Mo-K α) (Å)	0.71069
Scan mode	$\omega - 2\theta$
ω scan angle	$0.66 + 0.35\tan\theta$
Horizontal aperture width (mm)	$2.7 + 0.1\tan\theta$
Scattering range (°)	$2 \leq \theta \leq 23$
μ (mm ⁻¹)	0.328
Absorption corrections	Semi empirical
Measured intensities	2508
Unique intensities	1923
Unique intensities with $[I > 2\sigma(I)]$	1652
Structure solution	Direct & Fourier
Refinement method	Full-matrix least-squares on F^2
Weighting scheme	$1/[\sigma^2(F_o^2) + (0.074P)^2 + 0.68P]$, where $P = 1/3 [\text{Max}(F_o^2, 0) + 2F_c^2]$
$R = \Sigma F_o - F_c / \Sigma F_o $	0.0411 $[I > 2\sigma(I)]$
	0.0516 (all data)
$wR = \{\Sigma[w(F_o^2 - F_c^2)^2] / \Sigma[wF_o^4]\}^{1/2}$	0.1168 $[I > 2\sigma(I)]$
	0.1298 (all data)
GooF on F^2	1.103
$(\Delta/\sigma)_{\max}$	-0.001
$\Delta\rho_{\max}$ (eÅ ⁻³)	0.45
Number of parameters	211

Table II.20 Non-hydrogen atomic coordinates ($\times 10^4$) and isotropic thermal factors ($\text{\AA}^2 \times 10^3$) for PSSP

	x	y	z	U(eq)
P(1)	3218(1)	6800(1)	594(1)	53(1)
S(1)	4720(1)	5464(1)	2658(1)	61(1)
C(1)	3667(4)	6226(1)	2334(4)	50(1)
C(2)	3293(4)	6338(2)	3630(4)	60(1)
C(3)	3835(5)	5821(2)	4849(4)	63(1)
C(4)	4639(3)	5308(1)	4525(3)	47(1)
C(5)	5212(4)	6786(2)	494(4)	53(1)
C(6)	6294(5)	7322(2)	1245(5)	78(1)
C(7)	7840(6)	7344(3)	1292(7)	98(2)
C(8)	8307(6)	6839(3)	566(6)	97(2)
C(9)	7271(5)	6299(3)	-170(6)	85(1)
C(10)	5719(5)	6275(2)	-208(5)	67(1)
C(11)	1814(3)	6313(2)	-1274(4)	52(1)
C(12)	1501(5)	6555(2)	-2867(4)	67(1)
C(13)	299(6)	6243(3)	-4329(5)	87(1)
C(14)	-601(6)	5697(3)	-4230(7)	101(2)
C(15)	-321(6)	5463(3)	-2679(7)	105(2)
C(16)	871(5)	5766(2)	-1226(5)	79(1)

$$U_{\text{(eq)}} = \frac{1}{3} \cdot \sum_i \sum_j U_{ij} a_i^* a_j^* (a_i \cdot a_j)$$

Table II.21 Hydrogen atomic coordinates ($\times 10^4$) and isotropic thermal factors ($\text{\AA}^2 \times 10^3$) for PSSP

	x	y	z	U(eq)
H(1)	2630(4)	6742(17)	3630(4)	67(9)
H(2)	3580(5)	5810(2)	5730(5)	89(12)
H(3)	6000(5)	7640(2)	1600(5)	75(13)
H(4)	8570(6)	7700(2)	1770(5)	95(13)
H(5)	9230(6)	6860(2)	650(6)	91(14)
H(6)	7610(5)	5950(2)	-560(5)	78(12)
H(7)	5060(5)	5941(18)	-600(5)	72(11)
H(8)	2070(5)	6933(19)	-2930(5)	77(12)
H(9)	20(6)	6410(2)	-5280(6)	104(16)
H(10)	-1490(6)	5510(2)	-5250(7)	119(16)
H(11)	-940(6)	5040(3)	-2550(6)	130(17)
H(12)	1120(5)	5590(2)	-190(6)	94(14)

Table II.22 Anisotropic thermal factors ($\text{\AA}^2 \times 10^3$) for PSSP

	U(11)	U(22)	U(33)	U(23)	U(13)	U(12)
P(1)	60(1)	51(1)	53(1)	2(1)	32(1)	4(1)
S(1)	78(1)	68(1)	51(1)	9(1)	42(1)	20(1)
C(1)	56(2)	51(2)	49(2)	-1(1)	30(1)	0(1)
C(2)	77(2)	57(2)	57(2)	-1(2)	42(2)	12(2)
C(3)	87(2)	69(2)	52(2)	1(2)	48(2)	12(2)
C(4)	47(2)	59(2)	38(2)	-3(1)	23(1)	-4(1)
C(5)	59(2)	54(2)	49(2)	5(1)	29(2)	-4(1)
C(6)	79(3)	75(3)	78(3)	-10(2)	36(2)	-16(2)
C(7)	77(3)	118(4)	97(3)	-10(3)	40(3)	-40(3)
C(8)	56(2)	152(5)	86(3)	20(3)	36(2)	-9(3)
C(9)	68(2)	110(3)	90(3)	6(3)	49(2)	10(3)
C(10)	65(2)	70(2)	76(2)	-1(2)	43(2)	-5(2)
C(11)	44(2)	61(2)	52(2)	2(1)	25(1)	7(1)
C(12)	71(2)	80(2)	56(2)	7(2)	34(2)	11(2)
C(13)	83(3)	130(4)	48(2)	2(2)	30(2)	29(3)
C(14)	63(3)	146(5)	81(3)	-35(3)	22(2)	-12(3)
C(15)	83(3)	139(4)	83(3)	-23(3)	30(3)	-44(3)
C(16)	72(2)	96(3)	63(2)	-1(2)	27(2)	-22(2)

The anisotropic thermal factor exponent takes the form:

$$-2\pi^2[h^2a^{*2}U(11) + \dots + 2hka^*b^*U(12)].$$

Table II.23 Interatomic distances (Å) for PSSP (* Atoms generated by symmetry)

P(1)-C(1)	1.800(3)	C(6)-C(7)	1.366(6)
P(1)-C(11)	1.816(3)	C(7)-C(8)	1.353(7)
P(1)-C(5)	1.828(3)	C(8)-C(9)	1.360(7)
S(1)-C(4)	1.720(3)	C(9)-C(10)	1.375(5)
S(1)-C(1)	1.722(3)	C(11)-C(16)	1.381(5)
C(1)-C(2)	1.358(4)	C(11)-C(12)	1.391(5)
C(2)-C(3)	1.395(5)	C(12)-C(13)	1.382(6)
C(3)-C(4)	1.347(4)	C(13)-C(14)	1.370(7)
C(4)-C(4)*	1.445(6)	C(14)-C(15)	1.360(7)
C(5)-C(10)	1.368(5)	C(15)-C(16)	1.367(6)
C(5)-C(6)	1.375(5)		

Table II.24 Interatomic angles (°) for PSSP (* Atoms generated by symmetry)

C(1)-P(1)-C(11)	103.50(14)	C(6)-C(5)-P(1)	116.6(3)
C(1)-P(1)-C(5)	101.61(13)	C(7)-C(6)-C(5)	120.9(5)
C(11)-P(1)-C(5)	102.84(14)	C(8)-C(7)-C(6)	119.8(5)
C(4)-S(1)-C(1)	92.83(14)	C(7)-C(8)-C(9)	120.6(4)
C(2)-C(1)-S(1)	109.4(2)	C(8)-C(9)-C(10)	119.5(5)
C(2)-C(1)-P(1)	125.5(2)	C(5)-C(10)-C(9)	120.8(4)
S(1)-C(1)-P(1)	125.04(17)	C(16)-C(11)-C(12)	117.6(3)
C(1)-C(2)-C(3)	113.9(3)	C(16)-C(11)-P(1)	123.7(3)
C(4)-C(3)-C(2)	114.0(3)	C(12)-C(11)-P(1)	118.1(3)
C(3)-C(4)-C(4)*	129.9(3)	C(13)-C(12)-C(11)	120.0(4)
C(3)-C(4)-S(1)	109.9(2)	C(14)-C(13)-C(12)	120.7(4)
C(4)*-C(4)-S(1)	120.2(3)	C(15)-C(14)-C(13)	119.8(4)
C(10)-C(5)-C(6)	118.4(3)	C(14)-C(15)-C(16)	120.0(5)
C(10)-C(5)-P(1)	125.0(3)	C(15)-C(16)-C(11)	121.9(4)

II.4.2.2 Single crystal X-ray diffraction study on PSNSP

Greenish blocks of PSNSP were grown by slow evaporation of hexane/ether (2:1, v:v) solution. Data were collected using an Enraf-Nonius CAD4 diffractometer (Appendix A). SHELXS-97²¹⁶ and SHELXL-97²¹⁷ were employed for the structure solution calculations (Appendix A). In the least-squares refinement, the hydrogen atoms were included as ideal contributors with standard idealisation parameters. No disorder was observed in the anisotropically refined thermal factors of the non-hydrogen atoms. Crystallographic data are given in Table II.25, the non-hydrogen atomic coordinates in Table II.26, the hydrogen atomic coordinates in Table II.27, the anisotropic thermal factors in Table II.28, the interatomic distances in Table II.29 and the interatomic angles in Table II.30. The observed and calculated structure factors may be found on the disk in an envelope fixed to the inside back cover.

Table II.25 Crystal data and details of data collection and structure refinement for PSNSP

Empirical formula	C ₃₇ H ₂₇ NP ₂ S ₂
Colour and description	Greenish block
Crystal dimensions (mm)	0.38 x 0.23 x 0.19
Molecular mass (g·mol ⁻¹)	611.66
Crystal system	Triclinic
Space Group	P $\bar{1}$
a (Å)	9.032(2)
b (Å)	13.312(3)
c (Å)	13.577(3)
α (°)	85.853(18)
β (°)	82.694(19)
γ (°)	73.772(18)
V (Å ³)	1553.4(6)
Z	2
D _c (g·cm ⁻³)	1.308
F(000)	636
T (K)	293(2)
λ (Mo-K α) (Å)	0.71069

Table II.25 continued...

Scan mode	$\omega - 2\theta$
ω scan angle	$0.72 + 0.35\tan\theta$
Horizontal aperture width (mm)	$2.7 + 0.1\tan\theta$
Scattering range ($^{\circ}$)	$2 \leq \theta \leq 23$
μ (mm^{-1})	0.302
Absorption corrections	Semi empirical
Measured intensities	4946
Unique intensities	4301
Unique intensities with $[I > 2\sigma(I)]$	3311
Structure solution	Direct & Fourier
Refinement method	Full-matrix least-squares on F^2
Weighting scheme	$1/[\sigma^2(F_o^2) + (0.051P)^2 + 0.43P]$, where $P = 1/3 [\text{Max}(F_o^2, 0) + 2F_c^2]$
$R = \Sigma F_o - F_c / \Sigma F_o $	0.0366 $[I > 2\sigma(I)]$
	0.0589 (all data)
$wR = \{\Sigma[w(F_o^2 - F_c^2)^2] / \Sigma[wF_o^4]\}^{1/2}$	0.0901 $[I > 2\sigma(I)]$
	0.0990 (all data)
GooF on F^2	1.033
$(\Delta/\sigma)_{\max}$	-0.001
$\Delta\rho_{\max}$ ($\text{e}\text{\AA}^{-3}$)	0.47
Number of parameters	487

Table II.26 Non-hydrogen atomic coordinates ($\times 10^4$) and isotropic thermal factors ($\text{\AA}^2 \times 10^3$) for PSNSP

	x	y	z	U(eq)
S(1)	5529(1)	-1095(1)	-2137(1)	52(1)
S(2)	3643(1)	2351(1)	-1217(1)	49(1)
P(1)	7799(1)	-2719(1)	-3592(1)	53(1)
P(2)	3862(1)	4664(1)	-1583(1)	50(1)
N(1)	3295(2)	250(2)	-673(2)	44(1)
C(1)	6391(3)	-2352(2)	-2522(2)	47(1)
C(2)	5826(4)	-3046(2)	-1907(2)	51(1)
C(3)	4710(3)	-2580(2)	-1147(2)	51(1)
C(4)	4418(3)	-1521(2)	-1166(2)	44(1)
C(5)	3347(3)	-763(2)	-491(2)	48(1)
C(6)	2447(4)	-1094(3)	304(2)	66(1)
C(7)	1469(4)	-362(3)	917(3)	76(1)
C(8)	1419(4)	671(3)	745(2)	64(1)
C(9)	2352(3)	955(2)	-58(2)	45(1)
C(10)	2384(3)	2043(2)	-263(2)	44(1)
C(11)	1565(3)	2916(2)	235(2)	53(1)
C(12)	1957(3)	3823(2)	-152(2)	51(1)
C(13)	3058(3)	3659(2)	-948(2)	47(1)
C(14)	5901(3)	3939(2)	-1890(2)	46(1)
C(15)	6950(4)	4026(3)	-1272(3)	63(1)
C(16)	8504(5)	3495(4)	-1469(4)	86(1)
C(17)	9005(5)	2887(3)	-2272(4)	87(1)
C(18)	7987(4)	2800(3)	-2887(3)	77(1)
C(19)	6442(4)	3318(2)	-2703(3)	62(1)
C(20)	3174(3)	4836(2)	-2807(2)	50(1)
C(21)	2058(4)	4421(3)	-3071(3)	77(1)

Table II.26 continued...

C(22)	1580(6)	4631(4)	-4010(4)	97(2)
C(23)	2196(5)	5243(3)	-4687(3)	84(1)
C(24)	3283(4)	5678(3)	-4427(3)	74(1)
C(25)	3762(4)	5474(2)	-3501(2)	60(1)
C(26)	6709(3)	-2062(2)	-4607(2)	49(1)
C(27)	5128(4)	-1910(3)	-4551(2)	61(1)
C(28)	4319(4)	-1530(3)	-5355(3)	71(1)
C(29)	5071(5)	-1295(3)	-6237(3)	70(1)
C(30)	6631(5)	-1435(3)	-6319(3)	75(1)
C(31)	7460(4)	-1821(3)	-5519(2)	66(1)
C(32)	9114(3)	-1925(2)	-3464(2)	52(1)
C(33)	8884(4)	-883(3)	-3769(3)	64(1)
C(34)	9944(5)	-354(3)	-3599(3)	81(1)
C(35)	11221(5)	-855(4)	-3140(3)	83(1)
C(36)	11470(4)	-1874(4)	-2843(3)	78(1)
C(37)	10431(4)	-2413(3)	-3014(2)	64(1)

$$\underline{U}_{(eq)} = \frac{1}{3} \cdot \sum_i \sum_j \underline{U}_{ij} \hat{a}_i \cdot \hat{a}_j (\hat{a}_i \cdot \hat{a}_j)$$

Table II.27 Hydrogen atomic coordinates ($\times 10^4$) and isotropic thermal factors ($\text{\AA}^2 \times 10^3$) for PSNSP

	x	y	z	U(eq)
H(1)	6190(3)	-3710(2)	-1980(2)	56(9)
H(2)	4200(3)	-2940(2)	-650(2)	59(8)
H(3)	2480(3)	-1790(2)	360(2)	70(10)
H(4)	790(4)	-590(3)	1450(3)	97(11)
H(5)	750(4)	1170(2)	1080(2)	69(10)
H(6)	860(3)	2910(2)	770(2)	63(9)
H(7)	1450(3)	4460(2)	110(2)	63(9)
H(8)	6640(4)	4400(3)	-770(3)	79(13)
H(9)	9050(4)	3590(3)	-1020(3)	86(12)
H(10)	10040(5)	2520(3)	-2400(3)	98(13)
H(11)	8300(4)	2390(3)	-3460(3)	96(13)
H(12)	5800(3)	3220(2)	-3100(2)	58(9)
H(13)	1600(4)	4060(3)	-2600(3)	81(11)
H(14)	940(5)	4350(3)	-4170(3)	106(15)
H(15)	1900(4)	5380(3)	-5350(3)	86(11)
H(16)	3710(4)	6090(3)	-4900(3)	95(13)
H(17)	4560(3)	5750(2)	-3360(2)	56(8)
H(18)	4580(3)	-2060(2)	-3910(2)	61(8)
H(19)	3220(4)	-1440(3)	-5320(3)	87(11)
H(20)	4500(4)	-990(3)	-6820(3)	93(12)
H(21)	7210(4)	-1320(3)	-6890(3)	79(11)
H(22)	8580(4)	-1940(2)	-5570(2)	65(9)
H(23)	7960(3)	-530(2)	-4040(2)	54(8)
H(24)	9780(4)	290(3)	-3820(2)	74(11)
H(25)	11900(4)	-500(3)	-3040(3)	86(12)
H(26)	12390(5)	-2290(3)	-2480(3)	121(14)
H(27)	10560(3)	-3110(2)	-2830(2)	62(9)

Table II.28 Anisotropic thermal factors ($\text{\AA}^2 \times 10^3$) for PSNSP

	U(11)	U(22)	U(33)	U(23)	U(13)	U(12)
S(1)	64(1)	42(1)	49(1)	3(1)	4(1)	-19(1)
S(2)	59(1)	46(1)	41(1)	-3(1)	5(1)	-16(1)
P(1)	52(1)	45(1)	58(1)	-6(1)	-6(1)	-8(1)
P(2)	56(1)	42(1)	53(1)	-3(1)	-8(1)	-15(1)
N(1)	48(1)	50(1)	39(1)	4(1)	-7(1)	-20(1)
C(1)	53(2)	44(2)	47(2)	3(1)	-12(1)	-16(1)
C(2)	62(2)	38(2)	54(2)	5(1)	-18(2)	-16(1)
C(3)	60(2)	49(2)	48(2)	10(1)	-10(2)	-25(2)
C(4)	48(2)	46(2)	43(2)	6(1)	-11(1)	-20(1)
C(5)	51(2)	54(2)	44(2)	7(1)	-11(1)	-22(1)
C(6)	79(2)	59(2)	62(2)	8(2)	8(2)	-30(2)
C(7)	91(3)	74(2)	64(2)	3(2)	23(2)	-39(2)
C(8)	71(2)	67(2)	53(2)	-7(2)	15(2)	-24(2)
C(9)	48(2)	53(2)	38(2)	1(1)	-6(1)	-18(1)
C(10)	41(2)	55(2)	36(1)	-2(1)	-5(1)	-14(1)
C(11)	46(2)	66(2)	47(2)	-6(2)	1(1)	-18(2)
C(12)	47(2)	51(2)	56(2)	-13(2)	-2(1)	-12(1)
C(13)	46(2)	49(2)	48(2)	-2(1)	-9(1)	-12(1)
C(14)	53(2)	42(2)	50(2)	9(1)	-12(1)	-22(1)
C(15)	68(2)	61(2)	71(2)	12(2)	-26(2)	-34(2)
C(16)	70(3)	90(3)	113(4)	29(3)	-49(3)	-40(2)
C(17)	50(2)	77(3)	131(4)	21(3)	-11(3)	-20(2)
C(18)	62(2)	72(2)	88(3)	-3(2)	7(2)	-9(2)
C(19)	53(2)	63(2)	67(2)	-4(2)	-10(2)	-12(2)

Table II.28 continued...

C(20)	45(2)	41(2)	60(2)	-3(1)	-11(1)	-5(1)
C(21)	80(2)	72(2)	93(3)	27(2)	-44(2)	-35(2)
C(22)	103(3)	86(3)	121(4)	12(3)	-69(3)	-35(3)
C(23)	98(3)	80(3)	71(3)	3(2)	-34(2)	-8(2)
C(24)	71(2)	79(2)	65(2)	8(2)	-11(2)	-9(2)
C(25)	57(2)	65(2)	57(2)	5(2)	-11(2)	-17(2)
C(26)	54(2)	46(2)	47(2)	-8(1)	-1(1)	-13(1)
C(27)	56(2)	74(2)	50(2)	5(2)	-4(2)	-16(2)
C(28)	63(2)	88(3)	59(2)	3(2)	-15(2)	-14(2)
C(29)	91(3)	63(2)	55(2)	1(2)	-16(2)	-16(2)
C(30)	102(3)	85(3)	44(2)	-2(2)	2(2)	-42(2)
C(31)	64(2)	84(2)	54(2)	-13(2)	5(2)	-28(2)
C(32)	42(2)	57(2)	54(2)	-10(1)	1(1)	-8(1)
C(33)	57(2)	58(2)	78(2)	-6(2)	-9(2)	-16(2)
C(34)	87(3)	69(3)	90(3)	-8(2)	6(2)	-34(2)
C(35)	56(2)	110(4)	91(3)	-35(3)	9(2)	-36(3)
C(36)	48(2)	103(3)	81(3)	-20(2)	-2(2)	-17(2)
C(37)	46(2)	72(2)	67(2)	-10(2)	2(2)	-6(2)

The anisotropic thermal factor exponent takes the form:

$$-2\pi^2[h^2a^{*2}U(11) + \dots + 2hka^*b^*U(12)]$$

Table II.29 Interatomic distances (Å) for PSNSP

S(1)-C(4)	1.714(3)	C(14)-C(15)	1.375(4)
S(1)-C(1)	1.725(3)	C(14)-C(19)	1.382(4)
S(2)-C(10)	1.717(3)	C(15)-C(16)	1.385(6)
S(2)-C(13)	1.725(3)	C(16)-C(17)	1.358(6)
P(1)-C(1)	1.804(3)	C(17)-C(18)	1.351(6)
P(1)-C(26)	1.823(3)	C(18)-C(19)	1.373(5)
P(1)-C(32)	1.827(3)	C(20)-C(21)	1.372(4)
P(2)-C(13)	1.810(3)	C(20)-C(25)	1.379(4)
P(2)-C(20)	1.824(3)	C(21)-C(22)	1.382(5)
P(2)-C(14)	1.834(3)	C(22)-C(23)	1.354(6)
N(1)-C(9)	1.338(3)	C(23)-C(24)	1.362(5)
N(1)-C(5)	1.342(3)	C(24)-C(25)	1.367(5)
C(1)-C(2)	1.362(4)	C(26)-C(27)	1.377(4)
C(2)-C(3)	1.394(4)	C(26)-C(31)	1.395(4)
C(3)-C(4)	1.359(4)	C(27)-C(28)	1.378(4)
C(4)-C(5)	1.468(4)	C(28)-C(29)	1.360(5)
C(5)-C(6)	1.389(4)	C(29)-C(30)	1.359(5)
C(6)-C(7)	1.369(5)	C(30)-C(31)	1.384(5)
C(7)-C(8)	1.367(5)	C(32)-C(37)	1.380(4)
C(8)-C(9)	1.388(4)	C(32)-C(33)	1.385(4)
C(9)-C(10)	1.463(4)	C(33)-C(34)	1.386(5)
C(10)-C(11)	1.364(4)	C(34)-C(35)	1.363(6)
C(11)-C(12)	1.400(4)	C(35)-C(36)	1.351(6)
C(12)-C(13)	1.358(4)	C(36)-C(37)	1.380(5)

Table II.30 Interatomic angles (°) for PSNSP

C(4)-S(1)-C(1)	92.28(13)	S(2)-C(13)-P(2)	125.31(16)
C(10)-S(2)-C(13)	92.28(13)	C(15)-C(14)-C(19)	118.3(3)
C(1)-P(1)-C(26)	101.99(12)	C(15)-C(14)-P(2)	117.7(3)
C(1)-P(1)-C(32)	101.29(12)	C(19)-C(14)-P(2)	124.0(2)

Table II.30 continued...

C(26)-P(1)-C(32)	104.05(13)	C(14)-C(15)-C(16)	120.1(4)
C(13)-P(2)-C(20)	104.75(13)	C(17)-C(16)-C(15)	120.5(4)
C(13)-P(2)-C(14)	101.81(12)	C(18)-C(17)-C(16)	120.0(4)
C(20)-P(2)-C(14)	100.93(12)	C(17)-C(18)-C(19)	120.4(4)
C(9)-N(1)-C(5)	118.4(2)	C(18)-C(19)-C(14)	120.7(4)
C(2)-C(1)-S(1)	109.9(2)	C(21)-C(20)-C(25)	117.6(3)
C(2)-C(1)-P(1)	124.0(2)	C(21)-C(20)-P(2)	124.8(3)
S(1)-C(1)-P(1)	126.10(15)	C(25)-C(20)-P(2)	117.5(2)
C(1)-C(2)-C(3)	113.9(3)	C(20)-C(21)-C(22)	120.1(4)
C(4)-C(3)-C(2)	113.1(3)	C(23)-C(22)-C(21)	121.2(4)
C(3)-C(4)-C(5)	129.2(2)	C(22)-C(23)-C(24)	119.2(4)
C(3)-C(4)-S(1)	110.8(2)	C(23)-C(24)-C(25)	119.9(4)
C(5)-C(4)-S(1)	119.97(19)	C(24)-C(25)-C(20)	121.8(3)
N(1)-C(5)-C(6)	122.1(3)	C(27)-C(26)-C(31)	117.0(3)
N(1)-C(5)-C(4)	117.1(2)	C(27)-C(26)-P(1)	121.1(2)
C(6)-C(5)-C(4)	120.8(3)	C(31)-C(26)-P(1)	121.3(2)
C(7)-C(6)-C(5)	118.8(3)	C(26)-C(27)-C(28)	121.7(3)
C(8)-C(7)-C(6)	119.5(3)	C(29)-C(28)-C(27)	120.4(4)
C(7)-C(8)-C(9)	119.1(3)	C(30)-C(29)-C(28)	119.5(4)
N(1)-C(9)-C(8)	122.0(3)	C(29)-C(30)-C(31)	120.7(3)
N(1)-C(9)-C(10)	116.3(2)	C(30)-C(31)-C(26)	120.7(3)
C(8)-C(9)-C(10)	121.6(3)	C(37)-C(32)-C(33)	118.1(3)
C(11)-C(10)-C(9)	129.2(2)	C(37)-C(32)-P(1)	116.5(2)
C(11)-C(10)-S(2)	110.7(2)	C(33)-C(32)-P(1)	125.4(2)
C(9)-C(10)-S(2)	120.14(19)	C(32)-C(33)-C(34)	119.9(4)
C(10)-C(11)-C(12)	113.0(3)	C(35)-C(34)-C(33)	120.5(4)
C(13)-C(12)-C(11)	113.8(3)	C(36)-C(35)-C(34)	120.4(4)
C(12)-C(13)-S(2)	110.2(2)	C(35)-C(36)-C(37)	119.8(4)
C(12)-C(13)-P(2)	124.4(2)	C(32)-C(37)-C(36)	121.3(4)

II.4.2.3 Single crystal X-ray diffraction study on PSNP

Colourless blocks of PSNP were grown by slow evaporation from petroleum ether/ether (6:1, v:v). Data were collected using an Enraf-Nonius CAD4 diffractometer (Appendix A). SHELXS-97²¹⁶ and SHELXL-97²¹⁷ were employed for the structure solution calculations (Appendix A). Observation of the anisotropic thermal factors from the least-squares refinement indicated that there was no disorder in the non-hydrogen atoms. The hydrogen atoms were included as ideal contributors with standard idealisation parameters. Crystallographic data are given in Table II.31, the non-hydrogen atomic coordinates in Table II.32, the hydrogen atomic coordinates in Table II.33, the anisotropic thermal factors in Table II.34, the interatomic distances in Table II.35 and the interatomic angles in Table II.36. The observed and calculated structure factors may be found on the disk in an envelope fixed to the inside back cover.

Table II.31 Crystal data and details of data collection and structure refinement for PSNP

Empirical formula	C ₃₃ H ₂₅ NP ₂ S
Colour and description	Colourless rectangular block
Crystal dimensions (mm)	0.27 x 0.08 x 0.19
Molecular mass (g·mol ⁻¹)	529.54
Crystal system	Monoclinic
Space Group	P2 ₁ /n
a (Å)	8.408(5)
b (Å)	15.978(6)
c (Å)	20.402(7)
α (°)	90
β (°)	101.11(4)
γ (°)	90
V (Å ³)	2690(2)
Z	4
D _c (g·cm ⁻³)	1.308
F(000)	1104
T (K)	293(2)
λ (Mo-K _α) (Å)	0.71069
Scan mode	ω - 2θ

Table II.31 continued...

ω scan angle	$0.59 + 0.35 \tan \theta$
Horizontal aperture width (mm)	$2.7 + 0.1 \tan \theta$
Scattering range ($^{\circ}$)	$2 \leq \theta \leq 23$
μ (mm^{-1})	0.263
Absorption corrections	Semi empirical
Measured intensities	3925
Unique intensities	3616
Unique intensities with $[I > 2\sigma(I)]$	2173
Structure solution	Direct & Fourier
Refinement method	Full-matrix least-squares on F^2
Weighting scheme	$1/[\sigma^2(F_o^2) + (0.000P)^2 + 4.40P]$ where $P = 1/3 [\text{Max}(F_o^2, 0) + 2F_c^2]$
$R = \Sigma F_o - F_c / \Sigma F_o $	0.0524 $[I > 2\sigma(I)]$
	0.1275 (all data)
$wR = \{\Sigma[w(F_o^2 - F_c^2)^2] / \Sigma[wF_o^4]\}^{1/2}$	0.0845 $[I > 2\sigma(I)]$
	0.1263 (all data)
GooF on F^2	1.186
$(\Delta/\sigma)_{\text{max}}$	0.001
$\Delta\rho_{\text{max}}$ ($\text{e}\text{\AA}^{-3}$)	0.284
Number of parameters	334

Table II.32 Non-hydrogen atomic coordinates ($\times 10^4$) and isotropic thermal factors ($\text{\AA}^2 \times 10^3$) for PSNP

	x	y	z	U(eq)
P(1)	-3950(2)	13650(1)	639(1)	53(1)
P(2)	1752(2)	9580(1)	2025(1)	54(1)
S(1)	-2372(2)	11970(1)	1230(1)	55(1)
N(1)	-1133(5)	10386(3)	1840(2)	45(1)
C(1)	-3937(6)	12676(3)	1089(2)	48(1)
C(2)	-5198(7)	12380(4)	1346(3)	60(2)
C(3)	-4905(6)	11597(4)	1655(3)	56(2)
C(4)	-3421(6)	11284(3)	1638(2)	46(1)
C(5)	-2685(6)	10495(3)	1897(2)	43(1)
C(6)	-3517(7)	9901(4)	2193(3)	58(2)
C(7)	-2739(8)	9173(4)	2435(3)	62(2)
C(8)	-1170(7)	9051(4)	2362(3)	57(2)
C(9)	-408(6)	9667(3)	2056(2)	47(1)
C(10)	-1834(7)	13788(3)	585(3)	51(1)
C(11)	-1003(7)	13274(4)	213(3)	67(2)
C(12)	603(8)	13427(5)	203(3)	76(2)
C(13)	1379(9)	14094(5)	557(4)	84(2)
C(14)	605(9)	14602(5)	926(4)	84(2)
C(15)	-1013(8)	14453(4)	932(3)	68(2)
C(16)	-4858(6)	13342(4)	-219(3)	52(1)
C(17)	-5040(8)	13960(4)	-696(3)	69(2)
C(18)	-5817(8)	13821(5)	-1341(3)	82(2)
C(19)	-6433(8)	13044(6)	-1521(3)	86(2)
C(20)	-6253(9)	12413(5)	-1062(3)	93(2)
C(21)	-5480(8)	12562(4)	-410(3)	71(2)
C(22)	2012(7)	8449(3)	2025(3)	51(1)

Table II.33 Hydrogen atomic coordinates ($\times 10^4$) and isotropic thermal factors ($\text{\AA}^2 \times 10^3$) for PSNP (the numbering of the H atoms is done according to the numbering of the C atoms, to which the hydrogens are respectively attached)

	x	y	z	U(eq)
H(2)	-6168	12669	1320	72
H(3)	-5661	11319	1854	67
H(6)	-4590	9993	2228	70
H(7)	-3269	8772	2644	74
H(8)	-624	8562	2515	68
H(11)	-1534	12828	-29	80
H(12)	1164	13082	-41	92
H(13)	2460	14198	543	101
H(14)	1151	15043	1169	101
H(15)	-1561	14807	1174	81
H(17)	-4621	14490	-578	82
H(18)	-5925	14251	-1654	99
H(19)	-6975	12946	-1956	103
H(20)	-6651	11881	-1187	112
H(21)	-5378	12132	-98	85
H(23)	3750	8422	2853	78
H(24)	4147	6982	2870	98
H(25)	2575	6152	2088	103
H(26)	648	6731	1280	97
H(27)	298	8156	1235	87
H(29)	3309	8912	1001	79
H(30)	3718	9338	-22	97
H(31)	2614	10573	-479	93
H(32)	1053	11371	89	90
H(33)	636	10942	1122	73

Table II.34 Anisotropic thermal factors ($\text{\AA}^2 \times 10^3$) for PSNP

	U(11)	U(22)	U(33)	U(23)	U(13)	U(12)
P(1)	54(1)	45(1)	60(1)	0(1)	11(1)	8(1)
P(2)	48(1)	50(1)	59(1)	-3(1)	1(1)	3(1)
S(1)	47(1)	57(1)	63(1)	9(1)	14(1)	8(1)
N(1)	47(3)	44(3)	43(3)	3(2)	6(2)	3(2)
C(1)	52(3)	45(3)	48(3)	-12(3)	10(3)	7(3)
C(2)	47(4)	64(4)	69(4)	5(3)	14(3)	13(3)
C(3)	44(3)	68(4)	60(4)	12(3)	18(3)	-3(3)
C(4)	39(3)	55(4)	47(3)	-2(3)	13(2)	-5(3)
C(5)	45(3)	45(3)	38(3)	-3(3)	3(2)	2(3)
C(6)	55(4)	64(4)	56(4)	6(3)	12(3)	-11(3)
C(7)	70(5)	56(4)	63(4)	8(3)	20(3)	-5(3)
C(8)	58(4)	41(3)	68(4)	7(3)	8(3)	6(3)
C(9)	48(3)	47(4)	42(3)	-3(3)	1(3)	-2(3)
C(10)	56(4)	41(3)	53(3)	16(3)	7(3)	0(3)
C(11)	57(4)	75(5)	72(4)	-11(4)	19(3)	-3(4)
C(12)	65(5)	81(5)	89(5)	11(4)	30(4)	11(4)
C(13)	61(5)	79(5)	107(6)	19(5)	6(4)	-10(4)
C(14)	81(6)	62(5)	102(6)	-2(4)	-3(4)	-22(4)
C(15)	65(4)	54(4)	82(4)	7(4)	12(3)	-5(4)
C(16)	43(3)	50(4)	60(4)	4(3)	4(3)	6(3)
C(17)	82(5)	56(4)	67(4)	6(4)	9(4)	6(4)
C(18)	84(5)	94(6)	63(5)	27(4)	0(4)	18(5)
C(19)	76(5)	121(7)	53(4)	4(5)	-5(4)	6(5)
C(20)	114(6)	92(6)	64(5)	-15(4)	-6(4)	-24(5)

Table II.34 continued...

C(21)	85(5)	58(4)	64(4)	4(3)	2(4)	-5(4)
C(22)	49(3)	55(4)	49(3)	2(3)	8(3)	2(3)
C(23)	47(4)	79(5)	64(4)	16(4)	2(3)	10(3)
C(24)	60(5)	93(6)	92(6)	43(5)	17(4)	27(4)
C(25)	106(6)	60(5)	102(6)	19(5)	44(5)	24(5)
C(26)	124(6)	49(4)	66(4)	4(3)	12(4)	10(4)
C(27)	96(5)	53(4)	59(4)	9(3)	-8(4)	17(4)
C(28)	37(3)	52(4)	56(4)	1(3)	5(3)	-3(3)
C(29)	58(4)	56(4)	87(5)	-3(4)	25(4)	8(3)
C(30)	94(5)	76(5)	84(5)	-7(4)	43(4)	-3(4)
C(31)	85(5)	85(5)	67(4)	1(4)	26(4)	-19(4)
C(32)	73(5)	71(5)	82(5)	16(4)	19(4)	-2(4)
C(33)	59(4)	57(4)	68(4)	4(3)	16(3)	3(3)

The anisotropic thermal factor exponent takes the form:

$$-2\pi^2[h^2a^{*2}U(11) + + 2hka^*b^*U(12)]$$

Table II.35 Interatomic distances (Å) for PSNP

P(1)-C(1)	1.807(6)	C(12)-C(13)	1.379(9)
P(1)-C(10)	1.817(6)	C(13)-C(14)	1.355(9)
P(1)-C(16)	1.835(6)	C(14)-C(15)	1.384(8)
P(2)-C(22)	1.820(6)	C(16)-C(17)	1.376(7)
P(2)-C(28)	1.832(5)	C(16)-C(21)	1.378(8)
P(2)-C(9)	1.835(5)	C(17)-C(18)	1.369(8)
S(1)-C(1)	1.714(5)	C(18)-C(19)	1.368(9)
S(1)-C(4)	1.719(5)	C(19)-C(20)	1.365(9)
N(1)-C(9)	1.336(6)	C(20)-C(21)	1.383(8)
N(1)-C(5)	1.343(6)	C(22)-C(27)	1.375(8)
C(1)-C(2)	1.355(7)	C(22)-C(23)	1.377(7)
C(2)-C(3)	1.400(7)	C(23)-C(24)	1.395(9)
C(3)-C(4)	1.351(7)	C(24)-C(25)	1.362(9)
C(4)-C(5)	1.458(7)	C(25)-C(26)	1.345(9)
C(5)-C(6)	1.385(7)	C(26)-C(27)	1.377(8)
C(6)-C(7)	1.379(8)	C(28)-C(29)	1.375(7)
C(7)-C(8)	1.370(7)	C(28)-C(33)	1.386(7)
C(8)-C(9)	1.386(7)	C(29)-C(30)	1.366(8)
C(10)-C(15)	1.385(8)	C(30)-C(31)	1.371(9)
C(10)-C(11)	1.395(7)	C(31)-C(32)	1.364(8)
C(11)-C(12)	1.377(8)	C(32)-C(33)	1.382(8)

Table II.36 Interatomic angles (°) for PSNP

C(1)-P(1)-C(10)	103.0(2)	C(11)-C(12)-C(13)	119.7(7)
C(1)-P(1)-C(16)	102.4(2)	C(14)-C(13)-C(12)	121.7(7)
C(10)-P(1)-C(16)	102.0(3)	C(13)-C(14)-C(15)	118.7(7)
C(22)-P(2)-C(28)	102.6(3)	C(14)-C(15)-C(10)	121.5(6)
C(22)-P(2)-C(9)	101.2(3)	C(17)-C(16)-C(21)	117.6(5)
C(28)-P(2)-C(9)	105.2(2)	C(17)-C(16)-P(1)	116.9(5)
C(1)-S(1)-C(4)	93.0(3)	C(21)-C(16)-P(1)	125.3(5)
C(9)-N(1)-C(5)	118.1(5)	C(18)-C(17)-C(16)	122.1(6)
C(2)-C(1)-S(1)	109.8(4)	C(19)-C(18)-C(17)	119.4(7)
C(2)-C(1)-P(1)	124.7(4)	C(20)-C(19)-C(18)	120.0(6)
S(1)-C(1)-P(1)	125.5(3)	C(19)-C(20)-C(21)	120.1(7)
C(1)-C(2)-C(3)	113.8(5)	C(16)-C(21)-C(20)	120.8(6)
C(4)-C(3)-C(2)	113.7(5)	C(27)-C(22)-C(23)	117.8(6)
C(3)-C(4)-C(5)	129.8(5)	C(27)-C(22)-P(2)	123.4(4)
C(3)-C(4)-S(1)	109.8(4)	C(23)-C(22)-P(2)	118.8(5)
C(5)-C(4)-S(1)	120.4(4)	C(22)-C(23)-C(24)	120.1(6)
N(1)-C(5)-C(6)	122.0(5)	C(25)-C(24)-C(23)	120.0(6)
N(1)-C(5)-C(4)	115.6(5)	C(26)-C(25)-C(24)	120.5(7)
C(6)-C(5)-C(4)	122.4(5)	C(25)-C(26)-C(27)	119.7(7)
C(7)-C(6)-C(5)	119.3(6)	C(22)-C(27)-C(26)	121.8(6)
C(8)-C(7)-C(6)	118.8(6)	C(29)-C(28)-C(33)	117.6(5)
C(7)-C(8)-C(9)	119.1(5)	C(29)-C(28)-P(2)	120.9(5)
N(1)-C(9)-C(8)	122.5(5)	C(33)-C(28)-P(2)	120.9(4)
C(8)-C(9)-P(2)	120.6(4)	C(29)-C(30)-C(31)	120.3(6)
C(15)-C(10)-C(11)	118.5(6)	C(32)-C(31)-C(30)	119.7(6)
C(15)-C(10)-P(1)	117.4(5)	C(31)-C(32)-C(33)	119.8(6)
C(11)-C(10)-P(1)	124.1(5)	C(32)-C(33)-C(28)	121.1(6)
C(12)-C(11)-C(10)	119.9(6)		

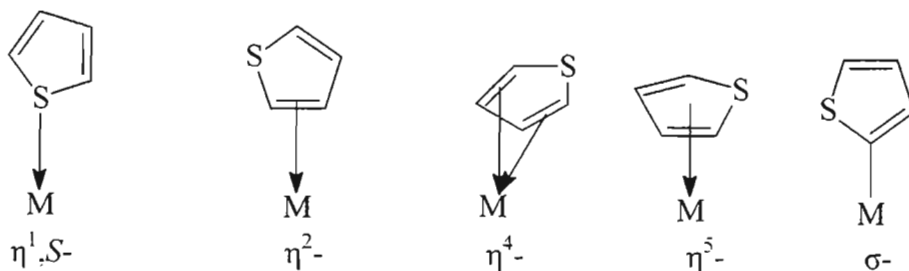
CHAPTER THREE

SYNTHESIS OF GOLD(I) COMPLEXES CONTAINING NOVEL THIENYLPHOSPHINE LIGANDS

III.1 INTRODUCTION

Thiophene and its derivatives are known to exhibit various coordination modes in complexes with transition metals. Evaluation of the interaction of thiophene with these metals requires knowledge of the electronic structure of the heterocycle. There are six valence orbitals, all of which having primarily *p*-orbital character. The five *p* orbitals orthogonal to the ring give rise to five non-degenerate π -states, with symmetries resembling those for the cyclopentadienyl moiety. One of the sulfur-localised lone pairs occupies such a *p*-orbital orthogonal to the plane of the thiophene ring. As such it participates in the π -delocalised bonding. *Ab initio* calculations show that the thiophene sulfur has a partial positive charge, while the carbon atoms at the positions 2 and 5 possess partial negative charges.²¹⁸

Studies involving the reactivity of thiophenes with transition metals have provided numerous examples of thiophene coordination via the S atom, as well as of the η^5 , π -bonding mode that involves all of the atoms in the thiophene framework. The η^4 - and η^2 - are 4 and 2 electron donor modes respectively and are observed less frequently. The thiophene ligand can also coordinate through the C-2 carbon atom, leading to σ -type coordination, or a metallated thiophene. The most commonly encountered thiophene coordination modes are presented in Scheme III.1.



SCHEME III.1

In the ruthenium complex, $[\text{Ru}(\text{PPh}_3)_2(\text{C}_5\text{H}_4\text{-CH}_2\text{-C}_4\text{H}_3\text{S})]^+$, thiophene is found bonded to the metal through the sulfur atom.²¹⁹ X-ray crystallographic investigations have established that in this coordination mode the metal lies out of plane such that the sulfur has trigonal pyramidal coordination (Figure III.1). This is in contrast to the "normal" coordination mode exhibited by another commonly used heterocyclic ligand *e.g.*, pyridine, where binding with the metal occurs in the plane of the pyridine ring.

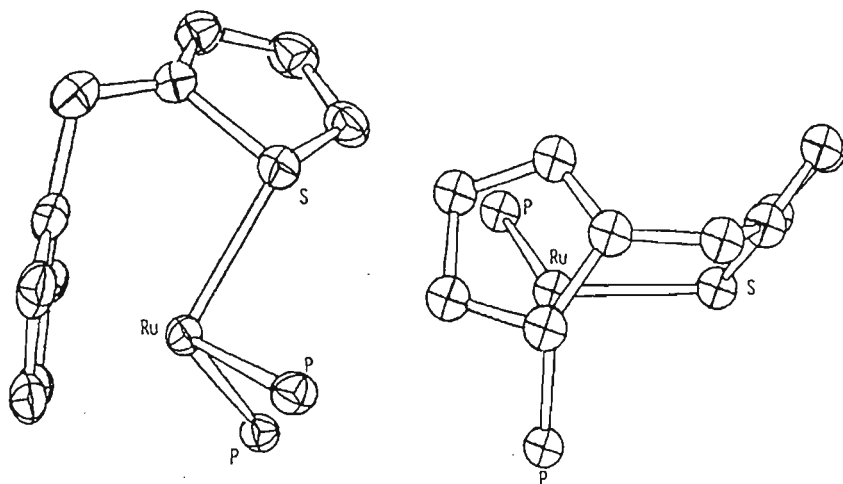
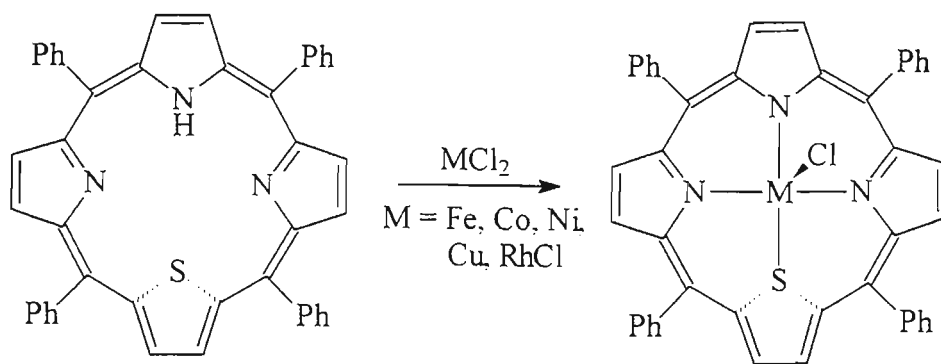


Fig. III.1 Structure of $[\text{Ru}(\text{PPh}_3)_2(\text{C}_5\text{H}_4\text{-CH}_2\text{-C}_4\text{H}_3\text{S})]^+$ (phenyl groups are omitted).²¹⁹

The strong tendency of the thiophene sulfur to be pyramidal when S-bound is evident in the coordination of thiophene when it is incorporated into a porphyrin by replacing a pyrrole unit. Tetraphenylthiaporphyrin, or HSTPP gives five-coordinate complexes of the type $[\text{M}(\text{STPP})\text{Cl}]$ upon reaction with the dichlorides of Fe, Co, Ni, Cu and Zn.²²⁰ Crystallographic studies for $\text{M} = \text{Fe}$, Ni and Cu reveal that the metallothiaporphyrinate distorts from the planar structure characteristic of the free ligand, being puckered at the metal-thiophene bond (Scheme III.2).



SCHEME III.2

The exposed face of the sulfur atom lies on the ring side opposite from the chloride. The pyramidalisation at sulfur varies from 110.5 to 116.7°. An interesting feature in the crystal structures of all of the above complexes is a slight bending of the thiophene ring along the C2-C5 vector.

Sulfur-bound thiophenes are normally labile and can be easily replaced by other ligands such as acetonitrile, CO and tetrahydrothiophene.²¹⁹ In the $[\text{CpRu}(\text{PPh}_3)_2(\eta^1\text{-C}_4\text{H}_4\text{S})]^+$ complex (Cp = cyclopentadienyl), the S-bound thiophene ligand rearranges upon standing into the more stable, η^5 -coordinated species, *i.e.* $[\text{CpRu}(\eta^5\text{-C}_4\text{H}_4\text{S})]^+$.²¹⁹

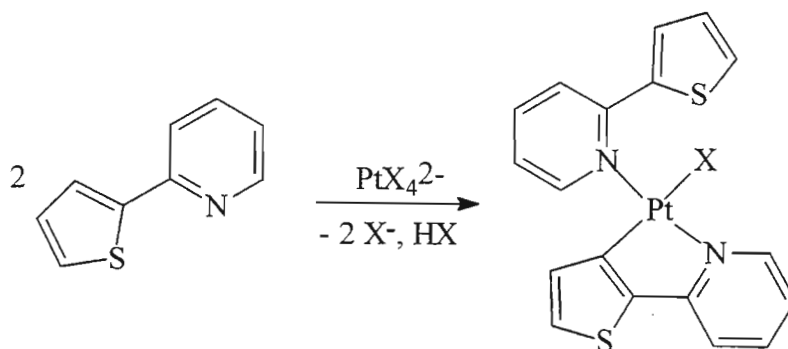
Constable *et al.*^{221,222} have demonstrated that the polydentate ligands 6-(2-thienyl)-2,2'-bipyridine (NNS) and 2,6-bis(2'-thienyl)pyridine (SNS) enforce the S-bonding mode of thiophene. Examples of complexes where the thiophene fragment of the ligand is bonded to the metal via the thiophene sulfur are $[\text{RuCl}(\text{N,N,S-NNS})(\text{N,N-NNS})]^+$ ²²¹ and $[\text{Pt}(\text{C,N,S-SNS}')\text{Cl}]$ ²²² (SNS' is the SNS ligand metallated at the 3-position of one of the thiophenes). Attempts to form analogous complexes under the same conditions using thiophene itself were not successful.

There are many examples in the literature of the η^5 -bound thiophenes, *i.e.* π -thiophene complexes. In these complexes all five atoms in the thiophene ring are bonded to the metal, although the M-C and M-S bond distances are somewhat different.²²³ The metals commonly used to form complexes with η^5 -bound thiophene are Cr, Mn, Fe, Ru, Rh, Ir, the structural types of the complexes varying from arene-carbonyl {*e.g.* $[\text{Cr}(\text{CO})_3(\eta^5\text{-C}_4\text{H}_2\text{Me}_2\text{S})]$ and $[\text{Mn}(\text{CO})_3(\eta^5\text{-C}_4\text{H}_4\text{S})]\text{O}_3\text{SCF}_3$ ²¹⁸} to ferrocene-like {*e.g.* $[\text{Fe}(\eta^5\text{-C}_5\text{H}_5)(\eta^5\text{-C}_4\text{H}_4\text{S})]$ and $[\text{Ru}(\eta^5\text{-C}_4\text{Me}_4\text{S})_2](\text{BF}_4)_2$ ²¹⁸} to mixed-ligand ones {*e.g.* $[\text{Ru}(\eta^5\text{-C}_4\text{Me}_4\text{S})\text{Cl}_2(\text{PR}_3)]$ ²¹⁸ and $[\text{Rh}(1,5\text{-cod})(\eta^5\text{-C}_4\text{H}_4\text{S})]^+$ ²²⁴}.

η^4 -Thiophene complexes can be prepared from the corresponding η^5 complexes. For example, $\text{Cp}^*\text{Ir}(\eta^4\text{-C}_4\text{H}_2\text{Me}_2\text{S})$ (Cp^* = permethylated Cp) was prepared by reduction of the relevant η^5 -coordinated species with $\text{NaAlH}_2(\text{OCH}_2\text{CH}_2\text{OCH}_3)$.^{225,226} The two-electronic reduction results in major spectroscopic and geometric changes, the latter manifesting itself most clearly in a pronounced folding of the coordinated thiophene ring along the C2-C5 axis.

Generally, η^2 -arene ligands are observed only for $16e^-$ metal centres that are exceptional π -donors and which have only one coordination site available for ligand binding. In the case of thiophene, coordination to a $16e^-$ metal fragment can lead to either η^2 -coordination of any pair of adjacent carbon atoms or oxidative addition of the C-S bond (also known as insertion).²¹⁸ Examples include $[\text{Os}_3(\eta^2\text{-C}_4\text{H}_4\text{S})\text{H}_2(\text{CO})_9]$ and $[\text{Fe}_2\{-\text{SC}_4\text{H}_3\text{-}(2\text{-Me})\}(\text{CO})_6]$, respectively. Angelici *et al.*²²⁷ demonstrated that benzo[b]thiophene (BT) forms both S-bound and η^2 -coordinated isomers of formula $[\text{Cp}'\text{Re}(\text{CO})_2(\text{BT})]$ ($\text{Cp}' = \text{Cp}$ or Cp^*); the formation of the η^2 -isomer is favoured to a greater extent by the presence of more electron-rich substituent (Cp^*) on the metal.

Synthetic access to σ -thienyl, also known as metallated thiophene complexes, is provided by electrophilic attack on the thiophene ring and by metathesis of thienyllithium reagents with metal halides. Electrophilic attack by a metal on the unsubstituted thiophene ring can occur at either 2-position, *e.g.* to give $2\text{-(HgOAc)C}_4\text{H}_3\text{S}$,²²⁸ or at position 3. A second example is provided in Scheme III.3.²²⁹



SCHEME III.3

On the other hand, complexes of platinum group metals containing thiophene and 2,2'-bithiophene σ -bonded at position 2 of the thiophene ring are prepared using metathesis reactions between correspondingly lithiated (or trimethylstannylated) heterocycles and *trans*- $[\text{M}(\text{PBU}_3)_2\text{Cl}_2]$ ($\text{M} = \text{Pt}, \text{Pd}$).¹⁸⁹ Also, nucleophilic attack on a thiophene via oxidative addition of $\text{Pd}(\text{PPh}_3)_4$ to $\text{C}_4\text{H}_{4-n}\text{Br}_n\text{S}$ ($n = 1\text{-}4$), leads selectively to complexes with the thiophene ring metallated at the 2-position *i.e.*, *trans*- $[\text{PdBr}(\sigma\text{-C}_4\text{H}_{4-n}\text{Br}_{n-1}\text{S})(\text{PPh}_3)_2]$ ($n = 1\text{-}4$).²³⁰

Carmona *et al.*²³¹ have reported a preparation of the iridium complex $[\text{Tp}^*\text{Ir}(\sigma\text{-C}_4\text{H}_4\text{S})_2(\eta^1\text{-C}_4\text{H}_4\text{S})]$ ($\text{Tp}^* = \text{hydrotris}\{3,5\text{-dimethylpyrazolyl}\}\text{borate}$) that contains

thiophene ligands in two different coordination modes. One of the thiophene ligands is coordinated through the sulfur atom, while the other two are metallated in the 2-position. Investigation of the chemical properties of this complex revealed that σ -bonded ligands are more difficult to replace than the η^1 , S-bound ligand.

Recently there has been increased interest in the synthesis of complexes where the thiophene ligand displays a bridging coordination mode, achieved in one of the following ways. The complex $[\text{Cp}^*(\text{CO})_2\text{Re}(\mu\text{-C}_4\text{H}_4\text{S})\text{Fe}(\text{CO})_3]^{232}$ provides one of many examples of the $\eta^1:\eta^4$ -binding mode of thiophene, where the heterocycle is S-bound to rhenium and is coordinated in the η^4 mode to the iron. (It is known that coordinating via S destroys the aromaticity of the thiophene ring, thereby causing diene-like reactivity for the heterocycle and promoting the η^4 coordination mode; the opposite is also true²¹⁸). Reaction of the trinuclear osmium cluster, $[\text{Os}_3(\text{CO})_{10}(\text{MeCN})_2]$ with 2,2'-bithiophene and 2,2':5',2''-terthiophene gives rise to the complexes $[\text{Os}_3(\mu\text{-H})(\mu\text{-C}_4\text{H}_2\text{S-C}_4\text{H}_3\text{S})(\text{CO})_{10}]$ and $[\text{Os}_3(\mu\text{-H})(\mu\text{-C}_4\text{H}_2\text{S-C}_4\text{H}_2\text{S-C}_4\text{H}_3\text{S})(\text{CO})_{10}]$, respectively, where only one thiophene unit of the polythiophene ligand participates in bonding with the metal atoms: it displays both σ -coordination to one osmium atom and vinyl, η^2 -binding to the other.²³³ Deeming *et al.*²³⁴ recently reported an example of a $\mu\text{-C,S}$ -bonded thienyl in the complex $[\text{Re}_2(\mu\text{-PPh}_2)(\mu\text{-C}_4\text{H}_3\text{S})(\text{CO})_8]$. An interesting metal exchange reaction has been observed in a heterobimetallic complex, $\sigma:\eta^5$ -bridged by thiophene, *viz.* $[(\text{CO})_3\text{Cr}(\mu\text{-C}_4\text{H}_3\text{S})\text{Mn}(\text{CO})_5]$.²³⁵ Here chromium is π -bonded to the thiophene ring, while manganese binds to the position 2 of the heterocyclic ring. It is proposed that this complex undergoes an intramolecular 'flip' to afford the thermodynamically more stable $[(\text{CO})_3\text{Mn}(\mu\text{-C}_4\text{H}_3\text{S})\text{Cr}(\text{CO})_5]$ species, where manganese is π -bonded to the thiophene ring, while chromium binds to the position 2 of the heterocyclic ring.

There have been only a few examples of transition metal complexes containing thiophene functionalised with a phosphine moiety such as the diphenylphosphino group. The diphenyl(2-thienyl)phosphine (PS) ligand has been the most studied so far. In the majority of the cases, *e.g.* *cis*- $[\text{Mo}(\text{CO})_4(\text{PS})_2]^{166}$ and $[\text{Co}_3(\mu_3\text{-CMe})(\text{CO})_7(\text{PS})_2]^{163}$ this ligand acts as a simple tertiary phosphine donating via the phosphorus atom only. Alternatively, it can serve as a bridging ligand coordinating to rhenium atoms through both the carbon and the sulfur atoms as in the complex $[\text{Re}_2(\text{CO})_8\{\mu\text{-PPh}_2(\text{C}_4\text{H}_3\text{S})\}]^{236}$. Furthermore, reaction of PS with $[\text{Ru}_3(\text{CO})_{12}]$ results in C-H bond cleavage and the formation of bimetallic products

in which the thiophene moiety of the ligand forms a σ, η^2 -vinyl type bridge between two metal atoms with phosphorus coordinating to the third centre.²³⁷

The donor properties of various tris(2-thienyl)-phosphines in complexes with Pt,¹⁶⁴ Rh and Pd^{146,160} have also been studied. In all these compounds the thienylphosphine ligand is bound to the metal through the P-atom only. Examples are $[\text{Pt}\{\text{P}(\text{C}_4\text{H}_3\text{S})_3\}_2\text{Cl}_2]$,¹⁶⁴ $[\text{Pd}\{\text{P}(5\text{-Me-C}_4\text{H}_2\text{S})_3\}_2\text{Cl}_2]$ ¹⁶⁰ and $[\text{RhH}(\text{CO})\{\text{P}(\text{C}_4\text{H}_3\text{S})_3\}_3]$.¹⁴⁶

Introduction of a 'spacer' between the phosphorus atom and the thiophene ring, *e.g.* an ethylene bridge, improves the chances for the molecule to act as a chelating ligand. Thus, two 4-diphenylphosphinodibenzothiophene (DPDBT) ligands coordinate to Ru via both P and S atoms in the stable complex *cis*- $[\text{RuCl}_2(\text{DPDBT})_2]$, with the Ru-S bond being as short as 2.34 Å.²³⁸ Mathieu and co-workers^{239,240} showed that both 2,5-bis[2-(diphenylphosphino)ethyl]- and 2,5-bis[3-(diphenylphosphino)propyl]-thiophene (BDPPT) could serve as tridentate ligands, binding through phosphorus and sulfur in complexes with metals such as Mo(0), Co(I) and Rh(I). Interestingly, the complex $[\text{Rh}(\text{CO})(\text{BDPPT})]^+ [\text{ClO}_4]^-$, in which the BDPPT ligand exhibits this coordination mode, is readily decarbonylated with the thiophene moiety becoming π -bound and the Rh-P bonds remaining intact.

There has been no information reported so far on the coordination of thienylphosphine ligands to gold(I). Indeed, the coordination of the unsubstituted thiophenes towards gold(I) has only been sparsely investigated. In this Chapter we report the preparation of a number of gold(I) complexes with the new thienylphosphine ligands reported in Chapter 2. Of particular interest is the mode of coordination of the thienylphosphine ligands to gold(I).

III.2 SYNTHESIS AND CHARACTERISATION OF GOLD(I) COMPLEXES WITH THE NOVEL THIENYLPHOSPHINE LIGANDS

The various types of gold(I) complexes with tertiary phosphine ligands were discussed in detail in Chapter I. As discussed, complexes of gold(I) with phosphine ligands can be broadly classified as either ionic or neutral. A further sub-classification depends on the number of gold atoms in the complex *i.e.*, on whether the complex is mono-, di- or trinuclear. Here, the complexes which have been synthesised and characterised, are

initially grouped according to the denticity of the thienylphosphine ligand *i.e.*, on the number of phosphorus atoms in the ligand molecule.

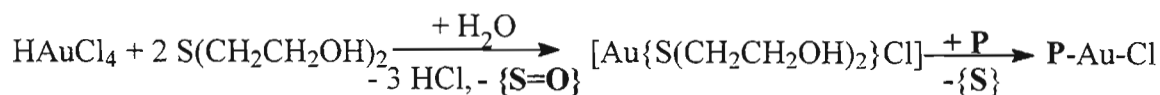
III.2.1 Gold(I) complexes with monophosphine ligands

III.2.1.1 Neutral mononuclear complexes containing two-coordinate gold

Preparation

A commonly used precursor for the synthesis of neutral gold(I) complexes is tetrachloroauric acid, HAuCl_4 ,^{9,17,104} as well as its sodium and potassium salts.^{32,100} Gold(I) complexes with labile thioether ligands such as $[\text{ClAu}(\text{tth})]$ (tth = tetrahydrothiophene) and $[\text{ClAu}\{(\text{CH}_3)_2\text{S}\}]$ can also be employed,^{93,241} although they are generally less stable than the above gold(III) compounds, tending to decompose slowly with release of elemental gold even at decreased temperatures.

A convenient route to a two-coordinate neutral gold(I)-phosphine complex lies through *in situ* preparation of a gold(I)-thioether complex with subsequent replacement of the labile ligand with the desired phosphine, as shown in Scheme III.4.



where

$\{\text{S}\} = \text{S}(\text{CH}_2\text{CH}_2\text{OH})_2$ (tdg), $\{\text{S}=\text{O}\} = \text{OS}(\text{CH}_2\text{CH}_2\text{OH})_2$ and

P = monodentate phosphine

SCHEME III.4

The reaction sequence was used for the following monodentate thiophene-based phosphines: PS, PDS, PTS, PSBr, PSS, PSSS, PSN and PNS. In all cases a clean reaction took place with the exclusive formation of complexes of general formula $[\text{ClAu}(\eta^1\text{-L})]$, where L represents a thienylphosphine molecule. For simplicity, they will later be referred to as just $[\text{ClAuL}]$ complexes.

The experimental conditions for the syntheses are essentially the same for all the phosphines and involve dissolution of the required amount of tetrachloroauric acid in an acetone/water mixture, cooling the solution (in order to minimise side-reactions during the

following step), addition of neat thiodiglycol (tdg) until the orange colour of gold(III) disappears, and finally addition of a solution containing a stoichiometric amount of the phosphine dissolved in a suitable solvent. The precipitate that forms is collected and after washing and drying normally affords the target neutral gold(I) complex in nearly quantitative yields. Variations in the synthetic procedures from one phosphine to another generally involved differences in the composition of the solvents both for the phosphine and for the gold(III) precursor. The reason for this was the need to find an optimum balance between (i) dissolving a non-polar phosphine in order for it to be able to react with the gold(I)-tdg complex and (ii) having a more polar reaction medium which ensures fuller precipitation of the neutral complex formed as a result of the reaction. Thus, the phosphine was generally dissolved in a reasonably polar solvent, such as acetone or a mixture of chloroform (or dichloromethane) and methanol, while the tetrachloroauric acid was dissolved in aqueous acetone to which a small amount of methanol was sometimes added. Cold methanol was also often added during the last step of the reaction to maximise precipitation of the gold(I) complex. Table III.1 presents the physical data for the eight gold(I)-phosphine complexes prepared according to the above method.

The complexes are generally very stable in air at room temperature, being non-hygroscopic and resistant to oxidation or reduction (due to the strong bond between phosphorus and gold(I)). However the complexes containing light-sensitive ligands, such as PTS or PSSS, are best kept in the dark, as some discoloration was noticed upon their exposure to ambient

Table III.1 Physical data for the neutral di-coordinate gold(I) complexes with monodentate thiophene-based ligands

Compound number	Formula	Molar mass, $\text{g}\cdot\text{mol}^{-1}$	Colour	Yield, %
[1]	[ClAuPS]	500.73	white	92
[2]	[ClAuPDS]	506.76	white	89
[3]	[ClAuPTS]	512.78	off-white	87
[4]	[ClAuPSBr]	579.63	white	88
[5]	[ClAuPSS]	582.85	off-white	78
[6]	[ClAuPSSS]	664.52	yellow	92
[7]	[ClAuPSN]	577.82	white	90
[8]	[ClAuPNS]	577.82	white	95

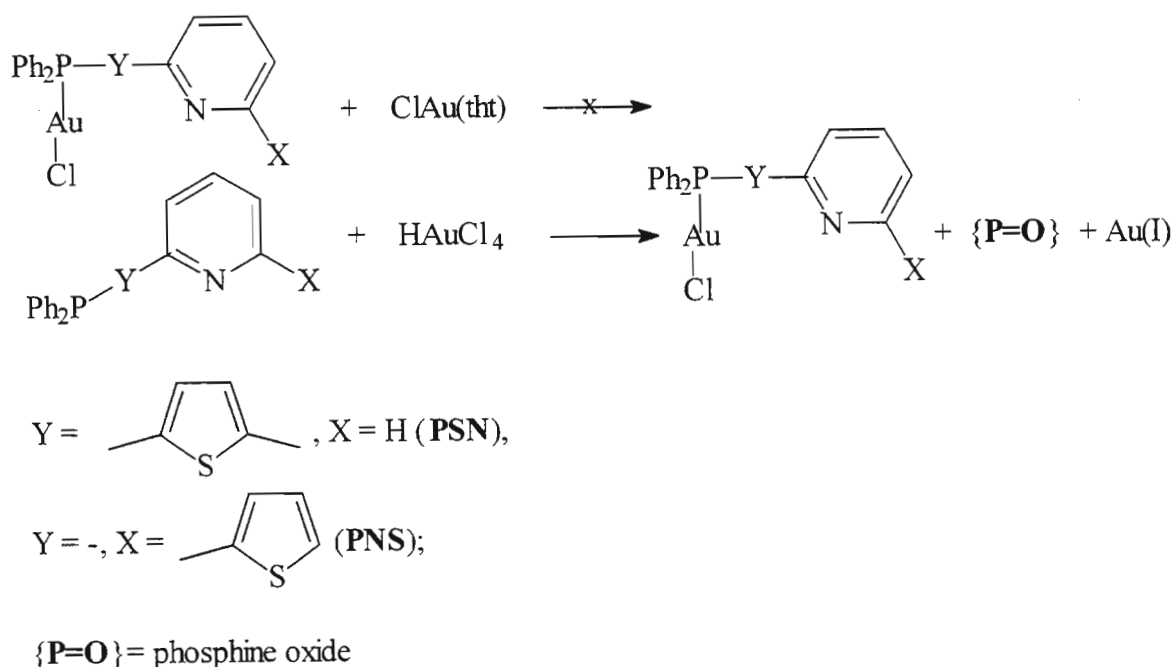
light for a week or longer. All the complexes are highly crystalline compounds, melting (with decomposition) at temperatures above 200°C.

In all of the complexes [1]-[8] the thienylphosphine ligand bonds to gold(I) through the P-atom only. As all of the above ligands contain at least one additional donor atom (thiophene S as well as pyridine N in the ligands PSN and PNS), it was decided to investigate the possibility of formation of a stable complex where the thienylphosphine ligand coordinates through both P and S donor atoms. It is expected from the geometry of the 2-thienylphosphine moiety that if the S atom does coordinate, the resultant molecule will be a dinuclear P,S-bridged complex rather than a mononuclear complex with chelating ligand, as the S-Au-P angle would be too small and cause destabilisation. (No chelating complexes of gold(I) with dppm, *i.e.* the ligand where two donor atoms are also separated by a single carbon atom, have ever been discovered.)

Changing the ratio of the reagents in the reaction shown in Scheme III.4 to L:Au = 1:2 (L = PS) did not lead to the formation of any new compound, as the only complex that could be isolated from the mixture was identical to [1]. Increasing further the amount of Au per molecule of phosphine effected the same result. Using [ClAu(tht)] as the starting material with a 4-fold excess over the amount of PS also resulted in production of [ClAuPS] as the only isolated product. Attempts to vary the temperature and the solvent ($\pm 50^\circ\text{C}$, reactions carried out in chloroform or acetonitrile/dichloromethane mixtures) also did not provide any evidence for formation of a product with the μ -S,P-mode of coordination.

Clearly, the sulfur of the thiophene ring is too weak a donor atom to displace the divalent sulfur of the thioethers tdg and tht from their respective complexes with gold(I). In order to eliminate the presence of competing thioether ligands in the mixture it was decided to carry out a direct reaction between the gold(III) precursor and the phosphine ligand. In this case the phosphine molecule serves not only as a ligand, but as a reducing agent as well, converting gold(III) into gold(I) without any other interfering ligands being present in the mixture. As one molecule of a phosphine is required to reduce gold(III), the stoichiometry of the reaction had to be chosen as 2:3 (Au:L). However even in this case the reaction only produced the complex [1]. It appears that the thiophene sulfur is too weak a donor to displace chloride ligands from either gold(III) or gold(I) precursors.

The unsuccessful attempts to make the thiophene S coordinate to gold(I) were followed by an investigation of the possibility of coordination of the pyridine N and the P-atom of the PSN and PNS ligands to separate gold atoms, with the aim of obtaining dinuclear species. Scheme III.5 shows the reactions attempted with the two ligands.



SCHEME III.5

As can be seen from the above Scheme the products isolated from these reactions were identical to the previously synthesised mononuclear complexes [7] and [8] *i.e.*, no complex with both N and P coordinating to gold(I) (either bridging or chelating) could be obtained. There was still a possibility that the nitrogen of the pyridine ring could not coordinate simply due to the low pH values of aqueous solutions of HAuCl₄ that caused its protonation. However increasing the pH of the solution in the second reaction by addition of a sufficient amount of NaHCO₃, followed by gentle heating to eliminate the CO₂ formed and then cooling to $\pm 10^\circ\text{C}$ did not change the outcome of the reaction. Thus, the novel thienylphosphine ligands PS, PDS, PTS, PSBr, PSS, PSSS, PSN and PNS appear to only form gold(I) complexes that are mononuclear, neutral and di-coordinate, and where coordination between the ligand and the metal is achieved via a P-Au bond only. Certainly, this is true in the reactions of these ligands with precursors that contain an Au-Cl moiety. This finding is in agreement with the results of Schmidbaur *et al.*⁵⁷ who have prepared several chlorogold(I) complexes with 2-pyridyl-based phosphines by reacting an

appropriate ligand with the [ClAuCO] precursor; in all cases it was established that the phosphorus is the exclusive coordination site for these ligands to the metal.

Characterisation

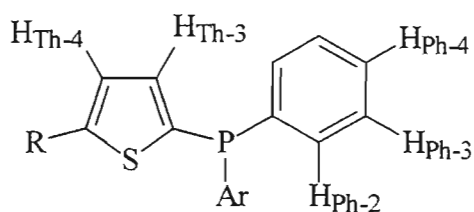
The ^1H and ^{31}P NMR spectroscopic data for the complexes [1]-[8] are given in Table III.2. It can be noted from this Table that the ^{31}P NMR chemical shifts of the complexes are markedly different from the values obtained for the corresponding ligands. The former signals appear downfield with respect to the latter, a general property for phosphine complexes. The analogous complex, [ClAuPPh₃], was reported to have the ^{31}P chemical shift of 33.2 ppm - approximately 39 ppm downfield from the chemical shift of the ligand ($\delta[\text{PPh}_3] = -6$ ppm).⁴⁵

The assignments of the signals in the ^1H NMR spectra of the complexes were carried out based on the assignments done for the ligands alone, taking into account the effect of coordination to the metal centre (*e.g.* an increase in the $J_{\text{H-P}}$ values) and by using 2-dimensional NMR techniques (COSY). However, even with the help of COSY spectroscopy, it proved impossible to resolve signals due to individual hydrogens in most of the spectra, especially in the case of the [ClAuPSN] and [ClAuPNS] complexes, because of the extensive overlap between aromatic proton resonances arising from the benzene, thiophene and pyridine nuclei.

Examination of the ^1H NMR chemical shifts of the protons in the coordinated ligands of these complexes also reveals overall downfield shift when compared to those in the non-coordinated ligands, a shift that is clearly the result of coordination of the phosphine ligand to gold(I). In the next Table, Table III.3, a quantitative estimate is provided of this change; specifically, the value of $\Delta = \delta(\text{complex}) - \delta(\text{ligand})$ is given, which is known as coordination chemical shift (CCS).⁴³ This has been done for both ^{31}P and ^1H NMR chemical shifts.

Table III.2 ^1H and ^{31}P NMR spectroscopic data for the complexes [1]-[8], as measured in CDCl_3 ; the atom numbering scheme for all the ligands is given in the Figure III.2 below

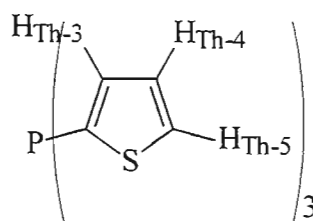
Complex	$\delta^{31}\text{P}$, ppm	$\delta^1\text{H}$, ppm
[1]	19.18 (s)	7.26 (ddd, 1 H, $\text{H}_{\text{Th-4}}$), 7.41-7.65 (m, 11 H, 10 H_{Ph} + $\text{H}_{\text{Th-3}}$), 7.82 (ddd, 1 H, $\text{H}_{\text{Th-5}}$)
[2]	5.77 (s)	7.25 (ddd, 2 H, $\text{H}_{\text{Th-4}}$), 7.42-7.70 (m, 7 H, 5 H_{Ph} + 2 $\text{H}_{\text{Th-3}}$), 7.81 (ddd, 2 H, $\text{H}_{\text{Th-5}}$)
[3]	-6.41 (s)	7.24 (ddd, 3 H, $\text{H}_{\text{Th-4}}$), 7.63 (ddd, 3 H, $\text{H}_{\text{Th-3}}$), 7.81 (ddd, 3 H, $\text{H}_{\text{Th-5}}$)
[4]	18.85 (s)	7.15-7.37 (ABX system, 2 H, $\text{H}_{\text{Th-4}}$ + $\text{H}_{\text{Th-3}}$), 7.42-7.65 (m, 10 H, H_{Ph})
[5]	19.43 (s)	7.03 (dd, 1 H, $\text{H}_{\text{Th-4'}}$), 7.22 (dd, 1 H, $\text{H}_{\text{Th-3'}}$), 7.26 (part of ABX system, 1 H, $\text{H}_{\text{Th-3}}$), 7.31 (dd, 1 H, $\text{H}_{\text{Th-5'}}$), 7.43 (part of AB system, 1 H, $\text{H}_{\text{Th-4}}$), 7.46-7.70 (m, 10 H, H_{Ph})
[6]	18.45 (s)	7.04 (dd, 1 H, $\text{H}_{\text{Th-4''}}$), 7.11 (m, 2 H, $\text{H}_{\text{Th-3'}}$ + $\text{H}_{\text{Th-4'}}$), 7.19 (dd, 1 H, $\text{H}_{\text{Th-3''}}$), 7.22-7.27 (m, 2 H, $\text{H}_{\text{Th-3}}$ + $\text{H}_{\text{Th-5''}}$), 7.45 (part of AB system, 1 H, $\text{H}_{\text{Th-4}}$), 7.48-7.69 (m, 10 H, H_{Ph})
[7]	20.63 (s)	7.22 (ddd, 1 H, $\text{H}_{\text{Py-5}}$), 7.40-7.80 (m, 14 H, 10 H_{Ph} + $\text{H}_{\text{Th-3}}$ + $\text{H}_{\text{Th-4}}$ + $\text{H}_{\text{Py-3}}$ + $\text{H}_{\text{Py-4}}$), 8.55 (m, 1 H, $\text{H}_{\text{Py-6}}$)
[8]	31.32 (s)	7.10 (dd, 1 H, $\text{H}_{\text{Th-4}}$), 7.40 (dd, 1 H, $\text{H}_{\text{Th-5}}$), 7.43-7.56 (m, 7 H, 4 $\text{H}_{\text{Ph-3}}$ + 2 $\text{H}_{\text{Ph-4}}$ + $\text{H}_{\text{Py-3}}$), 7.58 (dd, 1 H, $\text{H}_{\text{Th-3}}$), 7.66-8.00 (m, 6 H, 4 $\text{H}_{\text{Ph-2}}$ + $\text{H}_{\text{Py-5}}$ + $\text{H}_{\text{Py-4}}$)



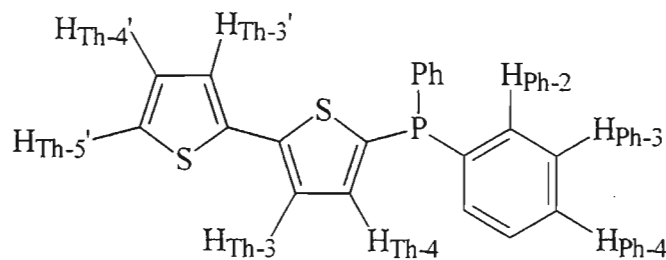
R = H_{Th-5}, Ar = Ph: L = **PS**;

R = H_{Th-5}, Ar = Th: L = **PDS**;

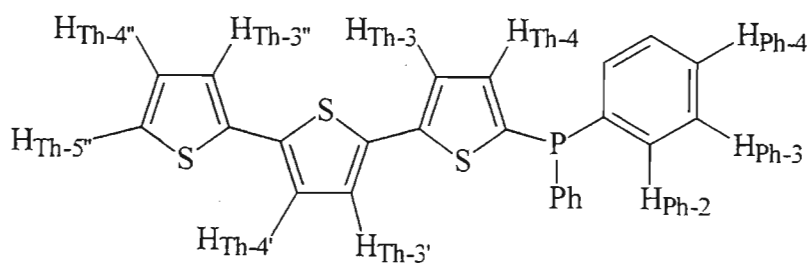
R = Br, Ar = Ph: L = **PSBr**



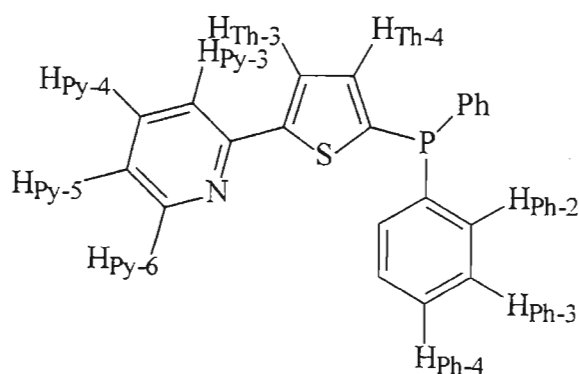
L = **PTS**



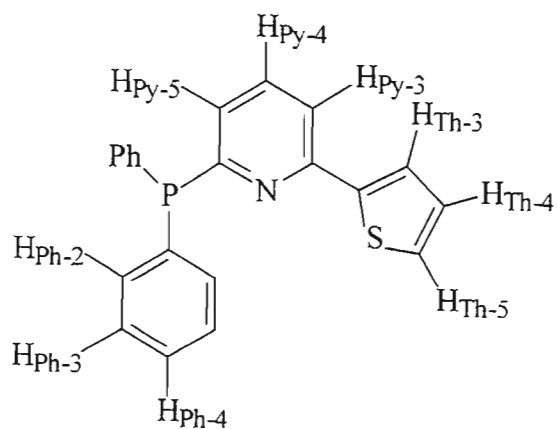
L = **PSS**



L = **PSSS**



L = **PSN**



L = **PNS**

Fig. III.2 Numbering schemes for the hydrogen atoms in the ligands of the complexes [ClAuL], [1]-[8].

Table III.3 CCS[#] values for the complexes [1]-[8] expressed in the form $\Delta = \delta(\text{complex}) - \delta(\text{ligand})$

Complex	³¹ P, Δ , ppm	¹ H, Δ , ppm [*]
[1]	39.08	- ^{***} , H _{Th-3}
[2]	39.03	- ^{***} , H _{Th-3}
[3]	39.86	0.27, H _{Th-3}
[4]	36.73	0.24, H _{Th-3}
[5]	38.26	- ^{***} , H _{Th-4}
[6]	37.16 ^{**}	- ^{***} , H _{Th-4}
[7]	38.98	- ^{***} , H _{Th-4}
[8]	34.96	- ^{***#} , H _{Py-5}

[#] CCS stands for coordination chemical shift

^{##} Although it was not possible to determine the CCS value exactly, it appeared from the comparison of the spectra of the coordinated and non-coordinated PNS, that the signal due to the H_{Py-5} shifted downfield by greater than 0.5 ppm

^{*} The chemical shifts of the protons nearest to the P atom were used to determine the ¹H CCS value

^{**} The chemical shift for the ligand was obtained in CDCl₃, while that for the complex was measured in CD₂Cl₂

^{***} The value could not be determined because either the corresponding signal in the ligand or the complex spectrum was not sufficiently resolved

It can be seen from the Table III.3 that the chemical shifts of phosphines experience a downfield shift of approximately 38 ppm upon coordination to gold(I) in two-coordinate neutral complexes with chloride as the second ligand. The value is slightly higher for phosphines with substituents that include one thiophene ring, but appears to decrease slightly with an increase in the number of the thiophene rings joined together in the substituent. Introduction of a bromine substituent in a thiophene ring also reduces the CCS value (for both ³¹P and ¹H chemical shifts). For the pyridine-based phosphine ligand, PNS, the ³¹P Δ value is noticeably smaller (± 35 vs. ± 38 ppm), while the CCS value for the hydrogen nearest to the phosphorus appears to be greater (± 0.5 vs. 0.27 ppm).

The effect of coordination of a thienylphosphine ligand to chlorogold(I) moiety on the proton chemical shift can be further illustrated by tabulating the Δ values for all thiophene

hydrogens together with the $J_{\text{H-P}}$ coupling constants for both complexes and ligands in the compounds [1]-[3].

Table III.4 Coupling constants between the thiophene hydrogens and the phosphorus in the chlorogold(I) complexes of PS, PDS, PTS (the corresponding $J_{\text{H-P}}$ value for the ligand is given in brackets) and related Δ values, where $\Delta = \delta(\text{complex}) - \delta(\text{ligand})$

Hydrogen Complex	$\text{H}_{\text{Th-3}}$		$\text{H}_{\text{Th-4}}$		$\text{H}_{\text{Th-5}}$	
	$^3J_{\text{H-P}}$, Hz	Δ , ppm	$^4J_{\text{H-P}}$, Hz	Δ , ppm	$^5J_{\text{H-P}}$, Hz	Δ , ppm
[ClAuPS] ([1])	- [*] (4.63)	- [*]	1.38 (1.28)	0.13	3.23 (0)	0.23
[ClAuPDS] ([2])	- [*] (4.57)	- [*]	1.33 (1.27)	0.12	3.33 (0)	0.20
[ClAuPTS] ([3])	9.65 (5.71)	0.27	1.43 (1.40)	0.16	3.52 (0)	0.25

^{*} The relevant value could not be obtained due to overlap of this signal with the signals of the phenyl hydrogens

The data from the Table III.4 clearly show that coordination of a thiophene-based phosphine to gold(I) results in a considerable change in electron density at $\text{H}_{\text{Th-3}}$ and $\text{H}_{\text{Th-5}}$, while that around $\text{H}_{\text{Th-4}}$ remains nearly unchanged: the corresponding coupling constants for the first two in the gold(I) complexes are generally markedly larger than the relevant values in the ligands themselves.

The coordination to metal affects the electron density not only in the aromatic ring directly bound to the phosphorus atom but also in the rings adjacent to them, although to a smaller extent. Thus comparison of the spectra of PSS and its complex gives $\Delta = 0.06$ ppm ($\text{H}_{\text{Th-4'}}$) and those of PSSS give $\Delta = 0.10$ ppm ($\text{H}_{\text{Th-4''}}$) and $\Delta > 0.15$ ppm ($\text{H}_{\text{Th-3'}} + \text{H}_{\text{Th-4'}}$). Similarly, for PSN and PNS complexes $\Delta = 0.08$ ppm ($\text{H}_{\text{Py-5}}$) and $\Delta = 0.04$ ppm ($\text{H}_{\text{Th-4}}$).

IR and UV-vis spectroscopy were also employed for characterisation of the chlorogold(I) complexes. Unfortunately the limitations of the IR instrument do not allow any measurements to be conducted at the frequencies below 400 cm^{-1} . This region is the most informative for characterisation of the complexes since both the $\nu(\text{Au-Cl})$ and $\nu(\text{Au-P})$ frequencies are found between 300 and 400 cm^{-1} . Thus the data we report is of only marginal importance: most of the IR absorption bands of the complexes occur in the

'fingerprint' part of the spectra. More useful are IR spectra of those phosphines (and the corresponding complexes) that contain pyridine rings, since these exhibit moderately intense C-N stretching bands between 1500 and 1600 cm^{-1} . The IR data are presented in the Experimental section of this Chapter.

The UV-vis spectra of the complexes [1]-[8] recorded in dichloromethane strongly resemble those of the ligands, as there are no electronic transitions associated with the metal d-electrons due to gold(I) having the d^{10} electronic configuration. In fact the wavelengths of the absorption maxima recorded for the complexes and the ligands are essentially the same. However differences in the shapes of the peaks can be discerned, those for the complexes appearing narrower and with more fine structure (*e.g.* two shoulders at 268 and 276 nm are observed in the spectra of all the gold complexes, but not in the ligand spectra).

Changing the solvent from dichloromethane to acetonitrile does not markedly change the spectral behaviour of the complexes [1]-[8]. This suggests that the complexes do not dissociate in solution and that acetonitrile (a potential ligand!) does not interact with the gold(I) centre in these complexes. The full description of the UV-vis spectra of the gold(I)-phosphine complexes can be found in the Experimental section of this Chapter.

Crystal structures of the [ClAuPSS] and [ClAuPNS] complexes

Single crystals of three neutral two-coordinate gold(I)-phosphine complexes, namely [ClAuPS], [ClAuPSS] and [ClAuPNS] were obtained during this study. Although the quality of the [ClAuPS] crystal appeared to be satisfactory for the data collection, the refinement of the structure proved to be dubious as the sulfur and carbon atoms of the thiophene ring could not be unequivocally found and essentially had to be placed in calculated positions, *i.e.* all substituents on phosphorus appeared to be phenyl rings. In absence of another good quality single crystal of [1] it was decided to abandon the structure refinement and to discard the data. The crystals of the other two compounds, on the other hand, provided suitable data to carry out successful structure determination, though it should be noted that the thiophene rings in [ClAuPSS] show evidence of disorder (see Experimental section of this Chapter).

Crystallisation of [ClAuPSS] ([5]) from an acetone-water mixture afforded pale yellow needles which were employed for X-ray diffraction studies. Figure III.3 represents the molecular structure of [5] and the crystallographic data are discussed with respect to the numbering scheme shown. The bond lengths and angles, crystallographic parameters as well as the other structural information are given in Tables III.24-29 at the end of the Experimental section.

There are 2 molecules per asymmetric unit cell in the crystal structure of [ClAuPSS]. The shortest distance between any two gold atoms within the unit cell is as large as 7.661(2) Å and there appears to be no metal-metal bonding between gold atoms from different unit cells. There is also no interaction between the aromatic rings of two molecules as none of the rings is parallel to each other.

The geometry around the gold atoms is nearly linear for both molecules [176.3(3) and 178.6(2)°] with the Au-P and Au-Cl bond lengths being within the accepted limits for two-coordinate chlorogold(I)-phosphine complexes (see Table I.1 in the Section I.1.1). It should be noted though, that the respective values for the first molecule [2.217(7) and 2.256(8) Å] are somewhat smaller than those reported for [ClAuPPh₃] [2.235(3) and 2.279(3) Å],²¹ while those for the second, *i.e.* 2.232(6) and 2.282(6) Å, are on the par with the triphenylphosphine complex.

The geometry around both phosphorus atoms is tetrahedral with the angles ranging from 105.6(1) to 114.4(8)° [105.6(1) to 107.2(1)° for the three substituents on the phosphorus] for the first molecule and from 102.6(1) to 113.7(7)° [102.6(1) to 108.6(1)° for the three substituents on the phosphorus] for the second. There is an indication of a slight 'opening-up' effect of the ligand upon coordination to the metal as the angles between the substituents on phosphorus in both [ClAuPSS] molecules are greater than the angles of 101.6(1) to 103.5(1)° found in the non-coordinated PSSP molecule, which is the closest available free ligand for which the structure is known. The distances between the phosphorus atom and the carbons of the substituents are close to the expected value of 1.8 Å, with the only exception being P(1)-C(1) which is rather short at 1.68(2) Å. The bonds and angles between carbon atoms in the phenyl substituents fall within normal range.

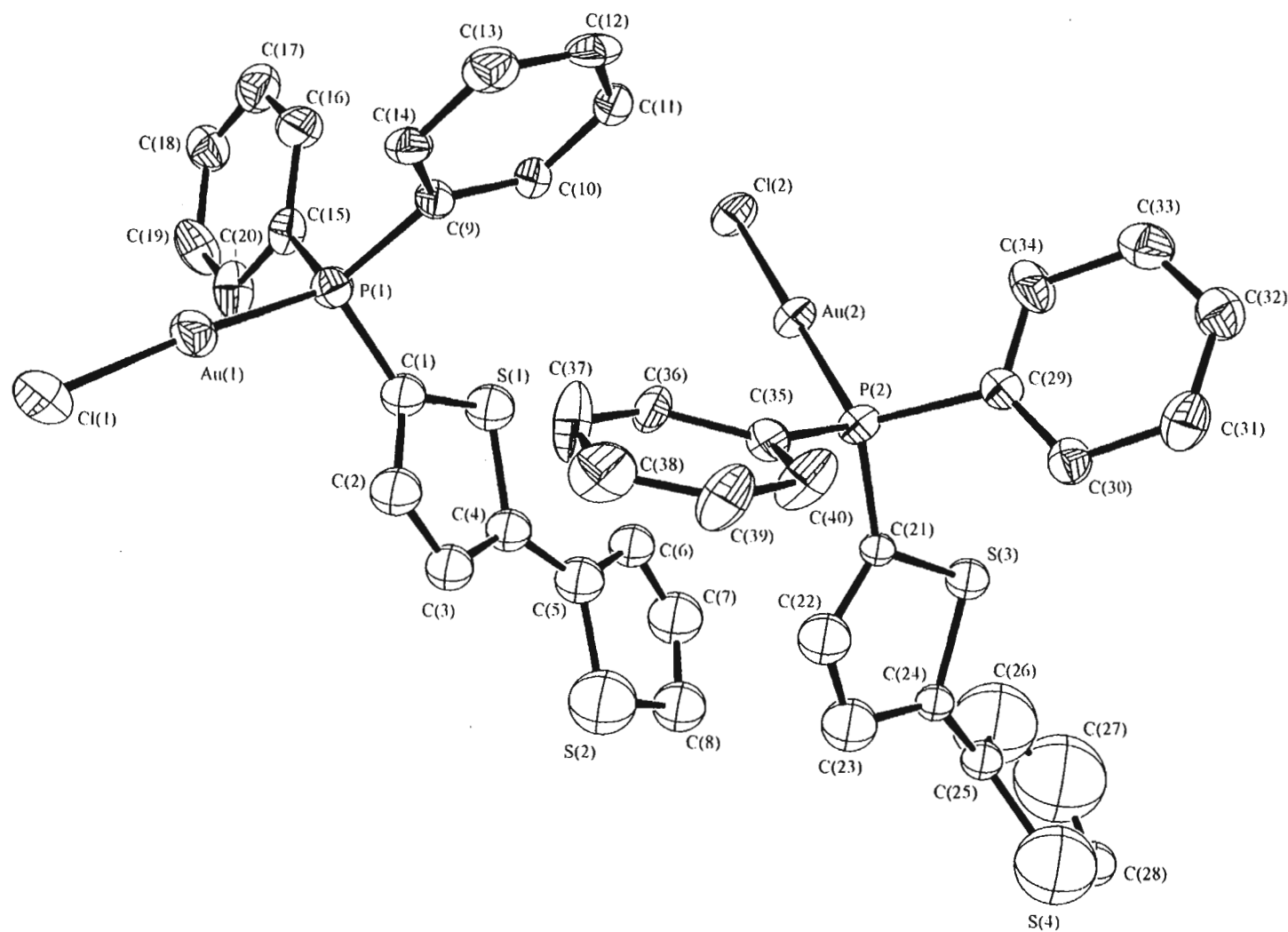


Fig. III.3 Structure of [ClAuPSS] ([5]), showing the atom numbering scheme

The conformations adopted by PSS ligands in the two molecules are markedly different. Firstly, the angles between the thiophene rings of the bithienyl substituents in PSS molecules are 3.43 and 57.50° for the first molecule [*i.e.* the one containing the Au(1) atom] and the second molecule [*i.e.* the one containing the Au(2) atom] respectively. Secondly, the angles between the plane of the thiophene ring attached to the phosphorus and the planes of the phenyl substituents are 60.62 and 73.58° for the first molecule and 107.51 and 78.10° for the second molecule. Comparison of these observed angle values with those in the molecule of the PSSP ligand - the angles between the thiophene and two phenyl rings are 105.7 and 77.3° - shows that it is the ligand in the first [ClAuPSS] molecule which has acquired most conformational changes upon coordination to gold(I). However the bithienyl moiety in the first molecule is much less distorted than in the second molecule: the S(1)..C(4) and S(2)..C(8) thiophene rings adopt a *S,S-transoid* and nearly planar geometry, which is very similar to the geometry of the bithienyl fragment in PSSP, while in the second molecule the second thiophene ring [S(4)..C(28)] is noticeably rotated out of the plane of the first ring. The thermal ellipsoids of S(4), C(26) and C(27) atoms are very large indicating considerable disorder and instability in the ring and the likelihood of the presence of several rotamers of the second molecule in the crystal lattice. The distortion of the molecules is likely a consequence of their packing in the crystal.

It is interesting to note that the corresponding torsion angles Au(1)-P(1)-C(1)-S(1) and Au(2)-P(2)-C(21)-S(3) in both molecules are markedly different, the first being 166.8 and the second 66.5°. This implies that in the first molecule the nearest to gold thiophene sulfur faces the direction nearly opposite that of the metal, while in the second molecule the sulfur is positioned roughly on the same side as the gold. [Note, however, that there is no gold-sulfur non-bonding interactions, the Au(2)...S(3) distance being as large as 4.074(5) Å.] The idealised calculations given in Appendix B for the PSSP, PSNP and PSNSP ligands show that the thiophene conformation with the sulfur atom facing the same way as the lone pair of the phosphorus (or P-M bond) causes greater steric effects in comparison to the conformation where the sulfur is facing opposite. This finding may help to explain the greater disorder of the PSS ligand in the second molecule as it has adopted a less sterically viable conformation.

It is worth noting at this stage that disorder in thiophene rings of thienylphosphine ligands has been reported before.^{160,163} In particular, Gol'dfarb *et al.*¹⁶⁰ have demonstrated that all 3

thiophene rings of the PTS ligand in the $[\text{Pd}(\text{PTS})_2\text{Cl}_2]$ complex are disordered to certain extent. However the ring with the sulfur facing the direction opposite to that of the metal had the least disorder, while the other two with the S being turned towards the gold both appeared as equally weighted rotamers with different conformations obtained by rotation around the P-C bond. In the complex $[\text{Co}_3(\mu_3\text{-CMe})(\text{CO})_7(\text{PS})_2] \cdot 0.5\text{C}_6\text{H}_{14} \cdot \text{H}_2\text{O}$,¹⁶³ some atoms of one phenyl ring and the thienyl ring belonging to one of the two PS ligands exhibited unrealistic thermal ellipsoids and bond distances. Orientational disorder in the phosphine cone was proposed and the successful refinement of the structure was made by constructing a model incorporating two orientations of the phosphine ligand related by a 120° rotation around the Co-P axis.

Crystallisation of $[\text{ClAuPNS}]$ ([8]) from dichloromethane-hexane afforded colourless prisms which were employed for X-ray diffraction studies. Figure III.4 represents the molecular structure of [8] and the crystallographic data are discussed with respect to the numbering scheme shown. The bond lengths and angles, crystallographic parameters as well as the other structural information are given in Tables III.30-35 at the end of the Experimental section.

The molecules exist as discrete entities in the crystal there being no intermolecular non-bonded contact distances less than the sum of the van der Waals radii for the two atoms concerned. In particular, there is no evidence for intermolecular Au...Au interaction in the crystal.

The geometry around the gold atom is linear $[\text{Cl}(1)\text{-Au}(1)\text{-P}(1) = 177.0(4)^\circ]$ with the bond lengths Au(1)-P(1) and Au(1)-Cl(1) being 2.227(1) and 2.278(1) Å respectively, values very close to those reported for the $[\text{ClAuPPh}_3]$ complex of 2.235(3) and 2.279(3) Å.²¹ The bond lengths and angles appear to be within the normal limits and correlate well with the values found for the PSNP ligand molecule, the latter being the closest available free ligand for which the structure is known (see Section II.2.5.4).

The geometry around the phosphorus atom is tetrahedral with the angles subtended at the P atom ranging from $104.4(2)$ to $114.7(1)^\circ$. The angles subtended at the P atom by the three ring substituents between the three ring substituents span the range from $104.4(2)$ to

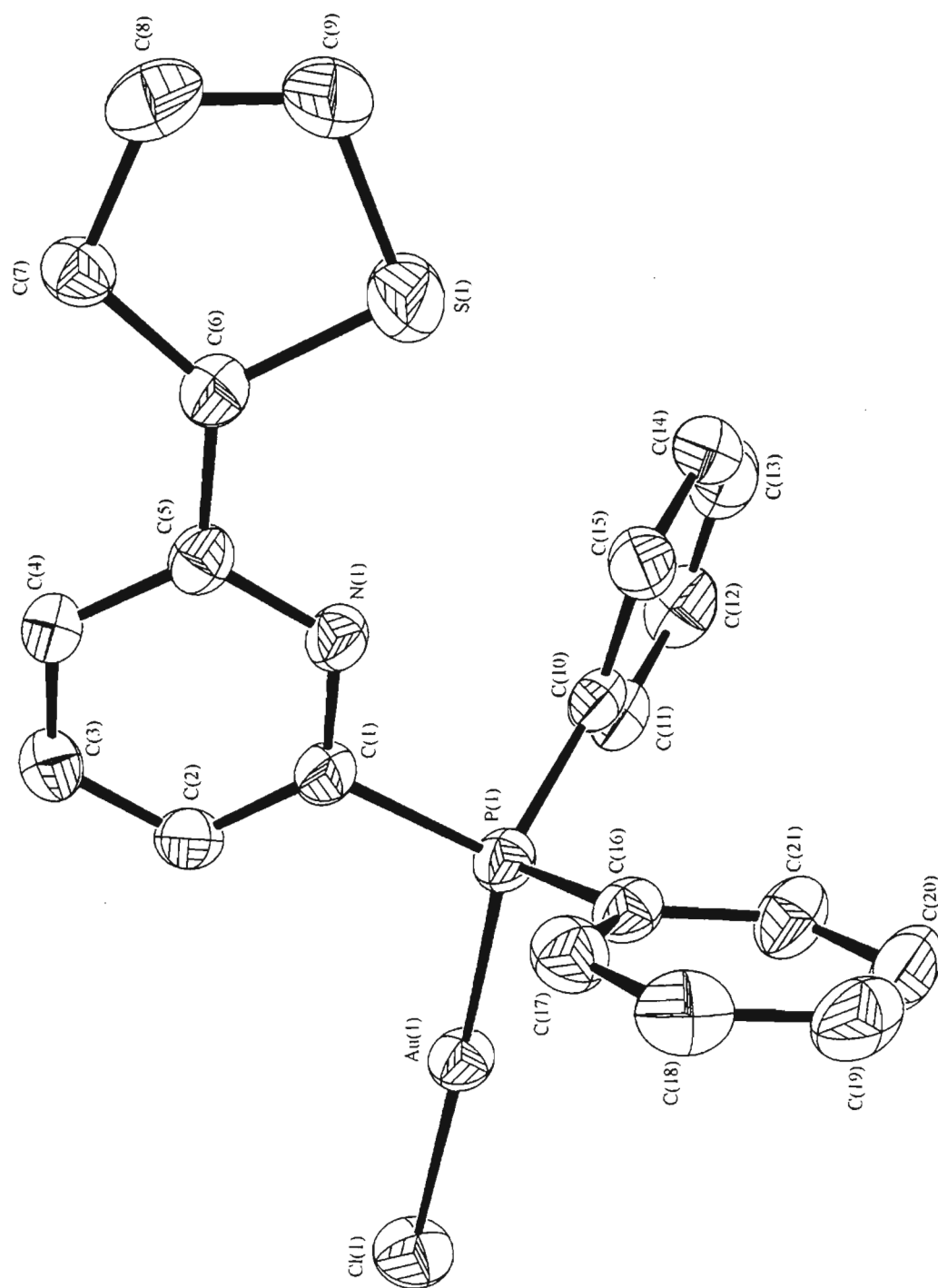


Fig. III.4 Structure of [ClAuPNS] (8), showing the atom numbering scheme

106.0(2)° and appear somewhat greater than the corresponding values in the PSNP ligand ('pyridine side' of the molecule) of 101.2(3) to 105.2(2)° (see Section II.2.5.4). This indicates that the ligand is 'opened-up' to some extent of coordination. The torsion angle Au(1)-P(1)-C(1)-N(1) is 179.6(1)°, which implies that the pyridine N is pointing in the opposite direction to the P-Au bond. Cone angle calculations given in Appendix B suggest that the conformation adopted when the pyridine N faces the phosphorus lone pair (or P-M bond), labelled P-C-N, is somewhat less sterically hindered than the one in which the lone pairs face opposite directions, *i.e.* the one labelled P-C-C-H.

The dihedral angles between the plane of the pyridine ring and each of the phenyl groups are 116.38 and 110.73°, while the angle between the two phenyl rings is 73.71°. The corresponding angles for the 'pyridine' part of the PSNP ligand are 68.54, 43.56 and 112.10° respectively. This shows (with assumption that the structure of the non-coordinated PNS is very similar to that of PSNP) that the PNS ligand underwent a conformational change upon coordinating to gold(I).

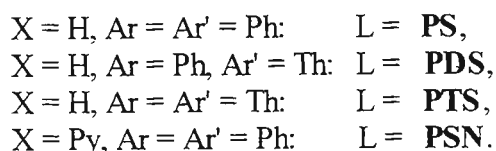
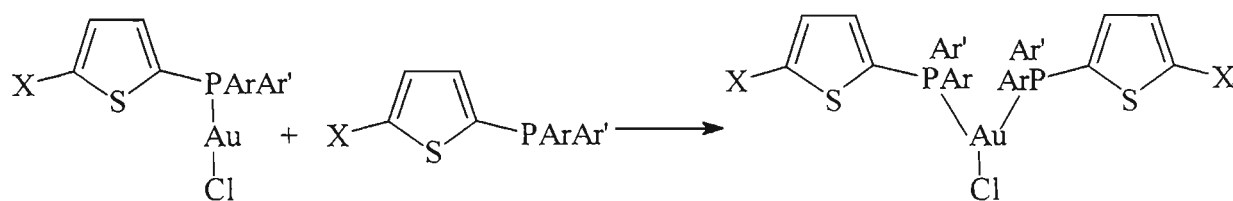
The thiophene and pyridine rings of the PNS ligand possess the *N,S-cisoid* arrangement found in the PNS fragment of the PSNP molecule (see Section II.2.5.4). However the angle between the two planes of 11.30° is higher than the corresponding angle in the PSNP molecule of 3.56°. The distance between the pyridine nitrogen and the thiophene sulfur has remained at around 2.90(1) Å (2.95(1) Å in the PSNP).

III.2.1.2 Neutral mononuclear complexes containing three-coordinate gold

Preparation

Two-coordinate chlorogold(I)-phosphine complexes can serve as convenient precursors for complexes where gold(I) displays a coordination number greater than 2.

Addition of an extra equivalent of the appropriate phosphine ligand to a solution of the chlorogold(I) complex resulted in the formation of the new three-coordinate complexes of general formula $[\text{ClAu}(\eta^1\text{-L})_2]$, where L = PS, PDS, PTS and PSN (Scheme III.6).



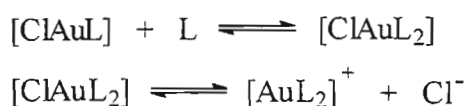
SCHEME III.6

This synthetic approach was chosen over the alternative one *i.e.* where 2 molar equivalents of ligand are added directly to either the Au-tdg intermediate (see Scheme III.4) or the [ClAu(tht)] precursor. The disadvantage of the latter approach is the almost inevitable formation of a mixture of complexes even when the exact stoichiometric amounts of the gold precursor and the ligand are used. This is probably the result of (i) incomplete reduction of Au(III) to Au(I) (in case of the Au-tdg intermediate) or (ii) partial decomposition of [ClAu(tht)], which always takes place to some extent, leading to a change in the actual Au:L ratio. Although this method did prove successful for the preparation of the [ClAu(PSN)₂] complex, the yield of the target compound was only 53%, compared to 82% obtained using the method outlined in Scheme III.6.

The reaction was carried out in dichloromethane for $L = \text{PS}$, while for the other three phosphines ($L = \text{PDS}$, PTS and PSN) acetone was found to be the most suitable solvent; in all four cases hexane was used to precipitate the desired product. In fact, the choice of the solvent system determines the outcome of the reaction. For example, if a dichloromethane/hexane solvent system is used, the material isolated is either the desired product ($L = \text{PS}$), the starting two-coordinate species ($L = \text{PSBr}$, PSN and PNS) or a mixture of the two- and three-coordinate complexes ($L = \text{PDS}$, PTS , PSS and PSSS). Substitution of hexane as the precipitating solvent by benzene or ether did not drastically change the outcome of the syntheses.

Solvents other than dichloromethane and acetone, such as chloroform, ethanol and acetonitrile as well as mixtures thereof were investigated with a view to synthesising three-

coordinate complexes of PSBr, PNS, PSS and PSSS; none was successful in affording a pure product. A plausible explanation for this is based on the known fact (see Chapter I) of the existence of an equilibrium in solution between two-coordinate and three-coordinate complexes of gold(I) of the type shown in Scheme III.7.



SCHEME III.7

The position of these equilibria obviously depends on the solubility of each of the species in the chosen medium, itself a function of the solvent polarity. The first equilibrium tends to shift so as to afford the species which is most easily precipitated, while the second is directly affected by the polarity of the solvent as well as by the strength of the bond between the gold and chlorine in the complex. Thus, the successful preparation of three-coordinate complexes with PNS, PSBr, PSS and PSSS as ligands should be possible once the composition of the solvent(s) which specifically causes precipitation of the three-coordinate species and/or suppresses its dissociation is found. Addition of a semi-saturated aqueous NaCl solution to a solution of the complex was found to assist formation of three-coordinate chlorogold(I) complexes. However, due to the lack of time, the problem of appropriate solvent selection could not be exhaustively investigated.

Table III.5 gives the physical properties of the new three-coordinate chlorogold(I) complexes.

Table III.5 Physical data for the neutral tri-coordinate gold(I) complexes with monodentate thiophene-based ligands

Compound number	Formula	Molar mass, g·mol ⁻¹	Colour	Yield, %
[9]	[ClAu(PS) ₂]	769.05	white	64
[10]	[ClAu(PDS) ₂]	781.10	white	82
[11]	[ClAu(PTS) ₂]	793.14	white	87
[12]	[ClAu(PSN) ₂]	923.12	white	82

The three-coordinate complexes are stable as solids. However in solution the compounds tend to dissociate and with time, precipitation of the starting two-coordinate complex can be observed. Also in solution, the three-coordinate complexes appear to undergo discolouration upon exposure to light to a much higher extent than the corresponding two-coordinate species.

The three-coordinate chlorogold(I)-phosphine complexes are generally more soluble in organic solvents than their two-coordinate precursors. They dissolve in a wide range of solvents such as acetone, acetonitrile, dichloromethane, chloroform, DMSO and alcohols. The complexes also tend to decompose more easily when heated *e.g.*, the melting point of $[\text{ClAu}(\text{PS})_2]$ was determined to be in the region of 180°C , while that for the corresponding two-coordinate complex was greater than 200°C .

Characterisation and ^{31}P NMR solution studies

The ^{31}P and ^1H NMR data for the complexes [9]-[12] are given in Table III.6. To illustrate the effect of coordination of the second phosphine ligand to the chlorogold(I) moiety, the following Table, Table III.7, summarises the differences between the ^{31}P chemical shifts of the three-coordinate complexes and those for the two-coordinate complexes as well as for the ligands alone: $\Delta_{\text{C}} = \delta(3\text{-coord}) - \delta(2\text{-coord})$, $\Delta_{\text{L}} = \delta(3\text{-coord}) - \delta(\text{ligand})$ (CCS).

Table III.6 ¹H and ³¹P NMR spectroscopic data of the complexes [9]-[12], as measured in CDCl₃; the atom numbering scheme for all the ligands was given in the Figure III.2 earlier in this Chapter

Complex	δ ³¹ P, ppm	δ ¹ H, ppm
[9]	11.02 (s)	7.17 (ddd, 1 H, H _{Th-4}), 7.33-7.59 (m, 11 H, 10 H _{Ph} + H _{Th-3}), 7.69 (ddd, 1 H, H _{Th-5})
[10]	-2.98 (s)	7.17 (ddd, 2 H, H _{Th-4}), 7.33-7.60 (m, 7 H, 5 H _{Ph} + 2 H _{Th-3}), 7.70 (ddd, 2 H, H _{Th-5})
[11]	-15.93 (s)	7.16 (ddd, 3 H, H _{Th-4}), 7.54 (ddd, 3 H, H _{Th-3}), 7.70 (ddd, 3 H, H _{Th-5})
[12]	10.56 (s)	7.18 (ddd, 1 H, H _{Py-5}), 7.31-7.72 (m, 14 H, 10 H _{Ph} + H _{Th-3} + H _{Th-4} + H _{Py-3} + H _{Py-4}), 8.52 (m, 1 H, H _{Py-6})

Table III.7 Comparison of the chemical shifts of the tri-coordinate complexes [9]-[12] with those of the corresponding di-coordinate complexes and the ligands; for the definition of Δ_C, Δ_L, see text

Complex	Δ _L ³¹ P, ppm	Δ _C ³¹ P, ppm	Δ _L ¹ H, ppm [*]	Δ _C ¹ H, ppm [*]
[9]	30.92	-8.16	- ^{**} , H _{Th-3}	- ^{**} , H _{Th-3}
[10]	30.28	-8.75	- ^{**} , H _{Th-3}	- ^{**} , H _{Th-3}
[11]	30.34	-9.52	0.18, H _{Th-3}	-0.09, H _{Th-3}
[12]	28.91	-10.07	- ^{**} , H _{Th-4}	- ^{**} , H _{Th-4}

* The chemical shifts of the protons nearest to the P atom were used to determine the ¹H Δ_L value

** The value could not be determined because either the corresponding signal in the ligand or the complex spectrum was not sufficiently resolved

The data presented in Tables III.6 and III.7 show that both the ^{31}P and ^1H chemical shifts due to the ligands in the three-coordinate complexes have moved downfield in relation to the values in the non-coordinated phosphines. However they are situated upfield from the signals of the corresponding two-coordinate complexes. Although little information is available regarding the synthesis and characterisation of three-coordinate chlorogold(I) complexes with monophosphines (only a handful having been isolated and characterised so far), several NMR studies conducted in the early 80's^{11,41-44} established that the order of the ^{31}P NMR chemical shifts should be [bis]>[mono]>[tris]>[ligand]. In this sequence 'mono' stands for the two-coordinate complex $[\text{XAuL}]$ ($\text{X} = \text{Cl}, \text{Br}, \text{L} = \text{phosphine}$), 'bis' - for the three-coordinate $[\text{XAuL}_2]$ *etc.*

Hence the results obtained in this study appear to contradict the previously established trend. As the compositions of the complexes [9]-[12] were unequivocally determined using elemental analysis, the reason for the lack of agreement of our results with those in the literature should be rather associated with the NMR experiments. During the measurement of our NMR spectra, the complex established to be a three-coordinate species by elemental analysis was normally dissolved in deuterated chloroform to give a solution of moderate concentration ($\pm 0.1\text{M}$). The spectra were then recorded at ambient temperature, which was approximately 33°C . Due to the known tendency of the three-coordinate complexes to dissociate in solution, the observed spectrum then must have represented the overall spectrum of all species present in solution averaged by rapid nuclear exchange. On the other hand, the literature experiments, which generally involved either trialkylphosphines or dialkylphenylphosphines, were designed to determine the chemical shift of the species obtained upon titration of a known amount of the gold complex with an exact number of equivalents of the phosphine ligand. In this way, the ratio of ligand to gold was known; also the solution was cooled down to a very low temperature to slow down the exchange, thus allowing for observation of clearly resolved peaks belonging to particular species.

In order to prove that the unexpected ^{31}P NMR results for the new complexes are caused by the behaviour of these compounds in solution several NMR experiments were designed.

Firstly, equal amounts of the $[\text{ClAu}(\text{PS})_2]$ complex [9] were dissolved in the same volume of two deuterated solvents of different polarity, CDCl_3 and acetone- d_6 , and their spectra compared. The ^{31}P NMR chemical shifts recorded for the two solutions (at ambient

temperature) were found to be 10.88 and 12.34 ppm respectively, showing that the different solvents have different stabilising effect on the species in the equilibria given in Scheme III.5. Acetone, being a more polar solvent, is likely to shift the equilibrium towards a three-coordinate complex which can then form ionic species.

Secondly, the ^{31}P NMR spectra of solutions with varying concentrations of complex [9] were recorded in dichloromethane. The chemical shifts at two different concentrations of the complex, $\pm 0.15\text{ M}$ and $\pm 0.03\text{ M}$, were found to be 12.16 and 6.87 ppm respectively. This suggests that a change in the overall concentration of the complex results in different proportions of the various species present in solution. Therefore the weighted average of the signals for each of these species appears at a different position.

Finally, a short variable temperature study was undertaken for the $[\text{ClAuPS}] + n\text{ PS}$ system with the chemical shifts for different values of n and the temperature being recorded. The spectroscopic data for this experiment are presented in Table III.8.

Table III.8 ^{31}P NMR data for $\text{CD}_2\text{Cl}_2\text{-CH}_2\text{Cl}_2$ solutions of $[\text{ClAuPS}]$ with added PS at various temperatures, where n is the number of equivalents of the added phosphine

Temperature, °C	δ , ppm				
	33.5	- 2.5	-69.1	-97.5	-104.2
$n = 0$	20.90, s*	20.42, s	19.97, s	19.81, s	19.72, s
$n = 0.5$	13.21, s	18.55, br**	22.79, br	25.35, br	27.02, s & 19.78, s
$n = 1$	5.14, s	16.71, br	24.58, br	26.71, br	27.06, s
$n = 2$	-0.62, s	11.48, s	25.19, s	25.66, br	25.67, vbr***
$n = 4$	-5.81, s	4.92, s	9.79, br	5.37, vbr	4.55, vbr

* s - a sharp signal

** br - a broad signal

*** vbr - a very broad signal

It can be seen from the results that the spectra of the $\{[\text{ClAuPS}] + n\text{ PS}\}$ solutions usually only become resolved at the temperature below -100°C . Above this temperature the signals coalesce producing broad peaks, which become sharp again upon warming to room temperature. The original two-coordinate complex, $[\text{ClAuPS}]$, is the only complex which

retains its integrity in solution, as evidenced by its signal remaining sharp and staying at nearly the same value throughout the whole range of temperatures employed.

Addition of a half equivalent of the ligand to this complex resulted in a small upfield shift of the signal in relation to that of the starting material at room temperature. However, upon lowering the temperature, the signal became broader and started moving downfield until it eventually was resolved into two signals when the temperature dropped below -100°C . The two peaks appear to have the same intensity and on the basis of the employed stoichiometry, they were assigned to $[\text{ClAuPS}]$ ($\delta = 19.78$ ppm) and $[\text{ClAu}(\text{PS})_2]$ ($\delta = 27.06$ ppm).

Addition of exactly one equivalent of the phosphine also initially resulted in a sharp signal with a chemical shift upfield from that of the starting material. Reducing the temperature, though, caused a gradual downfield move until only a single sharp peak was observed at -104°C , indicating the formation of the single stable species, $[\text{ClAu}(\text{PS})_2]$. It is interesting to note that at intermediate temperatures the peak appeared to be broad, which is a possible indication that other species (*e.g.* products of dissociation of the complex) may be present in the solution at higher temperatures.

Increasing the number of equivalents of the added phosphine further did not lead to isolation of any other single species: only broad peaks were observed. Surprisingly, even an obvious excess of ligand ($n = 4$) and a very low temperature are unable to prevent rapid exchange of a ligand between the inner and outer coordination spheres of the complex (note that a further decrease in temperature was not feasible as the solvent began crystallising). Therefore a tentative conclusion can be made that PS is capable of forming at least three complexes including the chlorogold(I) precursor, *i.e.* $[\text{ClAuPS}]$, $[\text{ClAu}(\text{PS})_2]$ and either $[\text{Au}(\text{PS})_3]\text{Cl}$ (or $[\text{ClAu}\{\text{PS}\}_3]$) or $[\text{Au}(\text{PS})_4]\text{Cl}$. The existence of the first two complexes is confirmed by the clearly resolved signals in the ^{31}P NMR spectra at low temperature. The existence of a further complex is assumed on the basis of ligand exchange taking place in the solution at low temperatures resulting in a broad peak, rather than just two sharp peaks due to the $[\text{ClAu}(\text{PS})_2]$ and free ligand present in excess.

The chemical shift of the three-coordinate complex at -104.2°C , 27.06 ppm, is indeed greater than that of the two-coordinate complex, 19.72 ppm, - in full agreement with the

literature findings (*vide supra*). Unfortunately, the uncertainty about the existence of the complex with three or four PS ligands does not allow comment on whether its chemical shift fits in with the established chemical shift sequence *i.e.*, [bis] > [mono] > [tris] > [ligand].

The corrected Δ_C and Δ_L values for the three-coordinate complex $[\text{ClAu}(\text{PS})_2]$ therefore are 7.34 and 46.96 ppm respectively. In general, the coordination chemical shift (Δ_L) values for the 'bis'-complexes are known to vary and are strongly dependent on the nature of the phosphine, in particular on its electronic and steric properties *e.g.*, for $[\text{BrAu}(\text{PPhMe}_2)_2]$ Δ_L is 62.2 ppm⁴⁴ while for $[\text{BrAu}(\text{n-BuPPh}_2)_2]$ Δ_L is 53.4 ppm.⁴³

The conclusion which can be drawn from the above NMR study is that the three-coordinate chlorogold(I)-phosphine complexes dissociate in solution to an extent which is determined by the polarity of the solvent used and which increases with dilution of the sample. The process can be monitored by measuring NMR spectra at low temperatures, specifically below -100°C. There is a possibility, however, that other gold(I) complexes with more than two PS ligands per gold atom can be formed if an excess of the phosphine is employed. It follows from the above conclusion that the characterisation of the three-coordinate complexes of the $[\text{ClAuL}_2]$ type by means of NMR spectroscopy at ambient temperature is not very meaningful as the signal collected will simply be the weighted average of more than one possible species in solution.

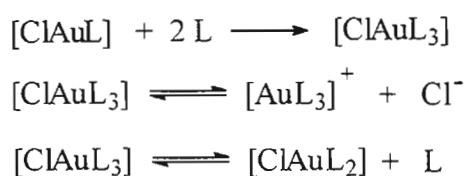
The IR spectra of the four three-coordinate complexes [9]-[12] in the solid state (KBr pellets) do not produce any additional information. This is because with the instrumentation available it was not possible to measure the Au-P and Au-Cl stretching frequencies as these occur at very low wavenumbers (300-400 cm^{-1}). Hence the observed spectra are again essentially identical to those of the ligands themselves.

III.2.1.3 Neutral mononuclear complexes containing four-coordinate gold

Several attempts were made to prepare complexes of the $[\text{ClAuL}_3]$ type using methodology analogous to that used for the synthesis of tri-coordinate complexes. The phosphines PS, PDS, PTS and PSN were added to an acetone solution of the relevant $[\text{ClAuL}]$ complex in a 2:1 ratio. The products that precipitated out after evaporation of most of the solvent were analysed for %C, %H and %N where appropriate. None of them appeared to have a

composition corresponding to that of a four-coordinate complex. Recrystallisation from acetone afforded single crystals only from the solution obtained in the reaction with PDS as the ligand. However X-ray diffraction study on one of the crystals showed it to be a three-coordinate complex, $[\text{ClAu}(\text{PDS})_2]$. The crystal structure of the complex will be discussed later in this Section. The elemental analysis and the ^{31}P chemical shift recorded in CDCl_3 for this compound match closely to those obtained for complex [10], described in the previous Section.

Formation of a three-coordinate complex in this case is not surprising taking into account the general lability of the ligands in complexes of gold(I) where the metal has a coordination number greater than two. If a complex of the $[\text{ClAuL}_3]$ type is formed in solution it is very likely to be in equilibrium with other species as shown in the Scheme III.8 below.



SCHEME III.8

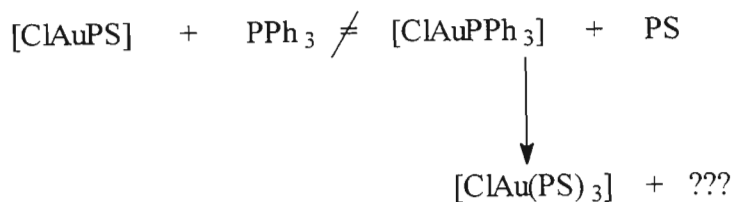
As was demonstrated during the low temperature ^{31}P NMR studies described in the previous Section, on occasion even an excess of the ligand and reduced temperatures cannot shift the equilibria towards the exclusive formation of the four-coordinate species.

A further attempt was made to prepare a four-coordinate gold(I) complex by using a different gold precursor: indeed, works by Baker *et al.*⁸ and Fackler *et al.*¹⁰⁶ have shown that the eventual product formed when coordination numbers higher than 2 for gold are achieved is strongly influenced by the choice of the starting material.

The complexes $[\text{ClAu}(\text{tht})]$, $[\text{ClAuPPh}_3]$ and $[\text{ClAuPEt}_3]$ were employed as alternative precursors by reacting them in dichloromethane solution with a stoichiometric amount of the PS ligand *i.e.*, in the ratio of 1:3. After evaporation of the solvent and addition of hexane or by partially removing the solvent and cooling to low temperatures, solids separated and were subsequently analysed. None of the products appeared to correspond to the desired species.

Fortuitously, however, a 1:1 mixture of PS and the $[\text{ClAuPPh}_3]$ complex prepared in a high concentration ($\pm 1 \text{ M}$) in CD_2Cl_2 for a NMR analysis, afforded single crystals upon standing. The results of an elemental analysis as well as a subsequent X-ray diffraction study showed that the crystals corresponded to the four-coordinate complex $[\text{ClAu}(\text{PS})_3] \cdot 2\text{CH}_2\text{Cl}_2$ (or $[\text{ClAu}(\text{PS})_3] \cdot 2\text{CD}_2\text{Cl}_2$ - complex [13]). This structure will be discussed in detail later in this Section. Attempts to analyse the composition of the solution left in the NMR tube after precipitation of the crystals failed: there were several peaks in the ^{31}P NMR spectrum of the mixture which could not be assigned to any of the known species. The chemical shift of the CD_2Cl_2 solution of the pure crystals was recorded to be 13.71 ppm, which is most likely again an overall averaged signal from several species.

It is interesting to note that an attempt to reproduce exactly the same conditions but using $[\text{ClAuPEt}_3]$ as a precursor did not yield any precipitate. The shifts in the ^{31}P NMR spectrum of the mixture were as expected different from those with $[\text{ClAuPPh}_3]$, but still unidentifiable, which made it difficult to establish the reason for the reaction failure. The reaction between $[\text{ClAuPS}]$ and PPh_3 was also monitored using ^{31}P NMR spectroscopy in order to see if an equilibrium is established between triphenylphosphine- and PS-containing species. Upon mixing the compounds (1:1 molar ratio) at room temperature in CD_2Cl_2 two peaks are observed at 35.10 and 11.79 ppm with small shoulders at 34.42 and 10.44 ppm. This spectrum was different from the one where $[\text{ClAuPPh}_3]$ and PS were mixed which consisted of only two peaks at 34.28 and 11.22 ppm. The latter spectrum remained unchanged after 15 hours, while the former changed with time with two sharp peaks appearing at 34.86 and 11.27 ppm. However the two spectra still did not appear the same as the relative intensities of the two peaks are opposite. Cooling both solution to below -100°C did not clarify the situation: the first solution gave rise to 2 major sharp peaks at 42.71 and 41.16 ppm and five broad peaks between 39 and 20 ppm, while the second exhibited two sharp peaks at 30.22 and 22.92 ppm, with 2 small broad peaks at around 39 ppm, and two large broad peaks between 26 and 22 ppm. Overall the spectra appeared to be different allowing one to conclude that a different combination of species is produced in the two different reactions between a gold(I) complex and a ligand (Scheme III.9).



SCHEME III.9

Although it was not possible to propose a reaction pathway for the formation of the four-coordinate compound, it is clear that the PS ligand can displace triphenylphosphine from its two-coordinate chlorogold(I) complex, while formation of a higher-coordination compound is promoted by employing high concentrations of the reagents.

Crystal structures of [ClAu(PDS)₂] ([10]) and [ClAu(PS)₃]·2CH₂Cl₂ ([13])

Crystallisation of [ClAu(PDS)₂] ([10]) from acetone afforded colourless prisms which were employed for X-ray diffraction studies. Figure III.5 represents the molecular structure of [10] and the crystallographic data are discussed with respect to the numbering scheme shown. The bond lengths and angles, crystallographic parameters as well as the other structural information are given in Tables III.36-41 at the end of the Experimental section.

There appears to be no intermolecular metal-metal bonding or significant non-bonded interactions in the crystal structure of the complex. The asymmetric unit of the complex [10] contains one half of the molecule with the Au and Cl atoms being on the 2-fold rotation axis. Consequently the gold atom lies in the plane formed by the two phosphorus atoms and the chlorine with the angles Cl(1)-Au(1)-P(1) and P(1)-Au-P(1)* being 107.35(4) and 145.31(8)° respectively. The Au-Cl and Au-P distances are 2.569(3) and 2.307(2) Å. The same parameters for the analogous complex with PPh₃ as a ligand are 118.7(1) and 132.1(1)°, 2.500(4) and 2.330(9) [or 2.320(3)] Å.²⁴² The PDS ligand shows an obvious increase in bonding between Au and P as the bond length in our complex is shorter. This is accompanied by the decrease in the Au-Cl bond strength, as the relevant bond in the PDS complex appears longer by nearly 0.07 Å. The angles between the two phosphine substituents in both complexes are significantly different (13.2°) indicating that the ligands have electronic and steric properties noticeably different from each other. It has been established¹⁶⁴ that 2-thienylphosphine based ligands have a greater *s*-character of the phosphorus lone pair than PPh₃ as a result of the electron-withdrawing nature of thiophene,

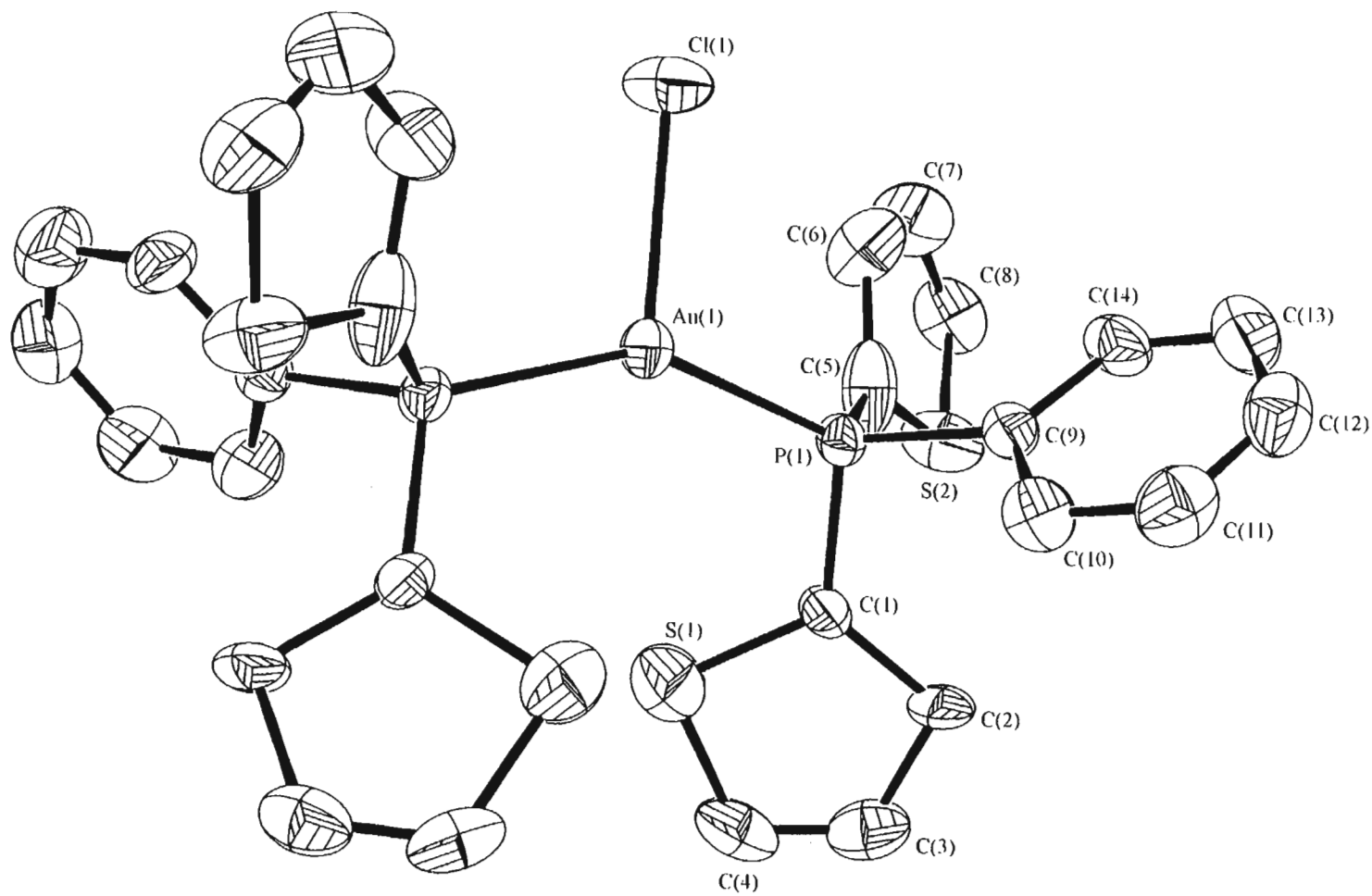


Fig. III.5 Structure of [ClAu(PDS)₂] ([10]), showing the atom numbering scheme

thus forming complexes where the length of the M-P bond is shorter than the corresponding value in triphenylphosphine complexes [M = Pt(II)].¹⁶⁴

The steric effects of a ligand are normally estimated by calculating its Tolman cone angle. The cone angle for the triphenylphosphine is known to be $\pm 152^\circ$.²⁴³ However cone angles for thienylphosphine ligands have not been reported. As no sophisticated computer software was available for the exact determination of cone angles during this work, the values were estimated using certain assumptions and basic trigonometric formulae. Appendix B gives the results of calculations, based on the X-ray structural data obtained for PSSP, PSNP and PSNSP, for idealised conformations of a phosphine ligand with phenyl, 2-thienyl and 2-pyridyl substituents. The values obtained via this method are obviously not exactly equal to Tolman's cone angles (the 'cone angle' for PPh₃ was found to be $\pm 165^\circ$) but, nevertheless, can serve as indicators of the steric demands of a substituent. From the calculations in Tables B.1-B.3 it is easy to see that the 'half-angle' contribution of phenyl and 2-thienyl are approximately the same provided the thiophene S is facing the direction opposite to that of the phosphorus lone pair. However if the thienyl substituent is rotated 180° around the P-C bond, its contribution becomes noticeably greater. In the complex under question, [ClAu(PDS)₂], the conformation of the ligands is such that one thiophene S is turned towards the M-P bond [the Au(1)-P(1)-C(1)-S(1) torsion angle is 24.40°] and the other is turned away [the Au(1)-P(1)-C(5)-S(2) torsion angle is 166.0°]. Therefore it is likely that in such a conformation the PDS ligand has a cone angle larger than that of PPh₃ and is, therefore, more sterically demanding. Thus both the steric and electronic effects exhibited by the PDS ligand appear to be responsible for the marked difference in bond angles and lengths around the gold(I) in this three-coordinate complex compared to the analogous structure with PPh₃ as the phosphine ligand.

The angles at the phosphorus atom vary considerably between $98.3(2)^\circ$ [C(5)-P(1)-C(1)] and $118.8(8)^\circ$ [Au(1)-P(1)-C(5)] indicating a distortion from the expected tetrahedral geometry. The P(1)-C(5) bond is also noticeably short at $1.674(2)$ Å. The angles between the planes of the substituents on phosphorus are 66.59° (between the two thiophene rings), 64.58° (between the first thiophene and the phenyl) and 91.83° (between the second thiophene and phenyl). Although it is positioned relatively close to the gold atom in space [Au(1)...S(1) is $3.43(1)$ Å], the sulfur on the first thiophene ring is considerably disordered

as judged by its high anisotropic temperature factors. The PDS ligand displays a disorder, similar to that observed during the determination of the crystal structure of [ClAuPSS]: the S(2)..C(8) thiophene ring exhibits significant deviations in bond length and angle values from average values previously measured for this heterocycle. For instance the C(5)-S(2)-C(8) angle is $101.77(1)^\circ$ and the C(5)-C(6) bond is $1.533(2) \text{ \AA}$, although they are typically $92.0(3)^\circ$ and $1.370(4) \text{ \AA}$ in a thiophene unit.²⁴⁴

The crystals of [ClAu(PS)₃] \cdot 2CH₂Cl₂ ([13]) were separated from a saturated dichloromethane solution (*vide supra*) as off-white rectangular blocks. They were found to be of suitable quality and used for X-ray diffraction studies. Figure III.6 represents the molecular structure of [13] and the crystallographic data are discussed with respect to the numbering scheme shown. The bond lengths and angles, crystallographic parameters as well as the other structural information are given in Tables III.42-47, at the end of the Experimental section. Note that there is considerable disorder associated with the thiophene rings in the [ClAu(PS)₃] complex, the treatment of which being given in the Experimental section. Thus, although the basic structure is correct, the standard errors in the bonding parameters as obtained from the least-squares analysis, are certainly underestimates. The disorder associated with thiophene rings in complexes containing thienylphosphine ligand is not unexpected: it has been reported by Gol'dfarb *et al.*^{160,163} and it has also been observed during this work in the case of the [ClAuPSS] complex (see Section 2.1.1 of this Chapter).

Similar to the other three chlorogold(I) complexes described so far, there appears to be no metal-metal interactions between the gold atoms from separate [ClAu(PS)₃] units in the crystal; nor is there any association between the gold complexes and the solvent molecules of crystallisation. The individual molecules do not possess any crystallographically imposed symmetry elements.

The geometry around gold is intermediate between that expected for ideal three- and four-coordination: the relevant angles around the metal range from $115.1(3)$ to $121.5(3)^\circ$ (between the phosphines) and from $92.2(3)$ to $104.1(3)^\circ$ (between the chlorine and the phosphorus atoms). The Au-P distances vary from $2.363(8)$ to $2.405(10) \text{ \AA}$ while the Au(1)-Cl(1) bond is very long at $2.776(9) \text{ \AA}$. The distance between the gold atom and the mean P₃ plane is 0.33 \AA . Overall, the structure is very similar to that of a related complex

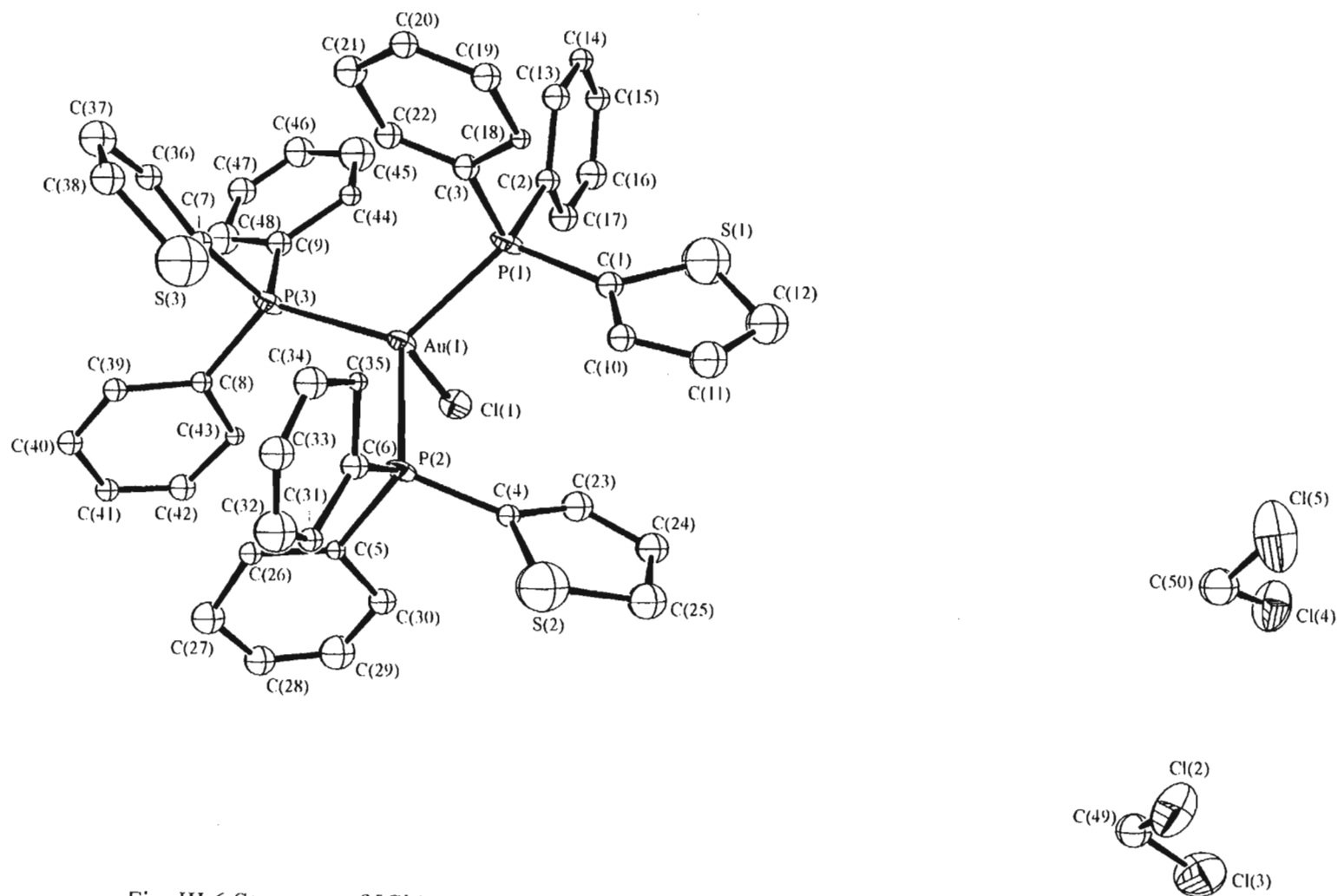


Fig. III.6 Structure of [ClAu(PS)₃]·2CH₂Cl₂ ([13]), showing the atom numbering scheme

with triphenylphosphine ligand, $[\text{ClAu}(\text{PPh}_3)_3]$.⁴⁵ In the latter complex the angles around gold between the phosphorus atoms range from $116.1(1)$ to $119.6(1)^\circ$, while those between the chlorine and the phosphorus atoms range from $92.0(1)$ to $107.7(1)^\circ$. The Au-P distances are on average longer at 2.41 \AA and the Au-Cl bond is shorter at $2.710(2) \text{ \AA}$. Shortening of the Au-P bonds in the PS complex in comparison to the PPh_3 complex is associated with the greater *s*-character of the lone pair on phosphorus in the former (*vide supra*). Strengthening of the Au-P bonds in turn results in some weakening of the Au-Cl bond; hence its length increases. However the angles between the phosphine substituents in the two complexes do not seem to differ significantly. This is not surprising taking into account that, being part of a distorted triangular geometry, the three ligands in each of the complexes are already nearly maximally separated.

The three PS ligands adopt different conformations around the gold atom: the first phosphine ligand is positioned in such a way that the torsion angle $\text{Au}(1)\text{-P}(1)\text{-C}(1)\text{-S}(1)$ is $130(2)^\circ$; for the second ligand the corresponding angle is $153(2)^\circ$, while for the third ligand it is $42(2)^\circ$. Thus, only one of the ligands adopts a conformation in which the sulfur is turned towards the Au-P bond [the $\text{Au}(1)\text{...S}(3)$ distance is 4.07 \AA]. The mutual arrangement of the aromatic rings on the three ligands does not appear to result in any intramolecular π -interactions as might appear from a glance at Figure III.6. Although the $\text{S}(1)\text{...C}(12)$ and $\text{S}(2)\text{...C}(25)$ rings look as if they are antiparallel, the actual angle between the planes is 163.62° . (The angles between the above thiophene rings and the third one are 129.93 and 33.72° , respectively.) On the other hand, the planes of the two phenyl rings, $\text{C}(5)\text{...C}(30)$ and $\text{C}(8)\text{...C}(43)$, are nearly coplanar, the dihedral angle between them being only 9.33° . However, there is no possibility of a π -interaction between the rings as the distance between their planes is too large (about 4 \AA).

It is instructive at this stage to compare the Au-P and Au-Cl distances in the two-, three- and four-coordinate gold complexes the structures of which have been determined in this work. Table III.9 presents the Au-Cl and Au-P distances as well as the P-Au-Cl and P-Au-P angles for $[\text{ClAuPSS}]$, $[\text{ClAu}(\text{PDS})_2]$ and $[\text{ClAu}(\text{PS})_3]\cdot 2\text{CH}_2\text{Cl}_2$.

Table III.9 Bonding parameters at the gold atom in the chlorogold(I) complexes

Complex	Au-P, Å	Au-Cl, Å	P-Au-P, °	P-Au-Cl, °
[ClAuPSS]: molecule 1	2.217(7)	2.256(8)	-	176.3(3)
molecule 2	2.232(6)	2.282(6)	-	178.6(2)
[ClAuPNS]	2.227(1)	2.278(1)	-	177.02(4)
[ClAu(PPh ₃)] ²¹	2.235(3)	2.279(3)	-	179.63(8)
[ClAu(PDS) ₂]	2.307(2)	2.569(3)	145.31(8)	107.35(4)
[ClAu(PPh ₃) ₂] ²⁴²	2.330(9)	2.500(4)	132.1(1)	118.7(1)
	2.320(3)			
[ClAu(PS) ₃]·2CH ₂ Cl ₂	2.405(10)	2.776(9)	121.5(3)	104.1(3)
	2.380(8)		118.9(3)	94.5(3)
	2.363(8)		115.1(3)	92.2(3)
[ClAu(PPh ₃) ₃] ⁴⁵	2.431(2)	2.710(2)	119.6(1)	107.7(1)
	2.404(2)		116.6(1)	98.3(1)
	2.395(2)		116.1(1)	92.0(1)

The data in this Table confirm the established trend of increasing Au-P and Au-Cl distances with an increase in the coordination number of the gold atom. At the same time the P-Au-Cl angles and, where appropriate the P-Au-P angles, become smaller. The Au-P distances in 2-thienylphosphine complexes appear shorter than those of the PPh₃ analogues, while the Au-Cl bonds are longer. The P-Au-Cl angles tend to be larger in triphenylphosphine complexes.

III.2.1.4 Cationic complexes containing two-coordinate gold

Preparation

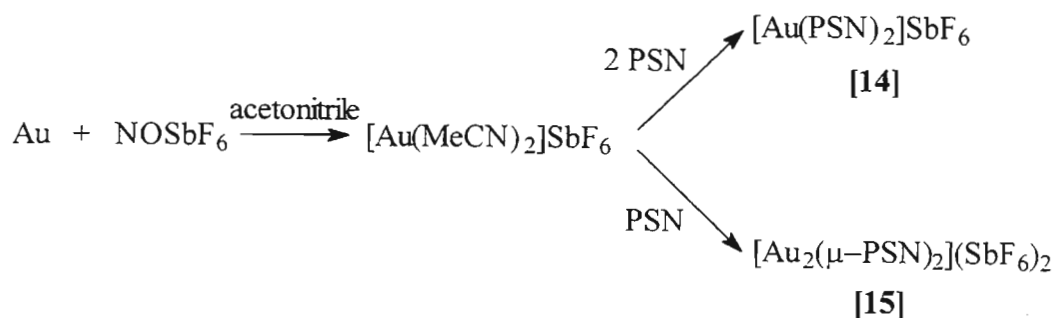
There are two general approaches to the synthesis of cationic gold(I) complexes. The first involves addition of the required number of molar equivalents of the ligand to a neutral gold(I) precursor, *e.g.* [ClAuPEt₃], followed by the displacement of the chloride ligand and formation of a salt with a non-coordinating counterion, *e.g.* hexafluorophosphate.²⁴⁵ The second approach makes use of a cationic gold(I) precursor, for instance [Au(tht)₂]PF₆,²⁴⁶ to which the required amount of the ligand is added.

The second approach was chosen as we were aiming at exploring the coordination chemistry of thienylphosphine ligands with *N*-donor atoms in their structure *e.g.*, PSN and PNS. It was shown earlier that the nitrogen of pyridine ring on these ligands does not coordinate to gold(I) if a chloro-precursor is used.

A convenient gold(I) precursor with labile ligands is the complex $[\text{Au}(\text{MeCN})_2]\text{SbF}_6$. The preparation of this precursor is given in the Experimental section and is a modification of the original procedure suggested by Bergerhoff.²⁴⁷ The complex is prepared *in situ* by oxidising metallic gold with NOSbF_6 in acetonitrile. The gold is normally taken in excess and the calculation of the amount of the complex formed is based on the amount of NOSbF_6 used. The precursor is quite stable in acetonitrile solution under nitrogen but cannot be isolated in solid form without decomposition.

Reaction of two molar equivalents of PSN dissolved in dichloromethane with one mole of $[\text{Au}(\text{MeCN})_2]\text{SbF}_6$ afforded the mononuclear di-coordinate complex [14] shown in Scheme III.10. Changing the stoichiometry of the reaction to a 1:1 ratio afforded the dinuclear two-coordinate complex [15].

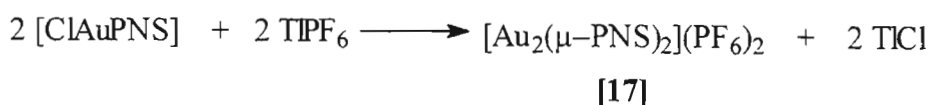
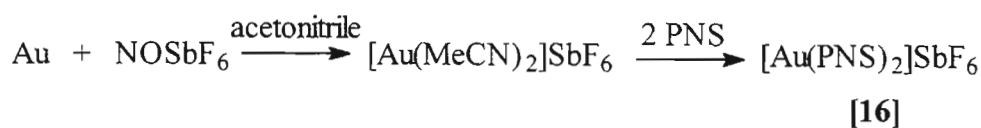
The same approach was used for the PNS ligand, affording the mononuclear two-coordinate complex $[\text{Au}(\text{PNS})_2]\text{SbF}_6$ [16]. Although a dinuclear complex with PNS analogous to [15] could have been prepared following the same pathway, it was decided to try a different approach.



SCHEME III.10

This approach is based on the work by Schmidbaur *et al.*,⁵⁷ who synthesised the related dinuclear complexes $[\text{Au}_2(\mu\text{-PN})_2]\text{X}_2$ (PN = 2-diphenylphosphinopyridine, X = BF_4 and

PF₆) via the reaction between [ClAuPN] and AgX. Our approach was to react the [ClAuPNS] complex with the thallium(I) salt, TlPF₆. The reaction was carried out in a mixture of THF and acetonitrile. Using a 1:1 complex to thallium ratio, the target dinuclear compound, [Au₂(μ-PNS)₂](PF₆)₂ ([17]) was formed in only 25% yield. Doubling the amount of TlPF₆ led to a considerable increase in the yield. The procedure was found to be more convenient in comparison to the one involving [Au(MeCN)₂]SbF₆ as a precursor, for the following reasons. First, there is always an exact stoichiometric 1:1 ratio between gold and PNS due to the composition of the starting material. Second, the reaction takes considerably less time as both [ClAuPNS] and [Au₂(μ-PNS)₂](PF₆)₂ can be prepared within 8 hours, while the preparation of the [Au(MeCN)₂]SbF₆ precursor alone takes 12 hours. Lastly, any contamination of complex [17] with the starting material can be easily eliminated by simple washing of the product with chloroform in which the former is insoluble. This is not possible when both the starting material and the product are ionic, as is the case when [Au(MeCN)₂]SbF₆ is used as the starting complex. The reactions used to obtain the complexes [16] and [17] are summarised in Scheme III.11. The composition of the complexes is confirmed by elemental analysis.



SCHEME III.11

With regard to the mechanism of formation of the dinuclear species [17] this probably involves abstraction of the chloride from the neutral complex [8] with Tl⁺ and possible formation of a solvated intermediate. The nitrogen atom of the pyridine ring (unattached in complex [8]) being a stronger donor than a molecule of solvent (THF or acetonitrile) now displaces the solvent from a neighbouring gold(I) atom forming a bridge between two metal centres. The nitrogen of the PNS ligand on the second gold(I) in turn displaces the solvent molecule on the first gold(I) thus resulting in formation of a macrocycle. The physical data for the complexes [14]-[17] are given in Table III.10.

Table III.10 Physical data for the di-coordinate gold(I) complexes with monodentate thiophene-based ligands PSN and PNS

Compound number	Formula	Molar mass, g·mol ⁻¹	Colour	Yield, %
[14]	[Au(PSN) ₂]SbF ₆	1123.60	white	63
[15]	[Au ₂ (μ-PSN) ₂](SbF ₆) ₂	1556.21	white	89
[16]	[Au(PNS) ₂]SbF ₆	1123.60	white	74
[17]	[Au ₂ (μ-PNS) ₂](PF ₆) ₂	1374.65	white	70

The complexes [14]-[17] are crystalline air-stable materials readily soluble in polar solvents such as acetonitrile and acetone as well as in dichloromethane. They are not soluble in ether, chloroform, hexane or benzene. The dinuclear complex with PNS as a ligand, [17], is somewhat light-sensitive - it slowly becomes discoloured when left exposed to ambient light for prolonged periods of time.

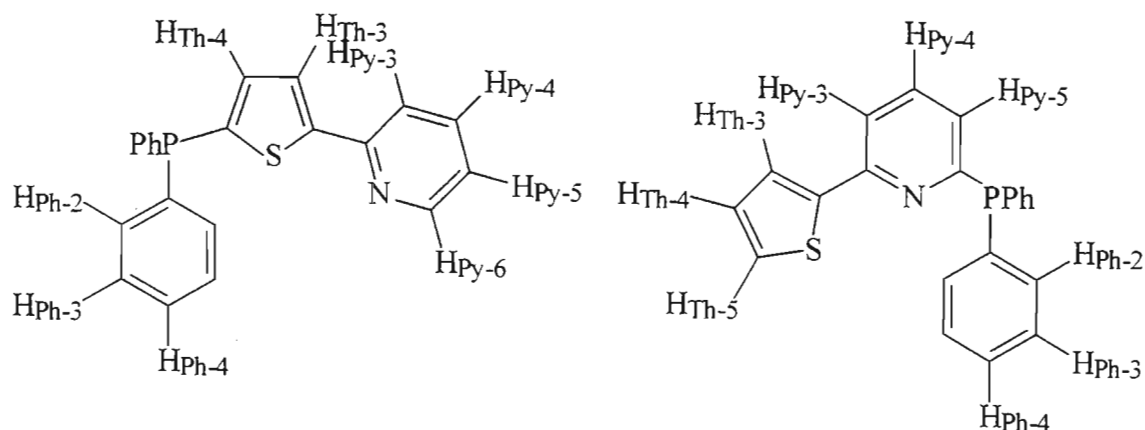
Characterisation

The ¹H and ³¹P NMR spectroscopic data for the complexes [14]-[17] are given in Table III.11. The spectra were measured in CD₃CN for the PSN complexes and in acetone-*d*₆ for the PNS complexes.

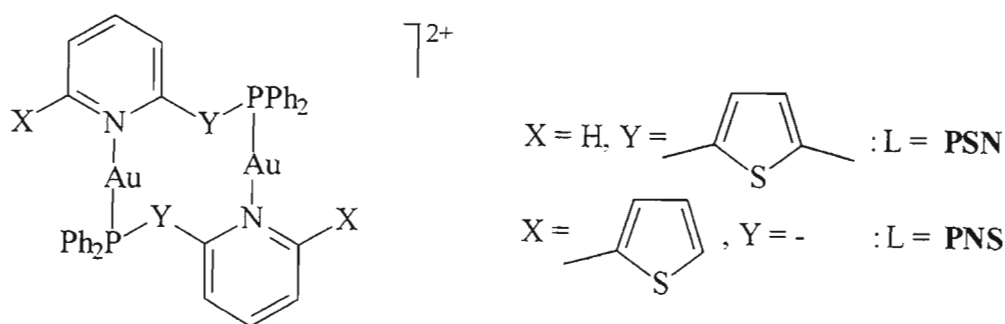
Each of the four complexes produces a single peak in the ³¹P NMR spectra. Noteworthy is that the ³¹P NMR chemical shifts for the mononuclear complexes are consistently downfield from those in their dinuclear counterparts. For comparison purposes it can be noted that the [Au(PS)₂]⁺ species exhibits a ³¹P chemical shift of *ca.* 32 ppm. In the mononuclear complexes, [14] and [16], the coordination to gold(I) is undoubtedly achieved via two phosphorus atoms affording a [P-Au-P]⁺ unit. In the dinuclear complexes the gold is most likely bonded to one phosphorus and one nitrogen forming a [P-Au-N]⁺ unit *i.e.*, the ligands bridge the two gold atoms in a 'head-to-tail' fashion. This assumption is supported by relative values of the ³¹P chemical shifts in the two units: due to the σ-donating property of a pyridine nitrogen, its coordination to gold brings about an increase in the back-donation to phosphorus, causing an upfield displacement of the phosphorus shift in the dinuclear complexes.

Table III.11 ^1H and ^{31}P NMR spectroscopic data of the complexes [14]-[17], the atom numbering scheme for all the ligands is given in the Figure III.7

Complex	$\delta^{31}\text{P}$, ppm	$\delta^1\text{H}$, ppm
[14]*	33.51 (s)	7.19 (dd, 1 H, $\text{H}_{\text{Th-4}}$), 7.29 (ddd, 1 H, $\text{H}_{\text{Py-5}}$), 7.33-7.86 (m, 13 H, 10 H_{Ph} + $\text{H}_{\text{Th-3}}$ + $\text{H}_{\text{Py-3}}$ + $\text{H}_{\text{Py-4}}$), 8.46 (m, 1 H, $\text{H}_{\text{Py-6}}$)
[15]*	19.13 (s)	7.49 (dd, 1 H, $\text{H}_{\text{Th-4}}$), 7.59-7.84 (m, 10 H), 7.95 (ddd, 1 H, $\text{H}_{\text{Py-5}}$), 8.02 (dd, 1 H, $\text{H}_{\text{Th-3}}$), 8.20-8.48 (m, 2 H, $\text{H}_{\text{Py-3}}$ + $\text{H}_{\text{Py-4}}$), 8.91 (m, 1 H, $\text{H}_{\text{Py-6}}$)
[16]**	45.82 (s)	7.01 (m, 1 H, $\text{H}_{\text{Py-3}}$), 7.09 (dd, 1 H, $\text{H}_{\text{Th-4}}$), 7.20-7.65 (m, 14 H, 10 H_{Ph} + $\text{H}_{\text{Th-3}}$ + $\text{H}_{\text{Th-5}}$ + $\text{H}_{\text{Py-3}}$ + $\text{H}_{\text{Py-4}}$)
[17]**	36.46 (s)	7.18 (dd, 1 H, $\text{H}_{\text{Th-4}}$), 7.51-8.28 (m, 15 H, 10 H_{Ph} + $\text{H}_{\text{Th-3}}$ + $\text{H}_{\text{Th-5}}$ + $\text{H}_{\text{Py-3}}$ + $\text{H}_{\text{Py-4}}$ + $\text{H}_{\text{Py-6}}$)

* The spectra are measured in CD_3CN ** The spectra are measured in acetone- d_6 **Fig. III.7** Numbering scheme for the hydrogen atoms in the PSN and PNS ligands

A schematic diagram of the dinuclear complexes with the ligands bridging in the μ - P,N -fashion is shown in Scheme III.12.

**SCHEME III.12**

The ^1H NMR spectra of the dinuclear complexes also support the proposed mode coordination of the bridging ligand *i.e.*, the participation of the pyridine ring in bonding with gold(I). This is especially pronounced in the case of PSN which has a hydrogen in the position-6 of the pyridine ring. In the non-coordinated ligand this hydrogen has a chemical shift of 8.5 ppm, while in $[\text{Au}_2(\text{PSN})_2](\text{SbF}_6)_2$ the signal due to this hydrogen moves to 8.91 ppm - the difference of 0.41 ppm! This is not a mere solvent effect since in $[\text{Au}(\text{PSN})_2]\text{SbF}_6$, where no N-coordination is expected, the chemical shift of that hydrogen is still close to the 8.5 ppm value.

In the PNS ligand-bridged complex there is unfortunately no such clear-cut indication for pyridine N-coordination. There is no hydrogen in the position-6 in the PNS molecule and the effect of the nitrogen coordination on other protons of the pyridine ring is either not as strong or could not be determined, being obscured by overlap with other aromatic hydrogens. Nevertheless the overall view of the ^1H NMR spectrum of $[\text{Au}_2(\mu\text{-PNS})_2](\text{PF}_6)_2$ shows a downfield shift from the spectrum of the corresponding mononuclear complex indicating a depletion of electron density on the atoms through donation to the metal.

The IR spectra recorded as KBr pellets of the cationic complexes [14]-[16] exhibit a strong absorption band at 657 cm^{-1} , characteristic of the Sb-F stretching vibration of the SbF_6^- counterion; and at 839 cm^{-1} for complex [17], characteristic of the PF_6^- ion. There are some small variations between the spectra of the pure ligands and those of their corresponding dinuclear complexes in the $1500\text{-}1620\text{ cm}^{-1}$ region, where C-N stretches are normally found. However as the intensities of these bands vary from moderate to weak, they provide little useful information.

The UV-vis spectra of the mononuclear complexes [14] and [16] resemble the corresponding spectra of the ligands themselves irrespective of the solvent used (dichloromethane or acetonitrile). However, in the dinuclear complexes, only the spectra obtained in acetonitrile were similar to those of the ligands. Employing dichloromethane as a solvent resulted in considerable drop in intensity of the lowest energy absorption bands ($\pi \rightarrow \pi^*$ transition) for complexes [15] and [17].

Numerous attempts were made to obtain single crystals of these cationic complexes in order to unequivocally establish their structures. Unfortunately in 3 out of 4 instances the crystals quickly lost solvent and thus could not be used. However, single crystals could be obtained of the fourth complex, $[\text{Au}_2(\mu\text{-PSN})_2](\text{SbF}_6)_2$, and thus its crystal structure was determined.

Crystal structure of $[\text{Au}_2(\mu\text{-PSN})_2](\text{SbF}_6)_2$

The colourless crystals of $[\text{Au}_2(\mu\text{-PSN})_2](\text{SbF}_6)_2$ were obtained by vapour diffusion of ether into a dichloromethane solution of the complex. Figure III.8 represents the structure of the cation $[\text{Au}_2(\mu\text{-PSN})_2]^{2+}$. The crystallographic data are discussed with respect to the numbering scheme shown. The bond lengths and angles, crystallographic parameters as well as other structural information are given in Tables III.48-53, at the end of the Experimental section.

The crystal structure of the complex confirms the proposed configuration of the cation *i.e.*, 'head-to-tail' bridging arrangement of the ligands. The $[\text{Au}_2(\mu\text{-PSN})_2]^{2+}$ cations pack in the crystal in such a way that there is no evidence for either intra- or intermolecular Au...Au contacts. The Au(1)...Au(2) distance is 5.7021(4) Å, which is much greater than the sum of the Van der Waals radii of two gold atoms. There is also no interaction between any of the gold and sulfur atoms as the shortest Au...S distance in this cation is 3.0326(21) Å [Au(1)...S(2)]. The coordination around both gold ions is approximately linear with the P(1)-Au(1)-N(2) and P(2)-Au(2)-N(1) angles being 178.1(2) and 176.9(2) Å respectively. The Au-N distances fall in the range 2.078(7) to 2.087(8) Å, while the Au-P distances fall in the range 2.228(2) to 2.239(2) Å, all values being typical for these types of complexes.⁵⁷ The P-Au-N axes on each gold atom are staggered with respect to each other, the appropriate torsion angle around the Au...Au axis being around 68°.

The arrangement of the substituents around the phosphorus atoms is tetrahedral in both ligands. The angles vary from 103.7(4) to 107.5(4)° between the P-C bonds in the first PSN ligand, *i.e.* the one containing P(1), S(1) and N(1) heteroatoms; while in the second PSN ligand, the corresponding angles vary from 106.5(4) to 107.4(4)°. For comparison, the corresponding angles in the PSNSP molecule range from 100.9(1) to 104.8(1)° (see Section II.2.5.2), thus being on average smaller than those in the coordinated PSN ligand. (Unfortunately, a crystal structure of the PSN ligand could not be obtained so a direct

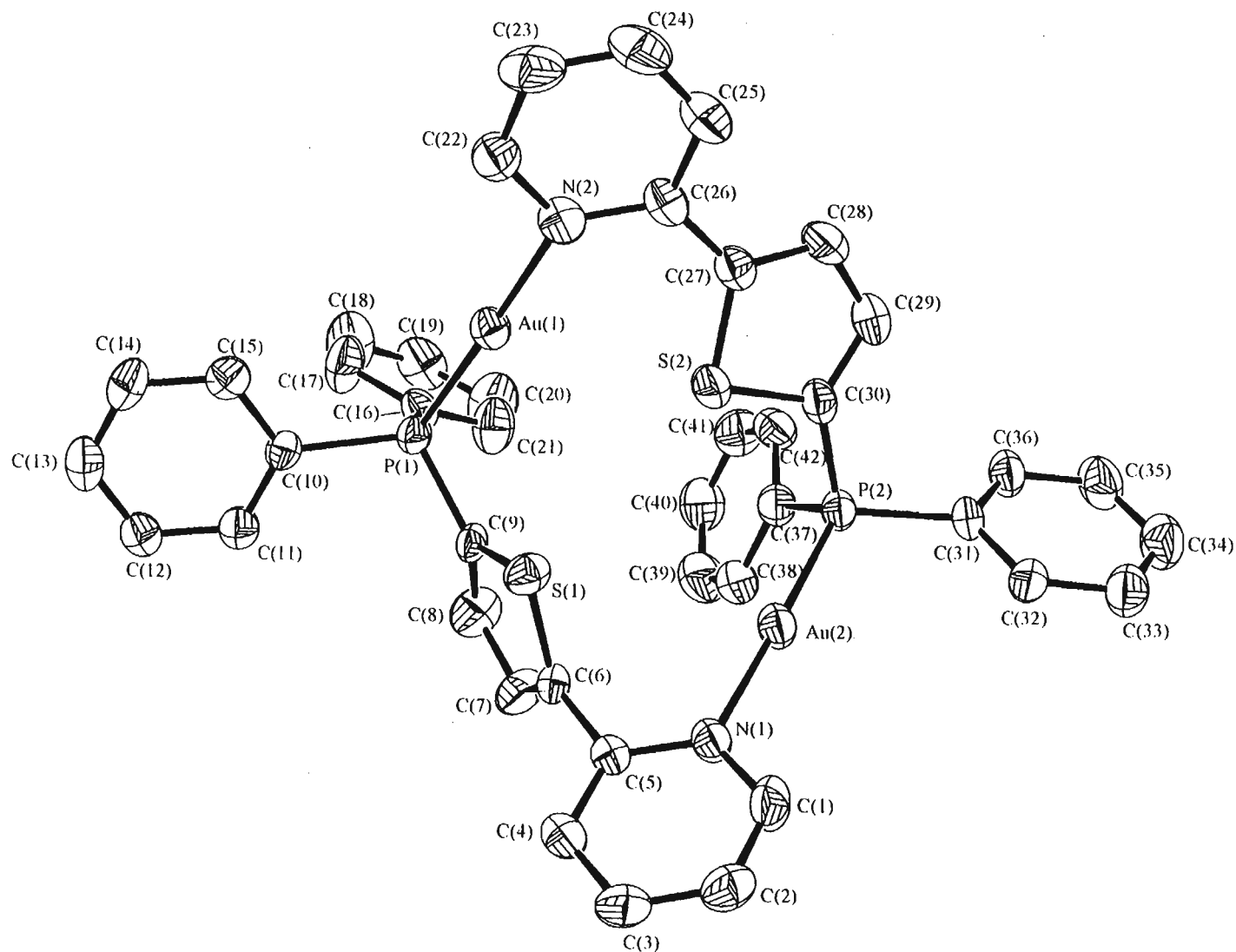


Fig. III.8 Structure of the $[\text{Au}_2(\mu\text{-PSN})_2]^{2+}$ cation ([15]), showing the atom numbering scheme

comparison is not possible.) This phenomenon has been encountered before during the analysis of the structure of other gold(I) complexes prepared during this work and is attributed to increase of the *s*-character of the phosphorus orbitals as a result of coordination. The angles around both nitrogen atoms are very close to 120° consistent with the *sp*²-hybridisation of nitrogen in the pyridine ring. The remaining bond lengths and angles in the cation are within expected limits and require no further discussion.

The conformations of the two bridging ligands are different from each other: in the first ligand [containing P(1), S(1) *etc.*] the thiophene and pyridine rings are twisted with respect to each other around the C(5)-C(6) bond by 72.9°, while in the second the angle of rotation around the C(26)-C(27) bond is only 29.4°. This is probably the result of mutual repulsion between the electron pairs of the two sulfurs which are separated by a distance of 3.599(4) Å in this arrangement of the two ligands. If the two thiophene rings were coplanar the distance between the sulfur atoms would be much smaller (less than 3 Å) causing considerable destabilisation of the structure.

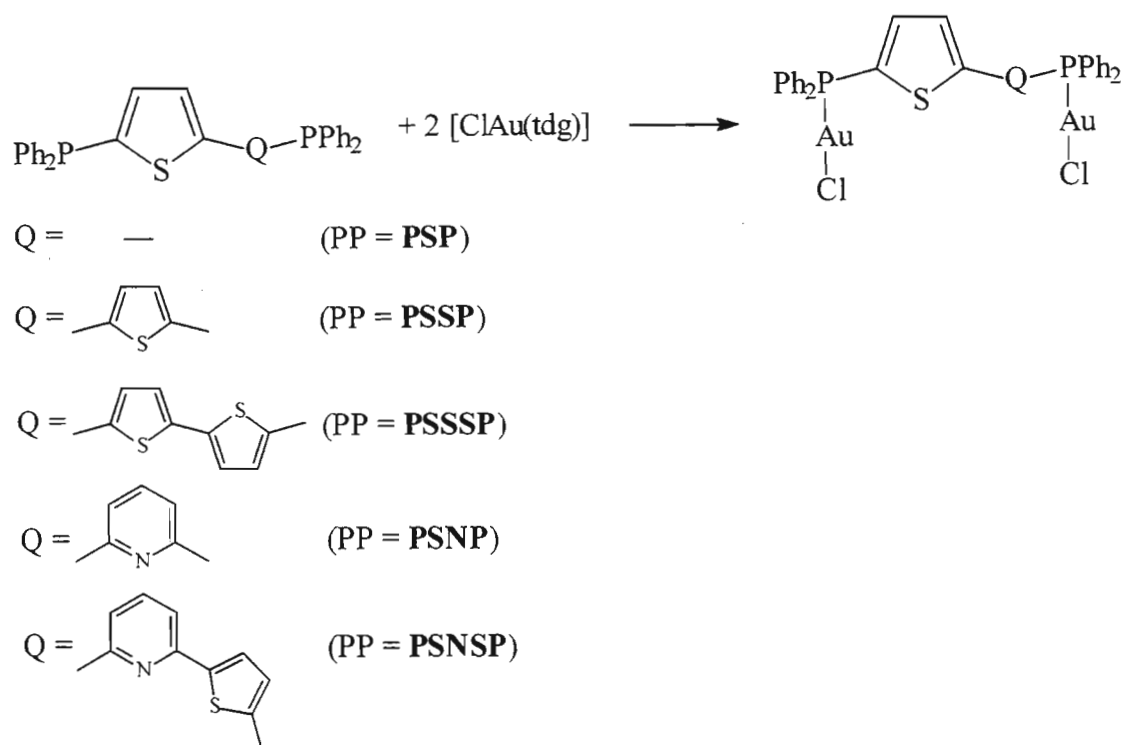
III.2.2 Gold(I) complexes with diphosphine ligands

III.2.2.1 Neutral dinuclear complexes containing two-coordinate gold

Preparation

Since the thiophene-based diphosphine ligands, PSP, PSSP, PSSSP, PSNP and PSNSP, have rigid backbone structures, it seems highly unlikely that they will form complexes where they would chelate a gold atom through both phosphorus atoms. Rather, they provide an ideal opportunity for bridging between two metal centres.

Indeed, reactions between these ligands and an *in situ* prepared gold(I) precursor (the Au-tdg complex, see Scheme III.4) in 1:2 molar ratio led to formation of dinuclear di-coordinate complexes of the [ClAu(μ-PP)AuCl] type in high yield. The composition of all the complexes was established by elemental analysis. No incidents of *S*- or *N*-coordination alongside the μ-*P,P* coordination mode were observed. Scheme III.13 shows the general reaction sequence.



SCHEME III.13

The experimental conditions for the above syntheses are very similar to those employed for the preparation of the neutral mononuclear chlorogold(I) analogues with monophosphines described in the Section 2.1.1 of this Chapter. The main variation in the procedure in case of complexes with diphosphine ligands is associated with using a dichloromethane-ethanol mixed solvent to dissolve the ligands before reacting them with the Au-tdg complex, as most of them are poorly soluble in acetone-based solvents (particularly, PSSP and PSNSP). Table III.12 presents the yields of the dinuclear complexes obtained as well as some of their physical data.

Table III.12 Physical data for the neutral di-coordinate chlorogold(I) complexes with thiophene-based diphosphine ligands

Compound number	Formula	Molar mass, $\text{g} \cdot \text{mol}^{-1}$	Colour	Yield, %
[18]	$[\text{ClAu}(\mu\text{-PSP})\text{AuCl}]$	917.33	white	82
[19]	$[\text{ClAu}(\mu\text{-PSSP})\text{AuCl}]$	999.45	white	75
[20]	$[\text{ClAu}(\mu\text{-PSSSP})\text{AuCl}]$	1081.57	yellow	71
[21]	$[\text{ClAu}(\mu\text{-PSNP})\text{AuCl}]$	994.41	white	86
[22]	$[\text{ClAu}(\mu\text{-PSNSP})\text{AuCl}]$	1076.53	off-white	75

The complexes [18]-[22] are air-stable solids which decompose when heated above 220°C. However the complex with the PSSSP ligand, [20], is light sensitive as a consequence of the light-sensitivity of the ligand and should be kept in the dark. The complexes are soluble in chlorinated organic solvents and DMSO but are poorly soluble in the more polar acetone and acetonitrile. The PSSP complex [19], is moderately soluble both in dichloromethane and chloroform.

Characterisation

The ^1H and ^{31}P NMR spectroscopic data for complexes [18]-[22] are given in Table III.13. The peaks due to the phosphorus nuclei in the dinuclear complexes are positioned downfield from the corresponding signals in the spectra of the ligands, in accordance to what was observed for the analogous mononuclear complexes. The values of the chemical shifts are also similar to the values determined earlier for di-coordinate chlorogold(I) complexes with thiophene-based monophosphine ligands (see Section 2.1.2 of this Chapter).

Table III.13 ^1H and ^{31}P NMR spectroscopic data for the complexes [18]-[22], as measured in CDCl_3 ; the atom numbering scheme for the ligands is given in the Figure III.9

Complex	$\delta^{31}\text{P}$, ppm	$\delta^1\text{H}$, ppm
[18]	19.92 (s)	7.35-7.66 (m, 22 H, 20 H_{Ph} + 2 $\text{H}_{\text{Th-3}}$)
[19]	19.53 (s)	7.31 (part of ABX system, 2 H, $\text{H}_{\text{Th-3}}$), 7.41 (part of ABX system, 2 H, $\text{H}_{\text{Th-4}}$), 7.45-7.67 (m, 20 H, H_{Ph})
[20]	19.48 (s)	7.13 (s, 2 H, $\text{H}_{\text{Th-3}}$), 7.27 (part of ABX system, 2 H, $\text{H}_{\text{Th-3}}$), 7.42 (part of ABX system, 2 H, $\text{H}_{\text{Th-4}}$), 7.46-7.69 (m, 20 H, H_{Ph})
[21]	31.84 (s) & 19.47 (s), 1:1	7.38-7.97 (m, 25 H, 20 H_{Ph} + 2 H_{Th} + 3 H_{Py})
[22]	19.43 (s)	7.43-7.83 (m, 27 H, 20 H_{Ph} + 4 H_{Th} + 3 H_{Py})

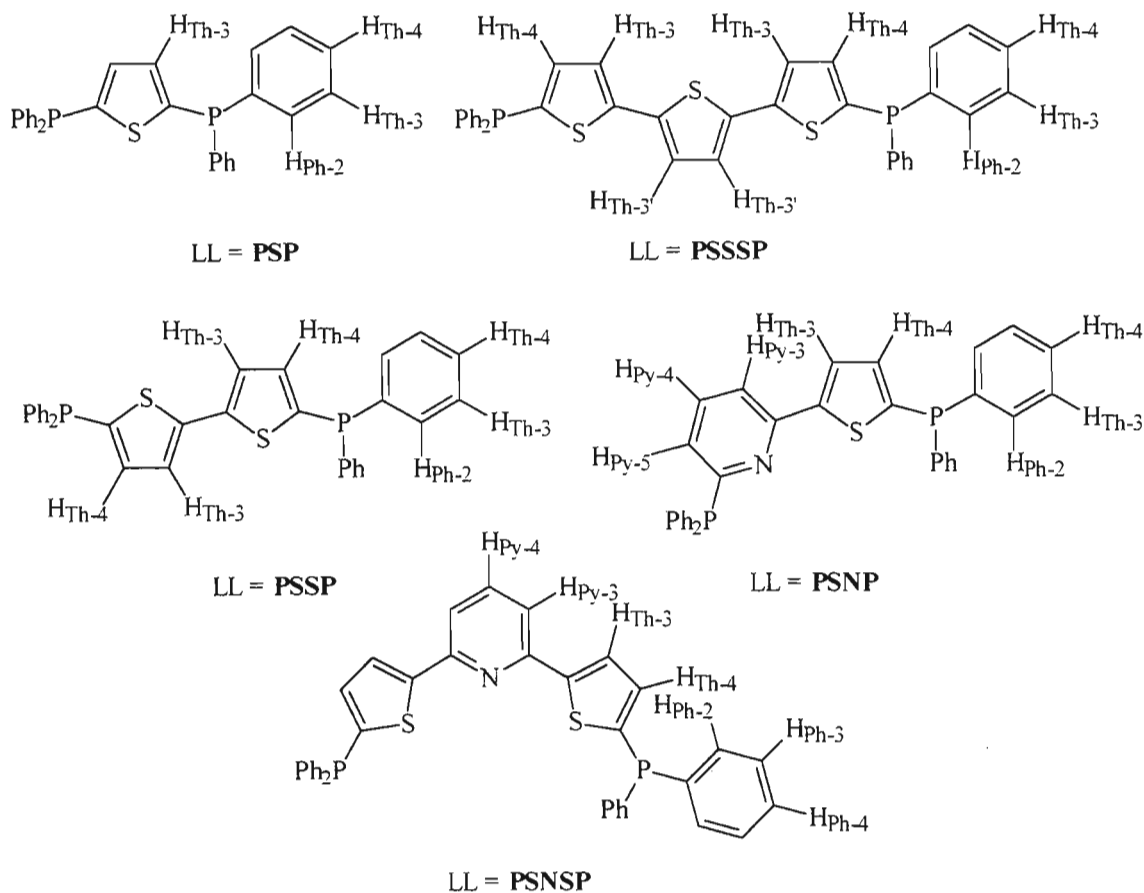


Fig. III.9 Numbering schemes for the hydrogen atoms in the ligands of the complexes [18]-[22].

Assignments of the hydrogen signals in the ^1H spectra of the complexes are based on the assignments of the relevant signals in the spectra of the ligands. Unfortunately, in three out five of the complexes the peaks due to phenyl and thienyl (and also pyridyl) hydrogens were not resolved and assignment of individual signals was impossible.

The effect of coordination of the bidentate ligands to gold(I) can, as before, be quantified by calculating their coordination chemical shift (CCS) values [$\Delta = \delta(\text{complex}) - \delta(\text{ligand})$]. The results for the ^{31}P NMR chemical shifts for the complexes [18]-[22] as well as for the ^1H shifts of the ring hydrogens nearest to phosphorus in the complexes [19] and [20] are shown in Table III.14.

Table III.14 CCS values for the complexes [18]-[22] expressed in the form $\Delta = \delta(\text{complex}) - \delta(\text{ligand})$

Complex	^{31}P , Δ , ppm	^1H , Δ , ppm [*]
[18]	38.76	- ^{**} , H _{Th-3}
[19]	38.28	0.21, H _{Th-4}
[20]	38.19	0.21, H _{Th-4}
[21]	35.44 & 37.81	- ^{**} , H _{Py-5} & - ^{**} , H _{Th-4}
[22]	38.25	- ^{**} , H _{Th-4}

^{*} The chemical shifts of the protons nearest to the P atom were used to determine the ^1H CCS value

^{**} The value could not be determined because the signal under question in the spectrum of the complex was obscured by other aromatic signals

The Δ values for the molecules where phosphorus atoms are attached to thiophene rings are around 38 ppm correlating well with the values obtained for analogous mononuclear complexes with the PS, PSS, PSSS and PSN ligands. The coordination chemical shift of the phosphorus attached to a pyridine ring in the PSNP complex [21] is lower at about 35 ppm, a value similar to that found for the [ClAuPNS] complex (see Table III.3). The effect of coordination of phosphorus to gold(I) on the chemical shift of the adjacent hydrogen atom appears to be somewhat lower for the dinuclear complexes than it was for the related mononuclear complexes (0.21 vs. ± 0.25 ppm, respectively). The values of the $^3J_{\text{H-P}}$ coupling constants for the complexes [19] and [20] are 8.78 and 9.03 Hz respectively, a significant increase from the 6.14 Hz value found in both uncoordinated ligands, but very similar to the $^3J_{\text{H-P}}$ value of 9.65 Hz found in the [ClAuPTS] complex. This confirms the general trend of the increase in the $^3J_{\text{H-P}}$ thiophene hydrogen-phosphorus coupling constants upon coordination to gold(I), which was established earlier (see Table III.4).

The IR spectra of the complexes [18]-[22] strongly resemble the spectra of the corresponding ligands. As they are only useful in the 'fingerprint' region, the data are only given in the Experimental section. As mentioned before (Section 2.1.1 of this Chapter), the UV-vis spectra of the gold(I)-phosphine complexes are simply metal-perturbed UV-vis spectra of the corresponding ligands. For the complexes [18], [19] and [20] there is not

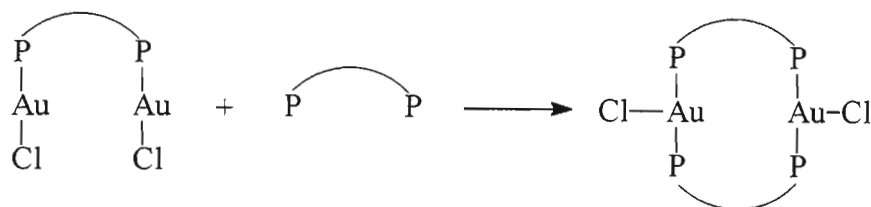
much difference between the spectra of the complexes and the ligands, with the small variation in appearance being due to small shoulder peaks at 269 and 276 nm, which were observed in the mononuclear complexes [1]-[8] as well. There are, however, noticeable perturbations in the UV-vis spectra of the complexes [21] and [22], when compared to those of their ligands. Upon coordination to gold(I) the broad intense band at approximately 265 nm present in the spectra of both PSNP and PSNSP ligands disappears giving rise to two small peaks at 269 and 277 nm. Furthermore, the band at 324 nm present in the spectrum of the PSNSP ligand apparently experiences a shift towards a lower wavelength (315 nm), in the complex. Similar, the band at 336 nm in the spectrum of the PSNP ligand shifts to 324 nm. As a detailed study of the absorption spectra and assignment of individual bands in the spectra of phosphines and their complexes lies beyond the scope of this work, the reason behind the changes in spectral appearances has not been established. Unfortunately, no good quality crystals could be obtained of any of the complexes [18]-[22] to carry out an X-ray diffraction study.

III.2.2.2 Neutral dinuclear complexes containing three-coordinate gold

Diphosphine ligands are known to form three-coordinate chlorogold(I) complexes of the $[\text{XAu}(\mu\text{-LL})_2\text{AuX}]$ type ($\text{X} = \text{Cl}, \text{Br}$ etc.).^{86,87} The complexes have annular, usually 8-membered, structures with the geometry around the both gold atoms being T-shaped, although there are some examples of non-equivalent arrangements of substituents around the two metal atoms. (More detailed information can be found in Chapter I of this Thesis.) The ligands employed for the preparation of this type of complex were based on bis(diphenylphosphino)methane, dppm, the diphosphine ligand which is known to stabilise intramolecular Au...Au interactions due to the small distance between the two phosphorus atoms. The other characteristic of dppm enabling it to promote formation of a macrocyclic bridging structure is that the ligand is very unlikely to chelate to gold(I). In our case the backbones of the diphosphine ligands (PSP, PSSP, PSSSP, PSNP and PSNSP) are sufficiently rigid to render chelation impossible. Moreover, the distances between the phosphorus atoms in all of the ligands are considerably larger, with the smallest in PSP being at around 6 Å, which rules out stabilising effect of intramolecular Au...Au interaction. (The stability of the complexes of the $[\text{XAu}(\mu\text{-LL})_2\text{AuX}]$ type, where LL = dppe, dppb etc., is known to be lower than that of the related complexes with dppm ligand.⁶⁷) Therefore it was of interest to investigate the possibility of the formation of

macrocyclic structures containing two three-coordinate gold(I) atoms bridged by the thiophene-based diphosphine ligands.

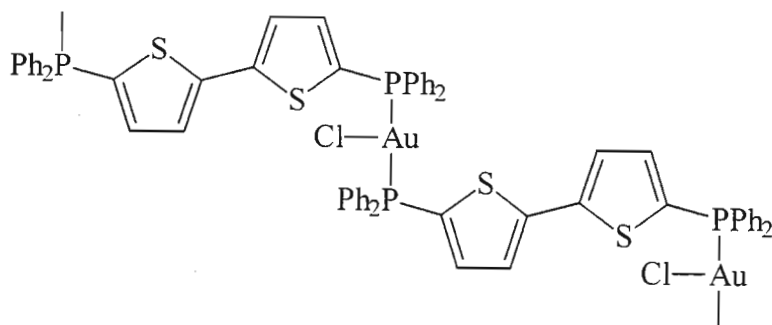
The synthetic approach chosen for the synthesis of dinuclear di-bridged complexes $[\text{ClAu}(\mu\text{-LL})_2\text{AuCl}]$ was based on the similar procedure employed for the preparation of mononuclear three-coordinate chlorogold(I) complexes with monophosphine ligands. One equivalent of the diphosphine ligand was reacted with one equivalent of the corresponding dinuclear complex according to Scheme III.14 below.



SCHEME III.14

The same type of approach was used by Schmidbaur *et al.*⁸⁶ during the synthesis of $[\text{ClAu}(\mu\text{-dppm})_2\text{AuCl}]$ and Sadler and Berners-Price⁶⁷ during the ^{31}P NMR study of the reaction between dppm and its homologues with gold(I).

The diphosphines were dissolved in dichloromethane and added with stirring to a dichloromethane solution of the appropriate chlorogold(I) complex. With the PSP and PSSSP ligands this resulted in clear solutions while the PSSP, PSNP and PSNSP ligands afforded insoluble products. These products were not soluble in most common organic solvents tried, including DMSO, which suggests that they were of polymeric nature. The elemental analysis obtained on the solid precipitated from the reaction with PSSP corresponded to the composition $[\text{ClAu}(\text{PSSP})]_n$. A possible structure (based on a similar reported structure by Baker⁸) is proposed with the PSSP bridging intermolecularly and is shown below:



However the results of elemental analysis for the other two compounds did not match the calculated values for the expected composition $[\text{ClAu}(\mu\text{-LL})]_n$ where LL = PSNP and PSNSP. It is likely that these two ligands gave rise to mixtures of a more complex nature.

The elemental analysis for the compounds isolated from the reactions with the PSP and PSSSP (the yields were 76 and 83% respectively) confirmed the ratio between the ligand and gold in the complexes to be 1:1. It is assumed, but at present cannot be proved beyond reasonable doubt, that their formulae are $[\text{ClAu}(\mu\text{-PSP})_2\text{AuCl}]$ ([23]) and $[\text{ClAu}(\mu\text{-PSSSP})_2\text{AuCl}]$ ([24]) respectively. Further characterisation of these complexes was based on ^1H and ^{31}P NMR spectroscopy. The ^{31}P chemical shifts of the complexes were measured in CDCl_3 and were found to be 11.88 ppm (PSP complex) and 13.42 ppm (PSSSP complex). The corresponding CCS values of about 30.7 and 32.1 ppm are smaller than the CCS values of *ca.* 38 ppm in the original two-coordinate ligand-bridged complexes [18] and [20]. This is unexpected result given the findings of Sadler and Berners-Price⁶⁷ that in stable annular complexes of the $[\text{ClAu}(\mu\text{-LL})_2\text{AuCl}]$ type the coordination chemical shift of the phosphorus is greater than that in two-coordinate complexes.

The reason for this apparent inconsistency is most likely to be the same as the one discussed in the Section describing the characterisation of mononuclear three-coordinate chlorogold(I) complexes (Section III.2.1.2). This is that the thiophene-based phosphines form less stable three-coordinate gold(I) complexes than their alkane-based analogues, resulting in a fast rate exchange between coordinated and non-coordinated ligands in solution on the NMR time-scale. The solution of a "three-coordinate" complex with two thienylphosphine ligands is therefore a mixture of several species providing an averaged and single signal in ^{31}P NMR spectra. Evidence for the exchange taking place in the solutions of PSP and PSSSP complexes can also be found in their ^1H NMR spectra which contain broad poorly resolved peaks, unlike the sharp peaks seen in the spectra of the two-coordinate precursors. In this connection it is noteworthy that when preparation of $[\text{ClAu}(\mu\text{-PSSSP})_2\text{AuCl}]$ was attempted using acetonitrile as the solvent, the resultant product gave 3 different signals in its ^{31}P NMR spectrum, at 18.56, 19.03 and 24.34 ppm. According to Sadler and Berners-Price,⁶⁷ acetonitrile and acetone stabilise three-coordinate complexes much better than chloroform and dichloromethane do. Possibly, the peak at 24 ppm is associated with such a species. However, the presence of the other two peaks

indicates clearly that even employment of a more polar solvent has not led to exclusive formation of a single product.

It follows from the above discussion that a definite characterisation of the potentially three-coordinate complexes cannot be made in solution. Although thin yellow crystals of "[ClAu(μ -PSSSP) $_2$ AuCl]" were isolated upon diffusion of ether into concentrated dichloromethane solution of the compound, they unfortunately proved to be too inferior quality to be used for X-ray diffraction studies. Thus, although two complexes formally fitting the composition [ClAu(μ -LL)] $_n$ (LL = PSP and PSSSP) were synthesised, their structure as well as the value for n could not be unequivocally determined.

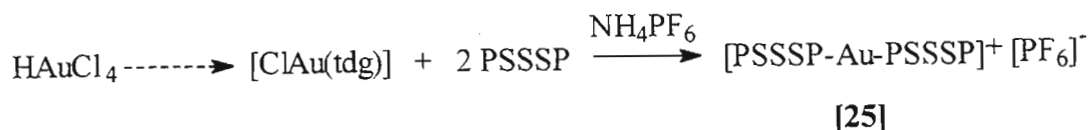
III.2.2.3 The cationic mononuclear complex [Au(η^1 -PSSSP) $_2$]PF $_6$ ([25])

There are two possibilities for the synthesis of a mononuclear gold(I) complex with diphosphine ligands. One is to have the ligand chelating and the other is to have the ligand coordinating via a single donor atom only. When the crystal structure of the PSNSP was discussed (Section 2.5.2 of Chapter II) it was mentioned that the cavity formed by the three heterocyclic rings might provide an opportunity for chelation. An attempt was made to use this ligand for the preparation of a cationic mononuclear gold(I) complex starting with a cationic gold(I) precursor, [Au(MeCN) $_2$]SbF $_6$.

Addition of 1 molar equivalent of PSNSP in dichloromethane or acetonitrile to this precursor did not afford the desired product. The clear solution which was formed originally, quickly turned turbid and the precipitate separated with time. Attempts to dissolve this precipitate in a range of organic solvent including DMSO proved fruitless. This indicates that the product is polymeric in nature. Variations in reaction time and temperatures did not change the outcome. Thus it was concluded that PSNSP is more likely to act as a bridging ligand (via both phosphorus atoms and the nitrogen) rather than a chelating one.

Diphosphines are potentially capable of acting as monodentate phosphine ligands in complexes *i.e.*, where one of the phosphorus sites is coordinated to the metal and the other remains pendant. There have been no previous examples of such complexes with gold(I) reported in the literature, although this mode of coordination is known for complexes with other metals.

Reaction of 2 equivalents of PSSSP dissolved in a 1:1 mixture of dichloromethane and ethanol with one equivalent of the chlorogold(I) precursor in aqueous acetone, followed by addition of saturated NH_4PF_6 , afforded a clear solution from which the yellow microcrystalline product was isolated upon addition of water and *iso*-propanol (Scheme III.15).



SCHEME III.15

The elemental analysis of the product was consistent with the proposed structure. The compound was analysed using ^{31}P and ^1H NMR as well as IR spectroscopies. Table III.15 summarises the essential characterisation details for this complex ([25]).

Table III.15 Characterisation details for the compound [25], the numbering scheme for the hydrogens is identical to that in Figure III.9

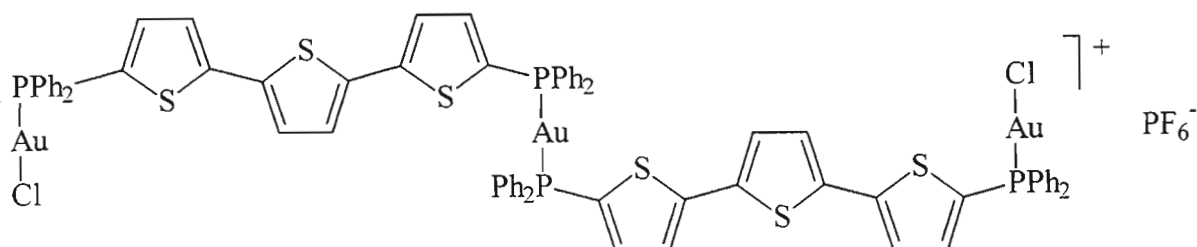
Formula	Yield, %	Colour	$\delta^{31}\text{P}$, ppm*	$\delta^1\text{H}$, ppm*
$[\text{Au}(\text{PSSSP})_2]\text{PF}_6$	92	yellow	26.5 (s, br)	6.64 (s, 2 H, $\text{H}_{\text{Th-3}}$), 6.92 (d, br, 2 H, $\text{H}_{\text{Th-3}}$), 7.10-7.40 (m, 22 H, 20 H_{Ph} + 2 $\text{H}_{\text{Th-4}}$)

* The value measured in acetone- d_6

The ^{31}P NMR spectrum of the compound recorded in deuterated acetone appears as a broad peak with the maximum at approximately 26.5 ppm. Likewise the ^1H NMR spectrum consists of broad, mainly unresolved lines. This situation implies that an exchange, taking place between the coordinated and uncoordinated phosphorus atoms, is fast on the NMR time scale. The IR spectrum shows an intense absorption band at 838 cm^{-1} confirming the presence of PF_6^- as the counterion.

The following reaction was carried out in order to confirm that the two phosphorus atoms in complex [25] are indeed pendant. The gold(I) precursor $[\text{ClAu}(\text{tht})]$ was first added to a solution of [25] in dichloromethane in a 2:1 mole ratio. As it turned out the order of addition in this reaction is crucial.

Addition of complex [25] to $[\text{ClAu}(\text{tht})]$ results in exclusive formation of the dinuclear two-coordinate complex $[\text{ClAu}(\mu\text{-PSSSP})\text{AuCl}]$ ([20]), as confirmed by means of ^{31}P NMR spectroscopy and C, H microanalysis. The product of the addition of the precursor to [25] is different however, and is assigned the trinuclear structure shown below.



The latter species could not be obtained sufficiently pure for the elemental analysis. However its ^{31}P NMR spectrum recorded in CDCl_3 is informative. The spectrum consists of two sharp peaks at 30.37 and 19.53 ppm, in a 1:1 ratio. The latter chemical shift is nearly the same as that found for complex [20] $\{[\text{ClAu}(\mu\text{-PSSSP})\text{AuCl}]\}$ *i.e.*, 19.72 ppm, which therefore should be ascribed to the 2 phosphorus atoms attached to the chlorogold moieties. Hence the chemical shift at 30.37 ppm belongs to the two phosphorus atoms bonded to the central gold ion. {This value is quite close to that observed for the phosphorus signals in the dinuclear cationic complex $[\text{Au}_2(\text{PSP})_2](\text{PF}_6)_2$ which is discussed in the Section 2.2.4 of this Chapter *i.e.*, 32.43 ppm. The complex contains a similar P-Au-P⁺ moiety.} The trinuclear complexes with dppm and related diphosphines as ligands have been obtained before¹⁰³⁻¹⁰⁵ although via different reaction pathways. The relationship between the chemical shifts of the phosphorus atoms in the $[\text{Cl}_2\text{Au}_3(\mu\text{-dppm})_2]\text{ClO}_4$ complex was found to be the same, *i.e.* the downfield peak is assigned to the two *trans* inner phosphorus atoms.¹⁰⁵

The IR spectrum of the solid shows a strong band at 837 cm^{-1} , confirming the presence of the PF_6^- counterion. The complex does not appear to be very stable in solution as after 24 hours several small peaks appear in the ^{31}P NMR spectrum, and eventually an unknown solid precipitates out. This fact seems to support the idea that a trinuclear species is formed in the reaction and that this undergoes rapid inter- and possibly intramolecular ligand exchange resulting in the formation of other species. The alternative, namely that the product solution contains a mixture of the dinuclear complexes $[\text{ClAu}(\mu\text{-PSSSP})\text{AuCl}]$ and $[\text{Au}_2(\mu\text{-PSSSP})_2](\text{PF}_6)_2$ is unlikely, as the ^{31}P NMR spectrum of such a mixture should not be affected with time.

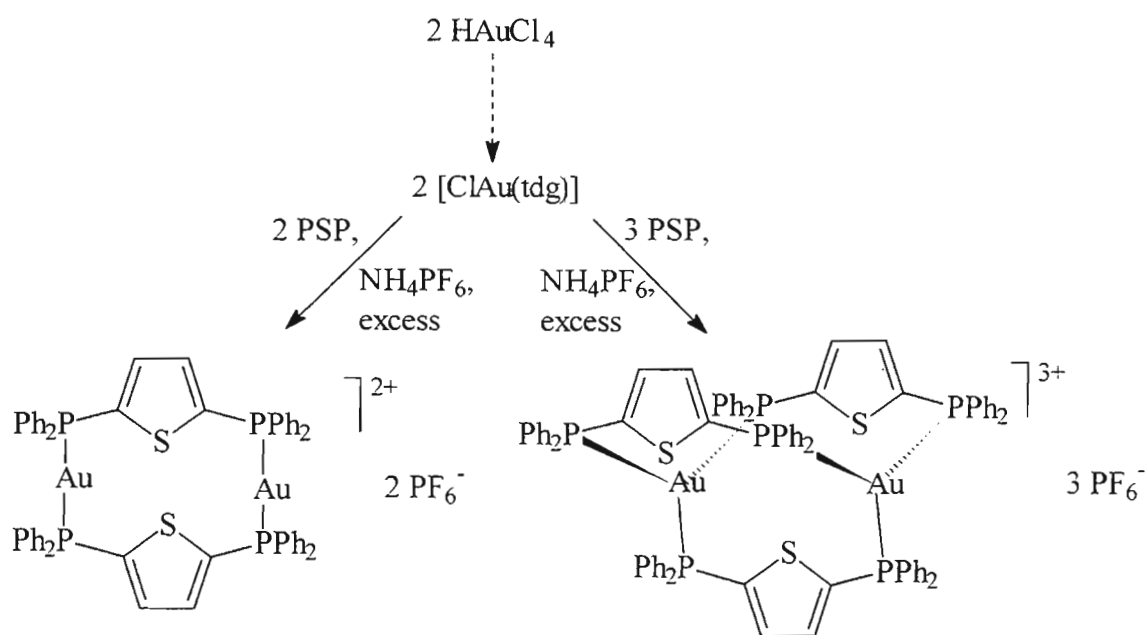
A final comment is that Laguna *et al.*¹⁰⁵ have demonstrated that stable trinuclear complexes of gold(I) are best stabilised through use of dppm as the bridging ligand. It is likely that intramolecular gold-gold interactions are responsible for the greater stability of the dppm-bridged complexes, as analogous complexes with dppe tend to disproportionate. This conclusion is consistent with our observations regarding the stability of the PSSSP-bridged trinuclear complex.

III.2.2.4 Cationic dinuclear complexes

Preparation

Complexes of the type where two gold(I) cations are bridged by two diphosphine ligands are quite common.^{43,90-92,99} They can be prepared from the neutral halide gold(I) precursors by displacing the halide with large non-coordinating counterions in the presence of the diphosphine ligand. This synthetic approach was investigated using PSP as the model ligand. This thienylphosphine was chosen due to its relative structural rigidity, as there is no possibility of rotation around interannular C-C bonds in this molecule, unlike in the other thienylphosphines reported here. This rigidity is believed to be beneficial for maintaining the annular structure of the target dibridged dinuclear complex.

Scheme III.16 below presents the reaction sequence employed for the preparation of the cationic dinuclear gold(I) complexes with PSP as a ligand.



SCHEME III.16

A solution of a stoichiometric amount of the PSP ligand in acetone was added to a solution of the neutral chlorogold(I) precursor in aqueous acetone. The 1:1 ligand to gold ratio afforded the complex with two-coordinate gold(I), while a 3:2 mole ratio afforded the complex with three-coordinate gold(I). The composition of the complexes was established by means of elemental analysis. With regard to the structures illustrated in Scheme III.16, these take into account the propensity for the PSP ligand to bridge two metal atoms. In particular, an alternative arrangement for the ligands in the three-coordinate complex, which has one PSP ligand bridging and each of the other two chelating, is extremely unlikely because of the rigidity of this ligand. The physical data for the complexes are given in Table III.16.

Table III.16 Physical data for the cationic dinuclear gold(I) complexes with the PSP ligand

Compound number	Formula	Molar mass, $\text{g}\cdot\text{mol}^{-1}$	Colour	Yield, %
[26]	$[\text{Au}_2(\mu\text{-PSP})_2](\text{PF}_6)_2$	1588.84	white	52
[27]	$[\text{Au}_2(\mu\text{-PSP})_3](\text{PF}_6)_2$	2041.3	white	55

The complexes [26] and [27] appear to be very stable both in the solid state and in solution. They are microcrystalline compounds which behave as typical cationic complexes in solution *i.e.*, they dissolve more readily in polar solvents like acetone and acetonitrile than non-polar solvents like chloroform, though they do dissolve in dichloromethane.

Attempts to carry out similar reactions with the ligands PSSP and PSSSP did not lead to single identifiable products. Furthermore in case of PSSP, polymerisation tended to occur before the NH_4PF_6 salt was added.

Characterisation

Analysis of the complexes using various spectroscopic methods revealed large similarities as well as differences between the data for the two compounds, which can be expected for complexes containing the same ligand but with different geometries around the metal centre. Table III.17 lists ^{31}P and ^1H chemical shifts for complexes [26] and [27].

Table III.17 ^1H and ^{31}P NMR spectroscopic data for the complexes [26] and [27], as measured in acetone- d_6

Compound	$\delta^{31}\text{P}$, ppm	$\delta^1\text{H}$, ppm
[26]	32.43 (s)	7.33 (br s, 2 H, $\text{H}_{\text{Th-3}}$), 7.40-7.65 (m, 20 H, H_{Ph})
[27]	34.83 (s)	7.05 (br s, 2 H, $\text{H}_{\text{Th-3}}$), 7.25-7.60 (m, 20 H, H_{Ph})

The ^{31}P chemical shift of the three-coordinate complex is slightly downfield from that recorded for the two-coordinate complex. As no ^{31}P NMR data for similar complexes has been described to date it is difficult to account for such unexpected behaviour. Both on the grounds of reduced σ -donation by each phosphorus atom and increased π -back donation to the P-atoms, we would expect a relatively higher electron density on the P-atom in the three-coordinate complex and an upfield shift in the ^{31}P chemical shift. This is what is indeed observed in the ^1H NMR spectra of the complexes for the $\text{H}_{\text{Th-3}}$ peak: the chemical shift of this hydrogen in the two-coordinate complex lies downfield with respect to that in the three-coordinate complex, indicating that there is slightly greater electron density on the latter. Perhaps there are some unknown factors responsible for the shift of the ^{31}P signal in the three-coordinate complex in the 'wrong' direction. They will only become clear if more investigations on similar types of complexes are performed. This "anomaly" cannot serve as an indication of possible thiophene coordination as a downfield shift in the ^{31}P NMR chemical shift of a three-coordinate dinuclear complex (in comparison to the related two-coordinate species) has been observed before for a complex containing purely phosphine ligands. McCleskey and Gray²⁴⁸ reported ^{31}P NMR chemical shifts for acetonitrile- d_3 solutions of $[\text{Au}_2(\mu\text{-dcpe})_2](\text{PF}_6)_2$ and $[(\eta^2\text{-dcpe})\text{Au}(\mu\text{-dcpe})\text{Au}(\eta^2\text{-dcpe})](\text{PF}_6)_2$ [dcpe = 1,2-bis(dicyclohexylphosphino)ethane] complexes. The former complex as well as the dicyanoaurate salt¹⁰² of the latter have been structurally characterised, thus providing unambiguous proof of gold coordination environment. In the latter complex, each gold is three-coordinate, which is achieved by chelation by one dcpe ligand [δ = 64.20 ppm (d)] and bridging by another [δ = 57.49 ppm (t)], while in the former each gold is linear two-coordinate [δ = 52.4 ppm (s)].

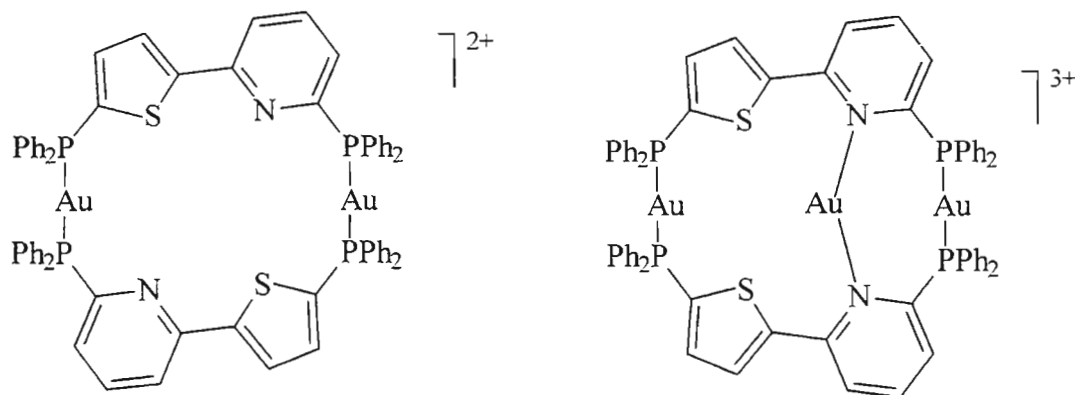
The IR spectra of both complexes recorded as KBr pellets exhibit a strong band at 838 cm^{-1} , characteristic of the P-F stretching frequencies of the PF_6^- counterion. The spectra are

essentially the same apart from the region at around 1600 cm^{-1} . In the spectrum of [26] there is only a broad band of weak intensity at $\pm 1650\text{ cm}^{-1}$, while in the spectrum of [27] there are two moderate intensity bands at 1616 and 1684 cm^{-1} . As the PSP ligand itself does not absorb in this region, the bands must be associated with the formation of respective complexes.

The UV-vis spectra of acetonitrile solutions of both complexes exhibit broad continuous bands from 200 (apparent maximum) to about 340 nm with several more or less distinguishable shoulders. The main difference in the spectrum of the complex [27] when compared to that of [26] is, apart from the obvious extinction coefficient difference, the presence of a noticeable shoulder at $\pm 310\text{ nm}$ alongside the bigger shoulder at 260-270 nm characteristic for both complexes. The absorbance of the complex [26] at 310 nm, on the other hand, is negligible. The full IR and UV-vis characterisation data for both complexes are given in the Experimental section of this Chapter.

III.2.2.5 Attempted preparation of cationic dinuclear and trinuclear complexes using the PSNP ligand

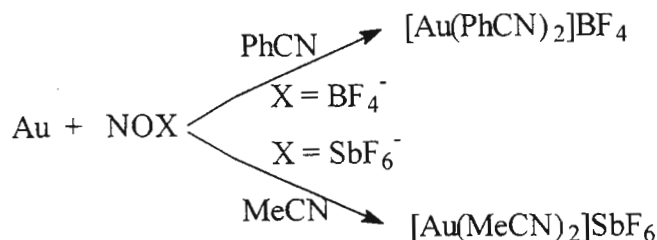
The PSNP ligand presents a very interesting example of a ligand with 3 inequivalent coordination sites *i.e.*, the phosphorus adjacent to the thiophene ring, the phosphorus adjacent to the pyridine ring and the nitrogen of the pyridine ring. Thus it provides a good opportunity for studying various types of coordination modes this ligand can adopt in different type of complexes. Unfortunately due to the lack of time a comprehensive investigation could not be managed during the present work. The study carried out with this ligand only included attempts to prepare dinuclear two-coordinate and trinuclear two-coordinate complexes, aiming at the structures depicted below:



The structures shown are examples only, as the formation of complexes in which the two ligands bridge 'head-to-tail' as opposed to 'head-to-head' complexes is difficult to predict or guarantee.

During several attempts to use neutral chlorogold(I) precursors obtained *in situ* from HAuCl_4 as starting materials for the preparation of these cationic complexes, precipitation of polymeric products inevitably occurred. On the basis that one mole of the phosphine was added to one mole of the chlorogold(I) species, we speculate that the polymeric products consist of three-coordinate gold(I) units bridged intermolecularly by the PSNP ligand (see Section 2.2.2 of this Chapter). In order to avoid the formation of polymeric species cationic gold(I) precursors were employed.

The two cationic precursors used have a similar structure and are prepared according to similar methods (Scheme III.17).



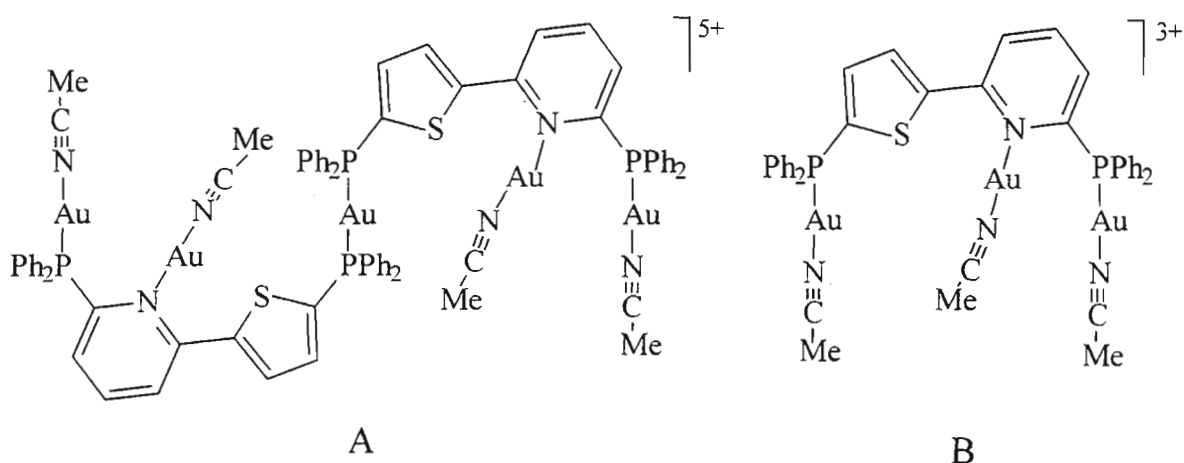
SCHEME III.17

When a solution of 1 equivalent of PSNP in acetonitrile was added to 1 equivalent of $[\text{Au}(\text{PhCN})_2]\text{BF}_4$ also in acetonitrile, a clear solution resulted. The ^{31}P NMR spectrum of this solution showed at least 9 clearly distinguishable peaks with chemical shifts ranging from 15 to 35 ppm. The same behaviour was observed with the other gold(I) precursor. Addition of approximately 1.5 equivalents of the ligand instead brought about a change in the colour of the solution to yellow. But there were still 6 different peaks of various intensities in the ^{31}P NMR spectrum of the solution, making it impossible to isolate a single product. Increasing the ligand to gold ratio to 2:1 caused the solution to become colourless again, but it still did not simplify the appearance of the spectrum. A smaller ratio of 2:3, consistent with the stoichiometry of the second of the desired structures illustrated above, also gave rise to a complex spectrum with approximately 10 lines. It is therefore clear that

PSNP forms a large variety of species with gold(I) in solution and there seems to be no specificity towards formation of the annular complexes shown above.

Interestingly, using a large excess of the gold precursor, $[\text{Au}(\text{PhCN})_2]\text{BF}_4$, over the ligand, afforded a solution with a simple ^{31}P NMR spectrum containing just two peaks, at approximately 33 and 15 ppm, in a 1:1 ratio. Unfortunately the compound(s) represented by these peaks is air-, moisture- and light-sensitive in solution and for this reason it could not be isolated. To improve on the stability of the reaction product, the other gold precursor was used as it contained a larger counterion. The reaction between $[\text{Au}(\text{MeCN})_2]\text{SbF}_6$ and PSNP in acetonitrile in a 5:1 mole ratio afforded a colourless solution which was reduced in volume and treated with dry degassed ether. The white powder isolated was washed with ether and dried gently under vacuum. The compound is stable in the dark under nitrogen for up to several hours. However even brief contact with air leads to reduction of the complex and the appearance of metallic gold, which initiates a further auto-catalysed decomposition.

The elemental analysis conducted on the solid gave values corresponding closely to two different formulae: $[\text{Au}_5(\mu\text{-PSNP})_2(\text{CH}_3\text{CN})_4](\text{SbF}_6)_5$ (A) and $[\text{Au}_3(\mu\text{-PSNP})(\text{CH}_3\text{CN})_3](\text{SbF}_6)_3$ (B). The possible structures consistent with the ^{31}P NMR spectrum are given in the Scheme III.18 below.



SCHEME III.18

The IR spectrum of the solid product contains a very strong absorption band at 653 cm^{-1} , the frequency associated with the Sb-F stretching vibration in the SbF_6^- counterion. An

interesting feature of the spectrum is a smallish band at 2350 cm^{-1} which can be attributed to the coordinated acetonitrile. This band has not been observed in any of the previously studied complexes whether cationic or neutral. However those data are still insufficient to distinguish between the proposed structures as both include coordinated acetonitrile, with SbF_6^- as the counterion.

Structure B appears more likely due to its simplicity. The first structure could have other isomers in solution *e.g.*, the two phosphorus atoms adjacent to the pyridine ring could also coordinate to the central gold, thus resulting in 4 rather than 2 signals in ^{31}P NMR spectrum. Unfortunately, recrystallisation of the product from dichloromethane-ether or acetonitrile-ether did not help produce a cleaner compound for the purposes of obtaining a more informative elemental analysis. Prolonged handling of the product resulted, instead, in partial decomposition.

III.3 LUMINESCENT PROPERTIES OF A SELECTION OF GOLD(I) COMPLEXES WITH NOVEL THIENYLPHOSPHINE LIGANDS

The luminescent properties of gold(I) complexes have attracted considerable attention during the past decade.^{27,71-74,100-102,111} Linear mononuclear complexes of the $[\text{XAuL}]$ type ($\text{X} = \text{Cl}, \text{Br}, \text{L} = \text{phosphine}$) have been shown not to exhibit luminescence either in solution or in the solid state, although low temperature luminescence (77 K) has been observed for these complexes.²⁵ Visible metal-centred luminescence in mononuclear gold(I) complexes appears to be associated with a trigonal, noncentrosymmetric structure about the metal ion, achieved either through three-coordination by certain ligands²⁴⁶ or via intermetallic $\text{Au}\dots\text{Au}$ interactions.^{88,249,250} In the complexes containing three-coordinate gold(I) with phosphine ligands, the luminescence has been assigned to a metal-centred $p_z \rightarrow d_\sigma$ phosphorescence.¹⁰² Several three-coordinate mononuclear gold(I) complexes are now known to luminesce both in the solid state and in solution.²⁴⁶ A di-gold(I) complex with 3 bridging phosphine ligands, $[\text{Au}_2(\mu\text{-PNP})_3](\text{ClO}_4)_2$ (PNP = 2,6-bis[diphenylphosphino]pyridine),¹⁰⁰ and in which there is no intramolecular $\text{Au}\dots\text{Au}$ interaction, is also emissive.

With few exceptions, linear gold(I) complexes having a Au...Au contact of less than 3.6 Å, are luminescent in the solid state (especially at liquid nitrogen temperatures). However, while the presence of a Au...Au interaction has been linked to photoluminescence,^{249,250} Bruce *et al.*⁷⁴ have shown that such a relationship does not always exist. In practice, emission by a gold(I)-phosphine complex cannot be taken as proof for the presence of a gold(I)-gold(I) interaction as the luminescence of these complexes can originate, for example, from a ligand-to-metal-charge-transfer (LMCT) transition.⁷⁴ The observed emission may also have its origins in a ligand-centred (LC) transition.³⁸ Due to the interest shown by numerous research groups in the phenomenon of luminescence in gold(I)-phosphine complexes, the luminescent properties of a selection of the new thienylphosphine ligand complexes of gold(I) have been investigated.

Table III.18 presents the emission wavelengths of the 8 such complexes obtained after excitation at 350 nm, both in the solid state and in dichloromethane solution. (Dichloromethane was chosen as a universal solvent in these studies as opposed to acetonitrile since it could dissolve all of the compounds studied.)

Table III.18 Emission of the selected gold(I)-phosphine complexes at room temperature in the solid state and in solution ($\lambda_{\text{ex}} = 350 \text{ nm}$)

Complex	$\lambda_{\text{em}}(\text{max}), \text{nm}$	
	in solid state	in solution*
[ClAuPDS]	NE**	NE**
[ClAuPTS]	NE**	NE**
[ClAu(PDS) ₂]	464, 487	NE**
[ClAu(μ -PSSSP) ₂ AuCl]	470, 489, 496	NE**
[Au ₂ (μ -PSP) ₂](PF ₆) ₂	522 ⁼	NE**
[Au ₂ (μ -PSP) ₃](PF ₆) ₂	526	520
[Au ₂ (μ -PSN) ₂](SbF ₆) ₂	531, 558, 619 (sh)	536, 566
[Au ₂ (μ -PNS) ₂](PF ₆) ₂	450, 467, 560, 643 (sh)	-***

* The measurements were carried out in deoxygenated dichloromethane

** NE stands for the complex being non-emissive

*** The available amount of this complex was not sufficient for studying its luminescence in solution

= The intensity of emission of this complex is far lower than that of the tri-coordinate complex. See the text for details

Although detailed assignment of the different kinds of luminescence exhibited by the above complexes lies beyond the scope of this work, it will nevertheless be useful to comment on their luminescent properties as given in Table III.18.

The mononuclear linear complexes [ClAuPDS] and [ClAuPTS] do not luminesce in either solution or the solid state, as expected. However, the presence of an extra ligand in the three-coordinate species [ClAu(PDS)₂] has as a result that the compound luminesces strongly in the solid state. Dissolving [ClAu(PDS)₂] in dichloromethane leads to dissociation of this extra ligand (see Section 2.1.2 of this Chapter); hence no luminescence is observed in solution. The dinuclear complex, [ClAu(μ-PSSSP)₂AuCl], shows a similar trend: it emits light upon excitation in the solid state, but not in solution - in full agreement with the tendency of three-coordinate complexes to lose the third ligand in dichloromethane solutions (see Section 2.2.2 of this Chapter). This complex is not expected to have intramolecular Au...Au interactions due to the large bite of the PSSSP ligand.

The two PSP ligand-bridged complexes, [Au₂(μ-PSP)₂](PF₆)₂ and [Au₂(μ-PSP)₃](PF₆)₂, illustrate the effect of the geometry around the gold(I) ion on the luminescent properties of the complex. The complex with two-coordinate gold emits light of low intensity upon excitation in the solid state but does not luminesce in solution. The complex with three-coordinate gold emits strongly both in the solid state and solution, with both spectra being very similar *i.e.*, having broad gaussian shapes. These observation suggest that the third PSP ligand in this complex is bonded firmly and does not dissociate upon dissolution in dichloromethane, unlike for [ClAu(PDS)₂] and [ClAu(μ-PSSSP)₂AuCl]. The energy of the emission is very similar to the value reported by Che *et al.*¹⁰⁰ for analogous complex, [Au₂(μ-PNP)₃](ClO₄)₂ [PNP = 2,6-bis(diphenylphosphino)pyridine]: *i.e.* 520 nm. Che assigned the emission of this complex to be of metal-perturbed intraligand character.

Based on literature findings, the two-coordinate complex, [Au₂(μ-PSP)₂](PF₆)₂, should not exhibit luminescence (except, possibly, intraligand emission) even in the solid state. The weak luminescence observed in the solid state is most likely the result of the presence of a small amount of some impurity *e.g.*, the three-coordinate complex; alternatively, defects in the crystal lattice of the two-coordinate complex that disturb the centrosymmetric structure of the [P-Au-P]⁺ unit could be responsible for the weak luminescence.

To the best of our knowledge, the luminescent properties of di-coordinate gold(I) complexes containing an asymmetric $[P-Au-N]^+$ unit have never been reported. The two complexes, $[Au_2(\mu-PSN)_2](SbF_6)_2$ and $[Au_2(\mu-PNS)_2](PF_6)_2$, provide examples of complexes containing an asymmetric $[P-Au-N]^+$ unit. Unlike complexes with the $[P-Au-P]^+$ or $[P-Au-Cl]$ units, they emit strongly in the solid state giving rise to quite complex spectra. The spectra of the two solids have similar band profiles, except that that of PNS ligand-bridged complex exhibits additional peaks of moderate intensity at 450 and 467 nm. Also for this compound the low energy shoulder on the peak is red-shifted in comparison to that in the spectrum of the PSN complex by approximately 25 nm. We speculate that the red shift is associated with an intramolecular Au...Au interaction in this complex. (The PNS complex uniquely exhibits orange-yellow luminescence in the solid state.) Although we could not determine the crystal structure of the $[Au_2(\mu-PNS)_2](PF_6)_2$, Schmidbaur *et al.*⁵⁷ have reported a very short distance of 2.77 Å between the metal centres in the similar complex, $[Au_2(\mu-P'N)_2](BF_4)_2$ ($P'N$ = 2-dimethylphosphinopyridine). On the other hand, the crystal structure of the PSN complex reveals no such contacts (see Section 2.1.3 of this Chapter). The emission spectrum of the PSN complex remains nearly unchanged in solution indicating that the observed luminescence is likely to be the property of the $[P-Au-N]^+$ unit.

The results of the luminescence studies allow one to distinguish between two- and three-coordinate species in the solid state. Specifically, a hand-held mercury lamp with two filter settings (254 and 360 nm) was used to produce low energy excitation light and the resultant emission by the complex was observed in the dark. Weak, bluish-white luminescence is normally of intraligand origin and is characteristic of two-coordinate complexes (neutral or cationic) with one or two phosphine ligands attached to the gold atom. Bright yellow emission was observed from complexes with three-coordinate gold. Disappearance of the luminescence in solution normally indicated lability of the ligands and, in particular, dissociation of a ligand in the three-coordinate complexes to produce a two-coordinate species.

The few results described above demonstrate the wide scope for a full investigation of the optical properties of the new gold(I)-phosphine complexes prepared in this work. However, due to time constraints, this will have to be the subject of an independent investigation.

III.4 SUMMARY AND CONCLUSION

Given that the synthesis and characterisation of a number of new gold(I) complexes is reported in this Chapter, it seems appropriate to briefly summarise their properties.

III.4.1 Properties of the new gold(I) complexes with thienylphosphine ligands

Table III.19 gives an overview of the types of gold(I) complexes prepared during this work as well as providing their basic characteristics, such as yield, colour and ^{31}P NMR shift.

Table III.19 Selected properties of the novel phosphines and related compounds obtained during this work

Complex Type	Formula	Yield, %	Colour	$\delta^{31}\text{P}$, ppm
COMPLEXES WITH MONOPHOSPHINE LIGANDS				
<u>I. Neutral, mononuclear</u>				
I.1 Containing two-coordinate gold	$[\text{ClAu}(\text{PS})]$ ([1])	92	white	19.18^* (s)
	$[\text{ClAu}(\text{PDS})]$ ([2])	89	white	5.77^* (s)
	$[\text{ClAu}(\text{PTS})]$ ([3])	87	off-white	-6.41^* (s)
	$[\text{ClAu}(\text{PSBr})]$ ([4])	88	white	18.85^* (s)
	$[\text{ClAu}(\text{PSS})]$ ([5])	78	off-white	19.43^* (s)
	$[\text{ClAu}(\text{PSSS})]$ ([6])	92	yellow	18.45^{**} (s)
	$[\text{ClAu}(\text{PSN})]$ ([7])	90	white	20.63^* (s)
	$[\text{ClAu}(\text{PNS})]$ ([8])	95	white	31.32^* (s)
I.2 Containing three-coordinate gold	$[\text{ClAu}(\text{PS})_2]$ ([9])	64	white	11.02^* (s)
	$[\text{ClAu}(\text{PDS})_2]$ ([10])	82	white	-2.98^* (s)
	$[\text{ClAu}(\text{PTS})_2]$ ([11])	87	white	-15.93^* (s)
	$[\text{ClAu}(\text{PSN})_2]$ ([12])	82	white	10.56^* (s)
I.3 Containing four-coordinate gold	$[\text{ClAu}(\text{PS})_3]$ ([13])	- ⁼	off-white	13.71^{**} (s)

⁼ The yield was not measured

^{*} The spectrum was recorded in CDCl_3

^{**} The spectrum was recorded in CD_2Cl_2

Table II.19 continued...

COMPLEXES WITH MONOPHOSPHINE LIGANDS				
<u>II. Cationic</u>				
II.1 Mononuclear, two-coordinate gold	$[\text{Au}(\text{PSN})_2]\text{SbF}_6$ ([14])	63	white	33.51 ^{***} (s)
	$[\text{Au}(\text{PNS})_2]\text{SbF}_6$ ([16])	74	white	45.82 ^{****} (s)
II.2 Dinuclear, two-coordinate gold	$[\text{Au}(\text{PSN})_2](\text{SbF}_6)_2$ ([15])	89	white	19.13 ^{***} (s)
	$[\text{Au}(\text{PSN})_2](\text{PF}_6)_2$ ([17])	70	white	36.46 ^{****} (s)
COMPLEXES WITH DIPHOSPHINE LIGANDS				
<u>I. Neutral. dinuclear</u>				
I.1 Containing two- coordinate gold	$[\text{ClAu}(\mu\text{-PSP})\text{AuCl}]$ ([18])	82	white	19.92 [*] (s)
	$[\text{ClAu}(\mu\text{-PSSP})\text{AuCl}]$ ([19])	75	white	19.53 [*] (s)
	$[\text{ClAu}(\mu\text{-PSSSP})\text{AuCl}]$ ([20])	71	yellow	19.48 [*] (s)
	$[\text{ClAu}(\mu\text{-PSNP})\text{AuCl}]$ ([21])	86	white	31.84 [*] (s), & 19.47 [*] (s), 1:1
	$[\text{ClAu}(\mu\text{-PSNSP})\text{AuCl}]$ ([22])	75	off-white	19.43 [*] (s)
I.2 Containing three- coordinate gold	$[\text{ClAu}(\mu\text{-PSP})_2\text{AuCl}]$ ([23])	63	white	11.88 [*] (s)
	$[\text{ClAu}(\mu\text{-PSSSP})_2\text{AuCl}]$ ([24])	70	yellow	13.42 [*] (s)
<u>II. Cationic</u>				
II.1 Mononuclear, two-coordinate gold	$[\text{Au}(\eta^1\text{-PSSSP})_2]\text{PF}_6$ ([25])	92	yellow	26.52 ^{****} (br s)
II.2 Dinuclear, two-coordinate gold	$[\text{Au}_2(\mu\text{-PSP})_2](\text{PF}_6)_2$ ([26])	52	white	32.43 ^{****} (s)
II.3 Dinuclear, three-coordinate gold	$[\text{Au}_2(\mu\text{-PSP})_3](\text{PF}_6)_3$ ([27])	55	white	34.83 ^{****} (s)
[*] The spectrum was recorded in CDCl_3 ^{**} The spectrum was recorded in CD_2Cl_2 ^{***} The spectrum was recorded in CD_3CN ^{****} The spectrum was recorded in acetone- d_6				

As can be seen from the above Table, complexes of 10 different structural types have been prepared during this work, five of them with monophosphine ligands and five with diphosphine ligands. The yields of the complexes differ from very good (95%) to moderate

(52%). Syntheses of neutral two-coordinate gold(I) complexes with both mono- and diphosphine ligands are normally high yielding, while syntheses of three-coordinate complexes, particularly with bidentate ligands, are much less successful. This is in full agreement with the known preference of gold(I) for low coordination numbers (see Chapter I).

All the complexes obtained here are air-stable, microcrystalline materials. Most of them are also light-stable. However, the complexes containing phosphine ligands with polythiophene moieties are affected by light, especially in solution. Their prolonged exposure to light, while in contact with a polar solvent, results in discoloration within a few days, possibly as a result of ligand decomposition. (Exposure of a dichloromethane solution of [ClAuPSSS] to sunlight for a week did not produce any new peaks in the ^{31}P NMR spectrum, in the region characteristic of coordinated phosphorus species.)

The wide range of structural types of complexes synthesised during this work has ensured a wide range of polarities and hence, their solubility in various solvents. Neutral complexes containing two-coordinate gold(I) seem to be the least polar and the least soluble, with chlorinated hydrocarbons and DMSO being their solvents of choice. Such complexes are completely insoluble in alcohols and acetonitrile. Dinuclear complexes of this type with diphosphine ligands are considerably less soluble than their mononuclear analogues. Neutral complexes containing three-coordinate gold(I) are significantly more soluble than the related two-coordinate species, the solubility process most likely being aided by chemical reactions of the dissolved species (dissociation). The good solvents will include, together with chlorinated hydrocarbons, more polar acetone and aromatic hydrocarbons. These complexes are not soluble in aliphatic hydrocarbons. It is difficult to comment on the solubility of the four-coordinate gold(I) complex, [ClAu(PS)₃] ([13]), as upon dissolving it in any solvent (dichloromethane, acetone *etc.*) it could never be recovered.

The cationic complexes, being ionic in nature, are very different from the neutral ones as far as their solubility is concerned. However, amongst the different types of cationic complexes there is no significant difference in the solubility pattern (even complexes of the same cation containing counterions of different size *e.g.*, SbF_6^- and PF_6^- , do not show differences in solubility). All cationic complexes are soluble in dichloromethane, acetone and acetonitrile, but not in chloroform or hydrocarbons. They can also dissolve in

methanol, but the poor hydrophilic properties of the ligands do not make it possible for the complexes to dissolve in water.

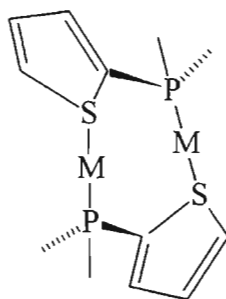
III.4.2 Conclusion

A wide range of gold(I) complexes with thienylphosphine ligands has been obtained during this work. The structural types prepared include (according to the classification given in Chapter I): mononuclear neutral with two-coordinate gold (*e.g.* [ClAuPSS]), mononuclear neutral with three-coordinate gold (*e.g.* [ClAu{PDS}₂]), mononuclear neutral with four-coordinate gold (*e.g.* [ClAu(PS)₃]), mononuclear cationic with two-coordinate gold (*e.g.* [Au{PNS}₂]{SbF₆}), dinuclear cationic with two-coordinate gold (*e.g.* [Au₂{μ-PNS}₂]{SbF₆}₂), dinuclear neutral with two-coordinate gold (*e.g.* [ClAu{μ-PSSP}AuCl]), dinuclear neutral with three-coordinate gold (*e.g.* [ClAu{μ-PSP}₂AuCl]), mononuclear cationic with two-coordinate gold ([Au{η¹-PSSSP}₂]{PF₆}), dinuclear cationic with two-coordinate gold ([Au₂{μ-PSP}₂]{PF₆}₂) and dinuclear cationic with three-coordinate gold ([Au₂{μ-PSP}₃]{PF₆}₂).

Five of the twenty seven complexes prepared were characterised structurally using X-ray analysis. Yet, amongst this wide range there is not one example of coordination by the thienylphosphine ligand either through a S-atom or via any other mode of thiophene coordination. In all cases the thienylphosphine coordinates through the P-atom (or atoms), with the thienyl group being merely a "spectator" substituent insofar as coordination to the metal is concerned. This is in contrast to the pyridine fragment, which can coordinate via nitrogen to gold(I). Although this could not be observed in any of the neutral complexes synthesised, this mode of coordination was present in the cationic complexes [Au₂{μ-PNS}₂]{SbF₆}₂ and [Au₂{μ-PNS}₂]{PF₆}₂.

The lack of coordination of thiophene to gold(I) in the thienylphosphine complexes can be attributed to several factors. Firstly, thiophene sulfur, although a "soft ligand", is a very weak donor, much weaker than sulfur in thiolates or mercapto compounds.²¹⁸ Thus it struggles to compete for coordination sites in the presence of stronger ligands such as chloride or phosphine. Secondly, gold(I) tends to form complexes with lower coordination numbers, with *n* = 2 being the most stable. Thus, after gold has already formed two bonds with phosphorus atoms (or P and Cl, or P and aliphatic S), it is quite unlikely for the metal

to expand its coordination number by coordinating to such a poor ligand as thiophene S, as this is not going to bring any gain in energy. Thirdly, in the case when there is an excess of gold ions over the phosphorus atoms and one might expect the thienylphosphine fragment to bridge via P and S, the coordination still does not occur as a result of the geometric constraints. It is described in the Section 1 of this Chapter, that coordinated thiophene sulfur forms an angle between the thiophene plane and the S-M vector; thus for a dinuclear complex to be formed the structure shown below would have to be formed and a considerable strain would have to be overcome. It should also be recalled (see Appendix B) that the conformation, in which the thiophene S points towards the phosphorus lone pair is sterically more demanding than the one where it is rotated around the P-C bond by 180° .



A good illustration of the difficulty for the thienylphosphine fragment to bridge is the $[\text{Au}_2\{\mu\text{-PSN}\}_2]\{\text{SbF}_6\}_2$ complex, where bridging between the two metal centres is achieved not via the P and S atoms, but via the P and N atoms, although the former pair are closer to each other.

To conclude, the thienylphosphine ligands synthesised during this project do not exhibit coordination to gold(I) via the thiophene sulfur; however this does not exclude the possibility of other ligands, combining thiophene and phosphine moieties in a different arrangement, to do so. Further research in this direction is definitely needed.

III.5 EXPERIMENTAL

All reactions involving synthesis of gold(I) complexes were carried out in air unless otherwise stated. The final products in nearly all cases were air-stable compounds. General experimental details and sources of chemicals are given in Appendix A. The elemental analyses, ^1H NMR, IR and UV-vis data for the complexes obtained are summarised in Section III.5.1.8.

III.5.1 Syntheses

III.5.1.1 Synthesis of neutral chlorogold(I) complexes with monophosphine ligands of the general formula $[\text{ClAuL}]$

General procedure for the synthesis of the chlorogold(I) complexes with $\text{L} = \text{PS}$ ([1]), PDS ([2]), PTS ([3]), PSBr ([4]), PSS ([5]) and PSSS ([6])

Tetrachloroauric acid, $\text{HAuCl}_4 \cdot 3\text{H}_2\text{O}$ (0.0394 g, 0.1 mmol) was dissolved in 15 ml water/ethanol/acetone mixture (4:1:1, v:v:v ratio). It was cooled down to 0°C and neat thiodiglycol (0.012 g, 0.1 mmol) was added slowly with stirring until the solution became colourless. The solution was stirred for 15 minutes until it reached room temperature. At that point, a solution containing 0.1 mmol of the ligand dissolved in 5 ml ethanol/acetone mixture (the composition was selected individually in each case depending on the solubility of the ligand) was added dropwise. The mixture was left to stir for 0.5 - 2 hours and then filtered. Where necessary, the volume of the mixture was reduced first and 10 ml methanol added to aid precipitation. The crude product was washed with 20 ml water/methanol (1:1, v:v ratio) mixture, filtered, washed with 5 ml cold methanol and dried under vacuum.

Yields [1]: 0.0465 g, 92%;
[2]: 0.0471 g, 89%;
[3]: 0.0447 g, 87%;
[4]: 0.0507 g, 88%;
[5]: 0.0454 g, 78%;
[6]: 0.0612 g, 92%.

Synthesis of the chlorogold(I) complexes with L = PSN ([7]) and PNS ([8])

Tetrachloroauric acid, $\text{HAuCl}_4 \cdot 3\text{H}_2\text{O}$ (0.197 g, 0.5 mmol) was dissolved in a mixture of 10 ml water and 4 ml acetone. To this solution 50 mg solid NaHCO_3 were added, the mixture was warmed up to 35°C , stirred for 10 minutes and then cooled to 0°C . The rest of the procedure was analogous to the described above.

Yields [7]: 0.2610 g, 90%;

[8]: 0.2753 g, 95%.

III.5.1.2 Synthesis of neutral chlorogold(I) complexes with monophosphine ligands of the general formula $[\text{ClAuL}_2]$

Synthesis of bis[diphenyl(2-thienyl)phosphine] chlorogold(I) $[\text{ClAu}(\text{PS})_2]$ ([9])

The complex $[\text{ClAuPS}]$ (0.332 g, 0.663 mmol) was dissolved in 5 ml of dichloromethane. Then a solution of 0.178 g (0.663 mmol) diphenyl(2-thienyl)phosphine (PS) in 1.5 ml dichloromethane was added and allowed to stir for 15 minutes. Hexane (10 ml) was added to the clear solution to the cloudiness point and the solution was left at -15°C for 72 hours. Crystals separated out; they were collected and dried under vacuum.

Yield [9]: 0.327 g, 64%.

Synthesis of chlorogold(I) complexes with L = PDS ([10]), PTS ([11]) and PSN ([12])

The relevant mononuclear two-coordinate chlorogold(I) complex $[\text{ClAuL}]$ (0.2 mmol) was dissolved in 4 ml of acetone and a solution of the corresponding ligand (0.2 mmol) in 2 ml acetone was added. The solution was stirred for 30 minutes, the volume of the solvent was reduced and the mixture cooled to -15°C . A white precipitate was collected and dried under vacuum.

Yield [10]: 0.128 g, 82%;

[11]: 0.139 g, 87%;

[12]: 0.151 g, 82%.

Alternative synthesis of bis{diphenyl[5-(2'-pyridyl)-2-thienyl]phosphine} chlorogold(I) $[\text{ClAu}(\text{PSN})_2]$ ([12])

Tetrachloroauric acid, $\text{HAuCl}_4 \cdot 3\text{H}_2\text{O}$ (0.0788 g, 0.2 mmol) was dissolved in a mixture of 10 ml water and 4 ml acetone. To this solution 20 mg solid NaHCO_3 were added, the mixture was warmed to 35°C and stirred for 10 minutes. It was subsequently cooled to 0°C

and neat thiodiglycol (0.024 g, 0.2 mmol) was added slowly with stirring until the solution became colourless. The solution was stirred for 15 minutes, allowing to reach room temperature. To this mixture a solution of 0.138 g (0.4 mmol) diphenyl[5-(2'-pyridyl)-2-thienyl]phosphine (PSN) in 10 ml acetone was added. The solution first turned murky, but then the precipitate gradually dissolved yielding clear slightly yellowish solution. It was added with stirring to concentrated aqueous NaCl solution, and an off-white precipitate separated. It was triturated with water, filtered and dried.

Yield [12]: 0.097 g, 53%.

III.5.1.3 Isolation of tris[diphenyl(2-thienyl)phosphine] chlorogold(I) $[\text{ClAu}(\text{PS})_3]$ ([13])

Triphenylphosphine chlorogold(I) (0.0989 g, 0.2 mmol) was dissolved in 0.2 ml CD_2Cl_2 (in a 5-mm NMR tube). To this solution 0.0536 g (0.2 mmol) solid diphenyl(2-thienyl)phosphine (PS) was added. The mixture was allowed to react for 1 hour, after which changes in the ^{31}P NMR could no longer be observed. After standing for 3 days at room temperature, large crystals precipitated out. They were analysed using X-ray crystallographic analysis and found to correspond to the solvate $[\text{ClAu}(\text{PS})_3] \cdot 2\text{CH}_2\text{Cl}_2$ {or $[\text{ClAu}(\text{PS})_3] \cdot 2\text{CD}_2\text{Cl}_2$ }.

III.5.1.4 Synthesis of cationic gold(I) complexes with monophosphine ligands

Synthesis of the mononuclear complexes of the general formula $[\text{Au}(\eta^1\text{-L})_2]\text{SbF}_6$, where L = PSN ([14]) and PNS ([16])

Nitrosyl hexafluoroantimonate (0.0665 g, 0.25 mmol) was dissolved in 10 ml dry oxygen-free acetonitrile under the atmosphere of dry nitrogen. Gold powder (0.0750 g, 0.38 mmol) was added to the solution and the mixture was stirred at ambient temperature for 16 hours. Excess of gold powder was carefully filtered off under nitrogen to leave a clear solution containing 0.25 mmol $[\text{Au}(\text{MeCN})_2]\text{SbF}_6$. This solution was added under nitrogen to 5 ml dichloromethane solution containing 0.5 mmol of the ligand (PSN or PNS: 0.1725 g). The mixture was stirred at ambient temperature for 2 hours. The solution was evaporated to dryness and the residue re-dissolved in a small amount of dichloromethane. Addition of hexane led to formation of a powdery precipitate.

Yield [14]: 0.177 g, 63%;

[16]: 0.208 g, 74%.

Synthesis of the dinuclear complex $[\text{Au}_2(\mu\text{-PSN})_2](\text{SbF}_6)_2$ ([15])

The general procedure described in the Section 5.1.4 was followed in order to obtain a solution containing 0.4 mmol $[\text{Au}(\text{MeCN})_2]\text{SbF}_6$. To this solution the PSN ligand (0.138 g, 0.4 mmol) dissolved in 15 ml dry oxygen-free acetonitrile was added with stirring. The mixture was stirred at ambient temperature for 2 hours, the volume reduced and ether added. The resulting white powder was recrystallised from dichloromethane/ether.

Yield [15]: 0.2770 g, 89%.

Synthesis of the dinuclear complex $[\text{Au}_2(\mu\text{-PNS})_2](\text{PF}_6)_2$ ([17])

Single crystals of diphenyl[6-(2'-thienyl)-2-pyridyl]phosphine chlorogold(I) (ClAuPNS) (0.0351 g, 0.06 mmol) were dissolved in 10 ml dry degassed THF and solid TiPF_6 (0.035 g, excess) added. The clear mixture was allowed to react at room temperature for one hour, then the solvent was removed and 8 ml acetonitrile added. The solution was filtered through microfibre filter. The volume of the filtrate was reduced and ether added. The off-white precipitate was recrystallised from dichloromethane/ether.

Yield [17]: 0.0412 g, 70%.

III.5.1.5 Synthesis of neutral bis[chlorogold(I)] complexes with diphosphine ligands

Synthesis of dinuclear bis[chlorogold(I)] complexes of the general formula $[\text{ClAu}(\mu\text{-LL})\text{AuCl}]$ with LL = PSP ([18]), PSSP ([19]), PSSSP ([20]), PSNP ([21]) and PSNSP ([22])

Tetrachloroauric acid, $\text{HAuCl}_4 \cdot 3\text{H}_2\text{O}$ (0.0394 g, 0.1 mmol) was dissolved in 15 ml water/acetone mixture (2:1, v:v ratio). It was cooled to 0°C and neat thiodiglycol (0.012 g, 0.1 mmol) was added slowly with stirring until the solution became colourless. The solution was stirred for 15 minutes, allowing to reach room temperature. At that point a solution containing 0.05 mmol of the ligand dissolved in 5 ml dichloromethane/ethanol mixture (normally 1:1 volume ratio) was added dropwise. Some acetone was added to the mixture on certain occasions to avoid separation into aqueous and organic phases. The solution was left to stir for 1 hour and then filtered. Wherever necessary, the volume of the mixture was reduced first and some methanol or ethanol added to aid precipitation. The crude product was washed with 2 x 10 ml water/methanol (1:1, v:v ratio) mixture, filtered, washed with 5 ml cold methanol and dried under vacuum.

Yield [18]: 0.0376 g, 82%;

[19]: 0.0375 g, 75%;

[20]: 0.0383 g, 71%;

[21]: 0.0427 g, 86%;

[22]: 0.0403 g, 75%.

Synthesis of neutral bis[chlorogold(I)] complexes of the general formula $[\text{ClAu}(\mu\text{-LL})_2]$, where LL = PSP ([23]) and PSSSP ([24])

The relevant dinuclear μ -bis[chlorogold(I)] complex $[\text{ClAu}(\mu\text{-LL})\text{AuCl}]$ (0.1 mmol) was dissolved in 5 ml dichloromethane and a solution of the corresponding ligand (0.1 mmol) in 5 ml dichloromethane was added. The solution was stirred for 30 minutes, the volume of the solvent was reduced and ether added to the cloudiness point. The mixture was cooled to -15°C and the precipitate collected and dried under vacuum.

Very low solubility of the complex formed (in analogous reaction) by the PSSSP ligand in chloroform (as well as dichloromethane and even DMSO) indicated formation of polymeric species as a result of this reaction. Elemental analysis of the product showed the composition to correspond to the empirical formula $[\text{ClAu}(\mu\text{-PSSSP})]_n$.

Yield [23]: 0.0578 g, 63%;

[24]: 0.0757 g, 70%.

III.5.1.6 Synthesis of cationic gold(I) complexes with diphosphine ligands

Synthesis of the mononuclear complex $[\text{Au}(\eta^1\text{-PSSSP})_2]\text{PF}_6$ ([25])

Tetrachloroauric acid, $\text{HAuCl}_4 \cdot 3\text{H}_2\text{O}$ (0.0394 g, 0.1 mmol) was dissolved in 12 ml water/acetone mixture (1:1, v:v ratio). It was cooled to 0°C and neat thiodiglycol (0.012 g, 0.1 mmol) was added slowly with stirring until the solution became colourless. The solution was stirred for 15 minutes, allowing to reach room temperature. A solution of the PSSSP ligand (0.1232 g, 0.2 mmol) in 10 ml dichloromethane/ethanol (1:1, v:v) was added slowly with stirring at that point, producing a clear mixture. A saturated aqueous solution of NH_4PF_6 (10 ml) was added to the mixture followed by 20-25 ml water/*iso*-propanol (2:1, v:v). The yellow precipitate was filtered off and triturated with 2 x 25 ml of distilled water, filtered again and dried.

Yield [25]: 0.1448 g, 92%.

Synthesis of the dinuclear complexes with the general formula $[\text{Au}_2(\mu\text{-PSP})_n](\text{PF}_6)_2$, where $n = 2$ ([26]), 3 ([27])

Tetrachloroauric acid, $\text{HAuCl}_4 \cdot 3\text{H}_2\text{O}$ (0.0788 g, 0.2 mmol) was dissolved in a mixture of 15 ml water and 15 ml acetone. It was cooled to 0°C and neat thiodiglycol (0.024 g, 0.2 mmol) was added slowly with stirring until the solution became colourless. The solution was allowed to stir for 15 minutes and to reach room temperature. A solution of the required amount 2,5-bis(diphenylphosphino)thiophene (PSP) (0.0908 g or 0.2 mmol, $n = 2$ and 0.136 g or 0.3 mmol, $n = 3$) in 20 ml acetone was added to the mixture and the temperature increased to 35°C . It was stirred at this temperature for 30 minutes, then cooled to ambient temperature and 20 ml *iso*-propanol were added. Saturated aqueous solution of NH_4PF_6 (25 ml) was added to precipitate the product. It was triturated with water and *iso*-propanol, washed thoroughly with water, filtered and dried.

Yield [26]: 0.165 g, 52%;

[27]: 0.224 g, 55%.

III.5.1.7 Synthesis of other cationic gold(I) complexes with diphosphine ligands

Attempted synthesis of the complex $[\text{ClAu}(\mu\text{-PSSSP})\text{Au}(\mu\text{-PSSSP})\text{AuCl}]\text{SbF}_6$

The complex $[\text{Au}(\eta^1\text{-PSSSP})_2]\text{PF}_6$ ([25], 0.0787 g, 0.05 mmol) was dissolved in 10 ml dichloromethane. To this solution $[\text{ClAu}(\text{tht})]$ (0.0321 g, 0.1 mmol) in 6 ml dichloromethane was added at once. The mixture was stirred for 15 minutes at room temperature, after which the solution was partially evaporated and ether added. The precipitate was filtered off and dried under vacuum.

Reaction of an excess of the cationic gold precursors $[\text{Au}(\text{RCN})_2]\text{X}$, where $\text{X} = \text{BF}_4$, $\text{R} = \text{Ph}$ and $\text{X} = \text{SbF}_6$, $\text{R} = \text{Me}$, with PSNP

METHOD A

Gold(I) bis(benzonitrile) tetrafluoroborate (0.245 g, 0.5 mmol: see Appendix A for preparation details) was dissolved in 10 ml dry, degassed acetonitrile. A solution of 0.0529 g (0.1 mmol) diphenyl{5-[2'-(6'-diphenylphosphino)pyridyl]-2-thienyl}-phosphine (PSNP) in 5 ml degassed dichloromethane was added. The mixture was stirred for one hour. After that the volume was reduced and degassed ether added. A white powdery precipitate was thoroughly triturated with ether to remove excess of the starting material. The product was filtered and dried. However after storing the product for 24 hours at -10°C , partial

decomposition to metallic gold was observed. The compound proved to be too labile to carry out normal characterisation procedures.

METHOD B

A solution containing 0.5 mmol $[\text{Au}(\text{MeCN})_2]\text{SbF}_6$ was obtained as described in section III.5.1.4. The rest of the procedure was exactly the same as described in Method A above, with $[\text{Au}(\text{MeCN})_2]\text{SbF}_6$ being used instead of $[\text{Au}(\text{PhCN})_2]\text{BF}_4$. The final product of the reaction was purified by recrystallisation from dry, degassed acetonitrile/ether. It was reasonably stable to allow some basic characterisation procedures to be carried out. Decomposition of the complex to metallic gold was observed after storing in the fridge for several days.

Yield: 0.112 g, 38% {based on the product formula as $[\text{Au}_3(\mu\text{-PSNP})(\text{MeCN})_3](\text{SbF}_6)_3$ }.

III.5.1.8 Characterisation data for the complexes [1]-[27]

Table III.20 Elemental analysis of the complexes

COMPLEX	Found (Calculated), %		
	C	H	N
[1]	38.20 (38.38)	2.43 (2.26)	-
[2]	33.04 (33.18)	1.97 (2.19)	-
[3]	28.12 (28.11)	1.59 (1.77)	-
[4]	33.00 (33.22)	1.93 (2.09)	-
[5]	40.98 (41.21)	2.24 (2.59)	-
[6]	43.29 (43.35)	2.29 (2.58)	-
[7]	43.63 (43.65)	2.64 (2.79)	2.34 (2.42)
[8]	43.64 (43.65)	2.67 (2.79)	2.18 (2.42)
[9]	50.43 (49.98)	3.54 (3.41)	-
[10]	42.71 (43.06)	2.68 (2.84)	-
[11]	36.98 (36.34)	2.44 (2.29)	-
[12]	54.18 (54.64)	3.22 (3.49)	2.81 (3.03)
[13]	49.56 (49.58)	3.34 (3.55)	-
[14]	45.21 (44.90)	3.12 (2.87)	2.63 (2.49)
[15]	32.90 (32.42)	2.01 (2.07)	1.99 (1.80)
[16]	44.86 (44.90)	2.95 (2.87)	2.30 (2.49)
[17]	36.72 (36.70)	2.29 (2.35)	1.86 (2.04)
[18]	36.96 (36.66)	2.37 (2.42)	-
[19]	38.27 (38.46)	2.24 (2.42)	-
[20]	39.97 (39.98)	2.08 (2.42)	-
[21]	39.77 (39.86)	2.33 (2.53)	1.36 (1.41)
[22]	40.90 (41.28)	2.27 (2.53)	1.30 (1.30)
[23]	48.37 (49.10)	3.09 (3.24)	-
[24]	50.72 (50.92)	3.09 (3.09)	-
[25]	54.31 (54.89)	3.40 (3.33)	-
[26]	43.01 (42.33)	2.89 (2.79)	-
[27]	48.98 (49.42)	3.26 (3.26)	-

Table III.21 ^1H and ^{31}P NMR spectroscopic data of the complexes (spectra recorded in CDCl_3 , unless otherwise stated)

Complex	$\delta^{31}\text{P}$, ppm	$\delta^1\text{H}$, ppm (J , Hz)
[1]	19.18 (s)	7.26 (ddd, $^4J_{\text{H-P}} = 1.38$, $^3J_{\text{H-H}} = 4.50$, $^3J_{\text{H-H}} = 3.65$; 1 H), 7.41-7.65 (m, 11 H), 7.82 (ddd, $^5J_{\text{H-P}} = 3.23$, $^3J_{\text{H-H}} = 4.42$, $^4J_{\text{H-H}} = 1.13$; 1 H)
[2]	5.77 (s)	7.25 (ddd, $^4J_{\text{H-P}} = 1.33$, $^3J_{\text{H-H}} = 4.90$, $^3J_{\text{H-H}} = 3.60$; 2 H), 7.42-7.70 (m, 7 H), 7.81 (ddd, $^5J_{\text{H-P}} = 3.33$, $^3J_{\text{H-H}} = 4.93$, $^4J_{\text{H-H}} = 1.18$; 2 H)
[3]	-6.41 (s)	7.24 (ddd, $^4J_{\text{H-P}} = 1.43$, $^3J_{\text{H-H}} = 4.86$, $^3J_{\text{H-H}} = 3.62$; 3 H), 7.63 (ddd, $^3J_{\text{H-P}} = 9.67$, $^3J_{\text{H-H}} = 3.66$, $^4J_{\text{H-H}} = 1.13$; 3 H), 7.81 (ddd, $^5J_{\text{H-P}} = 3.52$, $^3J_{\text{H-H}} = 4.89$, $^4J_{\text{H-H}} = 1.15$; 3 H)
[4]	18.85 (s)	7.15-7.37 (ABX system, $^4J_{\text{H-P}} = 1.56$, $^3J_{\text{H-P}} = 9.60$, $J_{\text{A-B}} = 3.84$; 2 H), 7.42-7.65 (m, 10 H)
[5]	19.43 (s)	7.03 (dd, $^3J_{\text{H-H}} = 5.13$, $^3J_{\text{H-H}} = 3.67$; 1 H), 7.22 (dd, $^3J_{\text{H-H}} = 3.66$, $^4J_{\text{H-H}} = 1.11$; 1 H), 7.26 (part of ABX system, $^4J_{\text{H-P}} = 1.49$, $J_{\text{A-B}} = 3.77$; 1 H), 7.31 (dd, $^3J_{\text{H-H}} = 5.10$, $^4J_{\text{H-H}} = 1.12$; 1 H), 7.43 (part of ABX system, $^3J_{\text{H-P}} = 9.17$, $J_{\text{A-B}} = 3.76$; 1 H), 7.46-7.70 (m, 10 H)
[6]	18.45 (s)	7.04 (dd, $^3J_{\text{H-H}} = 5.07$, $^3J_{\text{H-H}} = 3.64$; 1 H), 7.11 (m, 2 H), 7.19 (dd, $^3J_{\text{H-H}} = 3.59$, $^4J_{\text{H-H}} = 1.11$; 1 H), 7.22-7.27 (m, 2 H), 7.45 (part of ABX system, $^3J_{\text{H-P}} = 8.98$, $J_{\text{A-B}} = 3.75$; 1 H), 7.48-7.69 (m, 10 H)
[7]	20.63 (s)	7.22 (ddd, $^3J_{\text{H-H}} = 6.77$, $^3J_{\text{H-H}} = 4.86$, $^4J_{\text{H-H}} = 1.83$; 1 H), 7.40-7.80 (m, 14 H), 8.55 (m, 1 H)
[8]	31.32 (s)	7.10 (dd, $^3J_{\text{H-H}} = 3.73$, $^3J_{\text{H-H}} = 5.05$; 1 H), 7.40 (dd, $^3J_{\text{H-H}} = 5.09$, $^4J_{\text{H-H}} = 1.14$; 1 H), 7.43-7.56 (m, 7 H), 7.58 (dd, $^3J_{\text{H-H}} = 3.76$, $^4J_{\text{H-H}} = 1.16$; 1 H), 7.66-8.00 (m, 6 H)
[9]	11.02 (s)	7.17 (ddd, $^4J_{\text{H-P}} = 1.35$, $^3J_{\text{H-H}} = 4.92$, $^3J_{\text{H-H}} = 3.57$; 1 H), 7.33-7.59 (m, 11 H), 7.69 (ddd, $^5J_{\text{H-P}} = 2.01$, $^3J_{\text{H-H}} = 4.94$, $^4J_{\text{H-H}} = 1.12$; 1 H)
[10]	-2.98 (s)	7.17 (ddd, $^4J_{\text{H-P}} = 1.27$, $^3J_{\text{H-H}} = 4.82$, $^3J_{\text{H-H}} = 3.56$; 2 H), 7.33-7.60 (m, 7 H), 7.70 (ddd, $^5J_{\text{H-P}} = 2.03$, $^3J_{\text{H-H}} = 4.89$, $^4J_{\text{H-H}} = 1.15$; 2 H)
[11]	-15.93 (s)	7.16 (ddd, $^4J_{\text{H-P}} = 1.41$, $^3J_{\text{H-H}} = 4.93$, $^3J_{\text{H-H}} = 3.50$; 3 H), 7.54 (ddd, $^3J_{\text{H-P}} = 8.17$, $^3J_{\text{H-H}} = 3.54$, $^4J_{\text{H-H}} = 1.18$; 3 H), 7.70 (ddd, $^5J_{\text{H-P}} = 2.10$, $^3J_{\text{H-H}} = 4.96$, $^4J_{\text{H-H}} = 1.17$; 3 H)
[12]	10.56 (s)	7.18 (ddd, $^3J_{\text{H-H}} = 6.70$, $^3J_{\text{H-H}} = 4.85$, $^4J_{\text{H-H}} = 1.91$; 1 H), 7.31-7.72 (m, 14 H), 8.52 (m, 1 H)
[13] ^a	13.71 (s)	7.14 (ddd, $^4J_{\text{H-P}} = 1.32$, $^3J_{\text{H-H}} = 4.87$, $^3J_{\text{H-H}} = 3.66$; 1 H), 7.31-7.58 (m, 11 H), 7.63 (ddd, $^5J_{\text{H-P}} = 0.87$, $^3J_{\text{H-H}} = 4.82$, $^4J_{\text{H-H}} = 1.10$; 1 H)

Table III.21 continued...

[14]**	33.51 (s)	7.19 (dd, $^3J_{\text{H-P}} = 7.96$, $^3J_{\text{H-H}} = 3.77$; 1 H), 7.29 (ddd, $^3J_{\text{H-H}} = 7.07$, $^3J_{\text{H-H}} = 4.81$, $^4J_{\text{H-H}} = 1.49$; 1 H), 7.33-7.86 (m, 13 H), 8.46 (m, 1 H)
[15]**	19.13 (s)	7.49 (dd, $^3J_{\text{H-P}} = 7.36$, $^3J_{\text{H-H}} = 3.69$; 1 H), 7.59-7.84 (m, 10 H), 7.95 (ddd, $^3J_{\text{H-H}} = 7.57$, $^3J_{\text{H-H}} = 4.78$, $^4J_{\text{H-H}} = 1.57$; 1 H), 8.02 (dd, $^4J_{\text{H-P}} = 1.18$, $^3J_{\text{H-H}} = 3.92$; 1 H), 8.20-8.48 (m, 2 H), 8.91 (m, 1 H)
[16]***	45.82 (s)	7.01 (m, 1 H), 7.09 (dd, $^3J_{\text{H-H}} = 5.10$, $^3J_{\text{H-H}} = 3.73$; 1 H), 7.20-7.65 (m, 13 H), 7.49 (dd, $^3J_{\text{H-H}} = 3.73$, $^4J_{\text{H-H}} = 1.01$; 1 H)
[17]***	36.46 (s)	7.18 (dd, $^3J_{\text{H-H}} = 4.55$, $^3J_{\text{H-H}} = 4.11$; 1 H), 7.51-8.28 (m, 14 H), 7.91 (dd, $^3J_{\text{H-H}} = 3.63$, $^4J_{\text{H-H}} = 0.94$; 1 H)
[18]	19.92 (s)	7.35-7.66 (m, 22 H)
[19]	19.53 (s)	7.31 (part of ABX system, $^4J_{\text{H-P}} = 1.50$, $J_{\text{A-B}} = 3.82$; 2 H), 7.41 (part of ABX system, $^3J_{\text{H-P}} = 8.86$, $J_{\text{A-B}} = 3.79$; 2 H, $\text{H}_{\text{Th-4}}$), 7.45-7.67 (m, 20 H)
[20]	19.48 (s)	7.13 (s, 2 H), 7.27 (part of ABX system, $^4J_{\text{H-P}} = 1.47$, $J_{\text{A-B}} = 3.65$; 2 H), 7.42 (part of ABX system, $^3J_{\text{H-P}} = 9.00$, $J_{\text{A-B}} = 3.71$; 2 H), 7.46-7.69 (m, 20 H)
[21]	31.84 (s) & 19.47 (s), 1:1	7.38-7.97 (m, 25 H)
[22]	19.43 (s)	7.43-7.83 (m, 27 H, 20)
[23]	11.88 (s)	7.03 (br m, 2 H), 7.24-7.64 (m, 20 H)
[24]	13.42 (s)	6.80 (s, 2 H), 7.04-7.68 (m, 24 H)
[25]	26.5 (br s)	6.63 (s, 2 H), 7.03 (br d, $J = 3.64$; 2 H), 7.10-7.40 (m, 22 H)
[26]***	32.43 (s)	7.33 (br s, 2 H), 7.40-7.65 (m, 20 H)
[27]***	34.83 (s)	7.05 (br s, 2 H), 7.25-7.60 (m, 20 H)

* Spectra recorded in CD_2Cl_2 ** Spectra recorded in CD_3CN *** Spectra recorded in acetone- d_6

Table III.22 UV-vis parameters of the complexes (spectra recorded in dichloromethane, unless otherwise stated)

COMPLEX	λ_{max} , nm ($\epsilon \cdot 10^{-4}$, $\text{M}^{-1} \cdot \text{cm}^{-1}$)
[1]	233 (1.7), 261 (sh, 0.9), 269 (sh, 0.8), 275 (sh, 0.4)
[2]	237 (1.3), 266 (sh, 0.95), 276 (sh, 0.85)
[3]	241 (1.8), 267 (1.4)
[4]	230 (1.7), 272 (1.2), 277 (sh, 1.15)
[5]	232 (2.0), 266 (sh, 0.9), 276 (sh, 0.85), 329 (1.8)
[6]	232 (2.2), 266 (sh, 0.9), 275 (sh, 0.65), 377 (2.6)
[7]	231 (2.0), 267 (sh, 0.9), 277 (1.0), 316 (1.9)
[8]	234 (2.8), 269 (1.2), 277 (1.2), 300 (1.5), 315 (1.5)
[9]*	234 (2.9), 261 (sh, 2.2), 269 (sh, 2.0), 275 (sh, 1.5)
[10]*	236 (1.7), 266 (sh, 1.1), 274 (sh, 0.9)
[11]*	241 (3.5), 268 (2.3)
[12]*	231 (3.2), 266 (sh, 2.5), 276 (2.5), 316 (4.0)
[13]	not measured
[14]	231 (3.9), 270 (2.4), 276 (sh, 2.4), 317 (4.7)
[15]	234 (4.6), 270 (3.2), 276 (sh, 3.0), 315 (2.2)
[16]**	208 (8.0), 262 (3.4), 276 (sh, 3.1), 288 (2.9), 317 (2.7)
[17]	231 (3.8), 267 (sh, 1.7), 280 (sh, 1.8), 315 (sh, 1.3)
[18]	231 (3.4), 270 (1.7), 278 (1.8)
[19]	234 (3.0), 269 (1.0), 276 (1.0), 344 (2.4)
[20]	234 (4.2), 267 (sh, 1.2), 275 (sh, 1.0), 385 (3.8)
[21]	235 (3.4), 269 (1.0), 276 (1.0), 324 (2.1)
[22]	231 (2.3), 270 (1.0), 277 (1.1), 303 (1.5), 313 (sh, 1.3), 344 (1.2)
[23]*	230 (4.0), 269 (1.9), 276 (2.0)
[24]*	232 (4.0), 268 (sh, 1.5), 275 (sh, 1.3), 389 (4.1)
[25]	231 (3.6), 379 (3.3)
[26]	232 (7.6), 267 (sh, 4.1), 275 (sh, 3.9)
[27]	232 (9.0), 265 (sh, 5.4), 275 (sh, 4.5), 300 (sh, 1.8)

* It is unlikely that the measured spectra of these complexes belonged to three-coordinate species as the prepared dichloromethane solutions were highly diluted (concentration range for the complexes was within $2 \cdot 10^{-5}$ M) - see Sections 2.1.2 and 2.2.2 of this Chapter

** The spectrum was measured in acetonitrile

Table III.23 IR data for the complexes (spectra obtained as KBr disks)

COMPLEX	ν , cm^{-1}
[1]	498 (s), 510 (s), 542 (s), 573 (m), 690 (vs), 714 (s), 742 (s), 849 (m), 1000 (m), 1009 (m), 1026 (w), 1101 (vs), 1180 (w), 1220 (s), 1402 (m), 1434 (s), 1480 (m)
[2]	452 (m), 505 (vs), 534 (vs), 571 (s), 658 (m), 690 (s), 721 (vs), 740 (vs), 850 (m), 1008 (s), 1062 (w), 1099 (vs), 1220 (vs), 1331 (m), 1400 (s), 1434 (s), 1480 (m)
[3]	455 (m), 501 (s), 528 (s), 569 (m), 661 (m), 713 (vs), 738 (s), 748 (m), 852 (m), 1010 (s), 1060 (w), 1090 (m), 1220 (vs), 1331 (m), 1400 (s), 1496 (w)
[4]	503 (vs), 518 (s), 561 (m), 663 (m), 690 (vs), 702 (s), 708 (m), 748 (s), 806 (m), 962 (s), 999 (m), 1009 (m), 1101 (s), 1180 (w), 1209 (m), 1296 (m), 1400 (s), 1434 (s), 1481 (m)
[5]	490 (m), 517 (s), 540 (s), 692 (vs), 701 (s), 707 (s), 746 (m), 796 (m), 839 (m), 1004 (s), 1101 (s), 1182 (w), 1218 (w), 1419 (m), 1434 (s), 1480 (m)
[6]	480 (m), 517 (s), 538 (m), 549 (m), 692 (vs), 712 (m), 748 (m), 798 (s), 1002 (s), 1101 (s), 1184 (w), 1212 (w), 1425 (s), 1438 (s), 1456 (m), 1481 (w)
[7]	488 (m), 517 (s), 540 (s), 553 (m), 690 (vs), 702 (s), 714 (m), 744 (s), 777 (vs), 993 (m), 1016 (m), 1101 (s), 1184 (w), 1290 (w), 1424 (vs), 1437 (vs), 1465 (s), 1481 (m), 1563 (m), 1581 (s)
[8]	490 (w), 509 (s), 549 (vs), 690 (s), 703 (s), 714 (s), 744 (m), 800 (s), 1101 (m), 1228 (w), 1438 (s), 1446 (vs), 1481 (w), 1578 (m), 1590 (m)
[9]	507 (vs), 542 (m), 573 (m), 694 (vs), 719 (s), 743 (s), 850 (m), 999 (m), 1096 (s), 1182 (w), 1220 (s), 1333 (m), 1404 (m), 1435 (s), 1499 (m)
[10]	458 (s), 500 (s), 527 (m), 571 (m), 690 (s), 714 (s), 742 (m), 851 (m), 1010 (m), 1097 (vs), 1230 (s), 1328 (w), 1404 (m), 1437 (m), 1479 (m)
[11]	455 (m), 500 (s), 528 (m), 569 (s), 690 (m), 712 (vs), 742 (m), 849 (m), 1003 (s), 1085 (m), 1217 (s), 1331 (m), 1400 (s), 1437 (w), 1497 (m)
[12]	488 (m), 513 (s), 551 (m), 692 (vs), 714 (m), 743 (s), 775 (s), 991 (m), 1012 (m), 1097 (s), 1153 (w), 1290 (w), 1406 (s), 1425 (vs), 1435 (vs), 1454 (s), 1481 (m), 1529 (w), 1563 (m), 1581 (s)
[13]	not measured
[14]	482 (m), 507 (s), 551 (m), 573 (m), 658 (vs), 694 (s), 703 (m), 742 (s), 779 (s), 818 (m), 993 (m), 1097 (m), 1153 (w), 1184 (w), 1213 (w), 1425 (s), 1436 (s), 1458 (s), 1481 (m), 1556 (m), 1583 (s)

Table III.23 continued...

[15]	494 (w), 518 (s), 542 (m), 552 (s), 658 (vs), 694 (s), 701 (s), 715 (m), 754 (s), 781 (s), 999 (m), 1015 (m), 1102 (s), 1186 (w), 1258 (w), 1426 (s), 1442 (vs), 1476 (s), 1522 (m), 1566 (w), 1602 (s)
[16]	456 (m), 507 (s), 567 (w), 658 (vs), 690 (s), 712 (m), 746 (m), 800 (m), 1026 (w), 1099 (m), 1169 (w), 1284 (m), 1348 (w), 1419 (m), 1435 (s), 1440 (s), 1521 (m), 1550 (m), 1576 (s)
[17]	507 (s), 557 (vs), 690 (s), 701 (s), 714 (s), 746 (s), 835 (vs), 999 (w), 1102 (m), 1121 (m), 1147 (m), 1185 (w), 1270 (m), 1284 (m), 1310 (m), 1420 (w), 1438 (s), 1448 (s), 1484 (w), 1551 (m), 1577 (m), 1590 (m)
[18]	524 (s), 538 (s), 555 (s), 576 (m), 690 (vs), 701 (s), 714 (m), 748 (s), 814 (w), 999 (m), 1022 (s), 1101 (vs), 1184 (w), 1211 (m), 1436 (vs), 1481 (m)
[19]	507 (vs), 526 (m), 542 (s), 572 (w), 690 (vs), 701 (s), 712 (m), 748 (s), 804 (m), 1006 (s), 1101 (s), 1184 (w), 1215 (w), 1420 (m), 1435 (vs), 1481 (m)
[20]	498 (m), 520 (s), 542 (s), 588 (w), 690 (vs), 702 (s), 712 (m), 748 (s), 798 (s), 1001 (s), 1101 (s), 1183 (w), 1220 (w), 1425 (s), 1435 (s), 1481 (m)
[21]	478 (m), 513 (s), 543 (s), 570 (m), 630 (m), 690 (vs), 715 (m), 742 (s), 798 (m), 990 (m), 999 (m), 1022 (m), 1101 (s), 1182 (w), 1215 (w), 1388 (w), 1421 (s), 1437 (vs), 1448 (m), 1481 (m), 1553 (m), 1574 (s)
[22]	472 (w), 517 (vs), 544 (s), 638 (m), 690 (vs), 712 (m), 742 (s), 750 (s), 794 (s), 1000 (s), 1014 (s), 1101 (s), 1159 (m), 1182 (w), 1218 (w), 1267 (m), 1420 (s), 1434 (vs), 1458 (m), 1481 (m), 1562 (s), 1581 (m)
[23]	523 (s), 538 (s), 555 (s), 578 (m), 692 (vs), 746 (s), 812 (w), 1001 (m), 1017 (m), 1099 (s), 1184 (m), 1207 (m), 1435 (vs), 1481 (s)
[24]	507 (s), 522 (s), 551 (m), 692 (vs), 744 (s), 796 (m), 997 (s), 1026 (w), 1099 (s), 1184 (w), 1217 (w), 1420 (m), 1435 (s), 1479 (m)
[25]	509 (m), 558 (m), 692 (s), 744 (m), 798 (m), 839 (vs), 868 (m), 999 (m), 1097 (m), 1218 (w), 1424 (m), 1435 (s), 1479 (m)
[26]	526 (s), 557 (s), 690 (s), 708 (m), 744 (s), 837 (vs), 999 (m), 1018 (m), 1099 (s), 1186 (w), 1209 (m), 1280 (w), 1406 (w), 1437 (s), 1481 (m)
[27]	528 (m), 532 (m), 557 (s), 692 (s), 744 (m), 839 (vs), 999 (m), 1018 (s), 1097 (s), 1207 (w), 1436 (s), 1481 (w)

III.5.2 Crystal structure determinations

III.5.2.1 Single crystal X-ray diffraction study on chlorogold(I) diphenyl[5-(2,2'-bithienyl)]phosphine, [ClAuPSS] ([5])

Yellow rhombs of the [ClAuPSS] complex separated out upon standing from a cold water/acetone solution (in approximately 2:1 volume ratio). The crystallographic data were collected using an Enraf-Nonius CAD4 diffractometer (Appendix A). SHELXS-97²¹⁶ and SHELXL-97²¹⁷ were employed for the structure solution calculations (Appendix A). In the least-squares refinement, the hydrogen atoms were included as ideal contributors with standard idealisation parameters. As a result of considerable disorder in the thiophene groups, the constituent atoms were restrained to lie in a common plane (FLAT) and the bond lengths restrained to average C-C and C-S values (DFIX, SAME). Restraints on the anisotropic thermal factors (DELU, ISOR, SIMU) and refinement of the thiophene groups as parts did not improve the disorder. Hence the thiophene groups were refined isotropically. Crystallographic data are given in Table III.24, the non-hydrogen atomic coordinates in Table III.25, the hydrogen atomic coordinates in Table III.26, the anisotropic thermal factors in Table III.27, the interatomic distances in Table III.28 and the interatomic angles in Table III.29. The observed and calculated structure factors may be found on the disk in an envelope fixed to the inside back cover.

Table III.24 Crystal data and details of data collection and structure refinement [ClAuPSS] ([5])

Empirical formula	C ₂₀ H ₁₅ AuClPS ₂
Colour and description	Yellow rhomb
Crystal dimensions (mm)	0.50 x 0.12 x 0.08
Molecular mass (g·mol ⁻¹)	582.83
Crystal system	Monoclinic
Space Group	P2 ₁ /c
a (Å)	11.456(2)
b (Å)	13.487(2)
c (Å)	25.428(5)
α (°)	90
β (°)	90.551(16)

Table III.24 continued...

γ (°)	90
V (Å ³)	3928.6(13)
Z	8
D_c (g·cm ⁻³)	1.971
$F(000)$	2224
T (K)	293(2)
λ (Mo-K α) (Å)	0.71069
Scan mode	$\omega - 2\theta$
ω scan angle	$0.40 + 0.35\tan\theta$
Horizontal aperture width (mm)	$2.7 + 0.1\tan\theta$
Scattering range (°)	$2 \leq \theta \leq 23$
μ (mm ⁻¹)	7.920
Absorption corrections	Semi empirical
Measured intensities	6463
Unique intensities	5453
Unique intensities with $[I > 2\sigma(I)]$	3067
Structure solution	Direct & Fourier
Refinement method	Full-matrix least-squares on F^2
Weighting scheme	$1/[\sigma^2(F_o^2) + (0.1149P)^2 + 34.71P]$, where $P = 1/3 [\text{Max}(F_o^2, 0) + 2F_c^2]$
$R = \Sigma F_o - F_c / \Sigma F_o $	0.0826 $[I > 2\sigma(I)]$
	0.1619 (all data)
$wR = \{\Sigma[w(F_o^2 - F_c^2)^2] / \Sigma[wF_o^4]\}^{1/2}$	0.2055 $[I > 2\sigma(I)]$
	0.2384 (all data)
GooF on F^2	1.091
$(\Delta/\sigma)_{\max}$	0.002
$\Delta\rho_{\max}$ (eÅ ⁻³)	3.54 (Close to Au(I) centre)
Number of parameters	351
Number of restraints	48

Table III.25 Non-hydrogen atomic coordinates ($\times 10^4$) and isotropic thermal factors ($\text{\AA}^2 \times 10^3$) for [ClAuPSS] ([5])

	x	y	z	U(eq)
Au(1)	4051(1)	1384(1)	2374(1)	85(1)
Au(2)	1002(1)	1812(1)	5032(1)	70(1)
Cl(1)	5705(6)	1378(6)	1899(3)	106(2)
Cl(2)	-744(5)	1573(5)	4611(3)	86(2)
S(1)	1502(8)	3093(7)	3595(4)	128(3)
S(3)	2265(7)	3870(6)	6087(3)	97(2)
S(2)	2811(16)	5713(15)	4383(7)	250(8)
S(4)	3530(2)	6369(19)	6781(10)	346(13)
P(1)	2456(6)	1488(5)	2857(2)	76(2)
P(2)	2720(5)	2006(5)	5441(2)	64(2)
C(1)	2533(19)	2505(17)	3236(8)	100(9)
C(2)	3410(2)	3120(2)	3310(10)	132(12)
C(3)	3370(2)	3940(2)	3596(11)	122(11)
C(4)	2280(2)	4083(15)	3803(10)	108(9)
C(5)	2000(2)	4761(17)	4152(10)	130(12)
C(6)	910(2)	4920(2)	4359(11)	123(11)
C(7)	900(3)	5760(3)	4635(13)	178(17)
C(8)	1810(3)	6320(2)	4747(12)	169(16)
C(9)	2270(2)	466(16)	3305(8)	61(6)
C(10)	1420(2)	475(17)	3700(8)	71(7)
C(11)	1330(2)	-343(19)	4038(9)	79(7)
C(12)	2000(2)	-1145(17)	3959(11)	81(8)
C(13)	2840(2)	-1170(2)	3572(12)	90(8)
C(14)	2930(2)	-358(19)	3239(9)	78(7)
C(15)	1110(2)	1610(2)	2481(9)	74(7)
C(16)	350(3)	810(2)	2437(10)	98(9)

Table III.25 continued...

C(17)	-600(3)	890(3)	2110(12)	109(10)
C(18)	-820(3)	1750(3)	1832(12)	100(9)
C(19)	-40(2)	2530(3)	1881(11)	107(11)
C(20)	890(3)	2460(2)	2191(9)	89(9)
C(21)	3007(16)	3227(14)	5629(7)	62(6)
C(22)	3760(2)	3910(2)	5467(12)	144(13)
C(23)	3860(3)	4850(2)	5643(11)	153(14)
C(24)	3044(18)	4927(13)	6034(9)	76(7)
C(25)	2760(2)	5748(18)	6324(9)	91(8)
C(26)	1590(3)	6010(4)	6344(19)	660(11)
C(27)	1550(3)	6630(4)	6750(2)	430(6)
C(28)	2430(3)	7080(2)	6998(11)	123(11)
C(29)	2826(19)	1336(17)	6063(9)	60(6)
C(30)	3640(2)	1542(18)	6414(9)	72(7)
C(31)	3670(2)	950(3)	6868(10)	96(9)
C(32)	2920(3)	220(3)	6949(11)	98(9)
C(33)	2120(3)	10(2)	6602(13)	95(9)
C(34)	2090(3)	610(2)	6140(10)	88(8)
C(35)	3909(17)	1677(18)	5053(8)	65(6)
C(36)	3810(2)	1600(2)	4505(9)	79(7)
C(37)	4710(4)	1350(3)	4203(10)	142(15)
C(38)	5780(3)	1220(3)	4410(15)	123(12)
C(39)	5910(3)	1230(3)	4937(13)	115(12)
C(40)	5020(2)	1410(2)	5258(11)	103(10)

$$\underline{U}_{(eq)} = \frac{1}{3} \cdot \sum_i \sum_j \underline{U}_{ij} \mathbf{a}_i^* \mathbf{a}_j^* (\mathbf{a}_i \cdot \mathbf{a}_j)$$

Table III.26 Hydrogen atomic coordinates ($\times 10^4$) and isotropic thermal factors ($\text{\AA}^2 \times 10^3$) for [ClAuPSS] ([5]) (the numbering of the H atoms is done according to the numbering of the C atoms, to which the hydrogens are respectively attached)

	x	y	z	U(eq)
H(2)	4119	2971	3149	158
H(3)	3995	4370	3649	146
H(6)	266	4506	4311	147
H(7)	185	5968	4762	214
H(8)	1884	6872	4962	203
H(10)	924	1016	3737	86
H(11)	802	-329	4315	95
H(12)	1889	-1701	4170	97
H(13)	3335	-1711	3537	108
H(14)	3458	-380	2964	94
H(16)	483	236	2627	117
H(17)	-1110	349	2075	131
H(18)	-1481	1801	1617	120
H(19)	-173	3106	1692	129
H(20)	1401	2998	2215	107
H(22)	4277	3719	5206	173
H(23)	4369	5340	5526	184
H(26)	984	5805	6125	791
H(27)	806	6764	6885	513
H(28)	2442	7628	7222	147
H(30)	4168	2055	6363	87
H(31)	4241	1082	7122	115
H(32)	2972	-154	7256	118
H(33)	1592	-498	6653	114
H(34)	1532	476	5884	106

Table III.26 continued...

H(36)	3087	1724	4346	95
H(37)	4593	1258	3843	170
H(38)	6426	1125	4195	148
H(39)	6643	1106	5082	138
H(40)	5135	1356	5620	123

Table III.27 Anisotropic thermal factors ($\text{\AA}^2 \times 10^3$) for [ClAuPSS] ([5])

	U(11)	U(22)	U(33)	U(23)	U(13)	U(12)
Au(1)	91(1)	92(1)	72(1)	17(1)	-6(1)	-11(1)
Au(2)	67(1)	79(1)	65(1)	-15(1)	-8(1)	3(1)
Cl(1)	92(5)	110(6)	115(6)	27(5)	4(4)	-14(4)
Cl(2)	65(4)	107(5)	84(4)	-21(4)	-16(3)	4(4)
P(1)	97(5)	67(4)	62(4)	5(3)	-2(3)	-4(4)
P(2)	63(4)	66(4)	63(3)	-10(3)	-8(3)	2(3)
C(9)	83(16)	43(13)	57(13)	3(10)	9(12)	17(12)
C(10)	99(19)	57(15)	59(14)	-4(13)	10(13)	9(13)
C(11)	120(2)	68(17)	54(14)	-6(13)	10(13)	-4(16)
C(12)	100(2)	33(15)	100(2)	12(13)	-29(17)	-10(14)
C(13)	66(17)	90(2)	110(2)	-13(19)	2(16)	-4(15)
C(14)	110(2)	64(17)	64(15)	-1(13)	8(14)	-18(16)
C(15)	65(15)	90(2)	62(14)	-6(14)	3(11)	9(15)
C(16)	120(2)	100(2)	70(16)	25(16)	-45(17)	-30(2)
C(17)	130(3)	100(3)	100(2)	-10(2)	10(2)	0(2)
C(18)	80(2)	120(3)	90(2)	10(2)	9(16)	-20(2)
C(19)	76(19)	140(3)	110(2)	70(2)	11(17)	30(2)
C(20)	110(2)	80(2)	74(17)	24(15)	5(16)	45(17)
C(29)	59(14)	53(15)	69(15)	-2(12)	6(12)	4(12)

Table III.27 continued...

C(30)	89(18)	59(16)	68(16)	1(13)	14(14)	3(13)
C(31)	76(19)	140(3)	69(18)	-15(19)	-4(14)	20(2)
C(32)	100(2)	120(3)	71(19)	10(18)	17(17)	-20(2)
C(33)	90(2)	80(2)	120(2)	-5(19)	34(19)	-13(16)
C(34)	120(2)	65(18)	82(18)	25(15)	6(16)	19(17)
C(35)	39(11)	90(17)	68(15)	-12(13)	25(10)	-9(12)
C(36)	75(16)	110(2)	49(14)	-13(14)	-9(12)	-7(15)
C(37)	160(4)	220(4)	47(16)	-10(2)	30(2)	60(3)
C(38)	54(18)	180(4)	130(3)	-20(3)	10(19)	0(2)
C(39)	90(2)	160(3)	100(2)	-40(2)	-21(19)	50(2)
C(40)	48(14)	160(3)	96(19)	-50(2)	-19(14)	33(17)

The anisotropic thermal factor exponent takes the form:

$$-2\pi^2[h^2a^{*2}U(11) + \dots + 2hka^*b^*U(12)]$$

Table III.28 Interatomic distances (Å) for [ClAuPSS] ([5])

Au(1)-P(1)	2.217(7)	C(36)-C(37)	1.34(4)
Au(1)-Cl(1)	2.256(8)	C(37)-C(38)	1.35(4)
P(1)-C(1)	1.68(2)	C(38)-C(39)	1.35(4)
P(1)-C(9)	1.80(2)	C(39)-C(40)	1.33(4)
P(1)-C(15)	1.81(2)	S(1)-C(4)	1.688(15)
C(9)-C(14)	1.36(3)	S(1)-C(1)	1.696(14)
C(9)-C(10)	1.40(3)	C(1)-C(2)	1.322(15)
C(10)-C(11)	1.40(3)	C(2)-C(3)	1.325(15)
C(11)-C(12)	1.34(3)	C(3)-C(4)	1.373(15)
C(12)-C(13)	1.39(4)	C(4)-C(5)	1.31(3)
C(13)-C(14)	1.39(3)	S(3)-C(24)	1.688(14)
C(15)-C(16)	1.39(3)	S(3)-C(21)	1.689(13)
C(15)-C(20)	1.39(3)	C(21)-C(22)	1.332(15)
C(16)-C(17)	1.37(4)	C(22)-C(23)	1.350(16)
C(17)-C(18)	1.38(4)	C(23)-C(24)	1.375(15)
C(18)-C(19)	1.39(4)	C(24)-C(25)	1.37(3)
C(19)-C(20)	1.32(3)	S(2)-C(8)	1.688(15)
Au(2)-P(2)	2.232(6)	S(2)-C(5)	1.688(15)
Au(2)-Cl(2)	2.282(6)	S(2)-C(7)	2.29(3)
P(2)-C(21)	1.75(2)	C(5)-C(6)	1.379(15)
P(2)-C(35)	1.747(19)	C(6)-C(7)	1.328(15)
P(2)-C(29)	1.83(2)	C(7)-C(8)	1.316(16)
C(29)-C(34)	1.31(3)	C(25)-C(26)	1.384(16)
C(29)-C(30)	1.31(3)	C(25)-S(4)	1.676(15)
C(30)-C(31)	1.40(3)	S(4)-C(28)	1.677(15)
C(31)-C(32)	1.33(4)	S(4)-C(27)	2.30(4)
C(32)-C(33)	1.29(4)	C(26)-C(27)	1.339(16)
C(33)-C(34)	1.42(4)	C(27)-C(28)	1.332(16)
C(35)-C(36)	1.40(3)	C(35)-C(40)	1.42(3)

Table III.29 Interatomic angles (°) for [ClAuPSS] ([5])

P(1)-Au(1)-Cl(1)	176.3(3)	C(37)-C(38)-C(39)	118(3)
C(1)-P(1)-C(9)	105.6(11)	C(40)-C(39)-C(38)	123(3)
C(1)-P(1)-C(15)	105.6(11)	C(39)-C(40)-C(35)	121(3)
C(9)-P(1)-C(15)	107.2(12)	C(4)-S(1)-C(1)	99.9(12)
C(1)-P(1)-Au(1)	109.4(8)	C(2)-C(1)-P(1)	129.2(18)
C(9)-P(1)-Au(1)	114.0(8)	C(2)-C(1)-S(1)	99.5(18)
C(15)-P(1)-Au(1)	114.4(8)	P(1)-C(1)-S(1)	131.2(16)
C(14)-C(9)-C(10)	119(2)	C(1)-C(2)-C(3)	125(3)
C(14)-C(9)-P(1)	118.5(18)	C(2)-C(3)-C(4)	112(2)
C(10)-C(9)-P(1)	122.3(17)	C(5)-C(4)-C(3)	126(2)
C(11)-C(10)-C(9)	119(2)	C(5)-C(4)-S(1)	129(2)
C(12)-C(11)-C(10)	120(2)	C(3)-C(4)-S(1)	104.4(17)
C(11)-C(12)-C(13)	122(2)	C(24)-S(3)-C(21)	96.2(10)
C(14)-C(13)-C(12)	118(3)	C(22)-C(21)-S(3)	100.9(19)
C(9)-C(14)-C(13)	122(2)	C(22)-C(21)-P(2)	133.7(19)
C(16)-C(15)-C(20)	119(2)	S(3)-C(21)-P(2)	125.3(12)
C(16)-C(15)-P(1)	120(2)	C(21)-C(22)-C(23)	127(3)
C(20)-C(15)-P(1)	120(2)	C(22)-C(23)-C(24)	105(3)
C(17)-C(16)-C(15)	120(3)	C(25)-C(24)-C(23)	128(2)
C(16)-C(17)-C(18)	121(3)	C(25)-C(24)-S(3)	120.6(17)
C(17)-C(18)-C(19)	119(3)	C(23)-C(24)-S(3)	111.1(19)
C(20)-C(19)-C(18)	121(3)	C(8)-S(2)-C(5)	100.5(14)
C(19)-C(20)-C(15)	121(3)	C(8)-S(2)-C(7)	34.7(9)
P(2)-Au(2)-Cl(2)	178.6(2)	C(5)-S(2)-C(7)	65.9(10)
C(21)-P(2)-C(35)	104.3(10)	C(4)-C(5)-C(6)	126(2)
C(21)-P(2)-C(29)	102.6(10)	C(4)-C(5)-S(2)	129(2)
C(35)-P(2)-C(29)	108.6(11)	C(6)-C(5)-S(2)	104.3(18)
C(21)-P(2)-Au(2)	113.7(7)	C(7)-C(6)-C(5)	110(3)

Table III.29 continued...

C(35)-P(2)-Au(2)	113.4(8)	C(8)-C(7)-C(6)	126(3)
C(29)-P(2)-Au(2)	113.4(8)	C(8)-C(7)-S(2)	46.9(13)
C(34)-C(29)-C(30)	121(2)	C(6)-C(7)-S(2)	79.7(19)
C(34)-C(29)-P(2)	118(2)	C(7)-C(8)-S(2)	98(2)
C(30)-C(29)-P(2)	122(2)	C(24)-C(25)-C(26)	118(3)
C(29)-C(30)-C(31)	117(2)	C(24)-C(25)-S(4)	131(2)
C(32)-C(31)-C(30)	122(3)	C(26)-C(25)-S(4)	110(2)
C(33)-C(32)-C(31)	120(3)	C(25)-S(4)-C(28)	97.2(14)
C(32)-C(33)-C(34)	117(3)	C(25)-S(4)-C(27)	62.8(12)
C(29)-C(34)-C(33)	123(3)	C(28)-S(4)-C(27)	35.0(10)
C(36)-C(35)-C(40)	114(2)	C(27)-C(26)-C(25)	103(3)
C(36)-C(35)-P(2)	121.5(18)	C(28)-C(27)-C(26)	128(4)
C(40)-C(35)-P(2)	124.1(18)	C(28)-C(27)-S(4)	46.2(15)
C(37)-C(36)-C(35)	122(2)	C(26)-C(27)-S(4)	83(2)
C(36)-C(37)-C(38)	121(3)	C(27)-C(28)-S(4)	99(2)

III.5.2.2 Single crystal X-ray diffraction study on chlorogold(I) diphenyl[6-(2'-thienyl)-2-pyridyl]phosphine, [ClAuPNS] ([8])

Colourless crystals of [ClAuPNS] were grown from slow cooling of hexane/dichloromethane solution (in approximately 1:1 volume ratio). Data were collected using an Enraf-Nonius CAD4 diffractometer (Appendix A). SHELXS-97²¹⁶ and SHELXL-97²¹⁷ were employed for the structure solution calculations (Appendix A). In the least-squares refinement, the hydrogen atoms were included as ideal contributors with standard idealisation parameters. Crystallographic data are given in Table III.30, the non-hydrogen atomic coordinates in Table III.31, the hydrogen atomic coordinates in Table III.32, the anisotropic thermal factors in Table III.33, the interatomic distances in Table III.34 and the interatomic angles in Table III.35. The observed and calculated structure factors can be found on the disk in an envelope fixed to the inside back cover.

Table III.30 Crystal data and details of data collection and structure refinement for [ClAuPNS] ([8])

Empirical formula	C ₂₁ H ₁₆ AuClNPS
Colour and description	Colourless rhomb
Crystal dimensions (mm)	0.50 x 0.35 x 0.15
Molecular mass (g·mol ⁻¹)	577.79
Crystal system	Triclinic
Space Group	P $\bar{1}$
a (Å)	8.2680(15)
b (Å)	10.395(2)
c (Å)	11.860(2)
α (°)	105.443(15)
β (°)	95.501(15)
γ (°)	95.392(15)
V (Å ³)	970.4(3)
Z	2
D _c (g·cm ⁻³)	1.977
F(000)	552
T (K)	293(2)
λ (Mo-K α) (Å)	0.71069

Table III.30 continued...

Scan mode	$\omega - 2\theta$
ω scan angle	$0.60 + 0.35\tan\theta$
Horizontal aperture width (mm)	$2.7 + 0.1\tan\theta$
Scattering range ($^\circ$)	$2 \leq \theta \leq 23$
μ (mm^{-1})	7.913
Absorption corrections	Semi empirical
Measured intensities	3148
Unique intensities	2687
Unique intensities with $[I > 2\sigma(I)]$	2479
Structure solution	Direct & Fourier
Refinement method	Full-matrix least-squares on F^2
Weighting scheme	$1/[\sigma^2(F_o^2) + (0.028P)^2 + 0.443P]$, where $P = 1/3 [\text{Max}(F_o^2, 0) + 2F_c^2]$
Extinction coefficient	None
$R = \Sigma F_o - F_c / \Sigma F_o $	0.0187 $[I > 2\sigma(I)]$
	0.0226 (all data)
$wR = \{\Sigma[w(F_o^2 - F_c^2)^2] / \Sigma[wF_o^4]\}^{1/2}$	0.0480 $[I > 2\sigma(I)]$
	0.0491 (all data)
GooF on F^2	1.074
$(\Delta/\sigma)_{\text{max}}$	0.001
$\Delta\rho_{\text{max}}$ ($\text{e}\text{\AA}^{-3}$)	0.776
Number of parameters	235

Table III.31 Non-hydrogen atomic coordinates ($\times 10^4$) and isotropic thermal factors ($\text{\AA}^2 \times 10^3$) for [ClAuPNS] ([8])

	x	y	z	U(eq)
Au(1)	9823(1)	-1035(1)	6716(1)	44(1)
Cl(1)	8117(2)	165(1)	5902(1)	60(1)
P(1)	11422(1)	-2187(1)	7594(1)	39(1)
S(1)	15617(2)	-3294(1)	10603(1)	65(1)
N(1)	13184(4)	-1857(3)	9707(3)	38(1)
C(1)	12220(5)	-1237(4)	9113(4)	37(1)
C(2)	11869(5)	54(4)	9560(4)	42(1)
C(3)	12536(5)	727(4)	10711(4)	46(1)
C(4)	13503(5)	120(4)	11329(4)	43(1)
C(5)	13853(5)	-1191(4)	10804(4)	37(1)
C(6)	15016(5)	-1839(4)	11384(4)	39(1)
C(7)	15876(5)	-1361(4)	12575(4)	39(1)
C(8)	17002(6)	-2290(6)	12694(5)	62(1)
C(9)	16980(6)	-3343(5)	11739(5)	63(1)
C(10)	13198(5)	-2666(4)	6865(4)	40(1)
C(11)	13515(6)	-2229(4)	5905(4)	47(1)
C(12)	14867(7)	-2563(6)	5350(5)	65(1)
C(13)	15908(7)	-3336(6)	5745(5)	71(2)
C(14)	15593(6)	-3798(5)	6711(5)	61(1)
C(15)	14239(6)	-3461(4)	7270(4)	49(1)
C(16)	10375(5)	-3757(4)	7690(4)	40(1)
C(17)	9669(5)	-3881(4)	8671(4)	48(1)
C(18)	8766(6)	-5099(5)	8657(5)	56(1)
C(19)	8614(6)	-6165(5)	7693(5)	63(1)
C(20)	9324(6)	-6062(5)	6711(5)	63(1)
C(21)	10201(6)	-4865(4)	6699(4)	51(1)

Table III.32 Hydrogen atomic coordinates ($\times 10^4$) and isotropic thermal factors ($\text{\AA}^2 \times 10^3$) for [ClAuPNS] ([8]) (the numbering of the H atoms is done according to the numbering of the C atoms, to which the hydrogens are respectively attached)

	x	y	z	U(eq)
H(2)	11212	460	9111	51
H(3)	12313	1596	11052	55
H(4)	13942	565	12102	51
H(7)	15722	-593	13151	46
H(8)	17702	-2177	13385	75
H(9)	17644	-4023	11709	75
H(11)	12813	-1702	5627	56
H(12)	15071	-2260	4701	78
H(13)	16824	-3554	5371	85
H(14)	16293	-4332	6979	73
H(15)	14026	-3767	7917	59
H(17)	9793	-3156	9343	57
H(18)	8270	-5171	9312	67
H(19)	8027	-6974	7692	75
H(20)	9213	-6803	6051	76
H(21)	10672	-4800	6032	62

Table III.33 Anisotropic thermal factors ($\text{\AA}^2 \times 10^3$) for [ClAuPNS] ([8])

	U(11)	U(22)	U(33)	U(23)	U(13)	U(12)
Au(1)	45(1)	43(1)	45(1)	18(1)	-5(1)	8(1)
Cl(1)	59(1)	62(1)	69(1)	35(1)	-2(1)	18(1)
P(1)	41(1)	39(1)	37(1)	13(1)	-4(1)	5(1)
S(1)	80(1)	53(1)	57(1)	9(1)	-6(1)	22(1)
N(1)	41(2)	36(2)	36(2)	10(2)	-2(2)	4(2)
C(1)	33(2)	36(2)	38(2)	10(2)	1(2)	1(2)

Table III.33 continued...

C(2)	33(2)	42(2)	52(3)	14(2)	3(2)	6(2)
C(3)	46(3)	36(2)	52(3)	5(2)	4(2)	9(2)
C(4)	41(2)	43(2)	38(2)	1(2)	1(2)	6(2)
C(5)	35(2)	38(2)	37(2)	10(2)	4(2)	-3(2)
C(6)	41(2)	37(2)	37(2)	13(2)	2(2)	1(2)
C(7)	41(2)	42(2)	38(2)	18(2)	5(2)	11(2)
C(8)	61(3)	80(4)	48(3)	27(3)	-10(2)	9(3)
C(9)	69(3)	60(3)	62(3)	22(3)	-3(3)	26(3)
C(10)	40(2)	39(2)	36(2)	8(2)	-5(2)	-2(2)
C(11)	51(3)	45(2)	40(2)	10(2)	-3(2)	-4(2)
C(12)	66(3)	74(3)	51(3)	16(3)	10(3)	-6(3)
C(13)	54(3)	78(4)	66(4)	-5(3)	13(3)	-2(3)
C(14)	52(3)	62(3)	61(3)	4(3)	-2(3)	19(2)
C(15)	55(3)	49(3)	44(3)	12(2)	2(2)	11(2)
C(16)	38(2)	42(2)	39(2)	17(2)	-6(2)	5(2)
C(17)	47(2)	47(3)	52(3)	18(2)	4(2)	11(2)
C(18)	50(3)	62(3)	64(3)	33(3)	9(2)	5(2)
C(19)	49(3)	44(3)	94(4)	30(3)	-10(3)	-9(2)
C(20)	59(3)	48(3)	68(4)	6(3)	-18(3)	-9(2)
C(21)	56(3)	52(3)	41(3)	13(2)	-9(2)	-3(2)

The anisotropic thermal factor exponent takes the form:

$$-2\pi^2[h^2a^{*2}U(11) + \dots + 2hka^*b^*U(12)]$$

Table III.34 Interatomic distances (Å) for [ClAuPNS] ([8])

Au(1)-P(1)	2.2272(11)	C(7)-C(8)	1.427(7)
Au(1)-Cl(1)	2.2778(12)	C(8)-C(9)	1.347(7)
P(1)-C(16)	1.812(4)	C(10)-C(11)	1.372(6)
P(1)-C(10)	1.818(4)	C(10)-C(15)	1.386(6)
P(1)-C(1)	1.833(4)	C(11)-C(12)	1.376(7)
S(1)-C(9)	1.686(5)	C(12)-C(13)	1.363(8)
S(1)-C(6)	1.696(4)	C(13)-C(14)	1.392(8)
N(1)-C(1)	1.334(5)	C(14)-C(15)	1.382(7)
N(1)-C(5)	1.337(5)	C(16)-C(17)	1.380(7)
C(1)-C(2)	1.375(6)	C(16)-C(21)	1.394(6)
C(2)-C(3)	1.390(6)	C(17)-C(18)	1.403(6)
C(3)-C(4)	1.343(6)	C(18)-C(19)	1.350(7)
C(4)-C(5)	1.410(6)	C(19)-C(20)	1.377(8)
C(5)-C(6)	1.447(6)	C(20)-C(21)	1.384(7)
C(6)-C(7)	1.454(6)		

Table III.35 Interatomic angles (°) for [ClAuPNS] ([8])

P(1)-Au(1)-Cl(1)	177.02(4)	C(7)-C(6)-S(1)	112.5(3)
C(16)-P(1)-C(10)	104.41(19)	C(8)-C(7)-C(6)	107.1(4)
C(16)-P(1)-C(1)	105.72(19)	C(9)-C(8)-C(7)	115.5(4)
C(10)-P(1)-C(1)	105.99(18)	C(8)-C(9)-S(1)	112.6(4)
C(16)-P(1)-Au(1)	113.32(13)	C(11)-C(10)-C(15)	119.7(4)
C(10)-P(1)-Au(1)	114.68(14)	C(11)-C(10)-P(1)	119.5(3)
C(1)-P(1)-Au(1)	111.93(13)	C(15)-C(10)-P(1)	120.8(3)
C(9)-S(1)-C(6)	92.4(2)	C(10)-C(11)-C(12)	120.5(5)
C(1)-N(1)-C(5)	118.4(3)	C(13)-C(12)-C(11)	120.5(5)
N(1)-C(1)-C(2)	123.9(4)	C(12)-C(13)-C(14)	119.7(5)
N(1)-C(1)-P(1)	115.9(3)	C(15)-C(14)-C(13)	119.9(5)
C(2)-C(1)-P(1)	120.2(3)	C(14)-C(15)-C(10)	119.8(5)
C(1)-C(2)-C(3)	117.3(4)	C(17)-C(16)-C(21)	119.0(4)
C(4)-C(3)-C(2)	119.9(4)	C(17)-C(16)-P(1)	123.0(3)
C(3)-C(4)-C(5)	119.9(4)	C(21)-C(16)-P(1)	117.9(3)
N(1)-C(5)-C(4)	120.6(4)	C(16)-C(17)-C(18)	120.2(5)
N(1)-C(5)-C(6)	117.1(3)	C(19)-C(18)-C(17)	120.1(5)
C(4)-C(5)-C(6)	122.2(4)	C(18)-C(19)-C(20)	120.4(4)
C(5)-C(6)-C(7)	128.4(4)	C(19)-C(20)-C(21)	120.5(5)
C(5)-C(6)-S(1)	119.0(3)	C(20)-C(21)-C(16)	119.8(5)

III.5.2.3 Single crystal X-ray diffraction study on bis[phenyldi(2-thienyl)phosphine] chlorogold(I), [ClAu(PDS)₂] ([10])

The crystals of [ClAu(PDS)₂] were obtained by recrystallisation of the complex in acetone in the presence of the excess of the ligand. Data were collected using an Enraf-Nonius CAD4 diffractometer (Appendix A). SHELXS-97²¹⁶ and SHELXL-97²¹⁷ were employed for the structure solution calculations (Appendix A). These calculations indicated that both Au(1) and Cl(1) are located on a two-fold rotation axis (0,y,0). In the least-squares refinement, the hydrogen atoms were included as ideal contributors with standard idealisation parameters. The anisotropic thermal factor of S(1) was restrained to be approximately isotropic (ISOR) as a result of disorder in this atom. Crystallographic data are given in Table III.36, the non-hydrogen atomic coordinates in Table III.37, the hydrogen atomic coordinates in Table III.38, the anisotropic thermal factors in Table III.39, the interatomic distances in Table III.40 and the interatomic angles in Table III.41. The observed and calculated structure factors may be found on the disc in an envelope fixed to the inside back cover.

Table III.36 Crystal data and details of data collection and structure refinement for [ClAu(PDS)₂] ([10])

Empirical formula	C ₂₈ H ₂₂ AuClP ₂ S ₄
Colour and description	Colourless block
Crystal dimensions (mm)	0.23 x 0.38 x 0.31
Molecular mass (g·mol ⁻¹)	781.05
Crystal system	Monoclinic
Space Group	C2
a (Å)	17.610(6)
b (Å)	10.0917(16)
c (Å)	8.013(3)
α (°)	90
β (°)	100.68(3)
γ (°)	90
V (Å ³)	1399.5(7)
Z	2
D _c (g·cm ⁻³)	1.854

Table III.36 continued...

F(000)	760
T (K)	293(2)
λ (Mo-K α) (Å)	0.71069
Scan mode	$\omega - 2\theta$
ω scan angle	$0.47 + 0.35\tan\theta$
Horizontal aperture width (mm)	$2.7 + 0.1\tan\theta$
Scattering range (°)	$2 \leq \theta \leq 30$
μ (mm ⁻¹)	5.782
Absorption corrections	Semi empirical
Measured intensities	2822
Unique intensities	2365
Unique intensities with $[I > 2\sigma(I)]$	2318
Structure solution	Direct & Fourier
Refinement method	Full-matrix least-squares on F^2
Weighting scheme	$1/[\sigma^2(F_o^2) + (0.053P)^2]$, where $P = 1/3 [\text{Max}(F_o^2, 0) + 2F_c^2]$
Absolute structure parameter	0.024(9)
$R = \Sigma F_o - F_c / \Sigma F_o $	0.0297 $[I > 2\sigma(I)]$ 0.0322 (all data)
$wR = \{\Sigma[w(F_o^2 - F_c^2)^2] / \Sigma[wF_o^4]\}^{1/2}$	0.0764 $[I > 2\sigma(I)]$ 0.0780 (all data)
GooF on F^2	1.091
$(\Delta/\sigma)_{\max}$	0.000
$\Delta\rho_{\max}$ (eÅ ⁻³)	-1.07
Number of parameters	148

Table III.37 Non-hydrogen atomic coordinates ($\times 10^4$) and isotropic thermal factors ($\text{\AA}^2 \times 10^3$) for $[\text{ClAu}(\text{PDS})_2]$ ([10])

	x	y	z	U(eq)
Au(1)	0	0	0	37(1)
Cl(1)	0	-2546(3)	0	62(1)
S(1)	102(2)	3211(4)	2314(9)	128(2)
S(2)	1402	457	6074	67(1)
P(1)	977(1)	682(2)	2158(2)	35(1)
C(1)	938(4)	2399(7)	2712(9)	39(1)
C(2)	1611(5)	3274(6)	3454(11)	48(2)
C(3)	1246(7)	4575(11)	3547(12)	65(2)
C(4)	514(8)	4658(11)	3063(19)	88(4)
C(5)	1024	36	4099	73(2)
C(6)	930	-1462	4304	72(3)
C(7)	1115	-1940	6026	79(3)
C(8)	1355	-1002	7128	68(3)
C(9)	1934(3)	529(7)	1626(8)	38(1)
C(10)	2149(6)	1367(10)	373(11)	55(2)
C(11)	2866(7)	1228(12)	-49(14)	67(3)
C(12)	3350(4)	298(13)	689(11)	63(4)
C(13)	3162(5)	-532(13)	1903(13)	68(2)
C(14)	2470(5)	-406(9)	2336(10)	52(2)

$$U_{\text{(eq)}} = \frac{1}{3} \cdot \sum_i \sum_j U_{ij} a_i^* a_j^* (a_i \cdot a_j)$$

Table III.38 Hydrogen atomic coordinates ($\times 10^4$) and isotropic thermal factors ($\text{\AA}^2 \times 10^3$) for $[\text{ClAu}(\text{PDS})_2]$ ([10]) (the numbering of the H atoms is done according to the numbering of the C atoms, to which the hydrogens are respectively attached)

	x	y	z	U(eq)
H(2)	2129	3047	3773	58
H(3)	1539	5315	3946	78
H(4)	236	5436	3117	105
H(6)	766	-2021	3385	86
H(7)	1069	-2823	6324	94
H(8)	1480	-1113	8299	82
H(10)	1807	2006	-160	66
H(11)	3014	1787	-855	81
H(12)	3829	209	372	76
H(13)	3510	-1170	2414	82
H(14)	2342	-975	3154	63

Table III.39 Anisotropic thermal factors ($\text{\AA}^2 \times 10^3$) for $[\text{ClAu}(\text{PDS})_2]$ ([10])

	U(11)	U(22)	U(33)	U(23)	U(13)	U(12)
Au(1)	32(1)	44(1)	34(1)	0	0(1)	0
Cl(1)	91(2)	38(1)	56(2)	0	10(2)	0
S(1)	66(2)	75(2)	232(6)	-38(3)	-4(3)	18(2)
S(2)	102(2)	57(1)	38(1)	-1(1)	-1(1)	14(1)
P(1)	31(1)	37(1)	32(1)	0(1)	-2(1)	3(1)
C(1)	35(3)	36(3)	43(3)	-2(2)	0(2)	8(2)
C(2)	55(4)	25(3)	65(4)	-13(3)	14(3)	1(3)
C(3)	87(6)	50(4)	55(4)	-10(4)	10(4)	-11(4)
C(4)	87(7)	49(5)	124(11)	-4(5)	10(7)	25(5)
C(5)	41(3)	138(8)	38(3)	4(14)	2(2)	6(14)
C(6)	83(6)	84(7)	44(4)	17(4)	-3(4)	-25(6)

Table III.39 continued...

C(7)	98(8)	75(7)	63(6)	35(5)	16(5)	-4(6)
C(8)	80(6)	88(7)	38(3)	23(4)	13(4)	16(5)
C(9)	37(3)	41(3)	34(2)	-6(2)	2(2)	3(2)
C(10)	57(4)	63(5)	44(4)	4(3)	7(3)	5(4)
C(11)	70(6)	75(6)	64(5)	0(5)	30(5)	-10(5)
C(12)	48(3)	88(11)	56(4)	-21(5)	15(3)	-1(4)
C(13)	54(4)	76(5)	73(5)	-6(5)	10(4)	16(5)
C(14)	56(4)	46(3)	50(4)	7(3)	-3(3)	11(3)

The anisotropic thermal factor exponent takes the form:

$$-2\pi^2[h^2a^{*2}U(11) + \dots + 2hka^*b^*U(12)]$$

Table III.40 Interatomic distances (Å) for [ClAu(PDS)₂] ([10])

Au(1)-P(1)	2.3073(16)	C(3)-C(4)	1.279(15)
Au(1)-Cl(1)	2.569(3)	C(5)-C(6)	1.5328(2)
S(1)-C(1)	1.664(7)	C(6)-C(7)	1.4411(4)
S(1)-C(4)	1.690(13)	C(7)-C(8)	1.3100(2)
S(2)-C(5)	1.6547(5)	C(9)-C(14)	1.380(10)
S(2)-C(8)	1.7071(2)	C(9)-C(10)	1.416(11)
P(1)-C(5)	1.6742(16)	C(10)-C(11)	1.373(13)
P(1)-C(1)	1.793(7)	C(11)-C(12)	1.331(16)
P(1)-C(9)	1.819(6)	C(12)-C(13)	1.369(16)
C(1)-C(2)	1.509(10)	C(13)-C(14)	1.335(12)
C(2)-C(3)	1.469(13)		

Table III.41 Interatomic angles (°) for [ClAu(PDS)₂] ([10])

P(1)* refers to the phosphorous atom generated by symmetry

P(1)-Au(1)-P(1)*	145.31(8)	C(3)-C(4)-S(1)	113.2(8)
P(1)-Au(1)-Cl(1)	107.35(4)	C(6)-C(5)-S(2)	100.548(7)
P(1)*-Au(1)-Cl(1)	107.35(4)	C(6)-C(5)-P(1)	119.71(6)
C(1)-S(1)-C(4)	92.9(5)	S(2)-C(5)-P(1)	136.92(6)
C(5)-S(2)-C(8)	101.768(14)	C(7)-C(6)-C(5)	115.023(6)
C(5)-P(1)-C(1)	98.3(2)	C(8)-C(7)-C(6)	113.021(17)
C(5)-P(1)-C(9)	107.3(2)	C(7)-C(8)-S(2)	109.202(19)
C(1)-P(1)-C(9)	102.7(3)	C(14)-C(9)-C(10)	116.6(7)
C(5)-P(1)-Au(1)	118.79(8)	C(14)-C(9)-P(1)	123.6(6)
C(1)-P(1)-Au(1)	114.6(2)	C(10)-C(9)-P(1)	119.7(6)
C(9)-P(1)-Au(1)	113.2(2)	C(11)-C(10)-C(9)	119.5(8)
C(2)-C(1)-S(1)	112.9(5)	C(12)-C(11)-C(10)	120.3(9)
C(2)-C(1)-P(1)	126.9(5)	C(11)-C(12)-C(13)	121.9(8)
S(1)-C(1)-P(1)	120.2(4)	C(14)-C(13)-C(12)	118.6(9)
C(3)-C(2)-C(1)	103.0(7)	C(13)-C(14)-C(9)	123.1(9)
C(4)-C(3)-C(2)	118.0(9)		

III.5.2.4 Single crystal X-ray diffraction study on tris[diphenyl(2-thienyl)phosphine]chlorogold(I) bis(dichloromethane) solvate, $[\text{ClAu}(\text{PS})_3] \cdot 2\text{CH}_2\text{Cl}_2$ ([13])

The crystals of $[\text{ClAu}(\text{PS})_3] \cdot 2\text{CH}_2\text{Cl}_2$ precipitated from the concentrated deuterated-dichloromethane solution containing $[\text{ClAuPPh}_3]$ and PS (Section III.2.1.3). Data were collected using an Enraf-Nonius CAD4 diffractometer (Appendix A). SHELXS-97²¹⁶ and SHELXL-97²¹⁷ were employed for the structure solution calculations (Appendix A). The least-squares refinement indicated considerable disorder in this molecule. On anisotropic refinement of the C and S atoms, the majority became non-positive definite. Hence only the Au, P and Cl atoms were refined anisotropically. In addition, the constituent atoms of each of the phenyl and thiophene rings were restrained to lie in a common plane (FLAT), each of the phenyl rings was fitted to a regular hexagon (AFIX) and the bond lengths of the thiophene rings were restrained to average C-C and C-S values (DFIX). The hydrogen atoms were included as ideal contributors with standard idealisation parameters. Crystallographic data are given in Table III.42, the non-hydrogen atomic coordinates in Table III.43, the hydrogen atomic coordinates in Table III.44, the anisotropic thermal factors in Table III.45, the interatomic distances in Table III.46 and the interatomic angles in Table III.47. The observed and calculated structure factors may be found on the disk in an envelope fixed to the inside back cover.

Table III.42 Crystal data and details of data collection and structure refinement for $[\text{ClAu}(\text{PS})_3] \cdot 2\text{CH}_2\text{Cl}_2$ ([13])

Empirical formula	$\text{C}_{50}\text{H}_{43}\text{AuCl}_5\text{P}_3\text{S}_3$
Colour and description	Off-white (translucent) block
Crystal dimensions (mm)	0.35 x 0.12 x 0.23
Molecular mass ($\text{g} \cdot \text{mol}^{-1}$)	1207.15
Crystal system	Monoclinic
Space Group	$\text{P2}_1/\text{n}$
a (Å)	11.248(4)
b (Å)	22.578(7)
c (Å)	20.326(14)
α (°)	90
β (°)	94.12(5)
γ (°)	90

Table III.42 continued...

V (Å ³)	5148(4)
Z	4
D _c (g·cm ⁻³)	1.557
F(000)	2400
T (K)	293(2)
λ (Mo-K _α) (Å)	0.71069
Scan mode	ω - 2θ
ω scan angle	0.42 + 0.35tanθ
Horizontal aperture width (mm)	2.7 + 0.1tanθ
Scattering range (°)	2 ≤ θ ≤ 23
μ (mm ⁻¹)	3.365
Absorption corrections	Semi empirical
Measured intensities	7170
Unique intensities	6942
Unique intensities with [I > 2σ(I)]	335
Structure solution	Direct & Fourier
Refinement method	Full-matrix least-squares on F ²
Weighting scheme	1/[σ ² (F _o ²) + (0.111P) ² + 560.76P], where P = 1/3[Max(F _o ² , 0) + 2F _c ²]
R = Σ F _o - F _c / Σ F _o	0.1192 [I > 2σ(I)]
	0.2627 (all data)
wR = {Σ[w(F _o ² - F _c ²) ²] / Σ[wF _o ⁴]} ^{1/2}	0.2644 [I > 2σ(I)]
	0.3980 (all data)
GooF on F ²	1.035
(Δ/σ) _{max}	-0.001
Δρ _{max} (eÅ ⁻³)	4.37 (Close to Au(I) centre)
Number of parameters	258
Restraints	39

Table III.43 Non-hydrogen atomic coordinates ($\times 10^4$) and isotropic thermal factors ($\text{\AA}^2 \times 10^3$) for $[\text{ClAu}(\text{PS})_3] \cdot 2\text{CH}_2\text{Cl}_2$ ([13])

	x	y	z	U(eq)
Au(1)	1028(1)	2289(1)	196(1)	45(1)
Cl(1)	2102(9)	3085(4)	1093(5)	61(3)
Cl(2)	9010(2)	260(9)	5917(10)	167(8)
Cl(3)	10495(18)	938(10)	6814(11)	166(7)
Cl(4)	6366(18)	959(8)	7616(9)	152(7)
Cl(5)	4990(3)	139(9)	6861(9)	209(12)
S(1)	130(2)	1094(12)	2133(11)	187(9)
S(2)	4520(2)	871(11)	580(13)	200(10)
S(3)	-330(2)	2174(11)	-1655(13)	208(11)
P(1)	-312(8)	1756(4)	817(5)	50(2)
P(2)	2851(8)	1831(4)	-49(4)	45(2)
P(3)	355(8)	3070(4)	-544(5)	50(2)
C(1)	380(3)	1150(14)	1325(12)	56(10)
C(2)	-1210(3)	2149(13)	1391(15)	46
C(3)	-1410(3)	1358(15)	252(16)	52
C(4)	3590(2)	1452(12)	637(13)	41(8)
C(5)	4010(2)	2342(11)	-333(13)	30
C(6)	2630(3)	1275(15)	-708(16)	55
C(7)	-590(2)	2803(12)	-1234(13)	44(8)
C(8)	1480(3)	3497(13)	-926(15)	38
C(9)	-520(3)	3607(17)	-197(16)	56
C(10)	1110(3)	711(13)	1150(17)	58(10)
C(11)	1490(4)	352(19)	1660(2)	107(17)
C(12)	1070(4)	501(18)	2270(2)	130(2)
C(13)	-2430(3)	2076(14)	1427(16)	59

Table III.43 continued...

C(14)	-3010(3)	2417(13)	1861(14)	47
C(15)	-2460(3)	2812(15)	2250(16)	53
C(16)	-1300(4)	2870(19)	2220(2)	81
C(17)	-660(4)	2583(17)	1786(18)	71
C(18)	-1720(2)	765(12)	360(13)	28
C(19)	-2540(3)	507(17)	-55(16)	59
C(20)	-3060(3)	769(16)	-557(17)	54
C(21)	-2800(4)	1369(19)	-670(2)	75
C(22)	-1930(3)	1637(17)	-237(17)	55
C(23)	3580(3)	1565(17)	1285(14)	79(13)
C(24)	4250(3)	1240(16)	1740(2)	82(13)
C(25)	4900(4)	805(19)	1414(15)	109(17)
C(26)	3950(3)	2519(12)	-959(15)	42
C(27)	4930(4)	2934(18)	-1130(2)	90
C(28)	5690(4)	3065(18)	-640(2)	77
C(29)	5670(5)	2890(2)	-60(3)	105
C(30)	4880(3)	2516(15)	139(19)	60
C(31)	3550(3)	1070(13)	-1157(14)	41
C(32)	3310(6)	720(2)	-1590(3)	127
C(33)	2250(4)	519(19)	-1670(2)	81
C(34)	1370(4)	642(18)	-1350(2)	74
C(35)	1440(2)	1006(11)	-815(12)	25
C(36)	-1590(2)	3042(15)	-1551(14)	55(9)
C(37)	-2140(4)	2763(17)	-2074(17)	103(16)
C(38)	-1540(3)	2235(19)	-2208(18)	85(13)
C(39)	1510(3)	3596(13)	-1617(16)	47
C(40)	2280(3)	3935(14)	-1858(18)	52
C(41)	3080(3)	4192(14)	-1448(16)	47
C(42)	3150(3)	4143(17)	-819(19)	65

Table III.43 continued...

C(43)	2380(2)	3791(12)	-512(14)	30
C(44)	-1200(2)	3487(14)	379(14)	40
C(45)	-1860(4)	3890(3)	640(3)	118
C(46)	-1980(4)	4450(2)	390(2)	93
C(47)	-1410(3)	4590(2)	-73(19)	72
C(48)	-670(4)	4210(2)	-420(2)	102
C(49)	9580(5)	940(3)	6120(3)	118(19)
C(50)	5860(6)	750(3)	6840(3)	140(2)

$$\underline{U}_{(eq)} = \frac{1}{3} \cdot \sum_i \sum_j \underline{U}_{ij} \mathbf{a}_i \cdot \mathbf{a}_j (\mathbf{a}_i \cdot \mathbf{a}_j)$$

Table III.44 Hydrogen atomic coordinates ($\times 10^4$) and isotropic thermal factors ($\text{\AA}^2 \times 10^3$) for $[\text{ClAu}(\text{PS})_3] \cdot 2\text{CH}_2\text{Cl}_2$ ([13]) (the numbering of the H atoms is done according to the numbering of the C atoms, to which the hydrogens are respectively attached)

	x	y	z	U(eq)
H(10)	1336	661	722	70
H(11)	1985	29	1600	128
H(12)	1264	314	2672	161
H(13)	-2843	1800	1161	71
H(14)	-3827	2367	1881	56
H(15)	-2882	3042	2534	64
H(16)	-898	3124	2522	97
H(17)	140	2676	1750	85
H(18)	-1359	555	714	33
H(19)	-2756	117	25	70
H(20)	-3593	565	-844	65
H(21)	-3193	1578	-1018	90
H(22)	-1719	2029	-307	66
H(23)	3117	1872	1428	95

Table III.44 continued...

H(24)	4283	1296	2189	98
H(25)	5423	532	1615	131
H(26)	3358	2394	-1269	51
H(27)	4978	3087	-1548	108
H(28)	6316	3316	-727	93
H(29)	6254	3024	252	126
H(30)	4908	2377	571	72
H(31)	4317	1218	-1097	50
H(32)	3895	592	-1864	152
H(33)	2113	248	-2015	98
H(34)	640	478	-1490	89
H(35)	817	1075	-550	30
H(36)	-1892	3399	-1405	66
H(37)	-2820	2900	-2312	123
H(38)	-1760	1966	-2541	101
H(39)	942	3410	-1902	57
H(40)	2278	3998	-2310	63
H(41)	3651	4429	-1631	56
H(42)	3730	4353	-567	78
H(43)	2435	3743	-56	36
H(44)	-1166	3110	565	49
H(45)	-2262	3793	1009	141
H(46)	-2487	4716	571	111
H(47)	-1478	4977	-213	87
H(48)	-284	4350	-779	123
H(49a)	10012	1084	5756	142
H(49b)	8924	1210	6175	142
H(50a)	5397	1074	6636	170
H(50b)	6527	674	6583	170

Table III.45 Anisotropic thermal factors ($\text{\AA}^2 \times 10^3$) for $[\text{ClAu}(\text{PS})_3] \cdot 2\text{CH}_2\text{Cl}_2$ ([13])

	U(11)	U(22)	U(33)	U(23)	U(13)	U(12)
Au(1)	36(1)	45(1)	57(1)	1(1)	20(1)	0(1)
Cl(1)	66(6)	58(6)	60(6)	-17(5)	5(5)	-8(5)
Cl(2)	200(2)	134(16)	155(16)	12(13)	-56(14)	8(14)
Cl(3)	151(16)	160(18)	183(19)	-18(14)	-12(14)	-4(14)
Cl(4)	203(19)	118(13)	127(13)	9(11)	-47(13)	-28(13)
Cl(5)	400(4)	109(14)	119(14)	-15(11)	12(18)	-56(19)
P(1)	37(5)	44(5)	74(7)	-1(5)	30(5)	-3(4)
P(2)	35(5)	45(5)	58(6)	-4(4)	25(4)	5(4)
P(3)	41(6)	45(5)	67(6)	3(5)	27(5)	1(4)

The anisotropic thermal factor exponent takes the form:

$$-2\pi^2[h^2a^{*2}U(11) + \dots + 2hka^*b^*U(12)]$$

Table III.46 Interatomic distances (\AA) for $[\text{ClAu}(\text{PS})_3] \cdot 2\text{CH}_2\text{Cl}_2$ ([13])

Au(1)-P(1)	2.363(8)	C(3)-C(22)	1.28(5)
Au(1)-P(2)	2.380(8)	C(3)-C(18)	1.40(4)
Au(1)-P(3)	2.405(10)	C(18)-C(19)	1.34(4)
Au(1)-Cl(1)	2.776(9)	C(19)-C(20)	1.28(5)
P(1)-C(2)	1.83(3)	C(20)-C(21)	1.41(5)
P(1)-C(1)	1.85(3)	C(21)-C(22)	1.41(5)
P(1)-C(3)	1.86(4)	C(5)-C(26)	1.33(4)
P(2)-C(4)	1.79(3)	C(5)-C(30)	1.38(4)
P(2)-C(6)	1.84(4)	C(26)-C(27)	1.50(5)
P(2)-C(5)	1.86(3)	C(27)-C(28)	1.31(6)
P(3)-C(9)	1.74(4)	C(28)-C(29)	1.24(6)
P(3)-C(7)	1.80(3)	C(29)-C(30)	1.30(6)
P(3)-C(8)	1.81(3)	C(6)-C(35)	1.47(4)

Table III.46 continued...

C(1)-C(10)	1.351(19)	C(6)-C(31)	1.50(4)
C(1)-S(1)	1.691(18)	C(31)-C(32)	1.21(6)
S(1)-C(12)	1.716(19)	C(32)-C(33)	1.27(6)
C(10)-C(11)	1.353(19)	C(33)-C(34)	1.25(5)
C(11)-C(12)	1.41(2)	C(34)-C(35)	1.37(5)
C(4)-C(23)	1.341(19)	C(8)-C(39)	1.42(4)
C(4)-S(2)	1.692(18)	C(8)-C(43)	1.43(4)
S(2)-C(25)	1.724(19)	C(39)-C(40)	1.28(4)
C(23)-C(24)	1.358(19)	C(40)-C(41)	1.32(4)
C(24)-C(25)	1.406(19)	C(41)-C(42)	1.28(5)
C(7)-C(36)	1.369(19)	C(42)-C(43)	1.36(4)
C(7)-S(3)	1.695(18)	C(9)-C(48)	1.44(6)
S(3)-C(38)	1.707(19)	C(9)-C(44)	1.47(4)
C(36)-C(37)	1.347(19)	C(44)-C(45)	1.31(6)
C(37)-C(38)	1.407(19)	C(45)-C(46)	1.35(7)
C(2)-C(17)	1.38(5)	C(46)-C(47)	1.22(5)
C(2)-C(13)	1.39(5)	C(47)-C(48)	1.41(6)
C(13)-C(14)	1.37(5)	C(49)-Cl(3)	1.69(6)
C(14)-C(15)	1.31(4)	C(49)-Cl(2)	1.70(6)
C(15)-C(16)	1.32(5)	C(50)-Cl(5)	1.69(6)
C(16)-C(17)	1.35(5)	C(50)-Cl(4)	1.70(6)

Table III.47 Interatomic angles (°) for [ClAu(PS)₃] \cdot 2CH₂Cl₂ ([13])

P(1)-Au(1)-P(2)	118.9(3)	C(14)-C(13)-C(2)	119(3)
P(1)-Au(1)-P(3)	121.5(3)	C(15)-C(14)-C(13)	123(4)
P(2)-Au(1)-P(3)	115.1(3)	C(14)-C(15)-C(16)	118(4)
P(1)-Au(1)-Cl(1)	104.1(3)	C(15)-C(16)-C(17)	124(4)
P(2)-Au(1)-Cl(1)	94.5(3)	C(16)-C(17)-C(2)	119(4)
P(3)-Au(1)-Cl(1)	92.2(3)	C(22)-C(3)-C(18)	119(3)
C(2)-P(1)-C(1)	103.4(13)	C(22)-C(3)-P(1)	119(3)
C(2)-P(1)-C(3)	104.9(14)	C(18)-C(3)-P(1)	122(3)
C(1)-P(1)-C(3)	102.8(15)	C(19)-C(18)-C(3)	119(3)
C(2)-P(1)-Au(1)	119.8(10)	C(20)-C(19)-C(18)	123(4)
C(1)-P(1)-Au(1)	114.5(10)	C(19)-C(20)-C(21)	120(4)
C(3)-P(1)-Au(1)	109.7(11)	C(20)-C(21)-C(22)	117(4)
C(4)-P(2)-C(6)	105.8(14)	C(3)-C(22)-C(21)	122(4)
C(4)-P(2)-C(5)	104.2(13)	C(26)-C(5)-C(30)	124(3)
C(6)-P(2)-C(5)	104.9(14)	C(26)-C(5)-P(2)	120(2)
C(4)-P(2)-Au(1)	113.7(9)	C(30)-C(5)-P(2)	116(2)
C(6)-P(2)-Au(1)	112.1(12)	C(5)-C(26)-C(27)	115(3)
C(5)-P(2)-Au(1)	115.3(9)	C(28)-C(27)-C(26)	115(4)
C(9)-P(3)-C(7)	103.2(14)	C(29)-C(28)-C(27)	126(5)
C(9)-P(3)-C(8)	103.7(15)	C(28)-C(29)-C(30)	124(6)
C(7)-P(3)-C(8)	103.7(14)	C(29)-C(30)-C(5)	116(4)
C(9)-P(3)-Au(1)	114.7(12)	C(35)-C(6)-C(31)	116(3)
C(7)-P(3)-Au(1)	112.5(10)	C(35)-C(6)-P(2)	118(2)
C(8)-P(3)-Au(1)	117.4(10)	C(31)-C(6)-P(2)	126(3)
C(10)-C(1)-S(1)	110(3)	C(32)-C(31)-C(6)	122(4)
C(10)-C(1)-P(1)	129(2)	C(31)-C(32)-C(33)	119(6)
S(1)-C(1)-P(1)	120.3(18)	C(34)-C(33)-C(32)	128(6)
C(1)-S(1)-C(12)	94(2)	C(33)-C(34)-C(35)	123(4)
C(1)-C(10)-C(11)	114(4)	C(34)-C(35)-C(6)	111(3)

Table III.47 continued...

C(10)-C(11)-C(12)	115(4)	C(39)-C(8)-C(43)	116(3)
C(11)-C(12)-S(1)	106(4)	C(39)-C(8)-P(3)	125(2)
C(23)-C(4)-S(2)	105(3)	C(43)-C(8)-P(3)	119(2)
C(23)-C(4)-P(2)	130(2)	C(40)-C(39)-C(8)	122(3)
S(2)-C(4)-P(2)	124.9(18)	C(39)-C(40)-C(41)	118(4)
C(4)-S(2)-C(25)	96(2)	C(42)-C(41)-C(40)	125(4)
C(4)-C(23)-C(24)	121(4)	C(41)-C(42)-C(43)	121(4)
C(23)-C(24)-C(25)	110(4)	C(42)-C(43)-C(8)	117(3)
C(24)-C(25)-S(2)	107(3)	C(48)-C(9)-C(44)	112(3)
C(36)-C(7)-S(3)	105(2)	C(48)-C(9)-P(3)	126(3)
C(36)-C(7)-P(3)	131(2)	C(44)-C(9)-P(3)	122(3)
S(3)-C(7)-P(3)	124.1(18)	C(45)-C(44)-C(9)	122(4)
C(7)-S(3)-C(38)	96(2)	C(44)-C(45)-C(46)	122(5)
C(37)-C(36)-C(7)	120(3)	C(47)-C(46)-C(45)	119(6)
C(36)-C(37)-C(38)	111(4)	C(46)-C(47)-C(48)	126(5)
C(37)-C(38)-S(3)	108(3)	C(47)-C(48)-C(9)	118(4)
C(17)-C(2)-C(13)	117(3)	Cl(3)-C(49)-Cl(2)	113(3)
C(17)-C(2)-P(1)	118(3)	Cl(5)-C(50)-Cl(4)	111(4)
C(13)-C(2)-P(1)	125(3)		

III.5.2.5 Single crystal X-ray diffraction study on $[\text{Au}_2(\mu\text{-PSN})_2](\text{SbF}_6)_2$ ([15])

The crystals of $[\text{Au}_2(\mu\text{-PSN})_2](\text{SbF}_6)_2$ were obtained by vapour diffusion of ether in dichloromethane solution of the complex. Data were collected using an Enraf-Nonius CAD4 diffractometer (Appendix A). SHELXS-97²¹⁶ and SHELXL-97²¹⁷ were employed for the structure solution calculations (Appendix A). In the least-squares refinement, the hydrogen atoms were included as ideal contributors with standard idealisation parameters. An extinction coefficient was used in the refinement. Examination of the anisotropic thermal factors showed the F atoms in both SbF_6^- counterions to be disordered. Hence each counterion was considered as two molecules of different conformation. The site occupation factor of each conformation was refined as a free variable (52%/48% and 33%/67% for the counterions labelled with Sb(1) and Sb(2), respectively). The anisotropic thermal factors of the F atoms were initially restrained in the refinement to be approximately isotropic (ISOR), after which a rigid bond restraint (DELU) was added. Crystallographic data are given in Table III.48, the non-hydrogen atomic coordinates in Table III.49, the hydrogen atomic coordinates in Table III.50, the anisotropic thermal factors in Table III.51, the interatomic distances in Table III.52 and the interatomic angles in Table III.53. The observed and calculated structure factors may be found on the disk in an envelope fixed to the inside back cover.

Table III.48 Crystal data and details of data collection and structure refinement for $[\text{Au}_2(\mu\text{-PSN})_2](\text{SbF}_6)_2$ ([15])

Empirical formula	$\text{C}_{42}\text{H}_{32}\text{Au}_2\text{F}_{12}\text{N}_2\text{P}_2\text{S}_2\text{Sb}_2$
Colour and description	Colourless rectangular block
Crystal dimensions (mm)	0.19 x 0.31 x 0.46
Molecular mass ($\text{g}\cdot\text{mol}^{-1}$)	1556.19
Crystal system	Triclinic
Space Group	$\text{P}\bar{1}$
a (Å)	11.646(2)
b (Å)	11.9759(18)
c (Å)	18.397(5)
α (°)	90.640(16)
β (°)	103.537(19)
γ (°)	100.336(13)

Table III.48 continued...

V (Å ³)	2450.3(9)
Z	2
D _c (g·cm ⁻³)	2.109
F(000)	1456
T (K)	293(2)
λ (Mo-K _α) (Å)	0.71069
Scan mode	ω - 2θ
ω scan angle	0.60 + 0.35tanθ
Horizontal aperture width (mm)	2.7 + 0.1tanθ
Scattering range (°)	2 ≤ θ ≤ 23
μ (mm ⁻¹)	7.288
Absorption corrections	Semi empirical
Measured intensities	7553
Unique intensities	6797
Unique intensities with [I > 2σ(I)]	5522
Structure solution	Direct & Fourier
Refinement method	Full-matrix least-squares on F ²
Weighting scheme	1/[σ ² (F _o ²) + (0.056P) ² + 8.22P], where P = 1/3 [Max(F _o ² , 0) + 2F _c ²]
Extinction coefficient	0.00019(10)
$R = \Sigma F_o - F_c / \Sigma F_o $	0.0356 [I > 2σ(I)]
	0.0527 (all data)
$wR = \{\Sigma[w(F_o^2 - F_c^2)^2] / \Sigma[wF_o^4]\}^{1/2}$	0.0990 [I > 2σ(I)]
	0.1056 (all data)
GooF on F ²	1.103
(Δ/σ) _{max}	0.051
Δρ _{max} (eÅ ⁻³)	1.66 (Close to Au(I) centre)
Number of parameters	661

Table III.49 Non-hydrogen atomic coordinates ($\times 10^4$) and isotropic thermal factors ($\text{\AA}^2 \times 10^3$) for $[\text{Au}_2(\mu\text{-PSN})_2](\text{SbF}_6)_2$ ([15])

	x	y	z	U(eq)
Au(1)	10193(1)	3121(1)	793(1)	45(1)
Au(2)	13991(1)	4203(1)	3429(1)	53(1)
P(1)	9169(2)	3092(2)	1685(1)	38(1)
P(2)	14098(2)	2460(2)	3047(1)	43(1)
S(1)	11299(2)	4841(2)	2480(1)	46(1)
S(2)	12801(2)	3110(2)	1548(1)	49(1)
N(1)	13822(7)	5788(6)	3815(5)	53(2)
N(2)	11095(7)	3141(7)	-64(4)	50(2)
C(1)	14791(9)	6584(9)	4099(7)	71(3)
C(2)	14708(10)	7615(9)	4387(7)	66(3)
C(3)	13618(10)	7854(9)	4387(6)	66(3)
C(4)	12597(9)	7009(8)	4080(6)	55(3)
C(5)	12732(8)	6001(7)	3788(5)	40(2)
C(6)	11686(7)	5102(8)	3437(5)	40(2)
C(7)	10966(9)	4426(9)	3766(6)	57(3)
C(8)	10084(9)	3624(9)	3256(6)	61(3)
C(9)	10145(7)	3759(7)	2535(5)	36(2)
C(10)	7872(7)	3784(7)	1471(5)	36(2)
C(11)	7410(8)	4146(8)	2034(6)	48(2)
C(12)	6355(9)	4535(9)	1865(6)	53(2)
C(13)	5753(9)	4562(9)	1139(7)	61(3)
C(14)	6191(10)	4190(11)	573(7)	70(3)
C(15)	7267(9)	3820(9)	737(6)	54(3)
C(16)	8558(8)	1675(7)	1899(5)	43(2)
C(17)	7379(9)	1210(10)	1532(7)	71(3)
C(18)	6891(10)	94(9)	1669(9)	84(4)

Table III.49 continued...

C(19)	7547(11)	-514(10)	2140(8)	72(3)
C(20)	8697(12)	-80(10)	2485(8)	82(4)
C(21)	9198(10)	1016(9)	2360(7)	66(3)
C(22)	10480(10)	3401(9)	-736(6)	60(3)
C(23)	10900(12)	3338(9)	-1375(6)	68(3)
C(24)	11985(11)	3026(9)	-1326(6)	63(3)
C(25)	12623(10)	2785(9)	-651(6)	59(3)
C(26)	12180(8)	2831(7)	-12(5)	46(2)
C(27)	12867(8)	2535(8)	708(5)	46(2)
C(28)	13635(10)	1779(10)	810(6)	64(3)
C(29)	14171(9)	1691(9)	1565(6)	60(3)
C(30)	13795(8)	2341(8)	2046(6)	45(2)
C(31)	15527(8)	2038(8)	3407(5)	45(2)
C(32)	16508(8)	2855(8)	3746(5)	47(2)
C(33)	17590(9)	2564(11)	4047(6)	64(3)
C(34)	17700(10)	1433(11)	4043(7)	71(3)
C(35)	16725(10)	610(10)	3716(7)	67(3)
C(36)	15665(9)	924(9)	3415(6)	58(3)
C(37)	12976(8)	1405(8)	3316(6)	47(2)
C(38)	12581(9)	1655(10)	3952(6)	58(3)
C(39)	11813(11)	811(11)	4194(7)	74(3)
C(40)	11401(10)	-256(11)	3827(7)	70(3)
C(41)	11799(10)	-473(9)	3200(7)	69(3)
C(42)	12561(9)	325(8)	2933(6)	56(3)
Sb(1)	1503(1)	3171(1)	6033(1)	52(1)
F(1)	2392(6)	3347(8)	5312(4)	96(2)
F(2)	588(8)	2957(9)	6737(5)	120(3)
F(3a)	210(3)	2680(3)	5280(3)	130(10)
F(4a)	2920(2)	3880(3)	6691(15)	157(10)

Table III.49 continued...

F(5a)	1980(3)	1870(2)	6120(2)	158(11)
F(6a)	1620(3)	4646(17)	6200(12)	129(7)
F(3b)	110(3)	3080(4)	5330(3)	124(9)
F(4b)	2780(2)	3150(2)	6842(14)	129(8)
F(5b)	1300(3)	1558(19)	5944(19)	131(9)
F(6b)	1140(3)	4610(2)	5775(16)	149(10)
Sb(2)	6283(1)	2570(1)	-1679(1)	68(1)
F(7)	5986(12)	3843(11)	-2186(9)	188(5)
F(8a)	5270(6)	2370(6)	-1000(4)	188(17)
F(9a)	7700(4)	2400(4)	-1910(3)	157(15)
F(10a)	4930(4)	2460(5)	-2350(4)	224(18)
F(11a)	6920(4)	4020(2)	-1160(2)	145(10)
F(12a)	7090(5)	1940(4)	-790(2)	181(16)
F(8b)	5090(2)	2670(2)	-1225(14)	126(7)
F(9b)	7369(19)	2634(18)	-2274(10)	112(5)
F(10b)	5190(2)	1700(2)	-2490(13)	194(8)
F(11b)	7451(14)	3190(2)	-955(8)	157(8)
F(12b)	6178(17)	1102(10)	-1614(15)	175(8)

$$U_{(eq)} = \frac{1}{3} \cdot \sum_i \sum_j U_{ij} a_i^* a_j^* (a_i \cdot a_j)$$

Table III.50 Hydrogen atomic coordinates ($\times 10^4$) and isotropic thermal factors ($\text{\AA}^2 \times 10^3$) for $[\text{Au}_2(\mu\text{-PSN})_2](\text{SbF}_6)_2$ ([15]) (the numbering of the H atoms is done according to the numbering of the C atoms, to which the hydrogens are respectively attached)

	x	y	z	U(eq)
H(1)	15547	6431	4101	85
H(2)	15400	8151	4583	79
H(3)	13542	8549	4583	79
H(4)	11832	7140	4077	66

Table III.50 continued...

H(7)	11025	4468	4279	69
H(8)	9529	3068	3403	73
H(11)	7818	4125	2531	58
H(12)	6045	4782	2247	63
H(13)	5038	4837	1026	74
H(14)	5762	4186	78	84
H(15)	7586	3595	353	64
H(17)	6919	1632	1200	85
H(18)	6102	-222	1429	100
H(19)	7207	-1246	2232	87
H(20)	9153	-517	2807	99
H(21)	9995	1306	2599	80
H(22)	9747	3630	-772	72
H(23)	10448	3507	-1834	82
H(24)	12282	2979	-1751	76
H(25)	13370	2586	-613	70
H(28)	13784	1370	421	76
H(29)	14734	1230	1727	72
H(32)	16429	3613	3768	57
H(33)	18254	3124	4255	77
H(34)	18432	1230	4262	85
H(35)	16795	-151	3702	81
H(36)	15002	363	3205	70
H(38)	12830	2369	4202	69
H(39)	11559	961	4622	89
H(40)	10873	-807	3999	85
H(41)	11538	-1187	2952	83
H(42)	12805	161	2503	67

Table III.51 Anisotropic thermal factors ($\text{\AA}^2 \times 10^3$) for $[\text{Au}_2(\mu\text{-PSN})_2](\text{SbF}_6)_2$ ([15])

	U(11)	U(22)	U(33)	U(23)	U(13)	U(12)
Au(1)	34(1)	55(1)	46(1)	2(1)	13(1)	9(1)
Au(2)	35(1)	47(1)	76(1)	-12(1)	6(1)	14(1)
P(1)	26(1)	45(1)	42(1)	2(1)	7(1)	5(1)
P(2)	31(1)	44(1)	55(2)	-5(1)	6(1)	12(1)
S(1)	37(1)	52(1)	44(1)	0(1)	11(1)	-3(1)
S(2)	45(1)	56(2)	51(2)	2(1)	11(1)	25(1)
N(1)	35(4)	44(5)	76(6)	-17(4)	8(4)	9(4)
N(2)	52(5)	51(5)	51(5)	11(4)	17(4)	14(4)
C(1)	28(5)	70(8)	108(10)	-20(7)	6(6)	7(5)
C(2)	51(7)	54(7)	80(8)	-17(6)	0(6)	-3(5)
C(3)	65(7)	52(6)	73(8)	-21(6)	2(6)	10(6)
C(4)	48(6)	54(6)	65(7)	-8(5)	14(5)	16(5)
C(5)	37(5)	41(5)	44(5)	-1(4)	8(4)	12(4)
C(6)	25(4)	48(5)	46(5)	-2(4)	4(4)	10(4)
C(7)	43(6)	81(8)	42(6)	8(5)	7(5)	-1(5)
C(8)	50(6)	65(7)	62(7)	12(6)	16(5)	-6(5)
C(9)	20(4)	49(5)	37(5)	4(4)	6(4)	7(4)
C(10)	32(5)	38(5)	36(5)	9(4)	6(4)	6(4)
C(11)_	41(5)	57(6)	48(6)	3(5)	9(5)	13(5)
C(12)	47(6)	62(6)	53(6)	2(5)	15(5)	19(5)
C(13)	41(6)	60(7)	85(9)	9(6)	10(6)	19(5)
C(14)	57(7)	93(9)	58(7)	10(6)	-7(6)	33(6)
C(15)	50(6)	66(7)	46(6)	2(5)	9(5)	15(5)
C(16)	33(5)	38(5)	60(6)	-3(4)	18(4)	5(4)

Table III.51 continued...

C(17)	36(6)	62(7)	105(10)	7(6)	-1(6)	7(5)
C(18)	44(7)	45(7)	149(13)	3(8)	16(8)	-13(5)
C(19)	67(8)	45(6)	109(10)	3(7)	36(8)	2(6)
C(20)	75(9)	56(7)	110(11)	31(7)	9(8)	13(6)
C(21)	44(6)	57(7)	96(9)	19(6)	14(6)	7(5)
C(22)	59(7)	81(8)	47(6)	11(5)	14(5)	28(6)
C(23)	102(10)	65(7)	40(6)	14(5)	17(6)	24(7)
C(24)	88(9)	57(7)	59(7)	11(5)	40(7)	22(6)
C(25)	63(7)	61(7)	65(7)	7(5)	33(6)	20(5)
C(26)	44(5)	41(5)	59(6)	7(4)	23(5)	11(4)
C(27)	39(5)	49(5)	53(6)	2(5)	17(5)	10(4)
C(28)	65(7)	84(8)	54(7)	-5(6)	18(6)	39(6)
C(29)	46(6)	67(7)	73(8)	4(6)	15(6)	28(5)
C(30)	29(5)	46(5)	63(6)	0(5)	14(4)	9(4)
C(31)	28(5)	56(6)	53(6)	1(5)	11(4)	14(4)
C(32)	35(5)	52(6)	52(6)	0(5)	5(4)	11(4)
C(33)	41(6)	82(8)	70(8)	6(6)	13(5)	12(6)
C(34)	54(7)	100(10)	66(8)	19(7)	10(6)	37(7)
C(35)	58(7)	55(7)	95(9)	6(6)	20(6)	27(6)
C(36)	37(5)	57(6)	81(8)	-7(5)	8(5)	19(5)
C(37)	37(5)	49(6)	56(6)	1(5)	9(5)	11(4)
C(38)	46(6)	69(7)	61(7)	-3(5)	17(5)	12(5)
C(39)	66(8)	87(9)	79(9)	8(7)	34(7)	16(7)
C(40)	56(7)	73(8)	86(9)	18(7)	27(6)	9(6)
C(41)	57(7)	48(6)	93(9)	-10(6)	9(7)	-1(5)
C(42)	48(6)	52(6)	68(7)	-11(5)	17(5)	11(5)
Sb(1)	41(1)	62(1)	53(1)	2(1)	9(1)	13(1)
F(1)	65(4)	152(7)	83(5)	11(5)	38(4)	21(4)
F(2)	114(6)	174(8)	93(5)	19(5)	62(5)	33(6)

Table III.51 continued...

F(3a)	60(10)	190(2)	101(9)	-44(16)	-9(9)	-25(15)
F(4a)	75(8)	250(3)	111(14)	-72(19)	-17(8)	1(12)
F(5a)	240(3)	108(13)	180(2)	50(13)	89(19)	114(17)
F(6a)	210(2)	58(7)	116(17)	-15(9)	34(12)	17(9)
F(3b)	44(7)	240(3)	86(11)	20(2)	-2(7)	37(14)
F(4b)	87(9)	200(2)	80(8)	18(13)	-20(7)	31(14)
F(5b)	190(3)	63(7)	148(18)	0(8)	71(16)	13(10)
F(6b)	190(2)	104(11)	200(3)	54(14)	88(17)	93(14)
Sb(2)	62(1)	55(1)	94(1)	-5(1)	39(1)	4(1)
F(7)	171(11)	155(9)	251(13)	101(9)	53(10)	57(8)
F(8a)	190(3)	140(3)	290(4)	-10(2)	210(3)	-30(2)
F(9a)	120(2)	150(3)	250(4)	-20(2)	130(3)	26(17)
F(10a)	118(19)	230(3)	270(3)	40(3)	-42(19)	20(2)
F(11a)	250(3)	45(10)	166(15)	-29(11)	138(15)	-27(12)
F(12a)	290(4)	160(3)	130(2)	40(2)	44(19)	120(3)
F(8b)	93(9)	130(16)	174(16)	-46(10)	80(10)	9(10)
F(9b)	131(11)	109(11)	110(10)	-6(8)	84(9)	-15(8)
F(10b)	148(14)	221(15)	177(14)	-123(12)	62(9)	-83(13)
F(11b)	98(8)	260(2)	79(8)	-45(10)	15(6)	-44(12)
F(12b)	179(15)	51(6)	350(2)	23(9)	183(14)	9(7)

The anisotropic thermal factor exponent takes the form:

$$-2\pi^2[h^2a^{*2}U(11) + \dots + 2hka^*b^*U(12)]$$

Table III.52 Interatomic distances (Å) for [Au₂(μ-PSN)₂](SbF₆)₂ ([15])

Au(1)-N(2)	2.087(8)	C(24)-C(25)	1.352(15)
Au(1)-P(1)	2.239(2)	C(25)-C(26)	1.396(13)
Au(2)-N(1)	2.078(7)	C(26)-C(27)	1.461(13)
Au(2)-P(2)	2.228(2)	C(27)-C(28)	1.368(13)
P(1)-C(9)	1.787(8)	C(28)-C(29)	1.397(15)
P(1)-C(16)	1.804(9)	C(29)-C(30)	1.367(13)
P(1)-C(10)	1.816(8)	C(31)-C(36)	1.372(13)
P(2)-C(30)	1.791(10)	C(31)-C(32)	1.379(13)
P(2)-C(31)	1.805(9)	C(32)-C(33)	1.361(14)
P(2)-C(37)	1.810(10)	C(33)-C(34)	1.383(16)
S(1)-C(9)	1.714(8)	C(34)-C(35)	1.374(16)
S(1)-C(6)	1.721(9)	C(35)-C(36)	1.351(14)
S(2)-C(27)	1.708(9)	C(37)-C(38)	1.401(14)
S(2)-C(30)	1.711(9)	C(37)-C(42)	1.414(13)
N(1)-C(5)	1.329(11)	C(38)-C(39)	1.377(15)
N(1)-C(1)	1.335(12)	C(39)-C(40)	1.388(17)
N(2)-C(22)	1.347(12)	C(40)-C(41)	1.378(16)
N(2)-C(26)	1.363(12)	C(41)-C(42)	1.361(15)
C(1)-C(2)	1.366(15)	Sb(1)-F(1)	1.856(7)
C(2)-C(3)	1.350(15)	Sb(1)-F(2)	1.854(7)
C(3)-C(4)	1.414(14)	Sb(1)-F(3a)	1.80(3)
C(4)-C(5)	1.365(13)	Sb(1)-F(4a)	1.85(2)
C(5)-C(6)	1.485(12)	Sb(1)-F(5a)	1.74(2)
C(6)-C(7)	1.316(13)	Sb(1)-F(6a)	1.76(2)
C(7)-C(8)	1.425(14)	Sb(1)-F(3b)	1.81(3)
C(8)-C(9)	1.355(13)	Sb(1)-F(4b)	1.84(2)
C(10)-C(11)	1.373(12)	Sb(1)-F(5b)	1.90(2)
C(10)-C(15)	1.375(13)	Sb(1)-F(6b)	1.89(2)
C(11)-C(12)	1.361(13)	Sb(2)-F(7)	1.840(11)

Table III.52 continued...

C(12)-C(13)	1.360(14)	Sb(2)-F(8a)	1.90(4)
C(13)-C(14)	1.364(16)	Sb(2)-F(9a)	1.849(16)
C(14)-C(15)	1.372(14)	Sb(2)-F(10a)	1.74(4)
C(16)-C(21)	1.353(14)	Sb(2)-F(11a)	1.92(2)
C(16)-C(17)	1.391(13)	Sb(2)-F(12a)	1.92(3)
C(17)-C(18)	1.405(16)	Sb(2)-F(8b)	1.80(2)
C(18)-C(19)	1.330(17)	Sb(2)-F(9b)	1.85(3)
C(19)-C(20)	1.346(16)	Sb(2)-F(10b)	1.879(16)
C(20)-C(21)	1.382(15)	Sb(2)-F(11b)	1.716(13)
C(22)-C(23)	1.381(15)	Sb(2)-F(12b)	1.747(12)
C(23)-C(24)	1.364(16)		

Table III.53 Interatomic angles (°) for [Au₂(μ-PSN)₂](SbF₆)₂ ([15])

N(2)-Au(1)-P(1)	178.1(2)	F(3a)-Sb(1)-F(4b)	160.6(17)
N(1)-Au(2)-P(2)	176.9(2)	F(3b)-Sb(1)-F(4b)	171.3(19)
C(9)-P(1)-C(16)	106.5(4)	F(5a)-Sb(1)-F(4a)	90.7(15)
C(9)-P(1)-C(10)	107.5(4)	F(6a)-Sb(1)-F(4a)	65.2(14)
C(16)-P(1)-C(10)	103.7(4)	F(3a)-Sb(1)-F(4a)	169(2)
C(9)-P(1)-Au(1)	109.7(3)	F(3b)-Sb(1)-F(4a)	156.7(19)
C(16)-P(1)-Au(1)	113.3(3)	F(4b)-Sb(1)-F(4a)	28.6(12)
C(10)-P(1)-Au(1)	115.5(3)	F(5a)-Sb(1)-F(2)	96.7(12)
C(30)-P(2)-C(31)	107.4(4)	F(6a)-Sb(1)-F(2)	87.4(10)
C(30)-P(2)-C(37)	106.7(4)	F(3a)-Sb(1)-F(2)	91.9(17)
C(31)-P(2)-C(37)	106.5(4)	F(3b)-Sb(1)-F(2)	87.5(17)
C(30)-P(2)-Au(2)	110.1(3)	F(4b)-Sb(1)-F(2)	84.3(9)
C(31)-P(2)-Au(2)	115.0(3)	F(4a)-Sb(1)-F(2)	96.2(10)
C(37)-P(2)-Au(2)	110.9(3)	F(5a)-Sb(1)-F(1)	82.4(12)
C(9)-S(1)-C(6)	91.6(4)	F(6a)-Sb(1)-F(1)	94.0(10)

Table III.53 continued...

C(27)-S(2)-C(30)	92.8(5)	F(3a)-Sb(1)-F(1)	86.7(17)
C(5)-N(1)-C(1)	119.8(8)	F(3b)-Sb(1)-F(1)	91.5(17)
C(5)-N(1)-Au(2)	119.2(6)	F(4b)-Sb(1)-F(1)	96.7(9)
C(1)-N(1)-Au(2)	120.9(6)	F(4a)-Sb(1)-F(1)	85.2(10)
C(22)-N(2)-C(26)	118.7(8)	F(2)-Sb(1)-F(1)	178.3(4)
C(22)-N(2)-Au(1)	115.2(7)	F(5a)-Sb(1)-F(6b)	168.0(15)
C(26)-N(2)-Au(1)	125.9(6)	F(6a)-Sb(1)-F(6b)	26.4(11)
N(1)-C(1)-C(2)	122.1(9)	F(3a)-Sb(1)-F(6b)	83.0(16)
C(3)-C(2)-C(1)	119.8(10)	F(3b)-Sb(1)-F(6b)	67.4(18)
C(2)-C(3)-C(4)	117.6(10)	F(4b)-Sb(1)-F(6b)	116.3(14)
C(5)-C(4)-C(3)	120.0(9)	F(4a)-Sb(1)-F(6b)	89.3(14)
N(1)-C(5)-C(4)	120.5(8)	F(2)-Sb(1)-F(6b)	95.2(10)
N(1)-C(5)-C(6)	117.4(7)	F(1)-Sb(1)-F(6b)	85.6(9)
C(4)-C(5)-C(6)	122.1(8)	F(5a)-Sb(1)-F(5b)	25.1(15)
C(7)-C(6)-C(5)	128.2(9)	F(6a)-Sb(1)-F(5b)	173.7(14)
C(7)-C(6)-S(1)	111.8(7)	F(3a)-Sb(1)-F(5b)	72.8(19)
C(5)-C(6)-S(1)	119.9(7)	F(3b)-Sb(1)-F(5b)	88.5(16)
C(6)-C(7)-C(8)	113.1(9)	F(4b)-Sb(1)-F(5b)	88.0(12)
C(9)-C(8)-C(7)	112.6(9)	F(4a)-Sb(1)-F(5b)	114.6(15)
C(8)-C(9)-S(1)	110.7(7)	F(2)-Sb(1)-F(5b)	86.4(10)
C(8)-C(9)-P(1)	130.5(7)	F(1)-Sb(1)-F(5b)	92.2(10)
S(1)-C(9)-P(1)	118.5(5)	F(6b)-Sb(1)-F(5b)	155.8(14)
C(11)-C(10)-C(15)	119.7(8)	F(11b)-Sb(2)-F(10a)	157(3)
C(11)-C(10)-P(1)	120.7(7)	F(11b)-Sb(2)-F(12b)	106.5(12)
C(15)-C(10)-P(1)	119.2(7)	F(10a)-Sb(2)-F(12b)	94(2)
C(12)-C(11)-C(10)	120.1(9)	F(11b)-Sb(2)-F(8b)	97.0(11)
C(13)-C(12)-C(11)	120.1(10)	F(10a)-Sb(2)-F(8b)	70(3)
C(12)-C(13)-C(14)	120.5(10)	F(12b)-Sb(2)-F(8b)	95.5(10)

Table III.53 continued...

C(13)-C(14)-C(15)	119.7(10)	F(11b)-Sb(2)-F(7)	99.3(10)
C(14)-C(15)-C(10)	119.8(10)	F(10a)-Sb(2)-F(7)	62.3(19)
C(21)-C(16)-C(17)	118.1(9)	F(12b)-Sb(2)-F(7)	152.9(10)
C(21)-C(16)-P(1)	124.0(7)	F(8b)-Sb(2)-F(7)	89.6(9)
C(17)-C(16)-P(1)	117.8(8)	F(11b)-Sb(2)-F(9a)	72.0(19)
C(16)-C(17)-C(18)	119.1(11)	F(10a)-Sb(2)-F(9a)	123(3)
C(19)-C(18)-C(17)	120.6(11)	F(12b)-Sb(2)-F(9a)	80.0(16)
C(18)-C(19)-C(20)	120.7(11)	F(8b)-Sb(2)-F(9a)	166(2)
C(19)-C(20)-C(21)	119.8(11)	F(7)-Sb(2)-F(9a)	100.6(16)
C(16)-C(21)-C(20)	121.6(11)	F(11b)-Sb(2)-F(9b)	88.3(8)
N(2)-C(22)-C(23)	122.2(10)	F(10a)-Sb(2)-F(9b)	101(3)
C(24)-C(23)-C(22)	119.3(10)	F(12b)-Sb(2)-F(9b)	91.9(8)
C(25)-C(24)-C(23)	119.1(10)	F(8b)-Sb(2)-F(9b)	169.3(10)
C(24)-C(25)-C(26)	121.1(10)	F(7)-Sb(2)-F(9b)	80.4(8)
N(2)-C(26)-C(25)	119.6(9)	F(9a)-Sb(2)-F(9b)	24.2(17)
N(2)-C(26)-C(27)	120.1(8)	F(11b)-Sb(2)-F(10b)	169.5(14)
C(25)-C(26)-C(27)	120.3(9)	F(10a)-Sb(2)-F(10b)	34(2)
C(28)-C(27)-C(26)	125.9(9)	F(12b)-Sb(2)-F(10b)	65.8(13)
C(28)-C(27)-S(2)	110.8(8)	F(8b)-Sb(2)-F(10b)	91.1(11)
C(26)-C(27)-S(2)	123.3(7)	F(7)-Sb(2)-F(10b)	87.6(12)
C(27)-C(28)-C(29)	112.4(9)	F(9a)-Sb(2)-F(10b)	99(2)
C(30)-C(29)-C(28)	114.1(9)	F(9b)-Sb(2)-F(10b)	84.9(10)
C(29)-C(30)-S(2)	109.8(8)	F(11b)-Sb(2)-F(8a)	89(3)
C(29)-C(30)-P(2)	132.2(8)	F(10a)-Sb(2)-F(8a)	84(3)
S(2)-C(30)-P(2)	117.9(5)	F(12b)-Sb(2)-F(8a)	83(2)
C(36)-C(31)-C(32)	118.0(8)	F(8b)-Sb(2)-F(8a)	18(3)
C(36)-C(31)-P(2)	122.8(7)	F(7)-Sb(2)-F(8a)	107(2)
C(32)-C(31)-P(2)	119.0(7)	F(9a)-Sb(2)-F(8a)	149(3)

Table III.53 continued...

C(33)-C(32)-C(31)	120.7(10)	F(9b)-Sb(2)-F(8a)	173(2)
C(32)-C(33)-C(34)	119.9(11)	F(10b)-Sb(2)-F(8a)	97(3)
C(35)-C(34)-C(33)	119.9(10)	F(11b)-Sb(2)-F(11a)	40.6(13)
C(36)-C(35)-C(34)	118.9(10)	F(10a)-Sb(2)-F(11a)	116(3)
C(35)-C(36)-C(31)	122.5(10)	F(12b)-Sb(2)-F(11a)	145.0(16)
C(38)-C(37)-C(42)	120.2(9)	F(8b)-Sb(2)-F(11a)	80.9(14)
C(38)-C(37)-P(2)	118.1(8)	F(7)-Sb(2)-F(11a)	62.1(14)
C(42)-C(37)-P(2)	121.6(8)	F(9a)-Sb(2)-F(11a)	95(2)
C(39)-C(38)-C(37)	117.8(11)	F(9b)-Sb(2)-F(11a)	97.5(12)
C(38)-C(39)-C(40)	122.8(11)	F(10b)-Sb(2)-F(11a)	148(2)
C(41)-C(40)-C(39)	118.1(11)	F(8a)-Sb(2)-F(11a)	85(2)
C(42)-C(41)-C(40)	122.0(11)	F(11b)-Sb(2)-F(12a)	49.8(14)
C(41)-C(42)-C(37)	119.2(10)	F(10a)-Sb(2)-F(12a)	145(3)
F(5a)-Sb(1)-F(6a)	155.8(15)	F(12b)-Sb(2)-F(12a)	58.7(14)
F(5a)-Sb(1)-F(3a)	95.3(16)	F(8b)-Sb(2)-F(12a)	88.3(16)
F(6a)-Sb(1)-F(3a)	108.4(16)	F(7)-Sb(2)-F(12a)	148.3(15)
F(5a)-Sb(1)-F(3b)	111.7(19)	F(9a)-Sb(2)-F(12a)	78(2)
F(6a)-Sb(1)-F(3b)	92.2(16)	F(9b)-Sb(2)-F(12a)	102.1(15)
F(3a)-Sb(1)-F(3b)	17(2)	F(10b)-Sb(2)-F(12a)	124.1(18)
F(5a)-Sb(1)-F(4b)	66.4(15)	F(8a)-Sb(2)-F(12a)	71(3)
F(6a)-Sb(1)-F(4b)	90.4(12)	F(11a)-Sb(2)-F(12a)	86.3(17)

CHAPTER FOUR

PRELIMINARY STUDIES OF THE BIOLOGICAL ACTIVITY OF SELECTED THIENYLPHOSPHINES AND THEIR GOLD(I) COMPLEXES

IV.1 INTRODUCTION

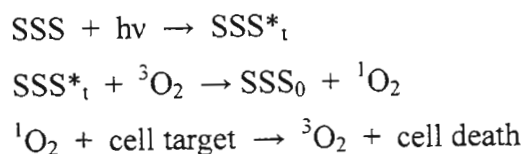
IV.1.1 Biological activity of α -bi- and terthiophenes

Uhlenbroek and Bijloo²⁵¹ in the late 1950s described the isolation of nematocidal heterocyclic compounds from the marigold *Tagetes erecta*. A bithienyl moiety was found to be a minimum structural requirement for the exhibited activity. Following a lapse of a few years, a steady succession of articles appeared concerning the toxicity of α -terthienyl (SSS) and related compounds to a wide variety of organisms as well as attempts to define the mechanism of their toxicity.

Gommers *et al.*²⁵² noticed that the toxicity of SSS markedly increased in the presence of sunlight or UV light. Originally, the increased potency was attributed to the effect of the UV component of sunlight. It was shown that the UV-absorption maximum of SSS coincided with the wavelength at which the light-induced enhancement of toxicity was the greatest. This observation led to conclusion that photoactivated terthienyl was the active species, rather than some other phototoxic compound whose level in the organism had been altered by the presence of SSS.

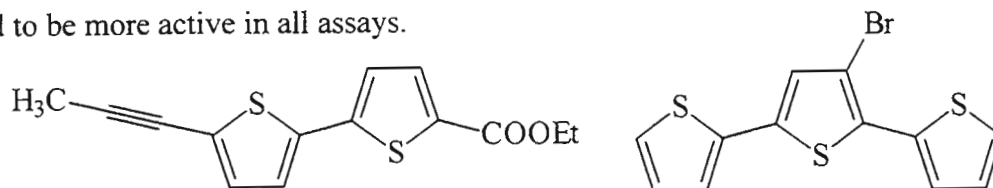
Further investigations, however, suggested that photoinduced damage caused by SSS and its derivatives was due to the generation of singlet oxygen ($^1\text{O}_2$) in a photosensitisation process analogous to that seen with dyes such as Rose Bengal and methylene blue.^{121,253} The experiments, which included the heterocycle, UV light and oxygen, revealed deactivation of enzymes exposed to this combination. The deactivation was inhibited by typical singlet oxygen scavengers such as NaN_3 and methionine, while superoxide scavengers – mannitol and superoxide dismutase – did not show any effect. As an additional test for $^1\text{O}_2$ generation, the reaction of the olefin adamantylidene adamantane with UV-irradiated oxygenated solutions of SSS was found to yield adamantanone by

decomposition of the olefin's single oxygen adduct.²⁵³ The formation of singlet oxygen occurs according to the sequence below (Scheme IV.1):²⁵⁴



SCHEME IV.1

Later studies focused on properties of both bithienyl and terthienyl derivatives.^{120,125,177,255,256} They revealed widely differing phototoxicities and selectivities towards several targets (bacteria and viruses). The activity was essentially determined by the compound hydrophobicity, ability to absorb near UV light and to generate singlet oxygen – in other words, to be an efficient photosensitiser.¹²⁰ Conjugated α -linked compounds with adjacent thiophene rings (bi- and terthienyls) – as shown below – were found to be more active in all assays.



Those compounds which did not have all these features, were much less active or inactive.^{120,125}

Most of the polythiophene derivatives that have been examined demonstrated high therapeutic potential by exhibiting antiviral, antimicrobial and even cytotoxic properties. The similar structural requirements for antiviral and cytotoxic activities are indicative of a common mechanism of action.

In general, the phototoxicity of thiophenes has been attributed to their action on membrane constituents via singlet oxygen¹²⁵ attack or by interaction with unsaturated fatty acids.²⁵⁷ It has also been suggested that other non-membrane targets – proteins or nucleic acids – should be taken in consideration.²⁵⁸ Kagan *et al.*²⁵⁹ proved that SSS incorporates into DNA during a photochemical reaction; however, no cross-linking was observed. Membrane proteins were also shown to be important sites of attack for SSS-generated singlet

oxygen.²⁶⁰ However, there are indications that toxicity is not always determined by successful formation of this active species: SSS shows cytotoxicity even in the dark, albeit not as high as under UV light.¹²⁰ (Note, however, that most of the other bi- and terthienyl derivatives are not cytotoxic in the dark.)

At present, the exact mechanism of biological action of polythiophenes remains unclear. Nevertheless, all available chemical, biochemical and photophysical studies suggest that these compounds represent a unique class of powerful phototoxic agents. This photosensitising property presents a high potential for their future use in photodynamic therapy – a relatively recent approach to the treatment of cancer by the combination of laser light, a photosensitising agent and molecular oxygen.²⁶¹⁻²⁶³

Photodynamic therapy has great potential in the treatment of a number of tumours. The technique involves the introduction of a photosensitiser which is selectively retained by the cancerous tissue as compared with surrounding tissue. The area is then irradiated with laser light causing the photosensitiser to fluoresce, thus transferring energy to triplet oxygen, resulting in its conversion to singlet oxygen. The singlet oxygen then oxidises the surrounding tissue, killing the cancer cells.²⁶³ Much development work has concentrated on cancers that lie close to the surface of the skin, such as basal cell carcinomas, but in principle, deeper lying and thicker tumours could be treated in this manner, provided the appropriate experimental conditions can be achieved.

There is, however, another side to photosensitising ability, namely a negative effect on the patient who has been administered a drug containing such agent and subsequently was exposed to sunlight or any other source of near UV light.²⁶⁴ Indeed, SSS has been known to cause dermatitis of human skin by oxidation of human skin surface lipids.²⁶⁵ This has to be taken into account during the design of drugs containing SSS and its derivatives. One possible solution to minimise this side effect would be to functionalise the compound in such a way that it accumulates selectively in the organelles (*e.g.* tumour sites) which require treatment.

IV.1.2 Biological activity of gold(I)-phosphine complexes

Gold compounds have long been used for the treatment of rheumatoid arthritis. Early formulations were based on water soluble oligomeric gold(I) thiolates. In the beginning of 1980s, a new lipophilic gold(I) phosphine complex Auranofin²⁶⁶ (see Figure IV.1) was introduced.

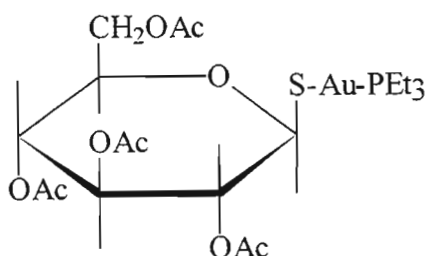


Fig. IV.1 Antiarthritic drug Auranofin – [(2,3,4,6-tetra-*O*-acetyl-1-thio-β-D-glucopyranosato-*S*)(triethylphosphine)gold(I)].

Auranofin has shown several advantages over preceding gold drugs. However results of numerous investigations seem to indicate that antiarthritic activity of gold complexes depends on the presence of gold(I) more than the ligands, although the ligands can markedly affect the absorption and distribution properties of the complex.³

During the studies devoted to antiarthritic properties of gold(I) drugs it was found that these compounds exert a number of effects on the immune response as a result of the interaction of gold with thiol groups on the proteins responsible for regulating the transcription of genes.¹¹⁵ Regulation of gene transcription plays an important part in a number of diseases: *i.e.* cytokine production in rheumatoid arthritis and oncogene expression in cancer.

Lorber *et al.*²⁶⁷ reported in 1979 that Auranofin had activity against HeLa cells in culture and followed this up with studies²⁶⁸ pointing out that the drug was active against P388 leukaemia in mice. However, it was inactive against solid tumours. Several other gold(I) phosphine complexes with thiosugar ligands were investigated with similar results.

More promising results were achieved with a series of dinuclear gold(I)-phosphine complexes. A large number of compounds of the diphosphine dppe and its derivatives were

investigated for antitumour activity.⁷⁵ While the ligands themselves showed some activity, the digold complexes had much greater potency. The dinuclear linear complex $[\text{ClAu}(\mu\text{-dppe})\text{AuCl}]$ was shown to rearrange upon reaction with thiols in blood plasma to give the mononuclear tetrahedral chelated species $[\text{Au}(\text{dppe})_2]^+$.²⁶⁹ Both the tetrahedral and the bridged complexes demonstrated significant and reproducible antitumour activity in a broad spectrum of murine tumours *in vivo* and potent cytotoxic activity to tumour cells *in vitro*.¹¹⁷ It is very likely that the bischelated complex is the major active metabolite of dinuclear complexes inside cells.

The substituents on the phosphine molecule are important for activity. For complexes of the type $[\text{ClAu}\{\mu\text{-R}_2\text{P}(\text{CH}_2)_n\text{PR}_2\}\text{AuCl}]$, highest activity was found with $\text{R} = \text{Ph}$, $n = 2, 3$ or *cis*- $\text{CH}=\text{CH}$. Substitution of phenyl groups by ethyl, pyridyl, fluorophenyl etc. substantially reduced or even eliminated antitumour activity.¹¹⁸

Low activity of Auranofin *in vivo* indicates that it is quickly detoxified by strong binding to albumin in blood plasma. On the other hand, $[\text{Au}(\text{dppe})_2]^+$ is stable in serum for several days. This stability and inertness is a result of two factors: the chelate effect and the greater stability of phosphine over thiolate ligands. The low reactivity of $[\text{Au}(\text{dppe})_2]^+$ towards thiols and high lipophilicity allow it to reach intracellular target sites which are inaccessible to Auranofin.

The mechanism of action of gold(I) phosphine complexes appears to be different to that of cisplatin $[\text{cis-Pt}(\text{NH}_3)_2\text{Cl}_2]$. As gold(I) forms only weak bonds with nitrogen ligands it can not form strong cross-links between purine bases of DNA as does Pt(II). However it can produce DNA-protein cross-links and DNA single strand breaks. The former are critical lesions, which can be repaired when the complex is removed, while the latter are only evident at supralethal doses.¹¹⁷ Electron microscope studies showed that $[\text{Au}(\text{dppe})_2]^+$ produces profound effects on mitochondrial morphology with subsequent uncoupling of mitochondrial oxidative phosphorylation.²⁷⁰

As many phosphines show cytotoxic and antitumour activities even without coordination to a metal,^{75,271} it was originally suggested that the function of gold(I) was merely to protect the ligand from oxidation when it enters cells. At the same time the phosphine

would stabilise gold(I) thus providing a mechanism for its transport into cells through the lipophilic cell membrane. This theory was supported by the following observations:

- a) activity was not limited to gold complexes, copper(II) also enhancing the cytotoxicity of dppe²⁷² as did Ni(II) and Pd(II),²⁷³
- b) phosphine oxides were inactive as antitumour agents and even non-toxic.⁷⁵

However, there are other facts which seem to indicate that gold(I) does have a role greater than that of a simple carrier: several gold complexes without phosphine ligands, *e.g.* [Au(Et₂S)Cl], were found to be active *in vivo*,²⁷⁴ also complexes of dppe with different metals show different activities per mole of dppe.²⁷⁵

Unfortunately, investigations into the antitumour activity of gold(I) complexes with bidentate phosphines were abruptly stopped when Hoke *et al.*²⁷⁶ discovered their significant cardiotoxicity. Nevertheless, the need for developing new cytotoxic gold(I) complexes that have antitumour activity is high. It is demonstrated by the broad-spectrum activity of gold(I) phosphine complexes against even cisplatin resistant tumours. Clearly, new ligand designs, new drug formulation methods and an even wider range of tumour systems need to be investigated in order to determine optimal activities and to reduce the side-effects of gold phosphine complexes.

IV.1.3 Design of new antitumour-active compounds

A new approach to the design of more efficient gold drugs has evolved over the last ten years. It consists of modification of the properties of known antitumour agents by coordinating them to gold(I). This ideally leads to at least one of the following:

- a) increased stability of some ligands,
- b) altered *in vivo* distribution of the drug,
- c) synergistic mechanism of cytotoxicity/antitumour activity.

Several examples of the application of this approach have appeared recently in the literature: [(Ph₃P)Au(5-fluorodeoxyuridine)]¹²³ was evaluated against leukaemia *in vivo* and found to be more active than fluorodeoxyuridine itself. Similarly, [ClAu(μ -dppf)AuCl] was also more active than ferrocene itself.²⁷¹ Gold(I) complexes with ligands that include a biologically active moiety, such as methyl sulfoxide, Ph₂PCH₂CH₂S(O)Me,¹²⁴ and sugar molecules such as n-MBPA,¹⁷ where MBPA = methyl

4,6-*O*-benzylidene-2-deoxy-2-(diphenylphosphino)- α -D-altropyranoside and $n = 2$ or 3 , showed high potential as antitumour agents.

To date there has been no report of attempts to combine the biological potential of gold(I) and polythiophene compounds. Thus, this work provides the first example of the incorporation of α -bi- and terthiophenes into phosphine ligands and the subsequent coordination of these ligands to gold(I). The combination of the two moieties – a thienylphosphine bonded to gold(I) – is expected to positively affect antitumour properties because:

- a) Thiophene-based phosphines are remarkably stable towards oxidation, thus ensuring that they are not deactivated *in vivo*;
- b) The mechanism of the cytotoxic action of polythiophenes is different to that of traditional phosphines and their gold(I) complexes, a synergistic effect therefore being anticipated.

It is well established that the mechanism of action of oligothiophene compounds is based on their photochemical properties. It is also true that a large number of publications has appeared in connection with the photophysics of various gold(I) compounds (see Section 3 in Chapter III), such as their luminescent properties in the solid state and in solution, significant advances having already been made in the elucidation of the nature of their emission. However, hardly any studies have been conducted concerning the chemical behaviour of the excited species. In fact it was only recently shown that Auranofin undergoes photodecomposition,²⁷⁷ but the product and intermediate species could not be identified. During the investigation of irradiation of a plasmid DNA in the presence of $[\text{Au}_3(\text{dmmp})_2]^{3+}$ [dmmp = bis(dimethylphosphinomethyl)methylphosphine], non-specific cleavage of DNA was observed as a result of the production of active oxygen species ($^1\text{O}_2$ or O_2^-) due to the photosensitising action of the gold complex.²⁷⁸ From these two studies it is difficult to estimate the effect UV irradiation has on the photocytotoxic properties of gold(I) compounds. Hence, this work aims to provide preliminary data on the possibility of use of gold(I) thienylphosphine complexes as cytotoxic agents not only under ambient conditions but also in the presence of near UV light.

IV.2 PHOTSENSITISING PROPERTIES OF THIENYLPHOSPHINES AND THEIR CHLOROGOLD(I) COMPLEXES

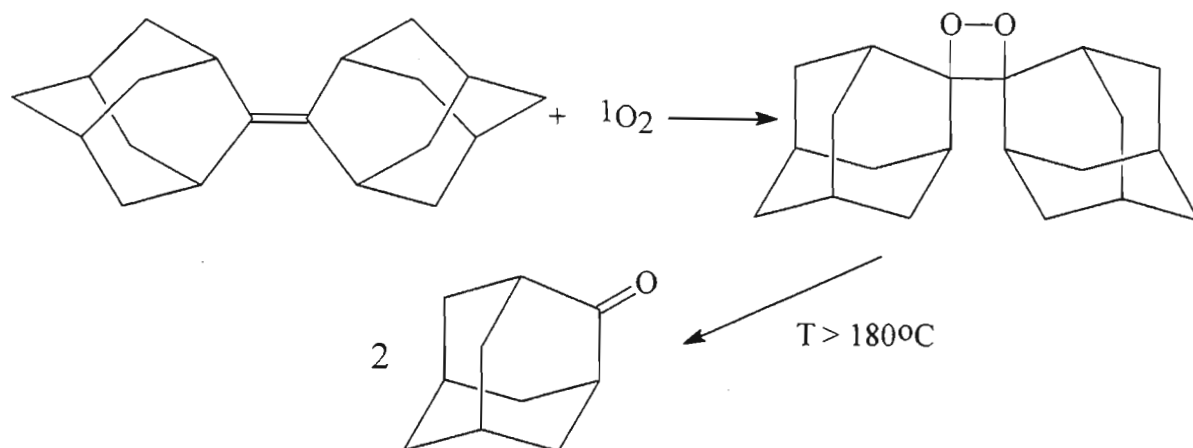
IV.2.1 Introduction

It was pointed out in the Section 1.1 of this Chapter, that the photocytotoxicity of terthiophene and its derivatives arises from their ability to sensitise the formation of singlet oxygen. Therefore, one of the first steps for the evaluation of the phototoxic properties of a polythiophene-containing compound has to be the estimation of its ability to generate singlet oxygen.

The quantum yield of singlet oxygen is the quantitative parameter employed to evaluate the photosensitising ability of a compound. Recently there has been significant interest in the spectroscopic properties of α -oligothiophene compounds as well as in their photosensitising efficiency.^{254,279-282} Several methods have been reported for measuring the quantum yield, the most reliable being laser flash photolysis and time-recorded phosphorescence.^{280,282} All available data on quantum yields for bithiophenes, terthiophenes and related compounds have been summarised by Scaiano *et al.*²⁸² The values of singlet oxygen quantum yields are shown to depend on both the method used for their determination and the solvent in which the measurements were conducted.²⁸² As a rule, the relative efficiency of singlet oxygen generation between different compounds remains unchanged by going from one solvent to another.

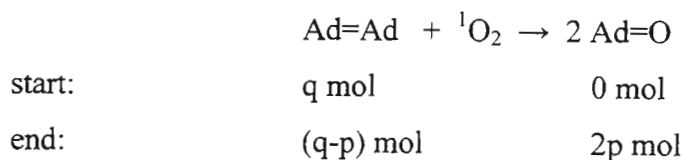
During this study, laser flash photolysis facilities were unavailable. Nevertheless it became possible to use an alternative method for estimating the efficiency of singlet oxygen production, *i.e.* the photochemical oxidation of adamantylidene adamantane (Ad=Ad) in the presence of a photosensitising agent.²⁵³ The results of this method are not as accurate as those of the spectroscopic technique, but they can still provide a reliable estimate of the relative photosensitising efficiency of a compound, provided a standard with a known efficiency is available. For this work α -terthiophene was selected as the reference compound and assigned a relative efficiency equal to 1.

The essence of the adamantylidene adamantane method is the determination of the amount of adamantanone formed after thermal decomposition of the dioxetane adduct. The latter is the result of the addition of singlet oxygen to the olefin (Scheme IV.2):



SCHEME IV.2

The conversion fraction of $\text{Ad}=\text{Ad}$ into the ketone ($\text{Ad}=\text{O}$) was chosen to be the quantitative parameter for estimating the photosensitising efficiency of a compound. It was calculated in the following way:



The ratio of adamantanone to the starting olefin – $Y = [\text{Ad}=\text{O}]/[\text{Ad}=\text{Ad}]$ – can be determined experimentally using gas chromatography. Therefore

$$Y = [\text{Ad}=\text{O}]/[\text{Ad}=\text{Ad}] = 2p/(q-p),$$

$$\therefore p = q \cdot Y/(2 + Y), \text{ or}$$

$$X = p/q = Y/(2 + Y), \text{ where } X \text{ is the conversion.}$$

IV.2.2 Photochemical oxidation of adamantylidene adamantane in presence of selected thiophene-based compounds

The photochemical oxidation of $\text{Ad}=\text{Ad}$ was carried out in dichloromethane using UVA light (a fluorescent lamp with a filter with a transmission maximum at 360 nm and cut-off

wavelengths of 320 nm and 400 nm) according to the modification of the method described by Gommers *et al.*²⁵³ The conditions are summarised in the Section 5.1 of this Chapter.

Using terthiophene SSS as a model sensitiser, it was established that:

- No reaction was observed, *i.e.* the $[Ad=O]/[Ad=Ad]$ ratio was zero, when no sensitiser was added; moreover use of three different concentrations of the sensitiser ($1 \cdot 10^{-4}$ M, $4 \cdot 10^{-5}$ M and $1 \cdot 10^{-5}$ M) but with the same amount of Ad=Ad did not significantly affect the conversion value;
- the conversion factor **X** depended on the initial amount of the olefin in the reaction mixture;
- the conversion factor **X** was directly proportional to the duration of the photochemical reaction (Fig. IV.2).

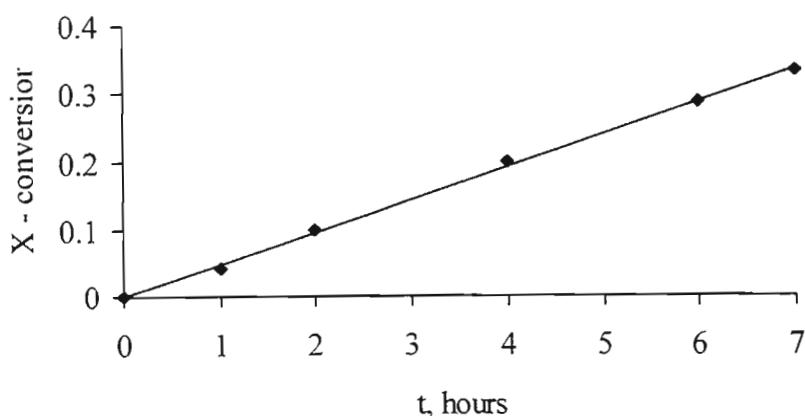


Fig. IV.2 The conversion factor **X** as a function of reaction time, $C(Ad=Ad) = 4 \cdot 10^{-4}$ M.

The following thiophene-based compounds were evaluated in the photochemical oxidation of adamantylidene adamantane: SS, SSS, SNS, PS, PSP, PSS, PSSP, PSSS, PSSSP, PSNSP, $[ClAuPS]$, $[ClAu(\mu-PSP)AuCl]$, $[ClAuPSS]$, $[ClAu(\mu-PSSP)AuCl]$, $[ClAuPSSS]$, and $[ClAu(\mu-PSSSP)AuCl]$. The results are presented in Table IV.1. The relative photosensitising efficiency of SSS in dichloromethane is taken as 1.

The mixed pyridine-thiophene heterocycle SNS was investigated in order to verify the meaningfulness of the results. Scaiano *et al.*²⁸² give the value of the singlet oxygen quantum yield for this compound as 0.27 in benzene. The value for SSS in the same solvent was 0.75. Therefore, the relative efficiency of SNS in comparison to SSS is 0.36. In this study, the value obtained for SNS was 0.38. Taking into account the differences in

the solvents and the experimental errors, the correlation between the two values appears good. Unfortunately, no other compound, evaluated by Scaiano *et al.*,²⁸² was available to confirm that this correlation is not a mere coincidence. Surprisingly, no quantum yield data have been reported for SS.

Table IV.1 Conversion factor **X**, % (Ad=Ad→Ad=O) and relative photosynthesising efficiencies of various thiophene containing compounds in dichloromethane.

Compound	Peak area ratio, Z^*	Conversion factor, X %	Relative efficiency
SS	0.046	4.8	0.17
SSS	0.367	28.5	1.00
SNS	0.111	10.8	0.38
PS	0	0	0
PSP	0	0	0
PSS	0.208	18.4	0.65
PSSP	0.206	18.3	0.64
PSSS	0.314	25.4	0.89
PSSSP	0.301	24.7	0.87
PSNSP	0.127	11.6	0.41
[ClAuPS]	0	0	0
[ClAu(μ -PSP)AuCl]	0	0	0
[ClAuPSS]	0.200	17.9	0.63
[ClAu(μ -PSSP)AuCl]	0.222	19.4	0.68
[ClAuPSSS]	0.399	30.3	1.06
[ClAu(μ -PSSSP)AuCl]	0.359	28.1	0.99

* $Z = 0.46 \cdot Y$ and $X = Z / (0.92 + Z)$ (see Section 5.2 of this Chapter)

Consideration of the data in Table IV.1 shows that the introduction of either one or two phosphine groups into 2,2'-bithiophene (SS) significantly increases the efficiency of generation of singlet oxygen. However, phosphine substituents on SSS reduce the efficiency somewhat. Coordination of the thienylphosphines PSS and PSSS to gold either leads to small increases in efficiency or very little change in efficiency. This is a significant

result in that it shows that the photosensitising of the thienylphosphine is not lost on coordination to gold(I). Compounds with a pyridine nucleus are less efficient sensitisers in comparison to their thiophene-containing analogues (compare SNS and SSS, PSNSP and PSSSP).

The photosensitising efficiencies of the thiophene-containing compounds are usefully considered in relation to their spectroscopic properties and, in particular, to their ability to absorb UV radiation (in the same solvent system). It was mentioned in the introduction to this chapter, that excitation of SSS with low-energy UV radiation produces the active species responsible for conversion of ground state triplet-oxygen into its singlet state. It is therefore expected that some correlation should exist between the efficiency of generation of singlet oxygen and the absorption of light in the near UV part of the spectrum. Table IV.2 presents the relative efficiencies of the compounds investigated taken in conjunction with λ_{\max} for their lowest energy UV-band as measured in dichloromethane.

The compounds with a pronounced photosensitising ability (relative efficiency not less than half of that for SSS) are given in bold in Table IV.2. As can be seen from the Table IV.2, those compounds which do not significantly absorb light above 300 nm do not generate singlet oxygen, while compounds that absorb between 350 and 390 nm are the most efficient in producing singlet oxygen. At the same time, there is no clear-cut relationship between the efficiency of generation of singlet oxygen and λ_{\max} or even between the efficiency normalised to the extinction coefficient ($\varepsilon \cdot 10^{-4}$) and λ_{\max} (Figures IV.3 and IV.4 - respectively).

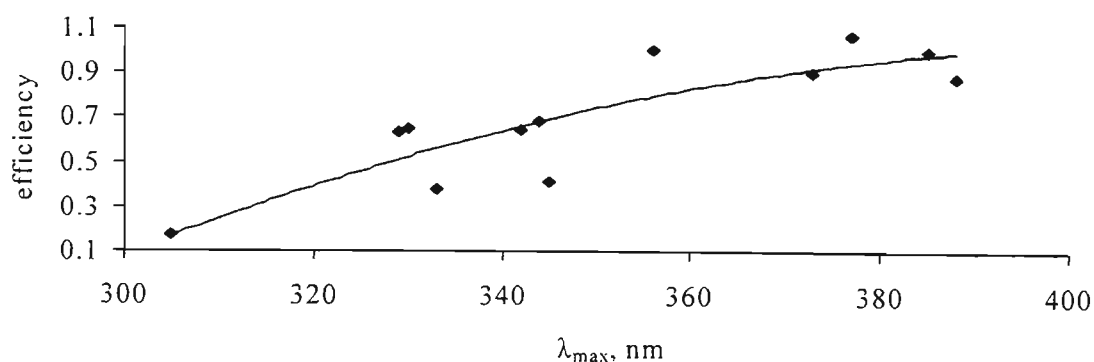
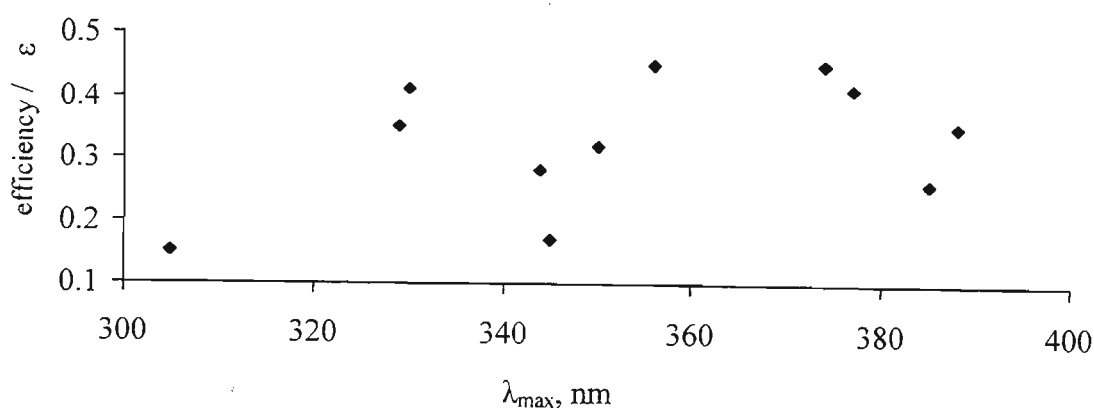


Fig. IV.3 Relative photosensitising efficiency vs. λ_{\max} of the lowest energy UV-absorption band.

Table IV.2 Relative photosensitising efficiency of thiophene-based compounds in dichloromethane and their lowest energy UV-absorption maxima as measured in dichloromethane.

Compound	Relative efficiency	λ_{\max} , nm ($\epsilon \cdot 10^{-4}$, $M^{-1} \cdot cm^{-1}$)
SS	0.17	305 (1.1)
SSS	1.00	356 (2.2)
PS	0	235* (1.2)
PSP	0	231* (2.8)
PSS	0.65	330 (1.6)
PSSP	0.64	350 (2.0)
PSSS	0.89	374 (2.0)
PSSSP	0.87	388 (2.5)
PSNSP	0.41	323 (2.7), 345 (2.8)
[ClAuPS]	0	233* (1.7)
[ClAu(μ -PSP)AuCl]	0	231* (3.4)
[ClAuPSS]	0.63	329 (1.8)
[ClAu(μ -PSSP)AuCl]	0.68	344 (2.4)
[ClAuPSSS]	1.06	377 (2.6)
[ClAu(μ -PSSSP)AuCl]	0.99	385 (3.8)
SNS	0.38	333 (1.0)

* UV-absorption of these compounds above 300 nm is less than 5% of its value at λ_{\max}

**Fig. IV.4** Relative normalised photosensitising efficiency vs. λ_{\max} of the lowest energy UV-absorption band.

The trend line on the Figure IV.4 seems to be shaped as parabola, resembling the transmission spectrum of the lamp filter. It is likely that the filter affects the amount of irradiation available to the sensitiser, thus influencing the photosensitising efficiency of compounds. Near the filter cut-off there is a proportionally lower amount of radiation is available to excite the molecules. Nevertheless, the relationship still cannot be considered as linear, there being a wide dispersion of data even in the middle of the graph, where filter transmission is 100%.

To summarise, it has been found that bithiophene and terthiophene-derived phosphines as well as their chlorogold(I) complexes show efficiency in the generation of singlet oxygen species comparable to that of α -terthiophene itself. At the same time, substitution of a thiophene ring by pyridine seems to be detrimental to the photosensitising ability.

IV.3 CYTOTOXIC PROPERTIES OF THIENYLPHOSPHINES AND THEIR GOLD(I) COMPLEXES

The next step in the evaluation of antitumour potential of the newly synthesised thiophene containing compounds is to test them against a suitable biological model. Historically, strategies for evaluation of new anticancer drugs have been predominantly based on an *in vivo* rodent model of disease. In recent years, a move has been seen from *in vivo* murine tumours to *in vitro* human tumour models.

In vitro cytotoxicity testing offers several advantages over the former method:

- a) It deals with the cells of a real human tumour, not its animal model, thus alleviating the need to extrapolate the results and make numerous assumptions,
- b) It prevents the unnecessary and costly sacrifice of animals,
- c) It provides a fast and efficient method of testing.

However, it still retains the innate drawback of any *in vitro* method, *i.e.* the inability to simulate the interaction with a whole living organism with its multitude of tissues and interrelationships. Quite often, compounds found to be cytotoxic *in vitro* are not active *in vivo* and vice versa.

Cell viability, *i.e.* the ratio of the amount of live cells after the treatment with the compound to the amount of live cells in the blank (blank refers to the treatment identical to the one with the compound with the only exception being the omission of the compound), is normally used as the quantitative measure of cytotoxicity. The compound is considered to be cytotoxic if it kills 50% or more of cells.

The cytotoxicity studies of compounds synthesised during this project are being presently carried out in the Department of Physiology, Medical School, University of Natal, Durban. The cell lines chosen for the testing are HepG2 – liver cancer and A549 – lung cancer. Using a variety of the cell lines rather than a single line is crucial in the determination of the selectivity of action (or the lack of it) of a compound against cancer cells. It is important that the compounds chosen as anticancer drugs show differential activity, otherwise they become overall toxic to the body. Selecting a liver cell line for testing allows one to predict a toxic effect the compound will have on a living organism, as liver is the major organ responsible for the detoxification of all chemicals entering the body.

It is also important to investigate cytotoxic effects of a compound in the presence of UV light due to the possibility of it inducing a photodynamic effect through generation of singlet oxygen. Photodynamic effects can play both positive and negative roles. On the positive side, they are currently used in medicine,^{262,263} as in photodynamic therapy (PDT is the combination of red laser or UV light, photosensitiser and molecular oxygen resulting in a therapeutic effect), for the treatment of a variety of diseases including cancer. On the negative side, they can cause skin and eye sensitivity and even tissue damage after uptake of the compound.^{264,265}

By the time this thesis was being written, only a part of the proposed investigation had been accomplished due to the problems associated with the handling and maintenance of the cell lines. So far, results are available for 8 compounds against the HepG2 cell line and for 16 compounds against the A549 cell line.

IV.3.1 Cytotoxic effects of selected compounds against the HepG2 cell line

The data on HepG2 cell viability upon incubation with various concentrations of six thiophene-containing compounds are given in Table IV.3.

Table IV.3 Cytotoxic effects for selected compounds against the HepG2 cell line in the dark

Compound/ Concentration	% Cell viability				
	1.56 µg/ml	3.12 µg/ml	6.25 µg/ml	12.5 µg/ml	25 µg/ml
SS	103	95	96	108	96
SSS	64	49	54	50	42
PSS	64	67	58	61	50
PSSP	91	114	95	130	86
[ClAuPSS]	86	54	25	7.4	7.2
[ClAu(µ-PSSP)AuCl]	88	87	101	92	88
dppe	101	92	82	71	63
[ClAu(µ-dppe)AuCl]	93	92	91	87	93

Known antitumour and cytotoxic agents dppe and its digold complex $[\text{ClAu}(\mu\text{-dppe})\text{AuCl}]$ have also been evaluated as reference compounds and are included in the Table. The results for the HepG2 cell line have only been obtained under conventional, 'in the dark' (*i.e.* without irradiation with UV light), conditions. The detailed procedure employed to obtain the results is outlined in the Experimental section of this Chapter.

From the Table above, it can be seen that only SSS (barely), PSS (barely and at a certain concentration) and $[\text{ClAuPSS}]$ can be regarded as cytotoxic. The effect of SS, $[\text{ClAu}(\mu\text{-PSSP})\text{AuCl}]$ and $[\text{ClAu}(\mu\text{-dppe})\text{AuCl}]$ on the cells is not much different from that of the control, while PSSP is even capable of promoting the cell growth at some concentrations (12.5 and 3.12 $\mu\text{g/ml}$). Dppe does not even achieve clear-cut cytotoxicity at the selected concentrations, but does show a clear trend of increasing toxicity with increasing concentration, and, therefore, is likely to become cytotoxic at higher concentrations. It is interesting to note that both dppe and $[\text{ClAu}(\mu\text{-dppe})\text{AuCl}]$ have previously been found to be cytotoxic against murine B16 melanoma cell line:⁷⁵ the latter was cytotoxic at concentrations as low as 8 μM , while in this study it did not have any effect on the HepG2 cell line at concentrations of up to 29 μM (\equiv 25 $\mu\text{g/ml}$).

Amongst the cytotoxic compounds, treatments with SSS and PSS show very little concentration dependency, while the toxicity of $[\text{ClAuPSS}]$ increases sharply with raising the concentration from 1.56 to 12.5 $\mu\text{g/ml}$ (21 μM) only then becoming constant. Indeed, the cytotoxicity of $[\text{ClAuPSS}]$ at concentrations of greater than 12.5 $\mu\text{g/ml}$ is dramatic with percentage cell viability values in single figures.

It must be stressed that the ability to kill cancerous cells increases from SS (non-cytotoxic) to PSS (mildly cytotoxic) to $[\text{ClAuPSS}]$ (highly cytotoxic). Thus, in this series, introduction of a phosphine moiety in the heterocycle structure proved beneficial. Even more so, coordination of this phosphine to gold(I) led to a remarkable improvement in the cytotoxic action. Mirabelli *et al.*⁷⁵ in their extensive study of antitumour activity of various phosphines and their chlorogold(I) complexes showed that coordination to gold often increases the antitumour potency of a ligand: *e.g.*, 1,2-bis[di(2-pyridyl)phosphino]ethane induced a negligible increase in the mouse life-span (ILS), while for its chlorogold(I) complex the ILS value was 60%. However cases with the opposite relationship are also

observed, as demonstrated by the same authors: 1,2-bis[di(2-thienyl)phosphino]ethane was active against P388 leukaemia, while its chlorogold(I) complex was not.

In this study comparison of the three ligand – chlorogold(I) complex pairs shows that only PSS/[ClAuPSS] couple possesses the ability to kill cancerous cells efficiently, implying that, perhaps, a certain structure of the phosphine is needed to induce cytotoxic effects. It might be significant that the inactive couples contained diphosphine moieties. However, more cytotoxicity data involving both mono- and diphosphine ligands as well as their complexes has to be obtained before a conclusion regarding structural requirements for cytotoxic activity is made. It will be of particular interest to examine the PSSS/[ClAuPSSS] couple because the thienylphosphine ligand, PSSS, is derived from the known cytotoxic compound, SSS.

The fact that [ClAuPSS] exhibits pronounced cytotoxic activity against HepG2 cell line whereas both dppe and [ClAu(μ -dppe)AuCl] are not effective suggests that the anti-neoplastic mechanism of the former is different. It has been established²⁸³ that the bis-chelated complex [Au(dppe)₂]Cl (formed *in vivo*) is responsible for the damaging effect of the dppe complex. In the case of PSS (or PSSS or any other of the thienylphosphines synthesised during this work) formation of the bis-chelated complex is clearly improbable and, thus, the observed cytotoxic effects must be induced by different means. This is a positive finding implying that there is a potential for the use of [ClAuPSS] against cell lines or cell line strains that are resistant to dppe and [ClAu(μ -dppe)AuCl].

Another factor to be considered when evaluating cytotoxicity is the delivery of compounds to the cancerous cells. In this light, poor (or the lack of) activity of PSSP and [ClAu(μ -PSSP)AuCl] might be the result of their poor solubility in solvents as polar as the water-based culture media (even with some 5% DMSO added). However, in order to prove or disprove this suggestion, a wider spectrum of related compounds with variable solubility patterns has to be tested.

IV.3.2 Cytotoxic effects of selected compounds against the A549 cell line

Cytotoxicity data for a number of thiophene-based compounds against the A549 cell line both in the dark (no UV light) and under near UV light (subsequently referred to as UVA

light) are presented in the Tables IV.4 and IV.5, respectively. The reference compounds dppe and $[\text{ClAu}(\mu\text{-dppe})\text{AuCl}]$ are also included in the Tables.

Table IV.4 Cytotoxic effects for selected compounds against the A549 cell line in the dark

Compound/ Concentration	% Cell viability			
	0.02 $\mu\text{g/ml}$	0.1 $\mu\text{g/ml}$	1.0 $\mu\text{g/ml}$	10 $\mu\text{g/ml}$
SN	78	74	87	82
SSS	70	70	72	63
SNS	96	110	80	80
NSN*	105	120	138	162
PS	151	130	129	107
PDS	196	153	108	106
PTS	209	214	95	90
PSS	82	103	37	108
PSSS	82	130	74	33
PSSP	124	111	112	90
PSSSP	107	86	83	58
PSNSP	125	137	88	74
$[\text{ClAuPSS}]$	132	154	126	128
$[\text{ClAu}(\mu\text{-PSSP})\text{AuCl}]$	133	120	146	98
dppe	118	89	58	31
$[\text{ClAu}(\mu\text{-dppe})\text{AuCl}]$	47	95	57	50

* NSN is 2,6 -bis(2'-thienyl)pyridine; it was evaluated here as an aid to understanding the effect of thiophene and pyridine rings on cytotoxic properties

In Table IV.4 only four compounds - PSS, PSSS, dppe and $[\text{ClAu}(\mu\text{-dppe})\text{AuCl}]$ - have potential cytotoxic properties as measured by a cell viability of less than 50% and given in the Table in bold. However, except in the case of dppe, there is no evidence of increasing toxicity with increasing concentration. The remaining compounds are generally inactive, some even promoting cell growth (for these, values are shown in the Table in *italics*). In fact, the monothiophene-containing phosphines PS, PDS and PTS are remarkable in their ability to promote cell growth, yielding proliferation increases of up to 100%! The greater number of thiophene rings in the molecules of these phosphines appears to elicit a larger

dependence of the percentage cell viability on the phosphine concentration *e.g.*, for PS the range of the cell viability is 44%, while it is 124% for PTS. The ligand NSN [NSN = 2,6-bis(2'-thienyl)pyridine – *vide infra*] also shows a tendency to promote cell growth, as evidenced by an increase in cell survival with an increase in concentration. Such a trend is entirely opposite to normal cytotoxic behaviour, when an increase in the concentration of a substrate leads to further cell destruction.

Also noteworthy is that the cytotoxic effect of SSS in the dark towards the A549 cell line seems to be insignificant – as opposed to its behaviour in the HepG2 experiment and contrary to the results of Hudson on the P815 mouse mastocytoma cell line.¹²⁰ Likewise, the compounds PSS and [ClAuPSS] – found to be cytotoxic (mildly, PSS and highly, [ClAuPSS]) against the HepG2 cells – do not appear to be cytotoxic toward the A549 cells. (Reduction of the cell viability to 37% at a single intermediate concentration can hardly be considered as a manifestation of true cytotoxic activity for the compound.)

Unfortunately the compound SS has not yet been evaluated against the A549 cell line which made the comparison of the cell killing abilities in the SS-PSS-[ClAuPSS] or SS-PSSP-[ClAu(μ -PSSP)AuCl] series impossible. Similarly, there are insufficient data to correlate cytotoxic properties in the SSS-PSSS-[ClAuPSSS] and SSS-PSSSP-[ClAu(μ -PSSSP)AuCl] series as neither of the two gold chlorogold(I) complexes has been tested. However both terthiophene-derived phosphines show somewhat better ability to damage the A549 cancer cells than the parent heterocycle at the highest concentration used (33 and 58% vs. 63% respectively).

Amongst the three ligand/chlorogold(I) complex couples, only dppe and its complex exhibit the cytotoxic properties. The trend is similar to what was observed during the HepG2 experiment: if the phosphine ligand exhibits cytotoxicity, its gold complex is cytotoxic as well. The fact that in this case there is very little improvement in the cell killing ability of dppe upon coordination to gold might be attributed to the logistical shortfall of the experimental technique. As all the concentrations were measured in $\mu\text{g/ml}$ rather than in more meaningful μM , the direct comparison of cytotoxic effects becomes difficult: *i.e.* the molar concentration of the gold complex of dppe was just less than a half that of the ligand at the same mass concentration, so that the critical concentration of the complex necessary for effective killing of the cells might not have been achieved.

Table IV.5 Cytotoxic effects for selected compounds against the A549 cell line under UVA light

Compound/ Concentration	% Cell viability			
	0.02 µg/ml	0.1 µg/ml	1.0 µg/ml	10 µg/ml
SN	36	60	81	36
SSS	37	56	7	11
SNS	54	62	51	16
NSN	116	65	38	16
PS	68	75	63	64
PDS	54	71	63	58
PTS	56	65	66	45
PSS	55	61	62	19
PSSS	74	96	65	52
PSSP	157	129	98	99
PSSSP	54	71	25	15
PSNSP	80	84	117	121
[ClAuPSS]	107	110	107	78
[ClAu(µ-PSSP)AuCl]	167	132	104	91
dppe	84	77	110	86
[ClAu(µ-dppe)AuCl]	53	35	57	50

As shown in Table IV.5, eight compounds show cytotoxic behaviour towards the A549 cell line under irradiation with UVA light: SN, SSS SNS, NSN, PTS, PSS, PSSSP and [ClAu(µ-dppe)AuCl]. For each of this thiophene containing compounds there is a significant enhancement in activity under UVA light compared to what was observed in the dark. Dramatic activity is exhibited by SSS and PSSSP at concentrations greater than 1 µg/ml. With regard to the remaining compounds, SN shows concentration dependent cytotoxicity – pronounced at both low and high concentrations, but poor at intermediate values. The SNS and PSS molecules are mildly cytotoxic becoming very potent at the highest concentration, while NSN shows a linear dependence of its potency on concentration. Both PTS and [ClAu(µ-dppe)AuCl] can be referred to as mildly cytotoxic without showing a strong concentration dependency.

Comparison of the data in the two Tables shows that the application of UVA light generally increases the cytotoxic properties of the compounds tested. The exception is PSNSP, which demonstrates a unique and quite remarkable behaviour, in that its effect under UVA light is reversed with the compound becoming a cell growth promoter as the concentration is increased.

The question arises as to whether the increase in activity is due to the photosensitising ability of the compound, *i.e.* to its ability to generate singlet oxygen. This will now be examined by correlating the activity of the cytotoxic compounds under UVA light with their photosensitising efficiency as determined in the Section 2 of this Chapter (see Table IV.2). Table IV.6a gives both the cytotoxic effects at the highest concentration of the eight compounds active under UVA light and their photosensitising efficiencies. (In only a couple of cases the cytotoxic response at this concentration is not the greatest achieved for the particular compound.)

Table IV.6a Cytotoxic responses against A549 cells of the eight cytotoxic compounds at 10 µg/ml under UVA light and their relative photosensitising efficiencies

Compound	Cell viability at 10 µg/ml	Relative photosensitising efficiency
SN	36	-*
SSS	11	1.0
SNS	16	0.38
NSN	16	-*
PTS	45	-*
PSS	19	0.65
PSSSP	15	0.87
(µ-dppe)(AuCl) ₂	50	-*

* Photosensitising efficiency was not measured

Before discussing the data in Table IV.6a it should be noted that the photosensitising efficiency and cell killing ability were determined under different conditions: the photochemical studies were conducted in dichloromethane, while the tissue culture experiments were carried out in aqueous culture medium with a small amount of DMSO added. Moreover, according to literature data,²⁸² the photosensitising efficiencies for the

same compound vary for different solvents and thus the values experimentally determined during this study cannot be taken as absolute. Nevertheless, the photosensitising efficiencies determined in dichloromethane may serve as qualitative guide as to how efficient the compound is in producing singlet oxygen in tissue culture experiments.

Although no measurements of the relative photosensitising efficiencies for PTS and $[\text{ClAu}(\mu\text{-dppe})\text{AuCl}]$ were carried out, one can deduce from their spectroscopic properties (both compounds do not absorb above 300 nm – the lamp filter cut-off), that they do not possess photosensitising properties. It is more difficult to estimate the photosensitising efficiencies of SN and NSN as they both absorb UV light between 300 and 400 nm, but it would be reasonable to believe that their efficiencies are greater than zero.

From the data in the Table IV.6a it is clear that good photosensitising ability is associated with good cell killing ability in the presence of light, at least for those four compounds for which the relative efficiency was measured. The non-photosensitising PTS and $[\text{ClAu}(\mu\text{-dppe})\text{AuCl}]$ show only mild cytotoxicity. However not all compounds with good photosensitising abilities kill A549 cells under UVA light: these are PSSS, PSSP, $[\text{ClAuPSS}]$, PSNSP and $[\text{ClAu}(\mu\text{-PSSP})\text{AuCl}]$. Table IV.6b combines the compounds which did not prove to be cytotoxic against A549 cell line under UVA light together with cytotoxic response and photosensitising efficiency values.

Table IV.6b Cytotoxic responses against A549 cells of the eight non-cytotoxic compounds at 10 $\mu\text{g/ml}$ under UVA light and their relative photosensitising efficiencies

Compound	Cell viability at 10 $\mu\text{g/ml}$	Relative photosensitising efficiency
PS	64	0
PDS	58	-*
PSSS	52	0.89
PSSP	99	0.64
PSNSP	121	0.41
$[\text{ClAuPSS}]$	78	0.63
$[\text{ClAu}(\mu\text{-PSSP})\text{AuCl}]$	91	0.68
dppe	86	-*

* Photosensitising efficiency was not measured

The analysis of the data in both Tables leads to the conclusion that the cytotoxicity of a compound is not directly proportional to its photosensitising ability, although in general the ability to produce singlet oxygen does seem to assist with cell destruction. To illustrate, let us take two similar compounds, PSSS and PSSSP. They are both good photosensitisers (relative efficiencies 0.89 and 0.87, respectively), but the former loses its activity under UVA light, while the latter becomes much more active in the presence of light. The reason behind such a difference in behaviour is not clear. Perhaps, quenching of photosensitising ability for some compounds in cell culture medium could be the cause. At present, the amount of the data accumulated is too limited to establish the true reason.

Looking at individual compounds, PSS and $[\text{ClAu}(\mu\text{-dppe})\text{AuCl}]$ are cytotoxic both in the dark and under UVA light. However it appears that their mechanisms of action in presence and absence of light are very different, as evidenced by the fact that the concentrations at which they act as non-cytotoxic in the dark are precisely those which caused the most cell mortality under UVA light.

The PSSP ligand and its gold complex, $[\text{ClAu}(\mu\text{-PSSP})\text{AuCl}]$, are not cytotoxic either in the dark or under UVA light. At the same time, they both affect the cells, although not in the way they were intended, *i.e.* they promote the cell growth at certain concentrations. This fact implies that the previously suggested hypothesis for the lack of the activity due to the solubility problems is probably not true. Thus a possible explanation for the poor cell-killing performance is that PSSP and $[\text{ClAu}(\mu\text{-PSSP})\text{AuCl}]$ are simply not capable of damaging any part of the cell either in the dark or under UVA light within the selected concentration range.

The third chlorogold(I) complex studied, $[\text{ClAuPSS}]$ – the compound showing remarkable activity against HepG2 cells, is not cytotoxic either in the dark or under UVA light against A549 cells. It is difficult to correlate cytotoxicity under UVA light and the presence of gold(I) in the compounds. So far, only three gold(I) complexes have been tested. Two of them – both containing bithiophene moiety – appear inactive, while the third, $[\text{ClAu}(\mu\text{-dppe})\text{AuCl}]$ shows moderate activity under UVA light. As, in general, their cytotoxic properties even in absence of light are quite similar to those in its presence, no definite conclusion on the effect of presence of gold(I) on the cytotoxicity of compounds under UVA conditions can be reached.

The phosphines containing monothiophene units – PS, PDS and PTS, do not have cytotoxic properties either in the dark or under UVA light. However they do seem to change their effect on cells in the presence of light: they can be generally considered as cell growth promoters in the dark, while inducing certain degree of cell mortality under UVA light. It is unlikely that this effect can be related to their photosensitising abilities as they do not absorb UV light above 300 nm.

From the results obtained with A549 cell line both in the dark and under UVA light, it can be seen that ability of a compound [a heterocycle, a phosphine or a gold(I)-phosphine complex] to generate singlet oxygen does affect its cytotoxicity under UVA light. Irradiation certainly changes responses of cells as well as the concentration-dependency trends for most of the compounds. We speculate that UVA light primarily affects targets inside the cells, which subsequently become more susceptible to an attack by phosphines or their complexes. However, at least four compounds appear to be genuinely photocytotoxic as their cytotoxic effects increase considerably in the presence of light and they have been proven to be quite efficient photosensitisers, at least in dichloromethane. The four compounds are SSS, SNS, PSS and PSSSP.

Finally, in order to establish a relationship between the structure of a compound and its cytotoxic behaviour, it is most meaningful to compare compounds with similar molar masses. The next six Figures present a graphical comparison of the cytotoxicity of compounds of similar molar masses towards the A549 cell line in the dark and under UVA light.

The following three sets of compounds are considered:

- a) SSS ($M = 248 \text{ g}\cdot\text{mol}^{-1}$), SNS ($M = 243 \text{ g}\cdot\text{mol}^{-1}$) and NSN ($M = 238 \text{ g}\cdot\text{mol}^{-1}$)
- b) PS ($M = 268 \text{ g}\cdot\text{mol}^{-1}$), PDS ($M = 274 \text{ g}\cdot\text{mol}^{-1}$) and PTS ($M = 280 \text{ g}\cdot\text{mol}^{-1}$)
- c) PSSSP ($M = 616 \text{ g}\cdot\text{mol}^{-1}$) and PSNSP ($M = 611 \text{ g}\cdot\text{mol}^{-1}$).

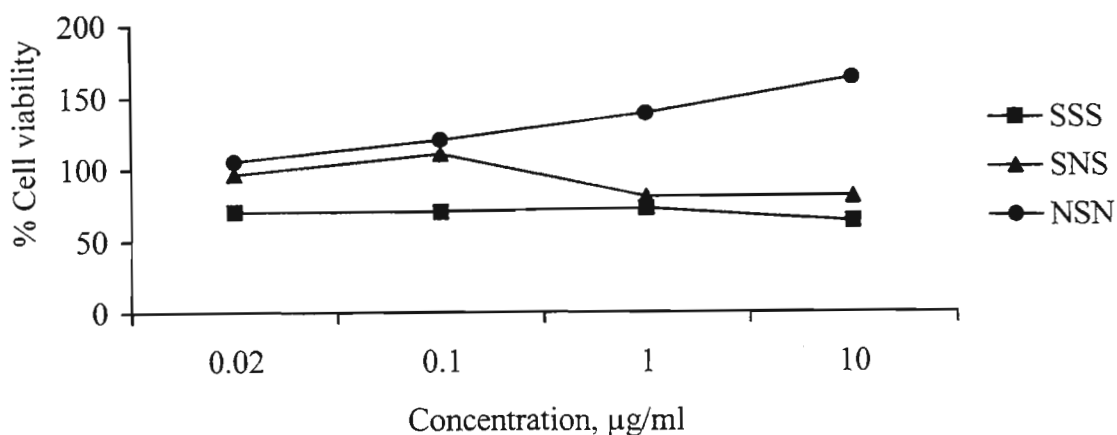


Fig. IV.5a Cytotoxic effects of the SSS, SNS and NSN heterocycles on the A549 cell line in the dark.

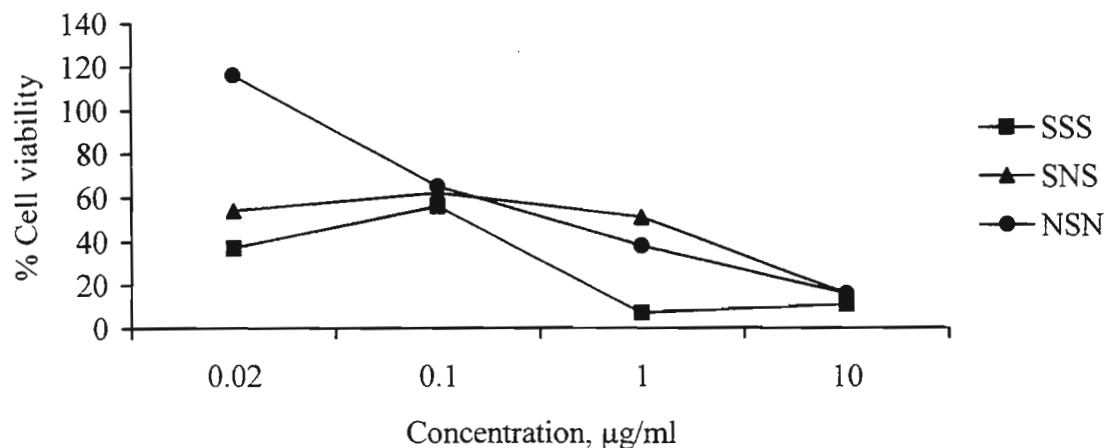


Fig. IV.5b Cytotoxic effects of the SSS, SNS and NSN heterocycles on the A549 cell line under UVA light.

It can be seen from Figures IV.5a and IV.5b, the SSS, SNS and NSN heterocycles show different trends both in the dark and under UVA light. However, at high concentrations under UVA light they all become very potent in killing the cells. In all cases SSS, the compound containing three α -linked thiophene units, shows the greatest cytotoxic effects.

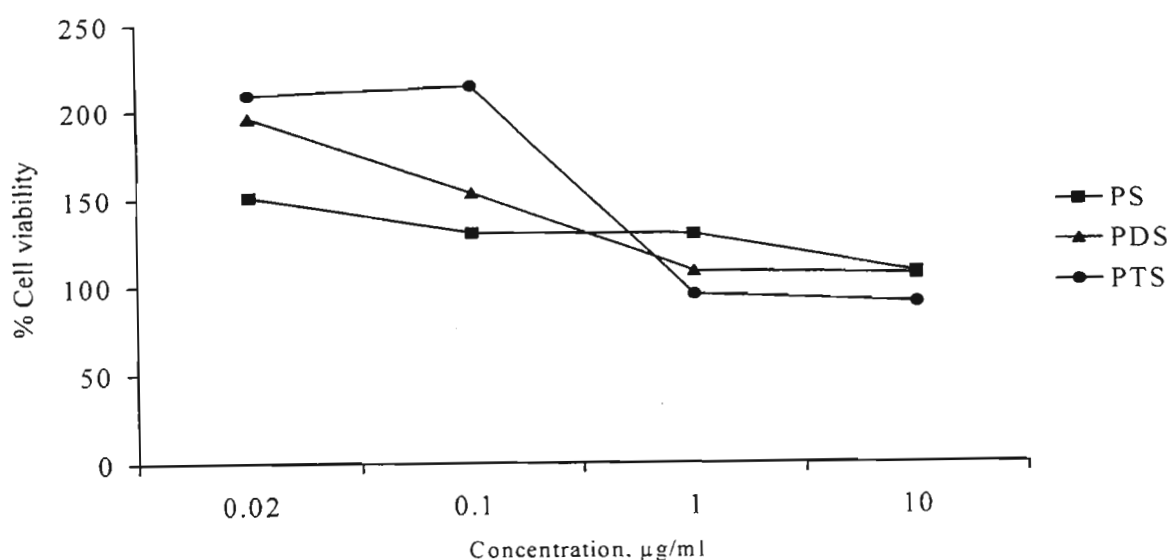


Fig. IV.6a Cytotoxic effects of the phosphines PS, PDS and PTS on the A549 cell line in the dark.

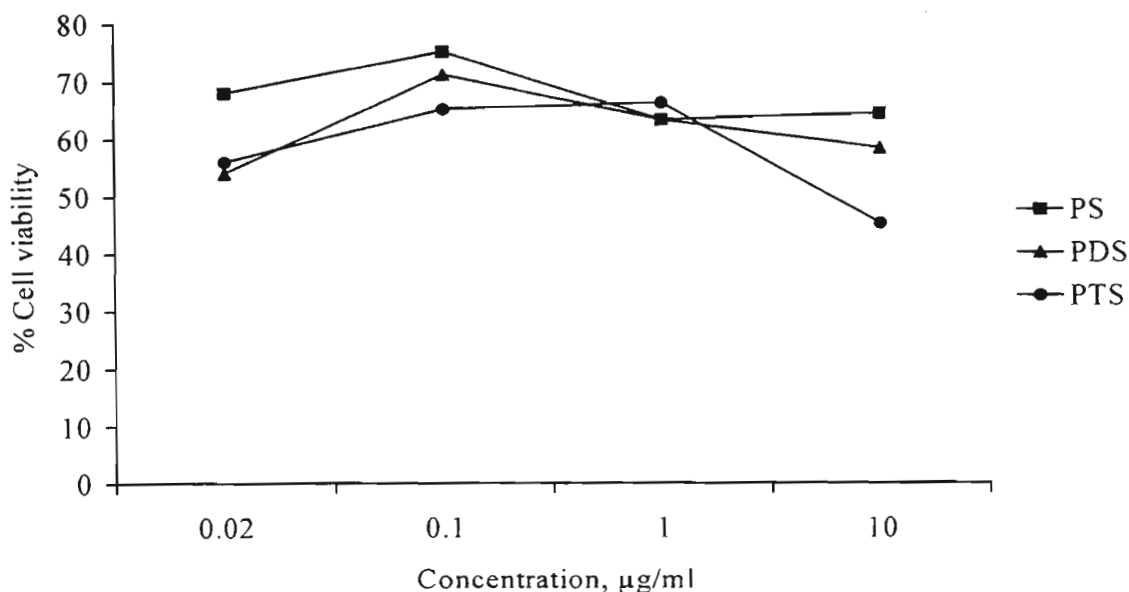


Fig. IV.6b Cytotoxic effects of the phosphines PS, PDS and PTS on the A549 cell line under UVA light.

As can be seen from Figures IV.6a and IV.6b the three phosphines PS, PDS and PTS show quite similar trends in their action on cells. The profiles showing cell growth promotion in the dark and cytotoxicity under UVA light are similar for all three compounds. The effect of PTS on the A549 cells is the greatest of the three phosphines, again suggesting that greater number of thiophene units (unlinked in this case) leads to a higher activity for a compound.

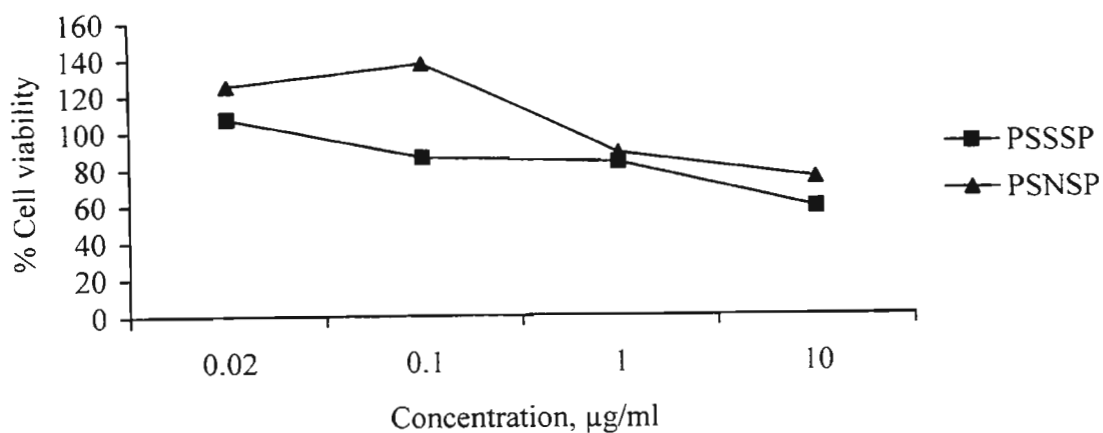


Fig. IV.7a Cytotoxic effects of the diphosphines PSSSP and PSNSP on the A549 cell line in the dark.

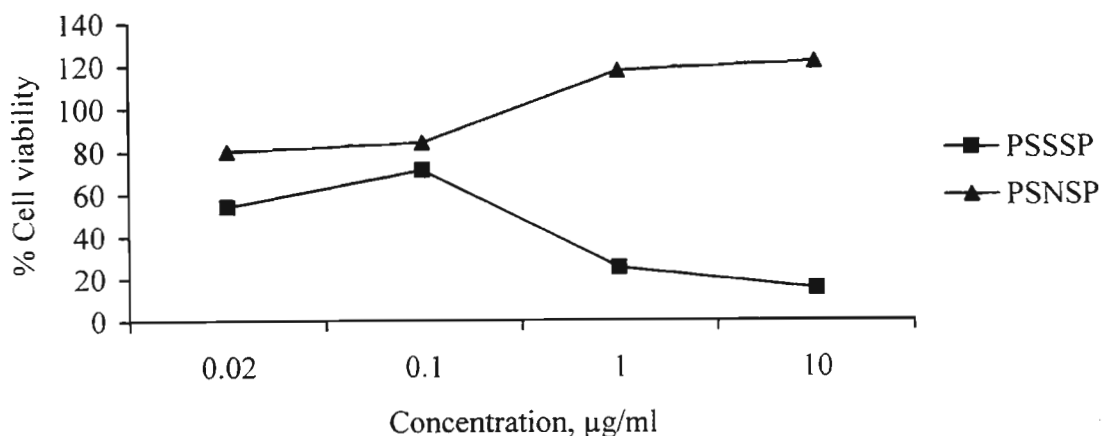


Fig. IV.7b Cytotoxic effects of the diphosphines PSSSP and PSNSP on the A549 cell line under UVA light.

Comparison of Figures IV.7a and IV.7b shows that PSSSP and PSNSP exhibit different trends of cytotoxic behaviour. In this case the phosphine derived from the most cytotoxic heterocycle, PSSSP, is more effective as a cell killing agent than PSNSP (where an α -linked pyridine unit was substituted for the middle thiophene) at all concentrations both in the dark and under UVA light.

A tentative conclusion can be made from the above discussion, that the more thiophene units are in a compound the more active it is; derivatives where a pyridine or a phenyl ring has been substituted for a thiophene unit are invariably less active.

IV.4 CONCLUSION

Phosphines derived from bi- and terthiophenes retain the photosensitising property characteristic of these heterocycles *i.e.*, thienylphosphines are also capable of absorbing and transferring light energy to ground state oxygen in order to produce singlet oxygen. This was conclusively demonstrated using the conversion of adamantylidene adamantane to adamantanone as a measure of the efficiency of singlet oxygen production. The relative photosensitising efficiency of the thienylphosphine as compared to the parent heterocycle does vary however. Thus, while phosphines derived from bithiophene (SS) are more efficient in converting oxygen to its singlet state than bithiophene itself, phosphines derived from terthiophene (SSS) are less efficient than terthiophene itself (see data in Table IV.1). Based on the data in Tables IV.1 and IV.2 it seems unlikely that the ability of the thienylphosphine to absorb UV light determines its ability to generate oxygen in its excited state. For example, SSS and PSSP have very similar absorption maxima and extinction coefficients of 356 nm ($2.2 \cdot 10^4 \text{ M}^{-1} \cdot \text{cm}^{-1}$) and 350 nm ($2.0 \cdot 10^4 \text{ M}^{-1} \cdot \text{cm}^{-1}$) respectively, yet their relative efficiencies of 1.0 and 0.64 respectively are very different. Nevertheless, absorption of UVA light is a prerequisite if activation of molecular oxygen is to take place.

There is a clear trend of increasing photosensitising ability with an increasing number of linked thiophene units in the molecule. Thus, SSS is more efficient than SS (relative sensitising efficiencies 1.0 and 0.17, respectively), which in turn is more efficient than thiophene itself (relative photosensitising efficiency of the latter was not measured but it is not expected to be different from zero, as it absorbs UV light only below 300 nm). Likewise, PSSSP is more efficient than PSSP and PSP (relative photosensitising efficiencies 0.87, 0.64 and 0), while PSSS is more efficient than PSS and PS (0.89, 0.65 and 0). The trend is retained even for the chlorogold(I) complexes: the relative photosensitising efficiencies drop from 0.99 {[ClAu(μ -PSSSP)AuCl]} to 0.68 {[ClAu(μ -PSSP)AuCl]} to 0 {[ClAu(μ -PSP)AuCl]} – in the digold series, and from 1.06 {[ClAuPSSS]} to 0.63 {[ClAuPSS]} to 0 {[ClAuPS]} – in the monogold series. The results obtained in this work also show that substitution of a pyridine for a thiophene unit either in the parent heterocycle or the thienylphosphine, has a detrimental effect on the ability of the compound to photosensitise the generation of singlet oxygen; for example SNS is less effective than SSS and PSNSP is less effective than PSSSP.

Interestingly, a thienylphosphine ligand and its gold(I) complex demonstrate the same photosensitising abilities. This indicates that the ability of a gold complex to sensitise the generation of singlet oxygen is determined by the optical properties of thienylphosphine chromophore. In general, the observed differences in the photosensitising abilities of the compounds studied in this work will depend on the properties of the excited state of the photosensitising molecule and, in particular, on what pathways are available for radiationless deactivation of the excited state. Extensive studies^{254,279-282} of the photophysics of terthiophene and its derivatives support this conclusion. However, a similar study of the photophysics of the new thienylphosphines is beyond the scope of this work.

Polythiophene-based phosphines show promising potential as cytotoxic agents. At reasonably low concentrations certain phosphines and their gold(I) complexes can kill a high number of cancerous cells. The PSS ligand kills 50% of the cells at concentration of 25 $\mu\text{g/ml}$ (71 μM), while upon coordinating to gold it becomes much more potent leaving only about 7% of viable HepG2 cells at 12.5 $\mu\text{g/ml}$ (21 μM). Another monophosphine ligand, PSSS, proves to be very active against A549 cells, killing two thirds of the cancerous cells at 10 $\mu\text{g/ml}$ (29 μM).

It is noteworthy that exposure of cells treated with a phosphine or its complex to UVA light generally results in higher cytotoxic effects, although exposure of cells to UVA light alone normally promotes cell growth. Indeed, the cell viability for the control rises upon irradiation (note the absorbance values for the controls in Tables IV.8a and IV.8b - see Experimental section). At least four of the compounds (SSS, SNS, PSS, PSSSP and possibly SN and NSN) tested are likely to be photocytotoxic; in addition to being singlet oxygen generators they exhibited increases in cell killing potency upon switching conditions from the dark to UVA light. In other instances it is likely that the UVA radiation affects certain targets inside the cells, which then respond to the chemical treatment. Different phosphines show different trends to kill (or grow) cells, so, perhaps, their modes of interaction with the tumour cells are not the same, those being strongly dependent on the fine structure of the molecule.

A brief attempt in correlating structure and activity amongst thienylphosphines as well as related compounds brings about a tentative conclusion that presence of thiophene nuclei is

important for a compound's cytotoxic ability, since its replacement with a pyridine (compare SSS and SNS, PSSSP and PSNSP) or a phenyl (compare activities of PS, PDS and PTS) moiety leads to a decrease in potency.

The thienylphosphines or their gold complexes exhibit variable potency against the two cell lines studied in this work, *i.e.* HepG2 and A549. It is reasonable to suggest that the nature of the cells plays an active role in the determination of a compound's mode of action – perhaps by supplying certain subcellular targets capable of interaction with the compound in question. As a consequence, the cytotoxic ability of a compound is a function of the nature of cells. Comparison of the data given for the two cell lines in Tables IV.3 and IV.4 for SSS, PSS, [ClAuPSS], dppe and [ClAu(μ -dppe)AuCl] shows that cell responses to the exposure to the above compounds are markedly different. For example, [ClAuPSS] is extremely toxic towards HepG2 cells, but growth promoting in A549 cell line, while [ClAu(μ -dppe)AuCl] is inactive towards the former and cytotoxic in the latter.

The limited amount of data available at present does not allow definite conclusions to be made about what features in a phosphine structure contribute to it being (or not being) cytotoxic, *i.e.* we cannot establish an overall structure-function relationship. In the near future extensive testing will have to be carried out in order to obtain sufficient information. First of all, a variety of monophosphines should be studied together with their chlorogold(I) complexes in order to determine which particular structural feature makes [ClAuPSS] so active against HepG2 cells. Also, a greater variety of thienyl-based phosphines should be tested on a variety of cell lines under both "dark" and "UVA" conditions in order to establish more definite links between their photosensitising abilities and possibility of photocytotoxic action.

At present, the most promising cytotoxic compound out of the 16 substances evaluated is the complex [ClAuPSS]. Future studies, possibly *in vivo*, are needed to determine the possibility of its use as an antitumour agent.

IV.5 EXPERIMENTAL

IV.5.1 Photochemical studies

Irradiation of adamantylidene adamantane (for preparation see Appendix A) solutions in the presence of a sensitizer was carried out at 22°C in a specific glass vessel with an open top, placed 25 cm below a Philips TLD 15W/05 UV lamp (filter: $\lambda_{\text{max. T}} = 100\% = 366 \text{ nm}$, $\lambda_{\text{T}=10\%} = 310 \text{ and } 410 \text{ nm}$). Both the lamp and the solution were sealed in a foil-lined box (50 x 60 x 50 cm³). Oxygen gas was bubbled through the solution at a constant rate of 5 ml·min⁻¹. The solvent (dichloromethane) was added every 15 min to counteract evaporation and to maintain the volume at 50 ml. All reactions were carried out in duplicate, and the results are given as an average of the two values.

Conditions of photochemical oxidation of adamantylidene adamantane in presence of a potential single oxygen sensitizer:

Concentration of Ad=Ad	$4 \cdot 10^{-4} \text{ M}$
Concentration of a sensitizer	$4 \cdot 10^{-5} \text{ M}$
Irradiation time	6 hours

IV.5.2 Gas chromatographic analysis of adamantylidene adamantane and adamantanone mixtures

Gas chromatographic analysis was carried out on a Varian Vista 4600 GC chromatograph. The data was processed by Delta Chromatography Software (1991, SMM Instruments, RSA).

In order to reproducibly quantify the relative amount of Ad=Ad and Ad=O in the solution, certain conditions for the gas chromatographic analysis had to be optimised.

1. Column temperature

An isothermal regime with a column temperature of 170°C, rather than that reported of 205°C,²⁵³ was found to be optimal for the separation of the Ad=O and Ad=Ad peaks. It also allowed for a fast analysis time, as both compounds had retention times of less than 3

min. Increased temperatures resulted in a deterioration of the chromatographic separation. By lowering the temperature somewhat the separation of peaks is also improved

2. Injector temperature

During this analysis, it was established that the injector temperature affects the reproducibility of the results. In other words, there was a significant deviation between the values of peak area ratios, taken in quintuplicate. The deviation was found to be the smallest and the mean ratio value to be nearly constant, when the injector temperature was kept between 220 and 240°C (see Figure IV.8; the solid line joins the mean ratio values). On this basis, for quantitative analysis the injector temperature was selected as 230°C. The dependence of the $[Ad=O]/[Ad=Ad]$ ratio on the injector temperature can be attributed to incomplete transfer of the compounds in the gaseous phase at lower temperatures, while at high temperatures decomposition tends to occur.

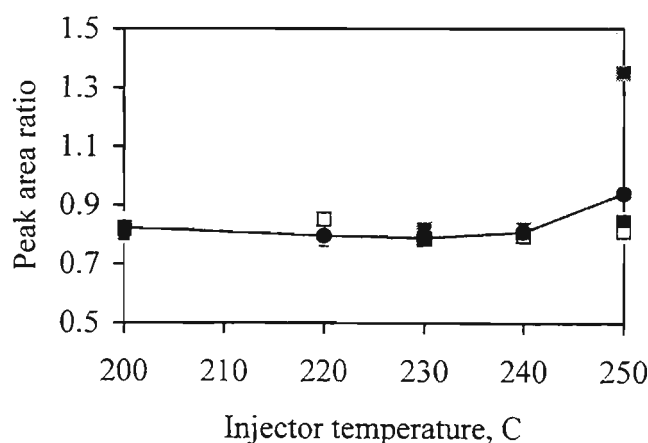


Fig. IV.8 The effect of injector temperature on the $[Ad=O]/[Ad=Ad]$ ratio.

The following chromatographic conditions were employed for the analysis:

Detection	FID, range 11;
Column	Carbowax 20M, 15m x 0.53 mm;
Carrier gas	He, flow rate 11 ml·min ⁻¹ , split ratio 2:1;
Injector temperature	230°C;
Detector temperature	250°C;
Column temperature	170°C, isothermal program;
Injection volume	1 µl.

All injections were made in quintuplicate.

Retention times:

Adamantanone	0.6 min,
Adamantylidene adamantane	2.1 min.

The calibration curve for Ad=Ad and Ad=O mixtures ($C = \pm 5 \cdot 10^{-4}$ M) is shown on Figure IV.9.

From this graph, the proportionality coefficient between the observed $[Ad=O]/[Ad=Ad]$ peak area ratio Z and the actual concentration ratio Y was obtained:

$$\underline{Z = 0.46 \cdot Y}$$

The value is quite close to the theoretically expected value of 0.5, as the sensitivity of a FID detector is proportional to the number of carbon atoms in the molecule.

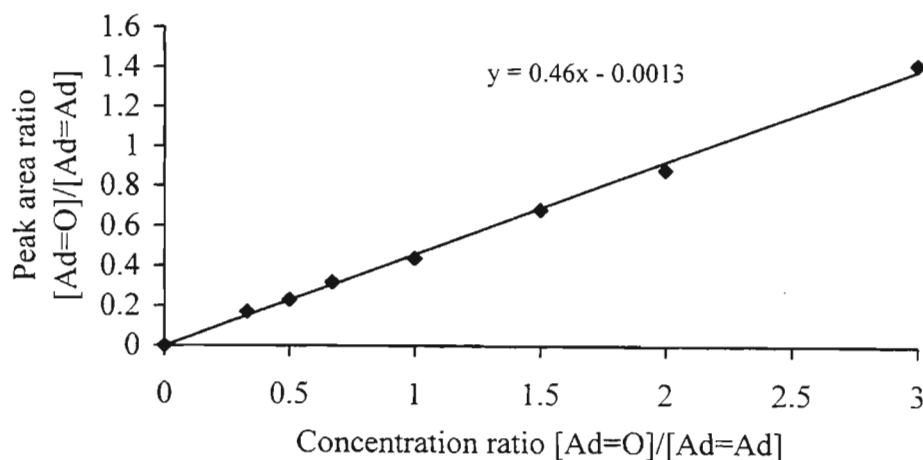


Fig. IV.9 Calibration curve for adamantylidene adamantane and adamantanone mixtures.

Thus, the final formulae used for the calculation of fractional conversion values are:

$$\underline{Y = Z/0.46} \text{ and } \underline{X = Z/(0.92 + Z)}$$

IV.5.3 Cytotoxicity measurements

These measurements were conducted by Ms D. Pillay at the Department of Physiology, Faculty of Medicine, University of Natal, Durban. The method used for the measurements has been adopted from Hudson¹²⁰ and modified according to the technique established in

that laboratory. All operations were performed under strictly sterile conditions (laminar flow). Cells were maintained according to the routine procedure.²⁸⁴

Aliquots of cell suspension (100 μ l) from one of the two human cell lines – HepG2 (liver carcinoma) or A549 (lung carcinoma) - were dispensed under minimal light from a stock suspension into wells of a 96-well microtitre plate. The cells were supplied with 100 μ l of cell culture medium (EMEM, BioWhittaker) and allowed to incubate for 0.5 hours. Thereafter, 100 μ l of the solution of the investigated compound (chosen concentration in 0.5% DMSO in the culture medium) was added to each well at a range of concentrations. For the HepG2 cell line the concentrations were 25 μ g/ml, 12.5 μ g/ml, 6.25 μ g/ml, 3.125 μ g/ml and 1.56 μ g/ml, and for the A549 – 10 μ g/ml, 1.0 μ g/ml, 0.2 μ g/ml and 0.02 μ g/ml.

For each concentration 5 assays were performed. The cells were then incubated for 48 hours. After the incubation, a solution of MTT {3-(4,5-dimethylthiazolyl)-2,5-diphenyl-2H-tetrazolium bromide} – 10 μ l, 5 mg/ml in cell culture medium – was added to each well. The plate was then incubated for a further 4 hours. A 100 μ l aliquot of DMSO was added to each cell to solubilise the formazan product formed. After 1 hour at 37°C the plate was then read spectrophotometrically on a microplate reader at 595 nm. As the formazan product is formed by live cells only (MTT is reduced by the succinate dehydrogenase enzymes present only in the mitochondria of live cells), absorbance is directly proportional to the amount of viable cells.

Cytotoxic measurement under UVA conditions were carried out in essentially the same way, apart from exposure of cells, treated with investigated compounds, to UVA light for 4 hours.

The following three Tables – Table IV.7 and Table IV.8a and IV.8b – present the raw data obtained for the viability of the HepG2 and A549 cells after treatment with a selection of the newly synthesised compounds.

The percentage cell viability was calculated from these tables as the ratio between absorbance of treated cells to that of the controls.

Table IV.7 Absorbance at 595 nm after treatment of the HepG2 cells with selected compounds in the dark

Compound/ Concentration	Absorbance at 595 nm				
	1.56 µg/ml	3.12 µg/ml	6.25 µg/ml	12.5 µg/ml	25 µg/ml
None (control)	0.758	0.758	0.758	0.758	0.758
SS	0.781	0.720	0.728	0.819	0.727
SSS	0.485	0.371	0.409	0.379	0.318
PSS	0.487	0.508	0.440	0.462	0.379
PSSP	0.690	0.864	0.720	0.985	0.652
[ClAuPSS]	0.653	0.409	0.190	0.056	0.055
[ClAu(µ-PSSP)AuCl]	0.667	0.659	0.766	0.697	0.665
dppe	0.767	0.697	0.622	0.538	0.478
[ClAu(µ-dppe)AuCl]	0.705	0.696	0.690	0.659	0.708

Table IV.8a Absorbance at 595 nm of the A549 cells after treatment with selected compounds in the dark

Compound/ Concentration µg/ml	Absorbance at 595 nm			
	0.02 µg/ml	0.1 µg/ml	1.0 µg/ml	10 µg/ml
None (control)	0.331	0.331	0.331	0.331
SN	0.261	0.248	0.290	0.274
SSS	0.229	0.229	0.238	0.210
SNS	0.323	0.369	0.268	0.261
NSN	0.348	0.402	0.429	0.536
PS	0.496	0.427	0.425	0.351
PDS	0.649	0.508	0.359	0.350
PTS	0.701	0.717	0.321	0.302
PSS	0.270	0.340	0.124	0.357
PSSS	0.271	0.432	0.243	0.107
PSSP	0.404	0.369	0.372	0.297

Table IV.8a continued...

PSSSP	0.355	0.282	0.277	0.194
PSNSP	0.410	0.438	0.293	0.246
[ClAuPSS]	0.434	0.518	0.415	0.426
[ClAu(μ -PSSP)AuCl]	0.442	0.397	0.482	0.321
dppe	0.390	0.296	0.194	0.102
[ClAu(μ -dppe)AuCl]	0.155	0.312	0.244	0.290

Table IV.8b Absorbance at 595 nm of the A549 cells after treatment with selected compounds under UVA light

Compound/ Concentration	Absorbance at 595 nm			
	0.02 μ g/ml	0.1 μ g/ml	1.0 μ g/ml	10 μ g/ml
None (control)	0.551	0.551	0.551	0.551
SN	0.200	0.336	0.448	0.199
SSS	0.200	0.309	0.038	0.062
SNS	0.299	0.311	0.285	0.091
NSN	0.634	0.356	0.211	0.087
PS	0.371	0.414	0.345	0.353
PDS	0.295	0.391	0.346	0.320
PTS	0.308	0.361	0.364	0.251
PSS	0.297	0.337	0.340	0.103
PSSS	0.406	0.528	0.356	0.281
PSSP	0.864	0.709	0.542	0.543
PSSSP	0.295	0.390	0.141	0.084
PSNSP	0.439	0.469	0.649	0.672
[ClAuPSS]	0.585	0.601	0.582	0.493
[ClAu(μ -PSSP)AuCl]	0.916	0.721	0.565	0.494
dppe	0.464	0.424	0.611	0.474
[ClAu(μ -dppe)AuCl]	0.290	0.201	0.314	0.278

APPENDIX A

EXPERIMENTAL DETAILS

A.1 GENERAL

A.1.1 Synthetic procedures

All operations requiring inert atmosphere were carried out on a vacuum line or in a glove box under atmosphere of dry nitrogen (or argon, when necessary) using the standard Schlenk technique.

Solvents required for air-sensitive reactions were purified according to the procedures, described by Perrin and Armarego,²⁸⁵ followed by distillation under nitrogen or degassing using freeze-pump-thaw technique prior to use. Water for preparation of gold(I) complexes was double distilled.

Disposal of all phosphorus containing compounds was carried out with utmost care. The compounds were reacted with large amount of cold bleach (5 % sodium hypochlorite) in the fume cupboard and left to stand until the reaction was complete. This method was found to give the quickest and the least odour-offensive result in comparison to applying KMnO_4/KOH or H_2O_2 solutions.

A.1.2 Chromatography

Merck plastic sheets, pre-coated with silica gel 60 F₂₅₄ were used for thin layer chromatography.

Merck silica gel 60 (particle size >60 μm) was used for flash column chromatography.

Centrifugal chromatography was carried out on a Harrison Research Chromatotron®, using glass plates, covered by a silica gel 60 (C/N 7749, E. Merck) layer of a certain thickness. Band separation was monitored by means of UV at 254 nm.

A.1.3 Characterisation and instrumentation

Melting points were recorded on a Kofler hot stage apparatus and were uncorrected.

C, H and N analyses were performed by the Microanalytical Laboratory of the Department of Chemistry and Chemical Technology, University of Natal, Pietermaritzburg, and by Gailbraith Laboratories, Inc., Knoxville, Tennessee, USA.

^1H NMR (200 MHz) and $^{13}\text{C}\{^1\text{H}\}$ NMR (50 MHz) spectra were recorded on a Gemini 200 spectrometer at 25°C with chemical shifts referenced to SiMe_4 . Deuterated solvents (E. Merck) were employed in all cases. $^{31}\text{P}\{^1\text{H}\}$ NMR spectra were recorded on a Varian FT-80A broad-band spectrometer, set at 32.086 MHz, at various temperatures, chemical shifts being quoted relative to 85% H_3PO_4 (external). Both deuterated and non-deuterated solvents were used.

Mass-spectra were obtained on a Hewlett-Packard HP5988A gas chromatographic mass-spectrometer, Department of Chemistry and Chemical Technology, University of Natal, Pietermaritzburg, and a Varian high resolution spectrometer, Mass-spectrometry unit, Cape Technikon, Cape Town.

UV-visible absorption spectra were recorded at 22°C using a Shimadzu UV-2101PC scanning spectrophotometer. Spectroscopic grade solvents (acetonitrile, dichloromethane) were employed in all cases. Emission spectra were recorded on a SLM-Aminco SPF-500C fluorometer in the Department of Chemistry, University of Zululand. The solvents for fluorescent measurements were of spectroscopic grade and degassed with argon prior to use.

Infra-red spectra were recorded as KBr disks using a Shimadzu Fourier Transform IR-4300 spectrometer.

A.1.4 Cytotoxicity testing

Cytotoxicity measurements were conducted by Ms D. Pillay at the Department of Physiology, Faculty of Medicine, University of Natal, Durban. The method used for the

measurements has been adapted from Hudson¹²⁰ and modified according to the technique established in that laboratory.

A.1.5 Crystal structure determination

A.1.5.1 Data collection

X-ray structures of each of the crystals in this work were obtained at 293 K using an Enraf-Nonius CAD-4 diffractometer with graphite monochromated Mo-K α radiation. For each crystal, the space group and cell constants were determined by first fitting the setting angles of 25 high-order reflections ($\theta > 12^\circ$). Intensity data were collected using an ω - 2θ scan where the vertical slit was fixed at 4 mm, the ω angle changed as $a_\omega + b_\omega \cdot \tan\theta$ ($^\circ$) and the horizontal aperture changed as $a_h + b_h \cdot \tan\theta$ (mm). The latter was limited to the range 1.3 to 5.9 mm. A critical evaluation of the peak shape for several reflections with different values of θ (OTPLOT) (Omega-Theta Plot; Enraf-Nonius diffractometer control program, 1988) established the optimum values of a_ω , b_ω , a_h and b_h for each crystal. Possible decomposition of the crystal was determined by measuring the intensities of three standard reflections hourly. Where required, a linear decay correction was applied to the final data set. Data were reduced using Lorentz and polarisation correction factors and where possible, corrected for absorption by the psi-scan (semi-empirical) method.²⁸⁶

A.1.5.2 Structure solution and refinement

The direct methods program, SHELXS-97,²¹⁶ as implemented in OSCAIL²⁸⁷ was used to solve all the crystal structures. For each structure, the remaining non-hydrogen atoms were located from the E-map and subsequent difference Fourier syntheses. The program, SHELXL-97,²¹⁷ was used to refine the structures anisotropically against F^2 using a full-matrix least-squares method with the following weighting scheme:

$$w = \frac{1}{\left[\sigma^2(F_o^2) + (aP)^2 + bP \right]}$$

where F_o is the observed structure factor, a and b are weight parameters determined by the program, and P is $1/3\{\text{Max}(F_o^2, 0) + 2F_c^2\}$. Here, F_c^2 is the calculated structure factor. Discrepancy indices used by the program are defined as follows:

$$R = \frac{\sum \|F_o\| - \|F_c\|}{\sum \|F_o\|}$$

$$wR = \sqrt{\frac{\sum [w(F_o^2 - F_c^2)^2]}{\sum [w(F_o^2)^2]}}$$

$$Goof = \sqrt{\frac{\sum [w(F_o^2 - F_c^2)^2]}{(n - p)}}$$

where n is the number of reflections and p is the total number of parameters refined. Plotting of structures and calculation of torsion angles and interplanar angles were performed using the program ORTEX v.7a.²⁸⁸ Tabulation of fractional coordinates, thermal parameters, interatomic distances and angles was achieved using the program CIFTAB.²¹⁷

A.2 CHEMICALS

A.2.1 Commercially available chemicals

The following chemicals were purchased from indicated suppliers and were generally used as received, unless otherwise stated.

Chemical	Supplier
Adamantanone	Aldrich Chemical Company Inc
Ammonium hexafluorophosphate	E. Merck
Benzonitrile	BDH
1,2-Bis(diphenylphosphino)butane	Fluka AG
1,2-Bis(diphenylphosphino)ethane	Aldrich Chemical Company Inc
1,2-Bis(diphenylphosphino)propane	Fluka AG
2-Bromopyridine ^a	Fluka AG
2-Bromothiophene	ACROS
n-Butyllithium, 1.6 M in hexane ^b	E. Merck

Copper(II) acetate, hydrated	BDH
1,8-Diazabicyclo[5.4.0]undec-7-ene	ACROS
1,2-Dibromoethane	E. Merck
2,6-Dibromopyridine	Fluka AG
2,5-Dibromothiophene ^c	Aldrich Chemical Company Inc
Dichlorophenylphosphine ^d	Fluka AG
Diethyl chlorophosphate ^d	Aldrich Chemical Company Inc
Diethyl phenylphosphonite	Aldrich Chemical Company Inc
Diisopropylamine	Fluka AG
Dimethoxymethane	BDH
Dimethylformamide	SAARChem
Dimethylsulfoxide	E. Merck
Diphenylacetic acid	Fluka AG
Diphenylchlorophosphine ^d	Strem Chemicals
Diphenylphosphine	Fluka AG
Ethylene glycol ^a	SAARChem
4-Fluorobenzenesulfonyl chloride	Aldrich Chemical Company Inc
Gold powder	Johnson Matthey GmbH
Lithium metal	SAARChem
Magnesium turnings	E. Merck
Magnesium bromide etherate	Aldrich Chemical Company Inc
Mercuric chloride	BDH
NBS ^e	Fluka AG
Nickel chloride, anhydrous ^e	Aldrich Chemical Company Inc
Nickel chloride, hydrated	SAARChem
Nitrosyl hexafluoroantimonate	Aldrich Chemical Company Inc
Nitrosyl tetrafluoroborate	Aldrich Chemical Company Inc
Palladium chloride	SAARChem
Phosphorus pentabromide	Aldrich Chemical Company Inc
Phosphorus tribromide	SAARChem
Phosphorus trichloride	E. Merck
Pyridine ^f	SAARChem
Tetrachloroauric acid, trihydrate	Aldrich Chemical Company Inc
Thallium(I) hexafluorophosphate	Strem Chemicals

2,2'-Thiodiethanol	Fluka AG
Thionyl chloride ^f	SAARChem
Tributyltin chloride ^d	ACROS
Trimethylchlorosilane ^f	E. Merck
Triphenylphosphine	Strem Chemicals
Triphenylphosphine chlorogold(I)	Strem Chemicals
Zinc shot	BDH

^a – dried and distilled prior to use, ^b – titrated with diphenylacetic acid prior to use, ^c – passed through silica and distilled, ^d – distilled under vacuum, ^e – dried prior to use, ^f – distilled under nitrogen

Other common consumables *e.g.*, acids and bases HCl, HBr, HIO₃, CH₃COOH, H₂SO₄, NH₃, NaOH, KOH, inorganic salts NaCl, NaHCO₃, MgSO₄, CaCl₂, KBr, KBrO₃, KI, Na₂S₂O₃, NaCH₃COO, were obtained from either SAARChem or BDH. Non-spectroscopic grade solvents – petroleum ether (40-60, 60-80 and 60-100), diethyl ether, acetonitrile, ethanol, acetone, THF, hexane, methanol, dichloromethane, chloroform were generally purchased from E. Merck and SAARChem.

Dichloromethane and acetonitrile used for spectroscopic measurements were purchased from E. Merck.

Deuterated chemicals (CDCl₃, CD₂Cl₂, CD₃CN, CD₃OD, C₆D₆, DMSO-*d*₆ and acetone-*d*₆) were purchased from E. Merck.

2-Chloro-1,3,2-dioxaphospholane [CIP(-OCH₂CH₂O-)]²⁰² 2,6-bis(2'-thienyl)pyridine (SNS),²¹⁴ 5,5'-dibromo-2,2'-bithiophene,¹⁹¹ (trimethylsilyl)diphenylphosphine,¹⁴¹ (tributylstannyl)diphenylphosphine,²⁸⁹ bis(benzonitrile)palladium dichloride,²⁹⁰ bis(triphenylphosphine)palladium dichloride,²⁹¹ (1,3-bis{diphenylphosphino}propane)nickel dichloride,²¹² (tetrahydrothiophene) chlorogold(I)²⁹² were prepared according to the published techniques.

A.2.2 Chemicals synthesised by adaptation of published methods

A.2.2.1 Preparation of adamantylidene adamantane²⁹³

A) 2,2-Dibromoadamantane

Adamantanone (6.6 g, 44 mmol) was added to \pm 32 g PBr_5 in the fume cupboard. The mixture turned liquid in the next 10 minutes. It was heated to 70°C and kept at that temperature for 1 hour, while stirring with a stirring rod. The mixture gradually became pale beige and started crystallising. At that stage, 100 ml warm water (60 - 70°C) was added and organic phase extracted with dichloromethane (2 x 50 ml). The solution was passed through a short layer of MgSO_4 and the solvent removed *in vacuo*. The white residue was dried under vacuum.

Yield = 11 g (85%). The compound is stable and can be kept for a long time before conversion to Ad=Ad.

B) Adamantylidene adamantane

Copper(II) acetate monohydrate (0.5 g) was dissolved in a small quantity of hot acetic acid. Then 8.8 g Zn shot was added. The mixture was heated for one hour, adding acetic acid when necessary, until the solution became nearly colourless (fumehood!). The solution was decanted and the solid washed with cold acetic acid (10 ml), ether (2 x 15 ml) and THF (15 ml). The Zn-Cu alloy thus formed was treated with 20 ml THF, followed by 4 g (13 mmol) 2,2-dibromoadamantane. The mixture was refluxed for 20 minutes and then cooled to room temperature. The solution was filtered and the solvent removed. The residue was extracted with 60 ml ether - 1 M H_2SO_4 mixture (1:1). The ether layer was separated, washed with water and dried and the solvent removed. The residue was recrystallised from methanol to give a white solid.

Yield = 1.07 g (59%), m.p. = 189 - 90°C (lit.²⁹³ 184 - 7°C).

^1H (CDCl_3), δ , ppm: 1.6-2.0 (br m, 24 H), 2.90 (br m, 4 H).

GCMS: m/z = 267.80 (M^+).

A.2.2.2 Preparation of 2,2'-bithiophene¹⁸³

2-Bromothiophene (16.3 g, 100 mmol) dissolved in 50 ml dry ether was added dropwise to 2.4 g Mg turnings under nitrogen. Nearly immediate reaction took place. The addition was kept at such a rate as to maintain a gentle reflux. When the reaction subsided, external heat was applied and the mixture refluxed for one more hour. It was transferred under nitrogen

to a dropping funnel and added slowly to a solution containing 16.3 g (100 mmol) 2-bromothiophene in 50 ml dry ether, containing 0.18 g Ni(dppp)Cl₂, at 0°C. When the addition was complete, the mixture was refluxed for one hour and stirred at the ambient temperature for 18 hours.

The mixture was hydrolysed by addition of 100 ml ice-cold semi-saturated NH₄Cl solution. The target compound was extracted with ether, the extracts combined, washed with brine and dried over MgSO₄. The solvent was removed, and the yellowish residue was distilled under vacuum.

Yield = 14.0 g (84%), m.p. = 31-2°C (lit.¹⁸³ 33°C), b.p. = 74-6°C/0.8 mmHg.

GCMS: m/z = 165.70 (M⁺).

A.2.2.3 Preparation of 2-bromo-5-(2-pyridyl)thiophene²⁹⁴

To the solution of 8.05 g (50 mmol) 2-(2'-pyridyl)-thiophene in 100 ml glacial acetic acid, solution of 2.7 ml (50 mmol) Br₂ in 25 ml acetic acid was added dropwise at room temperature. The addition took 1.5 hours, after which it was allowed to stir for further 2 hours. It was then hydrolysed with 1.5 l water and basified. Pinkish precipitate was filtered off, dissolved in chloroform, dried over MgSO₄ and the solvent evaporated *in vacuo*. Yellowish crystals were recrystallised from methanol.

Yield = 10.2 g (85%), m.p. = 92-93°C (lit.²⁹⁴ 91-93°C).

GCMS: m/z = 239.05 (⁷⁹Br: M⁺) and 240.95 (⁸¹Br: M⁺) – doublet.

A.2.2.4 Preparation of 5-bromo-2,2':5',2''-terthiophene¹⁹¹

To 0.5 g (2.0 mmol) 2,2':5',2''-terthiophene in 4.5 ml DMF (double-distilled from CaH₂ and kept over alumina under nitrogen), N-bromosuccinimide (NBS, 0.33 g, 1.9 mmol) was added portionwise over 8 hours. The reaction vessel was protected with thick aluminium foil from the daylight. The temperature was maintained between -20° and -10°C. The mixture was kept at -20°C for at least 12 hours and then it was warmed to ambient temperature. Ice-water (25 ml) was added and the solution extracted with CH₂Cl₂ (3 x 15 ml). After drying and evaporation of the solvent, the residue was recrystallised from hot hexane.

Yield = 0.485 g (77%, based on NBS), m.p. = 136-7°C (lit.¹⁹¹ 141-2°C).

GCMS: m/z = 325.95 (⁷⁹Br: M⁺) and 327.95 (⁸¹Br: M⁺) – doublet.

A.2.2.5 Preparation of bis(5-bromo-2-thienyl)methane¹⁸⁰

2-Bromothiophene (8.2 g, 50 mmol) and dimethoxymethane (1.9 g, 25 mmol) were dissolved in 50 ml glacial acetic acid. To this solution a mixture of 10 ml concentrated H₂SO₄ and 10 ml glacial acetic acid was added slowly (fumehood!). At the end of the reaction the solution had a large amount of brownish-black precipitate. Two portions (25 ml each) of chloroform were added to this mixture, so that all organic matter was extracted. The combined extracts were washed with water, dried over MgSO₄ and chloroform removed *in vacuo*. The dark solid residue was extracted four times with hot ethanol. The dark red solution was left at -20°C for 72 hours until off-white crystals separated. They were purified further by recrystallisation from ethanol with activated charcoal. The compound appeared to be light stable – contrary to the literature report.

Yield = 3.38 g (40%), m.p. = 43-44°C (lit.¹⁷⁹ 42-44°C).

¹H (CDCl₃), δ, ppm: 4.18 (s, 2H), 6.63 (d, 2H), 6.88 (d, 2H).

GCMS: *m/z* = 335.85 (⁷⁹Br + ⁷⁹Br: M⁺), 337.80 (⁷⁹Br + ⁸¹Br: M⁺), 339.80 (⁸¹Br + ⁸¹Br: M⁺) – doublet of doublets.

A.2.2.6 Preparation of 5-(chloromercurio)-2,2'-bithiophene¹⁹³

2,2'-Bithiophene (3.32 g, 20 mmol) was dissolved in 80 ml warm ethanol and was subsequently mixed with 5 ml warm aqueous solution containing 3.26 g (24 mmol) NaOAc·3H₂O. In another vessel 5.44 g (20 mmol) mercuric chloride were dissolved in 120 ml of warm distilled water. The second solution was slowly added to the first one. After 2 hours of stirring at ambient temperature it was cooled to 0°C, filtered and washed with water. The precipitate was air-dried on a Büchner funnel and washed with hexane followed by drying in air.

Yield = 7.5 g (92%), m.p. = 234-235°C (lit.¹⁹³ 234-235°C).

Elemental analysis: calculated C 23.49%, H 1.26%;

found C 23.60%, H 1.18%.

A.2.2.7 Preparation of potassium 4-fluorophenylsulfonate²⁰⁶

4-Fluorobenzenesulfonyl chloride (15.0 g, 71 mmol) was placed in 50 ml glacial acetic acid and refluxed for one hour. Then 100 ml of water was added to the hot solution and two layers separated. The mixture was refluxed for further 2 hours, and the solvent was distilled off. The white residue was dissolved in 50 ml water and neutralised with 3 M

KOH. Water was evaporated off under vacuum and the white solid dried in a dessicator over P_2O_5 .

Yield = 13.2 g (94%).

A.2.2.8 Preparation of 2,2':5',2''-terthiophene¹⁸³

2-Bromothiophene (3.2 g, 20 mmol) dissolved in 20 ml dry ether was reacted with 0.48 g (20 mmol) Mg turnings to produce the Grignard reagent in the manner described in the Section A.2.2.2. The solution was added dropwise to a solution of 2.4 g (10 mmol) 2,5-dibromothiophene in 20 ml dry ether, containing 0.08 g $Ni(dppp)Cl_2$, at 10°C for 15 minutes and then at 0°C until the addition was complete. The mixture was refluxed for two hours, cooled and worked up as described in the Section A.2.2.2. The residue was recrystallised from ethanol to give yellow crystalline material.

Yield = 1.88 g (75%), m.p. = 95-96°C (lit.¹⁸³ 89-90°C).

GCMS: m/z = 248.05 (M^+).

A.2.2.9 Preparation of 2-(2'-pyridyl)thiophene¹⁸³

2-Bromothiophene (8.2 g, 50 mmol) and Mg turnings (1.2 g, 50 mmol) were used to produce the Grignard reagent as described in the section A.2.2.2. This solution was added dropwise to a solution of 7.9 g 2-bromopyridine in ether, containing 0.09 g $Ni(dppp)Cl_2$, at 0°C. When the addition was complete, the mixture was gradually brought to reflux and refluxed for 20 hours. Then it was cooled to $\pm 5^\circ C$ and hydrolysed with ice-cold NH_4Cl solution. The solution was extracted with 4 M HCl, basified and extracted with ether. The ethereal extracts were combined, dried and evaporated. The residue was distilled under vacuum to give the desired product (white crystals).

Yield = 6.4 g (80%), m.p. = 63-5°C (lit.¹⁸³ 63-4°C), b.p. = 101-2°C/0.5 mmHg.

GCMS: m/z = 160.75 ($M^+ - 1$).

A.2.2.10 Preparation of μ -[1,2-bis(diphenylphosphino)ethane] bis[chlorogold(I)]¹⁴¹

Tetrachloroauric acid, $HAuCl_4 \cdot 3H_2O$ (0.788 g, 2 mmol), was dissolved in 25 ml of a 2:3 (v:v) water/methanol mixture. Neat 2,2'-thiodiethyleneglycol (tdg) was added from a pipette at 15°C until the solution became colourless. The mixture was stirred at this temperature for 30 minutes and a solution of dppe (0.398 g, 1 mmol) in 20 ml 1:1 (v:v) chloroform/methanol was added. The mixture was stirred at room temperature for two hours. A white precipitate was filtered off, washed with cold methanol and dried.

Yield = 0.665 g (77%), m.p. = 289-90°C (lit.¹⁴¹ 290-292°C).

^{31}P {H} (CDCl_3) = 31.78 ppm.

A.2.2.11 Preparation of (1,4-bis(diphenylphosphino)butane)palladium dichloride¹⁷⁵

Bis(benzonitrile)palladium dichloride (0.957 g, 2.5 mmol) was dissolved in 70 ml acetonitrile and heated to 70°C. Solid dppb (1.06 g, 2.5 mmol) was added to the clear solution. Pale yellow precipitate separated immediately and the solution turned yellow. It was cooled to 0°C, the precipitate filtered and washed with ether (2 x 10 ml).

Yield = 1.425 g (95%), m.p. > 300 (decomposition).

^{31}P {H} (C_6D_6) = 65.32 ppm (lit.¹⁷⁵ 65.84 ppm).

A.2.2.12 Preparation of bis(benzonitrile)gold(I) tetrafluoroborate²⁹⁵

In a glove box under an atmosphere of dry nitrogen, NOBF_4 (0.70 g, 6.1 mmol) was placed in a flask containing suspension of 1.2 g (6.1 mmol) gold powder in 100 ml 1:2 (v:v) acetonitrile/benzonitrile mixture, which was preliminarily dried and degassed. The mixture was allowed to react at ambient temperature (28°C) for 16 hours. Then the clear solution was transferred under nitrogen to another flask and most of the solvent removed under vacuum. Degassed dry ether (100 ml) was introduced under nitrogen and a white flaky precipitate appeared. More precipitate separated after storing the solution at -15°C for 14 hours. It was filtered under nitrogen in dry glassware and dried under vacuum. The compound was air-, moisture and light sensitive and could not be weighed without a certain degree of decomposition taking place. After storing the complex for two days in the fridge, decomposition to metallic gold was observed, hence the compound had to be recrystallised from dichloromethane/ether immediately before use.

APPENDIX B

CONE ANGLE CALCULATIONS

As a quantitative measure of the steric demands of phosphines, the cone angle concept was introduced by Tolman in 1977.²⁴³ In the original cone angle methodology, steric measurements of phosphines were achieved by placing the ligand phosphorus atom 2.28 Å from an apex, **M**, or a metal atom, and enclosing the ligand in a cone which just touches the van der Waals radii of the outermost atoms of the model (Figure B.1). If there were internal degrees of freedom, the substituents on the phosphorus atom were folded back to give a minimum cone. The angle values were then derived from molecular models or by using other simple mechanical tools.

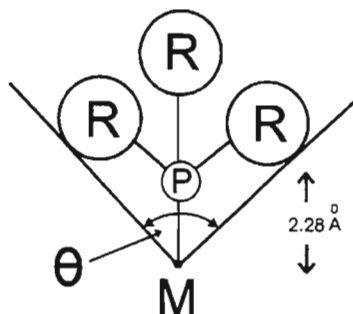


Fig. B.1 Measurement of a Tolman cone angle of a symmetrical ligand.

For symmetrical ligands the cone angle (θ) was measured at the point, which gave the largest value, and all cone angles were measured with a constant **M-P** bond distance to provide a comparative set of cone angle data. For unsymmetrical ligands $\text{PR}^1\text{R}^2\text{R}^3$, an effective cone angle can be defined as two times the average of half-angles as shown on Figure B.2.

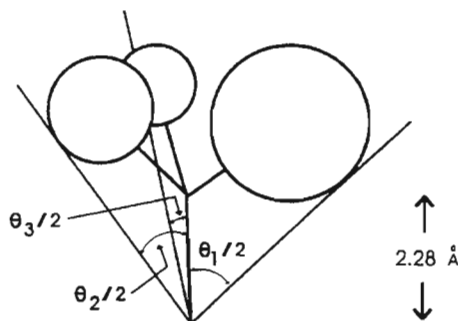


Fig. B.2 Measurement of a Tolman cone angle of an unsymmetrical ligand.

The Tolman method of measuring cone angle using molecular models has several limitations:

- a) in reality, even symmetrical ligands do not have cylindrical symmetry and can mesh into one another,
- b) with the models, it may be difficult to assess the minimum cone angle as unrealistic strain can be introduced,
- c) angles around phosphorus in molecular models are considered to be tetrahedral, whilst in real molecules they generally differ from 109° and can be changed by crowding,
- d) all bond lengths of the same type are considered to be equal and ascribed an idealised value, which seldom coincides with the distances observed in real molecules,
- e) the accuracy of the method is $\pm 4^\circ$.

In the past decade, other methodologies for calculation of Tolman cone angles have been proposed, which do not rely on usage of molecular models. Coville *et al.*²⁹⁶ made use of molecular mechanics, while Krüger²⁹⁷ and Mingos^{30,298} based their calculations on crystallographic data.

Most of the methods involve assumptions as well as certain simplifications. For example, Mingos *et al.*²⁹⁸ used an algorithm, which uses atomic centres instead of the van der Waals spheres of the atoms. The angle therefore has to be adjusted by the contribution of the van der Waals radius of the hydrogen atom (1.00 Å); in other words, a hypothetical atom **M** was placed only 1.28 Å from the phosphorus atom. Geometrically, this method was identical to the Tolman method only when a cone angle is equal to 180° . The difference between the two methods increases when angles are far from 180° .

As sophisticated molecular mechanics software was inaccessible to the author during this study, a different strategy was developed in order to estimate cone angle values for the new phosphines. The methodology, described herein, is based on the bond lengths and angles as determined from X-ray analysis of the ligands. The desired angle values were obtained by means of trigonometric calculations.

The following assumptions are made:

- A. The hypothetical atom **M** is placed 2.28 Å away from the phosphorus atom so that all **M-P-C** angles are equal. All atoms, except for the outermost ones are treated as dimensionless points.
- B. Van der Waals radii of the atoms are as given in HyperChem molecular modelling software:

Atom	Radius, Å
H	1.00
N	1.82
S	2.11

- C. The substituents on the phosphorus are folded back in such a way that the aromatic rings are perpendicular to the surface of the cone and parallel to the (**M-P-C**) plane.

The first two assumptions are in full agreement with Tolman's methodology, whilst the last clearly does not comply with the Tolman requirement of a minimum cone. It can be seen from observing molecular models as well as studying conformations of aromatic phosphines, available in the literature, that the minimum cone angle is normally achieved when aromatic rings are placed at an angle to the (**M-P-C**) plane. However, Mingos *et al.*,³⁰ showed that conformational differences have a relatively small effect on the overall cone angle, contributing to only $\pm 5\%$ of the variations, while other factors, such as the choice of van der Waals radii, have a more pronounced effect.

Nevertheless, as long as the methodology used remains the same, the values of cone angles thus determined, can be meaningfully compared.

The algorithm for measurements of $\theta/2$ is outlined below.

1. The aromatic rings are considered to be strictly planar.
2. If (**CXY**) indicates the plane of an aromatic ring, it can be shown that **M** \subset (**CXY**) - from the geometry of a sp^2 -hybridised carbon and from assumption C. Also, if atom X of the aromatic ring is connected to another atom, *e.g.* hydrogen, the latter has to belong to the same plane – again in accordance with the geometry of an aromatic ring. Therefore, all atoms in the diagram Figure B.3 lie in the same plane, and the

calculations become considerably simplified by being limited to two-dimensional space.

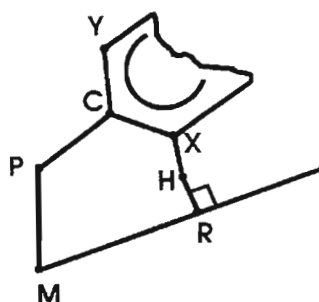


Fig. B.3 The aromatic ring plane and surrounding atoms.

3. By definition, $\theta_i/2$ is measured between (**MP**) and (**MR**), where (**MR**) is a tangent to the circumference drawn from the centre of the outermost atom with the radius equal to the van der Waals radius of this atom. Two different cases are presented on Figure B.4: $X = C'$ and $X = S$ or N .

In the first case $\theta_i/2 = PMC + CMC' + C'MH + HMR$,

while in the second: $\theta_i/2 = PMC + CMX + XMR$.

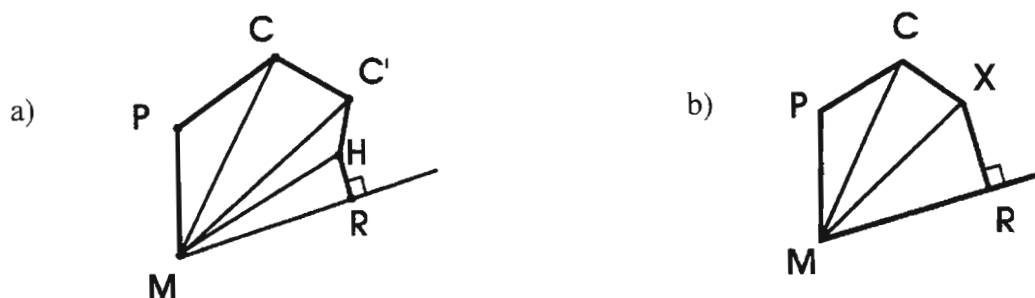


Fig. B.4 Calculation of $\theta_i/2$ for ligands with phenyl (a) and pyridyl and thienyl (b) substituents.

4. It is assumed here, but can also be easily demonstrated geometrically, that it is the *ortho*-H on the aromatic ring (as opposed to the *meta*-H), that determines the cone, which encapsulates the ligand. For thiophene and pyridine rings, the heteroatoms define the cone due to their large van der Waals radii.
5. The values of each component in the equations above can be determined from individual triangles. Using basic trigonometric formulae:

$$\sin(\text{PMC}) = \sin(\text{MPC}) \cdot \text{PC}/\text{MC} \quad (1)$$

$$\sin(\text{CMC}') = \sin(\text{MCC}') \cdot \text{CC}'/\text{MC}' \quad (2) \text{ or } \sin(\text{CMX}) = \sin(\text{MCX}) \cdot \text{CX}/\text{MX} \quad (2')$$

$$\sin(\text{C'MH}) = \sin(\text{HC'M}) \cdot \text{C'H}/\text{MH} \quad (3)$$

$$\sin(\text{HMR}) = \text{HR}/\text{MH} \quad (4) \text{ or } \sin(\text{XMR}) = \text{XR}/\text{MX} \quad (4')$$

Distances PC, CC', C'H or CX are known from the X-ray data, while MP = 2.28 Å and HR = 1.00 Å (XR = 1.82 or 2.11 Å for pyridine and thiophene, respectively) – by agreement. Angles PCC' and CC'H or CC'X are also available from the crystallographic data.

If the value of MPC is known, the rest of calculations can be done easily:

$$\text{MC}^2 = \text{MP}^2 + \text{PC}^2 - 2 \cdot \text{MP} \cdot \text{PC} \cdot \cos(\text{MPC}) \quad (5)$$

From (5) and (1) the values of MPC and PMC are derived, therefore $\text{PCM} = 180^\circ - (\text{MPC} + \text{PMC})$.

Therefore the values of MCC' or MCX can be calculated:

$$\text{MCC}' = \text{PCC}' - \text{PCM}, \text{ or } \text{MCX} = \text{PCX} - \text{PCM}.$$

From here MC' or MX can be found:

$$\text{MC}'^2 = \text{MC}^2 + \text{CC}'^2 - 2 \cdot \text{MC} \cdot \text{CC}' \cdot \cos(\text{MCC}') \quad (6)$$

$$\text{or } \text{MX}^2 = \text{MC}^2 + \text{CX}^2 - 2 \cdot \text{MC} \cdot \text{CX} \cdot \cos(\text{MCX}) \quad (6')$$

The values of MC' and MX help to calculate CMC' and CMX from the equations (6), (2) and (6'), (2') - respectively. The same algorithm is used to find the values of remaining angles.

6. It is known from the literature, that MPC depends on the steric requirements of the ligand. It is $\pm 115.6^\circ$ for PPh₃ and normally decreases with the increasing bulk of a substituent.

It is possible to calculate the exact value of MPC as a function of angles between the three substituents on the phosphorus - α , β , γ .

Consider the following picture (Figure B.5).

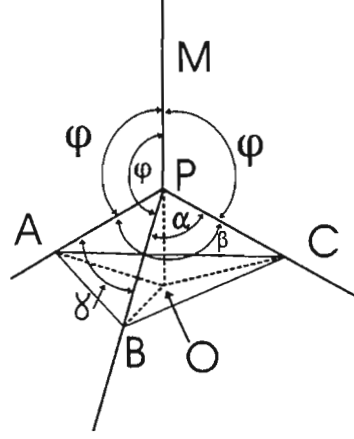


Fig. B.5 Calculation of the value of $MPC = \phi$ as a function of α , β and γ .

Cut equal distances on each of the four beams: $PM = PA = PB = PC$. By assumption, $MPA = MPB = MPC = \phi$. Therefore, $AM = BM = CM = 2 \cdot MP \cdot \sin \phi / 2$.

Also $AMP = BMP = CMP = 90^\circ - \phi / 2$. $APB = \gamma$, $APC = \beta$ and $BPC = \alpha$ – by agreement.

If we extend MP beyond P and drop the perpendicular from A, B and C, we will get a common point O, since $MO = MA \cdot \cos(AMP)$, which is exactly the same as $MB \cdot \cos(BMP)$ or $MC \cdot \cos(CMP)$.

The point O belongs to the same plane as (ABC), as it is only possible to have one line perpendicular to a plane at the point of intersection. And we have $(AO) \perp (MO)$, $(BO) \perp (MO)$, $(CO) \perp (MO)$, $\therefore (ABO) \perp (MO)$, but also $(ACO) \perp (MO)$ and $(BCO) \perp (MO)$. $\therefore (ABC) \perp (MO)$.

Also $AO = BO = CO = AM \cdot \sin(AMP) = 2 \cdot MP \cdot \sin \phi / 2 \cdot \cos \phi / 2 = MP \cdot \sin \phi$.

From triangles APB, APC and BPC:

$$c = AB = 2 \cdot AP \cdot \sin \gamma / 2 = 2 \cdot MP \cdot \sin \gamma / 2,$$

$$b = AC = 2 \cdot BP \cdot \sin \beta / 2 = 2 \cdot MP \cdot \sin \beta / 2,$$

$$a = BC = 2 \cdot MP \cdot \sin \alpha / 2 = 2 \cdot MP \cdot \sin \alpha / 2.$$

Consider the triangle ABC, O is the centre of the circumference drawn around ABC as $AO = BO = CO$ (Figure B.6).

Therefore $AOB = 2 \cdot ACB$ and $AB = 2 \cdot AO \cdot \sin(AOB/2) = 2 \cdot AO \cdot \sin \Delta$.

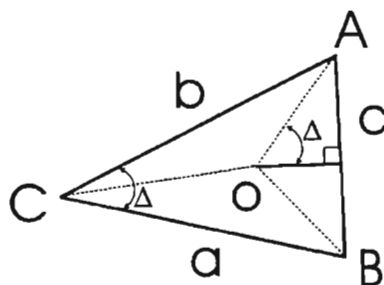


Fig. B.6 The triangle ABC.

$$\begin{aligned}\sin\Delta &= (1 - \cos^2\Delta)^{1/2}, \\ \text{but } \cos\Delta &= (a^2 + b^2 - c^2)/2ab = \\ &= \{(2 \cdot MP)^2(\sin^2\alpha/2 + \sin^2\beta/2 - \sin^2\gamma/2)\} / \{2 \cdot (2 \cdot MP)^2 \sin\alpha/2 \cdot \sin\beta/2\} = \\ &= (\sin^2\alpha/2 + \sin^2\beta/2 - \sin^2\gamma/2) / 2 \cdot \sin\alpha/2 \cdot \sin\beta/2.\end{aligned}$$

However $AB = 2 \cdot MP \cdot \sin\gamma/2$ and $AO = MP \cdot \sin\phi$,

$$\therefore 2 \cdot MP \cdot \sin\gamma/2 = 2 \cdot MP \cdot \sin\phi \cdot (1 - \cos^2\Delta)^{1/2},$$

$$\begin{aligned}\sin\phi &= \sin\gamma/2 \cdot (1 - \cos^2\Delta)^{-1/2} = \sin\gamma/2 \cdot \{(1 - \cos\Delta) \cdot (1 + \cos\Delta)\}^{-1/2} = \sin\gamma/2 \cdot \{(1 - [\sin^2\alpha/2 + \sin^2\beta/2 - \sin^2\gamma/2] / 2 \cdot \sin\alpha/2 \cdot \sin\beta/2) \cdot (1 + [\sin^2\alpha/2 + \sin^2\beta/2 - \sin^2\gamma/2] / 2 \cdot \sin\alpha/2 \cdot \sin\beta/2)\}^{-1/2} \\ &= 2 \cdot \sin\alpha/2 \cdot \sin\beta/2 \cdot \sin\gamma/2 \cdot \{(\sin^2\gamma/2 - [\sin\beta/2 - \sin\alpha/2]^2) \cdot ([\sin\beta/2 + \sin\alpha/2]^2 - \sin^2\gamma/2)\}^{-1/2} \\ &= 2 \cdot \sin\alpha/2 \cdot \sin\beta/2 \cdot \sin\gamma/2 \cdot \{(\sin\gamma/2 - \sin\beta/2 + \sin\alpha/2) \cdot (\sin\gamma/2 + \sin\beta/2 - \sin\alpha/2) \cdot (\sin\beta/2 + \sin\alpha/2 - \sin\gamma/2) \cdot (\sin\gamma/2 + \sin\beta/2 + \sin\alpha/2)\}^{-1/2}\end{aligned}$$

$$\phi = 180^\circ - \arcsin(\sin\phi), \text{ as } \phi > 90^\circ.$$

- After all necessary bond lengths and angles are established, the formulae and the values can be processed using a standard spread sheet software (QuatroPro/Lotus1-2-3/MS Excel *etc.*) to determine the angle $\theta_i/2$. The results of calculations for the 3 ligands, whose crystal structure were determined during this work, are presented in Tables B.1, B.2 and B.3. The results for phenyl rings are averaged if they belong to the same phosphorus atom.

Table B.1 $\theta_i/2$ values for the PSSP ligand ($\alpha = 101.7^\circ$, $\beta = 102.8^\circ$, $\gamma = 103.6^\circ$)

Substituent	φ	$\theta_i/2$
Thiophene – PCS conformation	115.8°	87.9°
Thiophene – PCC'H conformation	115.8°	82.0°
Phenyl (av. PCC'H conformation)	115.8°	82.5°

The results in Table B.1 reveal that for the thiophene ring θ_{PCS} is significantly larger than $\theta_{PCC'H}$; therefore the latter has to be used to obtain the minimum effective cone angle of the PSSP ligand*: $\theta = 2/3 \cdot (\theta_{PCC'H}/2 + 2 \cdot \theta_{PCC'H-Ph}/2) = 162.3^\circ = \pm 162^\circ$.

Table B.2 $\theta_i/2$ values for the PSNSP ligand ($\alpha_1 = 101.3^\circ$, $\beta_1 = 102.1^\circ$, $\gamma_1 = 104.0^\circ$, $\alpha_2 = 101.8^\circ$, $\beta_2 = 100.9^\circ$, $\gamma_2 = 104.7^\circ$)

Substituent	φ	$\theta_i/2$
Thiophene-1 – PCS conformation	115.8°	87.4°
Thiophene-2 – PCS conformation	115.8°	87.7°
Thiophene-1 – PCC'H conformation	115.8°	82.2°
Thiophene-2 – PCC'H conformation	115.8°	82.2°
Phenyl-1 (av. PCC'H conformation)	115.8°	83.1°
Phenyl-2 (av. PCC'H conformation)	115.8°	82.9°

The data in Table B.2 are consistent with the results from Table B.1. In other words, for both thiophene rings, θ_{PCS-1} and θ_{PCS-2} are considerably larger than the corresponding $\theta_{PCC'H-1}$ and $\theta_{PCC'H-2}$ values. Thus the latter have to be used to obtain the minimum effective cone angle of the ligand. The contribution of phenyl rings in the PSNSP molecule, $\pm 83^\circ$, is very close to that calculated for the PSSP ligand, $\pm 82.5^\circ$. Therefore, for the part of the molecule containing the thiophene substituent labelled "1", the cone angle is $\theta(1) = 2/3 \cdot (\theta_{PCC'H-1}/2 + 2 \cdot \theta_{PCC'H-Ph}/2) = 165.6^\circ = \pm 166^\circ$, while for the second part: $\theta(2) = 2/3 \cdot (\theta_{PCC'H-2}/2 + 2 \cdot \theta_{PCC'H-Ph}/2) = 165.4^\circ = \pm 165^\circ$.

* Strictly speaking, this cone angle refers to only one half of the molecule.

Table B.3 $\theta_i/2$ values for the PSNP ligand ($\alpha_{\text{thiophene}} = 101.8^\circ$, $\beta_{\text{thiophene}} = 102.5^\circ$, $\gamma_{\text{thiophene}} = 103.0^\circ$, $\alpha_{\text{pyridine}} = 101.2^\circ$, $\beta_{\text{pyridine}} = 102.6^\circ$, $\gamma_{\text{pyridine}} = 105.1^\circ$)

Substituent	ϕ	$\theta_i/2$
Thiophene – PCS conformation	115.8°	87.5°
Thiophene – PCC'H conformation	115.8°	81.8°
Pyridine – PCN conformation	115.4°	81.6°
Pyridine – PCC'H conformation	115.4°	83.1°
Phenyl (th) (av. PCC'H conformation)	115.8°	82.8°
Phenyl (py) (av. PCC'H conformation)	115.4°	83.2°

The results in Table B.3 demonstrate that for the thiophene substituent, θ_{PCS} is larger than $\theta_{\text{PCC'H}}$, while for the pyridine substituent it is θ_{PCN} which is somewhat smaller than the corresponding $\theta_{\text{PCC'H}}$ value; the contribution of phenyl rings at $\pm 83^\circ$ is similar for both "thiophene" and "pyridine" parts of the molecule and to the values found for the molecules PSSP and PSNSP. Therefore the minimum effective cone angles of the ligand are $\theta(\text{thiophene}) = 2/3 \cdot (\theta_{\text{PCC'H-Th}}/2 + 2 \cdot \theta_{\text{PCC'H-Th}}/2) = 165.0^\circ = \pm 165^\circ$, and $\theta(\text{pyridine}) = 2/3 \cdot (\theta_{\text{PCN}}/2 + 2 \cdot \theta_{\text{PCC'H-Ph}}/2) = 165.4^\circ = \pm 165^\circ$.

It can be seen from the above data, than the average effective cone angles of the three phosphines are very close at $\pm 165^\circ$, although individual contributions of half-angles varied from ligand to ligand. The values of the above cone angles can be compared to the one reported in the literature for triphenylphosphine, as the input from heteroaromatic rings appeared to be similar (within experimental errors) to that of phenyls. Tolman²⁴³ reported cone angle value for PPh_3 as $\pm 152^\circ$. The difference can be clearly attributed to the different algorithm used for the determination of the minimum cone, rather than the differences in bond lengths and angles. Although the current methodology does not provide the result equivalent to the Tolman cone angle, the values are still meaningful as they allow the comparison of steric effects of different conformations within a ligand. In other words, steric demands of a phosphine ligand increase if the thiophene substituent is rotated in such a way that the torsion angle between the C-S bond and the phosphorus lone pair is small (*i.e.* close to 0°), while for the pyridine substituent small torsion angle between C-N and the lone pair leads to a decrease in the cone angle.

REFERENCES

1. D. H. Brown and W. E. Smith, *Chem. Soc. Rev.*, 1980, **9**, 217.
2. R. J. Puddephatt, *The Chemistry of Gold*, Elsevier, Amsterdam, 1978.
3. O. M. Ni Dhubghaill and P. J. Sadler, in *Metal Complexes in Cancer Chemotherapy*, ed. B. K. Keppler, VCH Publishers, Weinheim, 1993; 223-248.
4. O. Pyykkö and J.-P. Deslaux, *Acc. Chem. Res.*, 1979, **12**, 276.
5. M. A. Mazid, M. T. Razi, P. J. Sadler, G. N. Greaves, S. J. Gurman, M. H. J. Koch and J. C. Phillips, *J. Chem. Soc., Chem. Commun.*, 1980, 1261.
6. R. C. Elder, K. Ludwig, J. N. Cooper and M. K. Eidsness, *J. Am. Chem. Soc.*, 1985, **107**, 5024.
7. M. Viotte, B. Gautheron, M. M. Kubicki, Y. Mugnier and R. V. Parish, *Inorg. Chem.*, 1995, **34**, 3465.
8. L.-J. Baker, R. C. Bott, G. A. Bowmaker, P. C. Healy, B. W. Skelton, P. Schwerdtfeger and A. H. White, *J. Chem. Soc., Dalton Trans.*, 1995, 1341.
9. S. Attar, W. H. Bearden, N. W. Alcock, E. C. Alyea and J. H. Nelson, *Inorg. Chem.*, 1990, **29**, 425.
10. R. C. Elder, E. H. K. Zeiher, M. Onady and R. R. Whittle, *J. Chem. Soc., Chem. Commun.*, 1981, 900.
11. C. A. McAuliffe, R. V. Parish and P. D. Randall, *J. Chem. Soc., Dalton Trans.*, 1978, 1730.
12. R. Colton, K. L. Harrison, Y. A. Mah and J. C. Traeger, *Inorg. Chim. Acta*, 1995, **231**, 65.
13. P. G. Jones, *Gold Bull.*, 1981, **14**, 102.
14. P. G. Jones, *Gold Bull.*, 1981, **14**, 159.
15. P. G. Jones, *Gold Bull.*, 1983, **16**, 114.
16. E. Cerrada, P. G. Jones, A. Laguna and M. Laguna, *Inorg. Chem.*, 1996, **35**, 2995.
17. J.-C. Shi, X.-Y. Huang, D.-X. Wu, Q.-T. Liu and B.-S. Kang, *Inorg. Chem.*, 1996, **35**, 2742.
18. K. Angermaier, E. Zeller and H. Schmidbaur, *J. Organomet. Chem.*, 1994, **472**, 371.
19. S. Ahrland, K. Dreisch, B. Norén and Å. Oskarsson, *Acta Chem. Scand., Ser. A*, 1987, **41**, 173.
20. E. R. T. Tiekink, *Acta Crystallogr., Sect. C*, 1989, **45**, 1233.

21. N. C. Baenziger, W. E. Bennett and D. M. Soboroff, *Acta Crystallogr., Sect. B*, 1976, **32**, 962.
22. P. F. Barron, L. M. Engelhardt, P. C. Healy, J. Oddy, and A. H. White, *Aust. J. Chem.*, 1987, **40**, 1545.
23. J. A. Muir, M. M. Muir, L. B. Pulgar, P. G. Jones, and G. M. Sheldrik, *Acta Crystallogr., Sect. C*, 1985, **41**, 1174.
24. Z. Assefa, B. G. McBurnett, R. J. Staples, J. P. Fackler, Jr., B. Assmann, K. Angermaier and H. Schmidbaur, *Inorg. Chem.*, 1995, **34**, 75.
25. L. J. Larson, E. M. McCauley, B. Weissbart and D. S. Tinti, *J. Phys. Chem.*, 1995, **99**, 7218.
26. H. Schmidbaur, *Gold Bull.*, 1990, **23**, 11.
27. R. Narayanaswamy, M. A. Young, E. Parkhurst, M. Ouellette, M. E. Kerr, D. M. Ho, R. C. Elder, A. E. Bruce and M. R. M. Bruce, *Inorg. Chem.*, 1993, **32**, 2506.
28. J. Guochen, R. J. Puddephatt, J. D. Scott and J. J. Vittal, *Organometallics*, 1993, **12**, 3565.
29. T. V. Baukova, L. G. Kuz'mina, N. A. Oleinikova, D. A. Lemenovskii and A. L. Blumenfel'd, *J. Organomet. Chem.*, 1997, **530**, 27.
30. D. M. P. Mingos and T. E. Müller, *J. Organomet. Chem.*, 1995, **500**, 251.
31. M. Malatesta, L. Naldini, G. Simonetta and F. Cariati, *Coord. Chem. Rev.*, 1966, **1**, 255.
32. A. D. Zotto, G. Nardin and P. Rigo, *J. Chem. Soc., Dalton Trans.*, 1995, 3343.
33. M. T. Razi, P. J. Sadler, D. T. Hill and B. M. Sutton, *J. Chem. Soc., Dalton Trans.*, 1983, 1331.
34. T. Jiang, G. Wei, C. Turmel, A. E. Bruce and M. R. M. Bruce, *Metal-Based Drugs*, 1994, **1**, 419.
35. A. K. H. Al-Sa'ady, C. A. McAuliffe, K. Moss, R. V. Parish and R. Fields, *J. Chem. Soc., Dalton Trans.*, 1984, 491.
36. J. A. Muir, M. M. Muir and E. Lorca, *Acta Crystallogr., Sect. B*, 1980, **38**, 931.
37. M. N. I. Khan, C. King, J. P. Fackler, Jr., and R. E. P. Winpenny, *Inorg. Chem.*, 1993, **32**, 2502.
38. Z. Assefa, R. J. Staples and J. P. Fackler, Jr., *Inorg. Chem.*, 1994, **33**, 2790.
39. W. Clegg, *Acta Crystallogr., Sect. B*, 1976, **32**, 2712.
40. J. G. Wijnhoven, W. P. J. H. Bosman and P. T. Beursbeur, *J. Cryst. Mol. Struct.*, 1972, **2**, 7.

41. M. J. Mays and P. A. Vergnano, *J. Chem. Soc., Dalton Trans.*, 1979, 1112.
42. C. B. Colburn, W. E. Hill, C. A. McAuliffe and R. V. Parish, *J. Chem. Soc., Chem. Commun.*, 1979, 218.
43. S. Al-Baker, W. E. Hill and C. A. McAuliffe, *J. Chem. Soc., Dalton Trans.*, 1985, 2655.
44. S. Al-Baker, W. E. Hill and C. A. McAuliffe, *J. Chem. Soc., Dalton Trans.*, 1986, 1297.
45. P. G. Jones, G. M. Sheldrick, J. A. Muir, M. M. Muir and L. B. Pulgar, *J. Chem. Soc., Dalton Trans.*, 1982, 2123.
46. G. A. Bowmaker and D. A. Rogers, *J. Chem. Soc., Dalton Trans.*, 1984, 1249.
47. C. King, J.-C. Wang, M. N. I. Khan and J. P. Fackler Jr., *Inorg. Chem.*, 1989, **28**, 2145.
48. J. F. Vollano, D. H. Picker and J. A. Statler, *Inorg. Chim. Acta*, 1989, **155**, 31.
49. J. J. Guy, P. G. Jones and G. M. Sheldrick, *Acta Crystallogr., Sect B.*, 1976, **32**, 1937.
50. W. Clegg, *Acta Crystallogr., Sect. B.*, 1978, **34**, 278.
51. R. V. Parish, O. Parry and C. A. McAuliffe, *J. Chem. Soc., Dalton Trans.*, 1981, 2098.
52. A. D. Westland, *Can. J. Chem.*, 1969, **47**, 4135.
53. H.-R. C. Jaw and W. R. Mason, *Inorg. Chem.*, 1989, **28**, 4370.
54. P. G. Jones, *Acta Crystallogr., Sect B.*, 1980, **36**, 3105.
55. P. G. Jones, *J. Chem. Soc., Chem. Commun.*, 1980, 1031.
56. E. L. Muetterties, W. G. Peet, P. A. Wegner and C. A. Alegranti, *Inorg. Chem.*, 1970, **9**, 2447.
57. Y. Inoguchi, B. Milewski-Mahrla and H. Schmidbaur, *Chem. Ber.*, 1982, **115**, 3085.
58. H. Schmidbaur, *Chem. Soc. Rev.*, 1995, 391.
59. J. S. Field, R. J. Haines, K. Lea, W. S. Schauerte, D. Wood, unpublished work.
60. M. Barron, H. B. Bnergi, D. K. Johnson and L. M. Venanzi, *J. Am. Chem. Soc.*, 1976, **98**, 2356.
61. R. T. Baker, J. C. Calabrese and S. A. Westcott, *J. Organomet. Chem.*, 1995, **498**, 109.
62. A. Houlton, D. M. P. Mingos, D. M. Murphy, D. J. William, L.-T. Phang and T. S. A. Hor, *J. Chem. Soc., Dalton Trans.*, 1993, 3629.
63. W. H. Chan, T. C. W. Mak and C.-M. Che, *J. Chem. Soc., Dalton Trans.*, 1998, 2275.

64. A.-M. Larssonneur, R. Turpin, P. Castan and G. Bernardinelli, *Inorg. Chim. Acta*, 1994, **227**, 85.
65. M. C. Gimeno, A. Laguna, C. Sarroca and P. G. Jones, *Inorg. Chem.*, 1993, **32**, 5926.
66. P. A. Bates and J. M. Waters, *Inorg. Chim. Acta*, 1984, **81**, 151.
67. S. J. Berners-Price and P. J. Sadler, *Inorg. Chem.*, 1986, **25**, 3822.
68. J. V. McArdle and G. E. Bossard, *J. Chem. Soc., Dalton Trans.*, 1990, 2219.
69. A. L. Balch, M. M. Olmstead, P. E. Reedy, Jr., and S. P. Rowley, *Inorg. Chem.*, 1988, **27**, 4289.
70. A. L. Balch, E. Y. Fung and M. M. Olmstead, *Inorg. Chem.*, 1990, **29**, 3203.
71. D. Li, X. Hong, C.-M. Che, W.-C. Lo and S.-M. Peng, *J. Chem. Soc., Dalton Trans.*, 1993, 2929.
72. S.-J. Shieh, X. Hong, S.-M. Peng and C.-M. Che, *J. Chem. Soc., Dalton Trans.*, 1994, 3067.
73. J. Foley, R. C. Fort, Jr., K. McDougal, M. R. M. Bruce and A. E. Bruce, *Metal-Based Drugs*, 1994, **1**, 405.
74. W. B. Jones, J. Yuan, R. Narayanaswamy, M. A. Young, R. C. Elder, A. E. Bruce and M. R. M. Bruce, *Inorg. Chem.*, 1995, **34**, 1996.
75. C. K. Mirabelli, D. T. Hill, L. F. Faucette, F. L. McCabe, G. R. Girard, D. B. Bryan, B. M. Sutton, J. O. Bartus, S. T. Crooke and R. K. Johnson, *J. Med. Chem.*, 1987, **30**, 2181.
76. H. Schmidbaur, A. Wohlleben, F. Wagner, O. Orama and G. Huttner, *Chem. Ber.*, 1977, **110**, 1748.
77. Z. Assefa, B. G. McBurnett, R. J. Staples and J. P. Fackler, Jr., *Inorg. Chem.*, 1995, **34**, 4965.
78. D. S. Eggleston, D. F. Chodosh, G. R. Girard and D. T. Hill, *Inorg. Chim. Acta*, 1985, **108**, 221.
79. D. S. Eggleston, J. V. McArdle and E. Zuber, *J. Chem. Soc., Dalton Trans.*, 1987, 677.
80. H. Schmidbaur, C. Paschalidis, O. Steigelmann and G. Müller, *Chem. Ber.*, 1989, **122**, 1851.
81. M. C. Cooper, L. E. Mitchell, K. Henrik, M. McPartlin and A. Scott, *Inorg. Chim. Acta*, 1984, **84**, L9.
82. P. G. Jones, *Acta Crystallogr., Sect. B*, 1980, **36**, 2775.

83. K. Dziwok, J. Lachmann, D. L. Wilkinson, G. Müller and H. Schmidbaur, *Chem. Ber.*, 1990, **123**, 423.
84. H. Schmidbaur, W. Graf and G. Müller, *Angew. Chem., Int. Ed. Engl.*, 1988, **27**, 417.
85. E. Colacio, R. Cuesta, J. M. Gutierrez-Zorilla, A. Luque, P. Roman, T. Giraldo and M. R. Taylor, *Inorg. Chem.*, 1996, **35**, 4232.
86. H. Schmidbaur, A. Wohlleben, U. Schubert, A. Frank and G. Huttner, *Chem. Ber.*, 1977, **110**, 2751.
87. J. Shain and J. P. Fackler, Jr., *Inorg. Chim. Acta*, 1987, **131**, 157.
88. C.-M. Che, H.-L. Kwong, C.-K. Poon and V. W.-W. Yam, *J. Chem. Soc., Dalton Trans.*, 1990, 3215.
89. A. Burini, R. Galassi, B. R. Pietroni and G. Rafaiiani, *J. Organomet. Chem.*, 1996, **519**, 161.
90. D. Perreault, M. Drouin, A. Michel, V. M. Miskowski, W. P. Schaefer and P. D. Harvey, *Inorg. Chem.*, 1992, **31**, 695.
91. V. W.-W. Yam and W.-K. Lee, *J. Chem. Soc., Dalton Trans.*, 1993, 2097.
92. H.-R. C. Jaw, M. M. Savas, R. D. Rogers and W. R. Mason, *Inorg. Chem.*, 1989, **28**, 1028.
93. W. P. Schaeffer, R. E. Marsh, T. M. McCleskey and H. B. Gray, *Acta Crystallogr., Sect. C*, 1991, **47**, 2553.
94. A. L. Balch, E. Y. Fung and M. M. Olmstead, *J. Am. Chem. Soc.*, 1990, **112**, 5181.
95. M. N. I. Khan, C. King, D. D. Heinrich, J. P. Fackler, Jr., and L. C. Porter, *Inorg. Chem.*, 1989, **28**, 2150.
96. H. Schmidbaur, R. Herr, G. Müller and J. Riede, *Organometallics*, 1985, **4**, 1208.
97. H. Schmidbaur, R. Herr, F. E. Wagner, R. Bau, J. Riede and G. Müller, *Organometallics*, 1986, **5**, 566.
98. M. Khan, C. Oldham and D. G. Tuck, *Can. J. Chem.*, 1981, **59**, 2714.
99. W. Bensch, M. Prelati and W. Ludwig, *J. Chem. Soc., Chem. Commun.*, 1986, 1762.
100. S.-J. Shieh, D. Li, S.-M. Peng and C.-M. Che, *J. Chem. Soc., Dalton Trans.*, 1993, 195.
101. R.-H. Uang, C.-K. Chan, S.-M. Peng and C.-M. Che, *J. Chem. Soc., Chem. Commun.*, 1994, 2561.
102. T. M. McCleskey, L. M. Henling, K. A. Flanagan and H. B. Gray, *Acta Crystallogr., Sect. C*, 1993, **49**, 1467.

103. R. Uson, A. Laguna, M. Laguna, E. Fernandez, M. D. Villacampa, P. G. Jones and G. M. Sheldrick, *J. Chem. Soc., Dalton Trans.*, 1983, 1679.
104. I. J. B. Lin, J. M. Hwang, D.-F. Feng, M. C. Cheng and Y. Wang, *Inorg. Chem.*, 1994, **33**, 3467.
105. M. Bardaji, A. Laguna and M. Laguna, *J. Chem. Soc., Dalton Trans.*, 1995, 1255.
106. M. N. I. Khan, R. J. Staples, C. King, J. P. Fackler, Jr., and R. E. P. Winpenny, *Inorg. Chem.*, 1993, **32**, 5800.
107. A. L. Balch and E. Y. Fung, *Inorg. Chem.*, 1990, **29**, 4764.
108. A. Stützer, P. Bissinger and H. Schmidbaur, *Chem. Ber.*, 1992, **125**, 367.
109. M. K. Cooper, K. Henrik, M. McPartlin and J. L. Latten, *Inorg. Chim. Acta*, 1982, **65**, L185.
110. V. W.-W. Yam, T.-F. Lai and C.-M. Che, *J. Chem. Soc., Dalton Trans.*, 1990, 3747.
111. D. Li, C.-M. Che, S.-M. Peng, S.-T. Liu, Z.-Y. Zhou and T. C. W. Mak, *J. Chem. Soc., Dalton Trans.*, 1993, 189.
112. C.-M. Che, H.-K. Yip, V. W.-W. Yam, P.-Y. Cheung, T.-F. Lai, S.-J. Shieh and S.-M. Peng, *J. Chem. Soc., Dalton Trans.*, 1992, 427.
113. K. Issleib and A. Brock, *Z. Anorg. Allg. Chem.*, 1957, **292**, 245.
114. H. J. Jakobsen, *Acta Chem. Scand.*, 1970, **24**, 2661.
115. C. F. Shaw, *Comments Inorg. Chem.*, 1989, **8**, 233.
116. T. M. Simon, D. H. Kunishima, G. J. Vibert and A. Lobert, *Cancer Res.*, 1981, **41**, 94.
117. S. J. Berners-Price, C. K. Mirabelli, R. K. Johnson, M. R. Mattern, F. L. McCabe, L. F. Faucette., C.-M. Sung, S.-M. Mong, P. J. Sadler and S. T. Crooke, *Cancer Res.*, 1986, **46**, 5486.
118. S. J. Berners-Price, G. R. Girard and D. T. Hill, *J. Med. Chem.*, 1990, **33**, 1386.
119. C. F. Shaw, in *Metal Compounds in Cancer Therapy*, ed. S. P. Fricker, Chapman & Hall, London, 1994; 47-64.
120. J. B. Hudson, E. A. Graham, N. Miki, G. H. N. Towers, L. L. Hudson, R. Rossi, A. Carpita and D. Neri, *Chemosphere*, 1989, **19**, 1329.
121. G. K Cooper and C. I. Nitsche, *Bioinorg. Chem.*, 1985, **13**, 362.
122. B. Cosimelli, D. Neri and G. Roncucci, *Tetrahedron*, 1996, **52**, 11281.
123. T. Amagai, T. K. Miyamoto, H. Ichida and Y. Sasaki, *Bull. Chem. Soc. Jpn.*, 1989, **62**, 1078.

124. S. Y. M. Chooi, P.-H. Leung, K. Y. Sim, K. S. Tan and O. L. Kon, *Tetrahedron: Assym.*, 1994, **5**, 49.
125. J. B. Hudson and G. H. N. Towers, *Photochem. Photobiol.*, 1988, **48**, 289.
126. M. M. T. Khan and A. E. Martell, *Inorg. Chem.*, 1975, **14**, 676.
127. H. Brunner and W. Z. Pieronczyk, *Angew. Chem., Int. Ed. Engl.*, 1979, **18**, 620.
128. K. Issleib and H. Weichmann, *Z. Chem.*, 1971, **11**, 188.
129. M. Antberg, L. Dahlenburg, N. Höck and C. Prengel, *Phosphorus Sulfur*, 1986, **26**, 143.
130. R. B. King, R. N. Kapoor, M. S. Saran and P. N. Kapoor, *Inorg. Chem.*, 1971, **10**, 1851.
131. R. B. King and J. C. Cloyd, Jr., *J. Am. Chem. Soc.*, 1975, **97**, 53.
132. L. Maier, *Helv. Chim. Acta*, 1965, **48**, 1034.
133. J. P. Amma and J. K. Stille, *J. Org. Chem.*, 1982, **47**, 468.
134. A. M. Aguiar and D. Daigle, *J. Am. Chem. Soc.*, 1964, **86**, 2299.
135. O. Herd, A. Heßler, K.P. Langhaus, O. Stelzer, W. S. Sheldrick and N. Weferling, *J. Organomet. Chem.*, 1994, **475**, 99.
136. E. C. Constable, C. E. Housecroft, M. Neuburger, A. G. Schneider and M. Zehnder, *J. Chem. Soc., Dalton Trans.*, 1997, 2427.
137. H. Zorn, H. Schindlbauer and H. Hagen, *Chem. Ber.*, 1965, **98**, 2431.
138. E. Lindner and D. Huebner, *Chem. Ber.*, 1983, **116**, 2574.
139. H. Brunner, M. E. Dylla, G. A. M. Hecht and W. Z. Pieronczyk, *Z. Naturforsch., B: Anorg. Chem., Org. Chem.*, 1982, **37**, 404.
140. O. Dahl, *Acta Chem. Scand., Ser. B*, 1976, **30**, 799.
141. S. E. Tunney and J. K. Stille, *J. Org. Chem.*, 1987, **52**, 748.
142. B. Chiswell and I. M. Venenzi, *J. Chem. Soc. A*, 1966, 617.
143. K. Issleib and A. Brack, *Z. Anorg. Allg. Chem.*, 1957, **292**, 245.
144. J. M. Brown and L. R. Canning, *J. Chem. Soc., Chem. Commun.*, 1983, 460.
145. E. Plazek and R. Tyka, *Zesz. Nauk. Politech. Wroclaw. Chem.*, 1957, 79; *Chem. Abstr.*, 1958, **52**, 20156.
146. Y. L. Gol'dfarb, A. A. Dudinov and V. S. Bogdanov, *Izv. Ak. Nauk SSSR, Ser. Khim.*, 1986, 2105.
147. G. Wittig, H. Braun and H.-J. Cristau, *Annalen*, 1971, **751**, 17.
148. W. J. Richter, *Angew. Chem.*, 1982, **94**, 932.

149. R. Benn, R. Mynott and W. J. Richter, *Z. Naturforsch. B: Anorg. Chem., Org. Chem.*, 1984, **39**, 79.
150. Z. S. Novikova, I. L. Odinets and I. F. Lutsenko, *Zh. Obsch. Khim.*, 1983, **53**, 699.
151. S. S. Moore and G. M. Whitesides, *J. Org. Chem.*, 1982, **47**, 1489.
152. D. B. Denney and F. J. Gross, *J. Org. Chem.*, 1967, **32**, 2445.
153. A. M. Aguiar, J. R. Smiley-Ireland, C. J. Morrow, J. P. John and G. W. Prejean, *J. Org. Chem.*, 1969, **34**, 2684.
154. G. Dyer and J. Roscoe, *Inorg. Chem.*, 1996, **35**, 4098.
155. M. Bentov, L. David and E. D. Bergman, *J. Chem. Soc.*, 1964, 4750.
156. E. A. Krasil'nikova, E. S. Sharafieva and A. I. Razumov, *Zh. Obsch. Khim.*, 1982, **52**, 2638.
157. A. A. Tolmachev, S. P. Ivonin, A. V. Kharchenko and E. S. Kozlov, *Zh. Obsch. Khim.*, 1991, **61**, 859.
158. K. Dziwok, G. Reber, G. Müller and H. Schmidbaur, *Helv. Chim. Acta*, 1987, **70**, 1905.
159. J. Green and L. H. Malcolm, *Eur. Pat.* 117.156, 1984; *Chem. Abstr.*, 1985, **102**, 6809s.
160. Y. L. Gol'dfarb, A. A. Dudinov, V. P. Litvinov, D. S. Yufit and Y. T. Struchkov, *Khim. Geterotsikl. Sojed.*, 1982, 1326.
161. A. Varshney and G. M. Gray, *Inorg. Chim. Acta*, 1988, **148**, 215.
162. D. W. Allen and D. F. Ashford, *J. Inorg. Nucl. Chem.*, 1976, **38**, 1953.
163. J. D. King, M. Monari and E. Nordlander, *J. Organomet. Chem.*, 1999, **573**, 272.
164. D. W. Allen and B. F. Taylor, *J. Chem. Soc., Dalton Trans.*, 1982, 51.
165. D. W. Allen, J. R. Charlton and B. G. Hutley, *Phosphorus*, 1976, **6**, 191.
166. *Comprehensive Organic Chemistry: Heterocyclic Compounds: The Synthesis and Reactions of Organic Compounds*, Vol. 4, ed. D. Barton, W. D. Ollis and P. G. Sammes, Pergamon Press, 1979; 789-838.
167. D. W. Allen, *J. Chem. Soc., B*, 1970, 1490.
168. D. W. Allen, S. J. Grayson, I. Harness, B. G. Hutley and I. W. Mowat, *J. Chem. Soc., Perkin Trans. II*, 1973, 1912.
169. C. E. Griffin, R. P. Peller, K. R. Martin and J. A. Peters, *J. Org. Chem.*, 1965, **30**, 97.
170. H. J. Jakobsen and J. A. Nielsen, *J. Mol. Spectrosc.*, 1970, **33**, 474.
171. S. Sørensen, R. S. Hansen and H. J. Jakobsen, *J. Am. Chem. Soc.*, 1972, **94**, 5900.
172. J. M. Brown and A. R. Lucy, *J. Organomet. Chem.*, 1986, **314**, 241.

173. R. Ziessel, *Tetrahedron Lett.*, 1989, **30**, 463.
174. H. C. Brookes, E. I. Lakoba and M. H. Sosabowski, *J. Chem. Res. (M)*, 1997, 1064.
175. E. I. Lakoba, M.Sc. Thesis, Moscow State University, Moscow, 1991.
176. K. R. Martin and C. E. Griffin, *J. Heterocycl. Chem.*, 1966, **3**, 92.
177. R. Rossi, A. Carpita, M. Ciofalo and V. Lippolis, *Tetrahedron*, 1991, **47**, 8443.
178. J. M. Tour, R. Wu and J.S. Schumm, *J. Am. Chem. Soc.*, 1991, **113**, 7064.
179. Y. L. Gol'dfarb and M. L. Kirmalova, *Zh. Obsch. Khim.*, 1956, **26**, 3409.
180. Z. Hu, J. L. Atwood and M. P. Cava, *J. Org. Chem.*, 1994, **59**, 8071.
181. R. J. Marles, R. L. Compadre, C. M. Compadre, C. Soucy-Breau, R. W. Redmond, F. Duval, B. Mehta, P. Morand, J. C. Scaiano and J. T. Arnason, *Pestic. Biochem. Physiol.*, 1991, **41**, 89.
182. J. C. Scaiano, A. MacEachern, J. T. Arnason, P. Morand and D. Weir, *Photochem. Photobiol.*, 1987, **46**, 193.
183. K. Tamao, S. Kodama, I. Nakajima and M. Kumada, *Tetrahedron*, 1982, **38**, 3347.
184. a) D. D. Cunningham, L. Laguren-Davidson, H. B. Mark, Jr., C. V. Pham and H. Zimmer, *J. Chem. Soc., Chem. Commun.*, 1987, 1021.
b) C. V. Pham, A. Burkhardt, R. Shabana, D. D. Cunningham, H. B. Mark, Jr., and H. Zimmer, *Phosphorus, Sulfur and Silicon*, 1989, **46**, 153.
185. G. J. Visser, G. J. Heers, J. Wolters and A. Vos, *Acta Crystallogr., Sect. B*, 1968, **24**, 467.
186. C. A. Veracini, D. Macciantelli and L. Lunazzi, *J. Chem. Soc., Perkin Trans. II*, 1973, 751.
187. J. S. Field, R. J. Haines, C. J. Parry and S. S. Sookraj, *S. Afr. J. Chem.*, 1993, **46**, 70.
188. H. Wynberg and A. Bentjes, *J. Am. Chem. Soc.*, 1960, **82**, 1447.
189. S. Kotani, K. Shiina and K. Sonogashira, *J. Organomet. Chem.*, 1992, **429**, 403.
190. A. Carpita, R. Rossi and C. A. Vernanzi, *Tetrahedron*, 1985, **41**, 1919.
191. P. Bäuerle, F. Würthner, G. Götz and F. Effenberger, *Synthesis*, 1993, 1099.
192. R. F. Curtis and G. T. Phillips, *J. Chem. Soc.*, 1965, 5134.
193. R. Rossi, A. Carpita and A. Lezzi, *Tetrahedron*, 1984, **40**, 2773.
194. Y. L. Gol'dfarb, A. A. Dudinov and V. P. Litvinov, *Izv. Ak. Nauk SSSR, Ser. Khim.*, 1982, 2388.
195. V. N. Kalinin, *Usp. Khim.*, 1991, **60**, 339.
196. E. G. Kuntz, *Chemtech*, 1987, **17**, 570.

197. W. A. Herrman, J. A. Kulpe, W. Konkol and H. Bahrmann, *J. Organomet. Chem.*, 1990, **389**, 85.
198. A. Hessler, S. Kucken, O. Steltzer, J. Blotevogel-Baltronat and W. S. Sheldrick, *J. Organomet. Chem.*, 1995, **501**, 293.
199. G. Muller and D. Sainz, *J. Organomet. Chem.*, 1995, **495**, 103.
200. B. Mohr, D. M. Lynn and R. H. Grubbs, *Organometallics*, 1996, **15**, 4317.
201. H. Bahrmann, K. Bergrath, H.-J. Kleiner, P. Lappe, C. Naumann, D. Peters and D. Regnat, *J. Organomet. Chem.*, 1996, **520**, 97.
202. H. J. Lucas, F. W. Mitchell, Jr., and C. N. Scully, *J. Am. Chem. Soc.*, 1950, **72**, 5491.
203. D. W. Allen, B. G. Hutley and M. T. J. Mellor, *J. Chem. Soc., Perkin Trans. II*, 1972, 63.
204. W. A. Herrman, J. A. Kulpe, J. Kellner, H. Riepl, H. Bahrmann and W. Konkol, *Angew. Chem.*, 1990, **102**, 408.
205. O. Herd, A. Heßler, K. P. Langhans, O. Stelzer, W. S. Sheldrick and N. Weferling, *J. Organomet. Chem.*, 1994, **475**, 99.
206. F. Bitterer, O. Herd, A. Heßler, M. Kühnel, K. Rettig, O. Stelzer, W. S. Sheldrick, S. Nagel and N. Rösch, *Inorg. Chem.*, 1996, **35**, 4103.
207. E. A. Krasil'nikova, O. L. Nevzorova and V. V. Sentemov, *Zh. Obsch. Khim.*, 1985, **55**, 1283.
208. P. Tavs, *Chem. Ber.*, 1970, **103**, 2428.
209. *Comprehensive Organic Chemistry: The Synthesis and Reactions of Organic Compounds*, Vol. 2, ed. D. Barton, W. D. Ollis and I. O. Sutherland, Pergamon Press, 1979; 1121-1187.
210. K. Sasse, *Methoden der Organischen Chemie (Houben Weyl)*, ed. H. Müller, G. Thieme, Stuttgart, 1963, **12**; 60, 241.
211. A. Buhling, J. W. Elgersma, S. Nkrumah, P. C. J. Kamer and P. W. N. M. van Leeuwen, *J. Chem. Soc., Dalton Trans.*, 1996, 2143.
212. M. H. Sosabowski, Ph. D. Thesis, London, Royal Holloway Colledge, 1991.
213. T. Kauffmann, *Angew. Chem., Int. Ed. Engl.*, 1979, **18**, 1.
214. A. Minato, K. Suzuki, K. Tamao and M. Kumada, *J. Chem. Soc., Chem. Commun.*, 1984, 511.
215. P. Ribereau and G. Quéguiner, *Tetrahedron*, 1983, **39**, 3593.
216. G. M. Sheldrick, *Acta Crystallogr. Sect. A*, 1990, **46**, 467.

217. G. M. Sheldrick and T. R. Schneider, "SHELXL: High-Resolution Refinement", *Methods in Enzymology*, 1997, **227**, 319.
218. T. B. Rauchfuss, in *Progress in Inorganic Chemistry*, Vol. 39, ed. S. J. Lippard, John Wiley & Sons, Inc., New York, 1991; 259-329.
219. M. Draganjac, C. J. Ruffing and T. B. Rauchfuss, *Organometallics*, 1985, **4**, 1909.
220. a) L. Latos-Graszynski, J. Lisowski, M. M. Olmstead and A. L. Balch, *Inorg. Chem.*, 1989, **28**, 1183.
220. b) L. Latos-Graszynski, J. Lisowski, M. M. Olmstead and A. L. Balch, *Inorg. Chem.*, 1989, **28**, 3328.
221. E. C. Constable, R. P. G. Henney and D. A. Tocher, *J. Chem. Soc., Chem. Commun.*, 1989, 913.
222. E. C. Constable, R. P. G. Henney and D. A. Tocher, *J. Chem. Soc., Dalton Trans.*, 1992, 2467.
223. R. J. Angelici, *Coord. Chem. Rev.*, 1990, **105**, 61.
224. J. R. Polam and L. C. Porter, *J. Organomet. Chem.*, 1994, **482**, 1.
225. J. Chen and R. J. Angelici, *Organometallics*, 1989, **8**, 2277.
226. J. Chen, L. M. Daniels and R. J. Angelici, *J. Am. Chem. Soc.*, 1990, **112**, 199.
227. M. G. Choi, M. J. Robertson and R. J. Angelici, *J. Am. Chem. Soc.*, 1991, **113**, 4005.
228. H. D. Hartough, *Thiophene and Its Derivatives*, Wiley-Interscience, New York, 1952.
229. T. J. Giordano and P. G. Rasmussen, *Inorg. Chem.*, 1975, **14**, 1628.
230. Y. Xie, S. C. Ng, B.-M. Wu, F. Xue, T. C. W. Mak and T. S. A. Hor, *J. Organomet. Chem.*, 1997, **531**, 175.
231. M. Paneque, M. L. Poveda, L. Rey, S. Taboada, E. Carmona and C. Ruiz, *J. Organomet. Chem.*, 1995, **504**, 147.
232. M. G. Choi and R. J. Angelici, *J. Am. Chem. Soc.*, 1989, **111**, 8753.
233. A. J. Arce, P. Arrojo, Y. De Sanctis and M. Márquez, *J. Organomet. Chem.*, 1994, **479**, 159.
234. A. J. Deeming, D. M. Speel, M. Shinhmar, A. Di Trapani, A. J. Arce and Y. De Sanctis, The 6th International Conference on Pt Group Metals, York, UK, July 21-26.
235. T. A. Waldbach, P. H. van Rooyen and S. Lotz, *Angew. Chem., Int. Ed. Engl.*, 1993, **32**, 710.
236. R. D. Adams and X. Qu, *Organometallics*, 1995, **14**, 2238.
237. A. J. Deeming, S. N. Jayasuriya, A. J. Arce and Y. De Sanctis, *Organometallics*, 1996, **15**, 786.

238. S. M. Bucknor, M. Draganjac, T. B. Rauchfuss and C. J. Ruffing, *J. Am. Chem. Soc.*, 1984, **106**, 5379.
239. M. Alvarez, N. Lugan and R. Mathieu, *Inorg. Chem.*, 1993, **32**, 5652.
240. M. Alvarez, N. Lugan, B. Donnadieu and R. Mathieu, *Organometallics*, 1995, **14**, 365.
241. D. V. Toronto, B. Weissbart, D. S. Tinti and A. L. Balch, *Inorg. Chem.*, 1996, **35**, 2484.
242. N. C. Baenzinger, K. M. Dittermore and J. R. Doyle, *Inorg. Chem.*, 1974, **13**, 805.
243. C. A. Tolman, *Chem. Rev.*, 1977, **77**, 313.
244. W. R. Harshbarger and S. H. Bauer, *Acta Crystallogr. Sect. B*, 1970, **26**, 1010.
245. M. M. Savas and W. R. Mason, *Inorg. Chem.*, 1987, **26**, 301.
246. C. King, M. N. I. Khan, R. J. Staples and J. P. Fackler, Jr., *Inorg. Chem.*, 1992, **31**, 3236.
247. G. Bergerhoff, *Z. Anorg. Allg. Chem.*, 1964, **327**, 139.
248. T. M. McCleskey and H. B. Gray, *Inorg. Chem.*, 1992, **31**, 1733.
249. C.-M. Che, H.-L. Kwong, V. W.-W. Yam and K.-C. Cho, *J. Chem. Soc., Chem. Commun.*, 1989, 885.
250. J. S. Field, J. Grieve, R. J. Haines, N. May and M. M. Zulu, *Polyhedron*, 1998, **17**, 3021.
251. J. H. Uhlenbroek and J. D. Bijloo, *Rec. Trav. Chim. Pays-Bas*, 1958, **77**, 1004.
252. F. J. Gommers, *Nematologia*, 1972, **18**, 458.
253. J. Bakker, F. J. Gommers, I. Nieuwenhuis and H. Wynberg, *J. Biol. Chem.*, 1979, **254**, 1841.
254. J. C. Scaiano, R. W. Redmond, B. Mehta and J. T. Arnason, *Photochem. Photobiol.*, 1990, **52**, 655.
255. J. Kagan, E. D. Kagan and E. Seigneurie, *Chemosphere*, 1986, **15**, 49.
256. R. J. Marles, J. B. Hudson, E. A. Graham, C. Soucy-Breau, P. Morand, R. L. Compadre, C. M. Compadre, G. H. N. Towers and J. T. Arnason, *Photochem. Photobiol.*, 1992, **56**, 479.
257. D. G. McRae, E. Yamamoto and G. H. N. Towers, *Biochem. Biophys. Acta*, 1985, **821**, 488.
258. J. B. Hudson, E. A. Graham, N. Micki, L. Hudson and G. H. N. Towers, *Photochem. Photobiol.*, 1986, **44**, 477.
259. J. Kagan, R. Gabriel and S. Reed, *Photochem. Photobiol.*, 1980, **31**, 465.

260. K. Downum, R. Hancock and G. H. N. Towers, *Photochem. Photobiol.*, 1982, **36**, 517.
261. T. J. Dougherty, *Photochem. Photobiol.*, 1987, **45**, 879.
262. T. J. Dougherty, in *Advances in Photochemistry*, Vol. 17, ed. D. Volman, G. Hammond and D. Neckers, John Wiley & Sons, Inc., New York, 1992; 275-311.
263. L. Milgrom and S. MacRobert, *Chemistry in Britain*, 1998, 45.
264. T. Oppenländer, *Chimia*, 1988, **42**, 331.
265. W. M. Rampone, J. L. McCullough, G. D. Weinstein, G. H. N. Towers, M. W. Berns and B. Abeysekera, *J. Invest. Dermatol.*, 1986, **87**, 354.
266. D. T. Walz, M. J. Dimartino and D. E. Griswold, *J. Rheumatol.*, 1982, **9**, 54.
267. T. M. Simon, D. H. Kushima, G. J. Vibert and A. Lerner, *Cancer*, 1979, **44**, 1965.
268. T. M. Simon, D. H. Kushima, G. J. Vibert and A. Lerner, *Cancer Res.*, 1981, **41**, 94.
269. S. J. Berners-Price, P. S. Jarret and P. J. Sadler, *Inorg. Chem.*, 1987, **26**, 3074.
270. C. K. Mirabelli, G. F. Rush, B. D. Jensen, J. O. Bartus, C.-M. Sung, D. W. Alberts, D. E. Gennaro, S. T. Hoffstein, R. K. Johnson and S. T. Crooke, *Proceed. AACR*, 1987, **28**, 313.
271. D. T. Hill, G. R. Girard, F. L. McCabe, R. K. Johnson, P. D. Stupik, D. H. Zhang, W. M. Reiff and D. S. Eggleston, *Inorg. Chem.*, 1989, **28**, 3529.
272. R. M. Snyder, C. K. Mirabelli and R. K. Johnson, *Cancer Res.*, 1986, **46**, 5054.
273. J. E. Schurig, H. A. Meinema, K. Timmer, B. H. Long and A. M. Casazza, *Progress in Clin. Biochem. Med.*, 1989, **10**, 205.
274. C. K. Mirabelli, R. K. Johnson, D. T. Hill, L. Faucette, G. R. Girard, G. Y. Kuo, C. M. Sung and S. T. Crooke, *J. Med. Chem.*, 1986, **26**, 218.
275. S. J. Berners-Price and P. J. Sadler, *Struct. Bond.*, 1988, **70**, 27.
276. G. D. Hoke, R. A. Macia, P. C. Menier, P. J. Bugelski, C. K. Mirabelli, G. F. Rush and W. D. Matthews, *Toxicol. Appl. Pharmacol.*, 1989, **100**, 293.
277. H. Kunkely and A. Vogler, *Z. Naturforsch.*, 1996, **51b**, 1067.
278. V. W.-W. Yam, S. W.-K. Choi, K. K.-W. Lo, W.-F. Dung and R. Y.-C. Kong, *J. Chem. Soc., Chem. Commun.*, 1994, 2379.
279. C. H. Evans and J. C. Scaiano, *J. Am. Chem. Soc.*, 1990, **112**, 2694.
280. M. Ciofalo and G. Ponterini, *Photochem. Photobiol. A: Chem.*, 1994, **83**, 1.
281. R. S. Becker, J. S. de Melo, A. L. Maçanita and F. Elisei, *Pure & Appl. Chem.*, 1995, **67**, 9.

-
282. R. Boch, B. Mehta, T. Connolly, T. Durst, J. T. Arnason, R. W. Redmond and J. C. Scaiano, *Photochem. Photobiol. A: Chem.*, 1996, **93**, 39.
283. S. J. Berners-Price and P. J. Sadler, *J. Inorg. Biochem.*, 1987, **31**, 267.
284. R. I. Freshney, *Culture of Animal Cells: a Manual of Basic Technique*, 2nd ed., Liss, New York, 1988.
285. D. D. Perrin, W. L. F. Armarego and D. R. Perrin, *Purification of Laboratory Chemicals*, 2nd ed., Pergamon Press, New York, 1980.
286. A. C. T. North, D. C. Phillips and F. S. Mathews, *Acta Crystallogr. Sect. A*, 1968, **24**, 351.
287. P. McArdle, *Oscail v. 7b*, Crystallography Centre, Chemistry Department, NUI Galway, Ireland.
288. P. McArdle, *J. Appl. Crystallogr.*, 1995, **28**, 65.
289. D. Dakternieks, B. F. Hoskins and C. L. Rolls, *Aust. J. Chem.*, 1986, **39**, 1221.
290. *Inorganic Syntheses*, Vol. 6, Wiley-Interscience, New York, 1960; 218.
291. A. O. King, E. Negishi, F. J. Villani and A. Silveira, *J. Org. Chem.*, 1978, **43**, 358.
292. *Inorganic Syntheses*, Vol. 26, Wiley-Interscience, New York, 1989; 86.
293. H. W. Geluk, *Synthesis*, 1970, 652.
294. M. H. Sosabowski and P. Powell, *J. Chem. Res. (M)*, 1997, 201.
295. D. M. P. Mingos and J. Yau, *J. Organomet. Chem.*, 1994, **479**, C16.
296. J. M. Smith, B. C. Taverner and N. J. Coville, *J. Organomet. Chem.*, 1997, **530**, 131.
297. J. Bruckman and C. Krüger, *Acta Crystallogr. Sect. C*, 1995, **51**, 1152.
298. T. E. Müller, S. W.-K. Choi, D. P. Mingos, D. Murphy, D. J. Williams and V. W.-W. Yam, *J. Organomet. Chem.*, 1994, **484**, 209.